Molecular and genetic cues influencing ovule development in barley (Hordeum vulgare)

Laura Gay Wilkinson

A thesis submitted to The University of Adelaide in fulfilment of the requirements for the degree of Doctor of Philosophy

The University of Adelaide

Faculty of Sciences

School of Agriculture, Food and Wine

THE UNIVERSITY of ADELAIDE

February 2019

Table of Contents

Declaration

I certify that this work contains no material which has been accepted for the award of any other degree or diploma in my name, in any university or other tertiary institution and, to the best of my knowledge and belief, contains no material previously published or written by another person, except where due reference has been made in the text. In addition, I certify that no part of this work will, in the future, be used in a submission in my name, for any other degree or diploma in any university or other tertiary institution without the prior approval of the University of Adelaide and where applicable, any partner institution responsible for the joint-award of this degree.

I acknowledge that copyright of published works contained within this thesis resides with the copyright holder(s) of those works.

I also give permission for the digital version of my thesis to be made available on the web, via the University's digital research repository, the Library Search and also through web search engines, unless permission has been granted by the University to restrict access for a period of time.

I acknowledge the support I have received for my research through the provision of an Australian Government Research Training Program Scholarship.

Laura Wilkinson

February 2019

Acknowledgements

I have been exceptionally lucky to have had a fantastic team of supervisors guide me throughout my PhD: Matthew Tucker, Rachel Burton and Caitlin Byrt. You have my most sincere thanks for the effort and support that you have given me over these four years. To my primary supervisor Matt in particular, I am deeply appreciative of how generous you are with your time, your patience with my endless questions and at times questionable priorities, and your ability to keep perspective on what matters both in science and in life.

I would like to thank the University of Adelaide for awarding me a Postgraduate Award, to support my PhD studies. I would also like to thank the Australian Research Council Centre of Excellence in Plant Cell Walls for additional scholarship support, both financially and professionally.

I would like to say a huge thank you to Neil Shirley, for making bioinformatics seem easy, and to Helen Collins and Lisa O'Donovan, for always being on call for microscopy questions. Thank you also to Kelly Houston and Ali Hassan for guidance on GWAS, and Rohan Singh and Kylie Neumann for your expertise and support with transgenic plants, and keeping everything growing happily. Thank you to all the students and staff of the Plant Cell Walls group, past and present, for making WIC West such a great place to work, particularly Nat B, Nat K, Dave, Stav and Julian for always keeping an eye on me, and having words of advice.

Thanks Tucker Lab! All of you lovely people near and far, thanks for all the knowledge sharing, trouble shooting, and endless banter. I couldn't imagine a more fun little band of lab monkeys to be part of. Aubert, thanks for being endlessly cheery, calm and cluey. It's going to be real weird showing up to work without you (how has it been 5 years?!).

To the people who keep me balanced: thank you Duncan, Royce, Morgan, Sophia, Carri, and Zoe for being a phone call away when times are tough, keen for adventures when times are good, and for always being so much fun that I wish I could pause the clock and do that labwork…. Later. Thank you to the Bell-O'Briens for being so kind, down to earth, and the most fantastic role models I could've ever imagined. Thank you to my music teachers, particularly Mr B, Rosemary, and Maxine, for years of fun and for teaching me invaluable life lessons like enjoying problem solving, finding joy in tiny details, and to always look at what's happening next.

To my family: Mum, Dad, Grandma, Grandpa, Granny Tuppy, Henry, Ollie, Charlie. Thank you for always being there with kindness, support and patience, even through all the Interesting Times we've been living in these last few years. I love you all to bits, far more than words can do justice, and I couldn't have gotten through this PhD without each of you.

Finally, Rhen. Love, thank you for being my anchor to weather the storms, and always pushing both of us to be our best. Times wouldn't nearly be as good, and I absolutely wouldn't be the person I am today without you.

Thank you to each and every one of you.

Chapter 1

Thesis Introduction

ꕥ • ꕥ

Thesis Introduction

Barley has been an important agricultural crop for thousands of years, and continues to be widely used for human nutrition, animal feed, malting and brewing in the present day. Each grain of barley is produced from an individual self-fertile flower. The floral structure of monocotyledonous cereal crops, including barley, is such that each individual flower generates thousands of pollen grains in the male reproductive organs, i.e. the anthers, and a single ovule within the female reproductive organ, i.e. the pistil, also called the ovary. As the site of fertilisation, the ovule is critical for both producing the female gamete and, together with the ovary, regulating transfer of nutrients into the developing grain. The abundance of pollen and its location within the relatively easily accessible anthers has facilitated much study regarding processes involved in male reproductive development. This provides useful insight into the molecular and genetic cues required for male fertility in cereal crops, especially under conditions of environmental stress. In contrast, until recently little work has been carried out to characterise cues regulating ovule development in cereals, largely due to the difficulty of isolating ovules in sufficient quantity for genetic and molecular analysis. Substantial knowledge is available regarding female reproductive development in model dicots such as *Arabidopsis thaliana*, and orthologous developmental regulatory systems are beginning to be described in cereals such as rice (*Oryza sativa*) and maize *(Zea mays*). However, there is key structural variation between the mature ovules produced by Arabidopsis and those produced by cereal crops that may influence the translation of this knowledge, or require unique description in the cereals. Generally speaking, the mature angiosperm ovule is composed of four tissues: the funiculus, embryo sac, nucellus, and integuments. The embryo sac is the site of fertilisation, giving rise to the embryo and endosperm, the nucellus acts as a nutrient transfer tissue for the developing endosperm and undergoes programmed cell death, and the integuments form the seed coat around the developing seed (Arabidopsis) or grain (cereals). The predominant difference between ovule morphology in Arabidopsis and cereal crops is the

lack of a true funiculus in the cereals, and the arrangement of the nucellus, which forms a single layer surrounding the embryo sac of Arabidopsis. In the cereals, proliferation of a multilayered nucellus during ovule development results in the nucellus contributing the majority of the volume in the ovule. Species with a "thin" nucellus, such as Arabidopsis, are described as having tenuinucellate ovules, while ovules of those with a multilayered nucellus, such as cereal crops, are described as crassinucellate. While tenuinucellate and crassinucellate ovule structure has been described in many species, to date it is not clear if there is any benefit of each nucellus type. Following fertilisation in *Triticeae* cereals, the role of the nucellus as a transfer tissue may require the presence of an enlarged nucellus at ovule maturity. However, whether this has any impact on eventual seed size or structure has not been determined. In addition, prior to fertilisation, little is known about the development or purpose of a multilayered nucellus in ovule development, especially with respect to the relationship between the nucellus and the developing embryo sac. Further, knowledge regarding the specific genes regulating ovule development has yet to be translated from Arabidopsis to barley. In this thesis, diverse genotypes of barley have been utilised to morphologically and transcriptionally analyse ovule development in barley with the aim of phenotypically and genetically quantifying variation in ovule development, and to provide resources for future study in this area.

Thesis Structure

This thesis contains seven chapters: a general thesis introduction (Chapter 1), a review of the literature (Chapter 2), a methods chapter in publication format (Chapter 3, published), three research chapters in publication format (Chapters 4 – 6, unpublished), and a final general discussion to summarise the findings and future perspectives of the presented work (Chapter 7). This structure is presented in Figure 1-1.

Chapter 2 aims to introduce the reader to the subject of ovule development, with a review paper that takes the place of a traditional literature review. Current research is summarised regarding key transcription factors required for ovule development in other species, the role of the ovule in grain development and maintaining fertility under conditions of environmental stress, and recent technical advances that facilitate greater investigation of female reproductive development. This review paper was published in Annual Plant Reviews Online, in 2018 (doi:10.1002/9781119312994.apr0609).

Chapter 3 presents optimisation of a clearing technique that is routinely used for observation of small, whole-mounted tissues, for use with much larger tissues, such as whole barley pistils. The technique allows whole barley pistils to be cleared sufficiently for observation and analysis of specific ovule features. The capacity for such analysis formed the foundation for phenotypic studies in subsequent chapters. This methods paper was published in Plant Methods in 2017, (doi: 10.1186/s13007-017-0217-z).

A forward-genetics screen is presented in Chapter 4, whereby the method presented in Chapter 3 was used to phenotype nine mature ovule traits among a population of 127 European two-row barley genotypes. Distinct components of ovule size were identified, although no clear relationship was identified between ovule and grain traits. Despite this, variation was coupled with genotypic data available from the James Hutton Institute (JHI, Scotland), and used to perform a genome wide association study (GWAS). This identified a total of 66 markers associated with variation in mature ovule morphology, of which many were located within four quantitative trait loci (QTL). These QTL may reflect genes that contribute to the development of distinct barley ovule tissues, and hence are of interest for further study. The results from this Chapter raised a number of questions including: 1) How early in reproductive development is the mature ovule phenotype “set”, 2) What is the contribution of

each of the ovule tissues towards ovule development over time, and 3) What are the genetic and molecular cues that underlie non-lethal variation in development of each ovule tissue?

Chapter 5 presents morphological and transcriptional characterisation of barley ovule development in four genotypes that show clear differences in mature ovule morphology (Chapter 4). The methodology presented in Chapter 3 was used to identify nine stages of ovule development, and to phenotype the growth of ovule tissues at six of these stages, spanning initiation of the embryo sac to reproductive maturity. Additionally, the cellular arrangement of the ovule and cell wall components of the ovule was assessed by immunolabelling semi-thin sections, leading to the revelation that the nucellus is composed of discrete domains, and that de-methylesterification of pectin is specifically regulated in the cell walls of the nucellus cells flanking the female reproductive lineage. RNA sequencing was undertaken for whole pistils across five of these stages, in order to provide a transcriptional resource for understanding ovule development and the differences between four variant genotypes. Additionally, laser capture microdissection was utilised to isolate six discrete ovule tissues and subsequently produce a second tissue-specific transcriptional data set. These datasets were queried using a set of key developmental genes, including MADS-box transcription factors, components of the auxin signalling pathway and pectin-related genes, which validated their utility. Thus, morphological and transcriptional data was generated in Chapter 5, providing fundamental phenotypic and genetic tools to address the questions raised in Chapter 4.

In Chapter 6, the two sets of transcriptional data were used to investigate the genes within the four QTLs identified in Chapter 4. Whole-pistil data was used to identify differentially expressed genes between each of the four genotypes, and between different developmental stages, while tissue-specific transcriptional data was used to assess the localisation of expression of these candidate genes within the ovule. This led to the identification of candidate

genes that may contribute to the natural variation observed in ovule development between 2-row spring barley genotypes.

Finally, Chapter 7 presents a general discussion of the work presented in this thesis, and explores future perspectives.

Figure 1-1: Schematic overview of thesis structure.

Chapter 2

Literature Review: Exploring the role of the ovule in cereal grain development and reproductive stress tolerance

ꕥ • ꕥ

Statement of Authorship

Title of Paper	Exploring the Role of the Ovule in Cereal Grain Development and Reproductive Stress Tolerance
Publication Status	☑ Published ☐ Accepted for Publication ☐ Submitted for Publication ☐ Unpublished and Unsubmitted work written in manuscript style
Publication Details	Laura G. Wilkinson[1,2], Dayton C. Bird[1,2], Matthew R. Tucker[1,*]

Principal Author

Name of Principal Author (Candidate)	Laura G. Wilkinson		
Contribution to the Paper	Compiled information and wrote the manuscript. I hereby certify that the statement of authorship is accurate.		
Overall percentage (%)	70%		
Certification:	This paper reports on original research I conducted during the period of my Higher Degree by Research candidature and is not subject to any obligations or contractual agreements with a third party that would constrain its inclusion in this thesis. I am the primary author of this paper.		
Signature		Date	14/2/19

Co-Author Contributions

By signing the Statement of Authorship, each author certifies that:

i. the candidate's stated contribution to the publication is accurate (as detailed above);
ii. permission is granted for the candidate in include the publication in the thesis; and
iii. the sum of all co-author contributions is equal to 100% less the candidate's stated contribution.

Name of Co-Author	Dayton C. Bird		
Contribution to the Paper	Compiled information and contributed to the preparation of the manuscript. I hereby certify that the statement of authorship is accurate.		
Signature		Date	14/2/19

Name of Co-Author	Matthew R. Tucker		
Contribution to the Paper	Compiled information and contributed to the preparation of the manuscript. I hereby certify that the statement of authorship is accurate.		
Signature		Date	14/2/19

Abstract

Maintaining and enhancing grain production in cereal crops is a key priority for global research efforts. The formation of floral organs impacts the number and quality of grain produced, and is an important component of cereal yield. The grain is derived predominantly from the ovule, a multifunctional tissue located in the ovary of the flower that specifies and nurtures the female germline, produces a female gametophyte, and supports embryo and endosperm development after fertilisation. Grain cannot form without successful production and fertilisation of the female gametophyte, and the stages of floral development encompassing gametophyte formation are particularly sensitive to environmental fluctuations. A deeper fundamental understanding of female reproductive development from a tissueand cell-type-specific perspective may provide opportunities to sustain and increase grain yields. In this article, we consider flower and ovule development, with a particular focus on pre-fertilisation stages in cereals and their role in stress tolerance and downstream grain formation.

Keywords: ovule, ovary, development, nucellus, cereal, grain, programmed cell death, fertilisation, stress

The Plant Ovule: Where, What and Why?

Plant reproduction in angiosperms begins with the formation of a flower and ends with the formation of seed. In general, the floral organs of both monocot and dicot species are arranged similarly, forming rings (whorls) that surround the central reproductive structures (Figure 2-1). Distinct differences can be found, however, in the identity, arrangement, and the number of organs present in each whorl. In dicot species such as *Arabidopsis thaliana* (Arabidopsis), the outer whorls form sepals and petals (Figure 2-1a), whereas in monocot species such as *Hordeum vulgare* (barley) they are occupied by the palea and lemma (Figure 2-1b). The inner whorls consist of the stamens, which support the anthers, and carpels, which house the ovule(s). The number of floral organs varies between species. Arabidopsis flowers produce two carpels that fuse to form the pistil, six stamens, four petals, and four sepals. Florets of barley and *Triticum aestivum* (wheat) consist of a single pistil, which terminates in two styles, three stamens, and two lodicules, enclosed by two 'empty glume' organs, the palea and lemma (Figure 2-1b; De Vries, 1971). The *Oryza sativa* (rice) floret is similar except that it includes six stamens (Itoh et al., 2005). *Zea mays* (maize) florets initiate development of three carpels, which fuse to form a single pistil that bears two silks, three stamens, and two lodicules, enclosed by the palea and lemma. However, during maturation, maize inflorescences become monoecious, meaning florets on the tassel abort the pistil, becoming male, and florets on the ear abort the stamens, becoming female (Bonnett, 1940; Nickerson, 1954). Despite this inter-species variation, a common feature within the cereals is the development of a single ovule within each pistil. The ovule is located in the ovary and at maturity consists of a haploid embryo sac (female gametophyte, FG) surrounded by diploid maternal nucellus tissue and one or two integuments (Figure 2-1c–h). Both Arabidopsis and barley ovules are bitegmic, meaning that two integuments form around the ovule, eventually giving rise to the seed coat. The mature FG is composed of an egg cell, two synergid cells, two polar nuclei within the central cell, and a cluster of between 3 (Arabidopsis) and ~100 (maize) antipodal cells (Diboll, 1968; Engell, 1994; Evans and Grossniklaus, 2009). The FG is located towards the distal, micropylar end of

the ovule and oriented such that the synergids, egg cell, and central cell are most proximal to the micropyle. The synergid cells lack a complete cell wall whereby the plasma membrane contacts that of the egg cell (Jensen, 1973). The role of the synergids is to guide the pollen tube towards the ovule, and upon pollen burst the egg cell and the polar nuclei are both fertilised, giving rise to the zygote and the endosperm (Higashiyama et al., 2001). The enlarged, persistent nucellus and a high number of antipodal cells are a distinguishing feature of cereal ovules compared to the three antipodal cells and reduced nucellus of Arabidopsis (compare Figure 2-1e and h).

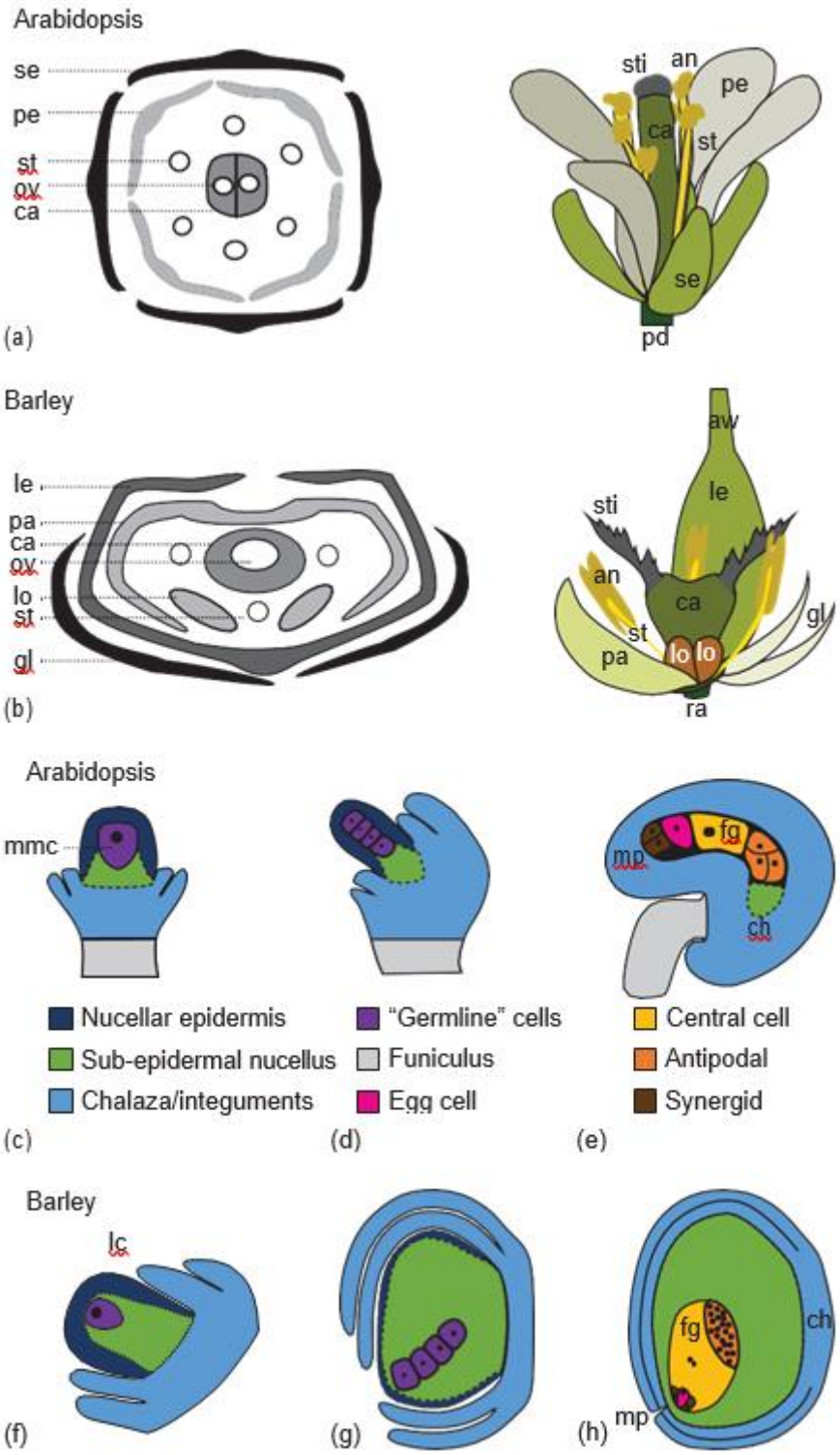

Figure 2-1: Flower and ovule development in Arabidopsis and barley. (a) In Arabidopsis, a representative of the dicots, the flower is arranged into concentric whorls of organs, each of which fulfils a specific role during reproductive development. The female reproductive organs are located in the centre of the flower. (b) In barley, a member of the

monocots, a whorl arrangement is also present, but organ types differ from those in Arabidopsis and show distinct identity relative to their position in the flower. The female reproductive organs are present in the centre of the flower. (c) Ovule development in Arabidopsis initiates from the placenta (at the junction of the two carpels) and requires the establishment of three distinct domains, the nucellus (which produces the germline), the chalaza (which produces the integuments), and the funiculus (which connects the ovule to the placenta and maternal plant). The nucellus can be divided into epidermal and sub-epidermal cell types. The accompanying legend uses colour coding to indicate the identity of the different cell types. (d) As the ovule grows, the megaspore mother cell undergoes meiosis to produce four megaspores in a linear or tetrahedral arrangement. The proximal megaspore initiates female gametophyte development. (e) At anthesis, the female gametophyte contains seven cells that represent four distinct cell types. The nucellus is restricted mainly to the chalazal end of the female gametophyte and is heavily reduced compared to species such as barley. (f) During early stages of ovule development in barley, the ovule appears similar to that of Arabidopsis, as indicated by the similar shading colours. However, a true funiculus is lacking, and the chalaza connects directly to the placental tissue. (g) As ovule development continues, the nucellus proliferates and expands, forming the bulk of the ovule. (h) Barley, similar to Arabidopsis, produces a Polygonum-type female gametophyte containing four different cell types. However, unlike Arabidopsis, the central cell nuclei do not fuse prior to fertilisation, and the antipodals continue proliferating independently of other gametophyte cells. se, sepal; pe, petal; st, stamen; ov, ovule; ca, carpel (ovary); sti, stigma; an, anther; pd, pedicel; le, lemma; pa, palea; lo, lodicule; gl, glume; ra, rachis; fg, female gametophyte; mmc, megaspore mother cell; lc, locule; mp, micropyle; ch, chalaza.

Genes involved in ovule development

Using forward and reverse genetics, diverse genes have been identified that influence ovule development. Table 2-1 lists a number of these from different species, dividing them into categories based on their role in floral meristem development, ovule formation and patterning, germline formation, and early gametophyte development. Many of these genes are potentially useful for the modification of flower, ovule, and seed development, affecting seed morphology or yield, and this has been discussed in various reviews (Cucinotta et al., 2014; Itoh et al., 2005; Noman et al., 2017). For the purposes of this article, we will mainly consider genes involved in the development of the most prominent somatic tissue within the ovule, the nucellus. The nucellus plays a multifunctional role in providing signals to support germline development prior to fertilisation, as well as establishing an environment that sustains and nourishes the downstream events of seed development after fertilisation has taken place.

Table 2-1: Selected genes involved in flower, ovary, and ovule development in species including Arabidopsis, rice, wheat, and maize.

Class	Gene	Species	Type	Function	Impact of altered function	Reference
Meristem development	KNOTTED1	*Z. mays*	HD TF	Regulator of meristem development	Additional carpels, altered ovule nucellus growth	Kerstetter et al. (1997)
	SUPERWOMAN (OsMADS16)	*O. sativa*	MADS TF (AP3)	Regulator of whorl-specific proliferation	Stamens and lodicules transformed into carpels and palea-like organs, altered ovule nucellus growth	Nagasawa et al. (2003)
	SILKY1	*Z. mays*	MADS TF (AP3)	Regulator of whorl-specific proliferation	Stamens and lodicules transformed into carpels and palea/lemma-like organs	Ambrose et al. (2000), Whipple et al. (2004)
	TaMADS51	*T. aestivum*	MADS TF (AP3)	Regulator of whorl-specific proliferation	Stamens transformed into pistil-like structures	Yamada et al. (2009), Zhao et al. (2006)
	PHOTOPERIOD DETERMINANT 1	*T. aestivum*/	PRR	Regulator of circadian clock	Modified architecture, additional paired spikelets (acts via FT)	Boden et al. (2015)
	INDETERMINATE FLORAL APEX1	*Z. mays*	YABBY TF	Regulator of meristem determinacy	Increased spikelets, ovule primordia	Laudencia-Chingcuanco and Hake (2002), Strable et al. (2017)
	RAMOSA1	*Z. mays*	ZF TF	Regulator of inflorescence architecture	Increased spikelets, altered spikelet development	Vollbrecht et al. (2005)

Class	Gene	Species	Type	Function	Impact of altered function	Reference
	TASSEL SEED 1 and 2	*Z. mays*	Putative alcohol dehydrogenase	Regulator of tassel pistil abortion	Carpels in tassel survive	Irish (1997)
	TASSEL SEED 4 and 6	*Z. mays*	miR172	Regulator of meristem development	Additional florets, tassel pistils, floral meristem indeterminacy	Chuck et al. (2007)
	REQUIRED TO MAINTAIN REPRESSION6	*Z. mays*	RNA polymerase d1	Regulator of tassel pistil abortion	Carpels in tassel survive, SILKY1 deregulated	Parkinson et al. (2007)
	INCOMPLETEY FUSED CARPELS	*Z. mays*	Unknown	Regulates carpel fusion, nucellus proliferation	Unfused carpels, protruding nucellus growth	Li et al. (2016), Li et al. (2017)
Ovule formation	SEEDSTICK	*A. thaliana*	MADS TF	Regulator of ovule identity	Ovules transformed to leaf- and carpel-like structures, elongated funiculus	Pinyopich et al. (2003)
	OsMADS13	*O. sativa*	MADS TF (STK)	Regulator of ovule identity	Ovule transformed to carpelloid structure	Dreni et al. (2007), Li et al. (2011)
	TaAGL2	*T. aestivum*	MADS TF (STK)	Regulator of ovule identity	Ectopic ovule growth in pistil-like stamens	Yamada et al. (2009), Zhao et al. (2006)
	WANDERING CARPEL	*Z. mays*	Unknown	Regulator of adaxial/abaxial orientation of floret	Double ovules formed in single pistil, carpel defects	Irish et al. (2003)
	INDETERMINATE GAMETOPHYTE1	*O. sativa*	LBD TF	Regulator ovule initiation and cell identity within FG	Double ovules, abnormal number of polar nuclei, egg cells, and synergids	Zhang et al. (2015)

Class	Gene	Species	Type	Function	Impact of altered function	Reference
Ovule patterning	SPOROCYTELESS	*A. thaliana*	TF	Regulator of transcription and megasporocyte development	Nucellus fails to elongate, FG development is blocked	Bencivenga et al. (2012), Schiefthaler et al. (1999), Yang et al. (1999)
	WUSCHEL	*A. thaliana*	HD TF	Regulator of MMC development, nucellus formation, and integument formation	Integuments do not form, MMC development terminates	Groß-Hardt et al. (2002), Zhao et al. (2017)
	WINDHOSE1, WINDHOSE2	*A. thaliana*	Small peptides	Regulator of MMC formation	Disrupted MMC development, ovule cell morphology	Lieber et al. (2011)
	DICER-LIKE 1	*A. thaliana*	RNAse III	Involved in miRNA production	Pleiotropic defects, short integuments, FG abortion	Kurihara and Watanabe (2004), Schauer et al. (2002)
	CORONA, PHABULOSA, PHAVOLUTA	*A. thaliana*	HD-ZIP III TF	Regulator of integument development and chalaza formation, repress WUSCHEL expression	Abnormal integument development, extra carpels	Yamada et al. (2016)

Class	Gene	Species	Type	Function	Impact of altered function	Reference
	ARGONAUTE1	*A. thaliana*	AGO	Effector of gene silencing	Altered ovule polarity	Lynn et al. (1999), Morel et al. (2002)
	ARGONAUTE10	*A. thaliana*	AGO	Modulator ofgene silencing	Altered ovule polarity	Mallory et al. (2009), Moussian et al. (1998)
	PIN-FORMED1	*A. thaliana*	PIN	Auxin efflux facilitator	Loss of integuments, FG abortion	Ceccato et al. (2013)
	INNER NO OUTER	*A. thaliana*	YABBY TF	Regulator of integument development	Lacking outer integument, impaired FG development	Baker et al. (1997)
	AINTEGUMENTA	*A. thaliana*	AP2-like TF	Regulator of integument development	No integument growth, failed meiosis and FG development	Klucher et al. (1996)
	BEL1	*A. thaliana*	HD TF	Regulator of integument specification and patterning, and chalaza development	Single integument formation which is converted into a carpel-like structure, disrupted FG formation	Brambilla et al. (2007), Ray et al. (1994), Robinson-Beers et al. (1992)

Class	Gene	Species	Type	Function	Impact of altered function	Reference
Female germline formation	ARGONAUTE9	*A. thaliana*	AGO	Effector of gene silencing	Extra germline-like cells	Olmedo-Monfil et al. (2010)
	RNA-DEPENDENT RNA POLYMERASE 6	*A. thaliana*	RDRP	Component of gene silencing pathways	Extra germline-like cells	Olmedo-Monfil et al. (2010), Peragine et al. (2004)
	SUPPRESSOR OF GENE SILENCING 3	*A. thaliana*	Uncharacterised protein	Component of gene silencing pathways	Extra germline-like cells	Olmedo-Monfil et al. (2010), Peragine et al. (2004)
	AUXIN RESPONSE FACTOR 3 (ETTIN)	*A. thaliana*	ARF TF	Regulator of gynoecium and integument development	Fused integuments, ovule abortion, extra germline-like cells	Sessions et al. (1997), Su et al. (2017)
	RETINOBLASTOMA1	*A. thaliana*	RB-like	Transcriptional repressor, regulator of MMC differentiation	Pleiotropic defects, extra germline-like cells	Ebel et al. (2004), Zhao et al. (2017)
	MULTIPLE SPOROCYTES 1	*O. sativa*	RLK	Suppressor of sporocyte differentiation	Extra germline-like cells	Nonomura et al. (2003)
	TAPETUM DETERMINANT-LIKE 1A (MAC1)	*Z. mays*	SP	Intercellular signalling component	Multiple nucellar cells adopt MMC identity	Sheridan et al. (1996), Wang et al. (2012a,b)
	AMEIOTIC1	*Z. mays*	AtSWI1-like	Regulator of meiosis: zygotene-leptotene transition	MMC undergoes mitosis instead of meiosis	Pawlowski et al. (2009)
	DOMINANT NON-REDUCTION4 (AGO104)	*Z. mays*	AGO	Effector of gene silencing	Unreduced female gametes	Singh et al. (2011)

Class	Gene	Species	Type	Function	Impact of altered function	Reference
Early gametophyte development	ARABIDOPSIS HISTIDINE KINASE1,2,3,4,5	*A. thaliana*	HK	Cytokinin receptor(s)	Knockouts lead to FG abortion	Cheng et al. (2013)
	ARABINOGALACTAN PROTEIN 18	*A. thaliana*	AGP	Cell wall glycoprotein, putative signalling molecule	Overexpression leads to multiple megaspores surviving	Demesa-Arevalo and Vielle-Calzada (2013)
	INDETERMINATE GAMETOPHYTE1	*Z. mays*	LBD TF	Regulator of cell identity	Additional egg cells, polar nuclei, and synergids	Evans (2007)
	DiSUMO-LIKE	*Z. mays*	SUMO	Regulates ubiquitylation/protein function	FG nuclei fail to polarise at stage FG5	Dresselhaus et al. (2010)
	ARGONAUTE5	*A. thaliana*	AGO	Effector of gene silencing	Dominant-negative version compromises FG development	Tucker et al. (2012)
	EA1-LIKE 1 (EAL1)	*Z. mays*	EAL1	Secreted peptide	Antipodal cells adopt CC identity, IG1 expression disrupted	Gray-Mitsumune and Matton (2006)

The Nucellus Fulfils Critical Roles as a Generative and Nutritive Tissue

The nucellus is also referred to as the megasporangium, and its main roles are to produce a germline progenitor cell, the megasporocyte (megaspore mother cell, MMC), and support the downstream events of germline development (megasporogenesis; Yadegari and Drews, 2004). In Arabidopsis, the nucellus is separated from maternal placental tissues through the growth of the chalaza and funiculus (Figure 2-1c). However, in species such as barley and wheat, a true funiculus is absent (Figure 2-1f–h). Similarly, in maize the funiculus is absent and the nucellus directly contacts the maternal plant through the pedicel, which is the site of sucrose supply from the phloem and selective uptake into the ovule (McLaughlin and Boyer, 2004; Tang and Boyer, 2013). Nucellar morphology varies greatly between species with regard to size and cell number (Lora et al., 2016). The model eudicotyledonous species Arabidopsis produces tenuinucellar ovules with a prominent unicellular layer surrounding the MMC (Figure 2-1c) and a small number of hypodermal nucellar cells (Lora et al., 2016). Cereals such as maize are crassinucellar, producing a large MMC deep within a multilayered nucellus (Rudall, 1997; Voronova et al., 2003). There are varying reports that describe the barley ovule as being crassinucellar, intermediate between those with massive and delicate nucelli (Norstog, 1974), as nearly tenuinucellate at anthesis (Engell, 1989), tenuinucellate (Bennett et al., 1973), or as medionucellate, syndermal, and multilayered (Shamrov, 1998). Despite this variation in terminology, it is clear that prior to fertilisation of the female gametophyte in barley, the nucellus is much more prominent than in tenuinucellate species such as Arabidopsis (compare Figure 2-1e and h). The role of an enlarged nucellus has been debated from an evolutionary perspective (Endress, 2011), but the question of how it forms in the cereals and acts to balance MMC formation, megasporogenesis, and downstream reproductive development, relative to what is known from Arabidopsis, is yet to be clearly addressed.

A One-way Street Ending in Female Gametophyte Production

At the mechanistic level, most of our molecular knowledge regarding nucellus development has been derived from Arabidopsis. In brief, the young ovule is produced through redundant activities of the MADS-box transcription factors SEEDSTICK (STK; Table 2-1) and SHATTERPROOF (SHP1/2) in the placenta, the tissue formed through fusion of the two carpels. Ovule primordia consist of three domains including the distal nucellus where the germline initiates, the central chalaza, and proximal funiculus (Figure 2-1c; Grossniklaus and Schneitz, 1998). These domains are initially defined by distinct gene expression patterns, rather than obvious differences in cellular morphology. In wild-type Arabidopsis, a single germline precursor cell (Megaspore mother cell; MMC) forms in the centre of the nucellus and expands much faster than the surrounding cells (Figure 2-1c; Lora et al., 2016). During expansion, the MMC exhibits a unique gene expression profile compared to the surrounding cells (Schmidt et al., 2011). Remarkably, many genes that influence female germline development in Arabidopsis are expressed in nucellar cells surrounding the MMC. In this sense, the nucellus appears to mimic the function of escort stem cells found in the drosophila ovary stem cell niche, which provide specific signals to maintain female gametogenesis (Decotto and Spradling, 2005). The Arabidopsis 'nucellus genes' include both positive and negative regulators of germline development (Table 2-1); for example, the nuclear protein encoded by *SPOROCYTLESS* (SPL) maintains nucellar cell identity (Wei et al., 2015; Yang et al., 1999), the WUSCHEL (WUS) transcription factor establishes the boundary between the distal and central ovule domains (Groß-Hardt et al., 2002) with support from HD-ZIP Class III genes and BEL1 (Yamada et al., 2016), and the small WINDHOSE (WIH) proteins appear to influence aspects of nucellar cell shape (Lieber et al., 2011). Plants lacking SPL, WUS, or WIH1/2 fail to form a functional female germline. Conversely, small RNA pathways acting downstream of ARGONAUTE9 (AGO9) restrict germline development, and mutants display additional germline-like cells in the ovule (Olmedo-Monfil et al., 2010). AGO9 appears to act with RNA-DEPENDENT RNA POLYMERASE 6 (RDR6) and a small RNA intermediate to

regulate gene expression via RNA-dependent DNA methylation (RdDM). The protein-coding targets of this pathway have proven elusive, but a recent report indicates that trans-acting small interfering RNA (tasiRNA)-mediated regulation of ETTIN/AUXIN RESPONSE FACTOR 3 (ARF3) is likely to be involved (Su et al., 2017). Regulation of phytohormone transport and response has also been linked to SPL, which modulates expression of the auxin efflux carrier PIN FORMED1 (PIN1), and WUS, which controls cytokinin response through the *ARABIDOPSIS RESPONSE REGULATOR* genes (Bencivenga et al., 2012; Leibfried et al., 2005). It is tempting to speculate that AGO9, SPL, and WUS form an interrelated regulatory network controlling signal flow and response in the developing ovule. Such a system would ensure a number of basic criteria: responsive cell types (the nucellus), positional information to direct the response (auxin flow through the epidermis and/or cytokinin accumulation), pathways that restrict the response to a single cell (sRNA molecules), and secondary signals that drive differentiation (such as cell wall genes; reviewed in Tucker and Koltunow, 2014). To date it remains unclear whether a similar molecular framework supports nucellus development in the cereals. Various MADS-box genes including *OsMADS13*, the rice D-class homologue of Arabidopsis *STK* (Dreni et al., 2007; Groß-Hardt et al., 2002), and the B_{sister} gene *OsMADS29* (Yang et al., 2012) impact ovule development. In terms of germline development, mutations in the maize *AGO104* gene (a homologue of Arabidopsis AGO9) lead to defects in female meiosis and megagametogenesis, despite being expressed outside the germline in nucellar cells (Singh et al., 2011). AGO104 is required for correct DNA methylation, suggesting that RdDM pathways may be conserved during ovule development between the dicots and the monocots. The *MULTIPLE SPOROCYTES* (*MSP1*) gene from rice encodes a leucine-rich repeat receptor-like protein kinase (Nonomura et al., 2003), while *MULTIPLE ARCHESPORIAL CELLS1* (*MAC1*) encodes the maize homologue of TAPETUM DETERMINANT-LIKE 1A (TDL1a; Sheridan et al., 1996; Wang et al., 2012a,b), a small peptide that appears to act as a ligand for MSP1-like receptors (Zhao et al., 2008). Mutations in these genes lead to the formation of extra germline-like cells. Although homologues of these

receptors and ligands are expressed in the Arabidopsis ovule, and ectopic expression causes infertility (Huang et al., 2015), a precise loss-of-function phenotype has yet to be demonstrated.

Life After Death: The Nutritive Role of the Nucellus

In species such as Arabidopsis, the epidermal layer of the nucellus collapses during germline development, and sub-epidermal nucellar cells are difficult to trace after the completion of gametogenesis. Xu et al. (2016) suggest that a cluster of cells positioned at the chalazal end of the ovule represent persistent nucellar cells, and these degenerate after fertilisation in a process dependent on AGAMOUS-like 62 (AGL62) and central cell fertilisation. Degradation of these cells is possibly required to make space for development of the chalazal endosperm. In cereal ovules, the bulk of the nucellus persists until after fertilisation, switching from a tissue that supports gametogenesis to one that transfers maternal nutrients to the nascent grain (Figure 2-2). During this transition, nucellus morphology changes dramatically; by 6 days after pollination (DAP), the majority of nucellar tissue is no longer present as it has undergone programmed cell death (PCD). However, the region of nucellus between the main vascular bundle and the ventral crease of the developing grain is retained and differentiates into the nucellar projection (NP; Figure 2-2a,b; Duffus and Cochrane, 1992). Instigated by an increase in the ratio of gibberellic acid to abscisic acid (Weier et al., 2014), differentiation of the NP is crucial for survival of the ovule and grain after fertilisation.

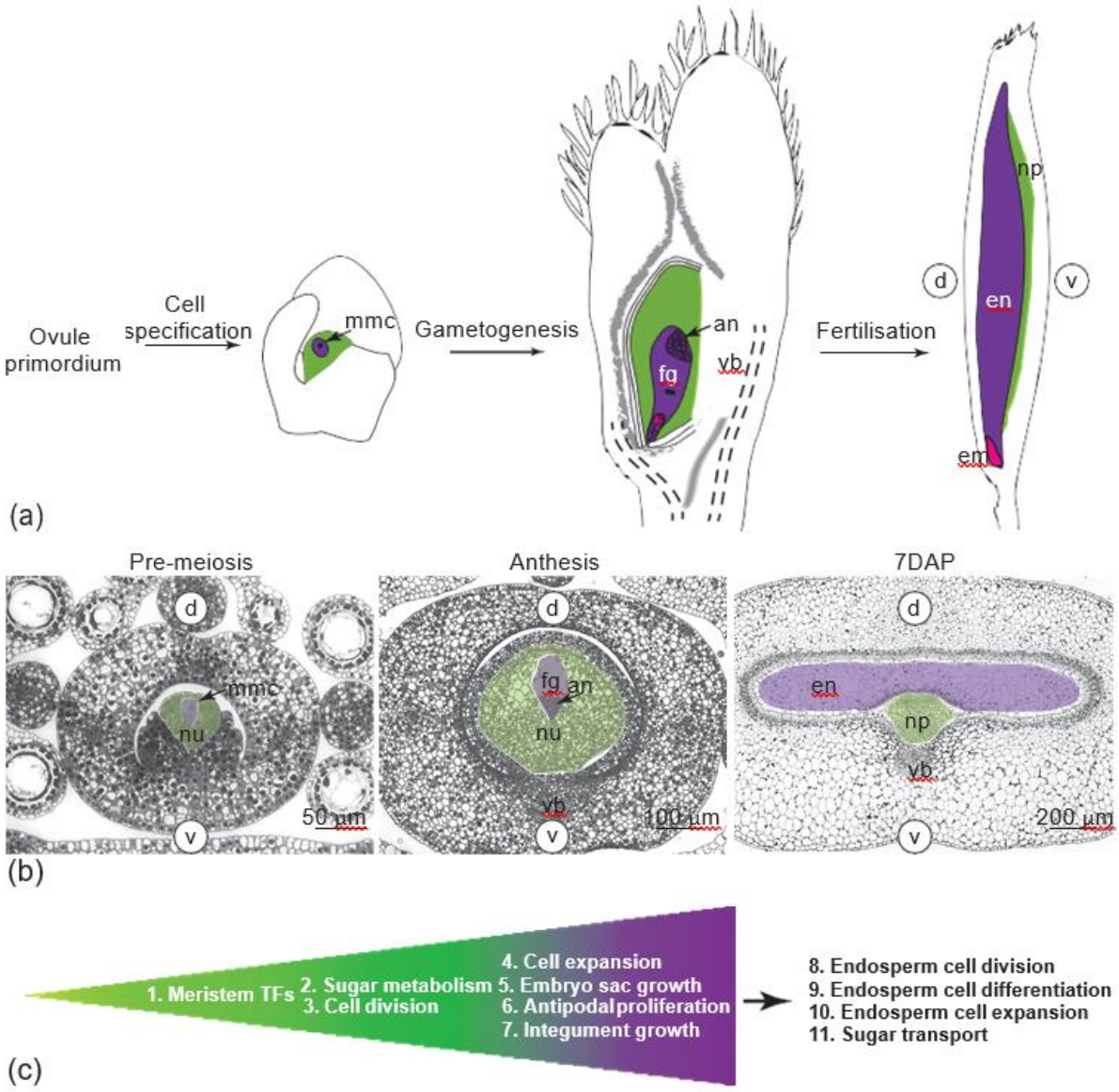

Figure 2-2: Nucellus development in barley. (a) A schematic representation of barley carpel, ovule, and grain development, presented in the sagittal plane. Different ovule tissues including the nucellus (green) and female gametophyte/embryo sac (purple) are indicated. (b) Transverse sections of barley ovules at pre-meiosis and anthesis stages, and a developing grain at 7 days after pollination. The ovule in barley forms from placental tissue, and the nucellus can be easily distinguished after integument initiation, consisting of both L1 and L2 cell types. Nucellar cells undergo divisions and expansion, concurrent with integument growth and female gametophyte development, and at anthesis contribute most of the ovule tissue. After fertilisation, the majority of the nucellar tissue degenerates via programmed cell death,

and the remainder differentiates to form the nucellar projection that funnels maternal nutrients into the endosperm through the endosperm transfer cells. (c) Many pathways contribute to ovule and nucellus development and function. Variation in the size of the nucellus might be explained by primary differences in floral meristem size or secondary changes in sugar metabolism, nucellar cell division and/or expansion, or variation in the size of other ovule tissues including the embryo sac, antipodals, and integuments. After fertilisation, the nucellus continues to influence grain development through control of sugar transport and endosperm division, differentiation, and expansion. an, antipodals; em, embryo; fg, female gametophyte; d, dorsal; en, endosperm; v, ventral; np, nucellar projection; DAP, days after pollination; nu, nucellus; mmc, megaspore mother cell; vb, main provascular bundle. Bars indicate the relative size of each transverse section.

Molecular Components of Nucellar Degeneration

Components of post-fertilisation nucellus development have been examined in several species. *OsMADS29* is expressed in the nucellus, NP, tapetum, and vascular bundle of the anther and stimulates production of a cysteine protease (LOC_Os02g07430) integral to nucellar PCD, as well as regulating other PCD-associated genes and auxin signalling pathways (Yin and Xue, 2012). Initially characterised in rice (Yin and Xue, 2012), homologues of *MADS29* have been isolated in maize (Chen et al., 2015) and barley (Thiel et al., 2008). Also in barley, eight vacuolar processing enzyme (VPE) isoforms have been characterised (HvVPE1, HvVPE2a, HvVPE2b, HvVPE2c, HvVPE2d, HvVPE3, HvVPE4, and LEG8; Radchuk et al., 2011; Julián et al., 2013) that participate in post-fertilisation ovary development. Initially called 'nucellain', *HvVPE2a*, a cysteine protease of the C13 protease family, was one of the initial genes identified in the barley ovule (Doan et al., 1996; Linnestad et al., 1998). Alongside research describing similar roles for the four *VPE* genes in Arabidopsis (Nakaune et al., 2005; Shimada et al., 2003), there is strong support for nucellain *HvVPE2b* and *HvVPE2d* acting in barley nucellar PCD. Most of the nucellar degeneration events initiate rapidly upon fertilisation. DNA fragmentation assays suggest that in barley, PCD initiates in the inner nucellus layers and spreads to outer layers within 2 days of pollination (Radchuk et al., 2011). At 2–4 DAP, an aspartic protease called 'nucellin' is expressed in nucellar tissues surrounding the vascular bundle (Chen and Foolad, 1997; Gubatz et al., 2007), as well as in the embryo, pollen, and apical meristems (Bi et al., 2005). A rice orthologue, *OsAsp1,* shows similar spatial and temporal expression (Bi et al., 2005) suggesting a conserved role in nucellar degeneration, although the targets of proteolysis remain unclear. Uniquely in barley, a protein encoded by *Jekyll* is expressed in the maternal tissue surrounding the male and female gametophytes (Radchuk et al., 2006). Peak expression of *Jekyll* occurs in the nucellar tissue around the vascular bundle at 4–6 DAP, concurrent with NP differentiation and nucellar PCD. Severe disruption of grain fill in *Jekyll* knockdown plants, in which differentiation and PCD of the

nucellar tissue is impaired, demonstrates that PCD of nucellar tissues is crucial for later stages of grain development (Radchuk et al., 2006).

The Nucellar Projection Feeds the Seed

Research in barley, wheat, and maize indicates that the NP (Figure 2-2b) is the site of release of photoassimilates and other nutrients from the maternal tissue for uptake by adjacent endosperm transfer cells (Sreenivasulu et al., 2002; Tang and Boyer, 2013; Thiel et al., 2009; Weschke et al., 2003). Sucrose, the major photoassimilate, is an essential source of carbon required for development of different cell types and energy reserves (e.g. starch) within the developing grain (reviewed by Ludewig and Flügge, 2013). Once unloaded from the phloem, invertase (INV), and sucrose synthase (SuSy) enzymes hydrolyse sucrose into its constituent hexoses, fructose, and glucose. This metabolism reduces the local sucrose concentration, thus maintaining a high concentration gradient between source and sink tissues, osmotically driving sucrose unloading (McLaughlin and Boyer, 2004; Ruan et al., 2012). Different invertase isoforms locate to the cell wall (CWIN), cytoplasm (CIN), or vacuole (VIN), and CWINs and VINs have their activity regulated by specific inhibitors (INVINH/PMEI). Expression of the sucrose transporters SUT1 and SUT2, and HvCWIN1/2, have been observed from 1 to 6 DAP in the NP, endosperm transfer cells, and nucellar tissues of barley and maize (Cheng et al., 1996; Weschke et al., 2000, 2003). A recent report suggests that HvSUT2 and HvSUT1 control sucrose homeostasis during grain fill, and downregulation leads to reduced endosperm starch content and dry weight (Radchuk et al., 2017). Other members of these sugar metabolism-related families accumulate in developing ovules of cotton (Wang et al., 2014) and the grass species *Brachiaria* (Dusi and Willemse, 1999). Furthermore, recent studies suggest that photoassimilates interact with hormonal pathways to regulate aspects of development, an area that has not been explored in detail in the cereals (see Liu et al., 2013 for review).

What does Nucellus PCD Achieve?

Although studies have demonstrated that changes in nucellus PCD can have negative impacts on grain development (Radchuk et al., 2006), the specific role of early post-fertilisation PCD remains elusive. This is partly due to the difficulty in disentangling the events of PCD from NP differentiation and early endosperm development. Concurrent with nucellar degeneration, the NP differentiates, which is critical for maternal nutrient transfer into the endosperm (Radchuk et al., 2006). In barley, however, the NP does not fully differentiate until around five DAP, suggesting that nutrients supporting the initial endosperm divisions may come from a local source rather than from the phloem. In the grasses, these nutrients may already be available within the embryo sac, where a large number of transient antipodal cells reside (Chettoor and Evans, 2015). Alternatively, it is also possible that remobilisation of reserves from nucellar cells by PCD provides a local nutrient source for early endosperm divisions and cellularisation, which would require local transport into the embryo sac. As discussed earlier, collapse of the nucellar cells coincides with expression of a diverse array of proteolytic enzymes, α-amylase and phosphoenolpyruvate carboxylase (Domínguez and Cejudo, 2014; Sreenivasulu et al., 2006; Tran et al., 2014; Van Hautegem et al., 2015), suggesting that specific amino acids and glucose may support differentiation of the NP and/or rapid endosperm proliferation. Alternatively (but not mutually exclusively), nucellus PCD may release physical constraints on the embryo sac, permitting expansion during endosperm divisions. Studies in barley suggest that nucellus size at anthesis varies between cultivars (Wilkinson and Tucker, 2017), but the mechanistic basis and contribution to grain development remains unclear (Figure 2-2c).

The Role of Pre-anthesis Female Tissues in Downstream Grain Development

The size of cereal carpels (ovaries) and grain varies along the inflorescence. In wheat (Benincasa et al., 2017; Calderini and Reynolds, 2000; Xie et al., 2015), barley (Guo et al., 2015, 2016; Scott et al., 1983), and sorghum (Yang et al., 2009), grain weight has a strong

genetic component determined before anthesis, which is in part due to carpel size. Florets in the middle of the spike tend to be bigger, make bigger grain, and are less influenced by environmental stress than those at the tips (Guo et al., 2015), while the size of barley carpels at distal positions along the spike is positively correlated with the number of grains per spike (Guo et al., 2015, 2016; Scott et al., 1983; Yang et al., 2009; Benincasa et al., 2017; Calderini and Reynolds, 2000; Xie et al., 2015). In a recent study, Reale et al. (2017) found that variation in wheat ovary size was due to increased cell numbers rather than cell size. In barley, the size of carpels during meiosis is positively correlated with carpel weight at anthesis (Scott et al., 1983), while in sorghum, floret meristem size is positively linked to ovary volume (Yang et al., 2009). In the same sorghum study, a positive correlation was identified between the number of ovary cells and grain weight (Yang et al., 2009). These studies indicate that changes in growth during early (pre-anthesis) stages of floral development impact downstream grain production. The basis for variation might range from the control of primordial size through to modified sugar metabolism, tissue-specific cell division, cell expansion, antipodal proliferation, and/or integument growth (Figure 2-2c). The genes underlying this variation may therefore be of interest for downstream application in breeding programs.

A Role for the Ovary in Stress Tolerance

The events of floral initiation, germline development, fertilisation, and grain fill may be compromised by environmental stress (Barnabas et al., 2008; Driedonks et al., 2016; Saini and Westgate, 1999). The specific effects of stress during early reproductive development have been most closely examined in anthers, and these include meiotic arrest, microspore abortion, and heat-induced differential expression of many genes (Giorno et al., 2013; Jain et al., 2010; Oshino et al., 2007). With regard to the ovary, less information is available, although studies indicate that both preand post-fertilisation stages of ovary development are sensitive (Bac-Molenaar et al., 2015; Sun et al., 2004; Zinn et al., 2010). In Arabidopsis, single treatments of heat stress compromise meiosis in both male and female reproductive organs,

leading to severe reductions in yield (Bac-Molenaar et al., 2015). Similarly in wheat, both male and female tissues are particularly sensitive to heat stress in the week preceding anthesis, which encapsulates meiosis and gametophyte development (Saini et al., 1983). In general, there is a negative correlation between ambient temperatures over 15 °C in the 30 days preceding anthesis and yield in cereal species (Ferris et al., 1998; Fischer, 1985; Sage et al., 2015). At the cellular level, Arabidopsis ovules show defects in megagametogenesis (Sun et al., 2004), ovule abortion, and reduced ovule number (Bac-Molenaar et al., 2015) after heat or salt stress. In one of the few studies to report cytological details of female development in cereals under stress, wheat exposed to severe heat stress at the start of meiosis experienced disrupted nucellus and integument development, or complete ovule abortion at a frequency of 30% (Saini et al., 1983). In both wheat and rice, heat stress also affects stigma receptivity and length, reflecting alteration of stigma structural development under conditions of stress (Jagadish et al., 2010; Saini et al., 1983). Similar to heat stress, pre-fertilisation water stress can have severe effects on downstream grain development (Bac-Molenaar et al., 2015; Saini et al., 1983; Ferris et al., 1998; Fischer, 1985; Sage et al., 2015; Giorno et al., 2013; Jain et al., 2010; Oshino et al., 2007; Sun et al., 2004; Zinn et al., 2010; Jagadish et al., 2010). Waterlogging during anthesis, for example reduces barley and wheat grain number by up to 79% and 92%, respectively (de San Celedonio et al., 2014). At the other extreme, wheat subjected to water deficit during meiosis exhibited a high level of pollen sterility and a 50% reduction in grain yield (Dorion et al., 1996). In general, the wheat anther is less tolerant of drought conditions than the ovary, and ovary tissue is better able to recover from short-term (4 days) water deficit upon water re-availability (Ji et al., 2010). Saini and Aspinall (1981) reported that wheat ovaries are unaffected by water deficit during meiosis, while pollen development aborts during microsporogenesis. In a recent study, however, Onyemaobi et al. (2016) examined the effect of water stress in 13 wheat genotypes and found that 4 showed reduced seed set as a result of reduced female fertility. Although the genetic basis for this variability remains unclear, molecular evidence suggests that wheat ovaries from different

cultivars show differential responses to stress. For example, in a study comparing sensitive and tolerant cultivars, Ji et al. (2010) showed that upon drought stress at the 'young microspore' stage, expression of cell wall invertase *IVR1* and sucrose 1-fructosyl-transferase (1-SST) are downregulated in the ovary of drought sensitive wheat cultivars, while in drought-tolerant cultivars, 1-SST is upregulated (Zinn et al., 2010).

Sugar as a Mediator of Pre-anthesis Female Stress Tolerance

Photoassimilates are an important determinant of reproductive resilience in both male and female tissues. Sugar limitation under heat and/or water stress is a major component of fruit and seed abortion (Barnabas et al., 2008; Boyer and McLaughlin, 2007), and studies show that modified sugar accumulation through the manipulation of INV or INVINH levels can alleviate some of these defects (see Liu et al., 2013 for review). In maize, for example water deficit imposed throughout anthesis leads to simultaneous accumulation of sucrose and depletion of sucrose metabolites in the ovary (Zinselmeier et al., 1995). This is accompanied by a reduction in invertase activity and increased ovule abortion, resulting in kernel number being reduced by 60% (Zinselmeier et al., 1999). Maize soluble acid invertase *IVR2* is expressed at the site of phloem unloading in the pedicel and within the basal region of the nucellus and is repressed by drought imposed 6 days before fertilisation (Andersen et al., 2002). Other studies show that invertase is active within the nucellus of diverse species including *Brachiaria* (Dusi and Willemse, 1999), *Gasteria* (Wittich and Willemse, 1999) and maize (McLaughlin and Boyer, 2004), creating a glucose gradient that enhances the sink strength of the ovule. McLaughlin and Boyer (2004) found that low water potential within the maize plant reduced photosynthesis and glucose and starch levels within the floret stem (pedicel) and led to high levels of ovule abortion. However, by feeding sucrose into water-deprived maize plants during anthesis, ovule abortion could be alleviated. Similar sugar-related pathways appear to modulate the response to salt stress. In maize, salt stress inhibits invertase activity and has a stronger effect on kernel number than drought stress (Hütsch et

al., 2015), limiting yield by reducing kernel number by 50% (Hütsch et al., 2014). Under salt stress conditions, plasma membrane H + ATPase activity is greatly inhibited within the ovary, lowering the pH gradient across the plasma membrane sufficiently to prevent proper function of hexose transporters and hexose metabolism within the maize ovary at anthesis and in the initial days of grain filling (Jung et al., 2017).

Collectively these studies suggest that photoassimilate accumulation and metabolism prior to fertilisation moderate the female response to stress. In the context of maize at least, water deficit and altered sugar metabolism during pre-anthesis stages have a more severe impact upon yield (grain number) than deficit after anthesis, as pre-anthesis stress causes female abortion rather than a reduction in kernel size. Based on the prominent size and position of the nucellus in the ovule surrounding the germline cells, and its role in nutrient accumulation and metabolism, it may represent a central component of female stress tolerance in different cereal species and cultivars.

Technical Advances to Expand Understanding of Germline Formation, Sugar Metabolism, and Stress Tolerance in Cereal Ovules

The diverse ovule signals and effectors balancing germline formation and nutrient flow have been difficult to identify, mainly because the tiny tissues involved are buried deep within the flower and are challenging to access for high-throughput imaging and molecular and cell biological analysis. However, recent technological advances have seen methods evolve to the level where interactions between ovule cell types can be examined in greater detail, both in model dicots and commercially relevant cereal species.

Cells within the ovule can be observed at high resolution through advances in whole-mount clearing (Kurihara et al., 2015; Wilkinson and Tucker, 2017) and deep-tissue live imaging (Kimata et al., 2016). The chemical composition of ovule cells can potentially be assessed

through mass spectroscopy (MS) imaging (Peukert et al., 2016) or infrared (IR) microscopy (Warren et al., 2015), while molecular signatures can be generated through laser capture microdissection (LCM; also known as laser-assisted microdissection, LAM) and high-throughput transcriptomics (Okada et al., 2013; Tucker et al., 2012; Wuest and Grossniklaus, 2014). In cereals such as rice, LCM has been used to generate stage-specific profiles of ovule development, which reveal the dynamic transcriptional behaviour of many regulatory (Figure 2-3a–d) and metabolic (Figure 2-3e–f) genes discussed in this article (Kubo et al., 2013). For example, specific members of the MADS-box (Figure 2-3a), WUSCHEL-RELATED HOMEOBOX (Figure 2-3b), and ARGONAUTE (Figure 2-3d) families show stage-specific expression patterns that may reflect important general or cell-type-specific roles in ovule and nucellus development. As an alternative to LCM, cell sorting via flow cytometry (fluorescence activated cell sorting; FACS) has recently been used to generate cell-type-specific profiles from the Arabidopsis placenta (Villarino et al., 2016) and MMC (Zhao et al., 2014). Although suited mainly to the diverse fluorescent marker gene resources available for Arabidopsis, the increased availability and flexibility of fluorescent tags provides an avenue by which FACS techniques might be applied more generally in cereal species (Yang et al., 2017). Even greater cell-type-specific resolution is available through the application of microfluidic systems such as the Fluidigm C1 (Clark et al., 2016), which has the potential to provide unique transcriptomic, genomic, and epigenetic profiles for individual reproductive cells. Once identified, key molecular signatures of the female reproductive cells can be dissected using genetic resources such as CRISPR/Cas9 (Zong et al., 2017), natural diversity panels (Muñoz-Amatriaín et al., 2014), and sequenced mutant resources (Cavanagh et al., 2008; Wang et al., 2012a,b). Moreover, nowadays routine biochemical techniques such as chromatin immuno-precipitation sequencing (ChIPSeq) can be used to identify cell-type-specific targets of regulatory transcription factors (Zhang et al., 2017). Techniques that were once suited solely to simple ‘model’ species are now broadly applicable, presenting new opportunities for fundamental discovery and application in relevant crops.

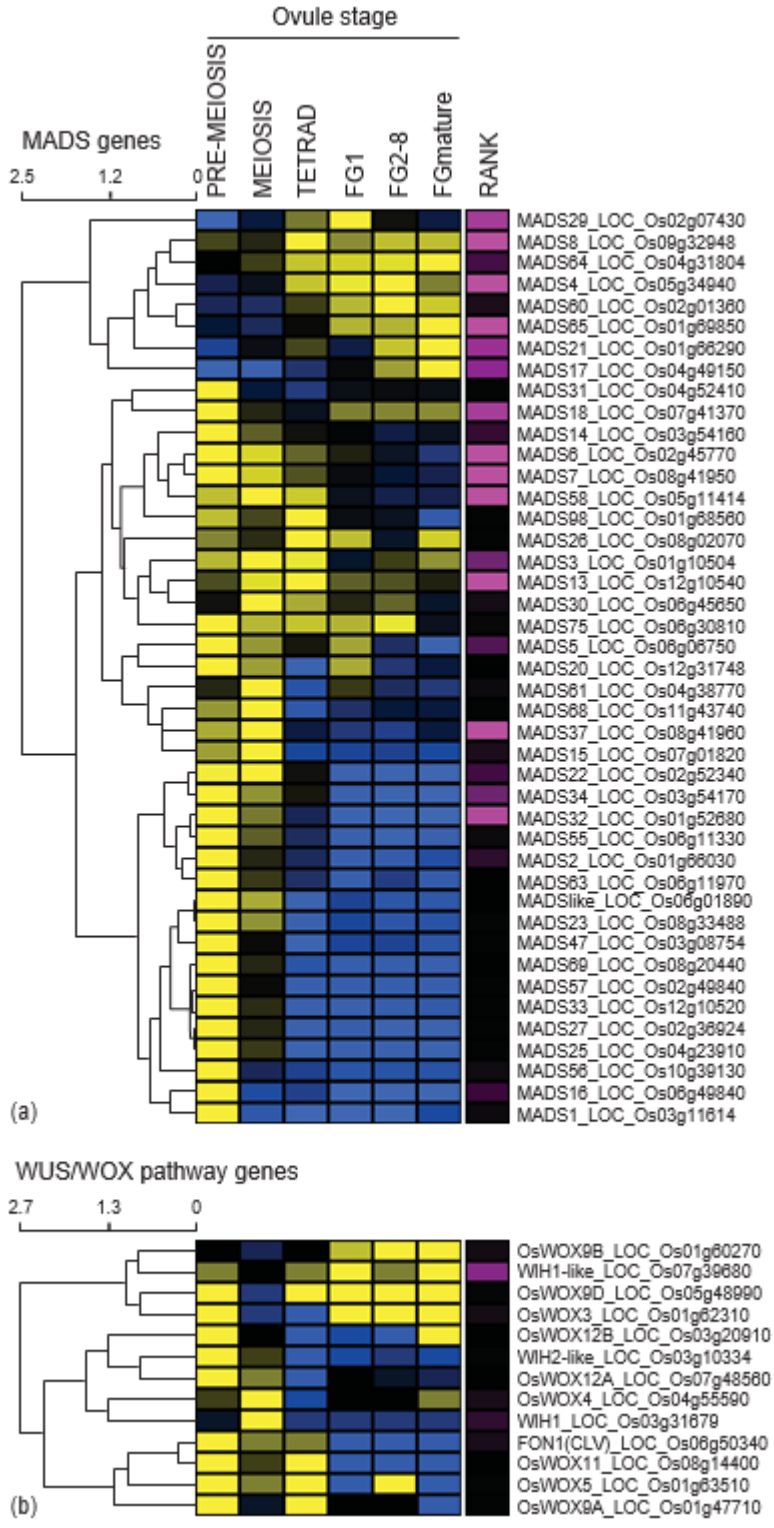
Ovule stage
PRE-MEIOSIS
MEIOSIS
TETRAD
FG1
FG2-8
FGmature
RANK
MADS genes
2.5
1.2
0
MADS29_LOC_Os02g07430
MADS8_LOC_Os09g32948
MADS64_LOC_Os04g31804
MADS4_LOC_Os05g34940
MADS60_LOC_Os02g01360
MADS65_LOC_Os01g69850
MADS21_LOC_Os01g66290
MADS17_LOC_Os04g49150
MADS31_LOC_Os04g52410
MADS18_LOC_Os07g41370
MADS14_LOC_Os03g54160
MADS6_LOC_Os02g45770
MADS7_LOC_Os08g41950
MADS58_LOC_Os05g11414
MADS98_LOC_Os01g68560
MADS26_LOC_Os08g02070
MADS3_LOC_Os01g10504
MADS13_LOC_Os12g10540
MADS30_LOC_Os06g45650
MADS75_LOC_Os06g30810
MADS5_LOC_Os06g06750
MADS20_LOC_Os12g31748
MADS61_LOC_Os04g38770
MADS68_LOC_Os11g43740
MADS37_LOC_Os08g41960
MADS15_LOC_Os07g01820
MADS22_LOC_Os02g52340
MADS34_LOC_Os03g54170
MADS32_LOC_Os01g52680
MADS55_LOC_Os06g11330
MADS2_LOC_Os01g66030
MADS63_LOC_Os06g11970
MADSlike_LOC_Os06g01890
MADS23_LOC_Os08g33488
MADS47_LOC_Os03g08754
MADS69_LOC_Os08g20440
MADS57_LOC_Os02g49840
MADS33_LOC_Os12g10520
MADS27_LOC_Os02g36924
MADS25_LOC_Os04g23910
MADS56_LOC_Os10g39130
MADS16_LOC_Os06g49840
MADS1_LOC_Os03g11614
(a)
WUS/WOX pathway genes
2.7
1.3
0
OsWOX9B_LOC_Os01g60270
WIH1-like_LOC_Os07g39680
OsWOX9D_LOC_Os05g48990
OsWOX3_LOC_Os01g62310
OsWOX12B_LOC_Os03g20910
WIH2-like_LOC_Os03g10334
OsWOX12A_LOC_Os07g48560
OsWOX4_LOC_Os04g55590
WIH1_LOC_Os03g31679
FON1(CLV)_LOC_Os06g50340
OsWOX11_LOC_Os08g14400
OsWOX5_LOC_Os01g63510
OsWOX9A_LOC_Os01g47710
(b)

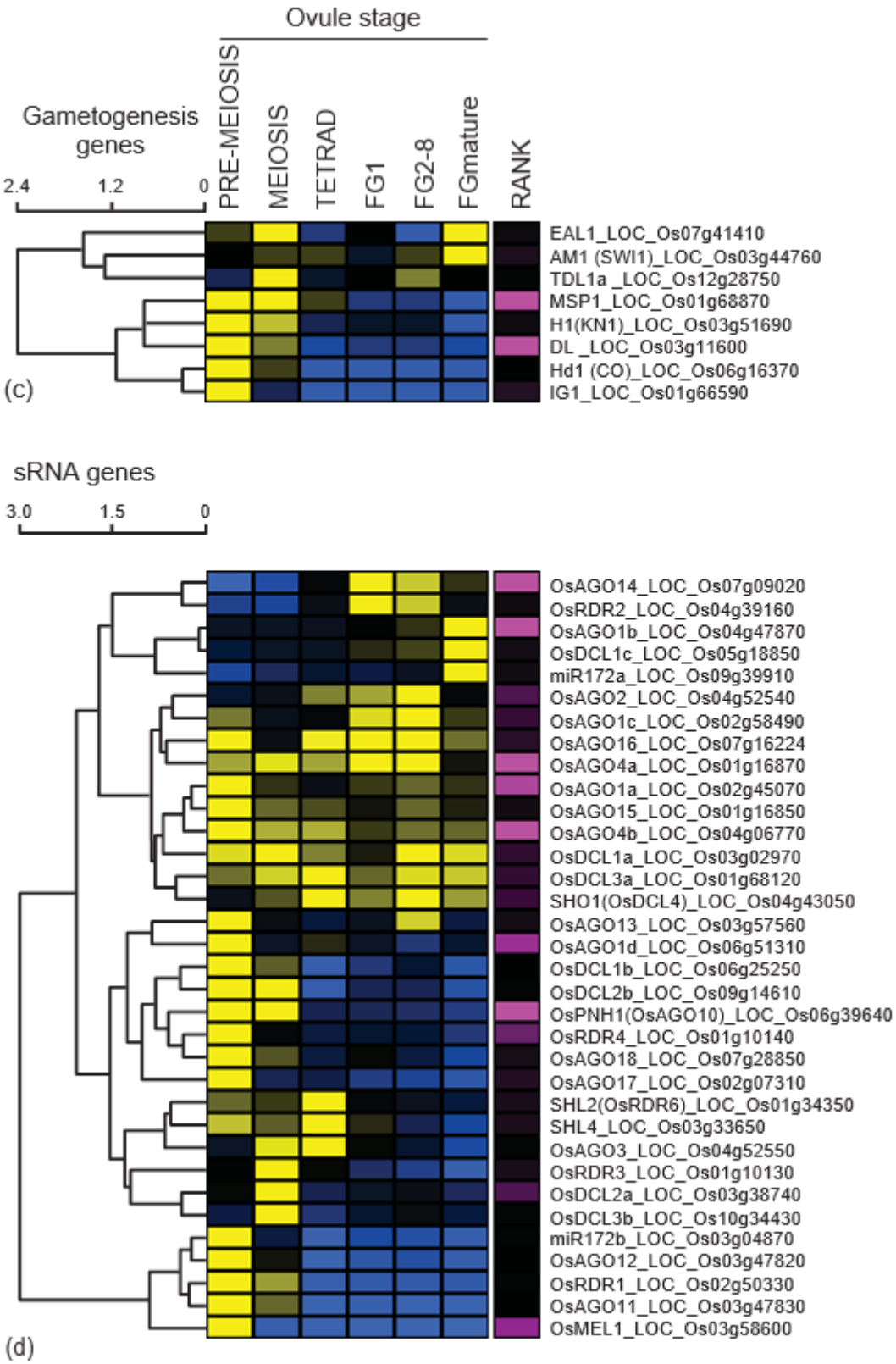
Ovule stage
PRE-MEIOSIS
MEIOSIS
TETRAD
FG1
FG2-8
FGmature
RANK
Gametogenesis genes
2.4
1.2
0
EAL1_LOC_Os07g41410
AM1 (SWI1)_LOC_Os03g44760
TDL1a _LOC_Os12g28750
MSP1_LOC_Os01g68870
H1(KN1)_LOC_Os03g51690
DL _LOC_Os03g11600
Hd1 (CO)_LOC_Os06g16370
IG1_LOC_Os01g66590
(c)
sRNA genes
3.0
1.5
0
OsAGO14_LOC_Os07g09020
OsRDR2_LOC_Os04g39160
OsAGO1b_LOC_Os04g47870
OsDCL1c_LOC_Os05g18850
miR172a_LOC_Os09g39910
OsAGO2_LOC_Os04g52540
OsAGO1c_LOC_Os02g58490
OsAGO16_LOC_Os07g16224
OsAGO4a_LOC_Os01g16870
OsAGO1a_LOC_Os02g45070
OsAGO15_LOC_Os01g16850
OsAGO4b_LOC_Os04g06770
OsDCL1a_LOC_Os03g02970
OsDCL3a_LOC_Os01g68120
SHO1(OsDCL4)_LOC_Os04g43050
OsAGO13_LOC_Os03g57560
OsAGO1d_LOC_Os06g51310
OsDCL1b_LOC_Os06g25250
OsDCL2b_LOC_Os09g14610
OsPNH1(OsAGO10)_LOC_Os06g39640
OsRDR4_LOC_Os01g10140
OsAGO18_LOC_Os07g28850
OsAGO17_LOC_Os02g07310
SHL2(OsRDR6)_LOC_Os01g34350
SHL4_LOC_Os03g33650
OsAGO3_LOC_Os04g52550
OsRDR3_LOC_Os01g10130
OsDCL2a_LOC_Os03g38740
OsDCL3b_LOC_Os10g34430
miR172b_LOC_Os03g04870
OsAGO12_LOC_Os03g47820
OsRDR1_LOC_Os02g50330
OsAGO11_LOC_Os03g47830
OsMEL1_LOC_Os03g58600
(d)

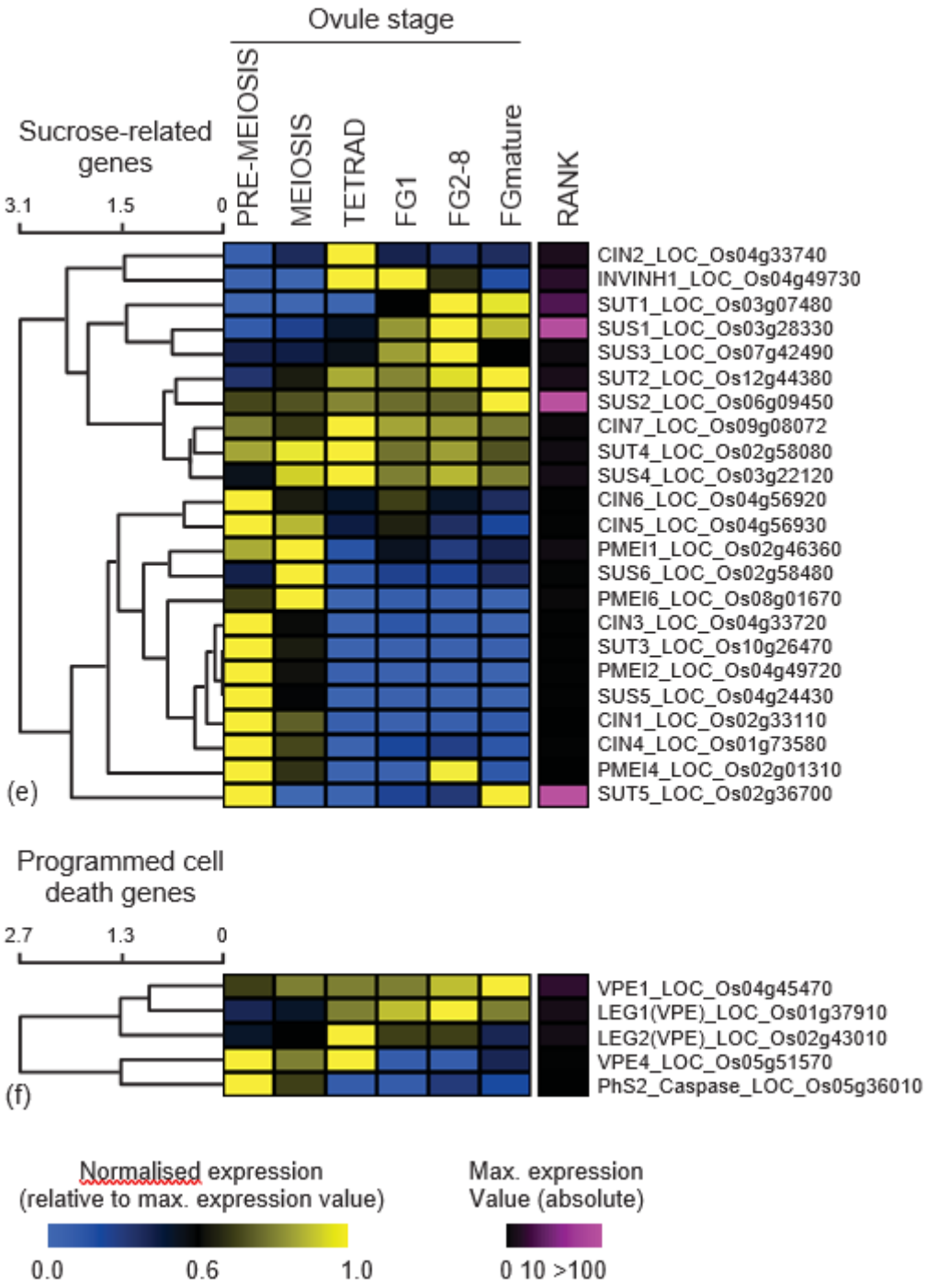

Figure 2-3: Transcript accumulation patterns of regulatory and metabolic genes during ovule development in rice. Kubo et al. (2013) used laser microdissection to capture tissues from consecutive stages of O. sativa ovule development. Transcript accumulation patterns are shown for various gene families discussed in this article, which have been implicated in ovule

development, gametogenesis, and/or nucellus growth. The stage names are assigned based on the staging reported in Kubo et al. (2013). Heatmaps show the expression at each stage relative to the maximum expression value for each gene (yellow indicates a stage where transcript is abundant) and the relative rank of each gene based on the absolute abundance of the maximum expression value (pink shows highly abundant genes). Genes were clustered using hierarchical clustering and Manhattan distance in Multiexperiment Viewer. Families examined include (a) MADS-box transcription factors, which have been shown to influence ovule and ovary development in many species (see Table 1); (b) WUSCHEL-related homeobox (WOX) genes that influence cell differentiation; (c) genes that are known to influence gametogenesis; (d) small-RNA pathway-related genes that influence many developmental events; (e) sucrose metabolism and transport-related genes, and (f) programmed cell death-related genes. Many of the genes examined are abundant during the earliest stage of ovule development examined. However, distinct clusters show stage-specific expression or gradual changes in transcript level over time, accompanying the progression of gametogenesis and nucellus development. Source: Kubo et al. (2013). Reproduced with permission of Oxford University Press.

Conclusions

The ovule is a complex organ that facilitates seed development and thus allows plant reproduction. Many years of research suggest that the ovule nucellus is a multifunctional tissue that balances generative and nutritive functions. Despite this, the capacity of the young growing nucellus to influence downstream events of seed development has not been explored in great detail. Avenues are now available to investigate this tissue further, with the overall aim of improving reproductive stress tolerance and grain traits.

Acknowledgements

We apologise to colleagues whose work we did not cite in this article. We wish to thank Matthew Aubert, Neil Shirley, Rachel Burton, Caitlin Byrt, Geoff Fincher, and Vincent Bulone for advice and support. Research in the Tucker lab is supported by an ARC Future Fellowship and DP180104092. L.G.W. is supported by a Research Training Program Scholarship and a top-up scholarship from the ARC Centre of Excellence in Plant Cell Walls.

References

Ambrose, B.A., Lerner, D.R., Ciceri, P. et al. (2000). Molecular and genetic analyses of the silky1 gene reveal conservation in floral organ specification between eudicots and monocots. *Molecular Cell* 5 (3): 569–579.

Andersen, M.N., Asch, F., Wu, Y. et al. (2002). Soluble invertase expression is an early target of drought stress during the critical, abortion-sensitive phase of young ovary development in Maize. *Plant Physiology* 130 (2): 591–604.

Bac-Molenaar, J.A., Fradin, E.F., Becker, F.F.M. et al. (2015). Genome-wide association mapping of fertility reduction upon heat stress reveals developmental stage-specific QTLs in *Arabidopsis thaliana*. *The Plant Cell* 27: 1857–1874.

Baker, S.C., Robinson-Beers, K., Villanueva, J.M. et al. (1997). Interactions among genes regulating ovule development in *Arabidopsis thaliana*. *Genetics* 145: 1109–1124.

Barnabas, B., Jager, K., and Feher, A. (2008). The effect of drought and heat stress on reproductive processes in cereals. *Plant Cell and Environment* 31 (1): 11–38.

Bencivenga, S., Simonini, S., Benkova, E., and Colombo, L. (2012). The transcription factors BEL1 and SPL are required for cytokinin and auxin signaling during ovule development in Arabidopsis. *The Plant Cell* 24 (7): 2886–2897.

Benincasa, P., Reale, L., Tedeschini, E. et al. (2017). The relationship between grain and ovary size in wheat: an analysis of contrasting grain weight cultivars under different growing conditions. *Field Crops Research* 210: 175–182.

Bennett, M., Rao, M., Smith, J., and Bayliss, M. (1973). Cell development in the anther, the ovule, and the young seed of *Triticum aestivum* L. var. Chinese Spring. *Philosophical Transactions of the Royal Society of London Series B, Biological Sciences* 39–81.

Bi, X.Z., Khush, G.S., and Bennett, J. (2005). The rice nucellin gene ortholog *OsAsp1* encodes an active aspartic protease without a plant-specific insert and is strongly expressed in early embryo. *Plant and Cell Physiology* 46 (1): 87–98.

Boden, S.A., Cavanagh, C., Cullis, B.R. et al. (2015). Ppd-1 is a key regulator of inflorescence architecture and paired spikelet development in wheat. *Nature Plants* 1: 14016.

Bonnett, O. (1940). Development of the staminate and pistillate inflorescences of sweet corn. *Journal of Agricultural Research* 60: 25–37.

Boyer, J.S. and McLaughlin, J.E. (2007). Functional reversion to identify controlling genes in multigenic responses: analysis of floral abortion. *Journal of Experimental Botany* 58 (2): 267–277.

Brambilla, V., Battaglia, R., Colombo, M. et al. (2007). Genetic and molecular interactions between BELL1 and MADS box factors support ovule development in Arabidopsis. *The Plant Cell* 19 (8): 2544–2556.

Calderini, D.F. and Reynolds, M.P. (2000). Changes in grain weight as a consequence of de-graining treatments at preand post-anthesis in synthetic hexaploid lines of wheat *Triticum durum* x *T. tauschii*. *Functional Plant Biology* 27 (3): 183–191.

Cavanagh, C., Morell, M., Mackay, I., and Powell, W. (2008). From mutations to MAGIC: resources for gene discovery, validation and delivery in crop plants. *Current Opinion in Plant Biology* 11 (2): 215–221.

Ceccato, L., Masiero, S., Sinha Roy, D. et al. (2013). Maternal control of PIN1 is required for female gametophyte development in Arabidopsis. *PLoS One* 8 (6): e66148.

Chen, F. and Foolad, M.R. (1997). Molecular organization of a gene in barley which encodes a protein similar to aspartic protease and its specific expression in nucellar cells during degeneration. *Plant Molecular Biology* 35 (6): 821–831.

Chen, J., Yi, Q., Song, Q. et al. (2015). A highly efficient maize nucellus protoplast system for transient gene expression and studying programmed cell death-related processes. *Plant Cell Reports* 34 (7): 1239–1251.

Cheng, C.Y., Mathews, D.E., Schaller, G.E., and Kieber, J.J. (2013). Cytokinindependent specification of the functional megaspore in the Arabidopsis female gametophyte. *The Plant Journal* 73 (6): 929–940.

Cheng, W.H., Taliercio, E.W., and Chourey, P.S. (1996). The *Miniature1 Seed* locus of maize encodes a cell wall invertase required for normal development of endosperm and maternal cells in the pedicel. *The Plant Cell* 8 (6): 971–983.

Chettoor, A.M. and Evans, M.M. (2015). Correlation between a loss of auxin signaling and a loss of proliferation in maize antipodal cells. *Frontiers in Plant Science* 6: 186. Chuck, G., Meeley, R., Irish, E. et al. (2007). The maize tasselseed4 microRNA controls sex determination and meristem cell fate by targeting Tasselseed6/indeterminate

spikelet1. *Nature Genetics* 39 (12): 1517–1521.

Clark, S.J., Lee, H.J., Smallwood, S.A. et al. (2016). Single-cell epigenomics: powerful new methods for understanding gene regulation and cell identity. *Genome Biology* 17 (1): 72.

Cucinotta, M., Colombo, L., and Roig-Villanova, I. (2014). Ovule development, a new model for lateral organ formation. *Frontiers in Plant Science* 5: 117.

de San Celedonio, R.P., Abeledo, L.G., and Miralles, D.J. (2014). Identifying the critical period for waterlogging on yield and its components in wheat and barley. *Plant and Soil* 378 (1): 265–277.

De Vries, A.P. (1971). Flowering biology of wheat, particularly in view of hybrid seed production—a review. *Euphytica* 20 (2): 152–170.

Decotto, E. and Spradling, A.C. (2005). The Drosophila ovarian and testis stem cell niches: similar somatic stem cells and signals. *Developmental Cell* 9 (4): 501–510.

Demesa-Arevalo, E. and Vielle-Calzada, J.P. (2013). The classical arabinogalactan protein AGP18 mediates megaspore selection in Arabidopsis. *The Plant Cell* 25 (4): 1274–1287.

Diboll, A.G. (1968). Fine structural development of the megagametophyte of *Zea mays*

following fertilization. *American Journal of Botany* 55 (7): 797–806.

Doan, D.N.P., Linnestad, C., and Olsen, O.A. (1996). Isolation of molecular markers from the barley endosperm coenocyte and the surrounding nucellus cell layers. *Plant Molecular Biology* 31 (4): 877–886.

Domínguez, F. and Cejudo, F.J. (2014). Programmed cell death (PCD): an essential process of cereal seed development and germination. *Frontiers in Plant Science* 5: 366.

Dorion, S., Lalonde, S., and Saini, H.S. (1996). Induction of male sterility in wheat by meiotic-stage water deficit is preceded by a decline in invertase activity and changes in carbohydrate metabolism in anthers. *Plant Physiology* 111 (1): 137–145.

Dreni, L., Jacchia, S., Fornara, F. et al. (2007). The D-lineage MADS-box gene OsMADS13 controls ovule identity in rice. *The Plant Journal* 52 (4): 690–699.

Dresselhaus, T., Srilunchang, K.O., and Krohn, N.G. (2010). DiSUMO-like DSUL is required for nuclei positioning, cell specification and viability during female gametophyte maturation in maize. *Development* 137 (2): 333–345.

Driedonks, N., Rieu, I., and Vriezen, W.H. (2016). Breeding for plant heat tolerance at vegetative and reproductive stages. *Plant Reproduction* 29 (1–2): 67–79.

Duffus, C. and Cochrane, M. (1992). Grain structure and composition. In: *Barley: Genetics, Biochemistry, Molecular Biology and Biotechnology* (ed. P.R. Shewry), 291–317. Wallingford: CAB International.

Dusi, D.M.A. and Willemse, M.T.M. (1999). Activity and localisation of sucrose synthase and invertase in ovules of sexual and apomictic *Brachiaria decumbens*. *Protoplasma* 208 (1–4): 173–185.

Ebel, C., Mariconti, L., and Gruissem, W. (2004). Plant retinoblastoma homologues control nuclear proliferation in the female gametophyte. *Nature* 429 (6993): 776–780. Endress, P.K. (2011). Angiosperm ovules: diversity, development, evolution. *Annals of*

Botany 107 (9): 1465–1489.

Engell, K. (1989). Embryology of barley: time course and analysis of controlled fertilization and early embryo formation based on serial sections. *Nordic Journal of Botany* 9 (3): 265–280.

Engell, K. (1994). Embryology of barley. IV. Ultrastructure of the antipodal cells of *Hordeum vulgare* L. cv. Bomi before and after fertilization of the egg cell. *Sexual Plant Reproduction* 7 (6): 333–346.

Evans, M.M.S. (2007). The indeterminate gametophyte1 gene of maize encodes a LOB domain protein required for embryo sac and leaf development. *The Plant Cell* 19 (1): 46.

Evans, M.M.S. and Grossniklaus, U. (2009). *Handbook of Maize: Its Biology*. New York: Springer.

Ferris, R., Ellis, R., Wheeler, T., and Hadley, P. (1998). Effect of high temperature stress at anthesis on grain yield and biomass of field-grown crops of wheat. *Annals of Botany* 82 (5): 631–639.

Fischer, R. (1985). Number of kernels in wheat crops and the influence of solar radiation and temperature. *The Journal of Agricultural Science* 105 (2): 447–461.

Giorno, F., Wolters-Arts, M., Mariani, C., and Rieu, I. (2013). Ensuring reproduction at high temperatures: the heat stress response during anther and pollen development. *Plants* 2 (3): 489–506.

Gray-Mitsumune, M. and Matton, D.P. (2006). The egg apparatus 1 gene from maize is a member of a large gene family found in both monocots and dicots. *Planta* 223 (3): 618–625.

Groß-Hardt, R., Lenhard, M., and Laux, T. (2002). WUSCHEL signaling functions in interregional communication during Arabidopsis ovule development. *Genes & Development* 16 (9): 1129–1138.

Grossniklaus, U. and Schneitz, K. (1998). The molecular and genetic basis of ovule and megagametophyte development. *Seminars in Cell & Developmental Biology* 9 (2): 227–238.

Gubatz, S., Dercksen, V.J., Brüß, C. et al. (2007). Analysis of barley (Hordeum vulgare) grain development using three-dimensional digital models. *The Plant Journal* 52 (4): 779–790.

Guo, Z., Chen, D., and Schnurbusch, T. (2015). Variance components, heritability and correlation analysis of anther and ovary size during the floral development of bread wheat. *Journal of Experimental Botany* 66 (11): 3099–3111.

Guo, Z., Slafer, G.A., and Schnurbusch, T. (2016). Genotypic variation in spike fertility traits and ovary size as determinants of floret and grain survival rate in wheat. *Journal of Experimental Botany* 67 (14): 4221–4230.

Higashiyama, T., Yabe, S., Sasaki, N. et al. (2001). Pollen tube attraction by the synergid cell. *Science* 293 (5534): 1480–1483.

Huang, J., Wijeratne, A.J., Tang, C. et al. (2015). Ectopic expression of TAPETUM DETERMINANT1 affects ovule development in Arabidopsis. *Journal of Experimental Botany* 67 (5): 1311–1326.

Hütsch, B., Jung, S., and Schubert, S. (2015). Comparison of salt and drought stress effects on Maize growth and yield formation with regard to acid invertase activity in the kernels. *Journal of Agronomy and Crop Science* 201 (5): 353–367.

Hütsch, B.W., Saqib, M., Osthushenrich, T., and Schubert, S. (2014). Invertase activity limits grain yield of maize under salt stress. *Journal of Plant Nutrition and Soil Science* 177 (2): 278–286.

Irish, E. (1997). Class II tassel seed mutations provide evidence for multiple types of inflorescence meristems in maize (Poaceae). *American Journal of Botany* 84 (11): 1502. Irish, E.E., Szymkowiak, E.J., and Garrels, K. (2003). The wandering carpel mutation of *Zea mays* (Gramineae) causes misorientation and loss of zygomorphy in flowers

and two-seeded kernels. *American Journal of Botany* 90 (4): 551–560.

Itoh, J.-I., Nonomura, K.-I., Ikeda, K. et al. (2005). Rice plant development: from zygote to spikelet. *Plant and Cell Physiology* 46 (1): 23–47.

Jagadish, S., Muthurajan, R., Oane, R. et al. (2010). Physiological and proteomic approaches to address heat tolerance during anthesis in rice (*Oryza sativa* L.). *Journal of Experimental Botany* 61 (1): 143–156.

Jain, M., Chourey, P.S., Boote, K.J., and Allen, L.H. (2010). Short-term high temperature growth conditions during vegetative-to-reproductive phase transition irreversibly compromise cell wall invertase-mediated sucrose catalysis and microspore meiosis in grain sorghum (*Sorghum bicolor*). *Journal of Plant Physiology* 167 (7): 578–582.

Jensen, W.A. (1973). Fertilization in flowering plants. *BioScience* 23 (1): 21–27.

Ji, X., Shiran, B., Wan, J. et al. (2010). Importance of pre-anthesis anther sink strength for maintenance of grain number during reproductive stage water stress in wheat. *Plant, Cell & Environment* 33 (6): 926–942.

Julián, I., Gandullo, J., Santos-Silva, L.K. et al. (2013). Phylogenetically distant barley legumains have a role in both seed and vegetative tissues. *Journal of Experimental Botany* 64 (10): 2929–2941.

Jung, S., Hütsch, B.W., and Schubert, S. (2017). Salt stress reduces kernel number of corn by inhibiting plasma membrane H+-ATPase activity. *Plant Physiology and Biochemistry* 113: 198–207.

Kerstetter, R.A., Laudencia-Chingcuanco, D., Smith, L.G., and Hake, S. (1997). Loss-of-function mutations in the maize homeobox gene, knotted1, are defective in shoot meristem maintenance. *Development* 124 (16): 3045–3054.

Kimata, Y., Higaki, T., Kawashima, T. et al. (2016). Cytoskeleton dynamics control the first asymmetric cell division in Arabidopsis zygote. *Proceedings of the National Academy of Sciences* 101 (49): 14157–14162.

Klucher, K.M., Chow, H., Reiser, L., and Fischer, R.L. (1996). The AINTEGUMENTA gene of Arabidopsis required for ovule and female gametophyte development is related to the floral homeotic gene APETALA2. *The Plant Cell* 8 (2): 137–153.

Kubo, T., Fujita, M., Takahashi, H. et al. (2013). Transcriptome analysis of developing ovules in rice isolated by laser microdissection. *Plant Cell Physiology* 54 (5): 750–765. Kurihara, D., Mizuta, Y., Sato, Y., and Higashiyama, T. (2015). ClearSee: a rapid optical clearing reagent for whole-plant fluorescence imaging. *Development* 142 (23):

4168–4179.

Kurihara, Y. and Watanabe, Y. (2004). Arabidopsis micro-RNA biogenesis through Dicer-like 1 protein functions. *Proceedings of the National Academy of Sciences* 101 (34): 12753–12758.

Laudencia-Chingcuanco, D. and Hake, S. (2002). The indeterminate floral apex1 gene regulates meristem determinacy and identity in the maize inflorescence. *Development* 129 (11): 2629–2638.

Leibfried, A., To, J.P, Busch, W. et al. (2005). WUSCHEL controls meristem function by direct regulation of cytokinin-inducible response regulators. *Nature* 438 (7071): 1172–1175.

Li, H., Liang, W., Yin, C. et al. (2011). Genetic interaction of OsMADS3, DROOPING LEAF, and OsMADS13 in specifying rice floral organ identities and meristem determinacy. *Plant Physiology* 156 (1): 263–274.

Li, H., Wu, Y., Zhao, Y. et al. (2016). Differential morphology and transcriptome profile between the incompletely fused carpels ovary and its wild-type in maize. *Science Reports* 6: 32652.

Li, H., Peng, T., Wang, Q. et al. (2017). Development of incompletely fused carpels in maize ovary revealed by miRNA, target gene and phytohormone analysis. *Frontiers in Plant Science* 8: 463.

Lieber, D., Lora, J., Schrempp, S. et al. (2011). Arabidopsis WIH1 and WIH2 genes act in the transition from somatic to reproductive cell fate. *Current Biology* 21 (12): 1009–1017.

Linnestad, C., Doan, D.N., Brown, R.C. et al. (1998). Nucellain, a barley homolog of the dicot vacuolar-processing protease, is localized in nucellar cell walls. *Plant Physiology* 118 (4): 1169–1180.

Liu, Y.-H., Offler, C.E., and Ruan, Y.-L. (2013). Regulation of fruit and seed response to heat and drought by sugars as nutrients and signals. *Frontiers in Plant Science* 4: 282.

Lora, J., Herrero, M., Tucker, M.R., and Hormaza, J.I. (2016). The transition from somatic to germline identity shows conserved and specialized features during angiosperm evolution. *New Phytologist* 216 (2): 495–509.

Ludewig, F. and Flügge, U.-I. (2013). Role of metabolite transporters in source-sink carbon allocation. *Frontiers in Plant Science* 4: 231.

Lynn, K., Fernandez, A., Aida, M. et al. (1999). The PINHEAD/ZWILLE gene acts pleiotropically in Arabidopsis development and has overlapping functions with the ARGONAUTE1 gene. *Development* 126 (3): 469–481.

Mallory, A.C., Hinze, A., Tucker, M.R. et al. (2009). Redundant and specific roles of the ARGONAUTE proteins AGO1 and ZLL in development and small RNA-directed gene silencing. *PLoS Genetics* 5 (9): e1000646.

McLaughlin, J.E. and Boyer, J.S. (2004). Sugar-responsive gene expression, invertase activity, and senescence in aborting maize ovaries at low water potentials. *Annals of Botany* 94 (5): 675–689.

Morel, J.B., Godon, C., Mourrain, P. et al. (2002). Fertile hypomorphic ARGONAUTE (ago1) mutants impaired in post-transcriptional gene silencing and virus resistance. *The Plant Cell* 14 (3): 629–639.

Moussian, B., Schoof, H., Haecker, A. et al. (1998). Role of the ZWILLE gene in the regulation of central shoot meristem cell fate during Arabidopsis embryogenesis. *EMBO Journal* 17 (6): 1799–1809.

Muñoz-Amatriaín, M., Cuesta-Marcos, A., Endelman, J.B. et al. (2014). The USDA barley core collection: genetic diversity, population structure, and potential for genome-wide association studies. *PLoS One* 9 (4): e94688.

Nagasawa, N., Miyoshi, M., Sano, Y. et al. (2003). SUPERWOMAN1 and DROOPING LEAF genes control floral organ identity in rice. *Development* 130 (4): 705–718.

Nakaune, S., Yamada, K., Kondo, M. et al. (2005). A vacuolar processing enzyme, δVPE, is involved in seed coat formation at the early stage of seed development. *The Plant Cell* 17 (3): 876–887.

Nickerson, N.H. (1954). Morphological analysis of the maize ear. *American Journal of Botany* 41 (2): 87–92.

Noman, A., Fahad, S., Aqeel, M. et al. (2017). miRNAs: Major modulators for crop growth and development under abiotic stresses. *Biotechnology Letters* 39 (5): 685–700.

Nonomura, K.-I., Miyoshi, K., Eiguchi, M. et al. (2003). The MSP1 gene is necessary to restrict the number of cells entering into male and female sporogenesis and to initiate anther wall formation in rice. *The Plant Cell* 15 (8): 1728–1739.

Norstog, K. (1974). Nucellus during early embryogeny in barley: fine structure. *Botanical Gazette* 135 (2): 97–103.

Okada, T., Hu, Y., Tucker, M.R. et al. (2013). Enlarging cells initiating apomixis in *Hieracium praealtum* transition to an embryo sac program prior to Entering Mitosis. *Plant Physiology* 163 (1): 216.

Olmedo-Monfil, V., Durán-Figueroa, N., Arteaga-Vandázquez, M. et al. (2010). Control of female gamete formation by a small RNA pathway in Arabidopsis. *Nature* 464 (7288): 628.

Onyemaobi, I., Liu, H., Siddique, K.H.M., and Yan, G. (2016). Both male and female malfunction contributes to yield reduction under water stress during meiosis in bread wheat. *Frontiers in Plant Science* 7: 2071.

Oshino, T., Abiko, M., Saito, R. et al. (2007). Premature progression of anther early developmental programs accompanied by comprehensive alterations in transcription during high-temperature injury in barley plants. *Molecular Genetics and Genomics* 278 (1): 31–42.

Parkinson, S.E., Gross, S.M., and Hollick, J.B. (2007). Maize sex determination and abaxial leaf fates are canalized by a factor that maintains repressed epigenetic states. *Developmental Biology* 308 (2): 462–473.

Pawlowski, W.P., Wang, C.J., Golubovskaya, I.N. et al. (2009). Maize AMEIOTIC1 is essential for multiple early meiotic processes and likely required for the initiation of meiosis. *Proceedings of the National Academy of Sciences* 106 (9): 3603–3608.

Peragine, A., Yoshikawa, M., Wu, G. et al. (2004). SGS3 and SGS2/SDE1/RDR6 are required for juvenile development and the production of trans-acting siRNAs in Arabidopsis. *Genes & Development* 18 (19): 2368–2379.

Peukert, M., Lim, W.L., Seiffert, U., and Matros, A. (2016). Mass spectrometry imaging of metabolites in barley grain tissues. *Current Protocols in Plant Biology* 1: 574–591.

Pinyopich, A., Ditta, G.S., Savidge, B. et al. (2003). Assessing the redundancy of MADS-box genes during carpel and ovule development. *Nature* 424 (6944): 85–88.

Radchuk, V., Borisjuk, L., Radchuk, R. et al. (2006). *Jekyll* encodes a novel protein involved in the sexual reproduction of barley. *The Plant Cell* 18 (7): 1652–1666.

Radchuk, V., Weier, D., Radchuk, R. et al. (2011). Development of maternal seed tissue in barley is mediated by regulated cell expansion and cell disintegration and coordinated with endosperm growth. *Journal of Experimental Botany* 62 (3): 1217–1227.

Radchuk, V., Riewe, D., Peukert, M. et al. (2017). Down-regulation of the sucrose transporters HvSUT1 and HvSUT2 affects sucrose homeostasis along its delivery path in barley grains. *Journal of Experimental Botany* 68 (16): 4595–4612.

Ray, A., Robinson-Beers, K., Ray, S. et al. (1994). *Arabidopsis* floral homeotic gene *BELL* (*BEL1*) controls ovule development through negative regulation of *AGAMOUS* gene (*AG*). *Proceedings of the National Academy of Sciences* 91: 5761–5765.

Reale, L., Rosati, A., Tedeschini, E. et al. (2017). Ovary size in wheat (*Triticum aestivum*

L.) is related to cell number. *Crop Science* 57: 914–925.

Robinson-Beers, K., Pruitt, R.E., and Gasser, C.S. (1992). Ovule development in wild-type Arabidopsis and two female-sterile mutants. *The Plant Cell* 4 (10): 1237–1249.

Ruan, Y.L., Patrick, J.W., Bouzayen, M. et al. (2012). Molecular regulation of seed and fruit set. *Trends in Plant Science* 17 (11): 656–665.

Rudall, P.J. (1997). The nucellus and chalaza in monocotyledons: structure and systematics. *The Botanical Review* 63 (2): 140–181.

Sage, T.L., Bagha, S., Lundsgaard-Nielsen, V. et al. (2015). The effect of high temperature stress on male and female reproduction in plants. *Field Crops Research* 182: 30–42.

Saini, H. and Aspinall, D. (1981). Effect of water deficit on sporogenesis in wheat (*Triticum aestivum* L.). *Annals of Botany* 48 (5): 623–633.

Saini, H., Sedgley, M., and Aspinall, D. (1983). Effect of heat stress during floral development on pollen tube growth and ovary anatomy in wheat (*Triticum aestivum* L.). *Functional Plant Biology* 10 (2): 137–144.

Saini, H.S. and Westgate, M.E. (1999). Reproductive development in grain crops during drought. *Advances in Agronomy* 68: 59–96.

Schauer, S.E., Jacobsen, S.E., Meinke, D.W., and Ray, A. (2002). DICER-LIKE1: blind men and elephants in Arabidopsis development. *Trends in Plant Science* 7 (11): 487–491.

Schiefthaler, U., Balasubramanian, S., Sieber, P. et al. (1999). Molecular analysis of NOZZLE, a gene involved in pattern formation and early sporogenesis during sex organ development in Arabidopsis thaliana. *Proceedings of the National Academy of Sciences* 96 (20): 11664–11669.

Schmidt, A., Wuest, S.E., Vijverberg, K. et al. (2011). Transcriptome analysis of the Arabidopsis megaspore mother cell uncovers the importance of RNA helicases for plant germline development. *PLoS Biology* 9 (9): e1001155.

Scott, W., Appleyard, M., Fellowes, G., and Kirby, E. (1983). Effect of genotype and position in the ear on carpel and grain growth and mature grain weight of spring barley. *The Journal of Agricultural Science* 100 (2): 383–391.

Sessions, A., Nemhauser, J.L., McColl, A. et al. (1997). *ETTIN* patterns the *Arabidopsis*

floral meristem and reproductive organs. *Development* 124: 4481–4491.

Shamrov, I. (1998). Ovule classification in flowering plants-new approaches and concepts. *Botanische Jahrbücher* 120: 377–407.

Sheridan, W.F., Avalkina, N.A., Shamrov, I.I. et al. (1996). The mac1 gene: controlling the commitment to the meiotic pathway in maize. *Genetics* 142 (3): 1009–1020.

Shimada, T., Yamada, K., Kataoka, M. et al. (2003). Vacuolar processing enzymes are essential for proper processing of seed storage proteins in Arabidopsis thaliana. *Journal of Biological Chemistry* 278 (34): 32292–32299.

Singh, M., Goel, S., Meeley, R.B. et al. (2011). Production of viable gametes without meiosis in maize deficient for an ARGONAUTE protein. *The Plant Cell Online* 23 (2): 443–458.

Sreenivasulu, N., Altschmied, L., Panitz, R. et al. (2002). Identification of genes specifically expressed in maternal and filial tissues of barley caryopses: a cDNA array analysis. *Molecular Genetics and Genomics* 266 (5): 758–767.

Sreenivasulu, N., Radchuk, V., Strickert, M. et al. (2006). Gene expression patterns reveal tissue-specific signaling networks controlling programmed cell death and ABA-regulated maturation in developing barley seeds. *The Plant Journal* 47 (2): 310–327.

Strable, J., Wallace, J.G., Unger-Wallace, E. et al. (2017). Maize YABBY genes drooping leaf1 and drooping leaf2 regulate plant architecture. *The Plant Cell* 29 (7): 1622–1641. Su, Z., Zhao, L., Zhao, Y. et al. (2017). The THO complex non-cell-autonomously represses female germline specification through the TAS3-ARF3 module. *Current*

Biology 27 (11): 1597–1609.

Sun, K., Hunt, K., and Hauser, B.A. (2004). Ovule abortion in *Arabidopsis* triggered by stress. *Plant Physiology* 135 (4): 2358–2367.

Tang, A.-C. and Boyer, J.S. (2013). Differences in membrane selectivity drive phloem transport to the apoplast from which maize florets develop. *Annals of Botany* 111 (4): 551–562.

Thiel, J., Weier, D., Sreenivasulu, N. et al. (2008). Different hormonal regulation of cellular differentiation and function in nucellar projection and endosperm transfer cells: a microdissection-based transcriptome study of young barley grains. *Plant Physiology* 148 (3): 1436–1452.

Thiel, J., Müller, M., Weschke, W., and Weber, H. (2009). Amino acid metabolism at the maternal–filial boundary of young barley seeds: a microdissection-based study. *Planta* 230 (1): 205–213.

Tran, V., Weier, D., Radchuk, R. et al. (2014). Caspase-like activities accompany programmed cell death events in developing barley. *PLoS One* 9 (10): e109426.

Tucker, M.R., Okada, T., Hu, Y. et al. (2012). Somatic small RNA pathways promote the mitotic events of megagametogenesis during female reproductive development in Arabidopsis. *Development* 139 (8): 1399–1404.

Tucker, M.R. and Koltunow, A.M. (2014). Traffic monitors at the cell periphery: the role of cell walls during early female reproductive cell differentiation in plants. *Current Opinions in Plant Biology* 17: 137–145.

Van Hautegem, T., Waters, A.J., Goodrich, J., and Nowack, M.K. (2015). Only in dying, life: programmed cell death during plant development. *Trends in Plant Science* 20 (2): 102–113.

Villarino, G.H., Hu, Q., Manrique, S. et al. (2016). Transcriptomic signature of the SHATTERPROOF2 expression domain reveals the meristematic nature of Arabidopsis gynoecial medial domain. *Plant Physiology* 171 (1): 42–61.

Vollbrecht, E., Springer, P.S., Goh, L. et al. (2005). Architecture of floral branch systems in maize and related grasses. *Nature* 436 (7054): 1119–1126.

Voronova, O.N., Shamrov, I.I., and Batygina, T.B. (2003). Ovule morphogenesis in normal and mutant *Zea mays*. *Acta Biologica Cracoviensia Series Botanica* 45 (1): 155–160. Wang, C.-J.R., Nan, G.-L., Kelliher, T. et al. (2012a). Maize multiple archesporial cells 1 (mac1), an ortholog of rice TDL1A, modulates cell proliferation and identity in

early anther development. *Development* 139 (14): 2594–2603.

Wang, L., Cook, A., Patrick, J.W. et al. (2014). Silencing the vacuolar invertase gene GhVIN1 blocks cotton fiber initiation from the ovule epidermis, probably by suppressing a cohort of regulatory genes via sugar signaling. *The Plant Journal* 78 (4): 686–696.

Wang, T.L., Uauy, C., Robson, F., and Till, B. (2012b). TILLING in extremis. *Plant Biotechnology Journal* 10 (7): 761–772.

Warren, F.J., Perston, B.B., Galindez-Najera, S.P. et al. (2015). Infrared microspectroscopic imaging of plant tissues: spectral visualization of *Triticum aestivum* kernel and Arabidopsis leaf microstructure. *The Plant Journal* 84 (3): 634–646.

Wei, B., Zhang, J., Pang, C. et al. (2015). The molecular mechanism of SPOROCYTELESS/NOZZLE in controlling Arabidopsis ovule development. *Cell Research* 25 (1): 121.

Weier, D., Thiel, J., Kohl, S. et al. (2014). Gibberellin-to-abscisic acid balances govern development and differentiation of the nucellar projection of barley grains. *Journal of Experimental Botany* 65 (18): 5291–5304.

Weschke, W., Panitz, R., Sauer, N. et al. (2000). Sucrose transport into barley seeds: molecular characterization of two transporters and implications for seed development and starch accumulation. *The Plant Journal* 21 (5): 455–467.

Weschke, W., Panitz, R., Gubatz, S. et al. (2003). The role of invertases and hexose transporters in controlling sugar ratios in maternal and filial tissues of barley caryopses during early development. *The Plant Journal* 33 (2): 395–411.

Whipple, C.J., Ciceri, P., Padilla, C.M. et al. (2004). Conservation of B-class floral homeotic gene function between maize and Arabidopsis. *Development* 131 (24): 6083–6091.

Wilkinson, L.G. and Tucker, M.R. (2017). An optimised clearing protocol for the quantitative assessment of sub-epidermal ovule tissues within whole cereal pistils. *Plant Methods* 13 (1): 67.

Wittich, P. and Willemse, M. (1999). Sucrose utilization during ovule and seed development of *Gasteria verrucosa* (Mill.) H. Duval as monitored by sucrose synthase and invertase localization. *Protoplasma* 208 (1): 136–148.

Wuest, S.E. and Grossniklaus, U. (2014). Laser-assisted microdissection applied to floral tissues. *Flower Development. Methods in Molecular Biology (Methods and Protocols)* 1110: 329–344.

Xie, Q., Mayes, S., and Sparkes, D.L. (2015). Carpel size, grain filling, and morphology determine individual grain weight in wheat. *Journal of Experimental Botany* 66 (21): 6715–6730.

Xu, W., Fiume, E., Coen, O. et al. (2016). Endosperm and nucellus develop antagonistically in Arabidopsis seeds. *The Plant Cell* 28 (6): 1343–1360.

Yadegari, R. and Drews, G.N. (2004). Female gametophyte development. *The Plant Cell*

16: S133–S141.

Yamada, K., Saraike, T., Shitsukawa, N. et al. (2009). Class D and Bsister MADS-box genes are associated with ectopic ovule formation in the pistil-like stamens of alloplasmic wheat (*Triticum aestivum* L.). *Plant Molecular Biology* 71 (1): 1–14.

Yamada, T., Sasaki, Y., Hashimoto, K. et al. (2016). CORONA, PHABULOSA and PHAVOLUTA collaborate with BELL1 to confine WUSCHEL expression to the nucellus in Arabidopsis ovules. *Development* 143 (3): 422–426.

Yang, J., Yuan, Z., Meng, Q. et al. (2017). Dynamic regulation of auxin response during rice development revealed by newly established hormone biosensor markers. *Frontiers in Plant Science* 8: 256.

Yang, W.C., Ye, D., Xu, J., and Sundaresan, V. (1999). The *SPOROCYTELESS* gene of *Arabidopsis* is required for initiation of sporogenesis and encodes a novel nuclear protein. *Genes & Development* 13: 2108–2117.

Yang, X., Wu, F., Lin, X. et al. (2012). Live and let die – The B(sister) MADS-box gene OsMADS29 controls the degeneration of cells in maternal tissues during seed development of rice (*Oryza sativa*). *PLoS One* 7 (12): e51435.

Yang, Z., van Oosterom, E.J., Jordan, D.R., and Hammer, G.L. (2009). Pre-anthesis ovary development determines genotypic differences in potential kernel weight in sorghum. *Journal of Experimental Botany* 60 (4): 1399–1408.

Yin, L.-L. and Xue, H.-W. (2012). The MADS29 transcription factor regulates the degradation of the nucellus and the nucellar projection during rice seed development. *The Plant Cell* 24 (3): 1049–1065.

Zhang, J., Tang, W., Huang, Y. et al. (2015). Down-regulation of a LBD-like gene, OsIG1, leads to occurrence of unusual double ovules and developmental abnormalities of various floral organs and megagametophyte in rice. *Journal of Experimental Botany* 66 (1): 99–112.

Zhang, S.-S., Yang, H., Ding, L. et al. (2017). Tissue-specific transcriptomics reveals an important role of the unfolded protein response in maintaining fertility upon heat stress in Arabidopsis. *The Plant Cell* 29 (5): 1007–1023.

Zhao, L., He, J., Cai, H. et al. (2014). Comparative expression profiling reveals gene functions in female meiosis and gametophyte development in Arabidopsis. *The Plant Journal* 80 (4): 615–628.

Zhao, T., Ni, Z., Dai, Y. et al. (2006). Characterization and expression of 42 MADS-box genes in wheat (*Triticum aestivum* L.). *Molecular Genetics and Genomics* 276 (4): 334.

Zhao, X., De Palma, J., Oane, R. et al. (2008). OsTDL1A binds to the LRR domain of rice receptor kinase MSP1, and is required to limit sporocyte numbers. *The Plant Journal* 54 (3): 375–387.

Zhao, X., Bramsiepe, J., Van Durme, M. et al. (2017). RETINOBLASTOMA RELATED1 mediates germline entry in Arabidopsis. *Science* 356 (6336).

Zinn, K.E., Tunc-Ozdemir, M., and Harper, J.F. (2010). Temperature stress and plant sexual reproduction: uncovering the weakest links. *Journal of Experimental Botany* 61 (7): 1959–1968.

Zinselmeier, C., Lauer, M.J., and Boyer, J.S. (1995). Reversing drought-induced losses in grain-yield sucrose maintains embryo growth in maize. *Crop Science* 35 (5): 1390–1400.

Zinselmeier, C., Jeong, B.R., and Boyer, J.S. (1999). Starch and the control of kernel number in maize at low water potentials. *Plant Physiology* 121 (1): 25–35.

Zong, Y., Wang, Y., Li, C. et al. (2017). Precise base editing in rice, wheat and maize with a Cas9-cytidine deaminase fusion. *Nature Biotechnology* 35 (5): 438–440.

Chapter 3

An optimised clearing protocol for the quantitative assessment of sub-epidermal ovule tissues within whole cereal pistils

Statement of Authorship

Title of Paper	Exploring the Role of the Ovule in Cereal Grain Development and Reproductive Stress Tolerance
Publication Status	☑ Published ☐ Accepted for Publication ☐ Submitted for Publication ☐ Unpublished and Unsubmitted work written in manuscript style
Publication Details	Laura G. Wilkinson[1] and Matthew R. Tucker[2,*]

Principal Author

Name of Principal Author (Candidate)	Laura G. Wilkinson		
Contribution to the Paper	Compiled information and wrote the manuscript. I hereby certify that the statement of authorship is accurate.		
Overall percentage (%)	90%		
Certification:	This paper reports on original research I conducted during the period of my Higher Degree by Research candidature and is not subject to any obligations or contractual agreements with a third party that would constrain its inclusion in this thesis. I am the primary author of this paper.		
Signature		Date	14/2/19

Co-Author Contributions

By signing the Statement of Authorship, each author certifies that:

i. the candidate's stated contribution to the publication is accurate (as detailed above);
ii. permission is granted for the candidate in include the publication in the thesis; and
iii. the sum of all co-author contributions is equal to 100% less the candidate's stated contribution.

Name of Co-Author	Matthew R. Tucker		
Contribution to the Paper	Conceived project and designed experiments. Contributed to the preparation of the manuscript. I hereby certify that the statement of authorship is accurate.		
Signature		Date	14/2/19

Abstract

Background: Seed development in the angiosperms requires the production of a female gametophyte (embryo sac) within the ovule. Many aspects of female reproductive development in cereal crops are yet to be described, largely due to the technical difficulty in obtaining phenotypic information at the cellular or sub-cellular level. Hoyer's solution is currently well established as a solution for clearing thin tissues samples, such as sections or whole tissues of bryophytes, mycorrhizal fungi, and small model organisms (e.g. *Arabidopsis thaliana)*.

Results: Here we report a Hoyer's solution-based clearing method to facilitate clearing of the whole barley pistil, with high reproducibility. The clearing process takes 10 days from fixation to visualisation, whereupon tissue is sufficiently clear to obtain multiple phenotypic measurements from sub-epidermal tissues and cells within the ovule.

Conclusion: Visualisation of cereal ovules that have not been dissected from the pistil allows an unprecedented capability to collect quantitative morphological information from the developing ovule, integument, nucellus and embryo sac. This will enable comparisons with genetic data to reveal the contribution of pre-fertilisation ovule tissues towards downstream seed development.

Keywords: Microscopy, Hoyer's solution, Barley, Ovule, Monocot, Development, Cereal, Clearing

Background

Sustaining food production above the level of food demand is a growing global challenge. Estimates suggest that crop yields will need to increase by 25% to 75% to ensure sufficient food production for the world's population in 2050 [1]. Cereal crop production is highly reliant upon development of flowers. In particular, the single ovule within each flower is essential, as it is the site of gametogenesis, fertilisation and downstream grain development. Environmental events such as drought, high temperatures and frost are known to disrupt flower and seed development, causing a reduction in both grain number and grain quality, thus compromising yield [2-4].

Our understanding of floral development and seed formation in flowering plants has been dramatically expanded by research in model dicots, such as *Arabidopsis thaliana*, *Hieracium* sp., and *Torenia fournieri* [5-7]. The formation of ovule primordia, the differentiation of a megaspore mother cell from somatic precursors and the production and fertilisation of an embryo sac have been described in intimate molecular, genetic and morphological detail [8]. Research in rice, maize, wheat and barley has contributed significant molecular and genetic knowledge of monocot inflorescence and flower development [9-12]. Despite this, remarkably little is known about ovule development in these important cereal species, particularly in regards to how different tissues contribute to eventual seed size, composition and shape. Studies have shown that ovary size is an important component of floret and grain survival [13], but the contribution of constituent tissues remains unclear. Determining the role of these tissues for downstream seed development requires robust, high throughput methods for quantitative two and three-dimensional analysis of developing ovule tissues, such that phenotypic information can be extracted and assessed.

Observation of the internal morphology of cleared floral organs is a powerful tool in understanding plant development, as it allows examination of phenotypic alterations in internal structures following genetic or environmental modification, without the need for thin-sectioning. Chemical treatment to clear small tissue samples is a well-established practice, with reagents ranging from the more traditional methyl salicylate, lactic acid and chloral hydrate based solutions [14-16] to recently developed methods such as ClearSee [17, 18] and PEA-CLARITY [19]. Despite this, observation of female reproductive tissues in cereal monocots remains technically challenging, contributing to a lack of specific genetic and mechanistic information about gametogenesis and ovule development. Two key technical challenges include the relatively large size of the pistils, which are sufficiently thick to remain opaque when treated using previously published clearing protocols designed for substantially smaller tissues (e.g. [20]), and the ease by which the physical structure of the ovule may be damaged during the process of dissection.

Here we report a robust method for clearing whole cereal ovaries with Hoyer's Solution [14], allowing visualisation of wheat and barley ovule ultrastructure in a manner that preserves the physical integrity of internal structures. Experimental variation of incubation time offers flexibility in sample preparation, yielding exceptionally clear tissue after a minimum of 10 days post tissue collection and up to a maximum of 16 weeks. The utility of the method was demonstrated by using optical sections through cleared ovaries to measure the dimensions of component tissues, enabling phenotypic variation in ovule development to be captured within a panel of barley cultivars.

Methods

Reagents

Chloral Hydrate C-IV (#15307, Sigma-Aldrich, Australia)

Ethanol (#EA043-2.5L, Chem-Supply, Australia)

Formaldehyde (#809, Ajax Finechem, Australia)

Glacial Acetic Acid (#2335, Ajax Finechem, Australia)

Glycerol (#242, Ajax Finechem, Australia)

Solutions

FAA fixative [21]**:** 50% Ethanol (v/v), 10% Formaldehyde (37% solution, also called formalin), 5% glacial acetic acid (v/v), and 35% sterile water (v/v).

Ethanol Series: 100% analytical grade EtOH diluted in water to a concentration of 70%, 80% and 90%, and 100% EtOH filtered through a molecular sieve.

Chloral hydrate solution: 250g chloral hydrate dissolved in 100mL sterile water

Hoyer's Solution [14]: A 3.0:0.8:0.2 mixture of chloral hydrate : water : glycerol.

Equipment

Greenhouse facility

Standard laboratory 4°C refrigerator

Fume cupboard

Compound microscope with differential contrast (DIC) and Nomarski filter for a 10X, 20X and/or 40X objective

Computer & free ZEN 2011 Blue (Zeiss) LE software

Ventilated microscopy slide box

Small exhaust fan

Glass pipettes

Fine point tweezers (Dumont #5, Emgrid, Australia)

Liquid scintillation vials (#Z190535, SigmaAldrich, Australia)

Polysine Slides (#P4981, ThermoFisher Scientific, Australia)

22x40mm Cover slips (#G422, ProSciTech, Australia)

Microflex 93-260 chemical resistant gloves (Ansell, Australia)

Plant Growth and Staging

Barley plants were grown in greenhouse facilities at The Plant Accelerator (Adelaide, Australia), under 22°C (day) and 17°C (night) temperatures without addition of supplemental light (Figure 3-1A). Florets were identified to be at anthesis by removing them from spikes (Figure 3-1B), gently reaching inside the palea and lemma with tweezers then assessing the colour of the anthers and how readily pollen was released upon gentle squashing. At anthesis, the anthers are a rich yellow colour and have yet to shed pollen, but readily release pollen with minimal application of pressure when pressed against a thumbnail. Any florets that contained green or green/yellow anthers, or anthers that had already shed pollen, were discarded.

Sample Collection and Fixation (Timing: 10 minutes per tiller + overnight fixation)

Whole pistils were removed from anthesis barley flowers by reaching inside the flower with fine tweezers and pinching the base of the pistil as low as possible (Figure 3-1C). Care was taken to avoid tearing the base of the pistil where the ovule is located. Lodicules were gently removed from the outside of the pistil before placing it in a flat bottomed glass scintillation vial containing 2mL of ice cold FAA fixative.

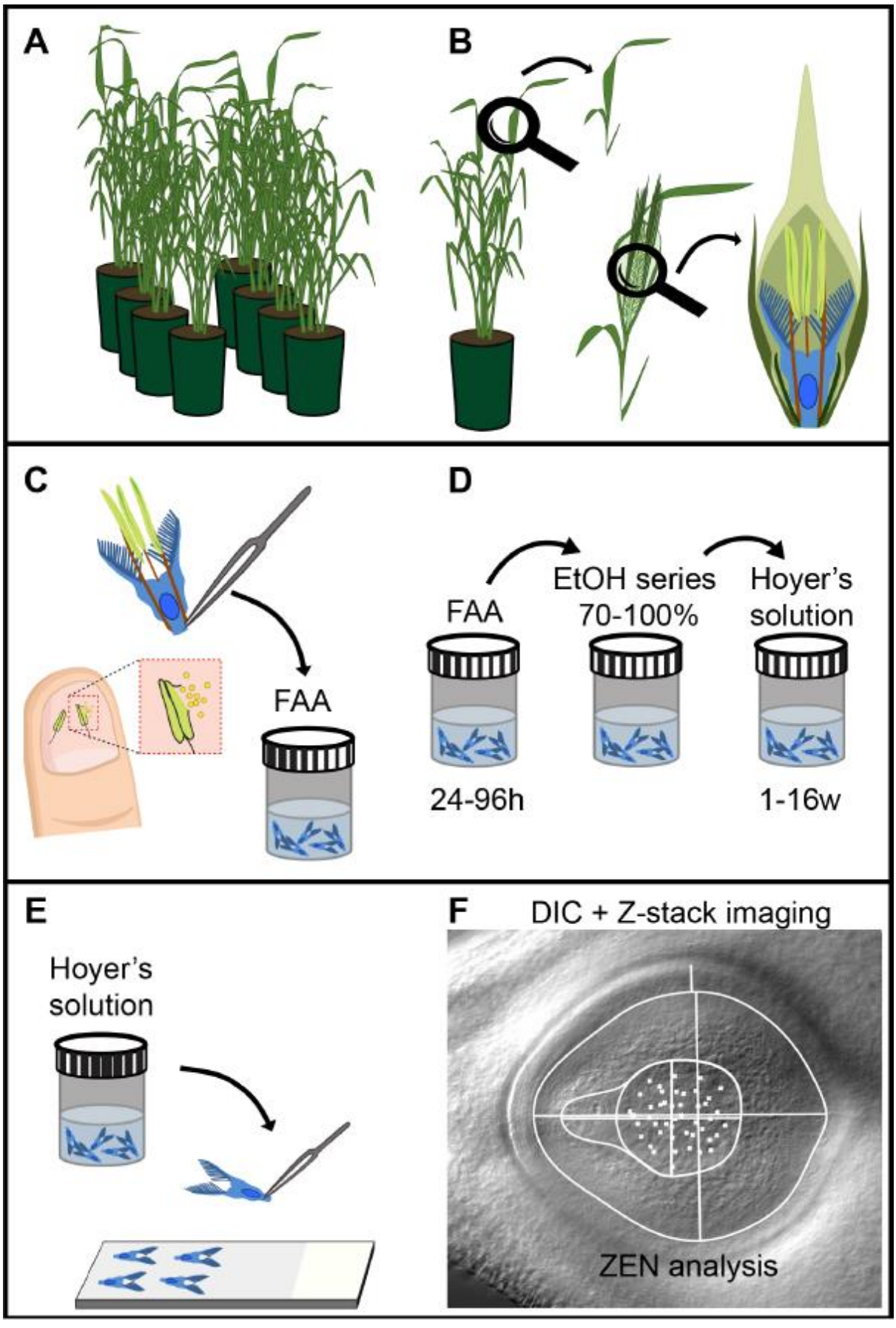
A
B
C
FAA
D
FAA
EtOH series
70-100%
Hoyer's
solution
24-96h
1-16w
E
Hoyer's
solution
F
DIC + Z-stack imaging
ZEN analysis

Figure 3-1: Schematic representation of the steps involved in visualising the internal structures of ovules within cleared cereal pistils. **A** Plants were examined to identify tillers containing developing spikes. **B-C** Individual florets were removed from spikes to identify those at anthesis stage, achieved via observation of pollen on fingernails after anther squashing. **C-D**, Whole pistils and anthers were gently removed and placed in fixative, followed by dehydration in an ethanol series and clearing in Hoyer's solution. **E** Ovaries were transferred to glass slides and covered with glass coverslips. **F** Samples were examined using DIC microscopy and Zeiss ZEN software.

Sample Dehydration (Timing: 4h + overnight dehydration + 4 to 120 days incubation)

Within 1 week of fixation barley pistils were dehydrated through an ethanol series and placed into Hoyer's solution (Figure 3-1D), using fine-tipped glass pipettes for each fluid exchange to minimise the possibility of damage to samples tissue. The EtOH series comprised of 3 x 20min washes at 70%, 80%, 90% and 100% EtOH at room temperature. Samples were left in the final 100% EtOH wash overnight before transfer into 4mL Hoyer's Solution. Samples must remain immersed in Hoyer's solution at room temperature for a minimum of 4 days. **Long protocol:** Samples may remain gently infiltrating in Hoyer's solution for up to 16 weeks. Incubation for 4 weeks preserves tissue quality ideally for imaging of embryo sac features. Vials must be tightly sealed if samples are to be stored for longer than 2 weeks.

Sample Mounting (Timing: 15 minutes per slide + 2 to 4 days incubation)

Pistil tissues were manipulated with fine point tweezers and only held by the stigma in order to avoid crushing the ovary wall, ovule or surrounding tissue. Pistils were placed on flat Poly-Lys coated glass microscopy slides with either the dorsal or ventral side down so that both stigma of each pistil lay "flat", rather than one stigma pointing up into the air (Figure 3-1E). On each slide, ovaries were placed equidistantly in a symmetrical arrangement and gently covered with a 22x40mm coverslip. This arrangement allows the ovaries to lie flat, ensures that variation in the relative viewing angle of the ovule is limited, and preserves the structural integrity of the ovule by preventing any damage to the tissue. Following sample arrangement and application of the cover slip, Hoyer's Solution was pipetted underneath the cover slip onto the slide until all air was evacuated. Slides were then placed flat into a slide storage box that allowed limited ventilation and left in a fume cupboard for four days. Samples stored in a well ventilated location are cleared in 24-48h depending upon the degree of ventilation. Conversely, samples stored after mounting with insufficient or no ventilation required up to 14 days to clear sufficiently to allow visualisation. Therefore, the degree of ventilation can be used to tailor the method to suit the user's time constraints. **Long protocol:** Samples incubated in

4mL Hoyer's Solution for longer than 2 weeks typically require less than 4 days to clear completely once mounted on the microscopy slide. For example, tissue stored in Hoyer's Solution for 8 – 16 weeks generally does not require a period of ventilated storage longer than 12h, and in some cases may be visualised immediately after mounting on slides.

Imaging (Timing: 2 minutes per piece of tissue)

Ovaries were imaged using differential contrast microscopy (DIC) at 10X resolution with a Zeiss AxioImager M2 equipped with a Nomarski filter. For comprehensive data collection, optical slices spanning from the dorsal to ventral integument were taken as a z-stack image, using Zeiss ZEN 2011 (Blue) software.

Image Analysis (Timing: 10 to 15 minutes per image)

Data were analysed using the Zeiss ZEN 2011 (Blue) software package. Diverse measurements were taken including the 2-dimensional area (μm^2) of each ovule tissue of interest, using the "contour (spline)" graphics tool to encircle the tissue, as well as the longitudinal and transverse dimensions (μm) of the same tissues, using the 'line' graphics tool, and the antipodal nuclei were counted using the 'event marker' graphics tool (Figure 4C). Measurements were taken by following tissue boundaries for each given trait throughout optical sections and placing contour markers at the widest point. Two-dimensional ovule area was measured at the boundary between integument and nucellus. Embryo sac area was measured by tracing the outline of the structure from the micropyle to the chalazal region. The residual somatic cell (nucellus) area was measured by subtracting the embryo sac area from the whole ovule area.

Results

Protocol timing optimisation

Clearing was most successful when fixative was removed through an ethanol dehydration series prior to a four-day infiltration step in Hoyer's solution, followed by a four day rest after mounting on microscopy slides (Figure 3-2A). Equally clear images were obtained from samples that were dehydrated, left to gently infiltrate in Hoyer's solution for 4 weeks, then imaged directly after mounting on microscopy slides (Figure 3-S1A). The maximum period of incubation that achieved acceptable clearing was approximately 16 weeks (Figure 3-S1B). Deterioration of cellular morphology was seen when samples were left in scintillation vials to gently infiltrate with Hoyer's solution for longer than 5 months (Figure 3-2B), or when samples were mounted on microscopy slides and stored in a well ventilated area for multiple days, or were imaged after 10 days in a semi-ventilated storage box (Figure 3-S1C). Evaporation of the Hoyer's solution was also a factor that prevented acquisition of acceptable images if the samples were over-ventilated.

Protocol reagent optimisation

Clearing was not successful when ethanol dehydration was omitted and fixed samples were placed directly in Hoyer's solution (Figure 3-2C). Similarly, it was found that use of pure chloral hydrate solution rather than Hoyer's solution yields unacceptably murky images (Figure 3-2D), a factor of both the harsher degradation process when chloral hydrate is used in isolation and the lack of glycerol lowering the refractive index of the mounting fluid. Rough sample collection or handling of tissue throughout the dehydration process often resulted in structural disruption of the sample (Figure 3-2E and Figure 3-S1D). In addition, a Nomarski filter is essential for image acquisition (Figure 3-2F).

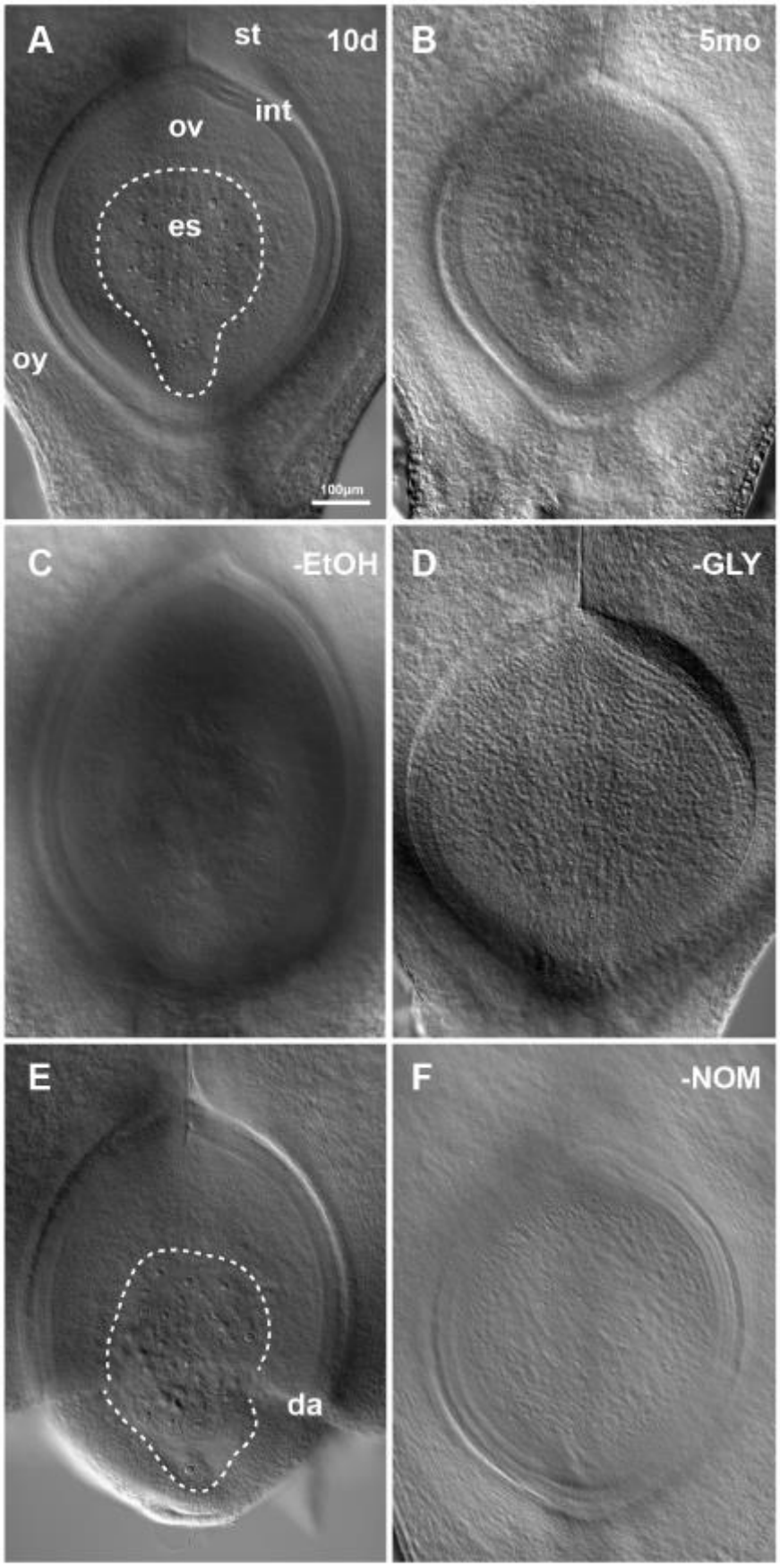
A
st
10d
int
ov
es
oy
100µm
B
5mo
C
-EtOH
D
-GLY
E
da
F
-NOM

Figure 3-2: Barley ovules imaged at 10X showing the outcomes of variations to the clearing protocol. Images presented as composites, generated by merging optical sections. **A** A 10-day (10d) method incorporating ethanol dehydration prior to a 4-day infiltration with Hoyer's solution, then a 4-day rest after mounting on microscopy slides produced the greatest clarity of results within a reasonably short time frame. es = embryo sac, ov = ovule, oy = ovary wall, st = style, int = integuments **B** Samples gently infiltrated with Hoyer's solution for over 5 months (5mo) deteriorated, resulting in unacceptably murky images. **C** Omitting ethanol (-EtOH) dehydration prior to incubation in Hoyer's solution results in the tissue becoming grainy, unacceptably murky. **D** Incubation of the sample in chloral hydrate without glycerol (-GLY) after fixing and dehydration results in the tissue becoming unacceptably murky. **E** Rough sample collection and careless handling of the tissues results in damaged ovaries, which may disrupt the internal morphology of the ovule. da = damaged region. **F** Samples cannot be imaged without a Nomarski filter (-NOM).

Optimised method results

Cleared pistils offer an excellent opportunity to visualise internal components of the ovule in their native spatial arrangement using a DIC microscope with a Nomarski filter (Figures 3-3 and 3-4). Imaging the entire ovule within the ovary is easily possible at 10X magnification, and is particularly powerful when captured in a series of optical sections, allowing construction of composite images and videos that represent all internal features of the ovule's cellular arrangement (Figure 3-3A and 3-S2) and measurement of some three-dimensional features such as embryo sac depth. At 40x magnification, intimate cellular details of the embryo sac and other ovule components could be obtained (Figures 3-3B-C), such as clear, prominent nuclei in the egg cell, central cell and antipodal cells. The quality of tissue resolution was similar in ovaries that were infiltrated in Hoyer's solution for 10 days (Figure 3-3D) and 10 weeks (Figure 3-3B).

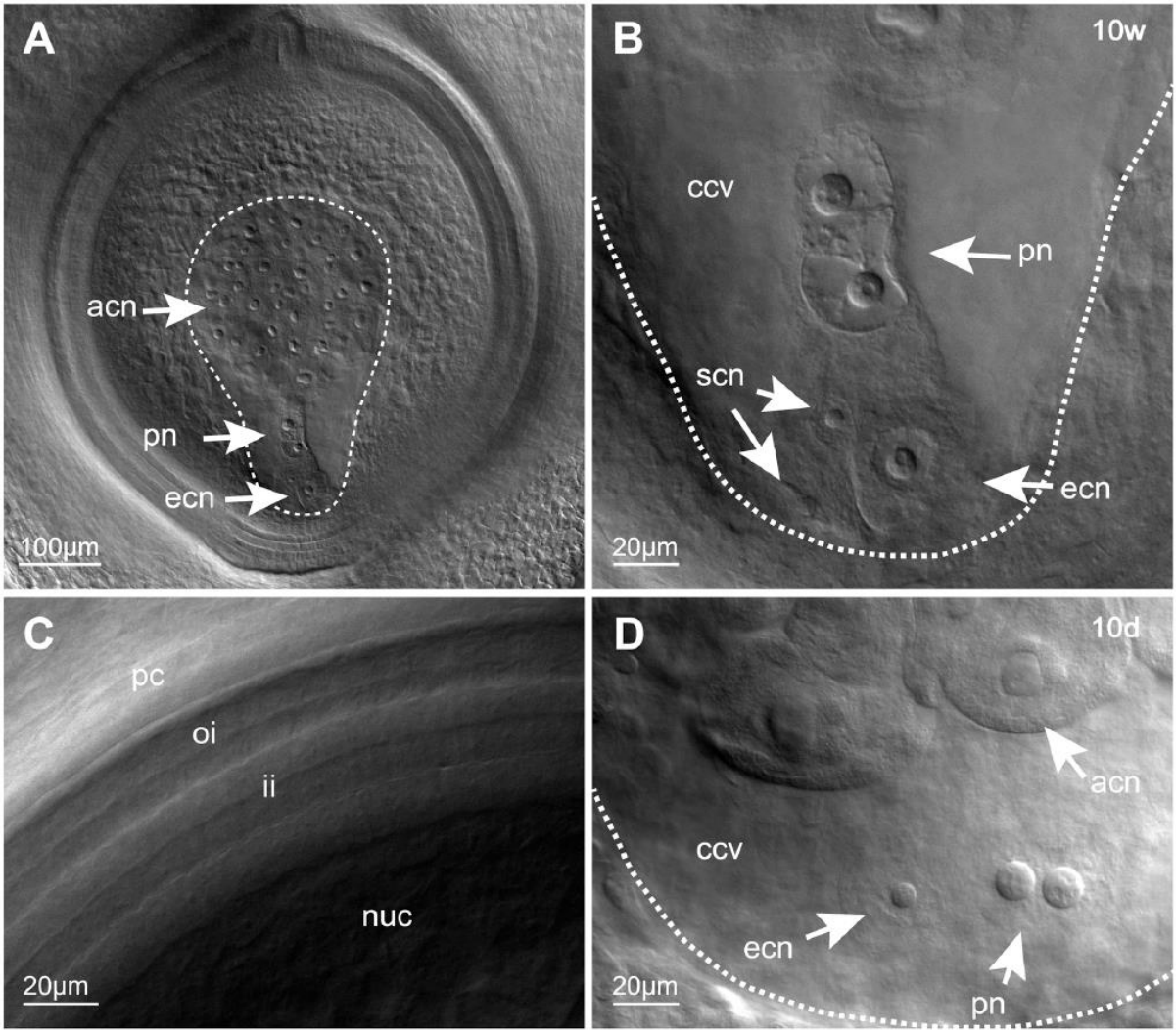

Figure 3-3: Structural details of the ovule are visible in cleared barley pistils (*H. vulgare* cv. Host). Images presented as composites, generated by merging optical sections. **A** Mature barley ovule imaged at 10X magnification without dissection from the pistil. **B-D** Cellular resolution may be achieved with a 40X objective, allowing clear visualisation of the egg cell nucleus, synergid nuclei, polar nuclei and antipodal cell nuclei using the “long method” ie. incubation for at least 10 weeks (10w) in Hoyer’s solution (**B**). The integument layers are also visible (**C**). Similar cellular resolution may also be achieved in samples processed with a 10-day (10d) “short” method (**D**). acn = antipodal cell nuclei, ccv = central cell vacuole, ecn = egg cell nucleus, ii = inner integument, int = integument, nuc = nucellus, oi = outer integument, pn = polar nuclei, pc = pericarp, scn = synergid cell nuclei. The embryo sac is indicated by a dashed white line.

Sup-epidermal details of ovule development differ between cultivars

A fundamental understanding of reproductive organ development in cereals ultimately aims to support breeding programs in generating high-yielding, high-quality cultivars. To demonstrate the utility of this clearing technique, we examined pistils from barley and wheat (Figure 3-4A-B). In both species, sub-epidermal details of ovule tissues, including the embryo sac, egg cell, central cell, antipodals, integument and nucellus could be discerned and measured (Figure 3-4C). To determine if intraspecific differences in ovule development could be identified, we examined a selection of 2-row spring barley cultivars. Quantification of morphological features such as tissue area, thickness and cell number in nine cultivars revealed natural variation in most traits (Table 3-1, Figures 3-4D-E and Figure 3-5). For example, ovule area in *H. vulgare* cv Horizon was almost 2-fold larger than *H. vulgare* cv Beryllium (Figures 3-4D-E and Figure 3-5A), antipodal number was lowest in *H. vulgare* cv. Toucan (~32±5) compared to *H. vulgare* cv. Horizon (~49±4) and integument width was thickest in *H. vulgare* cv Agenda (~50±4µm) and thinnest in *H. vulgare* cv Rainbow (~41±3µm). Correlation analysis indicated that multiple traits showed strong positive correlations, such as ovule area, embryo sac area and ovule height (Figures 3-5B-C), suggesting that these features are intimately related. However, other traits showed weak or no correlations with other ovule features, including integument width, antipodal number, nucellus area and ovule transverse width (Figures 3-5B-C).

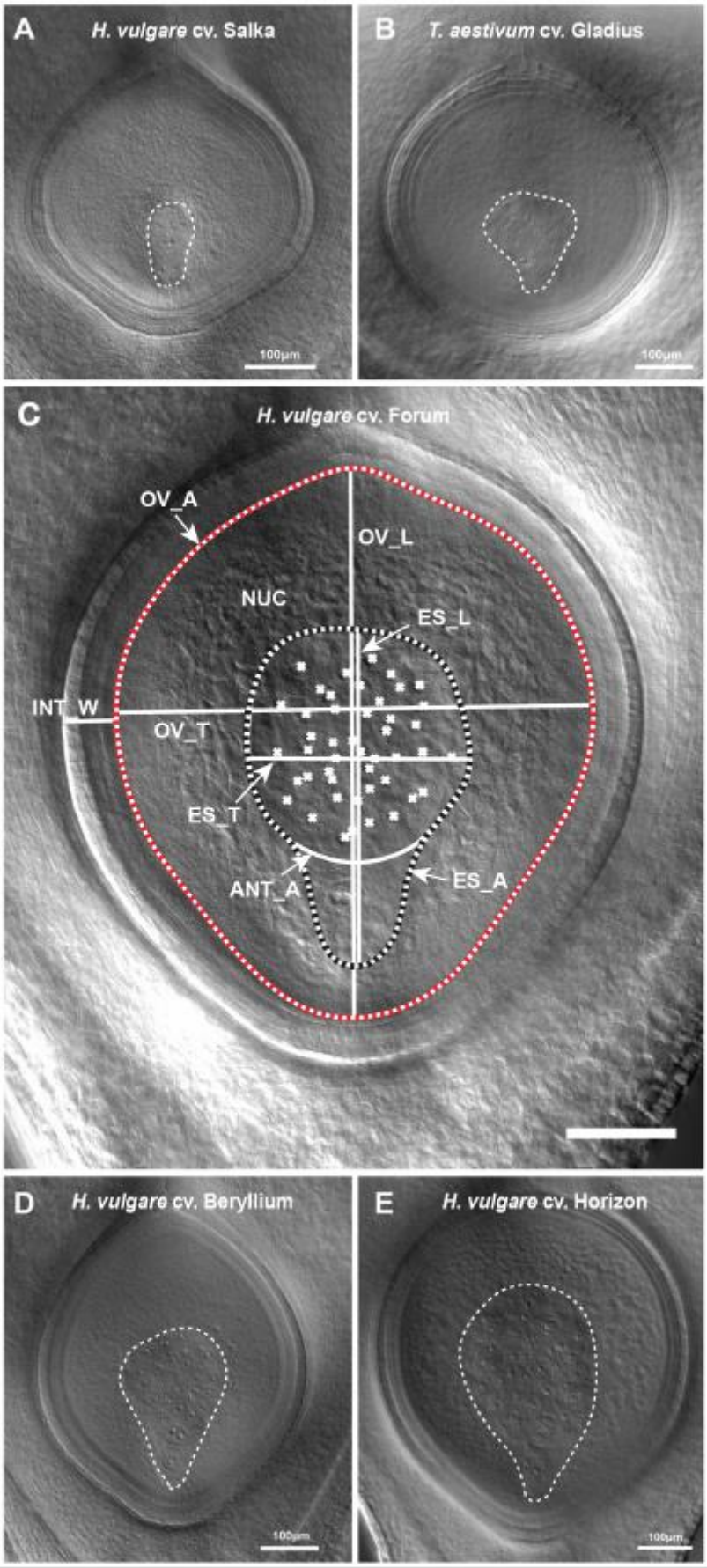
A
H. vulgare cv. Salka
100µm
B
T. aestivum cv. Gladius
100µm
C
H. vulgare cv. Forum
OV_A
OV_L
NUC
ES_L
INT_W
OV_T
ES_T
ANT_A
ES_A
D
H. vulgare cv. Beryllium
100µm
E
H. vulgare cv. Horizon
100µm

Figure 3-4: Ovule morphology after clearing. Ovule images are presented as composites, generated by merging optical sections. **A-B** The method worked equally well for barley (**A**) and wheat (**B**) ovaries at various stages. Pre-anthesis ovules are shown. **C** Measurement of traits at anthesis, including ovule area (OV_A), embryo sac area (ES_A), ovule and embryo sac transverse and longitudinal dimensions (OV_L, OV_T, ES_L, ES_T), integument width (INT_W), antipodal number (marked with crosses) and antipodal cluster area (ANT_A), using Zeiss ZEN Blue 2012 software. The ovule area is indicated with a dashed red and white line, while the embryo sac area is indicated by a dashed black and white line. NUC = nucellus. **D-E** Small (**D**) and large (**E**) mature barley ovules after clearing imaged at 10X magnification without dissection from the pistil. Bar = 100μm.

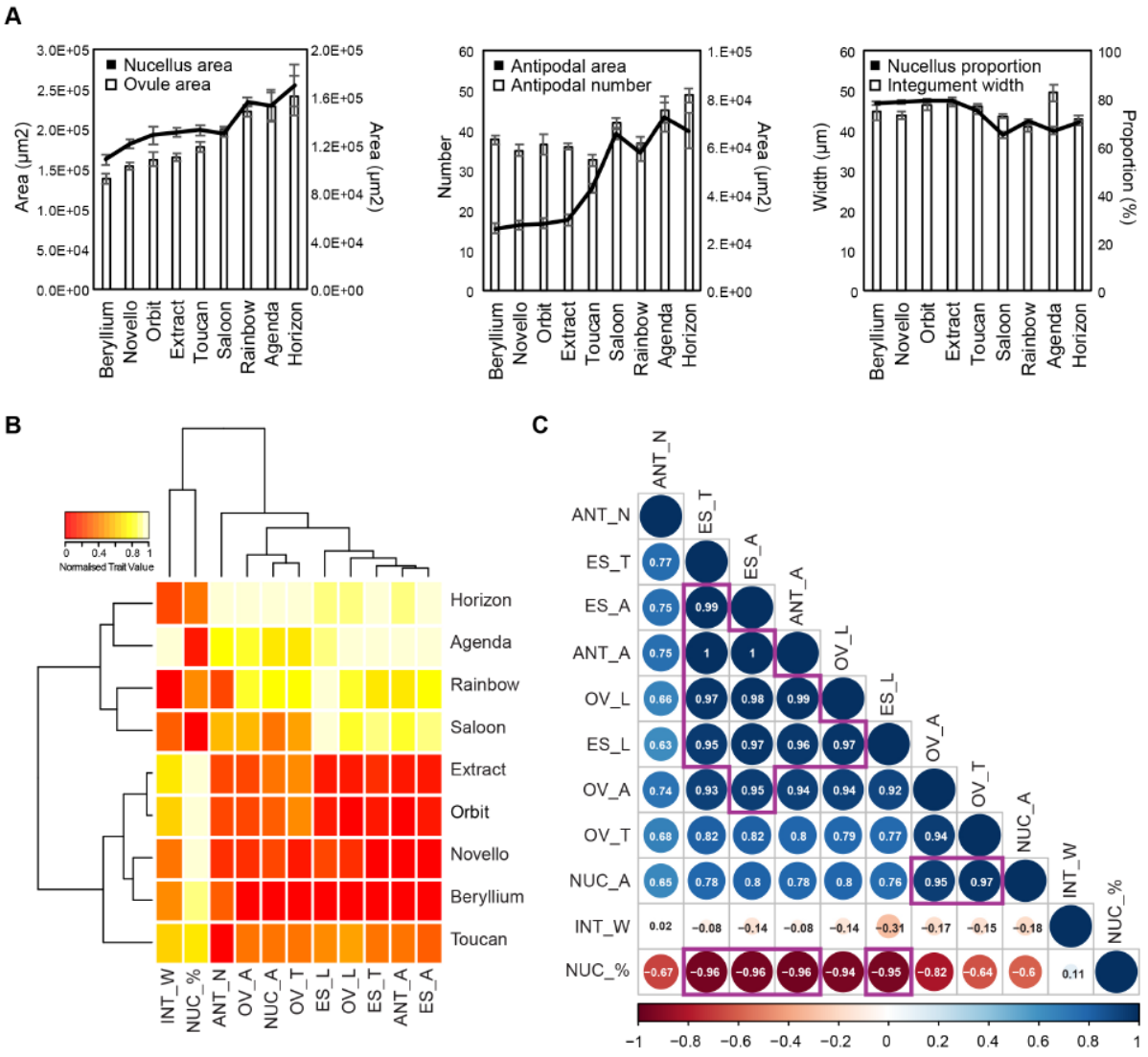

Figure 3-5: Analysis of barley ovule traits by pistil clearing**. A** Variation of ovule phenotypes was examined in nine cultivars of 2-row spring barley. Traits such as ovule area, nucellus area, antipodal number, antipodal area, nucellus proportion and integument width (see Fig 4) were compared between the cultivars. Error bars show standard error. **B** Heat map showing the normalised trait values (between 0 and 1) for 11 ovule traits in the 9 examined cultivars. Cultivars and traits were clustered via hierarchical clustering. **C** Correlation analysis of 11 different ovule traits. The size and colour of the circles indicates the degree of trait correlation, which is also indicated via a numerical value. R-squared values greater than 0.95 are indicated via purple boxes. INT_W = integument width, NUC_% = nucellus proportion, ANT_N = antipodal number, OV_A = ovule area, NUV_A = nucellus area, OV_T = ovule transverse

width, ES_L = embryo sac longitudinal height, OV_L = ovule longitudinal height, ES_T = embryo sac transverse width, ANT_A = entire antipodal area, ES_A = embryo sac area.

Table 3-1: Phenotypic measurements of ovule tissues from nine *H. vulgare* cultivars

		Ovule			Embryo Sac			Integument	Nucellus			Antipodal
Cultivar	**n**	**Area**	**Trans**	**Long**	**Area**	**Trans**	**Long**	**Width**	**Area**	**%**	**#**	**Area**
Beryllium	6	138197.8	396.9	484.3	30462.7	174.6	270.1	44.9	107735.1	78.1	37.7	25829.6
STDEV		15888.7	28.7	21.7	5597.7	26.0	25.5	5.7	11329.2	2.2	2.7	5562.9
Novello	12	154239.1	413.1	505.6	33330.3	171.7	298.0	43.9	120908.9	78.5	35.0	27401.0
STDEV		16522.7	19.1	42.8	6097.1	16.7	37.4	3.2	12418.2	2.5	4.7	6447.3
Orbit	6	161883.0	451.7	487.3	33816.5	182.2	281.0	46.4	128066.6	78.9	36.5	28026.6
STDEV		20556.0	32.4	20.9	4352.4	17.3	10.6	3.0	18494.2	2.6	6.6	4934.9
Extract	11	164652.1	448.3	497.6	34479.2	188.9	284.0	46.7	130172.9	79.1	36.0	29457.8
STDEV		14406.3	22.8	21.5	7094.9	25.8	27.4	2.7	11537.1	3.5	2.9	7992.9
Toucan	11	177561.6	444.7	554.2	45330.7	210.7	320.3	46.1	132230.9	74.7	32.6	42617.2
STDEV		21683.1	25.0	44.8	9374.7	22.8	46.4	2.1	14255.4	3.3	4.7	5469.6
Saloon	13	199385.6	456.7	598.7	70066.1	266.1	382.3	43.6	129319.5	64.9	41.8	65125.7
STDEV		11367.7	19.1	25.6	9071.9	21.7	25.0	1.7	10869.6	3.9	4.8	8283.8
Rainbow	6	221620.1	488.6	598.6	65471.9	242.4	375.2	41.0	156148.2	70.6	36.8	57424.8

STDEV		14500.2	20.3	19.8	8707.8	16.8	23.0	3.0	8030.2	2.5	3.5	7982.3
Agenda	6	227499.2	483.4	625.2	75121.6	272.9	367.9	49.5	152377.7	66.7	45.2	72000.8
STDEV		42467.0	42.0	60.6	13856.8	28.5	53.2	4.9	32315.5	4.3	8.5	14718.3
Horizon	6	241310.7	519.2	607.2	72158.9	268.8	371.9	43.0	169151.8	70.0	48.8	66487.6
STDEV		48703.9	48.0	59.0	14691.2	29.0	48.1	1.5	35130.8	2.2	3.6	14851.0

Legend: n = number of ovules, Trans = transverse width, Long = longitudinal height

Discussion

In this study a method for clearing tissue using Hoyer's solution has been designed to suit cereal ovaries such that internal structures of the ovule may be imaged with a high degree of clarity. Chloral hydrate-based clearing solutions have been successfully used in a wide range of biological fields [14, 22, 23], permitting a great deal of fundamental morphological and phenotypic information to be gathered. However, in our hands, previously reported protocols incorporating chloral hydrate that work well in Arabidopsis (e.g. [24]) did not result in sufficient clearing of barley ovaries to enable quantitative measurement of individual ovule tissues. Moreover, alternative methods that incorporate methyl salicylate [16, 25-27], lactic acid [28], sodium hypochlorite [29] or sodium hydroxide [30], lack the convenience and/or efficiency of our established Arabidopsis chloral hydrate-based method [20]. Other recently reported clearing reagents such as ClearSEE [17], PEA-CLARITY [19] and FocusClear [31] are designed to clear tissue while preserving fluorescent labelling, but are either too expensive for high-throughput analysis or provide insufficient cellular resolution without additional staining.

Although the chloral hydrate-based method we describe is not compatible with visualisation of fluorescently-tagged proteins, it can be applied to diverse cereals, allows customisable incubation times, requires minimal tissue handling, and consistently provided excellent clearing and an ability to detect quantitative differences in tissue development in unstained cereal ovary samples. The Zeiss ZEN software used for image analysis is freely available for download and easy to use, while the FIJI software suite was used to extract similar results [32]. In our pilot study of barley ovules at anthesis, 75 pistils were examined from 9 cultivars. The method was not specifically tested on a microscope containing a motorised 8-slide mounting frame or image stitching software, but such an approach would almost certainly be compatible, suggesting that image acquisition might be automated in future to allow for high-throughput data collection. Whether the scale of analysis required for germplasm screens in

breeding populations can be achieved is currently unclear. However, the method is compatible with pre-breeding efforts to dissect pre-fertilisation traits that contribute to downstream seed development and morphology. Furthermore, we anticipate that the method will be particularly useful for the rapid characterisation of mutant phenotypes and transgenic plants that effect ovule development in barley and wheat.

Conclusions

A clearing technique typically used in the analysis of tissues from dicot model organisms was successfully adapted to clear the much larger cereal pistil. This paves the way for further interrogation of sup-epidermal features of ovule development in barley and other cereal crop species. The application of this method to a large panel of genetically distinct or genetically modified cereal varieties may assist the identification of novel genes controlling ovule phenotypes as well as components of seed yield and quality.

Declarations

Ethics approval and consent to participate

Not Applicable.

Consent for publication

All authors give consent for the data to be published.

Availability of data and material

The datasets used and/or analysed during the current study are available from the corresponding author on reasonable request.

Competing interests

The authors declare that they have no competing interests.

Funding

This work was supported by an Australian Research Council (ARC) Centre of Excellence in Plant Cell Walls supplementary PhD scholarship (LGW) and an ARC Future Fellowship (MRT).

Authors' contributions

LGW collected and analysed the data. LGW and MRT designed and tested the method and jointly contributed to writing the manuscript. Both authors read and approved the final manuscript.

Acknowledgements

We wish to specifically thank Rachel Burton and Caitlin Byrt for advice, Ryan Whitford for wheat samples and Plant Accelerator staff for maintaining plants. We also wish to acknowledge members of the Tucker Laboratory and the ARC Centre of Excellence in Plant Cell Walls for useful discussions and suggestions.

References

1. Hunter MC, Smith RG, Schipanski ME, Atwood LW, Mortensen DA: **Agriculture in 2050: Recalibrating Targets for Sustainable Intensification**. *BioScience* 2017, **67**(4):386-391.

2. Onyemaobi I, Liu H, Siddique KHM, Yan G: **Both Male and Female Malfunction Contributes to Yield Reduction under Water Stress during Meiosis in Bread Wheat**. *Frontiers in Plant Science* 2016, **7**:2071.
3. Saini HS, Westgate ME: **Reproductive Development in Grain Crops during Drought**. *Advances in Agronomy* 1999, **68**:59-96.
4. Thakur P, Kumar S, Malik JA, Berger JD, Nayyar H: **Cold stress effects on reproductive development in grain crops: An overview**. *Environmental and Experimental Botany* 2010, **67**(3):429-443.
5. Susaki D, Takeuchi H, Tsutsui H, Kurihara D, Higashiyama T: **Live Imaging and Laser Disruption Reveal the Dynamics and Cell–Cell Communication During Torenia fournieri Female Gametophyte Development**. *Plant and Cell Physiology* 2015, **56**(5):1031-1041.
6. Tucker MR, Koltunow AMG: **Traffic monitors at the cell periphery: the role of cell walls during early female reproductive cell differentiation in plants**. *Current Opinion in Plant Biology* 2014, **17**:137-145.
7. Yang W-C, Sundaresan V: **Genetics of gametophyte biogenesis in Arabidopsis**. *Current Opinion in Plant Biology* 2000, **3**(1):53-57.
8. Yang W-C, Shi D-Q, Chen Y-H: **Female gametophyte development in flowering plants**. *Annual review of plant biology* 2010, **61**:89-108.
9. Boden SA, Weiss D, Ross JJ, Davies NW, Trevaskis B, Chandler PM, Swain SM: **EARLY FLOWERING3 regulates flowering in spring barley by mediating gibberellin production and FLOWERING LOCUS T expression**. *The Plant Cell* 2014, **26**(4):1557-1569.
10. Yoshida H, Nagato Y: **Flower development in rice**. *Journal of Experimental Botany* 2011, **62**(14):4719-4730.
11. Youssef HM, Eggert K, Koppolu R, Alqudah AM, Poursarebani N, Fazeli A, Sakuma S, Tagiri A, Rutten T, Govind G: **VRS2 regulates hormone-mediated inflorescence patterning in barley**. *Nature genetics* 2017, **49**(1):157-161.
12. Zhang D, Yuan Z: **Molecular control of grass inflorescence development**. *Annual review of plant biology* 2014, **65**:553-578.
13. Guo Z, Schnurbusch T: **Variation of floret fertility in hexaploid wheat revealed by tiller removal**. *Journal of experimental botany* 2015, **66**(19):5945-5958.
14. Anderson LE: **Hoyer's Solution as a Rapid Permanent Mounting Medium for Bryophytes**. *The Bryologist* 1954, **57**(3):242-244.
15. Cunningham JL: **A miracle mounting fluid for permanent whole-mounts of microfungi**. *Mycologia* 1972, **64**(4):906-911.

16. Stelly DM, Peloquin S, Palmer RG, Crane CF: **Mayer's hemalum-methyl salicylate: a stain-clearing technique for observations within whole ovules**. *Stain technology* 1984, **59**(3):155-161.
17. Kurihara D, Mizuta Y, Sato Y, Higashiyama T: **ClearSee: a rapid optical clearing reagent for whole-plant fluorescence imaging**. *Development* 2015, **142**(23):4168-4179.
18. Timmers AC: **Light microscopy of whole plant organs**. *Journal of microscopy* 2016, **263**(2):165-170.
19. Palmer WM, Martin AP, Flynn JR, Reed SL, White RG, Furbank RT, Grof CP: **PEA-CLARITY: 3D molecular imaging of whole plant organs**. *Scientific reports* 2015, **5**.
20. Tucker MR, Okada T, Hu Y, Scholefield A, Taylor JM, Koltunow AM: **Somatic small RNA pathways promote the mitotic events of megagametogenesis during female reproductive development in Arabidopsis**. *Development* 2012, 139(8):1399-404..
21. Young B, Sherwood R, Bashaw E: **Cleared-pistil and thick-sectioning techniques for detecting aposporous apomixis in grasses**. *Canadian Journal of Botany* 1979, **57**(15):1668-1672.
22. Berleth T, Jurgens G: **The role of the monopteros gene in organising the basal body region of the Arabidopsis embryo**. *Development* 1993, **118**(2):575-587.
23. Enugutti B, Schneitz K: **Microscopic analysis of Arabidopsis ovules**. *Flower Development: Methods and Protocols* 2014:253-261.
24. Franks RG: **Histological Analysis of the Arabidopsis Gynoecium and Ovules Using Chloral Hydrate Clearing and Differential Interference Contrast Light Microscopy**. *Oogenesis: Methods and Protocols* 2016:1-7.
25. Herr Jr J: **Recent advances in clearing techniques for study of ovule and female gametophyte development**. *Angiosperm pollen and ovules* 1992, **149**:154.
26. Koltunow AM: **Apomixis: Embryo Sacs and Embryos Formed without Meiosis or Fertilization in Ovules**. *The Plant Cell* 1993, **5**(10):1425-1437.
27. Ponitka A, Ślusarkiewicz-Jarzina A: **Cleared-ovule technique used for rapid access to early embryo development in Secale cereale x Zea mays crosses**. *Acta Biologica Cracoviensia Series Botanica* 2004, **46**:133-137.
28. Desfeux C, Clough SJ, Bent AF: **Female Reproductive Tissues Are the Primary Target ofAgrobacterium-Mediated Transformation by the Arabidopsis Floral-Dip Method**. *Plant physiology* 2000, **123**(3):895-904.
29. Aditya J, Lewis J, Shirley NJ, Tan HT, Henderson M, Fincher GB, Burton RA, Mather DE, Tucker MR: **The dynamics of cereal cyst nematode infection differ between susceptible and resistant barley cultivars and lead to changes in (1, 3; 1, 4)-β-**

glucan levels and HvCslF gene transcript abundance. *New Phytologist* 2015, **207**(1):135-147.

30. Tomer E, Gottreich M, Gazit S: **Defective ovules in avocado cultivars**. *Journal of the American Society for Horticultural Science* 1976, **101**(5):620-623.
31. Chung K, Wallace J, Kim S-Y, Kalyanasundaram S, Andalman AS, Davidson TJ, Mirzabekov JJ, Zalocusky KA, Mattis J, Denisin AK: **Structural and molecular interrogation of intact biological systems**. *Nature* 2013, **497**(7449):332-337.
32. Schindelin J, Arganda-Carreras I, Frise E, Kaynig V, Longair M, Pietzsch T, Preibisch S, Rueden C, Saalfeld S, Schmid B: **Fiji: an open-source platform for biological-image analysis**. *Nature methods* 2012, **9**(7):676-682.

Supplementary Data

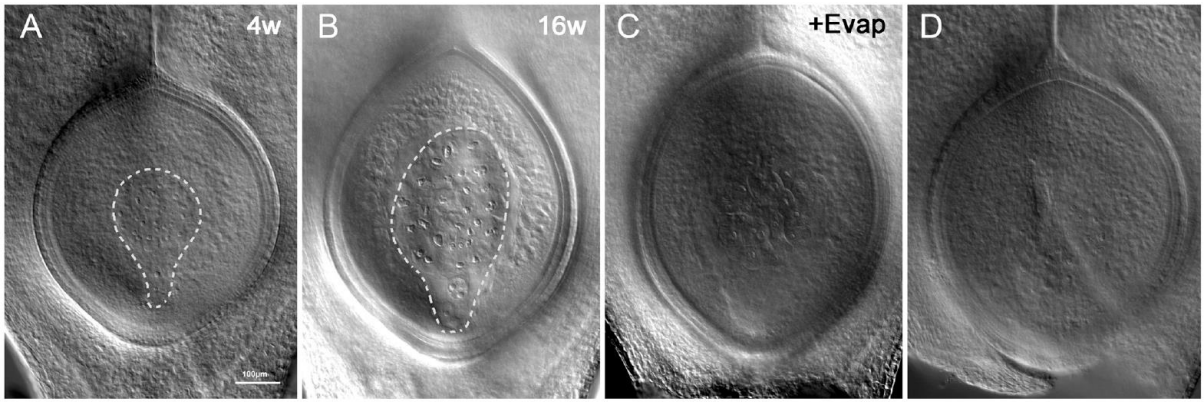

Supplementary Figure 3-1: Barley ovules imaged at 10X showing the outcomes of variations to the clearing protocol. Images presented as composites, generated by merging optical sections. **A** Ethanol dehydration prior to a 4-week (4w) gentle infiltration with Hoyer's solution, then imaging samples directly after mounting on microscopy slides produced high clarity results in a longer time frame. **B** Samples gently infiltrated with Hoyer's solution for 16 weeks (16w) then immediately imaged produced high-quality results. **C** Samples left mounted on microscope slides in a well ventilated storage box or for too long were not able to be imaged properly due to evaporation (+Evap) of the Hoyer's solution, causing uneven illumination of the sample and in some cases accelerated degradation of the tissue, resulting in an unacceptably grainy image. **D** Rough sample collection and careless handling of the tissues results in damaged ovaries, which may disrupt the internal morphology of the ovule. The embryo sac is indicated by a dashed white line.

Supplementary Figure 3-2: Sequential 2.4µm optical slices (n = 50) of a cleared *H. vulgare* cv. Gant ovule were combined to generate a movie file that moves through the pistil at anthesis.

Note: apologies, the movie has not been embedded in this thesis document. If you wish to view the movie, please see the publication online or contact Matthew Tucker.

Chapter 4

Natural variation in mature ovule morphology in barley (*Hordeum vulgare* L) has limited impact on downstream grain development

ଌ • ଓ

Statement of Authorship

Title of Paper	Natural variation in mature ovule morphology in barley (*Hordeum vulgare* L.) has limited impact on downstream grain development
Publication Status	☐ Published ☐ Accepted for Publication ☐ Submitted for Publication ☑ Unpublished and Unsubmitted work written in manuscript style
Publication Details	Laura G. Wilkinson[1,2], Kelly Houston[3], Tobias Würschum[4], Rachel A. Burton[1,2] and Matthew R Tucker[1]*.

Principal Author

Name of Principal Author (Candidate)	Laura G. Wilkinson		
Contribution to the Paper	Performed experiments, analysed all samples, interpreted data and wrote manuscript.		
Overall percentage (%)	80%		
Certification:	This paper reports on original research I conducted during the period of my Higher Degree by Research candidature and is not subject to any obligations or contractual agreements with a third party that would constrain its inclusion in this thesis. I am the primary author of this paper.		
Signature		Date	14/2/19

Co-Author Contributions

By signing the Statement of Authorship, each author certifies that:

i. the candidate's stated contribution to the publication is accurate (as detailed above);
ii. permission is granted for the candidate in include the publication in the thesis; and
iii. the sum of all co-author contributions is equal to 100% less the candidate's stated contribution.

Name of Co-Author	Kelly Houston		
Contribution to the Paper	Assisted with genome wide association study, interpretation of QTL data, and statistical analysis. I hereby certify that the statement of authorship is accurate.		
Signature		Date	14.02.19

Name of Co-Author	Tobias Würschum		
Contribution to the Paper	Assisted with statistical analysis and preparation. I hereby certify that the statement of authorship is accurate.		
Signature		Date	18. Feb 2019
Name of Co-Author	Rachel A. Burton		
Contribution to the Paper	Assisted with project conception and experimental design. I hereby certify that the statement of authorship is accurate.		
Signature		Date	24/02/2019

Name of Co-Author	Matthew R. Tucker		
Contribution to the Paper	Conceived project and designed experiments. Contributed to the preparation of the manuscript. I hereby certify that the statement of authorship is accurate.		
Signature		Date	14/2/19

Abbreviations

GWAS	Genome wide association study
QTL	Quantitative trait loci
SNP	Single nucleotide polymorphism
LOD	Logarithm of the odds, equal to $-\log_{10}$(p-value)
HORVU	Barley (*Hordeum vulgare*) gene sequence
O_A	Ovule area
O_T	Ovule transverse
O_L	Ovule longitude
ES	Embryo sac
ES_A	Embryo sac area
ES_T	Embryo sac transverse
ES_L	Embryo sac longitude
N_A	Nucellus area
N_P	Nucellus proportion (%)
I_W	Integument width
PCA	Principal component analysis
GO	Gene ontology
QTL1H_ES	QTL located on Ch 1H associated with embryo sac phenotype
QTL2H_NUC	QTL located on Ch 2H associated with nucellus phenotype
QTL2H_OV	QTL located on Ch 2H associated with ovule phenotype
QTL4H_INT	QTL located on Ch 4H associated with integument phenotype

Abstract

The ovule plays a critical role in cereal crop production as it is the site of fertilisation and grain development. The mature ovule is composed of four main tissue types: the funiculus, integuments, nucellus, and embryo sac. The size, structure and organisation of these ovule tissues varies between the model plant *Arabidopsis thaliana* and agriculturally important cereal crops, and to a lesser extent among genotypes of individual cereal crop species. However, the degree and functional significance of this variation present among genotypes of a single species is unclear. In this study, nine morphological traits of mature ovules were quantified in a population of 127 European two-row spring barley (*Hordeum vulgare* L.) genotypes. This provides information regarding the typical ovule phenotype of two-row spring barley and identifies cultivars showing significant natural variation. In contrast to previous studies of ovary size in barley and wheat, comparison of ovule phenotypic data with grain traits from the same genotypes indicated that mature ovule structure does not directly influence grain size. Genome wide association studies (GWAS) revealed sixty-six markers in six genomic regions significantly associated with the nine ovule traits. Although the results suggest ovule development is under complex multigenic control, four discrete quantitative trait loci (QTL) were notable in that multiple markers displayed clear associations with several ovule traits. Taken together, the results form a thorough morphological description of barley ovule phenotypes at maturity, thus providing a starting point to assess the multigenic regulation of ovule development in barley and the significance of structural variation in discrete tissues of the ovule to cereal crop reproduction.

Introduction

Barley is a cereal that has sustained humans for thousands of years (Eitam et al. 2015; Samuel 1996), and remains a crop of key agricultural and economical importance in the present era.

The effects of climate change have been predicted to negatively impact global barley yield, and as such efforts have been directed towards breeding elite barley genotypes with high yield and robust tolerance to environmental stress (Tester and Langridge 2010). A large portion of the economic value of barley comes from the starch stored in the grain's endosperm, as it is a key source of calories for direct consumption by humans and livestock (Sands et al. 2009), as well as the source of the fermentable sugars at the heart of the malting and brewing industries (Bokulich 2017). Each individual grain from cereal crops is produced by fertilisation of an ovule. A single ovule is located in the ovary of each cereal crop flower, thus in order for grain production to occur the development of the flower, ovary and ovule must not be compromised. Both the individual and combined effects of heat and drought stress have been demonstrated to compromise fertilisation and kernel development in other cereal crops such as wheat (*Triticum aestivum*) and maize (*Zea mays;* Jäger et al. 2008; Onyemaobi et al. 2018; Oury et al. 2016; Saini et al. 1983). Additionally, the number of mature florets has been linked to barley yield, while the size and number of cells within the pistil have been linked to mature dry weight of barley spikes (Guo et al. 2015; Guo et al. 2016). Together, such studies indicate that nutrient availability is a key determinant of floral survival and subsequent yield, especially under conditions of environmental stress. As such, greater understanding of the female developmental process in cereal crops may present targets for breeding genotypes with improved yield, and will therefore be of great importance in the years to come.

Much of our understanding of plant ovule development and fertilisation has been modelled on the dicot species *Arabidopsis thaliana*. The four tissues of the ovule are the funiculus, integuments, nucellus and embryo sac. In Arabidopsis, the tissues are arranged such that the embryo sac is at the centre, surrounded by a single layer of nucellus tissue, which is then enclosed by two layers of integuments (Schneitz et al. 1995; Willemse and De Boer-de 1981). The funiculus acts as a stalk to connect the ovule to the maternal plant. The integuments and nucellus are diploid maternal tissues, while the embryo sac consists of eight haploid nuclei

contained within seven cells of discrete function. At the most distal, or micropylar, end of the embryo sac are two synergid cells and the egg cell, while at the proximal, or chalazal, end of the embryo sac are three antipodal cells. The two groups of cells are separated by the central cell, a large vacuolated cell that contains two “polar” nuclei that fuse before fertilisation (Schneitz et al 1995). The synergid cells secrete chemoattractants that guide the pollen tube toward the micropylar end of the ovule (Higashiyama and Yang, 2017). Double fertilisation occurs upon arrival of the pollen tube, at which point the fertilised egg cell initiates embryonic development and the single, triploid nucleus of the central cell gives rise to the endosperm (Baroux et al. 2002). The three antipodal cells diminish as the ovule develops, such that antipodal cell death has been proposed to occur prior to fertilisation, and their role has not been determined (Song et al. 2014). Following fertilisation, the nucellus and integument tissues contribute to development of the seed coat (Roszak and Köhler 2011).

Embryo sac development in monocotyledonous cereal crops such as barley generally follows the same process as that of Arabidopsis, however there are some notable structural differences. Ovules of cereal crops are much larger than those of Arabidopsis, lack a true funiculus and at maturity form a more ovoid shape (Engell 1994; Maheswari 1950). The overall arrangement of the nucellus, embryo sac and integuments is generally the same as Arabidopsis, however ovules of cereal crops may be described as crassinucellar, as the nucellus is a thick, multilayered tissue that contributes up to 65% of the ovule area in barley (Wilkinson and Tucker 2017). The micropylar position of the egg apparatus, central cell and antipodal cells within the embryo sac is maintained between Arabidopsis and cereal crops. Despite this, the polar nuclei in wheat and barley do not fuse until fertilisation, and at least 30 antipodal cells indisputably persist until after fertilisation (Brink and Cooper 1944; Chaban et al. 2011; Diboll 1968).

The existence of interspecies variation in ovule morphology between model dicots and monocotyledonous cereal crops has been established for many years (Lloyd 1899), however the degree of intraspecies phenotypic variation in ovule morphology in a cereal crop such as barley does not appear to have been reported. This study defines the bounds of normal ovule morphology in a population of 127 two-row spring barley genotypes, investigates correlations between ovule morphology and grain traits, and uses a genome wide association study (GWAS) to identify four discrete genomic regions that influence mature ovule morphology.

Methods & Materials

Plant growth

A panel of 150 European two-row spring barley genotypes, representing a sub-panel of the genotypes described by Comadran et al. (2012), were sourced from the James Hutton Institute (Scotland). Plants were grown in greenhouses at The Plant Accelerator, Adelaide, Australia, in a 50:50 cocopeat:clay-loam soil mixture (v/v), under 22°C day, 15°C night conditions. The population was grown in triplicate, with pot sequence randomised within each group.

Sample collection and microscopy

Carpels were dissected from florets determined to be at anthesis by similarity of the pistil to that described in Stage 9.5 of the Waddington Scale (Waddington et al. 1983), and by the presence of bright yellow anthers that readily released pollen when gently crushed. Three carpels were hand dissected from one inflorescence (spike) of all three replicates of each genotype, where possible. All tissue was collected from florets located in the middle of each spike.

Clearing & microscopy

Carpels were fixed in FAA (10% formalin, 5% glacial acetic acid, 50% ethanol, 35% millipore H_2O, plus a drop of Triton X100) overnight, then dehydrated through an ethanol series (3 x 30mins at each of 70%, 80%, 90%, 95%, 100%) and placed into Hoyer's Solution as described in Wilkinson and Tucker (2017). Ovules within the cleared carpel tissue were captured as z-stack images, encompassing the entire ovule from dorsal to ventral aspect in 40 optical sections, using differential interference contrast (DIC) microscopy and Nomarski prisms on a Zeiss AxioImager M2. Composite images for figures were assembled in Adobe Photoshop and Illustrator (both version CC 2018; Adobe Inc., USA).

Quantitative analysis of ovule morphology

Nine morphological traits were measured from the z-stack images, using Zeiss Zen Blue (2012) software as described in Wilkinson and Tucker (2017). Each trait represents a one- or two-dimensional measurement, and data reflects the widest point of the region of interest visible within the z-stack. The nine measurements collected were: ovule area, ovule transverse, ovule longitude, embryo sac area, embryo sac transverse, embryo sac longitude, nucellus area, nucellus proportion and integument width. Measurements were averaged from a minimum of four ovules representing at least two plants from each genotype. Low sample numbers due to plant death and errors in staging resulted in elimination of 23 genotypes from analysis, reducing an initial population of 150 genotypes to a functional population of 127. Integument "area" was not measured as part of the ovule area due to difficulties in accurately scoring the boundaries. Thus, what is presented as ovule area is essentially nucellus plus embryo sac area.

Correlation analysis, PCA and dendrograms

Trait correlations, dendograms and principal component analysis were performed using default parameters in the "corrplot" package (https://cran.r-project.org/web/packages/corrplot/corrplot.pdf) in R with RStudio (R version 3.5.0; RStudio®,

USA). Figures were assembled in Adobe Illustrator CC 2018 (version 22.0.0, Adobe Inc., USA).

Grain trait analysis

Grain traits for 124 genotypes were analysed with a SeedCount^{TM} SC4 (Seed Count Australasia, Condell Park, Australia) at the University of Adelaide Barley Breeding Program/Laboratory, following manufacturer's instructions. Grain traits were analysed from the same generation of grain that was sown for ovule phenotype analysis. This grain was hand-threshed, according to Australian quarantine requirements. There was not sufficient grain for seed scanning of four of the genotypes from the population of 127 genotypes used for ovule analysis. These genotypes were Appaloosa, Calgary, Salka, and Turnberry.

Genome Wide Association Study

The population used for this study was previously genotyped on the 9K iSelect SNP Platform (Comadran et al. 2012). Following exclusion of SNP markers with allele frequency over 95% or missing data over 5%, 4117 markers were used for GWAS. Marker positions were compared between maps presented by Comadran et al. (2012) and Mascher et al. (2013) in order to ascertain the most reliable physical location for each marker. The average value for each ovule measurement was used as trait data. Marker-trait association analysis was performed using GenStat (15th Edition; VSN International, UK) with an Eigenanalysis relationship model to account for population structure and to minimise the risk of false positive associations, as described by Hassan et al. (2017). Markers with logarithm of the odds (LOD; $-\log_{10}$(p-value)) scores over 3 were considered to be significantly associated with the trait. False discovery rate (FDR) was calculated in R using the qvalue package (Storey 2011). Regions of interest were defined by groups of markers with a score of LOD > 3 proximal to the markers with the highest LOD scores. Genes (HORVUs) within each interval were identified using Barleymap (Cantalapiedra et al. 2015) to identify genes within +/-2.5cM of markers in

order to account for uncertainty in physical marker locations. Gene ontology (GO) terms were identified using AgriGO (Tian et al. 2017) and the EMBL QuickGO online tool (https://www.ebi.ac.uk/QuickGO/).

Results

Natural variation of ovule morphology is present among two-row spring barleys

Mature ovule morphology was measured in terms of two-dimensional area and one-dimensional distances, as described in Chapter 3. Two-dimensional areas were measured by following the widest boundary of the tissue of interest at any point within the z-stack. At the time of collection, flowers were assumed to be at anthesis if anthers were yellow and pollen was released when anthers were gently squeezed. In the majority of genotypes, ovules at this stage exhibited an overall similar appearance including a prominent embryo sac, large antipodal nuclei and enlarged central vacuole (Figure 4-1B). Fertilised ovules could easily be distinguished by the presence of irregularly shaped antipodal cell nuclei, clusters of small nuclei at the periphery of the embryo sac and a much larger ovule area (Figure 4-1C). At the other extreme, immature ovules were occasionally identified that showed an unusually small antipodal cluster, central cell and short distance between the micropyle and top of the embryo sac (Figure 4-1A). The incidence of ovules that were immature or fertilised may reflect sampling error, or indicate that reproductive maturity is not perfectly synchronous between the anther and ovule in all barley genotypes. After measurements relating to incorrectly staged ovules were eliminated, sufficient data remained to compare 127 genotypes (Table 4-S1).

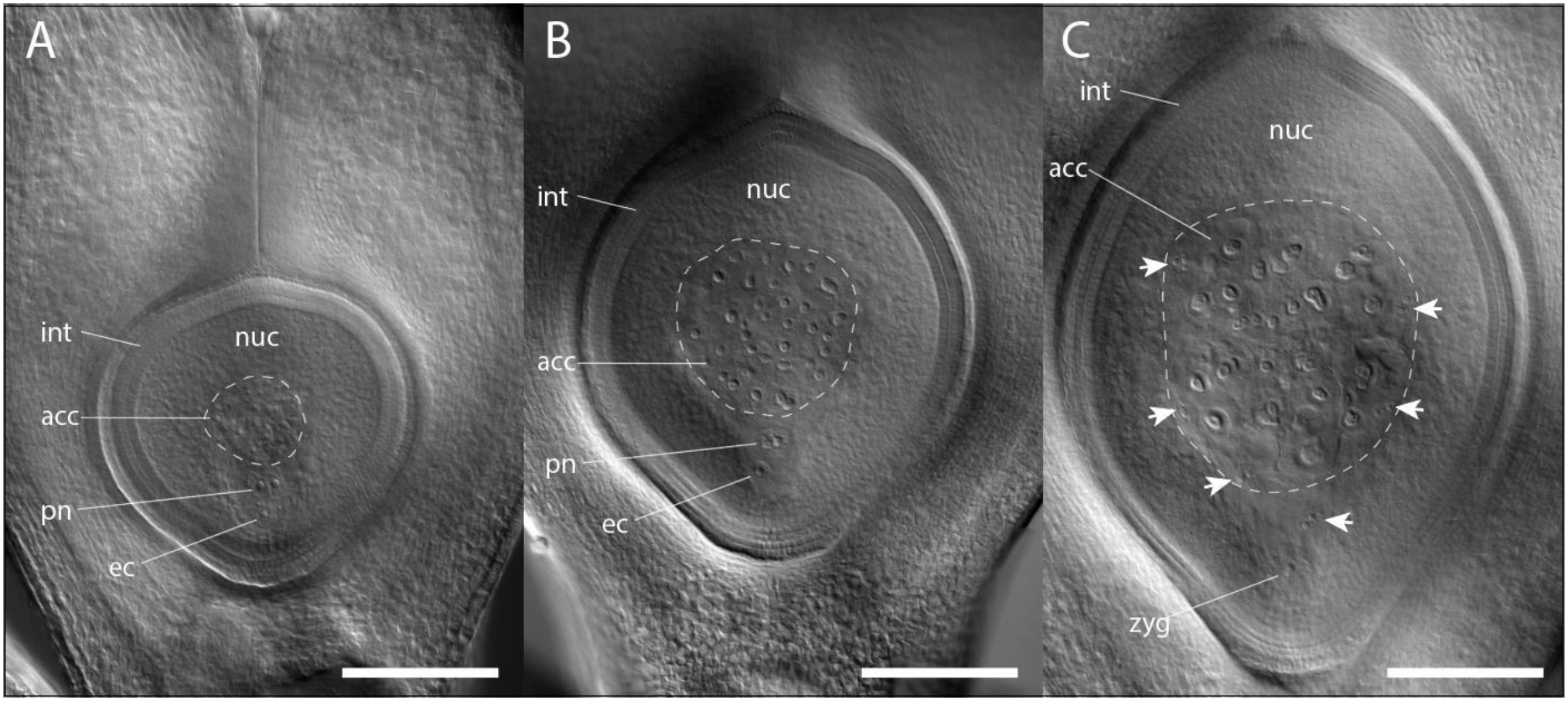

Figure 4-1: Staging of reproductive fertility in barley ovules with reference to morphological features. (A) Immature ovule (cv. Widre). (B) Reproductively mature, unfertilised ovule (cv. Scandium). (C) Fertilised ovule (cv. Scandium). acc, antipodal cell cluster; ec, egg cell nucleus; int, integument; pn, polar nuclei; nuc, nucellus; zyg, zygote. Arrowheads indicate small clusters of endosperm nuclei; dashed line indicates bounds of antipodal cell cluster. Scalebars = 200μm.

Quantification of ovule morphology revealed natural variation in all traits (Figure 4-2, Table 4-1). The most variable trait was found to be embryo sac area (ES_A), with an average size of 48876.2 ± 10844.2μm^2 (22.2%). Ovule area (O_A) and nucellus area (N_A) were comparatively less variable, observed to be 174421.2 ± 19857.8 μm^2 (11.4%) and 125560.8 ± 13408.7 μm^2 (10.7%), respectively. Similarly, the transverse and longitudinal measurements of the embryo sac (ES_T, ES_L) were observed to vary more than the transverse and longitudinal measurements of ovule area (O_T, O_L). Of all traits measured, the standard deviation of ovule transverse was the smallest, at 5.2%. Both integument width (I_W) and the proportion of nucellus within the ovule (calculated as nucellus area/ovule area; N_P) were found to vary relatively little, with standard deviation of 5.8%. For all traits, at least 30 genotypes were found to have phenotypic variation that fell outside the standard deviation (Table 4-S2). The trait with the most outlier genotypes was nucellus proportion, with 24 large and 22 small outliers, while the trait with the least outliers was ovule area, with 16 large and 18 small outliers. Several genotypes were found to have an “extreme” phenotype for multiple traits. Genotypes such as Salka and Wren were distinctly large for most phenotypes excepting nucellus proportion, Meanwhile, other genotypes presented an extreme phenotype for only one or few traits, such as Forum, which was notable for displaying small ovule area and nucellus area measurements, but presented average embryo sac (ES) measurements. This suggests different tissues may contribute to mature ovule morphology in a genotype-dependent manner.

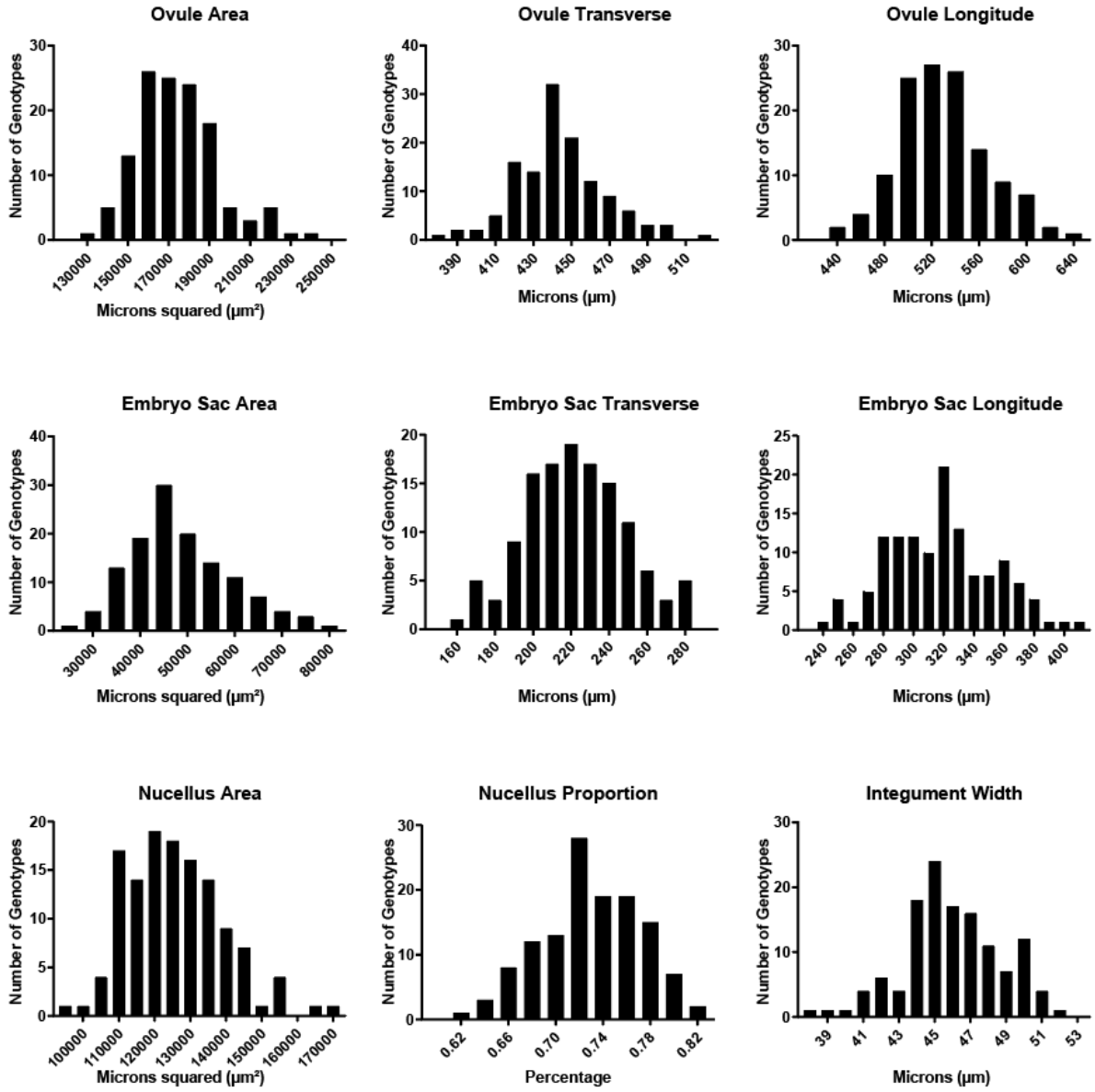

Figure 4-2: Natural variation in nine morphological traits of mature ovules observed among 127 genotypes of European two-row spring barley, represented as frequency distribution plots.

Table 4-1: Summary of natural variation in nine morphological traits of mature ovules observed among 127 genotypes of European two-row spring barley. O_A, ovule area (µm^2); O_T, ovule transverse (µm); O_L, ovule longitude (µm); ES_A, embryo sac area (µm^2); ES_T, embryo sac transverse (µm); ES_L, embryo sac longitude (µm); I_W, integument width (µm); N_A, nucellus area (µm^2); N_P, nucellus proportion (%).

	O_A	**O_T**	**O_L**	**ES_A**	**ES_T**	**ES_L**	**I_W**	**N_A**	**N_P**
Average	174421.2	444.8	529.1	48876.1	222.4	318.0	45.9	125560.8	0.724
St. Dev.	19857.8	23.2	38.6	10844.2	26.3	34.2	2.7	13408.7	0.042
St. Dev.as % Avg	11.4	5.2	7.3	22.2	11.8	10.8	5.8	10.7	5.820
Maximum	241310.7	519.2	639.8	77888.1	282.0	406.6	52.2	169151.8	0.821
Minimum	128009.3	384.0	440.0	25194.4	158.1	238.8	38.1	95875.3	0.608
Maximum as % Avg	138.3	116.7	120.9	159.4	126.8	127.9	113.6	134.7	113.511
Minimum as % Avg	73.4	86.3	83.2	51.5	71.1	75.1	83.0	76.4	84.017
Avg plus St. Dev. as % Avg	111.4	105.2	107.3	122.2	111.8	110.8	105.8	110.7	105.820
Avg minus St. Dev. as % Avg	88.6	94.8	92.7	77.8	88.2	89.2	94.2	89.3	94.180
No. Large Outliers	16.0	18.0	20.0	19.0	20.0	23.0	23.0	17.0	24.0
No. Small Outliers	18.0	18.0	16.0	20.0	20.0	22.0	17.0	21.0	22.0

Ovule component tissues develop in a variety of proportions among genotypes.

Correlation analysis was performed in order to determine if overall variation in ovule morphology is a result of coordinated development of component ovule tissues, or whether growth of one tissue is an important factor in determining mature ovule morphology (Figure 4-3). Nucellus area and ovule area were found to be more closely correlated ($R^2 = 0.86$, $p<0.001$) than ES area and ovule area ($R^2 = 0.77$, $p<0.001$), indicating that ES area is a slightly more independent trait (Figure 4-S1). Consistent with this, ES area and nucellus area showed a significant but relatively low correlation ($R^2 = 0.33$, $p<0.001$). Meanwhile, both ES area and ovule area were negatively correlated with nucellus proportion (ovule area to nucellus proportion: $R^2 = -0.38$, $p<0.001$; embryo sac area to nucellus proportion: $R^2 = -0.87$, $p<0.001$). This suggests that while an increase in nucellus area reliably leads to large ovule area, disproportionate growth of the ES with respect to the nucellus is a major driver of genotypic variation in ovule morphology. ES area was slightly more tightly correlated with related traits including ES transverse ($R^2 = 0.95$, $p<0.001$) and ES longitude ($R^2 = 0.91$, $p<0.001$) than ovule area was correlated with ovule transverse ($R^2 = 0.86$, $p<0.001$) and ovule longitude ($R^2 = 0.91$, $p<0.001$). Bigger ovules were more likely to have thinner integuments, as all ovule traits were negatively associated with integument width, particularly ovule area and nucellus area (ovule area to integument width: $R^2 = -0.25$, $p<0.01$; nucellus area to integument width: $R^2 = -0.24$, $p<0.005$).

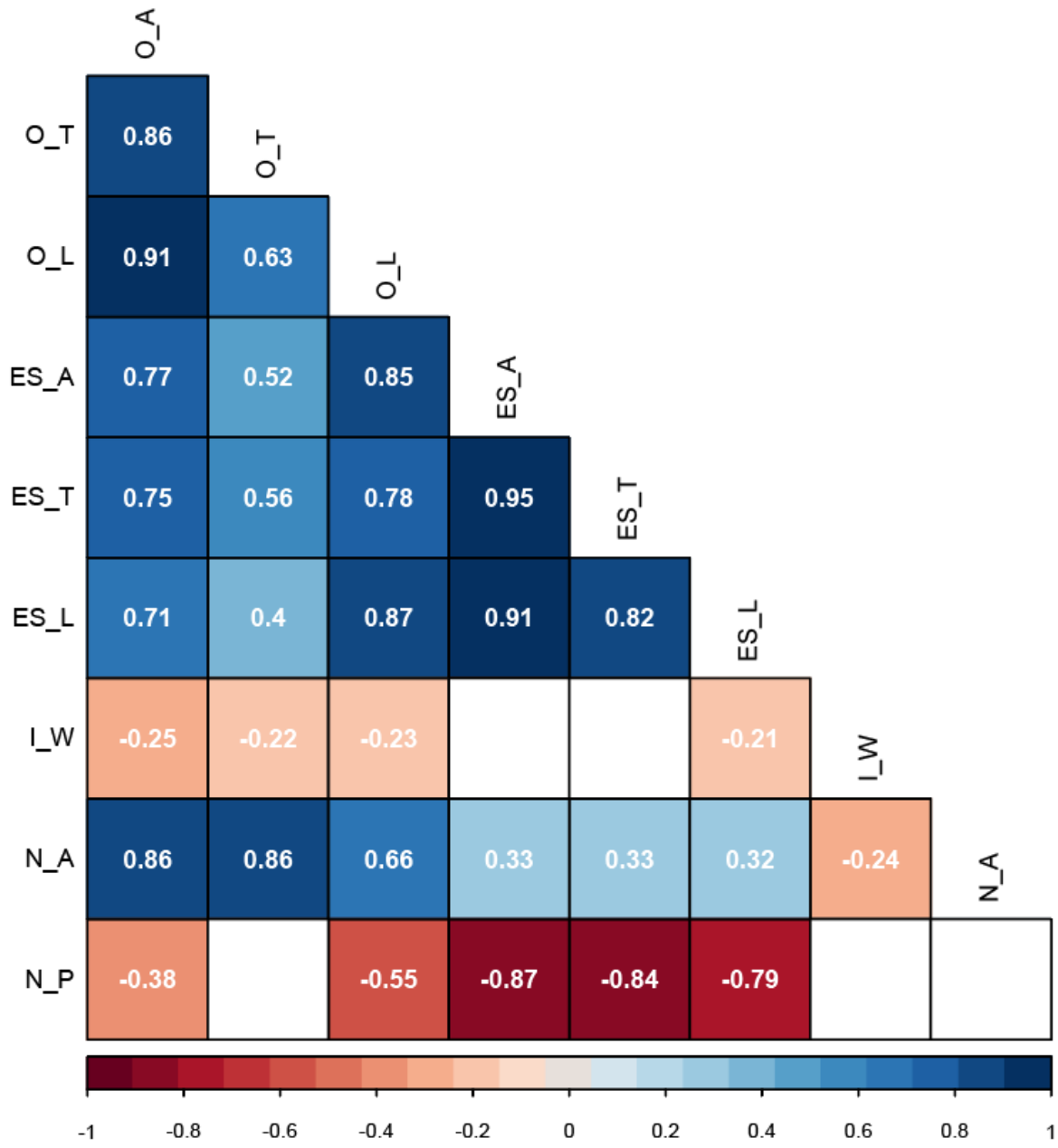

Figure 4-3: Heat map representing correlations between nine mature ovule traits measured in 127 genotypes of European two-row spring barley. Positive correlations are shaded blue, negative correlations are shaded red. Numbers within boxes represent the correlation coefficient (R^2) value. Both box colour and R^2 value are only shown for those with a p-value of < 0.05. O_A, ovule area (µm^2); O_T, ovule transverse (µm); O_L, ovule longitude (µm); ES_A, embryo sac area (µm^2); ES_T, embryo sac transverse (µm); ES_L, embryo sac longitude (µm); I_W, integument width (µm); N_A, nucellus area (µm^2); N_P, nucellus proportion (%).

The contribution of both ES and nucellus traits to ovule size was reflected in the principal component analysis (PCA) plot (Figure 4-4), which showed the location of ovule traits between those of the ES and nucellus area. The trait indicators for ES transverse and ES longitude (R^2 = 0.82, $p<0.001$) were closely positioned on the PCA plot in contrast to those of ovule transverse and ovule longitude (R^2 = 0.63, $p<0.001$). This suggests that variation in ES area is more likely to be due to variation in both transverse and longitude of the ES, whereas variation in ovule area may be due to genotype-dependent changes in either ovule transverse or ovule longitude. The PCA plot revealed an even spread of genotypes without obvious clustering, in addition to several clear outliers for each trait. Genotypes previously identified to have “extreme” phenotypes (Table 4-S2) were located at the periphery of the PCA plot, which provides some insight into how variation in either nucellus area or ES-related traits influence ovule area. For example, the large-ovule phenotypes of Salka and Wren appear to be due to a greater contribution of ES traits compared to other large-ovule genotypes such as Lina. Conversely, the small-ovule phenotype of the genotype Cecilia was not directly attributed to any specific nucellus and ES traits. This differed from genotypes such as Host, which produced an “average” sized ovule with a relatively large nucellus area, and the above-average ovule area of Foxtrot, which was predominantly due to enlarged ES traits. Other genotypes, such as Forum and Gant, had average ES-traits but an overall small-ovule phenotype due to low nucellus area. This is consistent with the correlation analysis and indicates that although variability in ES traits impacts ovule morphology, the overall “size” of the barley ovule is closely correlated to nucellus area.

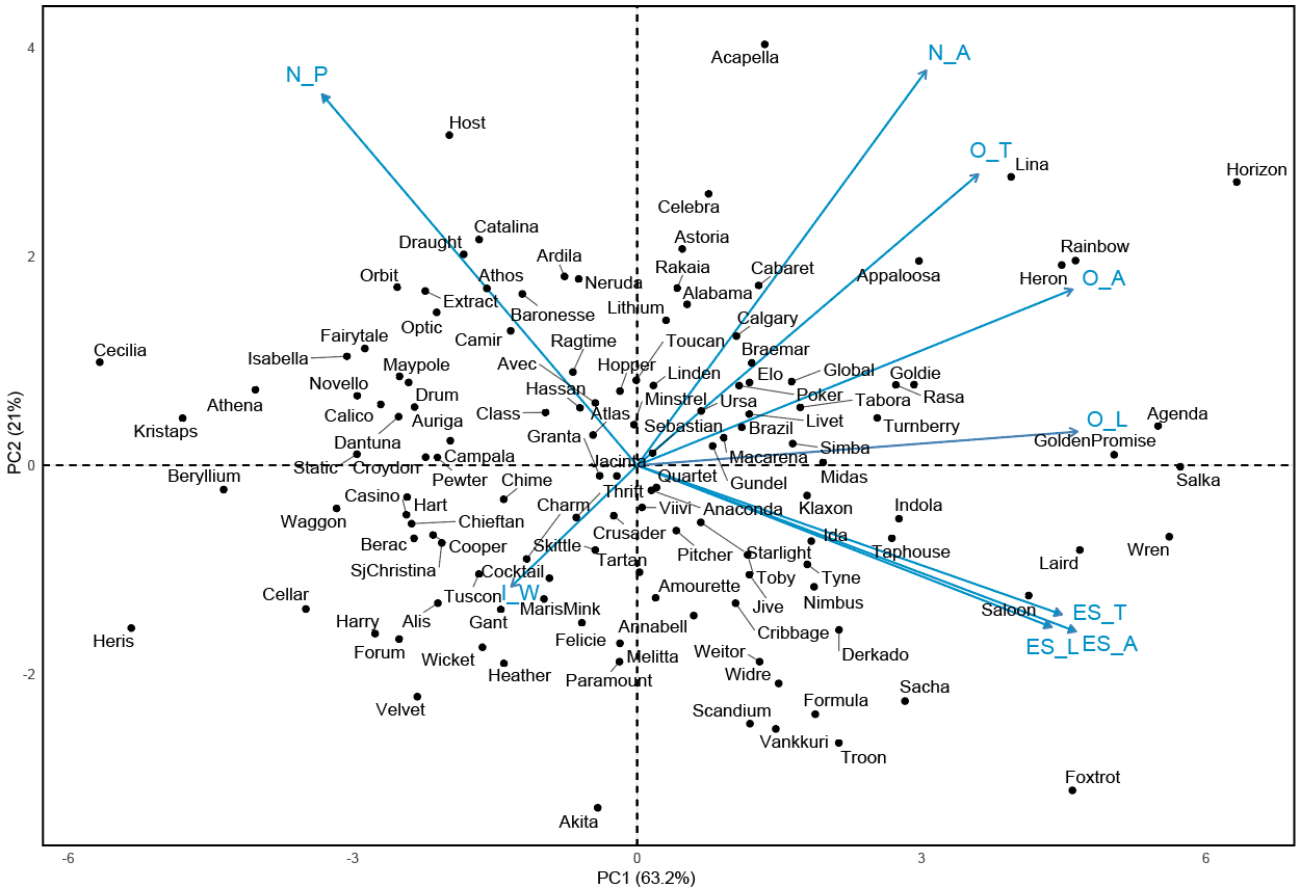

Figure 4-4: Principal Component Analysis of separating 127 genotypes of European two-row spring barley on the basis of phenotypic data for nine mature ovule traits. O_A, ovule area (µm^2); O_T, ovule transverse (µm); O_L, ovule longitude (µm); ES_A, embryo sac area (µm^2); ES_T, embryo sac transverse (µm); ES_L, embryo sac longitude (µm); I_W, integument width (µm); N_A, nucellus area (µm^2); N_P, nucellus proportion (%).

Despite the limited clustering according to the PCA plot, heatmap analysis suggested that in general, the 127 genotypes could be divided into two groups (Figure 4-5). The “large-ovule” group of genotypes is characterised by large ovule-related (ovule area, ovule transverse, ovule longitude) and ES-related (embryo sac area, embryo sac transverse, embryo sac longitude) traits, with small nucellus proportion and integument width, while the “small-ovule” group of genotypes is characterised by small ovule-related and ES-related traits, with greater nucellus proportion and integument width phenotypes. However, as noted above, within each of these two groups there was substantial variation for individual traits.

Grain traits vary among the same population but do not appear to be linked to ovule morphology

The evolutionary purpose of a large, crassinucellar ovule in cereal crops is yet to be determined. Before fertilisation, the nucellus gives rise to the germline and supports development of the embryo sac, while after fertilisation the nucellus acts as a transfer tissue, allowing nutrients from the maternal plant to be stored in the endosperm of the developing grain. To assess relationships between ovule morphology and grain traits in two-row spring barley, grain for 124 of the 127 genotypes was phenotyped using a SeedCount^{TM} SC4 (Seed Count Australasia, Condell Park, Australia), and correlation analysis was performed. The grain phenotyped was harvested in 2014, and was the generation that gave rise to the plants in which ovule morphology was assessed. There was insufficient grain to allow grain analysis for four genotypes: Appaloosa, Calgary, Salka and Turnberry. Variation was observed between all grain traits (Table 4-S3). However, few correlations with R^2 >0.5 were identified between ovule and grain traits (Figure 4-6. Figure 4-S2). A slight negative correlation was observed between integument width and grain length (R^2 = -0.22, $p < 0.05$), and nucellus proportion and grain length (R^2 = -0.20, $p < 0.05$) suggesting that genotypes with thicker integuments and a

greater ratio of nucellus to embryo sac within the ovule were slightly more likely to produce shorter grains.

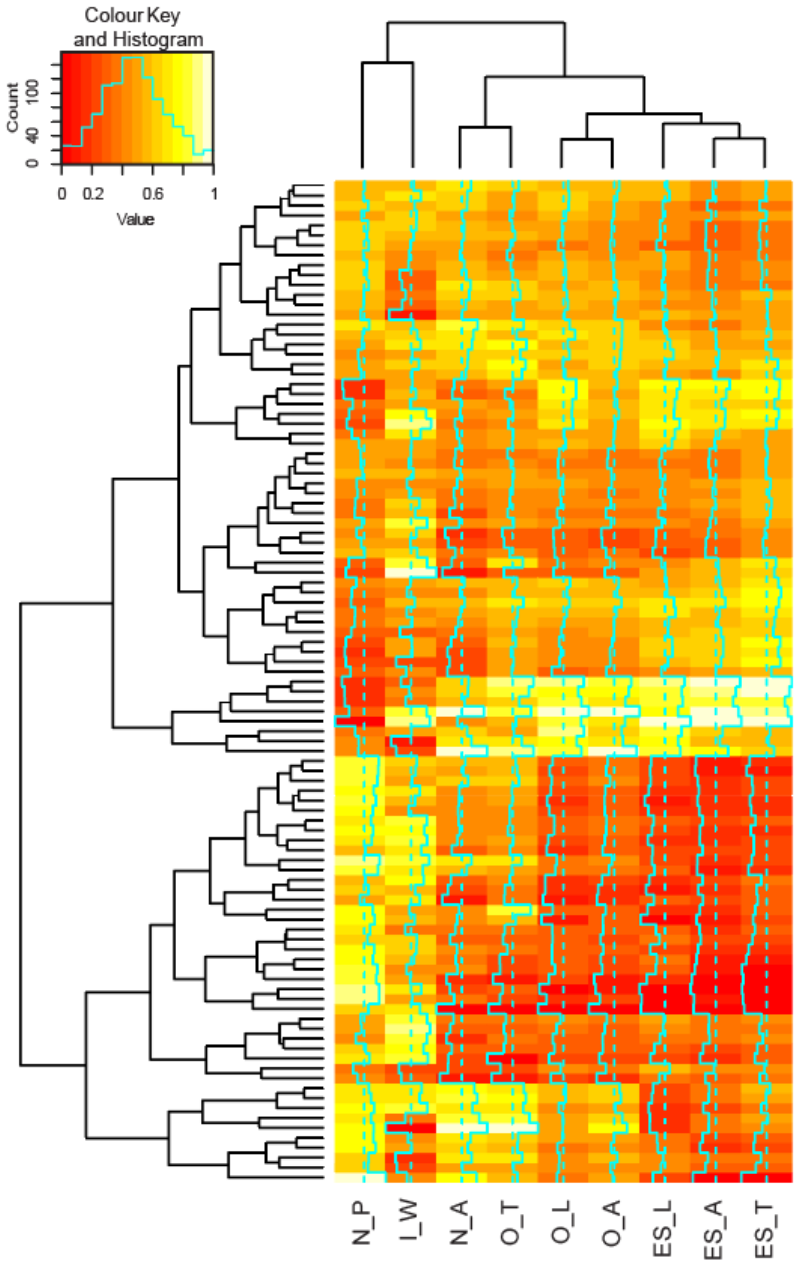

Figure 4-5: Genotypic similarities in variation of nine mature ovule traits among 127 genotypes of European two-row spring barley. Data for each trait was normalised to a value between 0 and 1, and both traits and genotypes were clustered based on similarity of traits. The relative degree of variation within each trait for each genotype is indicated by the blue line. O_A, ovule area (μm^2); O_T, ovule transverse (µm); O_L, ovule longitude (µm); ES_A, embryo sac area (μm^2); ES_T, embryo sac transverse (µm); ES_L, embryo sac longitude (µm); I_W, integument width (µm); N_A, nucellus area (μm^2); N_P, nucellus proportion (%).

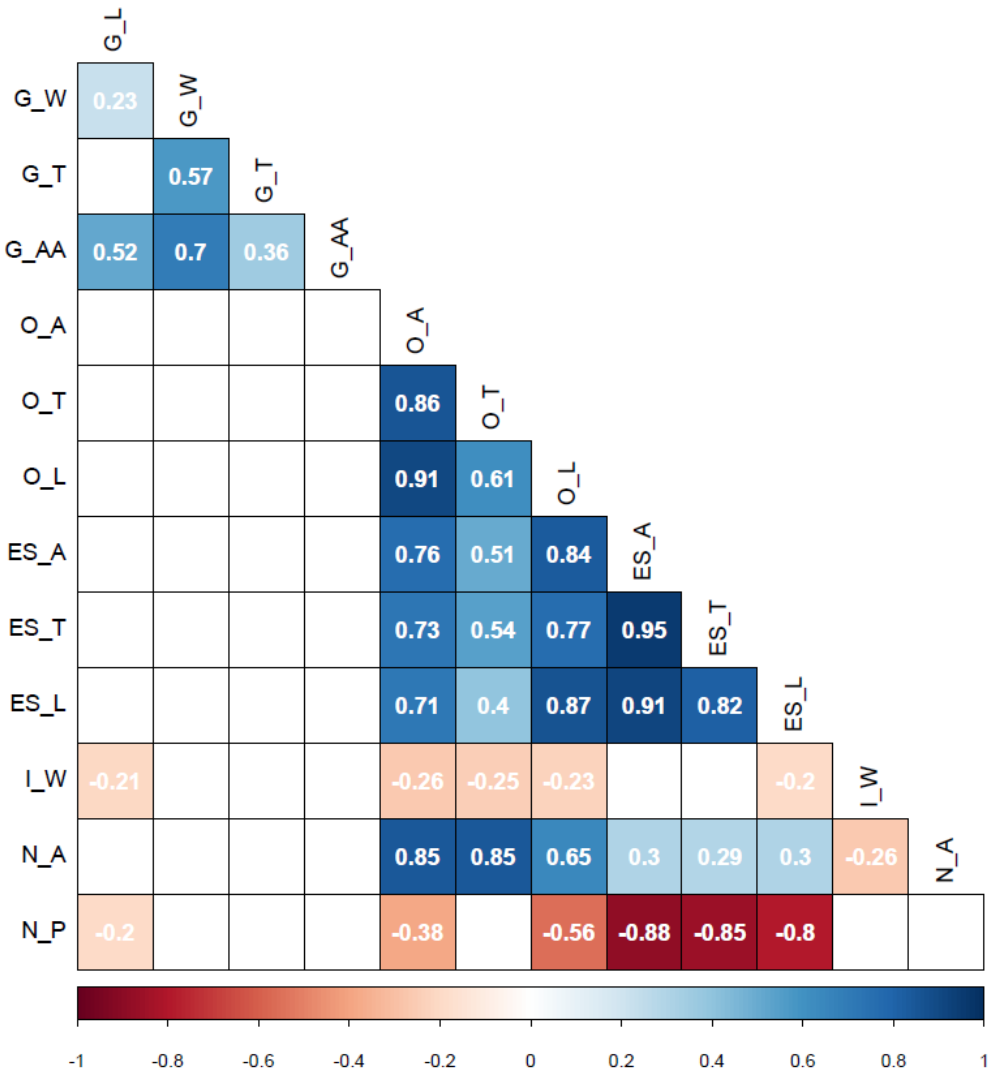

Figure 4-6: Heatmap representing correlations between grain traits and nine morphological traits of mature ovules measured in 124 genotypes of European two-row spring barley. Positive correlations are shaded blue, negative correlations are shaded red. Numbers within boxes represent the correlation coefficient (R^2) value. Both box colour and R^2 value are only shown for those with a p-value of < 0.05. G_L, grain length (mm); G_W, grain width (mm); G_T, grain thickness (mm); G_AA, grain average area (mm^2); O_A, ovule area (µm2); O_T, ovule transverse (µm); O_L, ovule longitude (µm); ES_A, embryo sac area (µm2); ES_T, embryo sac transverse (µm); ES_L, embryo sac longitude (µm); I_W, integument width (µm); N_A, nucellus area (µm2); N_P, nucellus proportion (%). Of the full panel of 127 genotypes, insufficient grain was available for four genotypes: Appaloosa, Calgary, Salka and Turnberry.

GWAS reveals 66 markers associated with mature ovule morphology

Despite the lack of evidence to suggest a global link between ovule morphology and grain development in two-row spring barley, the variation present in the panel provided a unique opportunity to investigate the genetic basis ovule tissue formation. Phenotypic data was used to conduct genome wide association studies (GWAS) in an attempt to identify genomic regions that significantly influence the nine traits measured. GWAS were carried out using panel of 4117 markers that had a minor allele frequency greater than 5%, and less than 5% missing data available for the 127 genotypes from which phenotypic data was collected.

Of these 4117 markers, 66 were found to have a LOD score (logarithm of the odds; $-\log_{10}$(p-value)) greater than 3 for at least one of the ovule traits used for GWAS (Table 4-S4). Fifty-seven of the markers were found to have an association of LOD>3 for multiple ovule traits. The majority of the 66 markers mapped to chromosomes 2H (29 markers, or 44%) and 4H (22 markers, or 33%), while only a single marker mapped to each of chromosomes 5H and 6H.

In total, 17 markers showed an association to an ovule trait with a LOD>4. Nine of these significant markers mapped to chromosome 2H, while four mapped to each of chromosomes 1H and 4H. The 17 markers found to associate to ovule traits with LOD>4 grouped into six genomic locations: two on Ch1, at 26.5cM and 41.2cM, three on Ch2, at 59cM, 73.8cM and ~120cM, and at 52.3cM on Ch4. The most significant associations were observed on Ch1 at 41.2cM, Ch2 at 59cM and Ch2 at 73.8cM, and were characterised as the highest associations with particular ovule traits, specifically, ES area, nucellus area and ovule area, respectively. All allele effects were positive with the exception of the two markers associated with ovule transverse at 120cM on Ch2. The associations of the two markers C16024 and C16995 on chromosome 2 with ovule area equally attained a LOD score of 6.652 and were thus the markers most highly associated with any trait observed.

Four major QTL influence mature ovule morphology

The most significant associations were located in four genomic regions (Table 4-2). For further analysis, these regions are referred to with a shorthand identity and taken to represent the trait for which the highest LOD score was observed within the region. Thus, these regions are QTL1H_ES, at 41.2cM on Ch1 representing the ES, QTL2H_NUC, at 59cM on Ch2 representing the nucellus, and QTL2H_OV at 73.8cM on Ch2 representing ovule area. A fourth region was included, referred to as QTL4H_INT and located at 52.3cM on Ch4. Associations between markers and integument traits were found exclusively within this region. These four QTLs were easily observed from Manhattan plots of marker associations for the four respective traits (Figure 4-7).

QTL1H_ES was defined by two markers, 11_20617 and SCRI_RS126734, for which associations of LOD score >4 were identified with ES area, ES longitude, ovule area and ovule longitude, and associations of between LOD 3 and 4 were identified with ES transverse and nucellus proportion. The most significant associations were shown with ES area (LOD = 5.695) and ES longitude (LOD = 5.265). Within QTL1H_ES, presence of the minor alleles of the markers 11_20617 and SCRI_RS_126734 were observed to have the greatest effect upon an ovule phenotype, contributing up to a 12.8% increase in ES area. This was the largest proportional effect upon any ovule phenotype among the markers within the four major QTLs.

Four markers form QTL2H_NUC, 11_10498, 11_10297, 12_30691 and 11_20674, all of which show an association of LOD>4 to nucellus area. When LOD values between 3 and 4 were considered, markers 11_10498, 12_30691 and 11_20674 were also observed to associate with ovule area, and 11_20198 was observed to associate with ovule transverse. Presence of the minor allele of the marker which showed the highest LOD score/association with nucellus area, 11_10498, was observed to confer a 5.6% increase in nucellus area.

Three major markers formed QTL2H_OV; SCRI_RS_150266, SCRI_RS_16024 and SCRI_RS_16995. These three markers were associated with ovule area, attaining LOD scores of 4.43 (SCRI_RS_150266) and 6.65 (SCRI_RS_16024, SCRI_RS_16995). The markers SCRI_RS_16024 and SCRI_RS_16995 were also associated with nucellus area and ovule transverse (LOD >5), and ovule longitude (LOD between 4 and 5). When associations of between LOD 3 and 4 were considered, a further six markers within 2cM of the major two markers at 73.8cM were found to associate with ovule traits. Notably, five of the nine markers within QTL2H_OV were also observed to associate with ES traits. These five markers were AA_10265, SCRI_RS_100476, SCRI_RS_16024, SCRI_RS_16995 and SCRI_RS_167713. Of the markers in QTL2H_OV, the greatest impact upon a trait was observed to be a 7.3% increase in ovule area, conferred by the both of SCRI_RS_16024 and SCRI_RS_16995. The association of these markers with nucellus area also conferred a 6.1% increase in nucellus area, which is notable as it is larger than the effect conferred by any marker within the QTL associated with nucellus area, QTL2H_NUC.

Four markers were associated with integument width (LOD >4) within the QTL4H_INT region. A further fourteen markers, predominantly with associations to nucellus area and ovule area rather than integument width, were observed in the QTL4H_INT region when associations of between LOD 3 and 4 were considered. Notably, markers within this region associated to nucellus or ovule area traits tended to confer a reduction of 2% to 5% area, while those associated with integument width consistently conferred a 2.3% increase in width.

Table 4-2: Summary of the four major QTLs and key SNP markers within each identified following GWAS performed for nine morphological traits of mature barley ovules among a population of 127 genotypes. Each major QTL is highlighted in a different colour. Within each QTL, the trait with the highest LOD score has been highlighted, as has the LOD score and the allele effect, calculated as % of the trait average phenotype. O_A, ovule area (μm^2); O_T, ovule transverse (µm); O_L, ovule longitude (µm); ES_A, embryo sac area (μm^2); ES_T, embryo sac transverse (µm); ES_L, embryo sac longitude (µm); I_W, integument width (µm); N_A, nucellus area (μm^2); N_P, nucellus proportion (%).

							Major Allele		Minor Allele					
QTL	Marker	Ch	cM	Trait	Trait Avg	LOD	Allele	Freq (%)	Allele	Freq (%)	Effect	s.e.	Effect%	s.e.%
QTL1H_ES	11_20617	1H	41.3	ES_A	48876.1	5.695	G	87%	C	13%	6257.7	1317.0	12.8	2.7
				ES_L	318.0	5.265	G	87%	C	13%	18.9	4.2	5.9	1.3
				O_A	174421.2	4.068	G	87%	C	13%	9718.3	2473.8	5.6	1.4
				O_L	529.1	5.171	G	87%	C	13%	21.2	4.7	4.0	0.9
	SCRI_RS_126734	1H	41.3	ES_A	48876.1	5.695	T	87%	C	13%	6257.7	1317.0	12.8	2.7
				ES_L	318.0	5.265	T	87%	C	13%	18.9	4.2	5.9	1.3
				O_A	174421.2	4.068	T	87%	C	13%	9718.3	2473.8	5.6	1.4
				O_L	529.1	5.171	T	87%	C	13%	21.2	4.7	4.0	0.9
QTL2H_NUC	11_10498	2H	58.3	N_A	125560.8	5.349	A	84%	G	16%	6987.2	1523.0	5.6	1.2
	11_10297	2H	59.2	N_A	125560.8	4.506	G	82%	A	18%	6076.7	1459.2	4.8	1.2
	12_30691	2H	59.2	N_A	125560.8	4.428	A	84%	C	17%	6245.0	1514.4	5.0	1.2
	11_20674	2H	59.5	N_A	125560.8	4.428	C	84%	A	17%	6245.0	1514.4	5.0	1.2
QTL2H_OV	SCRI_RS_150266	2H	73.8	O_A	174421.2	4.425	C	84%	T	16%	9598.8	2328.7	5.5	1.3
	SCRI_RS_16024	2H	73.8	N_A	125560.8	5.279	C	87%	T	13%	7653.7	1680.5	6.1	1.3
				O_A	174421.2	6.652	C	87%	T	13%	12676.0	2447.4	7.3	1.4
				O_L	529.1	4.155	C	87%	T	13%	19.5	4.9	3.7	0.9
				O_T	444.8	5.162	C	87%	T	13%	13.1	2.9	2.9	0.7

	SCRI_RS_16995	2H	73.8	N_A	125560.8	5.279	A	87%	G	13%	7653.7	1680.5	6.1	1.3
				O_A	174421.2	6.652	A	87%	G	13%	12676.0	2447.4	7.3	1.4
				O_L	529.1	4.155	A	87%	G	13%	19.5	4.9	3.7	0.9
				O_T	444.8	5.162	A	87%	G	13%	13.1	2.9	2.9	0.7
QTL4H_INT	SCRI_RS_144983	4H	52.3	I_T	45.9	4.263	C	73%	T	27%	1.0	0.3	2.3	0.6
	SCRI_RS_186944	4H	52.3	I_T	45.9	4.263	C	73%	T	27%	1.0	0.3	2.3	0.6
	SCRI_RS_230472	4H	52.3	I_T	45.9	4.263	G	73%	T	27%	1.0	0.3	2.3	0.6
	SCRI_RS_7401	4H	52.3	I_T	45.9	4.263	C	73%	T	27%	1.0	0.3	2.3	0.6

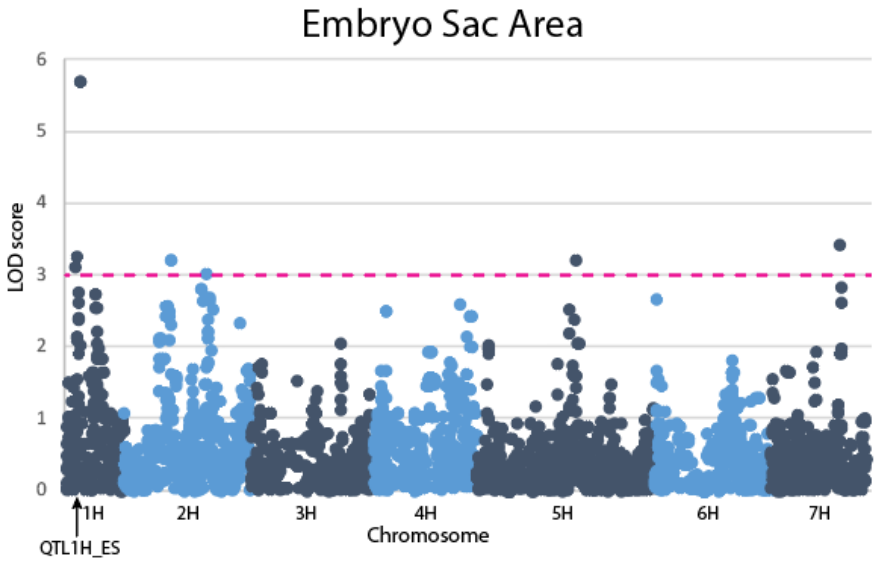
Embryo Sac Area
LOD score
Chromosome
1H
2H
3H
4H
5H
6H
7H
QTL1H_ES

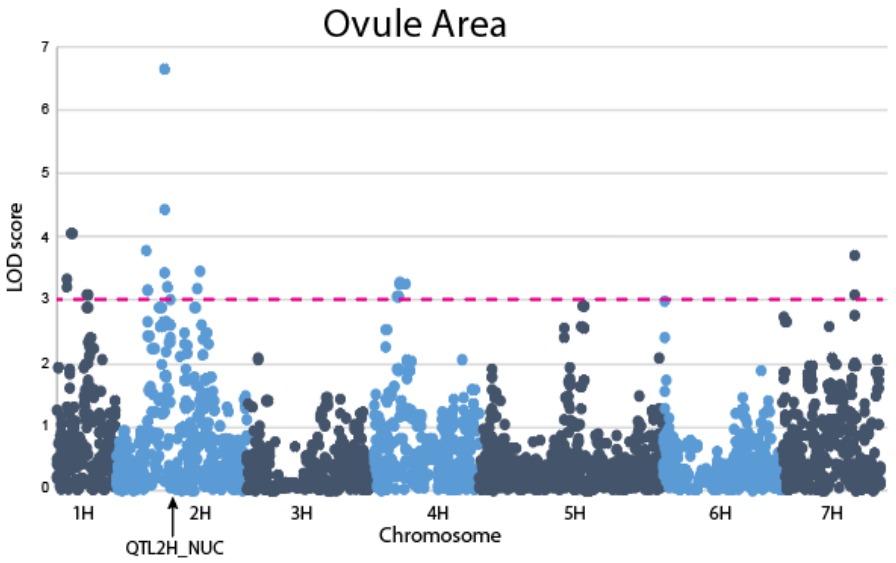
Ovule Area
LOD score
Chromosome
1H
2H
3H
4H
5H
6H
7H
QTL2H_NUC

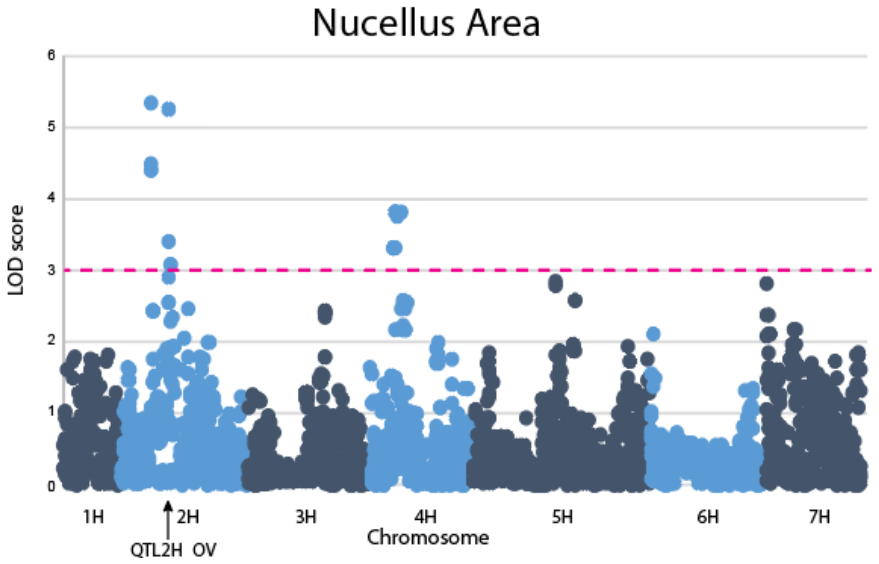
Nucellus Area
LOD score
Chromosome
1H
2H
3H
4H
5H
6H
7H
QTL2H_OV

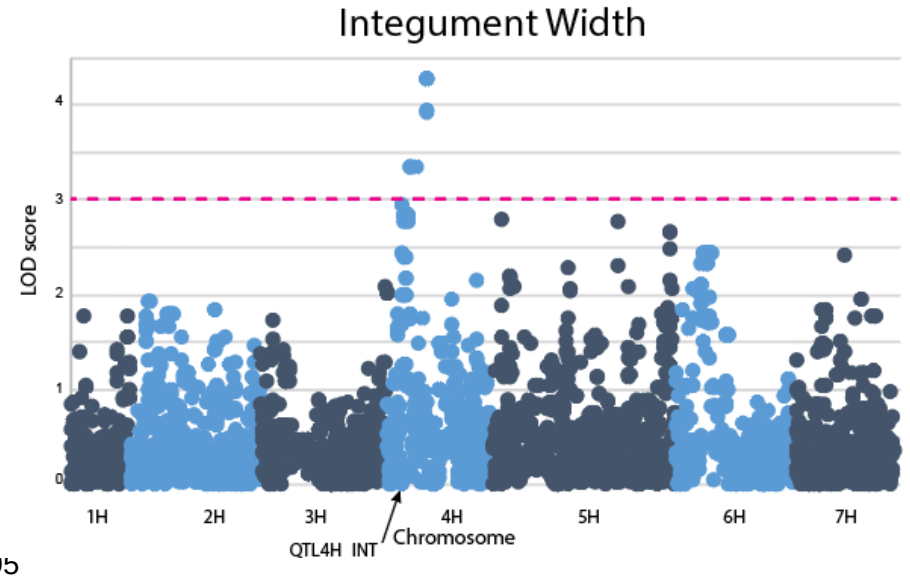
Integument Width
LOD score
Chromosome
1H
2H
3H
4H
5H
6H
7H
QTL4H_INT

Figure 4-7: Manhattan plots representing associations of 4117 single nucleotide polymorphism (SNP) markers with ovule area, embryo sac area, nucellus area, and integument width, as determined by GWAS using an Eigenstrat relationship model, and phenotypic data collected from 127 genotypes of European two-row spring barley. SNP markers with LOD ($-\log_{10}$(p-value)) score greater than 3 (dashed magenta line) were considered to be associated with the phenotype.

Identification of putative genes residing near QTL influencing ovule morphology

Candidate genes located near each of the 4 QTL were identified by entering all markers within the QTL that formed trait associations with LOD>3 into Barleymap (Cantalapiedra et al. 2015), using cv. Morex genome annotations (Mascher et al. 2017), and setting the range to +/-2.5cM, in order to account for uncertainty in physical marker locations. The total number of genes identified within these windows was 4211, of which QTL1H_ES contributed 399, QTL2H_NUC contributed 187, QTL2H_OV contributed 152 and QTL4H_INT contributed 3473. In order to assess the broad functionality of genes in each QTL, gene ontology (GO) terms were investigated. There were 90 unique GO terms associated with genes in QTL1H_ES, 78 unique GO terms associated with genes in QTL2H_NUC, 53 unique GO terms associated with genes in QTL2H_OV, and 364 unique GO terms associated with genes in QTL4H_INT. The most common GO terms annotated in the genes of each QTL (Figure 4-8) were similar, and tended to relate to basic cellular metabolism and replication activities, such as ATP binding, redox processes and transcription. In addition, several GO terms were found to be specifically enriched in each QTL. The GO term GO:0004867, relating to serine endopeptidase inhibitor activity, was enriched in genes underlying QTL1H_ES, the GO terms relating to esterase activity (GO:0016788) and methyltransferase activity (GO:008168) were common among genes underlying QTL2H_NUC, and the GO term for transporter activity (GO:0005215) was uniquely common in genes underlying QTL2H_OV. The most common GO terms for genes in QTL4H_INT were relatively unremarkable, perhaps reflecting the quantity of genes located in this region.

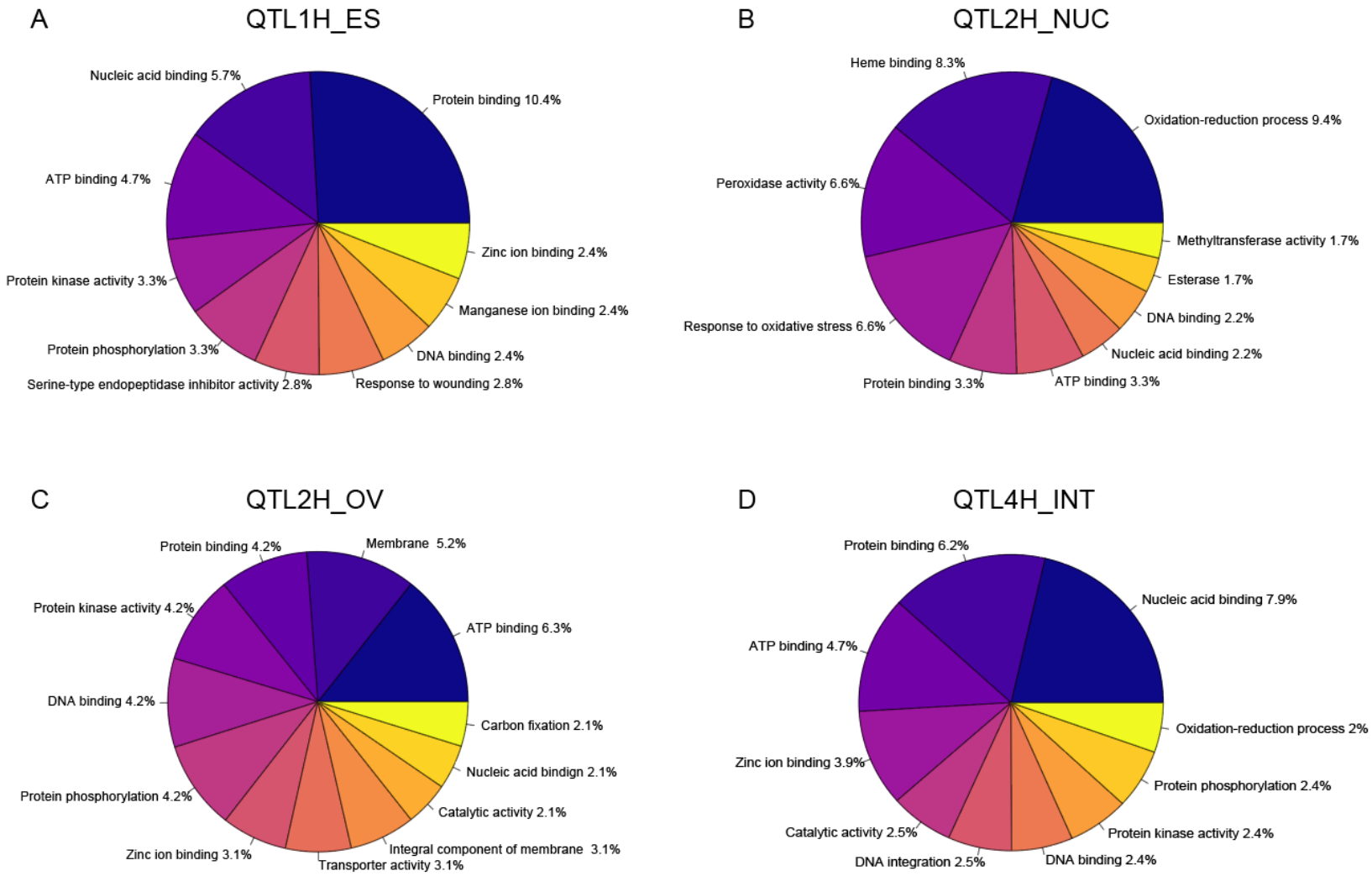

Figure 4-8: Pie charts indicating the most common gene ontology (GO) terms for genes underlying (A) QTL1H_ES, (B) QTL2H_NUC, (C) QTL2H_OV, and (D) QTL4H_INT

Discussion

As the site of fertilisation and grain initiation, the ovule fulfils a critical role in the life cycle of both eudicot and monocot plants, and is thus of critical importance to cereal crop industries. This study characterised the range of natural variation present in mature ovule phenotypes among a population of two-row spring barleys, establishing an average phenotype for ovule at maturity and identifying genotypes with variation among nine specific ovule traits, including: two-dimensional ovule area, ovule transverse, ovule longitude, two-dimensional embryo sac area, embryo sac transverse, embryo sac longitude, two-dimensional nucellus area, the proportion of the ovule occupied by nucellus, and the integument width. After elimination of cultivars due to staging and preparation errors, trait data was collected for 127 genotypes. Correlation analysis and principal component analysis (PCA) were used to assess relationships among ovule traits, and between the ovule and grain traits. Finally, the phenotypic data collected was used to perform a genome wide association study (GWAS), revealing sixty-six markers of which the majority were located in four key quantitative trait loci (QTL) associated with mature ovule morphology.

A key factor in quantifying morphological traits in the mature ovule was the accuracy of reproductive staging. It is generally accepted that male and female reproduction in cereals is synchronised (Kubo et al. 2013), thus the developmental stage of the much more easily accessible anthers should reflect the status of the ovule. Therefore, developmental stage was determined in this study both by similarity of the pistil to the description of the pistil at anthesis in a commonly used staging guide developed in barley and wheat, the Waddington Scale (Waddington et al. 1983), and by whether the anthers of each floret were yellow in colour and readily released pollen (Wilkinson and Tucker 2017). However, visualisation of ovule structure among the cleared tissue revealed greater morphological variation among ovules produced by individual genotypes than could be explained by natural variation of mature phenotypes

(Figure 4-1). In these instances trait variation was pronounced and accompanied by variation in features of the embryo sac that were not phenotyped for the purposes of this study, including: the density of the antipodal cell cluster, the size and shape of the antipodal cell nuclei, the presence of groups of small nuclei at the edge of the central cell, and the size of the central cell as evident by the distance between the micropylar end of the embryo sac and the most distal antipodal cell. Previous reports of the ultrastructure of cereal ovules have documented rapid expansion of the nucellus, central cell and the antipodal cells as fertilisation occurs, accompanied by degeneration of antipodal cells and multiplication of nuclei in the nascent endosperm over the following days (Diboll 1968; Engell 1994; Maeda and Miyake 1996). Thus regarding this data, small ovule, embryo sac and nucellus area traits in addition to the presence of two or more of tight clustering of antipodal nuclei, small antipodal nuclei with respect to others of that genotype, or a small central cell area was taken as an indicator of immaturity. Equally, the coincidence of enlarged ovule, embryo sac and nucellus area traits with the presence of irregularly shaped antipodal cell nuclei or clusters of small nuclei at the periphery of the embryo sac was taken as indicators that the ovule had been fertilised.

Data curation following quantification of morphological traits meant insufficient replicate ovule measurements were collected for 23 genotypes, thus reducing a total number of 150 barley genotypes to an effective population of 127 two-row spring genotypes. Collection of ovules at points before and after maturity despite attempts to stage for reproductive maturity may reflect sampling error. However, as anther and pistil phenotype were consistently used as a staging reference, it may be speculated that pistil structure varies among barley genotypes, and that male and female reproductive development are not perfectly synchronised among two-row spring barley genotypes.

Mature ovule morphology varies in barley

The mature barley ovule is composed of three main tissues; the integuments, the nucellus and the embryo sac, and lacks the fourth tissue present in Arabidopsis, the funiculus. The three ovule compartments form concentric rings within the pistil, and their relative proportions clearly differ in barley compared to ovules from eudicots such as Arabidopsis. Most notably, barley ovules develop to become crassinucellate upon maturity, meaning that the nucellus is a thick, multilayered tissue compared to the thin, often single layered nucellus in tenuinucellar species. Based on the data collected here, the typical two-row spring barley is 174421.2µm^2 ±19857.8µm^2, with 72.4% ±4.2% of the area composed of nucellus, and surrounded by an integument 45.9µm ±2.7µm thick. A range of cultivars were identified that showed distinct phenotypes compared to the average value. These cultivars include Akita, Cecilia, Forum, Foxtrot, Gant, Host, Lina, Optic, Salka and Wren, and may be considered useful for further studies of ovule development. Despite the variation in ovule traits between specific cultivars, analysis of the whole panel showed that nucellus area was tightly linked to the ovule area, indicating that ovules with more nucellus tissue tend to be larger, irrespective of the morphology of other ovule components. However, another major factor contributing to variations in ovule size between cultivars is expansion of the embryo sac. A simple summary explaining the relationship between the various ovule traits is summarised in a model (Figure 4-9). This highlights how the different component tissues of the ovule interact to determine final ovule size. These different components will be discussed further below.

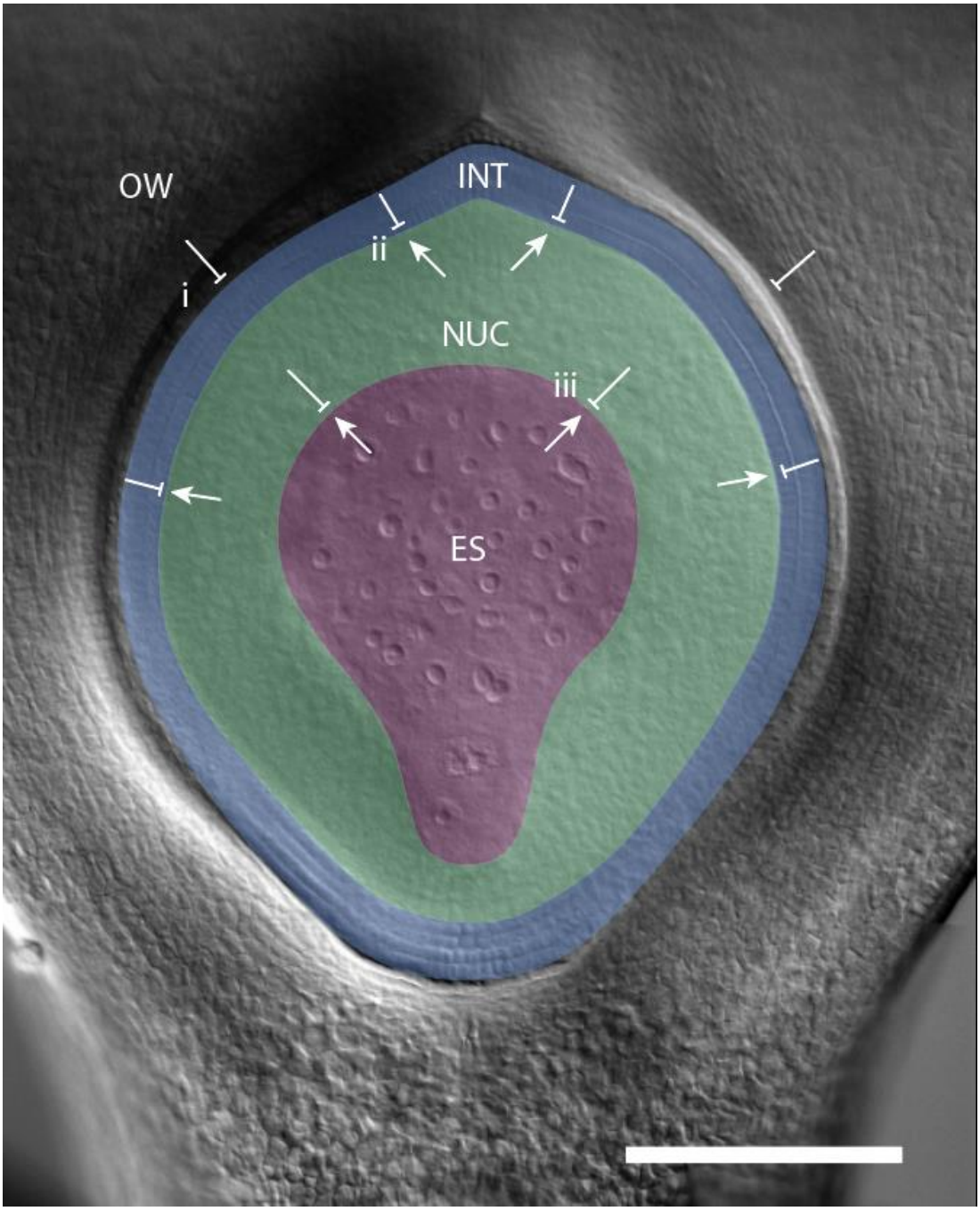

Figure 4-9: Model summarising the contribution of each sub-ovule tissue toward the overall mature structure of the barley ovule. Growth of the ovule occurs within the limits of the space available, as defined by the ovary wall (OW; i). As the outermost component of the ovule, growth of the integument (INT) may restrict development of the nucellus (NUC; ii). While growth of both the nucellus and embryo sac (ES) contribute to overall ovule growth, increase in either tissue occurs at the expense of the other (iii). ES, embryo sac; INT, integument; NUC, nucellus; OW, ovary wall.

Dissecting the role and components of nucellus size

As the megasporangium, or the tissue which ultimately gives rise to the female germ cell, the nucellus is a key component of ovule fertility. Nucellus area varied by up to 56.7% in the barley panel, and was tightly coupled to overall ovule size. Despite this, as ovule size increased, the proportion of nucellus tended to decrease. The reason for this appears to be embryo sac expansion, since embryo sac area showed a strong negative correlation with nucellus proportion. Hence, increased embryo sac and nucellus area both drive increases in ovule area, but the expanding embryo sac increases in size at the expense of the nucellus. This growth might be facilitated by pre-fertilisation induction of cell death in nucellus cells adjoining the embryo sac, or through compression of nucellus cells over time. With respect to the grain, the mild negative relationship between the proportion of nucellus and the grain length indicates that longer grains are slightly more likely to be produced from ovules that contain relatively more embryo sac than nucellus, which in turn, as mentioned above, is more likely to occur in larger ovules.

Despite many species producing crassinucellate ovules, the significance of a large nucellus remains unclear (Endress 2011; Rudall et al. 2008). Hypotheses suggest that a bigger nucellus could provide a larger repository of amino acids or sugar that are required for the early stages of grain development (discussed in Wilkinson et al. 2018), but this has yet to be conclusively shown. Alternatively, a larger nucellus may facilitate an ideal environment for signalling. Throughout ovule development, developmental signals such as auxin are transmitted through the nucellus (Cheng et al. 2006; Pagnussat et al. 2009), and models suggest that there may be nutritional transfer and signalling cross-talk between the nucellus and embryo sac prior to fertilisation (Juranić et al. 2018; Lora et al. 2017). However, information is currently lacking regarding the degree of symplastic connectivity and the molecular mechanisms of signal transduction between these two tissues. It is clear that after

fertilisation in barley and wheat, the nucellus undergoes programmed cell death (PCD) and forms the nucellar projection, which fulfils an important role as a transfer tissue facilitating movement of maternal nutrients to the developing embryo and endosperm (Thiel et al. 2008). Delayed PCD of nucellar cells dramatically reduces barley grain fill (Radchuk et al. 2006), however it is not known whether the size or number of cells in the nucellus or nucellar projection are important for nutrient transfer. This might be considered through thin sectioning and light microscopy of the cultivars described above.

Given the lack of a clear relationship between nucellus size and grain traits in this study, it is possible that simply having a nucellus is sufficient to satisfy the needs of downstream grain formation. Alternatively, it is also possible that the crassinucellate nature of barley ovules fulfils an important role in developmental regulation, stress tolerance and nutrition of the developing embryo sac, rather than the downstream stages of seed growth. Indeed, a number of studies have shown that female tissues are much more resilient against abiotic stress than male tissues (reviewed by Barnabás et al. (2008) and Wilkinson et al. (2018), and this may be due in part to the protection offered to the embryo sac by the ovule itself. Whether variations in nucellus size indirectly contribute to grain development by limiting ovule abortion under conditions of environmental stress was not tested. However, the identification of genotypes with variant nucellus phenotype in this study, such as Akita, Host, Lina and Wren will be a useful resource to investigate this question.

Embryo sac expansion contributes to ovule size at the expense of the nucellus

The embryo sac contains four discrete haploid cell types that arise by mitotic divisions of a cell known as the functional megaspore (Willemse and De Boer-de 1981). These four cell types are: synergid cells, of which there are two, the egg cell and the central cell, of which there are one of each, and the antipodal cells, of which there is a large cluster of indeterminate number

in cereal crops, generally accepted as being at least 30. By reproductive maturity the central cell and the antipodal cell cluster are prominent, and constitute the majority of the region occupied by the embryo sac (Chaban et al. 2011; Engell 1994; Maeda and Miyake 1997). Once a pollen tube enters the ovule, the two polar nuclei within the central cell are fertilised by a pollen sperm nucleus, fusing to form a single triploid nucleus (Mogensen 1990; You and Jensen 1985). In the five days following fertilisation, this triploid central cell nucleus undergoes mitosis without cytokinesis, thus forming the coenocytic endosperm. This is followed by cellularisation and subsequent differentiation of discrete endosperm cell types occurs (Olsen 2004). Prior to fertilisation, in Arabidopsis the central cell is responsible for production of developmental signals, such as the peptide ESF1 (EMBRYO SURROUNDING FACTOR 1), which is required for correct seed development (Costa et al. 2014). Previous work regarding maternal effects on barley endosperm development focussed on the role of the nucellus in post-fertilisation grain filling processes, but proposed that the central cell provides a “factor” critical for correct endosperm cell division (Felker et al. 1985). In maize, several maternal effect mutants have been identified in which defective growth and organisation of the central cell and antipodal cells impacts differentiation and patterning of endosperm cell types, ultimately altering kernel morphology (Chettoor et al. 2016; Gutiérrez-Marcos et al. 2006). The function of antipodal cells before and after fertilisation has been the subject of much debate but little detailed analysis, in part due to the technical difficulty of accessing this tissue (Lloyd 1899; Song et al. 2014). However, among historical studies comparing ovule structure in monocot and eudicot species (Lloyd 1899), the parents and progeny of a barley/rye cross (*Hordeum jubatum* x *Secale cereal;* Brink and Cooper, 1944), and more contemporary studies assessing antipodal ultrastructure in wheat and rice (Chaban et al. 2011; Maeda and Miyake 1997), there is some evidence to suggest that the antipodal cells are an important source of nutrition to the developing embryo and endosperm.

Cells of the embryo sac can be identified in barley using the methodology described in Chapter 3 (Wilkinson and Tucker 2017). However, one limitation of the imaging method used in this study was the lack of depth measurement, as optical sections were taken insufficiently far apart for 3-D reconstruction. Without this, it was not possible to separate the overlapping regions occupied by the central cell and the antipodal cell cluster. As such it could not be confirmed whether the proportional variation in embryo sac morphology is driven by an increase in central cell expansion, antipodal cell proliferation, antipodal cell expansion, or a combination of all three factors. Advances in tissue clearing, whole-mount imaging techniques, and image processing software capabilities will be useful for addressing this issue in future studies that aim to assess ovule morphology both with small sample sizes and in a high-throughput manner.

Within the population studied, the embryo sac was found to be the most variable ovule component, and as a result, its relationship with ovule area was slightly less than that of the nucellus. The transverse and longitude dimensions of the embryo sac were tightly correlated, meaning that variation of overall embryo sac area occurred proportionally rather than in only longitude or transverse. No significant correlations were directly identified between embryo sac traits and grain traits, however the proportion of nucellus is the direct inverse of the embryo proportion within the ovule. As such, it may be considered that there is a positive relationship between embryo sac proportion and grain length. Other than this, given the limitations of the method with respect to isolating specific central cell and antipodal cell cluster regions, the lack of other relationships being identified may either accurately reflect an absence of impact of embryo sac morphology upon grain development, or it may reflect that key traits were not phenotyped. Based on current literature, both the genotypic and mechanistic basis for embryo sac expansion remains unclear in dicots and monocots. Logically, embryo sac growth may result from activity within the embryo sac, such as accumulation of nutrients within the central cell and proliferation of the antipodal cells, or in response to changes in the surrounding

nucellus, such as substantial growth of the surrounding tissue throughout development stretching the embryo sac or conversely alteration of structural properties of nucellar cell walls allowing the embryo sac to crush the surrounding nucellus. Investigation of embryo sac development in variant genotypes identified in this study, such as Cecilia, Forum, Foxtrot and Salka may elucidate genetic inputs that contribute to structure of the embryo sac. Further, work utilising such genotypes to assess when and where cell division and expansion take place in the barley ovule, particularly in somatic components such as the nucellus and integuments, may begin to dissect the relationship between these tissues and their role in reproductive development and production of cereal crop grain.

The integuments

The integuments initiate from the chalazal region of the ovule primordium at the same time as selection of one nucellus cell to become the archesporial cell, then the megaspore mother cell, of which the daughter cells give rise to the embryo sac (Schneitz et al. 1995). Throughout ovule development, the bi-layered integument grows sufficiently rapidly to completely encapsulate the nucellus before the ovule reaches reproductive maturity. The point at which the integuments meet is known as the micropyle. This structure forms at the distal tip of the ovule, generally at the closest point to where the egg apparatus is located within the embryo sac, and has been found to be important for correct entrance of the pollen tube into the ovule prior to fertilisation (Lora et al. 2019). In addition to this role in facilitating fertilisation, in Arabidopsis, the integument has a critical role after fertilisation as it forms the seed coat (Nakaune et al. 2005; Windsor et al. 2000). Before fertilisation, the integument of Arabidopsis has also been demonstrated to be required for correct ovule development, by producing developmental signals such as KLUH/CYP78A5 (KLU) and CYP78A9 (Sotelo-Silveira et al. 2013; Zhao et al. 2018). These cytochrome P450 genes are required for proliferation of integument cells and subsequently the cells of the seed coat, ultimately regulating ovule

fertility and overall seed size (Adamski et al. 2009; Ito and Meyerowitz 2000). Silencing of *TaCYP78A5*, the wheat orthologue of the *KLU*, was found to restrict seed coat cell proliferation and cause a 10% reduction in grain size (Ma et al. 2015). In the barley panel investigated here, integument width was found to be the least variable of the nine ovule traits measured. Despite this, genotypes with larger ovule area tended to have thinner integuments, which may indicate they are less-resistant to compression by the nucellus and expanding embryo sac. Further, a mild negative relationship was identified between integument width and grain length (R^2 = -0.22, $p<0.05$), thus it may be speculated that mechanical constraint by the integuments could potentially play a role in grain filling processes. However, replication of both ovule and grain trait measurements must be undertaken before meaningful conclusions may be drawn from this analysis. Future study of genotypes identified to have variant integument phenotype at maturity, such as Akita, Forum, Gant and Wren may reveal genetic inputs into integument formation.

Characterisation of variation in mature ovule phenotype provides tools for the future

Shape and size of mature ovules is likely to be determined by a combination of factors such as nucellus cell divisions, expansion of cells within the embryo sac such as the central cell and antipodal cells, mechanical restriction from the integuments, or by the space within the carpel (the locule) that is available for the ovule to fill. Due to the unique challenges posed by the size and location of cereal ovules, accurate visualisation of physical structures such as the locule, and observation of processes such as cell expansion and division remains technically challenging. Prior to this study, morphological analysis of ovule development in cereal crops has been performed using time-consuming techniques that do not allow visualisation in more than two dimensions, such as histological staining of thick sections and transmission electron microscopy (Engell 1994; Maeda and Miyake 1997; You and Jensen 1985). While use of whole-mount clearing techniques such as ClearSee, PeaClarity and Hoyer's Solution can be

arduous and involve significant method optimisation (Anderson 1954; Kurihara et al. 2015; Palmer et al. 2015), this study demonstrates that it is possible to utilise such techniques for investigating genotypic differences in the physical arrangement of cereal crop ovules. These techniques will provide a powerful tool for future investigation of ovule development, especially upon identification of genes specifically expressed in discrete ovule cell types that can be used for generation of fluorescent reporter lines and mutational studies.

In this study, morphological quantification of the variation in nine mature ovule morphological traits facilitate the investigation between physical aspects of the mature barley ovule and the grain subsequently produced. Correlation analysis revealed only a single mild relationship between ovule and grain phenotypes, such that genotypes with thicker integuments were more likely to produce shorter grain. It must be acknowledged that only one generation of ovules and grain were analysed for this data, thus technical replications must be completed before meaningful conclusions are drawn from these correlation analyses. Further, it should be noted that it was not possible to phenotype several traits, such as nucellus cell number, and size of the central cell, thus the data presented in this study may not have captured the features of ovule development that contribute to mature grain traits. Future studies might also consider additional quantification of pistil traits, as recent work has identified a positive correlation between pistil and yield traits in wheat and sorghum (Guo et al. 2016; Yang et al. 2009). A positive relationship between pistil size and the number of grains produced per spike has been identified in wheat, which, alongside a further positive association between pistil size and floret survival, has led to the suggestion that floral nutrient allocation is a determinant of not only floral organ size but floral survival, and thus total yield (Guo et al. 2016). This hypothesis is in line with previous speculation that nutrient accumulation within the pistil, or even within the ovule, can support continuation of the metabolic processes of the ovule throughout conditions of environmental stress, thus accounting for the relatively robust environmental tolerance of the ovule as compared to that of the pollen in most species (reviewed by Wilkinson et al.,

2018). However, the relationship between ovule traits and ovary traits remains to be assessed.

Identification of morphological variation among 127 genotypes of two-row spring barley genotypes in this study raises several questions, particularly including: 1) What is the genetic basis for variation in ovule phenotype? 2) When in development does variant ovule morphology become apparent – is the mature ovule size determined upon ovule initiation, or can processes occurring mid-development influence the mature phenotype? 3) What is the role of cell proliferation and expansion in the nucellus and cells of the embryo sac with respect to mature ovule phenotype? Each of these questions requires future study of developing ovules, and assessment of genotypes with varied ovule phenotypes. Several suitable genotypes have been identified in this study, including Akita, Cecilia, Forum, Foxtrot, Gant, Host, Lina, Optic, Salka and Wren. In order to guide future investigation of the genetic basis for differences in mature ovule phenotype, the variation quantified in this study was used to perform a genome wide association study.

GWAS identifies four small-effect QTL that influence ovule morphology in two-row spring barley

The use of genome wide association studies (GWAS) in plants is relatively new. This technique compares phenotypic data collected from a population of related genotypes to marker data such as genotype-specific single nucleotide polymorphisms (SNP). These comparisons facilitate identification of quantitative trait loci (QTL) that influence the phenotypic trait in question, on the basis of how frequently phenotypic variation coincides with specific SNPs. Over the last decade, GWAS has been widely used to discover regions of the genome, and subsequently genetic components, of polygenic and pleiotropic traits, both in medical research fields and agricultural research (Qian et al. 2017). For example, the *NERD1 (NEW*

ENHANCER OF ROOT DWARFISM) gene was recently identified as a component of several fertility traits in Arabidopsis, following a GWAS using ovule number data in a population of 189 accessions (Yuan and Kessler 2018). Similarly, QTL of relevance to cereal crop breeding programs have been identified in wheat for genotypes showing tolerance against drought stress occurring at meiosis (Onyemaobi et al. 2018), heat-stress occurring in early grain fill (Shirdelmoghanloo et al. 2016), and a combination of heat and drought stress (Bennett et al. 2012). In this study, GWAS was used to identify QTL associated with the variation in mature ovule morphology present in a panel of 127 two-row spring barley genotypes. Marker associations with nine distinct ovule traits were analysed, including: ovule area, ovule transverse, ovule longitude, embryo sac area, embryo sac transverse, embryo sac longitude, nucellus area, nucellus proportion, and integument width. Sixty six SNP markers were identified that associated with variation in at least one these traits, and 17 markers exhibited particularly strong associations. The markers were grouped into six general regions throughout the barley genome, of which four were of particular interest. Although the maximum LOD score of any association was only 6.65, these four regions were notable in containing multiple markers that formed strong associations with multiple ovule traits. Interestingly, markers of greatest strength of association within each region related to combinations of either embryo sac and ovule traits, or nucellus and ovule traits, but not for the combination of embryo sac and nucellus traits, suggesting that development of the embryo sac and the nucellus are likely governed by distinct regulatory programs. Three of the four QTL were enriched for specific gene ontology (GO) terms unique to that QTLs, indicating that each QTL represents contribution of a different regulatory pathway to the observed variation in ovule phenotypes.

In relation to other GWAS studies, the strength of associations within the QTL identified in this study is relatively low. This, combined with the incidence of multiple marker associations for each trait, suggests that development of ovule morphological traits assessed are subject to complex small-effect multigenic regulation. In order to identify markers of greater significance,

future GWAS will require phenotypic data from larger populations and/or higher density genomic marker data. Alternatively, the genotypes identified as being outliers for each trait might be used to generate bi-parental populations for standard QTL mapping in the F2 generation. In parallel, a genomics approach could be used document expression patterns and filter for genes that vary between key cultivars and/or co-locate within QTL intervals. Further, study of these genes will be required throughout ovule development in order to assess at what developmental stage variant phenotype manifests, and ultimately to further our understanding of the reproductive purpose of the nucellus in cereal crops.

Conclusion

Microscopic technology has advanced sufficiently to allow quantification of morphological traits of mature barley ovules among a population. In this study a population screen identified variation among nine ovule traits, and revealed four QTL associated with variation in these traits. Correlation between ovule and grain traits would benefit from increased replication of the population grown in order to bulk grain production, to reduce the effects of plant loss on total yield and thus allow more rigorous grain trait analysis. Further study is required to determine whether variation of discrete ovule morphological traits confers an advantage to ovule development and fertility under stressful conditions.

References

Adamski NM, Anastasiou E, Eriksson S, O'Neill CM, Lenhard M (2009) Local maternal control of seed size by *KLUH/CYP78A5*-dependent growth signaling. Proceedings of the National Academy of Sciences 106 (47):20115-20120. doi:10.1073/pnas.0907024106

Anderson LE (1954) Hoyer's solution as a rapid permanent mounting medium for bryophytes. The Bryologist 57 (3):242-244

Barnabás B, Jäger K, Fehér A (2008) The effect of drought and heat stress on reproductive processes in cereals. Plant, Cell & Environment 31 (1):11-38. doi:doi:10.1111/j.1365-3040.2007.01727.x

Baroux C, Spillane C, Grossniklaus U (2002) Evolutionary origins of the endosperm in flowering plants. Genome Biology 3 (9):reviews1026-reviews1026

Bennett D, Reynolds M, Mullan D, Izanloo A, Kuchel H, Langridge P, Schnurbusch T (2012) Detection of two major grain yield QTL in bread wheat (*Triticum aestivum* L.) under heat, drought and high yield potential environments. Theoretical and Applied Genetics 125 (7):1473-1485

Bokulich NA (2017) Brewing Microbiology. Caister Academic Press,

Brink RA, Cooper DC (1944) The antipodals in relation to abnormal endosperm behavior in Hordeum jubatum x Secale cereale hybrid seeds. Genetics 29 (4):391-406

Cantalapiedra CP, Boudiar R, Casas AM, Igartua E, Contreras-Moreira B (2015) BARLEYMAP: physical and genetic mapping of nucleotide sequences and annotation of surrounding loci in barley. Molecular Breeding 35 (1):13. doi:10.1007/s11032-015-0253-1

Chaban I, Lazareva E, Kononenko N, Polyakov VY (2011) Antipodal complex development in the embryo sac of wheat. Russian Journal of Developmental Biology 42 (2):79-91

Cheng Y, Dai X, Zhao Y (2006) Auxin biosynthesis by the YUCCA flavin monooxygenases controls the formation of floral organs and vascular tissues in Arabidopsis. Genes & Development 20 (13):1790-1799. doi:10.1101/gad.1415106

Chettoor AM, Phillips AR, Coker CT, Dilkes B, Evans MMS (2016) Maternal gametophyte effects on seed development in maize. Genetics 204 (1):233-248. doi:10.1534/genetics.116.191833

Comadran J, Kilian B, Russell J, Ramsay L, Stein N, Ganal M, Shaw P, Bayer M, Thomas W, Marshall D, Hedley P, Tondelli A, Pecchioni N, Francia E, Korzun V, Walther A, Waugh R (2012) Natural variation in a homolog of Antirrhinum *CENTRORADIALIS* contributed to spring growth habit and environmental adaptation in cultivated barley. Nature Genetics 44:1388. doi:10.1038/ng.2447

https://www.nature.com/articles/ng.2447#supplementary-information

Costa LM, Marshall E, Tesfaye M, Silverstein KAT, Mori M, Umetsu Y, Otterbach SL, Papareddy R, Dickinson HG, Boutiller K, VandenBosch KA, Ohki S, Gutierrez-Marcos JF (2014) Central cell–derived peptides regulate early embryo patterning in flowering plants. Science 344 (6180):168-172. doi:10.1126/science.1243005

Diboll AG (1968) Fine structural development of the megagametophyte of *Zea mays* following fertilization. American Journal of Botany 55 (7):787-806

Eitam D, Kislev M, Karty A, Bar-Yosef O (2015) Experimental barley flour production in 12,500-year-old rock-cut mortars in Southwestern Asia. PLOS ONE 10 (7):e0133306

Endress PK (2011) Angiosperm ovules: diversity, development, evolution. Annals of Botany 107 (9):1465-1489. doi:10.1093/aob/mcr120

Engell K (1994) Embryology of barley. IV. Ultrastructure of the antipodal cells of *Hordeum vulgare* L. cv. Bomi before and after fertilization of the egg cell. Sexual Plant Reproduction 7 (6):333-346

Felker FC, Peterson DM, Nelson OE (1985) Anatomy of immature grains of eight maternal effect shrunken endosperm barley mutants. American Journal of Botany 72 (2):248-256. doi:doi:10.1002/j.1537-2197.1985.tb08289.x

Guo Z, Schnurbusch T, Chen D (2015) Variance components, heritability and correlation analysis of anther and ovary size during the floral development of bread wheat. Journal of Experimental Botany 66 (11):3099-3111. doi:10.1093/jxb/erv117

Guo Z, Slafer GA, Schnurbusch T (2016) Genotypic variation in spike fertility traits and ovary size as determinants of floret and grain survival rate in wheat. Journal of Experimental Botany 67 (14):4221-4230. doi:10.1093/jxb/erw200

Gutiérrez-Marcos JF, Costa LM, Evans MMS (2006) Maternal gametophytic *baseless1* is required for development of the central cell and early endosperm patterning in maize (*Zea mays*). Genetics 174 (1):317-329. doi:10.1534/genetics.106.059709

Hassan AS, Houston K, Lahnstein J, Shirley N, Schwerdt JG, Gidley MJ, Waugh R, Little A, Burton RA (2017) A Genome Wide Association Study of arabinoxylan content in 2-row spring barley grain. PLOS ONE 12 (8):e0182537

Ito T, Meyerowitz EM (2000) Overexpression of a gene encoding a cytochrome P450, *CYP78A9*, induces large and seedless fruit in *Arabidopsis*. The Plant Cell 12 (9):1541-1550

Jäger K, Fábián A, Barnabás B (2008) Effect of water deficit and elevated temperature on pollen development of drought sensitive and tolerant winter wheat (*Triticum aestivum* L.) genotypes. Acta Biologica Szegediensis 52 (1):67-71

Juranić M, Tucker MR, Schultz CJ, Shirley NJ, Taylor JM, Spriggs A, Johnson SD, Bulone V, Koltunow AM (2018) Asexual female gametogenesis involves contact with a sexually-fated megaspore in apomictic *Hieracium*. Plant Physiology 177 (3):1027-1049. doi:10.1104/pp.18.00342

Kubo T, Fujita M, Takahashi H, Nakazono M, Tsutsumi N, Kurata N (2013) Transcriptome analysis of developing ovules in rice isolated by laser microdissection. Plant and cell physiology 54 (5):750-765

Kurihara D, Mizuta Y, Sato Y, Higashiyama T (2015) ClearSee: a rapid optical clearing reagent for whole-plant fluorescence imaging. Development:dev. 127613

Lloyd FE (1899) The comparative embryology of the rubiaceae. Memoirs of the Torrey Botanical Club 8 (1):1-112

Lora J, Herrero M, Tucker MR, Hormaza JI (2017) The transition from somatic to germline identity shows conserved and specialized features during angiosperm evolution. New Phytologist 216 (2):495-509. doi:doi:10.1111/nph.14330

Lora J, Laux T, Hormaza JI (2019) The role of the integuments in pollen tube guidance in flowering plants. New Phytologist 221 (2):1074-1089

Ma M, Liu X, Li Z, Zhao H, Hu S, Song W (2015) *TaCYP78A5* regulates seed size in wheat (*Triticum aestivum*). Journal of Experimental Botany 67 (5):1397-1410. doi:10.1093/jxb/erv542

Maeda E, Miyake H (1996) Ultrastructure of antipodal cells of rice (*Oryza sativa*) after anthesis, as related to nutrient transport in embryo sac. Japanese Journal of Crop Science 65 (2):340-351

Maeda E, Miyake H (1997) Ultrastructure of antipodal cells of rice (oryza sativa) before anthesis with special reference to concentric configuration of endoplasmic reticula. Japanese Journal of Crop Science 66 (3):488-496. doi:10.1626/jcs.66.488

Maheswari P (1950) An introduction to the embryology of angiosperms. Tata Mcgraw-Hill Publishing Company Ltd; Bombay; New Delhi,

Mascher M, Gundlach H, Himmelbach A, Beier S, Twardziok SO, Wicker T, Radchuk V, Dockter C, Hedley PE, Russell J, Bayer M, Ramsay L, Liu H, Haberer G, Zhang X-Q, Zhang Q, Barrero RA, Li L, Taudien S, Groth M, Felder M, Hastie A, Šimková H, Staňková H, Vrána J, Chan S, Muñoz-Amatriaín M, Ounit R, Wanamaker S, Bolser D, Colmsee C, Schmutzer T, Aliyeva-Schnorr L, Grasso S, Tanskanen J, Chailyan A, Sampath D, Heavens D, Clissold L, Cao S, Chapman B, Dai F, Han Y, Li H, Li X, Lin C, McCooke JK, Tan C, Wang P, Wang S, Yin S, Zhou G, Poland JA, Bellgard MI, Borisjuk L, Houben A, Doležel J, Ayling S, Lonardi S, Kersey P, Langridge P, Muehlbauer GJ, Clark MD, Caccamo M, Schulman AH, Mayer KFX, Platzer M, Close TJ, Scholz U, Hansson M, Zhang G, Braumann I, Spannagl M, Li C, Waugh R, Stein N (2017) A chromosome conformation capture ordered sequence of the barley genome. Nature 544:427. doi:10.1038/nature22043

https://www.nature.com/articles/nature22043#supplementary-information

Mascher M, Muehlbauer GJ, Rokhsar DS, Chapman J, Schmutz J, Barry K, Muñoz-Amatriaín M, Close TJ, Wise RP, Schulman AH, Himmelbach A, Mayer KFX, Scholz U, Poland JA, Stein N, Waugh R (2013) Anchoring and ordering NGS contig assemblies by population sequencing (POPSEQ). The Plant Journal 76 (4):718-727. doi:doi:10.1111/tpj.12319

Mogensen HL (1990) Fertilization and early embryogenesis. Reproductive versatility in the grasses Cambridge Univ Press, Cambridge:76-99

Nakaune S, Yamada K, Kondo M, Kato T, Tabata S, Nishimura M, Hara-Nishimura I (2005) A vacuolar processing enzyme, deltaVPE, is involved in seed coat formation at the early stage of seed development. The Plant Cell 17 (3):876-887. doi:10.1105/tpc.104.026872

Olsen O-A (2004) Nuclear endosperm development in cereals and *Arabidopsis thaliana*. The Plant Cell 16 (suppl 1):S214-S227. doi:10.1105/tpc.017111

Onyemaobi I, Ayalew H, Liu H, Siddique KHM, Yan G (2018) Identification and validation of a major chromosome region for high grain number per spike under meiotic stage water stress in wheat (*Triticum aestivum* L.). PLOS ONE 13 (3):e0194075. doi:10.1371/journal.pone.0194075

Oury V, Tardieu F, Turc O (2016) Ovary apical abortion under water deficit is caused by changes in sequential development of ovaries and in silk growth rate in maize. Plant Physiology 171 (2):986-996

Pagnussat GC, Alandete-Saez M, Bowman JL, Sundaresan V (2009) Auxin-dependent patterning and gamete specification in the *Arabidopsis* female gametophyte. Science 324 (5935):1684-1689. doi:10.1126/science.1167324

Palmer WM, Martin AP, Flynn JR, Reed SL, White RG, Furbank RT, Grof CP (2015) PEA-CLARITY: 3D molecular imaging of whole plant organs. Scientific Reports 5:13492

Qian L, Hickey LT, Stahl A, Werner CR, Hayes B, Snowdon RJ, Voss-Fels KP (2017) Exploring and harnessing haplotype diversity to improve yield stability in crops. Frontiers in Plant Science 8:1534-1534. doi:10.3389/fpls.2017.01534

Radchuk V, Borisjuk L, Radchuk R, Steinbiss H-H, Rolletschek H, Broeders S, Wobus U (2006) *Jekyll* encodes a novel protein involved in the sexual reproduction of barley. The Plant Cell 18 (7):1652-1666. doi:10.1105/tpc.106.041335

Roszak P, Köhler C (2011) Polycomb group proteins are required to couple seed coat initiation to fertilization. Proceedings of the National Academy of Sciences 108 (51):20826-20831. doi:10.1073/pnas.1117111108

Rudall PJ, Remizowa MV, Beer AS, Bradshaw E, Stevenson DW, Macfarlane TD, Tuckett RE, Yadav SR, Sokoloff DD (2008) Comparative ovule and megagametophyte development in *Hydatellacea*e and water lilies reveal a mosaic of features among the earliest angiosperms. Annals of Botany 101 (7):941-956. doi:10.1093/aob/mcn032

Saini H, Sedgley M, Aspinall D (1983) Effect of heat stress during floral development on pollen tube growth and ovary anatomy in wheat (T*riticum aestivum* L.). Functional Plant Biology 10 (2):137-144

Samuel D (1996) Archaeology of ancient Egyptian beer. Journal of the American Society of Brewing Chemists 54 (1):3-12

Sands DC, Morris CE, Dratz EA, Pilgeram AL (2009) Elevating optimal human nutrition to a central goal of plant breeding and production of plant-based foods. Plant Science 177 (5):377-389

Schneitz K, Hülskamp M, Pruitt RE (1995) Wild-type ovule development in *Arabidopsis thaliana:* a light microscope study of cleared whole-mount tissue. The Plant Journal 7 (5):731-749. doi:doi:10.1046/j.1365-313X.1995.07050731.x

Shirdelmoghanloo H, Taylor JD, Lohraseb I, Rabie H, Brien C, Timmins A, Martin P, Mather DE, Emebiri L, Collins NC (2016) A QTL on the short arm of wheat (*Triticum aestivum* L.) chromosome 3B affects the stability of grain weight in plants exposed to a brief heat shock early in grain filling. BMC Plant Biology 16:100-100. doi:10.1186/s12870-016-0784-6

Song X, Yuan L, Sundaresan V (2014) Antipodal cells persist through fertilization in the female gametophyte of Arabidopsis. Plant Reproduction 27 (4):197-203

Sotelo-Silveira M, Cucinotta M, Chauvin A-L, Montes RAC, Colombo L, Marsch-Martínez N, de Folter S (2013) Cytochrome P450 *CYP78A9* is involved in Arabidopsis reproductive development. Plant Physiology:pp. 113.218214

Storey JD (2011) False discovery rate. In: International Encyclopedia of Statistical Science. Springer, pp 504-508

Tester M, Langridge P (2010) Breeding technologies to increase crop production in a changing world. Science 327 (5967):818-822. doi:10.1126/science.1183700

Thiel J, Weier D, Sreenivasulu N, Strickert M, Weichert N, Melzer M, Czauderna T, Wobus U, Weber H, Weschke W (2008) Different hormonal regulation of cellular differentiation and function in nucellar projection and endosperm transfer cells: a microdissection-based transcriptome study of young barley grains. Plant Physiology 148 (3):1436-1452. doi:10.1104/pp.108.127001

Tian T, Liu Y, Yan H, You Q, Yi X, Du Z, Xu W, Su Z (2017) agriGO v2.0: a GO analysis toolkit for the agricultural community, 2017 update. Nucleic Acids Research 45 (W1):W122-W129. doi:10.1093/nar/gkx382

Waddington S, Cartwright P, Wall P (1983) A quantitative scale of spike initial and pistil development in barley and wheat. Annals of Botany 51 (1):119-130

Wilkinson LG, Bird DC, Tucker MR (2018) Exploring the role of the ovule in cereal grain development and reproductive stress tolerance. Annual Plant Reviews:1-35

Wilkinson LG, Tucker MR (2017) An optimised clearing protocol for the quantitative assessment of sub-epidermal ovule tissues within whole cereal pistils. Plant Methods 13 (1):67

Willemse M, De Boer-de M (1981) Megasporogenesis and early megagametogenesis. Acta Societatis Botanicorum Poloniae 50 (1-2):111-120

Windsor JB, Symonds VV, Mendenhall J, Lloyd AM (2000) Arabidopsis seed coat development: morphological differentiation of the outer integument. The Plant Journal 22 (6):483-493. doi:doi:10.1046/j.1365-313x.2000.00756.x

Yang Z, van Oosterom EJ, Jordan DR, Hammer GL (2009) Pre-anthesis ovary development determines genotypic differences in potential kernel weight in sorghum. Journal of Experimental Botany 60 (4):1399-1408. doi:10.1093/jxb/erp019

You R, Jensen WA (1985) Ultrastructural observations of the mature megagametophyte and the fertilization in wheat (*Triticum aestivum*). Canadian Journal of Botany 63 (2):163-178

Yuan J, Kessler SA (2018) A genome-wide association study reveals a novel regulator of ovule number and fertility in *Arabidopsis thaliana*. BioRxiv:356600. doi:10.1101/356600

Zhao L, Cai H, Su Z, Wang L, Huang X, Zhang M, Chen P, Dai X, Zhao H, Palanivelu R (2018) KLU suppresses megasporocyte cell fate through SWR1-mediated activation of *WRKY28* expression in Arabidopsis. Proceedings of the National Academy of Sciences 115 (3):E526-E535

Supplementary Data

Table 4-S1: Measurements for nine morphological traits of mature ovules in 127 genotypes of European two-row spring barley. O_A, ovule area; O_T, ovule transverse; O_L, ovule longitude; ES_A, embryo sac area; ES_T, embryo sac transverse; ES_L, embryo sac longitude; I_W, integument width; N_A, nucellus area; N_P, nucellus proportion.

Genotype	O_A (µm^2)	O_T (µm)	O_L (µm)	ES_A (µm^2)	ES_T (µm)	ES_L (µm)	I_W (µm)	N_A (µm^2)	N_P (%)
Acapella	202777.7 ± 38935	499.1 ± 25.6	533.9 ± 19.7	46464.9 ± 9679.1	216.5 ± 4.8	279.5 ± 15.7	38.1 ± 2.5	156312.8 ± 30894.7	0.77 ± 0.024
Agenda	227499.2 ± 42467	483.4 ± 17.1	625.2 ± 24.7	75121.6 ± 13856.8	272.9 ± 11.6	367.9 ± 21.7	49.5 ± 2	152377.7 ± 32315.5	0.667 ± 0.043
Akita	159405.5 ± 21166.8	421.5 ± 5.4	500.8 ± 15.8	56263.6 ± 15762.1	242.9 ± 8.6	328.1 ± 16.2	52.2 ± 2.1	103142 ± 10601.4	0.653 ± 0.065
Alabama	188015.8 ± 22567.6	466.9 ± 10	543.3 ± 9.5	47066.8 ± 8037.7	233.3 ± 10.1	290.3 ± 8.7	48.1 ± 1.2	140949 ± 17452	0.75 ± 0.027
Alis	150012.3 ± 16751.1	432.3 ± 5.8	468.9 ± 15.9	44269.9 ± 9124.8	237 ± 13.1	266.1 ± 16.7	46.7 ± 0.8	105742.4 ± 9603.8	0.707 ± 0.037
Amourette	171066.4 ± 22210.5	435 ± 7.6	527.8 ± 12.7	53021.2 ± 11671.7	236.9 ± 9.4	320.1 ± 10.8	47.4 ± 0.6	118045.2 ± 12930.1	0.693 ± 0.038
Anaconda	175754.9 ± 24729.3	434.9 ± 12.6	544.4 ± 11.5	49135.6 ± 8349.3	225.1 ± 9.1	320.9 ± 11.7	46.6 ± 0.3	126619.3 ± 21639.9	0.719 ± 0.043
Annabell	169975.6 ± 17536.6	464.5 ± 23.1	514.9 ± 7	55868.4 ± 5977.1	246.6 ± 6.1	316 ± 6.7	49.6 ± 1.1	114107.2 ± 21672.8	0.666 ± 0.061
Appaloosa	211603.2 ± 24692	492 ± 11.6	576.9 ± 13.7	57511.7 ± 9111.2	260.2 ± 11	309.6 ± 15.7	49.5 ± 1.1	154091.6 ± 18946.2	0.728 ± 0.029
Ardila	180109.1 ± 18186.7	465.5 ± 8.2	519.5 ± 9.6	41395.2 ± 8153.9	214.4 ± 9.5	276.4 ± 8.2	49.7 ± 1.1	138714 ± 11530.8	0.772 ± 0.027
Astoria	190873.9 ± 16285	471.6 ± 5.3	543 ± 11.2	46474.6 ± 9324.7	224.7 ± 7.5	286.3 ± 12.1	47.5 ± 1.1	144399.3 ± 8488.4	0.759 ± 0.032
Athena	149659.1 ± 45201.7	412.8 ± 19	476.2 ± 26	32568.6 ± 18038.1	174.1 ± 15.8	254 ± 26.4	45.5 ± 1.3	117090.6 ± 31701.4	0.793 ± 0.07
Athos	160966.7 ± 27244.7	482.2 ± 49.1	497.9 ± 18.3	38129.9 ± 11155.5	201.4 ± 13.9	273 ± 17.2	44.7 ± 1.4	122836.7 ± 18501	0.766 ± 0.038
Atlas	171584.4 ± 32144.6	444.2 ± 18.4	530.7 ± 30.2	45944.1 ± 18271.2	207.3 ± 23.3	321.1 ± 27.1	46.4 ± 1.2	125640.3 ± 14108.7	0.742 ± 0.053

Auriga	161884.1 ± 38547.9	430.7 ± 15	503.2 ± 24.7	38298.6 ± 12018.4	191 ± 10	286.6 ± 18.1	48.8 ± 0.4	123585.5 ± 27274.8	0.768 ± 0.03
Avec	172691.2 ± 21624.7	447.1 ± 12.6	531.6 ± 10.2	44083.8 ± 8870.9	209.6 ± 4.2	312.6 ± 11.3	45.8 ± 1.8	128607.4 ± 22714.6	0.742 ± 0.055
Baronesse	171348.2 ± 28762.3	452 ± 13.7	514.5 ± 27.5	38308.1 ± 9522.4	197.4 ± 11.8	304.5 ± 16.8	45.3 ± 0.4	133040.1 ± 20688.9	0.778 ± 0.024
Berac	151120 ± 15047.7	419.8 ± 7.9	497.4 ± 23.9	38984.4 ± 8527.6	195.2 ± 3.7	310 ± 24.2	46.7 ± 0.5	112135.6 ± 9043.4	0.744 ± 0.037
Beryllium	138197.8 ± 15888.7	396.9 ± 11.7	484.3 ± 8.9	30462.7 ± 5597.7	174.6 ± 10.6	270.1 ± 10.4	44.9 ± 2.3	107735.1 ± 11329.2	0.781 ± 0.022
Braemar	187581.4 ± 11179.7	454.6 ± 10.1	562.9 ± 9.2	47076.2 ± 14935	239.7 ± 8.4	340 ± 19.3	47.5 ± 0.5	140505.2 ± 12090.8	0.751 ± 0.075
Brazil	182011.1 ± 23031.5	462.3 ± 11.3	542.3 ± 9.8	51241.6 ± 5545.8	242.9 ± 6.8	323.5 ± 8.4	45.5 ± 0.9	130769.6 ± 19270.8	0.717 ± 0.024
Cabaret	193191.6 ± 26708.1	466.6 ± 12.7	557.3 ± 16.3	48388.4 ± 10239.8	229.6 ± 7.9	321.9 ± 12.7	45.7 ± 0.8	144803.1 ± 19611.1	0.751 ± 0.033
Calgary	187296.8 ± 36417.7	472.4 ± 22	545.3 ± 22.5	49399.6 ± 10033.6	226.8 ± 13.2	325.5 ± 11	46.7 ± 1.2	137897.2 ± 27812.3	0.736 ± 0.021
Calico	156593.3 ± 21815.8	429.7 ± 10.5	495.7 ± 13.3	36313.5 ± 10750.5	186.6 ± 10	281.3 ± 10.2	46.6 ± 0.7	120279.8 ± 14262.8	0.772 ± 0.043
Camir	172567.8 ± 11254.8	461.2 ± 10	502.2 ± 6.1	39585 ± 4712.2	210.2 ± 6.7	286.9 ± 11.2	51.1 ± 0.5	132982.8 ± 12026.8	0.77 ± 0.032
Campala	162723.7 ± 30920	434.7 ± 11.6	503.4 ± 18.9	40636.5 ± 14579.3	201.7 ± 14.9	291.8 ± 14.6	49.5 ± 0.7	122087.3 ± 17067.7	0.759 ± 0.049
Casino	153786.7 ± 18049.9	435.5 ± 7.2	471.4 ± 8.3	40642.7 ± 6321.1	214.2 ± 6	278 ± 6.8	48.6 ± 0.7	113144 ± 14808.7	0.735 ± 0.031
Catalina	173326.2 ± 16742.5	461.7 ± 6.6	512.1 ± 13.5	35811.6 ± 10565.4	193.3 ± 10.8	286.7 ± 16.6	50.1 ± 0.8	137514.6 ± 12036.1	0.795 ± 0.049
Cecilia	136893.5 ± 27697.2	411.1 ± 17.7	440 ± 26.2	25194.4 ± 9330.6	158.1 ± 13	238.8 ± 24.3	46.1 ± 0.6	111699.2 ± 18406.4	0.821 ± 0.027
Celebra	193488.6 ± 15004.4	480 ± 7.8	533.3 ± 10	46708.3 ± 8401.9	229.2 ± 10.7	279.6 ± 13.1	43.5 ± 0.7	146780.3 ± 12442.5	0.759 ± 0.035
Cellar	148462 ± 34500.2	384 ± 26.2	485.2 ± 24.4	38385.3 ± 16361.6	200.2 ± 15.3	281.8 ± 21.2	49.8 ± 0.9	110076.7 ± 19948.7	0.752 ± 0.061
Charm	161985 ± 21394.4	421.9 ± 18.9	523.3 ± 8.4	45378.9 ± 10688.6	200.3 ± 18.5	327.1 ± 14.3	47.4 ± 2	116606.1 ± 11745.4	0.724 ± 0.038
Chieftan	155828.3 ± 12691.9	419.3 ± 4.5	511.5 ± 15.2	40089.8 ± 9515.4	196.7 ± 11.1	296.3 ± 19.9	50.8 ± 1.4	115738.5 ± 4680.8	0.746 ± 0.043
Chime	161668 ± 10602	434.8 ± 6.4	504.5 ± 10.5	43478.5 ± 6809.9	219.7 ± 7	288.9 ± 12.7	46.8 ± 0.7	118189.6 ± 7204.6	0.732 ± 0.031

Class	169898.4 ± 18278.3	436.2 ± 4.9	517.7 ± 20	43506.7 ± 13188.3	212.5 ± 18.5	300.6 ± 20.7	45 ± 0.3	126391.6 ± 6550.9	0.749 ± 0.053
Cocktail	163254.5 ± 25345	426.4 ± 10.7	525 ± 19.8	47006.1 ± 11979.9	215.3 ± 9.9	323.3 ± 18.3	49.6 ± 0.9	116248.3 ± 16431.4	0.715 ± 0.041
Cooper	155485.3 ± 25762.9	421.5 ± 8.5	504 ± 12.9	41315.4 ± 10263.4	205.8 ± 8.5	294 ± 11.6	48.6 ± 0.7	114169.8 ± 16507.1	0.737 ± 0.03
Cribbage	177799.4 ± 22963.1	443.1 ± 9.8	538.3 ± 12.5	57237.6 ± 10063.5	225.2 ± 4.3	358 ± 11.4	47.8 ± 0.7	120561.8 ± 15258.1	0.679 ± 0.029
Croydon	160034.6 ± 38047.1	437.1 ± 20.3	492.2 ± 36.1	41044.2 ± 15323.3	201.5 ± 12.1	277.7 ± 18.6	49.3 ± 0.5	118990.4 ± 23349.3	0.75 ± 0.033
Crusader	171243.3 ± 15637.8	444.1 ± 9.9	523.1 ± 9.8	48232.8 ± 12141	228.7 ± 13.4	317.5 ± 12.6	49.6 ± 0.6	123010.5 ± 9026	0.721 ± 0.054
Dantuna	158939.3 ± 22284.7	443.3 ± 11.3	482.3 ± 13.9	38076.7 ± 9948.8	198 ± 11.9	273.8 ± 14.1	49.6 ± 0.8	120862.5 ± 17061.1	0.762 ± 0.045
Derkado	186747.9 ± 22732.1	443 ± 8.2	565.1 ± 14.7	62685.7 ± 13968	252.9 ± 11.3	355.2 ± 16.3	49.3 ± 0.7	124062.2 ± 14565.2	0.667 ± 0.05
Draught	169698.7 ± 20772.6	455.8 ± 9.9	494.4 ± 9.3	36127.7 ± 3998	194.2 ± 4.6	282.4 ± 10.5	45.4 ± 0.7	133571.1 ± 17902.4	0.786 ± 0.017
Drum	160297.4 ± 21842.7	439.8 ± 9.2	491.5 ± 13.4	37227.3 ± 7495	195.9 ± 8.4	276.7 ± 10.9	47.5 ± 0.9	123070.1 ± 14843.9	0.77 ± 0.021
Elo	185090.6 ± 11378.9	458.4 ± 6.3	547.5 ± 7.2	50198.2 ± 5220.8	236.4 ± 3.5	329 ± 6.1	43.6 ± 0.5	134892.4 ± 9025.8	0.729 ± 0.022
Extract	164652.1 ± 14406.3	448.3 ± 6.9	497.6 ± 6.5	34479.2 ± 7094.9	188.9 ± 7.8	284 ± 8.3	46.7 ± 0.8	130172.9 ± 11537.1	0.791 ± 0.035
Fairytale	158521.2 ± 36092.7	440.4 ± 18.2	478.1 ± 21.3	35954.4 ± 13135.1	189.5 ± 17.3	264 ± 15.9	46.2 ± 1.6	122566.7 ± 24630.2	0.78 ± 0.046
Felicie	161461.4 ± 25734.5	430.3 ± 12.3	513.8 ± 10.3	49945.3 ± 10762.9	234.3 ± 8.8	305.8 ± 8.6	46.3 ± 0.7	111516.1 ± 20226.3	0.69 ± 0.048
Formula	179950.3 ± 16592.1	431.9 ± 7.1	570 ± 9.1	62091 ± 9557.1	247.6 ± 9.3	372.9 ± 10	50.7 ± 0.7	117859.4 ± 8938.8	0.657 ± 0.029
Forum	152996.3 ± 21356.1	398.6 ± 14.6	520.9 ± 15.2	43990.9 ± 15934.7	190.7 ± 22	295.7 ± 27.4	51.2 ± 1.1	109005.4 ± 16656.1	0.716 ± 0.084
Foxtrot	198862.9 ± 17717.3	449 ± 8.2	597.8 ± 10.5	77888.1 ± 8793.7	280.5 ± 7.8	406.6 ± 10.1	50.3 ± 1.3	120974.8 ± 13459.6	0.608 ± 0.032
Gant	158950.9 ± 39588.9	421.9 ± 12.8	511 ± 25.1	46619.9 ± 20650.8	209.9 ± 17	321.1 ± 19.9	50.4 ± 1.1	112331 ± 20229.6	0.719 ± 0.056
Global	192288 ± 17768	472.7 ± 12.1	551 ± 9.5	54115.5 ± 10936.5	224.5 ± 14.7	343.2 ± 11.4	47.8 ± 0.9	138172.5 ± 8588.4	0.721 ± 0.036
Golden Promise	216556.9 ± 14298.1	496 ± 10	590.7 ± 4.5	72314.9 ± 2290.7	281.7 ± 4	371.1 ± 3.8	48.7 ± 0.5	144242 ± 12135.2	0.665 ± 0.013

Goldie	204627.8 ± 14264.1	471.1 ± 12.4	572.7 ± 5.4	59582.5 ± 3252.3	245.4 ± 6.2	355.2 ± 9	47.4 ± 1.1	145045.3 ± 15604.8	0.707 ± 0.03
Granta	171594.5 ± 27088.2	428.8 ± 10.7	536.5 ± 14.9	47375.8 ± 11696.6	209.1 ± 9.6	322.9 ± 14	44.6 ± 1.5	124218.8 ± 18092.4	0.726 ± 0.034
Gundel	183395.7 ± 19038.4	444.8 ± 7.4	555.6 ± 10.2	50780.3 ± 10286.8	223.4 ± 9.9	341.2 ± 12.1	47.9 ± 0.8	132615.3 ± 9565.7	0.726 ± 0.033
Harry	143960.4 ± 15404.5	422.6 ± 7.6	463.9 ± 6.9	41114.3 ± 6085.6	206.4 ± 6	292.5 ± 5	47.6 ± 0.5	102846.1 ± 13370.9	0.713 ± 0.037
Hart	154955.7 ± 15849.2	435.8 ± 8.5	476.8 ± 10.4	40823.2 ± 5849.9	197.6 ± 6.1	288.3 ± 6.1	48 ± 0.7	114132.5 ± 14603.9	0.735 ± 0.036
Hassan	172938.6 ± 28604.2	440.3 ± 9.3	530.4 ± 14.2	44054.1 ± 10196.2	212.3 ± 7.2	311.7 ± 12.3	46.6 ± 0.5	128884.5 ± 21981.6	0.746 ± 0.04
Heather	155101.1 ± 9871.1	426 ± 4.9	498.2 ± 7.2	47387 ± 5030.5	217.8 ± 4.8	311.4 ± 6.4	49.5 ± 1.1	107714.1 ± 6795.3	0.695 ± 0.021
Heris	128009.3 ± 10397.5	386.8 ± 9.7	446.3 ± 5.7	32134 ± 2326	176.7 ± 4.5	251.7 ± 8.5	47.6 ± 0.5	95875.3 ± 10194.1	0.748 ± 0.024
Heron	219524.7 ± 33382.7	501.3 ± 19.3	584.6 ± 23.4	64910.8 ± 20208	264.5 ± 24.8	349 ± 24.3	43.7 ± 0.4	154613.9 ± 21015.5	0.71 ± 0.065
Hopper	176250.4 ± 2733.6	450.8 ± 1.5	522.3 ± 7.2	46541.8 ± 1841.5	222.4 ± 1.8	303.3 ± 12.1	44.9 ± 0.5	129708.7 ± 3117.5	0.736 ± 0.011
Horizon	241310.7 ± 48703.9	519.2 ± 24	607.2 ± 29.5	72158.9 ± 14691.2	268.8 ± 14.5	371.9 ± 24	43 ± 0.8	169151.8 ± 35130.8	0.7 ± 0.022
Host	174855.1 ± 22010.3	452 ± 12.2	513 ± 10.9	31372.8 ± 4873.2	170.3 ± 5.6	289.4 ± 8.5	44 ± 0.6	143482.3 ± 17884.2	0.821 ± 0.014
Ida	181751.8 ± 35204.9	452.9 ± 11.8	547.2 ± 18.9	57074.1 ± 16787.8	246.9 ± 11.3	359.6 ± 16.8	43.9 ± 0.8	124677.7 ± 20293.2	0.692 ± 0.043
Indola	192415.5 ± 25679.7	444.5 ± 8.8	607.5 ± 27.4	60038.8 ± 14732.8	233.4 ± 10.8	378.3 ± 21.3	45.2 ± 0.9	132376.7 ± 12874.2	0.692 ± 0.041
Isabella	155656.8 ± 32716.9	448.3 ± 16.4	458.7 ± 18.6	35115.4 ± 8884.8	196.4 ± 11.3	251.2 ± 12.1	46.1 ± 3.1	120541.4 ± 25453.2	0.774 ± 0.032
Jacinta	172285.4 ± 20494.2	444.2 ± 8.3	518 ± 9	47919 ± 11649.2	224.7 ± 9.5	312.6 ± 13.7	45.8 ± 0.6	124366.4 ± 14235.3	0.724 ± 0.05
Jive	177271.4 ± 48134.1	443.8 ± 19.5	528.6 ± 34.9	58553.1 ± 20528.7	241 ± 21.6	336.1 ± 22	42.1 ± 0.5	118718.3 ± 28599.7	0.676 ± 0.038
Klaxon	186547.5 ± 27052.2	451.5 ± 10.1	559.1 ± 16.8	57390 ± 14682	252 ± 13.2	331.4 ± 18.2	44.9 ± 0.6	129157.5 ± 16741.6	0.697 ± 0.059
Kristaps	141033.2 ± 16766.9	419.2 ± 7.9	451 ± 11.5	29149.3 ± 5087.3	172.1 ± 5.9	248.1 ± 10.6	48 ± 1.2	111883.9 ± 13941.6	0.793 ± 0.027
Laird	205907.9 ± 12201.4	478.3 ± 5.3	587.7 ± 9	72562.4 ± 9706.3	276.3 ± 6.1	379.3 ± 11.2	44.7 ± 0.6	133345.5 ± 8171.2	0.648 ± 0.036

Lina	218821.9 ± 23008.7	480.1 ± 14.6	618 ± 16.9	56061.7 ± 8325.2	245.8 ± 8.4	346.7 ± 12.2	41.8 ± 0.8	162760.2 ± 19881	0.743 ± 0.032
Linden	177054.9 ± 21240.3	440.6 ± 7.4	545 ± 8.8	45614.5 ± 7224.3	216.5 ± 5.5	322 ± 8.3	42 ± 0.4	131440.4 ± 20392.8	0.74 ± 0.047
Lithium	181754.7 ± 17181.1	453.5 ± 5.8	541.5 ± 6	45455.5 ± 6369	213.9 ± 3.9	317.5 ± 7.5	42.6 ± 0.5	136299.2 ± 14870.9	0.749 ± 0.031
Livet	185340 ± 16365.3	454.2 ± 12	555.3 ± 9.7	51007.7 ± 1965.7	228.7 ± 1.2	334.4 ± 7.1	45.2 ± 1.5	134332.3 ± 17738.9	0.722 ± 0.03
Macarena	179263.9 ± 28318	444.3 ± 18.2	539.9 ± 15.4	52068.4 ± 9691.3	228.3 ± 13.6	334.5 ± 6.4	39.1 ± 1.3	126477.7 ± 18769.5	0.715 ± 0.026
Maris Mink	159991.8 ± 16929.9	419.9 ± 12.5	503.8 ± 10.2	46703.7 ± 6238.6	220.4 ± 10.7	327.4 ± 9.3	45 ± 1.2	113288.1 ± 12547.9	0.708 ± 0.026
Maypole	159156.1 ± 31478.1	434.8 ± 16.4	486.1 ± 21	37549.7 ± 10722.4	192.2 ± 16	275.5 ± 11.4	44.5 ± 0.6	121606.4 ± 21810.1	0.767 ± 0.029
Melitta	162393.6 ± 22453.3	439.7 ± 8.6	494.5 ± 9	53423.8 ± 12408.2	236.3 ± 7.6	315.8 ± 8.4	43.8 ± 0.7	108969.8 ± 14518.4	0.673 ± 0.046
Midas	189991 ± 38369.1	458.8 ± 18.4	556.5 ± 29.1	56436.4 ± 12595.8	236 ± 12.6	353.3 ± 18.2	45.5 ± 0.9	133554.6 ± 25940.1	0.705 ± 0.011
Minstrel	175581.7 ± 17944.1	437.3 ± 6.4	541.7 ± 12.4	46950.9 ± 11014.2	215.7 ± 8.1	323.6 ± 15.3	44.4 ± 0.6	128927.6 ± 11016.1	0.742 ± 0.038
Neruda	177169.8 ± 19122.3	453.9 ± 8.1	531.6 ± 9.8	40801.9 ± 8715.7	200.3 ± 5.8	302.1 ± 10	44.3 ± 0.6	136367.9 ± 16535.1	0.769 ± 0.04
Nimbus	183543.5 ± 22967.5	435.6 ± 9.1	567.3 ± 10.9	58867.6 ± 13808.4	243.1 ± 11.8	357.5 ± 10.2	44.9 ± 1.1	124675.9 ± 14303.1	0.682 ± 0.046
Novello	154239.1 ± 16522.7	413.1 ± 5.5	505.6 ± 12.3	33330.3 ± 6097.1	171.7 ± 4.8	298 ± 10.8	43.9 ± 0.9	120908.9 ± 12418.2	0.785 ± 0.025
Optic	167477.1 ± 7342.4	439.9 ± 3.1	507.3 ± 7.4	35562.9 ± 3665.9	186.2 ± 6.3	294.3 ± 7.1	48.4 ± 0.6	131914.2 ± 5274.6	0.788 ± 0.016
Orbit	161883 ± 20556	451.7 ± 13.2	487.3 ± 8.5	33816.5 ± 4352.4	182.2 ± 7	281 ± 4.3	46.4 ± 1.2	128066.6 ± 18494.2	0.789 ± 0.026
Paramount	161360.3 ± 14144.7	413.7 ± 6.3	525.8 ± 15.4	51749.1 ± 13781.8	221.5 ± 14.4	342.1 ± 15.5	41.8 ± 0.9	109611.3 ± 2643.4	0.684 ± 0.061
Pewter	156268.5 ± 25146.1	423.6 ± 11	496.6 ± 10.3	37983.4 ± 5533.4	200.4 ± 6.5	298.6 ± 6.8	43.5 ± 0.5	118285.1 ± 21300.3	0.755 ± 0.026
Pitcher	172678.7 ± 11314.8	441.5 ± 5.6	532.4 ± 8.8	51923 ± 5262.5	234.8 ± 5.5	319.4 ± 7.8	44 ± 0.7	120755.7 ± 9224.1	0.699 ± 0.025
Poker	187373.3 ± 13702.9	455.1 ± 8.7	552.4 ± 11.7	50386.2 ± 9877.4	224.8 ± 9.1	334.2 ± 15.4	45.9 ± 0.9	136987.1 ± 11481.8	0.732 ± 0.045
Quartet	171754.4 ± 10072.4	450.7 ± 7.2	517.3 ± 7.1	48002.8 ± 10243.8	221.2 ± 14.3	348.8 ± 50.2	45.4 ± 1.1	123751.5 ± 7520.7	0.722 ± 0.048

Ragtime	170178.2 ± 26642.2	443.7 ± 14.7	519.3 ± 14.9	43434.9 ± 8846.7	202.3 ± 10.2	314.5 ± 13.8	41.2 ± 0.8	126743.3 ± 18976.8	0.746 ± 0.022
Rainbow	221620.1 ± 14500.2	488.6 ± 8.3	598.6 ± 8.1	65471.9 ± 8707.8	242.4 ± 6.9	375.2 ± 9.4	41 ± 1.2	156148.2 ± 8030.2	0.706 ± 0.025
Rakaia	183623.3 ± 16492.1	463.3 ± 8.6	521.5 ± 8.1	45941.3 ± 6966	213.7 ± 6.9	321.3 ± 6.8	40.9 ± 0.7	137682 ± 15001	0.749 ± 0.034
Rasa	194815.1 ± 36055.6	462 ± 18.7	582.6 ± 23.2	57361.3 ± 18451.3	230.1 ± 15.2	368.1 ± 26.5	39.6 ± 1.3	137453.8 ± 25536.5	0.707 ± 0.063
Sacha	183828.1 ± 29642.3	442.7 ± 9.5	580 ± 18.7	66886.2 ± 14705	255.3 ± 11.1	373.3 ± 13.4	45.5 ± 0.8	116941.9 ± 16409	0.639 ± 0.03
Salka	216504.3 ± 11109.6	476.6 ± 6.7	639.8 ± 8.9	72452.8 ± 7096.1	278.7 ± 7.5	396.9 ± 9.9	43.6 ± 0.4	144051.6 ± 11480.4	0.665 ± 0.032
Saloon	199385.6 ± 11367.7	456.7 ± 5.3	598.7 ± 7.1	70066.1 ± 9071.9	266.1 ± 6	382.3 ± 6.9	43.6 ± 0.5	129319.5 ± 10869.6	0.649 ± 0.039
Scandium	169544.2 ± 29001.2	437.8 ± 8.1	527.6 ± 17.7	60537.6 ± 17785.7	251.8 ± 11.9	350.2 ± 16.5	45.5 ± 0.5	109006.6 ± 14955.3	0.649 ± 0.055
Sebastian	177366.7 ± 12892	448.5 ± 10.9	535.3 ± 6.9	49655.6 ± 8576.6	214.8 ± 10	321.8 ± 19.5	46.7 ± 0.6	127711.1 ± 15658.4	0.719 ± 0.05
Simba	187989.2 ± 28982	470.9 ± 11.6	534.1 ± 15.6	55242.7 ± 13826	250.8 ± 15.7	332.8 ± 10.7	47.3 ± 0.8	132746.5 ± 17973.4	0.709 ± 0.041
Sj Christina	152980.5 ± 25152.2	420.8 ± 10.9	496.8 ± 12.3	42003.5 ± 10831.6	206 ± 9.4	295.5 ± 10.6	44.5 ± 0.9	110977.1 ± 16918.7	0.728 ± 0.041
Skittle	165843.4 ± 12277.1	429.9 ± 4.2	520.3 ± 8.2	47450 ± 8531.6	228.5 ± 8.8	316.8 ± 10.1	45.1 ± 0.6	118393.4 ± 9194	0.715 ± 0.04
Starlight	175739.2 ± 22371.3	440.8 ± 10.1	543 ± 14.5	52376.3 ± 15117.8	223.2 ± 14.7	348.9 ± 16	45.2 ± 0.5	123362.9 ± 10552	0.708 ± 0.056
Static	151390.8 ± 29178.8	412.4 ± 9.1	495.4 ± 18.9	34923.6 ± 6341.6	181.6 ± 6.1	301.5 ± 13.3	46.3 ± 0.8	118880.8 ± 24141.4	0.767 ± 0.024
Tabora	192978.2 ± 17445.3	450.4 ± 9.8	576.7 ± 8	53302 ± 5987.9	236.1 ± 6.7	334 ± 6.1	46.9 ± 1	139676.2 ± 12659	0.724 ± 0.016
Taphouse	192035.9 ± 29961.8	466 ± 9.4	556.7 ± 13.2	62763.8 ± 14264.2	253.1 ± 8.6	355.3 ± 10.3	46.1 ± 0.7	129272.1 ± 19587.2	0.675 ± 0.041
Tartan	166958.4 ± 19986.6	436 ± 7.8	524 ± 16.9	50389.5 ± 10818.3	231.5 ± 11.1	328.4 ± 11.1	44.7 ± 0.7	116568.9 ± 9242.8	0.702 ± 0.03
Thrift	163944.6 ± 13336.1	437.2 ± 6	516.9 ± 9.4	46666.3 ± 5608.5	224.4 ± 2.5	310.1 ± 9.1	44.5 ± 0.7	117278.2 ± 9335.9	0.716 ± 0.021
Toby	177399.8 ± 25090.6	449.9 ± 10.6	538.5 ± 11.6	55550.6 ± 12772.1	243 ± 11.1	338.7 ± 10.7	45.5 ± 0.7	121849.2 ± 15150.4	0.69 ± 0.041
Toucan	177561.6 ± 21683.1	444.7 ± 7.5	554.2 ± 13.5	45330.7 ± 9374.7	210.7 ± 6.9	320.3 ± 14	46.1 ± 0.6	132230.9 ± 14255.4	0.747 ± 0.033

Troon	178106.5 ± 15480.1	424 ± 7.7	580.2 ± 13.8	63375.3 ± 9998	253.2 ± 7.6	364 ± 12.6	46.5 ± 0.8	114731.2 ± 12625.3	0.644 ± 0.044
Turnberry	197208.8 ± 38990	458.2 ± 14.6	574.4 ± 34.1	58628.5 ± 24867.2	240.7 ± 25	355.1 ± 34.5	44.1 ± 0.9	138580.3 ± 19326.8	0.714 ± 0.082
Tuscon	154039 ± 30202.8	422.1 ± 10.7	502 ± 16.4	43908.6 ± 11936.7	218.2 ± 9.2	297.7 ± 13.6	44.9 ± 0.4	110130.4 ± 19497.2	0.718 ± 0.032
Tyne	183220.9 ± 29886.1	446.1 ± 14.2	547.9 ± 17.2	59202.6 ± 12854	257.8 ± 13.1	334.2 ± 11.3	44 ± 0.7	124018.3 ± 19111.5	0.679 ± 0.036
Ursa	180656.3 ± 16302.3	444.3 ± 7.1	551.3 ± 14	49858.8 ± 12481.4	227.8 ± 13.4	319.9 ± 16	42.7 ± 0.7	130797.5 ± 8571.4	0.727 ± 0.05
Vankkuri	172398.7 ± 53894.2	423.8 ± 32.9	549.8 ± 54.7	63755.6 ± 26969.7	240 ± 33.4	360.2 ± 48.7	42.5 ± 2.3	108643.1 ± 28393.1	0.652 ± 0.077
Velvet	143289.2 ± 27835.5	393.7 ± 9.1	491.1 ± 14.6	43372.5 ± 12077.3	210.7 ± 7.5	309.8 ± 13.7	42.4 ± 0.7	99916.7 ± 16250.7	0.702 ± 0.029
Viivi	170335.9 ± 32616.3	452.9 ± 19.9	506.4 ± 18.8	50929.4 ± 16704.8	234 ± 21.9	316.2 ± 17.2	44.6 ± 1	119406.6 ± 16508.7	0.707 ± 0.037
Waggon	146258.6 ± 24883.4	423.9 ± 9.1	471.6 ± 13.7	36657.3 ± 7066.1	203.9 ± 7.5	268.1 ± 8.6	46.3 ± 0.4	109601.3 ± 19976.5	0.748 ± 0.032
Weitor	169918.2 ± 21455.1	443.8 ± 8.8	521.7 ± 11	58549.7 ± 7184.3	256.3 ± 7.1	335.9 ± 8.5	41 ± 0.5	111368.5 ± 19181.1	0.653 ± 0.044
Wicket	152379.6 ± 17648.6	418.3 ± 7.3	499.9 ± 15.2	46210 ± 8823.6	222.2 ± 7.2	298.8 ± 12.4	46.6 ± 0.7	106169.6 ± 12074	0.698 ± 0.038
Widre	173886.7 ± 27079.8	448.3 ± 13.6	520.7 ± 12.7	60625.6 ± 11485.8	256 ± 12.4	349.8 ± 8.4	45.4 ± 0.9	113261.1 ± 18638.9	0.653 ± 0.041
Wren	210936.6 18576.4	488.7 ± 17.9	606.9 ± 11.7	76887.5 ± 15544.2	282 ± 11	387.8 ± 21.9	42.3 ± 0.9	134049.1 ± 15034.8	0.637 ± 0.056

Table 4-S2: Barley genotypes with (A) small and (B) large variant phenotypes for nine traits of mature ovule morphology, as determined by exceeding standard deviation from average trait values among a population of 127 genotypes. Genotypes are listed in descending order of variance from the average, i.e. smallest (A) and largest (B) genotypes are at the top of each table. O_A, ovule area (µm^2); O_T, ovule transverse (µm); O_L, ovule longitude (µm); ES_A, embryo sac area (µm^2); ES_T, embryo sac transverse (µm); ES_L, embryo sac longitude (µm); I_W, integument width (µm); N_A, nucellus area (µm^2); N_P, nucellus proportion (%).

A

	O_A	**O_T**	**O_L**	**ES_A**	**ES_T**	**ES_L**	**I_W**	**N_A**	**N_P**
1	Heris	Cellar	Cecilia	Cecilia	Cecilia	Cecilia	Acapella	Heris	Foxtrot
2	Cecilia	Heris	Heris	Kristaps	Host	Kristaps	Macarena	Velvet	Wren
3	Beryllium	Velvet	Kristaps	Beryllium	Novello	Isabella	Rasa	Harry	Sacha
4	Kristaps	Beryllium	Isabella	Host	Kristaps	Heris	Rakaia	Akita	Troon
5	Velvet	Forum	Harry	Heris	Athena	Athena	Weitor	Alis	Laird
6	Harry	Cecilia	Alis	Athena	Beryllium	Fairytale	Rainbow	Wicket	Saloon
7	Waggon	Static	Casino	Novello	Heris	Alis	Ragtime	Heather	Scandium
8	Cellar	Athena	Waggon	Orbit	Static	Waggon	Paramount	Beryllium	Vankkuri
9	Athena	Novello	Athena	Extract	Orbit	Beryllium	Lina	Vankkuri	Weitor
10	Alis	Paramount	Hart	Static	Optic	Athos	Linden	Melitta	Widre
11	Berac	Wicket	Fairytale	Isabella	Calico	Dantuna	Jive	Forum	Akita
12	Static	Kristaps	Dantuna	Optic	Extract	Maypole	Wren	Scandium	Formula

13	Wicket	Chieftan	Beryllium	Catalina	Fairytale	Ardila	Velvet	Waggon	Salka
14	Sj Christina	Berac	Cellar	Fairytale	Forum	Drum	Vankkuri	Paramount	Golden Promise
15	Forum	Maris Mink	Maypole	Draught	Auriga	Croydon	Lithium	Cellar	Annabell
16	Casino	Sj Christina	Orbit	Calico	Maypole	Casino	Ursa	Tuscon	Derkado
17	Tuscon	Cooper		Waggon	Catalina	Acapella	Horizon	Sj Christina	Agenda
18	Novello	Akita		Drum	Draught	Celebra		Weitor	Melitta
19				Maypole	Berac	Orbit		Felicie	Taphouse
20				Pewter	Drum	Calico		Cecilia	Jive
21						Cellar		Kristaps	Cribbage
22						Draught		Berac	Tyne

B

	O_A	**O_T**	**O_L**	**ES_A**	**ES_T**	**ES_L**	**I_W**	**N_A**	**N_P**
1	Horizon	Horizon	Salka	Foxtrot	Wren	Foxtrot	Akita	Horizon	Cecilia
2	Agenda	Heron	Agenda	Wren	Golden Promise	Salka	Forum	Lina	Host
3	Rainbow	Acapella	Lina	Agenda	Foxtrot	Wren	Camir	Acapella	Catalina
4	Heron	Golden Promise	Indola	Laird	Salka	Saloon	Chieftan	Rainbow	Athena
5	Lina	Appaloosa	Horizon	Salka	Laird	Laird	Formula	Heron	Kristaps
6	Golden Promise	Wren	Wren	Golden Promise	Agenda	Indola	Gant	Appaloosa	Extract
7	Salka	Rainbow	Saloon	Horizon	Horizon	Rainbow	Foxtrot	Agenda	Orbit

8	Appaloosa	Agenda	Rainbow	Saloon	Saloon	Sacha	Catalina	Celebra	Optic
9	Wren	Athos	Foxtrot	Sacha	Heron	Formula	Cellar	Goldie	Draught
10	Laird	Lina	Golden Promise	Rainbow	Appaloosa	Horizon	Ardila	Cabaret	Novello
11	Goldie	Celebra	Laird	Heron	Tyne	Golden Promise	Cocktail	Astoria	Beryllium
12	Acapella	Laird	Heron	Vankkuri	Weitor	Rasa	Annabell	Golden Promise	Fairytale
13	Saloon	Salka	Rasa	Troon	Widre	Agenda	Crusader	Salka	Baronesse
14	Foxtrot	Global	Troon	Taphouse	Sacha	Troon	Dantuna	Host	Isabella
15	Turnberry	Calgary	Sacha	Derkado	Troon	Vankkuri	Heather	Alabama	Ardila
16	Rasa	Astoria	Appaloosa	Formula	Taphouse	Ida	Campala	Braemar	Calico
17		Goldie	Tabora	Widre	Derkado	Cribbage	Appaloosa	Tabora	Drum
18		Simba	Turnberry	Scandium	Klaxon	Nimbus	Agenda		Camir
19			Goldie	Indola	Scandium	Taphouse	Croydon		Acapella
20			Formula		Simba	Derkado	Derkado		Neruda
21						Goldie	Auriga		Auriga
22						Turnberry	Golden Promise		Maypole
23						Midas	Casino		Static
24									Athos

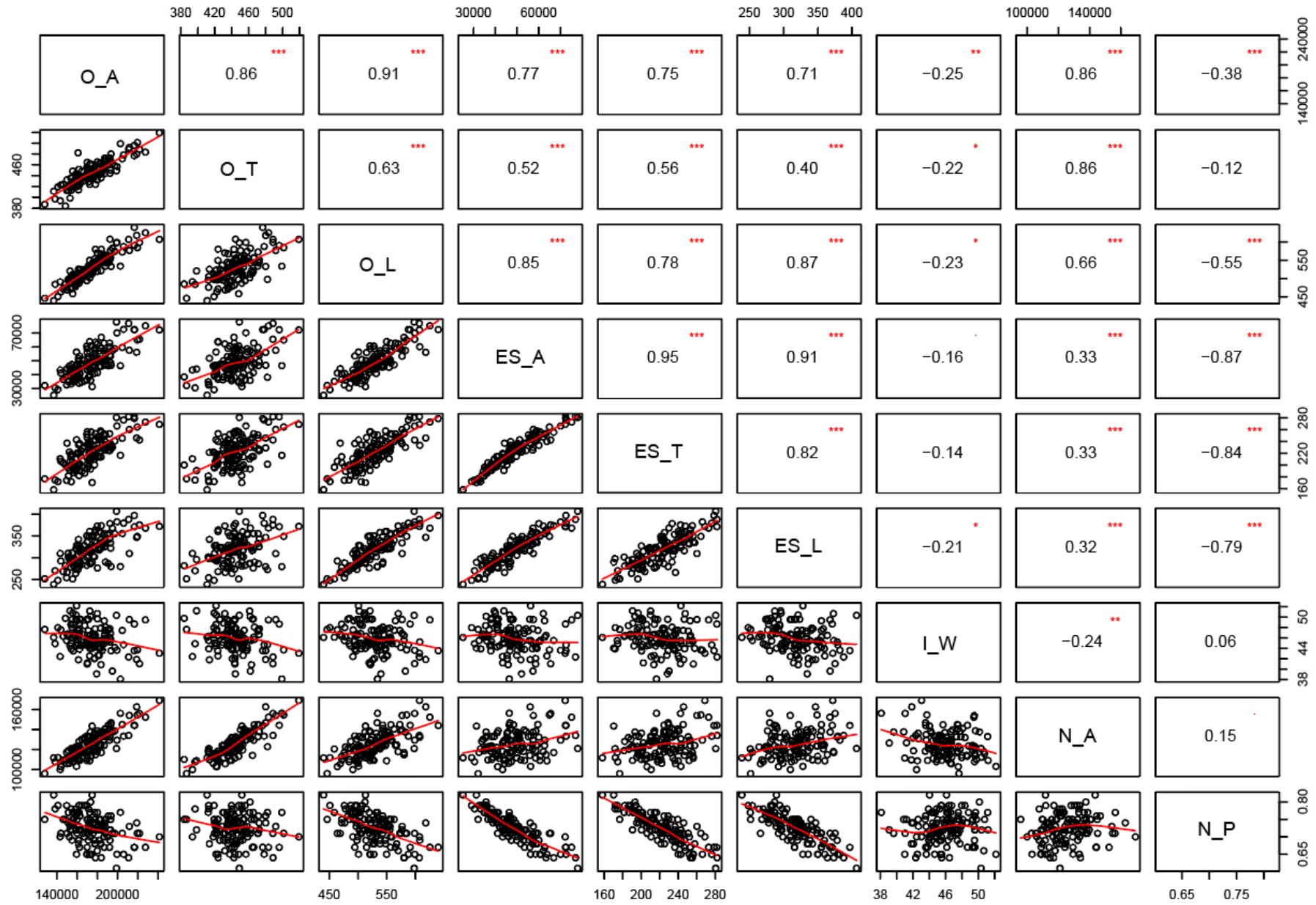
O_A
O_T
O_L
ES_A
ES_T
ES_L
I_W
N_A
N_P
0.86 *** 0.91 *** 0.77 *** 0.75 *** 0.71 *** −0.25 ** 0.86 *** −0.38 ***
0.63 *** 0.52 *** 0.56 *** 0.40 *** −0.22 * 0.86 *** −0.12
0.85 *** 0.78 *** 0.87 *** −0.23 * 0.66 *** −0.55 ***
0.95 *** 0.91 *** −0.16 . 0.33 *** −0.87 ***
0.82 *** −0.14 0.33 *** −0.84 ***
−0.21 * 0.32 *** −0.79 ***
−0.24 ** 0.06
0.15 .
380 420 460 500
30000 60000
250 300 350 400
100000 140000
140000 200000
450 550
160 200 240 280
38 42 46 50
0.65 0.75

Figure 4-S1: Correlation plots showing relationships between nine morphological traits of mature ovules measured in 127 genotypes of European two-row spring barley. Significance is given as: * = p <0.05; ** = p < 0.01; *** = p < 0.001. O_A, ovule area (µm^2); O_T, ovule transverse (µm); O_L, ovule longitude (µm); ES_A, embryo sac area (µm^2); ES_T, embryo sac transverse (µm); ES_L, embryo sac longitude (µm); I_W, integument width (µm); N_A, nucellus area (µm^2); N_P, nucellus proportion (%).

Table 4-S3: Grain traits measured in 123 genotypes of European two-row spring barley. TKW, thousand kernel weight. G_L, grain length (mm); G_W, grain width (mm); G_T, grain thickness (mm); G_AA, grain average area (mm^2); O_A, ovule area (µm2); O_T, ovule transverse (µm); O_L, ovule longitude (µm); ES_A, embryo sac area (µm2); ES_T, embryo sac transverse (µm); ES_L, embryo sac longitude (µm); I_W, integument width (µm); N_A, nucellus area (µm2); N_P, nucellus proportion (%). Of the full panel of 127 genotypes, insufficient grain was available for four genotypes: Appaloosa, Calgary, Salka and Turnberry.

Genotype	G_L (mm)	G_W (mm)	G_T (mm)	G_AA (mm^2)
Acapella	9.9 ± 0.73	3.43 ± 0.53	2.21 ± 1.18	22.6
Agenda	9.15 ± 0.68	3.08 ± 0.5	2.55 ± 1	18.2
Akita	9.6 ± 3.35	3.27 ± 1.09	2.95 ± 0.01	24.1
Alabama	8.87 ± 0.44	3.07 ± 0.42	2.21 ± 1.18	17.1
Alis	9.55 ± 0.81	2.8 ± 0.44	2.16 ± 0.42	17.8
Amourette	9.77 ± 0.53	3.21 ± 0.54	2.5 ± 0.24	21.3
Anaconda	9.98 ± 0.71	3.53 ± 0.37	2.8 ± 0.12	23
Annabell	9.14 ± 0.67	3.54 ± 0.39	2.66 ± 0.71	21.3
Ardila	9.1 ± 0.53	3.09 ± 0.5	2.32 ± 0.59	19.4
Astoria	9.68 ± 0.71	3.31 ± 0.39	2.56 ± 0.13	21.8
Athena	9 ± 1.34	3.38 ± 0.56	2.85 ± 0.18	20.6
Athos	9.8 ± 0.92	3.22 ± 0.43	2.67 ± 0.04	21.4
Atlas	9.66 ± 0.58	2.95 ± 0.33	2.22 ± 0.27	19.2
Auriga	10.08 ± 0.56	3.28 ± 0.51	2.66 ± 0.07	21.6
Avec	9.65 ± 0.53	3.26 ± 0.37	2.24 ± 0.64	20.7
Baronesse	9.65 ± 0.78	2.92 ± 0.49	2.43 ± 0.43	19.3
Berac	8.92 ± 3.25	3.11 ± 1.03	1.93 ± 0.96	21.2
Beryllium	9.78 ± 0.62	3.49 ± 0.47	2.02 ± 1.27	24.1
Braemar	9.88 ± 1.4	3.43 ± 0.55	2.67 ± 0.39	23.5
Brazil	9.45 ± 0.63	2.79 ± 0.39	2.33 ± 0.29	18.6
Cabaret	9.9 ± 0.42	3.44 ± 0.52	2.65 ± 0.05	21.9

Calico	10.19 ± 0.67	3.42 ± 0.58	2.59 ± 0.57	23.9
Camir	8.34 ± 0.38	2.96 ± 0.39	2.47 ± 0.11	16.3
Campala	8.87 ± 1.7	2.92 ± 0.53	2.18 ± 0.58	18
Casino	9.66 ± 0.27	2.46 ± 0.78	1.92 ± 0.17	17.9
Catalina	8.51 ± 4.1	2.97 ± 1.25	2.66 ± 0.08	24.3
Cecilia	9.32 ± 1.55	3.21 ± 0.55	2.35 ± 0.54	21.6
Celebra	9.3 ± 0.67	3.45 ± 0.37	2.76 ± 0.52	21.8
Cellar	10.1 ± 0.79	3.21 ± 0.31	2.32 ± 0.54	21.7
Charm	9.23 ± 0.67	3.05 ± 0.38	2.4 ± 0.12	17.1
Chieftain	9.31 ± 1.04	2.9 ± 0.56	2.32 ± 0.4	19.4
Chime	9.54 ± 0.82	3.14 ± 0.37	2.48 ± 0.57	19.7
Class	9.89 ± 0.69	3.44 ± 0.4	2.68 ± 0.19	22.6
Cocktail	8.26 ± 4.06	2.78 ± 1.33	2.43 ± 0.23	20.8
Cooper	9.5 ± 0.86	3.1 ± 0.53	2.7 ± 0.06	18.8
Cribbage	9.56 ± 0.6	3.26 ± 0.44	2.77 ± 1	20.5
Croydon	9.15 ± 0.59	3.36 ± 0.34	2.85 ± 0.11	20.5
Crusader	10.19 ± 1.02	3.08 ± 0.59	1.81 ± 1.07	20
Danuta	10.02 ± 0.86	3.33 ± 0.42	2.82 ± 0.18	21.3
Derkado	9.91 ± 0.84	3.43 ± 0.52	2.2 ± 1.1	21.6
Draught	9.15 ± 1.58	3.38 ± 0.62	2.65 ± 0.19	21.3
Drum	10.04 ± 0.85	3.4 ± 0.46	2.61 ± 0.32	23.4
Elo	9.1 ± 0.64	2.93 ± 0.35	2.53 ± 0.07	16.3
Extract	9.9 ± 0.68	3.37 ± 0.45	2.69 ± 0.13	21
Fairytale	8.89 ± 0.68	3.01 ± 0.48	2.67 ± 0.06	17
Felicie	9.45 ± 1.2	3.17 ± 0.52	2.54 ± 0.35	20.7
Formula	10.06 ± 0.71	3.3 ± 0.5	2.3 ± 0.63	23.8
Forum	9.83 ± 0.37	2.58 ± 0.5	2.01 ± 0.23	18.3
Foxtrot	10.15 ± 0.73	3.37 ± 0.39	2.96 ± 0.19	21.6
Gant	9.86 ± 0.74	3.22 ± 0.46	2.51 ± 0.18	21.5
Global	8.85 ± 0.7	3.41 ± 0.38	2.57 ± 0.65	19.7

Golden Promise	8.88 ± 0.63	3.31 ± 0.41	2.45 ± 0.27	19.5
Goldie	8.98 ± 0.69	3.36 ± 0.73	2.55 ± 0.2	20.7
Granta	10.63 ± 0.71	3.42 ± 0.47	2.78 ± 0.14	24.5
Gundel	10.1 ± 0.76	3.3 ± 0.31	2.6 ± 0.77	21.6
Harry	10.18 ± 0.65	3.24 ± 0.54	2.68 ± 0.14	22.5
Hart	9.26 ± 0.56	3.3 ± 0.48	2.74 ± 0.2	19.8
Hassan	9.31 ± 1.45	3.45 ± 0.54	2.64 ± 0.19	21.8
Heather	8.69 ± 0.22	3.05 ± 0.45	2.7 ± 1	17.4
Heris	9.04 ± 0.63	3.26 ± 0.36	2.27 ± 1	19.4
Heron	9.25 ± 0.7	3.43 ± 0.43	2.49 ± 0.56	21.6
Hopper	10.1 ± 0.76	3.43 ± 0.42	2.6 ± 0.15	22.9
Horizon	9.41 ± 1.27	3.4 ± 0.57	2.64 ± 0.18	22.1
Host	8.72 ± 1.97	3.12 ± 0.67	2.58 ± 0.13	19.4
Ida	10.46 ± 0.59	3.42 ± 0.57	2.31 ± 0.69	23.3
Indola	9.03 ± 0.69	3.08 ± 0.36	2.3 ± 0.83	18
Isabella	9.65 ± 0.59	3.75 ± 0.41	2.75 ± 0.41	23.4
Jacinta	9.33 ± 1.73	3.05 ± 0.61	2.53 ± 0.3	19.6
Jive	9.46 ± 1.43	3.14 ± 0.5	2.66 ± 0.17	21.1
Klaxon	9.62 ± 0.81	3.08 ± 0.34	2.68 ± 0.29	20
Kristaps	9.47 ± 0.43	3.05 ± 0.41	2.49 ± 0.22	18.7
Laird	8.73 ± 0.41	3.19 ± 0.58	2.45 ± 0.18	19.5
Lina	10.03 ± 0.49	3.04 ± 0.66	2.68 ± 0.14	20.8
Linden	10.85 ± 0.77	3.29 ± 0.43	2.99 ± 0.09	23.5
Lithium	9.8 ± 0.73	3.36 ± 0.44	2.53 ± 0.28	22.7
Livet	9.31 ± 0.61	2.7 ± 0.46	2.4 ± 0.34	16
Macarena	9.92 ± 0.62	3.21 ± 0.46	2.69 ± 0.18	22
Maris Mink	9.56 ± 0.8	3.41 ± 0.37	2.51 ± 0.58	22
Maypole	10.38 ± 0.84	3.37 ± 0.42	2.58 ± 0.5	23.6
Melitta	8.92 ± 0.9	3.27 ± 0.51	3.01 ± 0.08	17.8
Midas	9.13 ± 0.54	3.36 ± 0.48	2.59 ± 0.32	21

Minstrel	9.22 ± 0.74	3.43 ± 0.37	2.73 ± 0.24	20.5
Neruda	9.99 ± 0.78	3.39 ± 0.36	2.62 ± 0.44	23.2
Nimbus	10.13 ± 0.8	2.74 ± 0.45	2.14 ± 0.31	18.8
Novello	8.2 ± 3.5	2.85 ± 1.15	2.51 ± 0.37	20.8
Optic	9.12 ± 3.42	2.51 ± 0.88	1.81 ± 1.15	18.1
Orbit	9.52 ± 0.51	3.38 ± 0.43	2.41 ± 0.33	21.1
Paramount	10.7 ± 0.64	3.4 ± 0.41	2.52 ± 0.2	24.4
Pewter	10.14 ± 0.73	3.34 ± 0.37	2.9 ± 0.16	20.7
Pitcher	9.61 ± 0.69	2.76 ± 0.45	2.26 ± 0.22	18.6
Poker	9.79 ± 0.63	3.29 ± 0.35	2.68 ± 0.11	21.7
Quartet	9.31 ± 0.76	3.56 ± 0.47	2.8 ± 0.3	21.7
Ragtime	9.69 ± 1.9	3.18 ± 0.81	2.6 ± 0.17	23.2
Rainbow	9.56 ± 1.41	2.71 ± 0.49	1.33 ± 1.08	17.5
Rakaia	8.86 ± 0.75	3.03 ± 0.52	2.48 ± 0.44	17.7
Rasa	9.38 ± 0.62	3.31 ± 0.47	2.53 ± 0.4	20.8
Sacha	10.89 ± 0.59	3.38 ± 0.57	2.72 ± 0.19	23.7
Saloon	9 ± 3.15	2.85 ± 0.9	2.35 ± 0.2	20.6
Scandium	9.91 ± 0.66	3.27 ± 0.38	2.73 ± 0.17	21.3
Sebastian	9.26 ± 1.32	3.4 ± 0.51	2.7 ± 0.47	21.6
Simba	9.84 ± 0.67	3.57 ± 0.47	2.63 ± 0.58	23.3
Sj Christina	9.42 ± 0.68	3.46 ± 0.48	2.82 ± 0.24	21.6
Skittle	9.68 ± 0.83	3.39 ± 0.37	2.75 ± 0.53	21.6
Starlight	9.07 ± 1.6	3.41 ± 0.59	2.49 ± 0.71	20.7
Static	9.69 ± 0.9	3.34 ± 0.4	2.55 ± 0.33	21.7
Tabora	9.45 ± 0.5	3.01 ± 0.42	2.69 ± 0.14	18.6
Taphouse	9.35 ± 2.79	3.1 ± 0.8	2.74 ± 0.34	21.9
Tartan	10.16 ± 0.77	3.29 ± 0.41	2.59 ± 0.26	22.5
Thrift	9.48 ± 0.41	3.34 ± 0.47	2.87 ± 0.01	20
Toby	10.65 ± 0.71	3.56 ± 0.5	2.72 ± 0.19	24.1
Toucan	9.76 ± 1.37	3.37 ± 0.62	2.68 ± 0.41	22.7

Troon	9.82 ± 0.83	3.3 ± 0.32	2.7 ± 0.19	20.4
Tucson	9.76 ± 1.37	2.99 ± 0.52	2.36 ± 0.31	20.3
Tyne	9.48 ± 0.54	2.98 ± 0.34	2.31 ± 0.27	19.2
Ursa	10.12 ± 0.86	3.16 ± 0.4	2.54 ± 0.3	21.5
Vankkuri	11.33 ± 0.6	2.8 ± 0.38	2.28 ± 0.28	21.9
Velvet	10.09 ± 0.65	2.79 ± 0.62	2.34 ± 0.24	19.1
Viivi	9.83 ± 0.9	2.93 ± 0.48	2.49 ± 0.09	19.9
Waggon	9.55 ± 0.56	3.19 ± 0.33	2.78 ± 0.14	18.8
Weitor	9.52 ± 0.82	3.11 ± 0.5	2.57 ± 0.39	19.7
Wicket	9.83 ± 0.41	3.67 ± 0.44	3.08 ± 0.14	23.3
Widre	9.72 ± 0.61	2.64 ± 0.38	2.43 ± 0.09	16.6
Wren	9.67 ± 0.39	2.78 ± 0.43	2.56 ± 0.05	17.3

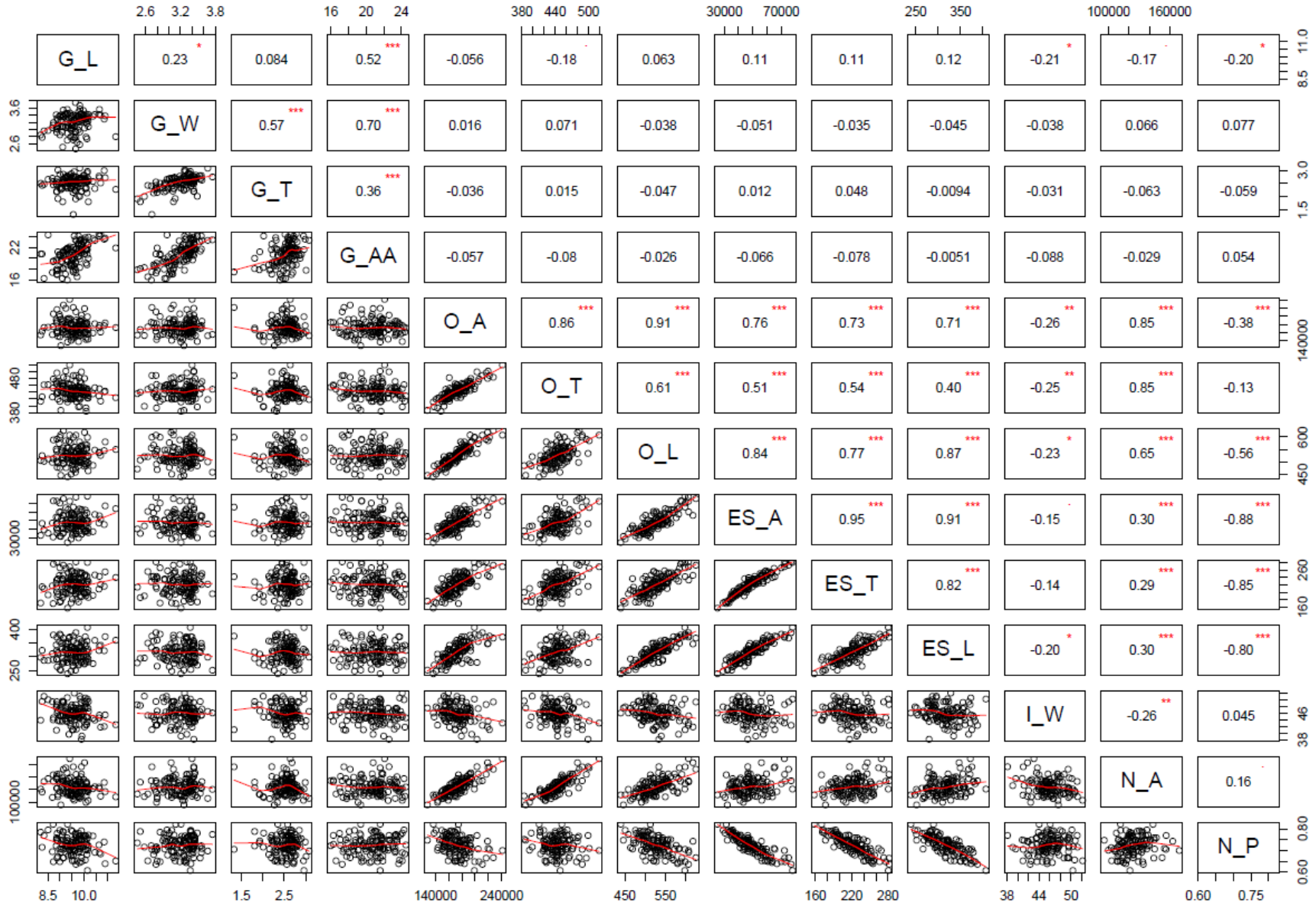
G_L
G_W
G_T
G_AA
O_A
O_T
O_L
ES_A
ES_T
ES_L
I_W
N_A
N_P
0.23 * 0.084 0.52 *** -0.056 -0.18 . 0.063 0.11 0.11 0.12 -0.21 * -0.17 . -0.20 *
0.57 *** 0.70 *** 0.016 0.071 -0.038 -0.051 -0.035 -0.045 -0.038 0.066 0.077
0.36 *** -0.036 0.015 -0.047 0.012 0.048 -0.0094 -0.031 -0.063 -0.059
-0.057 -0.08 -0.026 -0.066 -0.078 -0.0051 -0.088 -0.029 0.054
0.86 *** 0.91 *** 0.76 *** 0.73 *** 0.71 *** -0.26 ** 0.85 *** -0.38 ***
0.61 *** 0.51 *** 0.54 *** 0.40 *** -0.25 ** 0.85 *** -0.13
0.84 *** 0.77 *** 0.87 *** -0.23 * 0.65 *** -0.56 ***
0.95 *** 0.91 *** -0.15 . 0.30 *** -0.88 ***
0.82 *** -0.14 0.29 *** -0.85 ***
-0.20 * 0.30 *** -0.80 ***
-0.26 ** 0.045
0.16 .
2.6 3.2 3.8
16 20 24
380 440 500
30000 70000
250 350
100000 160000
3.6 2.6
22 16
480 380
400 250
46 38
8.5 10.0
1.5 2.5
140000 240000
450 550
160 220 280
38 44 50
0.60 0.75

Figure 4-S2: Correlation plots showing relationships between grain traits and nine morphological traits of mature ovules measured in 124 genotypes of European two-row spring barley. Significance is given as: * = p <0.05; ** = p < 0.01; *** = p < 0.001. G_L, grain length (mm); G_W, grain width (mm); G_T, grain thickness (mm); G_AA, grain average area (mm^2); O_A, ovule area (µm2); O_T, ovule transverse (µm); O_L, ovule longitude (µm); ES_A, embryo sac area (µm2); ES_T, embryo sac transverse (µm); ES_L, embryo sac longitude (µm); I_W, integument width (µm); N_A, nucellus area (µm2); N_P, nucellus proportion (%). Of the full panel of 127 genotypes, insufficient grain was available for four genotypes: Appaloosa, Calgary, Salka and Turnberry.

Table 4-S4: Summary of the 66 SNP markers identified to attain a LOD score greater than 3 for associations with nine morphological traits of mature barley ovules following GWAS performed using data collected from a population of 127 genotypes of European two-row spring barley. The bounds of each of the four major QTLs identified is highlighted in a different colour. Within each QTL, the trait with the highest LOD score has been highlighted, as has the LOD score and the allele effect, calculated as % of the trait average phenotype. O_A, ovule area (μm^2); O_T, ovule transverse (µm); O_L, ovule longitude (µm); ES_A, embryo sac area (μm^2); ES_T, embryo sac transverse (µm); ES_L, embryo sac longitude (µm); I_W, integument width (µm); N_A, nucellus area (μm^2); N_P, nucellus proportion (%).

							Major Allele		Minor Allele					
QTL	ID	Ch	cM	Trait	TraitAvg	LOD	Allele	Freq (%)	Allele	Freq (%)	Effect	s.e.	Effect (%)	s.e.
	SCRI_RS_128285	1H	26.5	ES_A	48876.1	3.13	T	63.8%	C	36.2%	3245.7	962.8	6.6	2.0
				ES_L	318.0	4.22	T	63.8%	C	36.2%	12.1	3.0	3.8	0.9
				O_A	174421.2	3.20	T	63.8%	C	36.2%	6059.7	1773.2	3.5	1.0
				O_L	529.1	3.29	T	63.8%	C	36.2%	12.0	3.4	2.3	0.7
	SCRI_RS_232660	1H	26.5	ES_A	48876.1	3.25	C	64.0%	T	36.0%	3325.5	963.8	6.8	2.0
				ES_L	318.0	4.33	C	64.0%	T	36.0%	12.3	3.0	3.9	1.0
				O_A	174421.2	3.33	C	64.0%	T	36.0%	6278.8	1795.4	3.6	1.0
				O_L	529.1	3.36	C	64.0%	T	36.0%	12.3	3.5	2.3	0.7
	SCRI_RS_117492	1H	33.3	ES_T	222.4	3.20	A	50.4%	G	49.6%	-7.7	2.2	-3.5	1.0
	SCRI_RS_151047	1H	33.3	ES_T	222.4	3.65	C	52.0%	T	48.0%	-8.2	2.2	-3.7	1.0
	SCRI_RS_217160	1H	33.3	ES_T	222.4	3.18	A	52.8%	G	47.2%	-7.6	2.2	-3.4	1.0
QTL1H_ES	11_20617	1H	41.3	ES_A	48876.1	5.70	G	86.6%	C	13.4%	6257.7	1317.0	12.8	2.7
				ES_L	318.0	5.27	G	86.6%	C	13.4%	18.9	4.2	5.9	1.3
				ES_T	222.4	3.98	G	86.6%	C	13.4%	12.7	3.3	5.7	1.5
				N_%	0.7	3.94	G	86.6%	C	13.4%	0.0	0.0	-2.8	0.7
				O_A	174421.2	4.07	G	86.6%	C	13.4%	9718.3	2473.8	5.6	1.4

				O_L	529.1	5.17	G	86.6%	C	13.4%	21.2	4.7	4.0	0.9
	SCRI_RS_126734	1H	41.3	ES_A	48876.1	5.70	T	86.6%	C	13.4%	6257.7	1317.0	12.8	2.7
				ES_L	318.0	5.27	T	86.6%	C	13.4%	18.9	4.2	5.9	1.3
				ES_T	222.4	3.98	T	86.6%	C	13.4%	12.7	3.3	5.7	1.5
				N_%	0.7	3.94	T	86.6%	C	13.4%	0.0	0.0	-2.8	0.7
				O_A	174421.2	4.07	T	86.6%	C	13.4%	9718.3	2473.8	5.6	1.4
				O_L	529.1	5.17	T	86.6%	C	13.4%	21.2	4.7	4.0	0.9
	SCRI_RS_21080	1H	75.3	O_A	174421.2	3.10	T	50.4%	C	49.6%	-5747.6	1714.8	-3.3	1.0
	SCRI_RS_4893	1H	75.3	O_A	174421.2	3.10	T	50.4%	C	49.6%	-5747.6	1714.8	-3.3	1.0
QTL2H_NUC	11_10498	2H	58.3	N_A	125560.8	5.35	A	84.3%	G	15.7%	6987.2	1523.0	5.6	1.2
				O_A	174421.2	3.80	A	84.3%	G	15.7%	8721.8	2310.8	5.0	1.3
				O_T	444.8	3.94	A	84.3%	G	15.7%	10.3	2.7	2.3	0.6
	11_10297	2H	59.2	N_A	125560.8	4.51	G	81.9%	A	18.1%	6076.7	1459.2	4.8	1.2
	12_30691	2H	59.2	N_A	125560.8	4.43	A	83.5%	C	16.5%	6245.0	1514.4	5.0	1.2
				O_A	174421.2	3.17	A	83.5%	C	16.5%	7787.3	2292.1	4.5	1.3
	11_20674	2H	59.5	N_A	125560.8	4.43	C	83.5%	A	16.5%	6245.0	1514.4	5.0	1.2
				O_A	174421.2	3.17	C	83.5%	A	16.5%	7787.3	2292.1	4.5	1.3
QT2H_OV	11_10265	2H	71.9	ES_L	318.0	3.13	G	56.7%	A	43.3%	-10.6	3.1	-3.3	1.0
	SCRI_RS_100476	2H	71.9	ES_L	318.0	3.13	C	56.7%	A	43.3%	-10.6	3.1	-3.3	1.0
	SCRI_RS_167713	2H	71.9	ES_L	318.0	3.13	C	56.7%	G	43.3%	-10.6	3.1	-3.3	1.0
	11_21251	2H	73.8	O_A	174421.2	3.43	A	85.8%	G	14.2%	8810.8	2474.8	5.1	1.4
	SCRI_RS_150266	2H	73.8	N_A	125560.8	3.42	C	84.3%	T	15.7%	5663.8	1594.9	4.5	1.3
				O_A	174421.2	4.43	C	84.3%	T	15.7%	9598.8	2328.7	5.5	1.3
				O_T	444.8	3.43	C	84.3%	T	15.7%	9.8	2.7	2.2	0.6
	SCRI_RS_16024	2H	73.8	ES_A	48876.1	3.21	C	87.4%	T	12.6%	4789.1	1399.2	9.8	2.9
				ES_T	222.4	3.35	C	87.4%	T	12.6%	11.8	3.4	5.3	1.5
				N_A	125560.8	5.28	C	87.4%	T	12.6%	7653.7	1680.5	6.1	1.3
				O_A	174421.2	6.65	C	87.4%	T	12.6%	12676.0	2447.4	7.3	1.4
				O_L	529.1	4.16	C	87.4%	T	12.6%	19.5	4.9	3.7	0.9

				O_T	444.8	5.16	C	87.4%	T	12.6%	13.1	2.9	2.9	0.7
	SCRI_RS_16995	2H	73.8	ES_A	48876.1	3.21	A	87.4%	G	12.6%	4789.1	1399.2	9.8	2.9
				ES_T	222.4	3.35	A	87.4%	G	12.6%	11.8	3.4	5.3	1.5
				N_A	125560.8	5.28	A	87.4%	G	12.6%	7653.7	1680.5	6.1	1.3
				O_A	174421.2	6.65	A	87.4%	G	12.6%	12676.0	2447.4	7.3	1.4
				O_L	529.1	4.16	A	87.4%	G	12.6%	19.5	4.9	3.7	0.9
				O_T	444.8	5.16	A	87.4%	G	12.6%	13.1	2.9	2.9	0.7
	SCRI_RS_219568	2H	75.5	N_A	125560.8	3.10	C	81.1%	T	18.9%	4959.8	1479.8	4.0	1.2
				O_A	174421.2	3.20	C	81.1%	T	18.9%	7635.0	2234.2	4.4	1.3
				O_T	444.8	3.25	C	81.1%	T	18.9%	9.2	2.7	2.1	0.6
	SCRI_RS_220533	2H	75.5	N_A	125560.8	3.10	C	81.1%	T	18.9%	4959.8	1479.8	4.0	1.2
				O_A	174421.2	3.20	C	81.1%	T	18.9%	7635.0	2234.2	4.4	1.3
				O_T	444.8	3.25	C	81.1%	T	18.9%	9.2	2.7	2.1	0.6
	SCRI_RS_171038	2H	83.1	O_A	174421.2	3.00	C	57.5%	T	42.5%	5878.5	1785.5	3.4	1.0
	11_10538	2H	112	O_A	174421.2	3.20	G	55.1%	A	44.9%	-6270.0	1835.7	-3.6	1.1
				O_T	444.8	3.28	G	55.1%	A	44.9%	-7.1	2.0	-1.6	0.5
	SCRI_RS_196100	2H	112	O_T	444.8	3.13	C	69.3%	T	30.7%	-8.1	2.4	-1.8	0.5
	SCRI_RS_132586	2H	113.1	ES_A	48876.1	3.03	T	50.4%	C	49.6%	-3430.7	1036.8	-7.0	2.1
				O_A	174421.2	3.46	T	50.4%	C	49.6%	-6274.0	1754.1	-3.6	1.0
				O_T	444.8	3.74	T	50.4%	C	49.6%	-7.5	2.0	-1.7	0.5
	11_10916	2H	114.2	O_T	444.8	3.44	A	61.4%	C	38.6%	-7.4	2.1	-1.7	0.5
	SCRI_RS_164608	2H	114.2	ES_L	318.0	3.19	A	81.9%	G	18.1%	-14.1	4.1	-4.4	1.3
	SCRI_RS_12444	2H	116.9	ES_L	318.0	3.19	T	81.9%	C	18.1%	-14.1	4.1	-4.4	1.3
	11_10092	2H	117.8	O_T	444.8	3.47	G	66.7%	A	33.3%	-8.0	2.2	-1.8	0.5
	11_20511	2H	117.9	O_T	444.8	3.59	G	66.9%	A	33.1%	-8.1	2.2	-1.8	0.5
	SCRI_RS_155161	2H	117.9	O_T	444.8	4.22	G	67.7%	A	32.3%	-8.9	2.2	-2.0	0.5
	SCRI_RS_174214	2H	117.9	O_T	444.8	3.59	A	66.9%	G	33.1%	-8.1	2.2	-1.8	0.5
	SCRI_RS_235261	2H	117.9	O_T	444.8	3.25	T	67.7%	C	32.3%	-7.9	2.3	-1.8	0.5
	11_11365	2H	122	O_T	444.8	4.22	A	67.7%	T	32.3%	-8.9	2.2	-2.0	0.5

	11_173490	2H	122	O_T	444.8	3.59	A	66.9%	G	33.1%	-8.1	2.2	-1.8	0.5
	12_20295	2H	122.3	O_T	444.8	3.32	A	68.5%	G	31.5%	-7.9	2.3	-1.8	0.5
	SCRI_RS_161030	2H	122.3	O_T	444.8	3.23	C	69.8%	A	30.2%	-7.9	2.3	-1.8	0.5
QTL4H_INT	SCRI_RS_187708	4H	52	I_T	45.9	3.34	C	66.1%	T	33.9%	0.8	0.2	1.8	0.5
	SCRI_RS_204773	4H	52	I_T	45.9	3.34	G	66.1%	A	33.9%	0.8	0.2	1.8	0.5
	11_10577	4H	52.1	N_A	125560.8	3.32	G	75.6%	A	24.4%	-5396.7	1546.4	-4.3	1.2
				O_A	174421.2	3.06	G	75.6%	A	24.4%	-8072.5	2427.2	-4.6	1.4
				O_T	444.8	3.01	G	75.6%	A	24.4%	-9.8	3.0	-2.2	0.7
				N_A	125560.8	3.82	G	74.8%	A	25.2%	-5810.3	1533.4	-4.6	1.2
				O_A	174421.2	3.26	G	74.8%	A	25.2%	-8245.7	2387.0	-4.7	1.4
	SCRI_RS_157290	4H	52.1	N_A	125560.8	3.32	T	75.6%	C	24.4%	-5396.7	1546.4	-4.3	1.2
				O_A	174421.2	3.06	T	75.6%	C	24.4%	-8072.5	2427.2	-4.6	1.4
				O_T	444.8	3.01	T	75.6%	C	24.4%	-9.8	3.0	-2.2	0.7
	SCRI_RS_157666	4H	52.1	N_A	125560.8	3.32	A	75.6%	G	24.4%	-5396.7	1546.4	-4.3	1.2
				O_A	174421.2	3.06	A	75.6%	G	24.4%	-8072.5	2427.2	-4.6	1.4
				O_T	444.8	3.01	A	75.6%	G	24.4%	-9.8	3.0	-2.2	0.7
	SCRI_RS_160373	4H	52.1	N_A	125560.8	3.82	T	74.8%	C	25.2%	-5810.3	1533.4	-4.6	1.2
				O_A	174421.2	3.26	T	74.8%	C	25.2%	-8245.7	2387.0	-4.7	1.4
	SCRI_RS_217322	4H	52.1	N_A	125560.8	3.32	T	75.6%	G	24.4%	-5396.7	1546.4	-4.3	1.2
				O_A	174421.2	3.06	T	75.6%	G	24.4%	-8072.5	2427.2	-4.6	1.4
				O_T	444.8	3.01	T	75.6%	G	24.4%	-9.8	3.0	-2.2	0.7
	SCRI_RS_226221	4H	52.1	N_A	125560.8	3.82	C	74.8%	T	25.2%	-5810.3	1533.4	-4.6	1.2
				O_A	174421.2	3.26	C	74.8%	T	25.2%	-8245.7	2387.0	-4.7	1.4
	12_30777	4H	52.2	N_A	125560.8	3.75	A	74.6%	G	25.4%	-5767.8	1538.1	-4.6	1.2
				O_A	174421.2	3.29	A	74.6%	G	25.4%	-8346.1	2404.3	-4.8	1.4
	SCRI_RS_145379	4H	52.2	I_T	45.9	3.34	A	66.1%	G	33.9%	0.8	0.2	1.8	0.5
	11_20782	4H	52.3	N_A	125560.8	3.82	G	74.8%	A	25.2%	-5810.3	1533.4	-4.6	1.2
	11_20782	4H	52.3	O_A	174421.2	3.26	G	74.8%	A	25.2%	-8245.7	2387.0	-4.7	1.4
	12_31310	4H	52.3	I_T	45.9	3.92	A	65.9%	C	34.1%	0.9	0.2	2.0	0.5

	SCRI_RS_144983	4H	52.3	I_T	45.9	4.26	C	73.2%	T	26.8%	1.0	0.3	2.3	0.6
	SCRI_RS_16811	4H	52.3	I_T	45.9	3.93	T	73.8%	A	26.2%	1.0	0.3	2.2	0.6
	SCRI_RS_186944	4H	52.3	I_T	45.9	4.26	C	73.2%	T	26.8%	1.0	0.3	2.3	0.6
	SCRI_RS_230472	4H	52.3	I_T	45.9	4.26	G	73.2%	T	26.8%	1.0	0.3	2.3	0.6
	SCRI_RS_7401	4H	52.3	I_T	45.9	4.26	C	73.2%	T	26.8%	1.0	0.3	2.3	0.6
	12_30620	4H	60	ES_L	318.0	3.10	A	60.6%	G	39.4%	10.6	3.2	3.3	1.0
	12_30455	4H	60.1	ES_L	318.0	3.10	C	60.6%	A	39.4%	10.6	3.2	3.3	1.0
	SCRI_RS_165031	4H	60.1	ES_L	318.0	3.10	G	60.6%	A	39.4%	10.6	3.2	3.3	1.0
	SCRI_RS_168478	4H	60.1	ES_L	318.0	3.10	G	60.6%	T	39.4%	10.6	3.2	3.3	1.0
	SCRI_RS_157334	5H	113.1	ES_A	48876.1	3.20	C	72.4%	T	27.6%	3719.6	1087.8	7.6	2.2
				ES_T	222.4	3.12	C	72.4%	T	27.6%	9.0	2.7	4.0	1.2
	SCRI_RS_9560	6H	3.2	O_L	529.1	3.63	C	85.0%	T	15.0%	17.3	4.7	3.3	0.9
	11_21335	7H	69.5	O_T	444.8	3.61	A	65.4%	G	34.6%	-7.6	2.1	-1.7	0.5
	SCRI_RS_152698	7H	69.5	O_T	444.8	3.61	C	65.4%	T	34.6%	-7.6	2.1	-1.7	0.5
	SCRI_RS_161285	7H	116.3	ES_A	48876.1	3.44	C	64.6%	A	35.4%	3523.5	988.8	7.2	2.0
				ES_T	222.4	3.74	C	64.6%	A	35.4%	8.9	2.4	4.0	1.1
				O_A	174421.2	3.71	C	64.6%	A	35.4%	6560.9	1761.5	3.8	1.0
				O_T	444.8	3.71	C	64.6%	A	35.4%	7.8	2.1	1.7	0.5
	SCRI_RS_174255	7H	116.3	O_A	174421.2	3.09	T	63.8%	C	36.2%	5928.4	1770.0	3.4	1.0
				O_T	444.8	3.12	T	63.8%	C	36.2%	7.1	2.1	1.6	0.5

Chapter 5

Phenotypic and transcriptional dynamics of ovule development in barley

ଌ • ଓ

Statement of Authorship

Title of Paper	Phenotypic and transcriptional dynamics of ovule development in barley
Publication Status	☐ Published ☐ Accepted for Publication ☐ Submitted for Publication ☑ Unpublished and Unsubmitted work written in manuscript style
Publication Details	Laura G. Wilkinson[1,2], Neil J. Shirley[1,2], Caitlin S. Byrt[1,3], Rachel A. Burton[1,2] and Matthew. R Tucker[1]

Principal Author

Name of Principal Author (Candidate)	Laura G. Wilkinson		
Contribution to the Paper	Performed experiments, analysed all samples, interpreted data and wrote manuscript.		
Overall percentage (%)	80%		
Certification:	This paper reports on original research I conducted during the period of my Higher Degree by Research candidature and is not subject to any obligations or contractual agreements with a third party that would constrain its inclusion in this thesis. I am the primary author of this paper.		
Signature		Date	14/2/19

Co-Author Contributions

By signing the Statement of Authorship, each author certifies that:

i. the candidate's stated contribution to the publication is accurate (as detailed above);
ii. permission is granted for the candidate in include the publication in the thesis; and
iii. the sum of all co-author contributions is equal to 100% less the candidate's stated contribution.

Name of Co-Author	Neil J. Shirley		
Contribution to the Paper	Performed quantitative PCR, assembled RNA sequencing library and helped with sample analysis. I hereby certify that the statement of authorship is accurate.		
Signature		Date	14/2/19

Name of Co-Author	Caitlin S. Byrt		
Contribution to the Paper	Assisted with project conception and experimental design. I hereby certify that the statement of authorship is accurate.		
Signature		Date	18/02/2019

Name of Co-Author	Rachel A. Burton		
Contribution to the Paper	Assisted with project conception and experimental design. I hereby certify that the statement of authorship is accurate.		
Signature		Date	24/02/2019

Name of Co-Author	Matthew R. Tucker		
Contribution to the Paper	Conceived project and designed experiments. Contributed to the preparation of the manuscript. I hereby certify that the statement of authorship is accurate.		
Signature		Date	14/2/19

Abstract

Development of reproductively competent ovules is a key factor in the production of cereal grain in species such as *Hordeum vulgare* (barley). Genetic factors required to initiate and sustain ovule development have been characterised in *Arabidopsis thaliana* and rice (*Oryza sativa*), however the barley ovule remains relatively unexplored. This study provides a detailed description of female reproductive development in barley, presenting morphological and transcriptional details of ovule development in five barley genotypes. Nine stages of reproductive development were determined, and genotypic variation in the rate of ovule tissue development throughout these stages was revealed by whole-mount microscopic analyses. Extraction and sequencing of RNA from whole pistils and specific ovule cell types revealed the expression dynamics of gene families known to influence reproductive development, including MADS-box genes, auxin-signalling genes, and genes involved in pectin biosynthesis and remodelling. Consistent with the abundance of pectin-related genes, immunolabelling detected pectin-related epitopes in a range of ovule cell types. Most notably, a discrete region of demethylestereified pectin was identified in the nucellus, specifically within the walls of nucellus cells adjoining the reproductive lineage. The proximity of this region to the germline cells suggests it may actively contribute to growth, expansion and/or signalling during female germline development.

Introduction

The formation and development of reproductive organs are critical for crop production. In cereal species such as barley, each flower produces thousands of pollen grains within the male reproductive organs, the stamens/anthers, and a single ovule within the female reproductive organ, the pistil (Kellogg 2015). The ovule is particularly important for seed development, since it produces the female germline and nourishes the female gametophyte

before and after fertilisation. At flower maturity, known as anthesis, the barley ovule contains an embryo sac, surrounded by nucellus, surrounded by a bi-layered integument. The nucellus and integument are diploid maternal tissues that differentiate into a nutrient transfer tissue and the seed coat, respectively, after fertilisation (You and Jensen 1985). The embryo sac (ES) is the site of fertilisation, and consists of two synergid cells, which attract the pollen tube, the egg cell, which is fertilised to form the embryo, and two polar nuclei in the central cell, which are also fertilised to form the endosperm. In addition, a cluster of over 30 antipodal cells is present that degenerates over the first few days after fertilisation, but for which an exact function remains yet to be precisely determined (Lloyd 1899; Weatherwax 1926; Maheswari 1950). Ovule tissue development must be carefully coordinated to support germline development, resist environmental stress and ensure the flower is capable of reproduction (Wilkinson et al. 2018).

The barley ovule develops from a primordial projection that extends into a locule, which is located in the centre of the pistil (Briggs 1978). The base of the primordium is known as the chalaza, and the distal end is the nucellus. Thus, already at this stage cereal ovule development differs from that of eudicots such as Arabidopsis, in which the primordial projection is tripartite; the tip is nucellus, the middle section is chalaza and there is additionally a basal region, known as the stalk-like funiculus (Bowman et al. 1994). Despite these differences, development of the female “germline” (i.e. the processes of megasporogenesis and megagametogenesis) is similar, and begins when a single sub-epidermal cell located toward the distal tip of the nucellus is selected to adopt a reproductive fate. This “archesporial” cell enlarges to become the megaspore mother cell (MMC), and undergoes meiosis. Four megaspores are produced, but only the megaspore closest to the chalaza survives, and this surviving cell is known as the functional megaspore (FM). The FM undergoes the process of megagametogenesis, meaning undergoing three rounds of mitosis, to form the female gametophyte (Schneitz et al. 1995; Willemse and De Boer-de 1981). The mature female

gametophyte is also known as the ES. Concurrent with the processes of megasporogenesis and megagametogenesis, two integument layers form from the chalaza, elongating until the nucellus is completely encapsulated and a micropyle is formed at the distal tip of the ovule (Ray et al. 1996). In contrast to eudicots, where the nucellus diminishes as the female gametophyte develops, in cereal crops the nucellus proliferates and by maturity contributes around 65% of the ovule area (see Chapters 3 and 4). Regarding the ES, the overall positioning of cells is similar between Arabidopsis and cereal crops, whereby the synergid cells and egg cell are located at the micropylar end of the ES, the antipodal cells are located at the chalazal end of the ES, and the central cell occupies a large space between the two groups of cells. However, in barley, the two polar nuclei remain unfused at anthesis as opposed to Arabidopsis where the nuclei are already fused prior to pollination. Moreover, while the three antipodal cells of Arabidopsis degenerate when the ES reaches maturity, in cereal crops the antipodal cells undergo several rounds of proliferation and endoreduplication, ultimately forming a cluster of over 30 cells with conspicuously large nuclei that does not begin degeneration until after fertilisation (Brink and Cooper 1944; Engell 1994). Neither the purpose of the antipodal cells nor the persistence of a thick nucellus has been precisely determined in barley, despite their occurrence in many other species (Endress 2011; Lora et al. 2017).

At the molecular level, ovule development requires a large number of inputs over a relatively short timeframe. Genes that contribute to cereal ovule development have been identified in rice and maize via mutagenesis, such as *MEIOSIS ARRESTED AT LEPTOTENE* (*OsMEL1;* Nonomura et al. 2007), *MULTIPLE SPOROCYTE 1* (*OsMSP1*; Nonomura et al. 2003); *MULTIPLE ARCHESPORIAL CELLS 1*; *ZmMAC1*, Wang et al. 2012), and *SEEDSTICK* (*AtSTK*; Pinyopich et al. 2003), as well as by transcriptional profiling (Jain and Khurana 2009; Johnston et al. 2007; Yu et al. 2005). However, little is known in barley. Similar to other angiosperms, it is likely that coordinated growth of multiple tissues is required to ensure stable ovule and germline development (Pinto et al. 2019). Desynchronization of developmental cues

can have a variety of effects, ranging from germline abortion (e.g. *mel1*), to extra germline cells (e.g. *msp1*) and altered tissue growth (e.g. *kluh*; Ito and Meyerowitz 2000), all of which impact downstream seed development. The identity of these cues is of particular interest in this study, especially those that may influence tissue or overall organ size (see Chapters 3 and 4). A number of cues that may facilitate ovule growth in barley have been reviewed in recent times and include organ formation genes (Callens et al. 2018), hormonal pathways (Shirley et al. 2018) and components of the cell wall (Tucker et al. 2018). Although these published reviews provide a comprehensive summary for readers, for the purposes of this thesis and the current Chapter, aspects are considered in further detail below.

MADS-box genes

The ABC model of floral development was proposed to explain the role of transcription factors in organising initiation of different organs from the floral meristem in angiosperms (Bowman et al. 2012; Coen and Meyerowitz 1991). The angiosperm flower is typically divided into four concentric rings, or whorls, each containing a specific floral organ, of which the descriptions are as follows: whorl 1 comprises the most outer tissues, namely sepals in eudicots or the palea and lemma in monocots, whorl 2 comprises the petals in eudicots or the lodicules in monocots, whorl 3 contains the anthers and whorl 4 contains the pistil. Within whorl 4 there is also a discrete region that may be considered its own whorl, which contains the ovule(s). Homeotic transcription factors (TFs) containing a conserved MADS-box motif, thus known as MADS-box genes, play a critical role in plant development, as well as a variety of key regulatory roles in animals and fungi. The name “MADS” is derived from four of the initial transcription factors identified, MCM1 (*Saccharomyces cerevisiae*), AGAMOUS (*Arabidopsis thaliana*), DEFICIENS (*Antirrhinum majus*), and SRF (*Homo sapiens*; Theißen et al. 1996). MADS-box genes are expressed in different whorls of the floral meristem in a highly regulated manner that has resulted in their designation as Class A, B, C, D, E, or B_{sister} genes. Class A

TFs are expressed in whorls 1 and 2, Class B TFs are expressed in whorls 2 and 3, Class C TFs are expressed in whorls 3 and 4, Class D TFs are expressed in only whorl 4, Class E TFs may be expressed in any whorl, and B_{sister} genes are predominantly expressed in the ovule. Identity and complete formation of the floral organs of each whorl relies upon the correct combination of MADS-box genes, resulting in the palea and lemma forming in whorl 1, lodicules in whorl 2, the anthers in whorl 3, and the pistil in whorl 4 (reviewed by Jack 2001; Theißen et al. 2016). Many of the MADS-box genes involved in floral development have been identified and functionally characterised in rice (Arora et al. 2007; Yoshida and Nagato 2011), allowing putative orthologues to be identified/predicted in wheat (Murai 2013) and barley (Callens et al. 2018). Of particular relevance to ovule development are the Class C genes *MADS3* and *MADS58*, which contribute to pistil formation (Dreni et al. 2011), the Class D genes *MADS13* and *MADS21* (Dreni et al. 2007) and the B_{sister} genes *MADS29, MADS30* and *MADS31* (Callens et al. 2018; Lee et al. 2013), which influence ovule initiation and germline development, and the Class E genes *MADS1, MADS5, MADS6, MADS7, MADS8* and *MADS34* (Dreni and Zhang 2016; Favaro et al. 2003), which are key components of most MADS-box protein complexes. Studies have indicated that MADS expression is not exclusive to the early stages of floral meristem development, suggesting that specific MADS genes may fulfil additional functions in growth and development in different stages and tissues (e.g. *STK/MADS13*; Mizzotti et al. 2014). Whether this is the case in barley has yet to be determined (Callens et al. 2018).

Auxin signalling genes

Similar to the MADS-box transcription factors, modulation of gene expression by auxin signalling plays a key role in ovule and flower development in a range of species (Shirley et al. 2018). Auxin is the general term for a class of plant hormones (characterised by an aromatic ring and a carboxylic acid group), the most abundant and potent member of which is indole-

3-acetic acid (IAA; Haagen-Smit et al. 1946; Kaethner 1977; Thimann 1958). In Arabidopsis, the auxin biosynthetic pathway involves conversion of tryptophan into indole-3-pyruvic acid (IPA), itself an auxin, which is then converted into IAA. Production of IPA is achieved by the combined action of TRYPTOPHAN AMINOTRANSFERASE OF ARABIDOPSIS (TAA1) and two TRYPTOPHAN AMINOTRANSFERASE RELATED genes (TAR1 and TAR2), while the conversion of IPA into IAA is catalysed by members of the YUCCA flavin monooxygenase-like enzyme family (Cheng et al. 2006; Stepanova et al. 2008; Won et al. 2011). Due to the chemical nature of auxin, direct observation of its short- and long-range movement is not currently possible, and as such, while it is proposed that movement occurs both actively and passively, the complete mechanisms of auxin transport are yet to be fully described. However, to counter the difficulty of directly observing auxin, activity of auxin responsive genes and abundance of transport proteins have been observed using fluorescent reporters (Chettoor and Evans 2017; Friml 2010; Yang et al. 2017). This has allowed inference of the fluctuation of auxin abundance in tissues over time. Models based on mutational studies indicate that ATP-BINDING CASSETTE SUBFAMILY B (ABCB) and PIN-FORMED (PIN) proteins are involved in active cellular IAA efflux of IAA (Carraro et al. 2006; Cho et al. 2007; Noh et al. 2001), while active cellular IAA import is facilitated by AUXIN1/LIKE AUX1 (AUX1/LAX) transport proteins (Swarup et al. 2008). Under low auxin conditions, AUXIN RESPONSE FACTOR (ARF) proteins are bound by AUXIN/INDOLE-3-ACETIC ACID INDUCIBLE (Aux/IAA) family proteins in a repressive manner (Tiwari et al. 2004; Ulmasov et al. 1999). TRANSPORT INHIBITOR RESPONSE 1/AUXIN SIGNALING F-BOX (TIR1/AFB) proteins are activated by cellular accumulation of auxin, and mediate degradation of Aux/IAA proteins, which effectively relieves repression of ARF function (Dharmasiri et al. 2005; Parry et al. 2009). The current model of auxin biosynthesis and transport within the developing ovule of Arabidopsis includes synthesis of IPA in the most basal nucellus / chalaza region and activity of YUCs, PIN1 and ARFs at the very distal tip of the nucellus at developmental stages between MMC and FG8. IAA may also be synthesised in the tip of the inner integument at stages after

FG1 (Crhak Khaitova et al. 2015; Larsson et al. 2013; Shirley et al. 2018). Mutants with overactive and defective auxin biosynthesis and transport exhibit compromised reproductive development, with ranging severity, including loss of antipodal cell proliferation in maize (Chettoor and Evans 2015) and defective embryo sac formation in Arabidopsis (Pagnussat et al. 2009). As such, it has been suggested that tight regulation of auxin biosynthesis and transport plays an important role in female reproductive development, recently summarised in several reviews (Larsson et al. 2013; Shirley et al. 2018).

Pectin-dependent cell wall remodelling during development

One of the mechanisms by which auxin signalling has been found to influence female reproductive development in Arabidopsis is by mediation of the pectin methylesterification status of cell walls (Andres-Robin et al. 2018). Pectin is a general term used to describe polysaccharide chains that are predominantly α-(1,4)-linked galacturonic acid, with a varying degree of sidechain substitution (O'Neill et al. 1990). Specific pectins include apiogalacturonan (AGA), homogalacturonan (HG), rhamnogalacturonan I and II (RG-I and RG-II), and xylogalacturonan (XG). Each of these types of pectin are distinguished by the other hexose present, and have different mechanical/structural properties and contribute different functionalities to the cell wall (reviewed by Ridley et al. 2001; Vincken et al. 2003). Of these, HG is the most well-studied. Longstanding models indicate that HG is synthesised and decorated in the Golgi apparatus, before vesicular transport and integration into the cell wall (Goldberg et al. 1996). Following synthesis by galacturonosyltransferases (GAUTs; Atmodjo et al. 2011), HG chains are methylesterified and acetylesterified on the carboxylic acid groups of the GalA backbone (Mouille et al. 2007), in a pattern that is highly regulated with respect to developmental processes and tissue identity (Tucker et al. 2018). Pectin methyltransferases decorate HG, which reduces the capacity of carboxylic acid groups on each GalA residue to interact with calcium ions present in the cell wall, meaning that the individual methylesterified

HG chains are prevented from crosslinking and forming a regular, densely packed matrix. Removal of methyl ester groups is performed by pectin methylesterase (PME) enzymes, allowing interaction with calcium ions, formation of a dense pectinaceous matrix, thereby conferring rigidity to the local cell wall region (Hongo et al. 2012; Morris et al. 1982). Alternatively, in the absence of calcium, de-methylesterified HG may be hydrolysed by endo-polygalacturonases (PGs), causing the plant cell wall structure to be degraded and thus become more flexible (reviewed by Cosgrove 1999; Wolf and Greiner 2012), and release short chains of HG known as oligogalacturonic acid (OGA), which may interact with auxin signalling pathways (Branca et al. 1988; Spiro et al. 2002). Activity of PMEs is regulated by pectin methylesterase inhibitors (PMEIs), and both PMEs and PMEIs are sensitive to pH fluctuation in the local cell wall (Sénéchal et al. 2017; Sénéchal et al. 2015). Methylation status of HG plays a regulatory role in organogenesis of floral organs (Peaucelle et al. 2008) and has been observed to be tightly regulated within different tissues of the ovule by immunolabelling in other species (Lora et al. 2017).

In summary, ovule development leads to the formation of distinct tissues that are essential for floral fertility and seed production. Function of these tissues depends upon a range of inputs, including MADS-box homeotic transcription factors, auxin signalling components, and the constant modification of cell wall properties to allow rapid cell proliferation to occur with the correct physical proportions. Much of this has been described in Arabidopsis, and to some extent in rice and maize, however morphological and transcriptional data is lacking in the *Triticeae* cereal crops such as barley. Here, we describe the morphological and transcriptional dynamics of barley ovule development in four distinct barley genotypes. Morphological features and cell wall modifications were analysed using cleared whole-mounted pistil tissue and immunostained thin sections, revealing discrete stages of reproductive development and differential cell wall modification within discrete sub-domains of the nucellus. RNA sequencing data from whole-pistil tissues collected throughout development was analysed in combination

with RNA sequence data from specific ovule tissues, collected using laser capture microdissection, to explore expression of genes involved in networks known to regulate floral development in other species, including MADS-box homeotic transcription factors and auxin biosynthesis.

Methods

Plant growth – 10 genotypes of interest and Sloop

Barley plants were grown in glasshouses at The Plant Accelerator, Adelaide, Australia, in a 50:50 cocopeat:clay-loam soil mixture (v/v), under 22°C day / 17°C night conditions. All genotypes used in this study were two-row spring barleys, and were grown in quintuplicate. Sloop is an elite malting genotype adapted to Australian conditions that has previously been used to study gene expression during grain development (Zhang et al. 2016). The remaining genotypes, including Akita, Cecilia, Forum, Foxtrot, Gant, Host, Lina, Optic, Salka and Wren, were part of an association panel provided by Prof Robbie Waugh (JHI, Scotland) and imported to Australia in 2013.

Collection of floral tissue for ovule morphological analysis, immunostaining and whole-pistil RNA sequencing

The Waddington scale (Waddington et al. 1983) was used to stage barley florets during spike development. For the genotypes Akita, Cecilia, Forum, Foxtrot, Gant, Host, Lina, Optic, Salka and Wren, florets were collected from the middle of tillers at Waddington Stage 7 until fertilisation. For each genotype, spikes at equivalent developmental stages were sampled from at least three of the five plants grown. Tissue collected from each spike was prepared for three end uses: clearing for morphological analysis, immunostaining, and whole-pistil RNA sequencing. This collection method enabled the developmental stage of each sample to be

determined by clearing prior to RNA extraction, allowing a more precise comparison of genotypes. To enable clearing, tissue was fixed in FAA (10% formalin, 5% glacial acetic acid, 50% ethanol, 35% millipore H_2O, plus a drop of Triton X100), dehydrated through an ethanol series (3 x 30mins at each of 70%, 80%, 90%, 95%, 100%) and placed into Hoyer's Solution (Wilkinson and Tucker 2017). Five samples were collected from each spike. At stages prior to Waddington Stage 8.5 whole florets were collected; for samples after this stage only the pistil was collected. After sampling and handling error, at least 10 samples were collected at each stage, from each genotype. To enable immunostaining, tissue was fixed in TEM fixative (4% paraformaldehyde, 0.25% glutaraldehyde, 4% sucrose, in phosphate buffered saline at pH 7.2), dehydrated in an ethanol series (3 x 30mins at each of 70%, 80%, 90%, 95%, 100%) and transitioned into LR White resin (ProSciTech, Australia) with overnight incubations in 50:50 100% ethanol:LR White resin then 100% LR White resin, before embedding in LR White resin, in gelatin capsules at 56°C for 72 hours. Three whole florets were prepared from each spike for immunostaining. To enable RNA sequencing, dissected pistils were frozen in liquid nitrogen and stored at -80^{o}C. At stages prior to Waddington Stage 8.5, ten pistils were collected from each spike; at later stages, five pistils were collected. In sum, for each genotype, and at all developmental stages assessed, a minimum of fifteen pistils were prepared for clearing, nine florets were prepared for immunolabelling, and either five or ten pistils were frozen for RNA extraction.

Analysis of cleared barley ovules during development

Ovules within the cleared carpel tissue were captured as z-stack images using differential contrast microscopy (DIC) on a Zeiss AxioImager M2, and analysed using Zeiss Zen Blue (2012) software (Carl Zeiss AG, Germany), as described in Wilkinson and Tucker (2017). Ovules were separated into nine reproductive developmental stages, called Stages 0 - 9, based on ovule morphology. From reproductive Stage 5 onwards (correlating to Waddington Stage 8.75) nine morphological traits were measured: ovule area, ovule transverse, ovule

longitude, embryo sac area, embryo sac transverse, embryo sac longitude, nucellus area, nucellus proportion and integument width. The ovule area trait was measured as the sum of embryo sac area and nucellus area, and did not include the integuments as it was not possible to reliably distinguish the outer integument layer from the locule. At all earlier developmental stages, ovule area was measured as the integuments plus the nucellus, because it was not possible to accurately separate them due to ovule curvature. Composite images for figures were generated to represent the key information captured by z-stack imaging using Adobe Photoshop and Illustrator (Adobe Inc., USA).

Immunostaining

LR-white embedded samples were sectioned at 0.8µm using a diamond knife with a Leica UM6 Ultramicrotome (Leica microsystems, Germany) and placed on poly-Lys coated glass slides (ProSciTech, Australia). Immunolabelling was performed as described by Betts et al., 2017. Primary antibodies included Rat LM19 monoclonal IgG which detects homogalacturonan (PlantProbes, UK), Rat LM20 monoclonal IgG that detects methyl-esterified homogalacturonan (PlantProbes, UK) and mouse BG1 that detects 1,3;1,4-β-glucan (BioSupplies, Australia). Secondary antibodies used included AlexaFluor 555 anti-rat monoclonal IgG and AlexaFluor 488 anti-mouse monoclonal IgG (ThermoFisher Scientific, USA). Immunolabelled sections were imaged using a Zeiss AxioImager M2. Immunolabelling of three replicate sections were used to quantify each ovule trait measured.

RNA extraction from whole barley pistils

Using tissue clearing and DIC microscopy, as per above, samples at equivalent developmental stages were selected from four genotypes: Forum, Gant, Salka and Wren. For each genotype, RNA was extracted from two replicate samples at each of five developmental stages. These stages, called 3, 4, 5, 6, and 7, were collected from florets of Waddington Stage 7.5 to Waddington Stage 9.5, and cover, with respect to reproductive development, a timepoint

shortly after selection of the functional megaspore until anthesis. RNA was extracted using the SpectrumTM Plant Total RNA kit (Sigma-Aldrich, Germany). RNA was treated with Ambion® TURBO DNA-*free*™ Post DNase kit (Life Technologies Corporation, USA). Poor RNA quality precluded sequencing of four samples. These samples were from: Forum at Stage 3, Salka at Stage 3, and Wren at Stages 5 and 7.

cDNA synthesis of RNA extracted from whole barley pistils

cDNA was synthesised from RNA extracted from all whole-pistil samples as described by Burton et al. (2008) with the SuperScript®III Reverse Transcriptase kit (Invitrogen, USA). qPCR was performed as described by Burton et al. (2008).

Primer design

Primers for HvMADS13 were designed to encompass a portion of the coding sequence, the stop codon, and the 3' untranslated region using Primer3 (v.0.4.0; (Untergasser et al. 2012). The sequences of the primers used were, forward: TCAGCTGAACCTAGGCTGC; reverse: TTTGACAGGAATAGTTGAGTACTGGT. Primers used for the housekeeping genes glyceraldehyde 3-phosphate dehydrogenase (HvGAPDH; HORVU7Hr1G074690), cyclophilin (HvCycl; HORVU6Hr1G012570), α-tubulin (HvTub; HORVU1Hr1G081280) and heat shock protein 70 (HvHSP70; HORVU5Hr1G113180) were determined as described by Burton et al (2004), and were as follows: HvGAPDH forward: GTGAGGCTGGTGCTGGATTACG; HvGAPDH reverse: TGGTGCAGCTAGCATTTGAGAC; HvCycl forward: CCTGTCGTGTCGTCGGTCTAAA; HvCycl reverse: ACGCAGATCCAGCAGCCTAAAG; HvTub forward: AGTGTCCTGTCCACCCACTC; HvTub reverse: AGCATGAAGTGGATCCTTGG; HvHSP70 forward: CGACCAGGGCAACCGCACCAC; HvHSP70 reverse: ACGGTGTTGATGGGGTTCATG.

Quantitative polymerase chain reaction

qPCR was performed as described by Burton et al. (2008) using the primers for HvMADS13 described above for all RNA samples extracted from whole pistils. Control genes were used to normalise data as described by Vandesompele et al. (2002).

Laser Capture Microdissection of specific ovule tissues

Whole flowers were collected from the reference barley cv. Sloop at approximately Stages 8, 8.75 and 9.5 on the Waddington Scale, corresponding to reproductive Stages 4, 5, and 7, which describe ovules at FG2-4, FG8, and Anthesis. For laser microdissection, the protocol described in Okada et al. (2013) was followed. Samples were fixed in an ice-cold mixture of 3:1 ethanol:acetic acid with 1mM 1,4-Dithiothreitol (DTT). Samples were stored at 4°C overnight, then transferred into 70% ethanol and stored at -20°C. Samples were dehydrated through an ethanol series (70%, 80%, 90%, 95%, 100%), and were gently agitated in each solution for at least 30 minutes. Each ethanol solution was prepared with 1mM DTT and kept ice-cold. Samples were infiltrated with BMM resin (composed of 40mL n-butyl methacrylate, 10mL methyl methacrylate, 250mg benzoin methyl ether (ProSciTech, Australia), and 1mM DTT), diluted with ethanol in a 1:3, 1:1, 3:1 ratio of BMM:ethanol over two days before being placed in pure BMM resin. Samples in BMM resin were placed in BEEM capsules (ProSciTech, Australia) for embedding, and kept in a Cryo Chamber under UVlight at -20°C for five days to allow polymerisation (Koltunow Lab, CSIRO, Adelaide). Embedded tissue was serially sectioned in a transverse aspect at 3µm, and all sections from the base of the ovule to the most apical integument cells were collected. Sectioning was performed on a Leica UM6 Ultramicrotome (Leica microsystems, Germany) with a glass knife. Sections were placed onto DEPC-treated water droplets on PEN-membrane glass slides (Thermo Fisher Scientific, USA) and evaporated using a 36°C slide warmer.

Prior to laser capture, BMM resin was removed from tissue sections by gently rinsing slides in acetone (Sigma) for 10 minutes. Various tissues were collected from each ovule using a Leica LMD Laser Dissection Microscope (Leica microsystems, Germany) at the Waite Adelaide Microscopy Facility. In total, 15 different samples were collected across three stages of ovule development. Tissues dissected from the most immature ovule (Stage 4) included: 1. Embryo Sac plus Nucellus, 2. Integument and 3. Ovary Wall. Tissues dissected from the Stage 5 ovule included: 1. Whole Embryo Sac, 2. Egg Apparatus (Egg and Synergid Cells) plus the Central Cell, 3. Antipodal Cell Cluster, 4. Nucellus, 5. Integuments, and 6. Ovary Wall. Tissues dissected from the anthesis-stage ovule included: 1. Egg Apparatus plus Central Cell, 2. Antipodal Cell Cluster, 3. Nucellus, 4. Integuments, 5. Chalaza, and 6. Ovary Wall.

RNA extraction, amplification and cDNA preparation from laser-dissected samples

Total RNA was extracted from each laser-dissected tissue sample using the Picopure RNA isolation kit (Molecular Devices, USA), with DNase I. Concentration and integrity of the resulting RNA was assessed by a NanoDrop One (Thermo Fisher Scientific, USA). The total RNA was amplified twice with the MessageAmp II aRNA Amplification kit (Thermo Fisher Scientific, USA).

RNA sequencing and transcript analysis

All RNA samples were sent to the Australian Genome Research Facility for sequencing on the Illumina Hiseq platform. Reads were assembled using the current barley reference genome (Mascher et al 2017) with CLC Genomics (Qiagen, Netherlands), and normalised to the previously mentioned housekeeping genes HvGAPDH, HvHSP70, HvTub and HvCycl. Normalised read counts (transcripts per million, TPM) were used to reflect the abundance of each gene in each sample. Gene names are annotated as HORVUs, as per the International Barley Sequencing Consortium (IBSC 2012).

Results

Developmental progression of ovule development in barley

Following analysis of inflorescence tissue across a time course, nine distinct stages of ovule development were discernible in cleared floral tissue using DIC microscopy, shown in Figure 5-1. In brief, Stages 0 through to 3 encapsulate outgrowth of the initial ovule primordium, megasporogenesis and integument growth (Figure 5-1A-D), Stages 4 through to 6 involve rapid cellular proliferation and expansion within the nucellus and embryo sac (Figure 5-1E-G), Stage 7 represents the mature, reproductively competent ovule at anthesis (Figure 5-1H), and Stage 8 represents the fertilised ovule (Figure 5-1I). This series of stages corresponds to the span of stages 6 to 10 on the Waddington scale, commonly used to assess floral development in barley and wheat (Waddington et al. 1983). Further details of each developmental stage are described in the following sections.

Stages 0 to 3: Ovule initiation, megasporogenesis and early female gametophyte development

Stage 0, “Ovule Initiation”, represents the initial stage of ovule development characterised in this study. At this stage the ovule is detected as a small protrusion of nucellus tissue extending out at a slight angle from the placental/carpel tissue, at the base of which the inner integument layer is just beginning to form (Figure 5-1A). Stage 0 correlates approximately to Stage 6 of the Waddington scale. Using the clearing method described in Chapter 3 it was not possible to indubitably or consistently identify an archesporial cell/megaspore mother cell at this stage, however a region containing an enlarged cell at the tip of the nucellus was often visible.

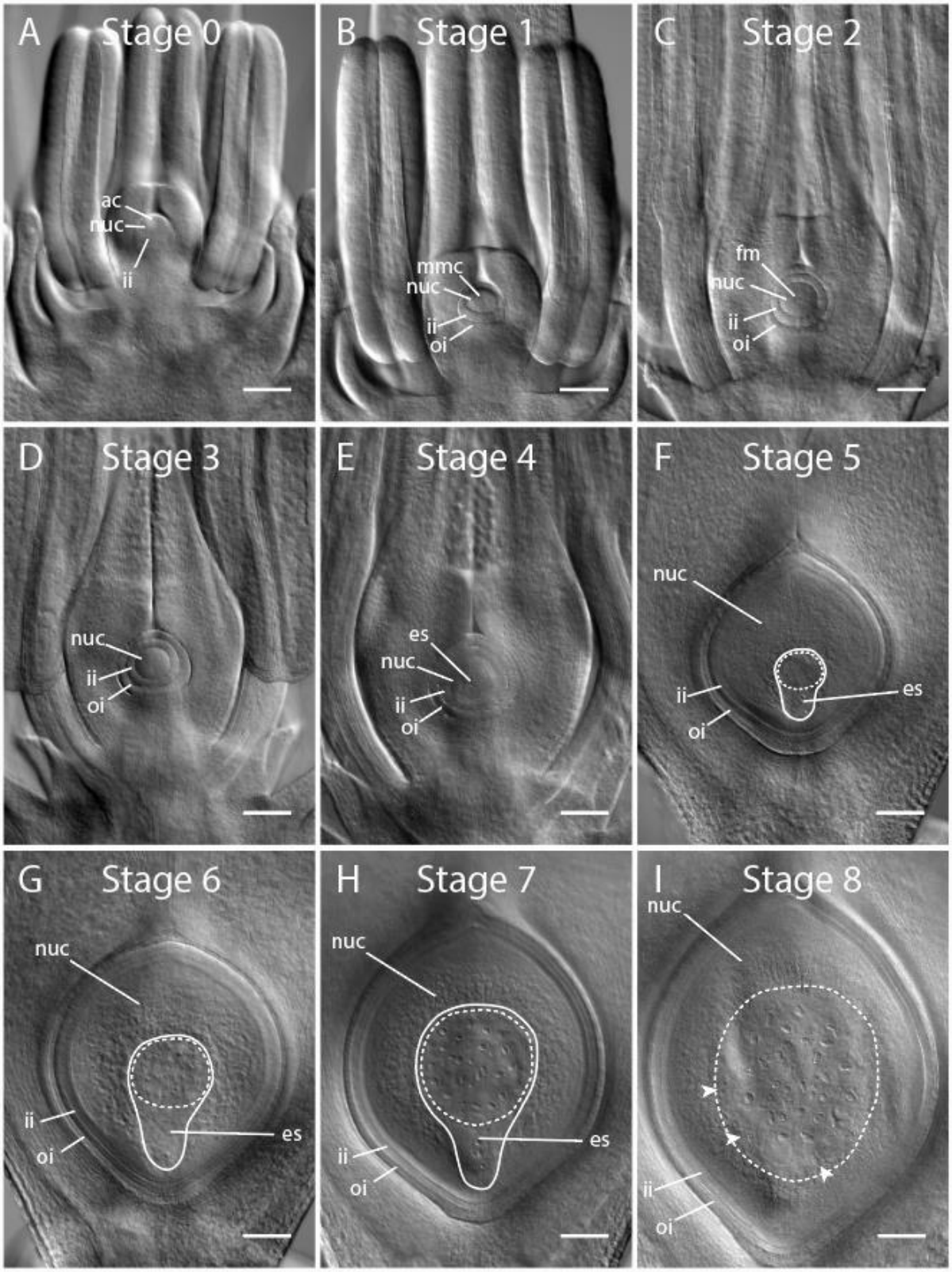

Figure 5-1: Female reproductive development of barley described in nine stages. (A) At Stage 0 the ovule is initiated from the ovule primordia by the selection of an archesporial cell and growth of the integuments; (B) at Stage 1 the selection of the megaspore mother cell (MMC)

develops from the archesporial cell; (C) at Stage 2 the MMC undergoes meiosis, giving rise to four haploid daughter cells, of which the single most chalazal survives and is known as the functional megaspore (FM); (D) at Stage 3 the FM undergoes several rounds of mitosis to form the cells that will become the embryo sac (ES); (E) at Stage 4 the integument has closed over the nucellus thus forming the micropyle, and the ES has cellularised, containing, arranged from proximal to the micropyle to most basal, two synergid cells, an egg cell, a central cell that contains the two polar nuclei, and at least three antipodal cells; (F) at Stage 5 growth of the ovule is driven by cell proliferation and expansion in the nucellus, and the antipodal cells proliferate to become a group of 15 to 45 small and tightly clustered cells; (G) at Stage 6 growth of the ovule is driven by cell proliferation and expansion within the nucellus and embryo sac, and the antipodal cells are distinctly less tightly clustered; (H), at Stage 7 the ovule reaches anthesis, or reproductive maturity, discernible from Stage 6 by both greater nucellus and embryo sac areas, and greater spacing of the antipodal cell nuclei; (I) at Stage 8 the ovule is fertilised, as determined by a combination of a further increase in ovule traits, visibility of extra pollen nuclei, lack of visibility of the polar nuclei, irregular nuclear shapes of antipodal cells, and clusters of small nuclei at the periphery of the embryo sac. ac = archesporial cell; es = embryo sac; fm = functional megaspore; ii = inner integument; mmc = megaspore mother cell; oi = outer integument; nuc = nucellus. Solid line indicates bounds of embryo sac, dashed line indicates bounds of antipodal cell cluster, arrowheads indicate additional clusters of nuclei after fertilisation. Images from the genotype Salka. Scale bars = 100µm.

Stage 1, “MMC”, represents the appearance of an enlarged megaspore mother cell (MMC), a single cell located in the sub-epidermal nucellus layer at the distal tip of the ovule primordia. This is the primary female germline cell (Pinto et al. 2019). At this stage the inner and outer integuments have both begun to differentiate forming rings around the base of the nucellar projection, and the nucellus appears to be tenuinucellate (containing a single-layered nucellar epidermis directly adjoining the MMC; Figure 5-1B). The pistils of ovules at this developmental stage resemble Waddington Stage 7.

Stage 2, “Meiosis”, represents the stage at which the megaspore mother cell undergoes meiosis. The pistils of ovules at this developmental stage resemble Waddington Stage 7.5. Cells containing enlarged nuclei appear to be visible at the distal tip of the ovule primordia and the integument layers extend to cover half the length of the projecting nucellus (Figure 5-1C). The nucellar projection itself is distinctly more angled away from its almost “upright” position with respect to the stigma, such that the inner integument is visible over the tip of the projection when the floret is viewed from the angle as shown in Figure 5-1. In terms of other floral organs, at this point the palea almost completely obscures the stigma, and the anthers elongate to nearly double their previous length.

Stage 3, “Mitosis”, represents the stage when megasporogenesis is complete and the functional megaspore has initiated megagametogenesis. Pistils at this stage of development resemble those between Waddington Stages 7.5 and 8. Due to the curvature of the ovule, more precise staging with regard to which phase of mitosis, or how many rounds of mitosis have occurred, was not possible using DIC microscopy and cleared wholemount floral tissue. At the distal tip of the nucellus, distinct cell walls mark the region of the nascent embryo sac. Integuments are in a similar position to Stage 2, extending slightly further around the nucellus but still leaving a large portion of the distal tip exposed (Figure 5-1D). By this stage the tip of the developing ovule, soon to form the micropyle, extends from the carpel at approximately a

90^{o} angle with respect to the stigma, i.e. it has become hemianatropous. This rotation from almost-upright to perpendicular generates asymmetry in the transverse aspect, visible in the sagittal aspect, as the ring of integument layers keeps pace with the growth and rotation of the distal tip, thus there is more integument on the “top” side (closest to the stigma) of the ovule.

Stages 4 to 7: Gametophyte maturity and ovule maturation

Stage 4, “Established Female Gametophyte”, represents the point at which a mature Polygonum-type female gametophyte has formed, as it is described in a range of model dicots such as Arabidopsis. At this stage the pistil resembles Stage 8 on the Waddington Scale. The female gametophyte exists as an embryo sac with at least 8 haploid nuclei within at least 7 cells. These cells are the egg cell, two synergid cells, the central cell containing two unfused polar nuclei, and at least three antipodal cells. By this stage the integuments have completely covered the nucellus, the inner integuments meeting to form the micropyle at the very distal tip of the ovule (Figure 5-1E). The micropyle is angled such that it now points more towards the base of the floret. This suggests it is transitioning from a hemianatropous position to an anatropous position.

Stage 5, “Antipodal Proliferation”, represents the point at which a massive proliferation of antipodal cells and expansion of the nucellus tissue has occurred. At this stage the pistil resembles Waddington Stages 8.5 to 8.75. Within the ovule, the antipodal cells form a distinct group of between 15 to 45 cells tightly clustered near the rest of the embryo sac cells (implying that the central cell is quite small), the ovule roughly doubles in overall size (see also: Figure 5-2), and the nucellus tissue and epidermal nucellus layer that flank the embryo sac undergo divisions such that the embryo sac is surrounded by at least two layers of nucellus at all points

other than the micropyle, i.e. the ovule becomes partially crassinucellar (Figure 5-1F). The position of the micropyle indicates that the ovule has become anatropous.

Stage 6, “Antipodal Expansion”, represents the stage where the antipodal cells have expanded from a tight cluster of cells into a group of much larger cells occupying the central region of the ovule, when viewed from the aspect as shown in Figure 5-1, making the shape of the embryo sac somewhat resemble a lightbulb (Figure 5-1G). The antipodal cells appear to be located along the “chalazal” side of the central cell. Notably, despite occupying a much greater region of the ovule, the nuclei of the antipodal cells do not appear to have increased in size. Between Stage 5 and Stage 6 the ovule once again increases approximately 50% in size and the pistil resembles Waddington Stages 9 to 9.25.

Stage 7, “Anthesis”, represents the stage at which the ovule is reproductively mature, and coincides with anther dehiscence (Figure 5-1H). The differences between Stage 6 and Stage 7 include an increase in ovule area by approximately 50% as compared to Stage 6 (Table 5-1), and the antipodal cell nuclei are more dispersed and much larger, meaning the embryo sac area is also increased and indicating that the antipodal nuclei have likely undergone endoreduplication. With the method used it was not possible to determine the area of the central cell, however as the antipodal cells are located along the flank of the central cell it is likely that central cell has expanded in proportion. This stage is equivalent to Stage 9.5 of the Waddington scale.

Stage 8: Post-fertilisation

Simply for the purposes of this study, Stage 8, “Fertilisation”, represents any ovules that were collected after fertilisation (Figure 5-1H). Fertilised ovules may include any of the following

phenotypic features: lack of distinct nuclei in the egg apparatus region, a single fused nucleus in the central cell, three nuclei in the central cell, non-spheroid antipodal nuclei, even-numbered clusters of small nuclei appearing at the edge of the embryo sac in the region where the polar nuclei would normally sit, and exaggerated elongation of the ovule. On the presented scale, Stage 8 is equivalent to Stage 10 on the Waddington scale.

In summary, using wholemount clearing and DIC microscopy, barley ovule development was divided into nine stages, called Stages 0 to 8. These stages were subsequently used to investigate variation in the relative size of embryo sac, nucellus, and overall ovule area among different genotypes showing variation in ovule traits at maturity (see Chapter 4).

Table 5-1: Quantification of five traits of ovule morphology in four barley genotypes with diverse mature morphologies, over six stages spanning initiation of the female reproductive lineage (Stage 2) to reproductive maturity (Stage 7).

Tissue	Stage	Forum	Gant	Salka	Wren
Ovule Area	2	5091.3 ± n/a	4982.3 ± 472.8	5270.6 ± 440.5	3307 ± 416.5
	3	9283.9 ± 3578.1	7463.8 ± 2179.5	6994.1 ± 1416.2	7252.1 ± 1879
	4	13890.6 ± 4686.2	17756.7 ± 5699.4	9974.2 ± 1727.7	14726.1 ± 6239
	5	61136.2 ± 20050.3	45275.7 ± 19816.6	72731.9 ± 24513.9	49503.3 ± 17302.7
	6	146006.5 ± 11843.2	134300 ± 34752.1	136426.9 ± 14316.6	133005.9 ± 25592.6
	7	160728.4 ± 20500.1	190807.8 ± 22657.3	200041.9 ± 14047.9	203119.9 ± 19874.5
Nucellus Area	2	5091.3 ± n/a	4982.3 ± 472.8	5270.6 ± 440.5	3307 ± 416.5
	3	9283.9 ± 3578.1	7463.8 ± 2179.5	6994.1 ± 1416.2	7252.1 ± 1879
	4	13890.6 ± 4686.2	17756.7 ± 5699.4	9974.2 ± 1727.7	14726.1 ± 6239
	5	54848.1 ± 17840.1	39949.5 ± 16306.2	63029.5 ± 19530.8	43723.8 ± 14191.4
	6	115120.6 ± 8231.1	98807 ± 22173.6	106537.2 ± 10527.5	102732.5 ± 15845.9
	7	115275.7 ± 15867.1	123623.6 ± 7262.1	134873.1 ± 8471.8	128484.5 ± 9665.8
Embryo Sac Area	5	6288.1 ± 3040.1	5326.3 ± 3848.2	9702.5 ± 5331	5779.5 ± 3242.3
	6	30885.9 ± 7720.4	35492.9 ± 13192.3	29889.7 ± 4744.5	30273.4 ± 10579.6
	7	45452.7 ± 5557.2	67184.2 ± 17216.4	65168.8 ± 11717.1	74635.3 ± 15221.5
Nucellus Proportion	5	0.897 ± 0.89	0.882 ± 0.823	0.867 ± 0.797	0.883 ± 0.82
	6	0.788 ± 0.695	0.736 ± 0.638	0.781 ± 0.735	0.772 ± 0.619
	7	0.717 ± 0.774	0.648 ± 0.321	0.674 ± 0.603	0.633 ± 0.486
Integument Width	5	51.6 ± 1.3	52.9 ± 4.7	52.8 ± 2.8	50.3 ± 4.2
	6	48 ± 3	53.4 ± 2.6	48.7 ± 1.5	50.3 ± 1
	7	50 ± 1.3	49.5 ± 1.7	46.4 ± 1.9	46.5 ± 2.2

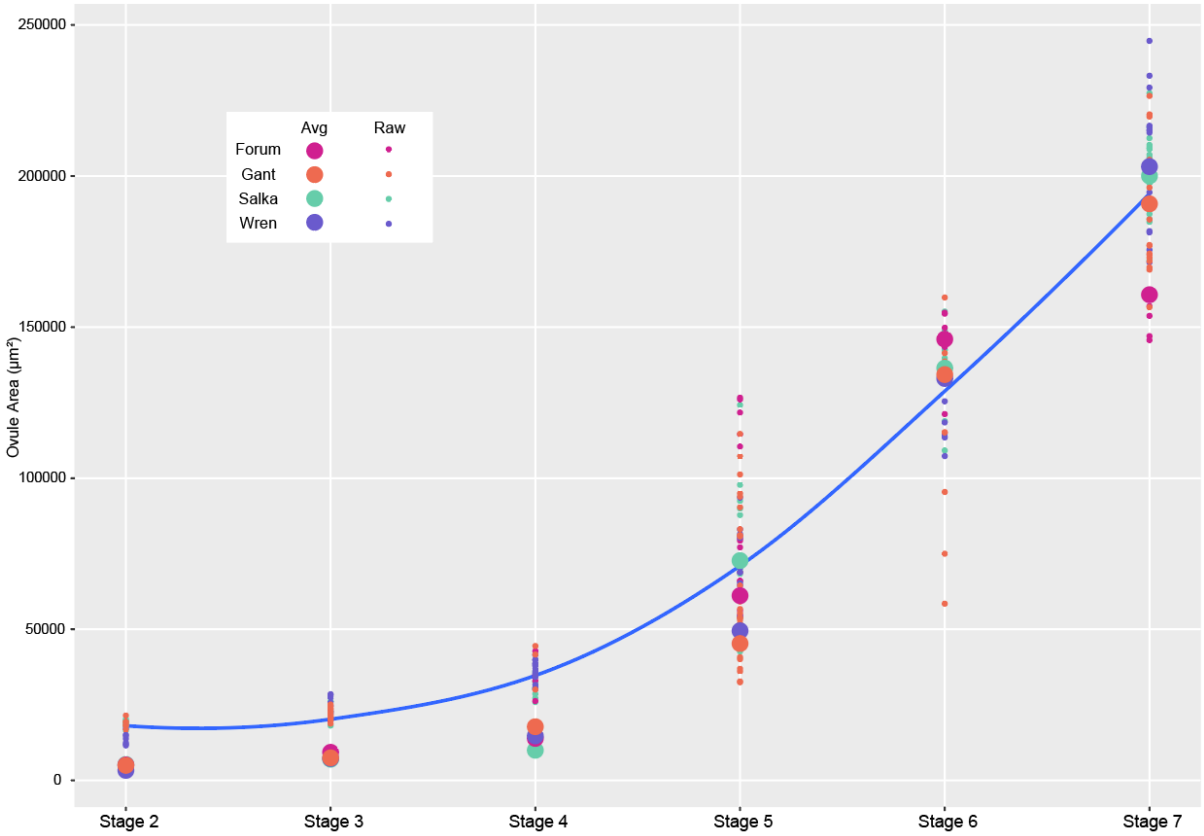

Figure 5-2: Change in ovule area (µm^2) at six stages (Stages 2 - 7) spanning initiation of the female reproductive lineage to reproductive maturity, as measured in four barley genotypes. Data for the genotype Forum is shown in pink, Gant in orange, Salka in green, and Wren in purple. The average value for each genotype at each developmental stage is indicated by a large circle, individual replicates are indicated by small circles. Blue line represents local regression curve calculated with the R ggplot2 package function geom_smooth, using data of all four genotypes.

Differences in ovule development between different genotypes are manifested at distinct developmental stages

Four genotypes were examined in detail, including Forum, Gant, Salka and Wren, in order to assess the development of ovule tissues among phenotypically variant genotypes. Forum and Gant represent genotypes that produce a smaller ovule at maturity compared to genotypes producing larger ovules, such as Wren and Salka (see Chapter 4). To assess the temporal variation in ovule development between these genotypes, measurements were compared from Stages 2 to 7 (Table 5-1; Figure 5-2). Samples were also collected for Stages 0, 1, and 8, but due to insufficient replicates, these were excluded from the analysis.

At Stage 2 the area of the ovule primordia in the smallest genotype (Wren, 3307.0µm^2) was 62.7% of the area of the largest genotype (Salka, 5270.6µm^2). At Stage 5, once the embryo sac had become established and the ovule had begun to undergo rapid proliferation and expansion, the ovule area of the smallest genotype at this stage (Gant, 45275.7µm^2) was 62.3% the size of the largest genotype (Salka, 72731.9µm^2). At Stage 5 the embryo sac was clearly visible, which allowed measurement of the nucellus and embryo sac in addition to total ovule area. At this stage, all four genotypes produced embryo sacs of similar area, occupying approximately 11% of the total ovule area.

Concurrent with an overall increase in ovule area between Stages 5 and 7, the proportion of embryo sac (relative to the ovule) in each genotype increased, demonstrating that expansion of the central cell and antipodal cells is likely to be a major contributor to the final mature ovule size. Further, as has previously been reported (Chapter 4), there was substantial variation in the contribution of the embryo sac to ovule area at Stage 7, ranging from 28.3% in Forum to 36.7% in Wren. Forum and Wren also presented the smallest and largest ovule area phenotypes at this stage, respectively, with Forum (160728.4µm^2) being 21% smaller than

Wren (203119.9μm^2). Despite ovules from Salka having a larger mature ovule area than those of Gant, the contribution of the embryo sac to ovule size in two genotypes was similar, 67% and 65% respectively, further supporting conclusions from Chapter 4 that embryo sac and nucellus development are independent processes.

Ovule area measurements from the four genotypes were plotted over time to assess growth dynamics during development (Figure 5-2). As discussed above, the different stages in each genotype were aligned based on morphological indicators such as the stage of germline development and integument growth. Hence, any differences in growth rate between genotypes should reflect inherent differences in size at the same developmental stage. The growth dynamic of all four genotypes was generally similar, with ovule size remaining relatively stable between Stages 2 to 4, and rapidly increasing from Stages 4 to 7. However, specific differences were identified between genotypes. For example, between Stages 4 and 5, ovule area in Forum increased much more rapidly than the other three genotypes. This difference was maintained until Stage 6, at which point the ovule area of Forum barely increased compared to Stage 7, contrasting with an increase in ovule area in the three other genotypes. Most notable of these was the increase in ovule area in Wren, which exhibited the smallest ovule size at both Stage 2 and Stage 6 but reached the largest size of all four genotypes by Stage 7. The area of embryo sac and nucellus tissue area also varied between genotypes over time, particularly in the final stage of development. However, when any two genotypes were compared, the variation at each stage with respect to the next was not consistent, meaning that the embryo sac and nucellus tissues of different genotypes do not grow at equivalent rates throughout ovule development.

In summary, these data indicate that genotype-dependent differences in ovule size at maturity arise at multiple stages of pistil development. Some genotypes, such as Salka, already show evidence of larger ovules at the primordial stage, while Wren only achieves a large size during

the rapid proliferation and expansion phase. By contrast, the smaller ovules of Gant and Forum produce intermediate-sized primordia that grow rapidly, but fail to maintain growth to the same degree as Wren and Salka.

Immunolabelling reveals discrete domains within the nucellus

A key question arising from the wholemount analysis is what drives the increase in ovule size; cell division, expansion or a combination of both? To observe the cellular arrangement of the ovule during growth, florets from the genotypes Forum, Gant, Salka and Wren were sectioned at three developmental stages: Stage 3 (Mitosis), Stage 5 (Antipodal proliferation), and Stage 7 (Anthesis). Transverse semi-thin sections (0.8µm) were generated in two regions of the ovule, cutting through the egg apparatus and antipodal cells. This enabled the integuments, nucellus and embryo sac to be compared at three distinct positions along the length of the ovule in the four genotypes. Cell nuclei and cytoplasmic contents were visualised by their autofluorescence in the DAPI channel (Zeiss FS 49), while cell walls were visualised by fluorescent immunolabelling of (1,3;1,4)-ß-glucan (BG), de-methylesterified homogalacturonan (LM19; Figure 5-3) and methylesterified homogalacturonan (LM20; Figure 5-4; negative controls Figure 5-S1). Visualisation of the cell walls and contents in replicate sections facilitated observation of the arrangement of the nucellus and embryo sac cells, and measurement of nucellus cell number. Observation of the ovule with semi-thin sections rather than whole-mount clearing yielded much more precise information about the organisation of ovule tissues. For example, autofluorescence in sections taken from all four genotypes indicated that the outer integument and inner integument have discrete properties; cells of the outer integument appeared mostly devoid of contents while cells of the inner integument were brightly autofluorescent.

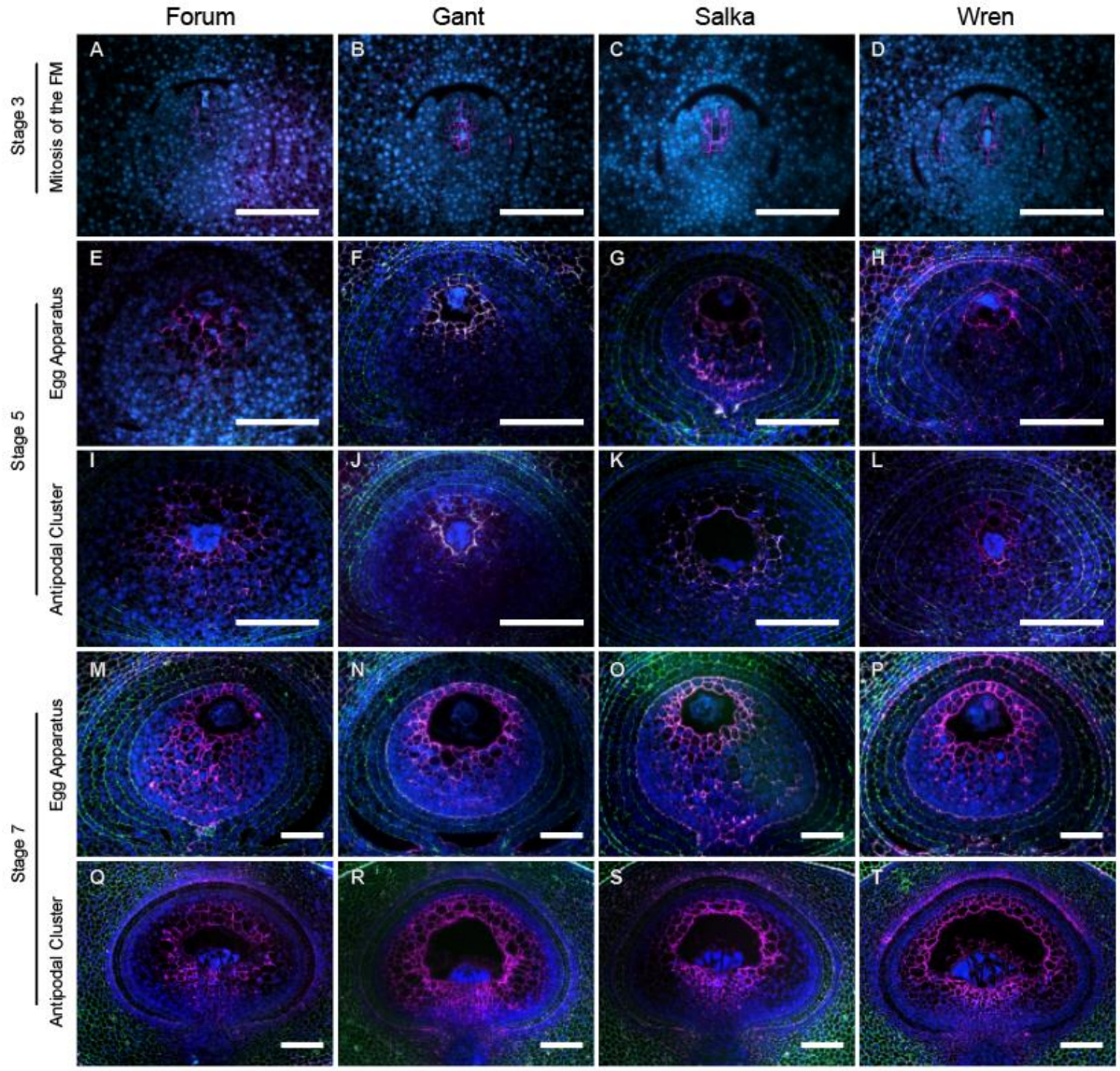

Figure 5-3: Immunolabelling of de-methylesterified homogalacturonan (pectin) and ß-(1,3;1,4)-glucan (BG) in the cell walls of barley ovules from four genotypes (Forum, Gant, Salka and Wren), at three stages of ovule development (Stages 3, 5 and 7). Labelling is shown in two different regions of the ovule at Stages 5 and 7. Pectin (magenta) was labelled with LM19, BG (green) was labelled with BG1, autofluorescence at 461nm is shown in blue. Sections were taken in the transverse aspect, with 0.8µm thickness. Scale bars = 100µm.

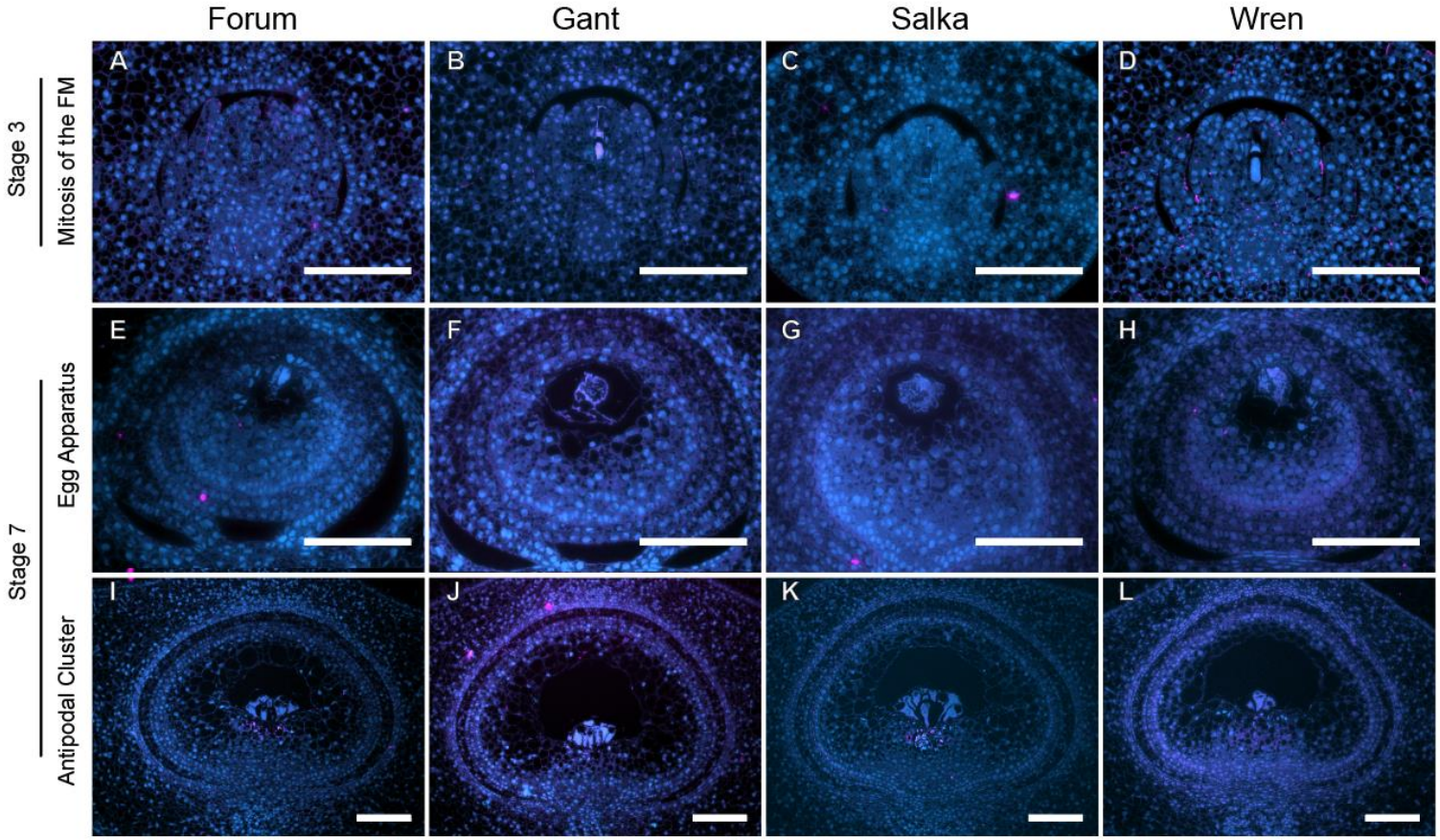

Figure 5-4: Immunolabelling of methylesterified homogalacturonan (pectin) in the cell walls of barley ovules from four genotypes (Forum, Gant, Salka and Wren), at three stages of ovule development (Stages 3, 5 and 7). Labelling is shown in two different regions of the ovule at Stages 5 and 7. Pectin (magenta) was labelled with LM20 , autofluorescence at 461nm is shown in blue. Sections were taken in the transverse aspect, with 0.8µm thickness. Scale bars = 100µ**m.**

Based on autofluorescence of the cellular contents and cell wall immunolabelling at Stages 5 and 7, the nucellus appears to consist of three discrete cell types: an epidermal layer, peripheral nucellus, and inner nucellus. The nucellar epidermis consists of a single, regularly organised layer of small cells with brightly autofluorescent cellular contents. The peripheral nucellus consists of relatively small, densely packed cells with brightly autofluorescent contents, starting near the chalaza and progressing around the whole ovule. The peripheral nucellus was the predominant cell type within all sections taken at Stage 3 (Figure 5-3A-D, Figure 5-4A-D), Stage 5 (Figure 5-3E-L), and through the egg apparatus plane at Stage 7 (Figure 5-3M-P, Figure 5-4E-H). The inner nucellus consists of large, vacuolated cells with irregular shape, which flank the embryo sac. This distinctive nucellus cell size and loss of cytoplasmic autofluorescence was observed at both Stage 5 and Stage 7, and was most evident in sections through the antipodal cell cluster in ovules at Stage 7 (Figure 5-3Q-T, Figure 5-4I-L). Finally, transverse sectioning confirmed that between Stage 5 and Stage 7 of reproductive development the barley ovule becomes crassinucellate, as multiple layers of nucellus were observed to surround the embryo sac as opposed to the single nucellus layer that defines tenuinucellate ovules.

Immunolabelling reveals discrete domains of differing pectin content within the nucellus

Different types of pectin have been associated with growth and development in diverse plant tissues, such as meristems (Iwai et al. 2002; Sobry et al. 2005) and ovules (Juranić et al. 2018; Lora et al. 2017) and can be detected using specific antibodies such as LM19 and LM20 (Verhertbruggen et al. 2009). These antibodies were used in immunolabelling assays to test for the presence and location of pectin epitopes in the growing barley ovule. Cell walls of the nucellus immediately flanking the embryo sac were specifically labelled with LM19 from its initiation (Stage 3; Figure 5-S2A) to maturity (Stage 7; Figure 5-S2B). At early stages of

development, represented here by Stage 3, the most prominent LM19 labelling was confined to nucellus cells within two cell layers flanking and three layers above and below the germline cells (i.e. the megaspore mother cell or the developing gametophyte). From Stage 5 onwards, labelling of nucellar cells with LM19 remained prominent in the two to three cell layers adjacent to the embryo sac, but additional weaker labelling was detected in inner nucellus cells located further away. Particularly at Stage 7, nucellus cells labelled with LM19 tended to match the inner nucellus phenotype, i.e. cells labelled with LM19 were located toward the centre of the ovule and tended to be large, vacuolated and irregularly shaped. Speckled LM19 labelling was also evident in the middle lamella between peripheral nucellus cells, and in cells at the junction of the chalaza, integuments and the "placental" region of the pistil where the ovule is attached. Notably, a near complete lack of LM20 labelling indicates that the pectin present is partially, if not completely, de-methylesterified (Figure 5-4).

Cell number and cell size contribute to variation in ovule area at anthesis.

Replicate transverse sections were used to measure the width of the carpel and the ovule, two-dimensional ovule area, and the total number of nucellus cells (Table 5-2, Table 5-3). To assess if there was any relationship between pectin labelling and ovule morphology, the number of LM19-labelled nucellus cells was also measured. To account for the variation in ovule shape at different points between its micropylar and chalazal ends, sections through the egg apparatus (region of the ES containing the egg cell and synergid cells) and the antipodal cell cluster were assessed. At Stage 3, ovule development involves asymmetric cell divisions causing a shift in orientation with respect to the orientation of the rest of the pistil. As such, the precise orientation of ovule sections was difficult to determine at Stage 3, thus only Stage 5 and Stage 7 were measured.

Table 5-2: Summary of data obtained from analysis of images taken following immunolabelling of pectin and ß-(1,3;1,4)-glucan in the cell walls of two regions of ovules at two developmental stages, in four barley genotypes.

Cultivar	Stage	Region	Ovule area (µm2)	Nucellus cell number	Area per cell (µm2)	Number of LM19-labelled cells	Proportion of nucellus with LM19 labelling (%)
Forum	5	Egg	30753.7 ± 3110.9	247.7 ± 14.8	124.2	81.3 ± 21.1	26.0
Gant	5	Egg	23789.3 ± 1684.3	217 19.9	109.6	56.7 ± 18.4	32.6
Salka	5	Egg	22265.2 ± 3438.6	195 26.5	114.2	132 ± 12.1	9.2
Wren	5	Egg	19534.2 ± 1828.5	141.7 11.9	137.9	72.3 ± 17.6	24.4
Forum	5	Antipodal	48017.2 ± 3027	396.7 29.2	121.1	185 ± 7.5	4.1
Gant	5	Antipodal	32667.5 ± 1053.6	303.3 12.1	107.7	87 ± 16	18.4
Salka	5	Antipodal	46913.7 ± 4094.6	328 27.9	143.0	182 ± 31.5	17.3
Wren	5	Antipodal	28288.5 ± 1249	217 3.6	130.4	105 ± 14.2	13.5
Forum	7	Egg	25430.3 ± 11051.9	283.3 94.4	89.8	205.7 ± 92.8	45.1
Gant	7	Egg	26974 ± 3206	286 24.9	94.3	238.7 ± 16.3	6.8
Salka	7	Egg	28952 ± 3158.2	333.7 44.8	86.8	280.7 ± 41	14.6
Wren	7	Egg	20031.1 ± 2975.7	213.7 19.5	93.7	151 ± 30.1	19.9
Forum	7	Antipodal	94118.6 ± 4572.4	635.3 33.9	148.1	342.3 ± 44.8	13.1
Gant	7	Antipodal	112599.5 ± 1495.5	736 19.5	153.0	479 ± 34.2	7.1
Salka	7	Antipodal	114690.6 ± 4383.2	697 43	164.5	394.7 ± 67.6	17.1
Wren	7	Antipodal	119680.1 ± 1981.8	773 14	154.8	727.7 ± 23.4	3.2

Table 5-3: Summary of data obtained from analysis of images taken following immunolabelling of pectin and ß-(1,3;1,4)-glucan in the cell walls of two regions of pistils at two developmental stages, in four barley genotypes.

Cultivar	Stage	Region	Carpel width (µm)	Ovule Width	Proportion of ovule to carpel
Forum	5	Egg	744.3 ± 16.8	326.4 ± 16.3	0.44
Gant	5	Egg	657.2 ± 8.3	265.2 ± 8.4	0.40
Salka	5	Egg	687.1 ± 27.4	292.4 ± 39.6	0.43
Wren	5	Egg	617.1 ± 23.6	246.5 ± 29.4	0.40
Forum	7	Antipodal	900.2 ± 18.3	452.6 ± 7.4	0.50
Gant	7	Antipodal	910.9 ± 3.4	468.2 ± 1.7	0.51
Salka	7	Antipodal	952.4 ± 6.3	524.7 ± 3.6	0.55
Wren	7	Antipodal	883.6 ± 10.2	510.6 ± 5.6	0.56

Slight variation of pistil width at anthesis was observed among the four genotypes, with the greatest proportion of ovule to pistil width (0.58) found in Wren and the smallest (0.50) found in Forum. At both Stage 5 and Stage 7, transverse area of the ovule was found to vary considerably between sections taken through the egg apparatus and the antipodal cell cluster. For example, in Forum at Stage 5 the ovule area at the plane of the egg apparatus was 30753.7± 3110.9μm^2, while at the plane of the antipodal cell cluster the ovule area was 48017.2 ± 3027.0μm^2, an increase of approximately 36%.

Generally speaking, both the ovule area and nucellus cell number of sections taken through the egg apparatus were similar between Stages 5 and 7. A decrease in ovule area at the egg apparatus from Stage 5 to Stage 7 in the genotype Forum may reflect a discrepancy in the angle at which the ovule was sectioned. Generally speaking, at Stage 5 the number of nucellus cells increased slightly in sections through the antipodal cell cluster as compared those through the egg apparatus, while the average area of nucellus cells was similar, indicating that the change in ovule area between these two different points of the ovule was likely driven by cell number. In contrast, at Stage 7 the number of nucellus cells was found to double between sections through the egg apparatus and the antipodal cell cluster, and the average area of nucellus cells increased by approximately 42%, indicating that, with respect to the contribution of the nucellus, the dramatic increase in ovule area previously observed between Stages 5 and 7 is driven by both cell number and cell expansion. Further, the lack of change in sections through the egg apparatus at each stage indicates that cell division and expansion occurs in nucellus cells located more centrally within the ovule, such as where the antipodal cell cluster is located, rather than at the micropylar tip.

At Stage 5, the genotypes with the greatest and least number of nucellus cells at the antipodal region of the ovule were Forum and Wren, respectively. Conversely, at Stage 7, the genotypes with the greatest and least number of nucellus cells at the antipodal region of the ovule were

Wren and Forum, respectively. Measurement of ovule area from the transverse plane could not be directly compared to area data collected from whole-mounted tissue, due to the difference in plane of viewing and the variation in ovule shape at different points throughout its structure. The proportion of nucellus cells labelled with LM19 varied substantially among genotypes, for example, among sections at anthesis through the antipodal cell cluster, 56.6% of nucellus cells were found to be labelled in Salka, compared to 94.1% labelled in Wren. The proportion of LM19 labelling tended to increase between Stage 5 and Stage 7. However, genotypic variation in the extent of LM19 labelling did not directly relate to ovule morphological variation observed among the four genotypes assessed.

Exploring the transcriptional landscape of the developing barley ovule

The differences in ovule development detected between genotypes Forum, Gant, Wren and Salka raised questions regarding genes that might be involved. The remarkable differences in overall ovule dimensions, component tissue proportions, cell number, cell size, and the timing of growth, provide a significant resource to investigate the molecular dynamics of barley ovule growth. Despite this, there is a general lack of information regarding the molecular details of pre-fertilisation ovule and pistil development in species such as barley and wheat. Some data is available for rice, where laser microdissection was coupled with microarrays to provide global transcriptional information across ovule development (Kubo et al. 2013) but this resource has limited usefulness in barley.

To address this gap, RNA sequencing (RNAseq) was used to generate transcriptional profiles from pistils at five stages of reproductive development, containing ovules ranging from Stage 3 to Stage 7. Moreover, profiles were generated from the four genotypes, Forum, Gant, Salka and Wren, which show differences in ovule morphology across development and at maturity. The RNAseq data corresponded directly to the stages analysed by microscopy (see above),

since pistils were collected for both microscopy and RNA extraction from adjacent florets on each spike. RNA was extracted from duplicate biological samples at all five stages in each of the four genotypes, however due to tissue loss and poor RNA quality, not every sample was sequenced. This meant that only one replicate was available for Forum at Stage 3, Salka at Stage 3, and Wren at Stages 5 and 7. In total, 36 individual samples of whole-pistil RNA were sequenced (Table 5-S1).

To provide some spatial context regarding the ovule, in addition to the whole pistil, RNA was also extracted and sequenced from specific ovule tissues harvested using laser capture microdissection. Different ovule tissues were collected from cv. Sloop, an elite Australian two-row spring genotype, to create a tissue-specific reference dataset. Although Sloop was not analysed as part of the ovule size experiments, thin sectioning and immunolabelling confirmed clear similarities in staging, ovule morphology and pectin deposition. Ovules were laser dissected at three developmental stages (approximately Stages 3, 5 and 7) that span a similar developmental period compared to the whole-pistil data. Rather than isolating replicate samples for every tissue, emphasis was placed on capturing similar tissues at sequential time points to assess the dynamic patterns of gene expression over time. In total, 15 tissue samples incorporating the nucellus, integuments, ovary wall, female gametophyte and chalaza were collected, amplified and submitted for RNAseq (Table 5-S2). RNAseq reads for all samples were aligned to the latest barley reference sequence that comprises 81,683 HORVUs. Samples were normalized and TPM values for each gene were assigned. For the pistil data, replicate TPM values were averaged, such that each developmental stage in each genotype was represented by a single set of expression data (20 in total). Among all whole-pistil samples, transcripts were identified for 15594 unique HORVUs at an expression level of at least 5TPM (Table 5-S3). In each individual sample (i.e. each of the 20 data sets representing five developmental stages in four genotypes), transcripts were identified for between 10,396 and 11,780 unique HORVUs ≥ 5 TPM, or between 67% and 75.5% of the total of 15,594

HORVUs identified (Table 5-S4). Approximately 13,500 HORVUs (+/- 450) were identified at TPM>5 in each genotype, across all developmental stages. The difference between the number of HORVUs identified to be expressed at TPM>5 between individual samples and between genotypes indicates the presence of stage- and genotype-specific gene expression. In the 15 tissue-specific RNA-seq samples (Table 5-S2), an average of 21,850 individual HORVUs were detected in any sample, and this was reduced to an average of 9,905 HORVUs when filtered for TPM greater than or equal to 5.

For the remainder of this Chapter, we consider these RNAseq data in terms of general expression trends during pistil and ovule development. Further analysis of differentially expressed genes is reported in Chapter 6.

Validation of whole-pistil and tissue-specific RNA-seq data by comparison to qPCR data and previously identified ovule-specific genes

To validate the whole-pistil RNA-seq data we assessed expression of *HvMADS13*, a key regulator of ovule identity (Figure 5-5; Dreni et al. 2007), by qPCR. Expression of the ovule identity factor was remarkably similar, increasing across ovule development in both datasets. To validate the tissue specificity of RNA-seq samples derived from small, laser-dissected tissues, the presence of genes previously identified as cell-specific ovule genes were assessed (Figure 5-6). For example, to determine if cell types within the embryo sac had been accurately dissected, expression of homologs of *EGG CELL 1* (*EC1*) and *DOWNREGULATED IN DIF1-29* (*DD29*, At2g47280) were assessed. EC1 has previously been identified to be specific to the egg cell in wheat and Arabidopsis (HORVU7Hr1G101980; Sprunck et al. 2012), while *DD29* is specifically expressed in Arabidopsis antipodal cells (Steffen et al. 2007) and shares homology with HORVU2Hr1G023830. The *JEKYLL* gene, associated with programmed cell death of the nucellus and nucellar projection after fertilisation

in barley (HORVU3Hr1G068150; Radchuk et al. 2006), was selected as a nucellus marker. The transcription factor *OsMADS21* is specifically expressed in the integument of rice ovules (HORVU1Hr1G064150; Dreni et al. 2011), thus the barley orthologue was selected to assess integument samples.

Transcripts of *HvEC1* were abundant in laser-dissected samples containing the egg apparatus plus the central cell, but were not identified at an appreciable level in the sample containing the whole embryo sac (Figure 5-6A). Conversely, transcripts of *HvDD29* were highly abundant in both antipodal samples, as well as the whole embryo sac sample (Figure 5-6B). Transcripts of *HvDD29* were also found at relatively very low abundance in the egg apparatus plus central cell samples. These two genes indicate that the egg apparatus plus central cell and antipodal cell samples were accurately dissected, contaminating neither the other embryo sac-derived samples nor nucellus samples, and that the whole embryo sac sample may be biased towards the antipodal cells. Expression of *HvJEKYLL* was identified in the nucellus at all developmental stages, as well as embryo sac derived samples, particularly the egg apparatus plus central cell sample at anthesis (Figure 5-6C). Notably, no expression was identified in the chalaza, integument, or ovary wall samples. As the expression pattern of *HvJEKYLL* has only been characterised as a nucellus-specific gene after fertilisation, this may be interpreted as indicating the integuments were not contaminated by nucellus, and may present new information regarding where *HvJEKYLL* is expressed and localised prior to fertilisation. Transcripts of *HvMADS21* was abundant in all three integument samples, as well as being identified in the chalaza sample at a reduced abundance, and several other samples at very low abundance (Figure 5-6D). Given the specificity of other samples assessed, this may indicate that integument samples were collected accurately, and the low abundance of *HvMADS21* in other tissue samples may present new insight regarding the site of *HvMADS21* function.

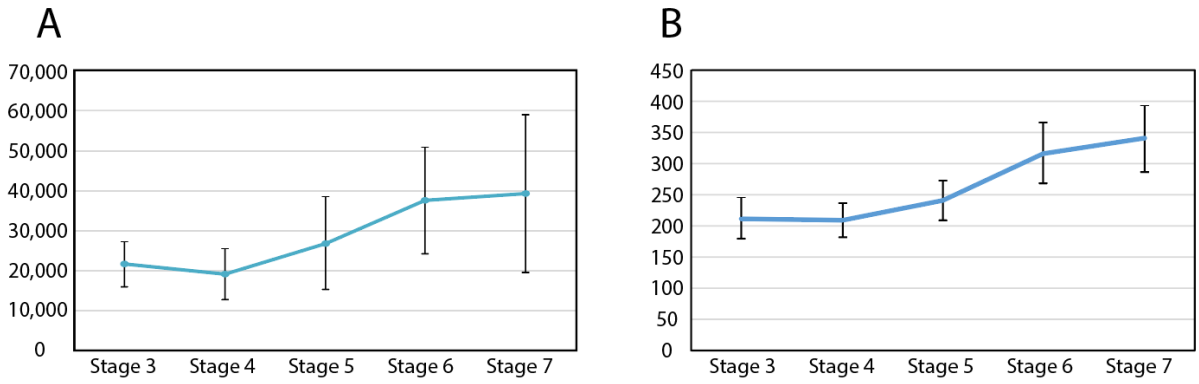

Figure 5-5. Comparison of transcript abundance of HvMADS13 (HORVU1Hr1G023620) as detected in RNA samples using (A) quantitative polymerase chain reaction (Q-PCR), and (B) an Illumina Hi-Seq platform. RNA was extracted from whole barley pistils at five stages of ovule development (Stages 3-7). Expression is presented as the average transcript abundance among samples of four genotypes at each developmental stage. Abundance is presented as arbitrary units in (A), and transcripts per million (TPM) in (B).

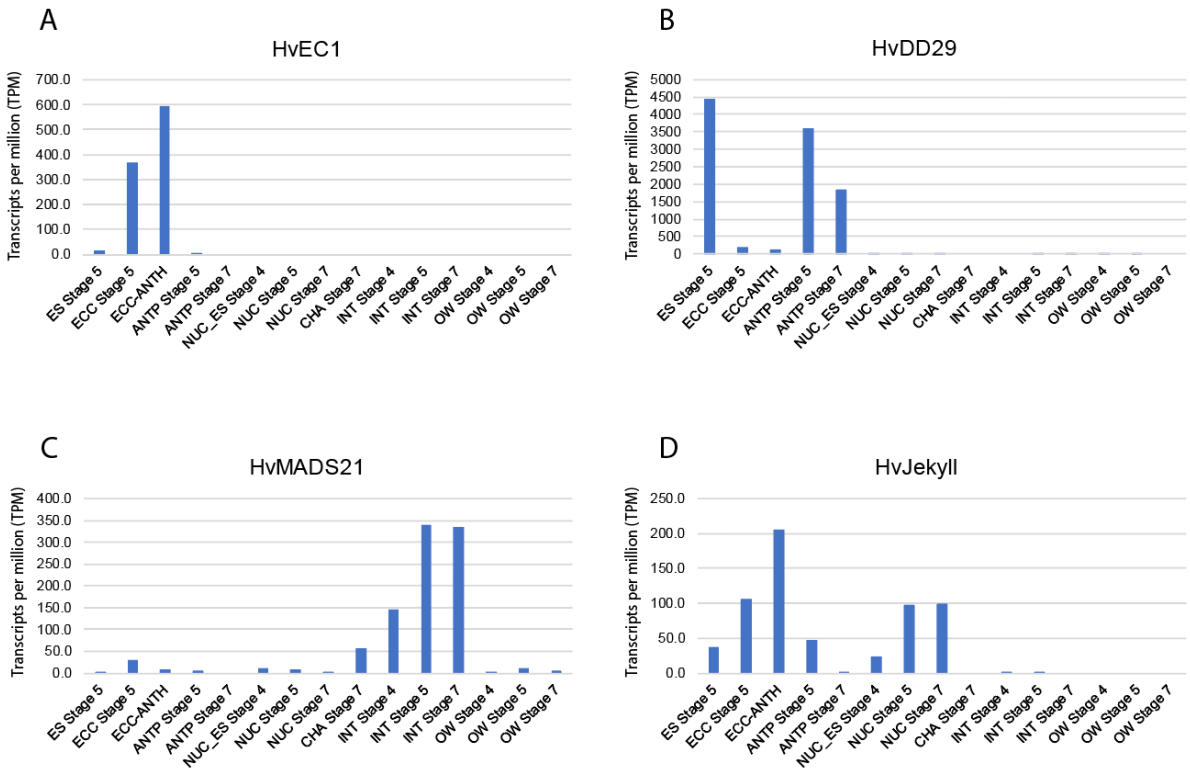

Figure 5-6: Expression of four tissue-specific genes among fifteen samples RNA sequencing data collected from specific ovule tissues of the genotype Sloop, at three stages of ovule development (Stages 4, 5 and 7) in order to assess successful tissue isolation. The four genes selected are specifically expressed in (A) the egg cell, (B) the antipodal cells, (C) the integuments, and (D) the nucellus. Transcript abundance is given as transcripts per million (TPM). ANTP, antipodal cell cluster; CHLZ, chalaza; ECC, egg apparatus and central cell; ES, embryo sac; INT, integument; NUC, nucellus; NUC_ES, nucellus and embryo sac; OW, ovary wall.

Expression analysis of gene families associated with flower and ovule development

The RNA-seq data provide an opportunity to establish novel information regarding gene expression patterns in barley pistils over time, and differences between genotypes and the location of expression in different regions of the ovule. To interrogate the RNA-seq data in detail, we first considered classes of genes that might be expected to be involved in ovule and/or flower development. Two classes of genes that are important for reproductive development in a number of species are the MADS box genes and auxin signalling genes (Favaro et al. 2003; Murai 2013; Larsson et al. 2013). Additionally, plasticity of the plant cell wall is necessary for organ growth, which requires extensive biosynthesis and modification of polysaccharides such as pectin (Sechet et al. 2018). In particular, the methylesterification status of HG has been identified to have an important role in plant development (Lora et al. 2017; Wolf et al. 2009). The roles of selected genes from these three families during floral development have been characterised in Arabidopsis, rice and maize, however this knowledge has not yet been translated to barley. Therefore, we identified barley orthologues of genes in each of these classes and used whole-pistil and tissue specific RNA sequencing data to assess their expression patterns throughout barley ovule development. This general "barley" timecourse was generated by averaging values from at least 6 replicates of RNAseq per stage, derived from the four genotypes described above.

Assessing the expression of barley MADS box genes during pistil and ovule development

Within the whole pistil timecourse, 18 of the 23 putative HvMADS genes showed expression >5TPM in at least one stage (Figure 5-S3, Table 5-S5). The most abundant genes were *HvMADS7* (E-class) and *HvMADS58* (C-class) that were expressed in every stage of development (Table 5-S6). Three main clusters of gene expression patterns were identified

when samples were normalised based on their maximum expression value. These clusters grouped genes that tended to show their highest expression (albeit weak) during early stages (i.e. *HvMADS4, HvMADS15, HvMADS56, HvMADS5*), genes that showed highest expression at maturity (i.e. *HvMADS57, HvMADS34, HvMADS14, HvMADS18*) and the remainder that appeared to be expressed in most stages of pistil development. In general, Stage 5 appeared to be a key stage for MADS-box gene expression.

Examination of the same genes in the tissue-specific data revealed considerably more information regarding expression location and dynamics (Figure 5-7, Table 5-S7). The MADS-box genes were clustered into four main groups based on expression pattern. These groups include putative non-germline genes, integument genes, nucellus genes, and germline genes. In this dataset, "germline" refers to the tissue-specific samples derived from the embryo sac (i.e. ES, EA/CC and ANT at three stages). Among the non-germline genes, relatively high transcript abundance was found for *HvMADS58* and *HvMADS6* (170.8TPM, 78.7TPM), Class C and Class E genes respectively, which have been demonstrated to interact in rice (Li et al. 2011). Maximum abundance of *HvMADS58* and *HvMADS6* was detected in the ovary wall samples, and decreased with time. Both genes were also found to be expressed in the integuments, but at lower abundance relative to the ovary wall.

A number of the MADS genes were most abundant in the integument samples and typically at the earliest stage (Stage 4). For example, transcript abundance peaked in the integument at Stage 4 for *HvMADS3, HvMADS13, HvMADS7 and HvMADS8* (135.7TPM, 432.5TPM, 417.9TPM, 63TPM), which are Class C, Class D, and two Class E genes respectively. Transcript abundance of the closest homologue of *HvMADS13*, *HvMADS21*, appeared to be specific to the integument (339.5TPM), similar to *HvMADS32*, also known as the orthologue of *CHIMERIC FLORAL ORGANS1* (*CFO1*; 134.4TPM). The B_{sister} genes *HvMADS29* and *HvMADS31* showed a distinct pattern that was unique to the nucellus (61.4TPM, 327.4TPM)

at the samples of Stages 4 and 5. Of the floral MADS-box genes showing at least 5 TPM in one tissue, only *HvAGL1* (putative annotation, class as yet undetermined) was observed to be abundant in the germline, and it was found to be specifically expressed in the egg/central cell (245.5TPM).

When comparing relative transcript abundance between the tissue-specific and whole-pistil data sets, it is evident that genes that have higher relative abundance in ovary wall samples, e.g. *HvMADS7* and *HvMADS58*, are more abundant in the pistil data. Similarly, genes that are not present in the ovary wall samples, but were enriched in the nucellus or integument samples, e.g. *HvMADS31, HvMADS29 and HvMADS21*, were identified to be expressed in the pistil data, but not found to be very abundant.

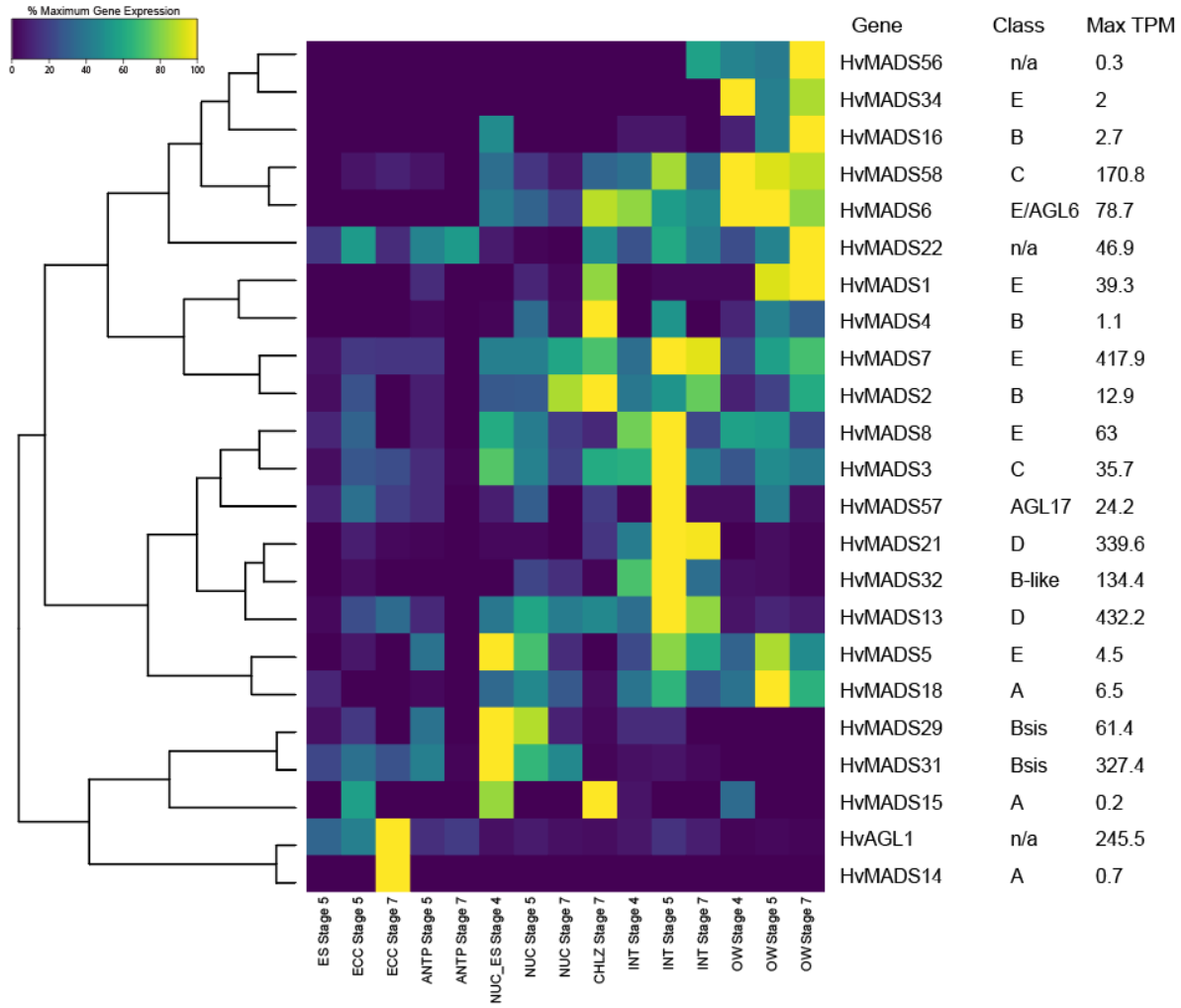

Figure 5-7: Heatmap showing expression of putative barley genes encoding MADS-box transcription factors in specific tissues of the barley ovule at three different stages of reproductive development, as determined by RNA sequencing. Transcript abundance values (TPM) have been normalised to 1. ANTP, antipodal cell cluster; CHLZ, chalaza; ECC, egg apparatus and central cell; ES, embryo sac; INT, integument; NUC, nucellus; NUC_ES, nucellus and embryo sac; OW, ovary wall.

Genes involved in auxin signalling show dynamic expression profiles in the pistil and ovule expression datasets

To gain insight into the transcriptional dynamics of the auxin pathway in barley, the ARF, Aux/IAA, PIN, TIR/AFB and YUC families were examined (Figure 5-8). Homology searches identified 23 ARF genes, 26 Aux/IAA genes, 13 PIN genes, 5 TIR/AFB genes and 11 YUC genes, many of which have recently been reported by (Shirley et al. 2018). Of the 78 genes, 36 were found to pass the abundance threshold of reaching TPM>5, and these formed the focus of subsequent expression analysis (Table 5-S8). Notably, all YUCCA family genes identified were excluded on the basis of low expression, both in the whole-pistil and tissue-specific data set. Examination of expression patterns in the whole pistil time course revealed distinct groups of “early” and “late” developmental genes, most abundant at Stage 3 or Stages 6 or 7, respectively (Figure 5-S4, Table 5-S9). These groups contained at least one member from each transport, signalling and response class. The most abundant early genes were *HvARF4a, HvARF4c*, and *HvIAA3*, while *ARF17*, *ARF25* and *HvIAA30* were abundant late genes at Stages 6 and 7. At least one member of each family was present during the entire timecourse, although patterns were distinct in each gene family. For example, *HvPIN1a*, *HvPIN1c*, *HvPIN1b* and *HvPIN2* showed different patterns (early, early, mid and late, respectively) suggesting they may be involved in different developmental events.

The same genes were examined in the tissue-specific data, and expression could be divided into three main categories: ovary wall genes, non-germline genes and germline genes, whereby expression was either entirely or predominantly observed in the ovary wall, all tissues other than germline tissues, or only in the germline tissues (Figure 5-8, Table 5-S10). Most genes were expressed in the ovary wall at all three developmental stages, while only a few genes were enriched in the germline tissues. Within all three groups, maximum gene

abundance was biased toward samples at earlier developmental stages. The only group with substantial abundance in mature-stage samples was the ovary wall group. Among the ovary wall genes, those that were observed to reach maximum transcript abundance in the Stage 4 sample included ARFs (*HvARF14, HvARF2, HvARF3, HvARF5*), a TIR/AFB (*HvAFB5*), and the orthologue of *OsPIN1b, HvPIN1b*. Transcript abundance for these genes was relatively low (none attained abundance over 35TPM). Three genes reached maximum abundance in the Stage 5 ovary wall sample; two AUX/IAAs (*HvIAA3, HvIAA14*) and a single ARF (*HvARF11*). Four additional ARFs were observed to reach maximum transcript abundance in the mature-stage ovary wall sample (*HvARF25, HvARF6, HvARF17, HvARF12*), as well as another single TIR/AFB (*HvAFB2*) and the orthologue of *OsPIN2, HvPIN2*. Notably, the most abundant genes within the ovary wall were *HvIAA3* and *HvIAA30*. This is consistent with the results of the pistil timecourse.

Among genes that were expressed in non-germline samples, all showed maximum transcript abundance at Stage 4 (in nucellus, integument, and ovary wall tissues), with the exception of *HvTIR1* and *HvARF22*, which reached maximum abundance in the Stage 7 ovule chalaza and Stage 5 integument, respectively. Notably, *HvTIR1* was one of only three genes, including *HvIAA1* and *HvIAA3*, that were highly abundant and expressed in the chalaza. Genes that reached maximum abundance in the nucellus samples i.e. *HvPIN1c, HvARF21, HvARF18*, *HvARF4c, HvARF8, HvAFB3, HvAFB4*, tended to only be expressed at low levels in other tissues, whereas genes observed to reach maximum abundance in the integument or ovary wall (*HvARF22, HvIAA19; HvARF4a, HvARF9*) tended to be expressed at 50-80% maximum abundance in other non-germline tissues. *HvARF4c, HvPIN1c* and *HvTIR1*, appeared to be particularly abundant in the Stage 4 nucellus. However, it is important to note that this early stage “nucellus” sample also contained the Stage 4 germline; thus it is possible that some expression is conferred by early germline cells.

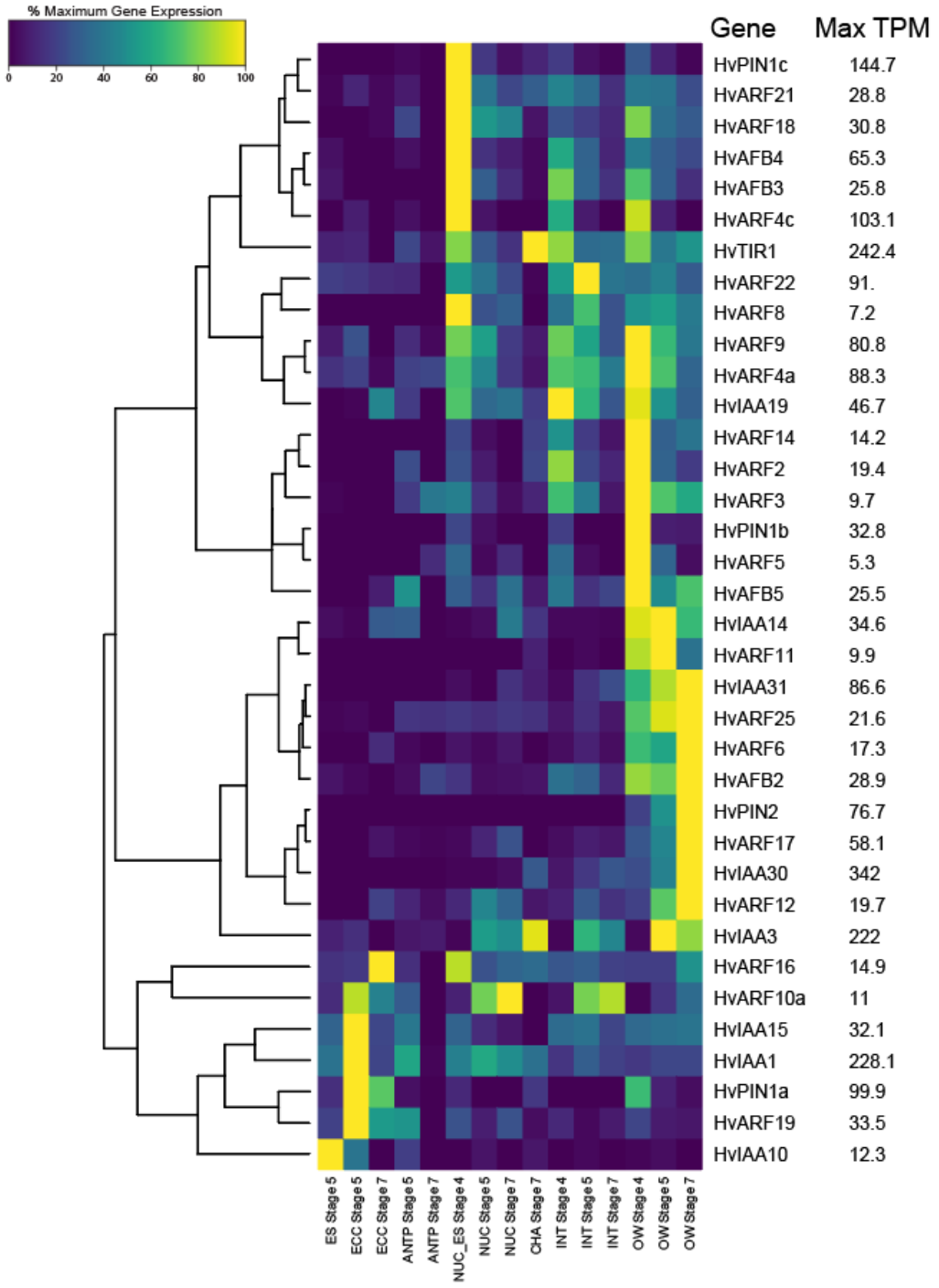

Figure 5-8: Heatmap showing expression of putative barley genes involved in auxin biosynthesis and transporter within specific tissues of the barley ovule at three different stages of reproductive development, as determined by RNA sequencing. Transcript abundance values (TPM) have been normalised to 1. ANTP, antipodal cell cluster; CHLZ, chalaza; ECC, egg apparatus and central cell; ES, embryo sac; INT, integument; NUC, nucellus; NUC_ES, nucellus and embryo sac; OW, ovary wall.

Among genes predominantly expressed in germline tissues, all bar *HvARF16* and *HvIAA10* reached maximum transcript abundance in the sample collected from the egg and central cell at Stage 5. Compared to other tissues, there was a greater proportion of Aux/IAA genes expressed in germline samples. Two genes had notably high transcript abundance in the germline cells; *HvIAA1* and *HvPIN1a*.

Comparing relative abundance of genes between tissue-specific and whole pistil-derived samples, it is evident that genes that were found to be abundant in small-tissue-derived samples of the tissue-specific data set, such as *HvIAA1*, *HvTIR1*, *HvPIN1a* and *HvPIN1c*, were detected but not observed to be very abundant in the whole-pistil data. Conversely, genes determined from the tissue-specific data to be active in the ovary wall, such as *HvARF4a, HvARF4c, HvIAA3* and *HvIAA30*, were observed to have high abundance among pistil samples relative to other genes analysed. This indicates that while detection of ovule expression within whole-pistil data may be possible for some genes, analysis of tissue specific data is necessary. Overall, the data suggests that localised auxin biosynthesis and signalling is occurring within the ovule, however future work is required to elucidate further, and improve the functional characterisation of, barley orthologues.

Genes involved in pectin biosynthesis and modification are expressed in tissues that accumulate pectin during ovule development

The analysis of the MADS and auxin families in the pistil and ovule datasets revealed dynamic patterns of gene expression that are generally consistent with previous publications and models. Therefore, the final set of genes chosen for analysis in this study were those involved in pectin biosynthesis and modification, for which far less is known. Specific patterns of pectin accumulation and methylesterification have been identified in the developing ovule and ovary of both monocots and eudicots (see Chapter 4; Lora et al. 2017). However, whether this

relates to specific domains of gene expression or mechanical stimuli that change wall composition during growth does not appear to have been addressed at the molecular level during ovule development.

In order to assess which regions of the ovule might be require pectin modification for development, barley genes were investigated for functional annotations and carbohydrate-active enzyme (CAZy; Drula et al. 2013) classification relating to HG biosynthesis and remodelling. These genes were then filtered based on expression of TPM>5 in at least one sample of the tissue specific RNA-seq data set, resulting in a list of 65 HORVUs encoding hexosyltransferases, polygalacturonases (PG), pectin esterases (PE), pectin lyases (PL), pectin methylesterases (PME) pectin methylesterase inhibitors (PMEI) and galacturonosyltransferases (GAUT) for analysis in this study (Table 5-S11).

Examination of gene expression in the whole pistil time course revealed groups of genes predominantly expressed at early or late developmental stages, and a group of genes that maintained expression throughout the time course (Figure 5-S5, Table 5-S12). Each group included members of all families assessed, meaning that expression of specific groups of hexosyltransferases, PEs, PLs, PMEs, PMEIs, and GAUTs was differentially up- or down-regulated, or maintained throughout the time course. Among the whole-pistil data, the most abundant genes included a pectin lyase (HORVU1Hr1G079140), beta-galactosidase (HORVU4Hr1G074280), and methylesterase (HORVU5Hr1G065680) abundant at Stages 3 and 4, and a methylesterase inhibitor (HORVU7Hr1G095080) and methylesterase (HORVU6Hr1G003900) abundant at Stages 6 and 7.

Genes involved in pectin biosynthesis and remodelling could be grouped into four clusters within the tissue-specific data: general genes, ovary wall genes, non-germline genes, and germline genes (Figure 5-9, Table 5-S13). Genes observed to be abundant in all ovule tissues and the ovary wall represented all functional categories of pectin biosynthesis and remodelling

analysed, reflecting the integral role of pectin within the plant cell wall structure of developing tissues. Of the 65 genes involved in pectin biosynthesis and remodelling, only 6 were observed to have high abundance specifically in the ovary wall tissues. These genes included two pectinesterase “11” genes (HORVU2Hr1G017220, HORVU2Hr1G097380), two genes encoding pectin lyase superfamily proteins (HORVU1Hr1G079130, HORVU3Hr1G054810), and two GT8 hexosyltransferases (HORVU2Hr1G091280, HORVU4Hr1G003590). This suggests that the ovary wall may be simultaneously undergoing pectin biosynthesis, modification and de-methylesterification in a manner unlike any ovule tissue. Future work involving immunolabelling of cell wall polysaccharides may investigate this hypothesis.

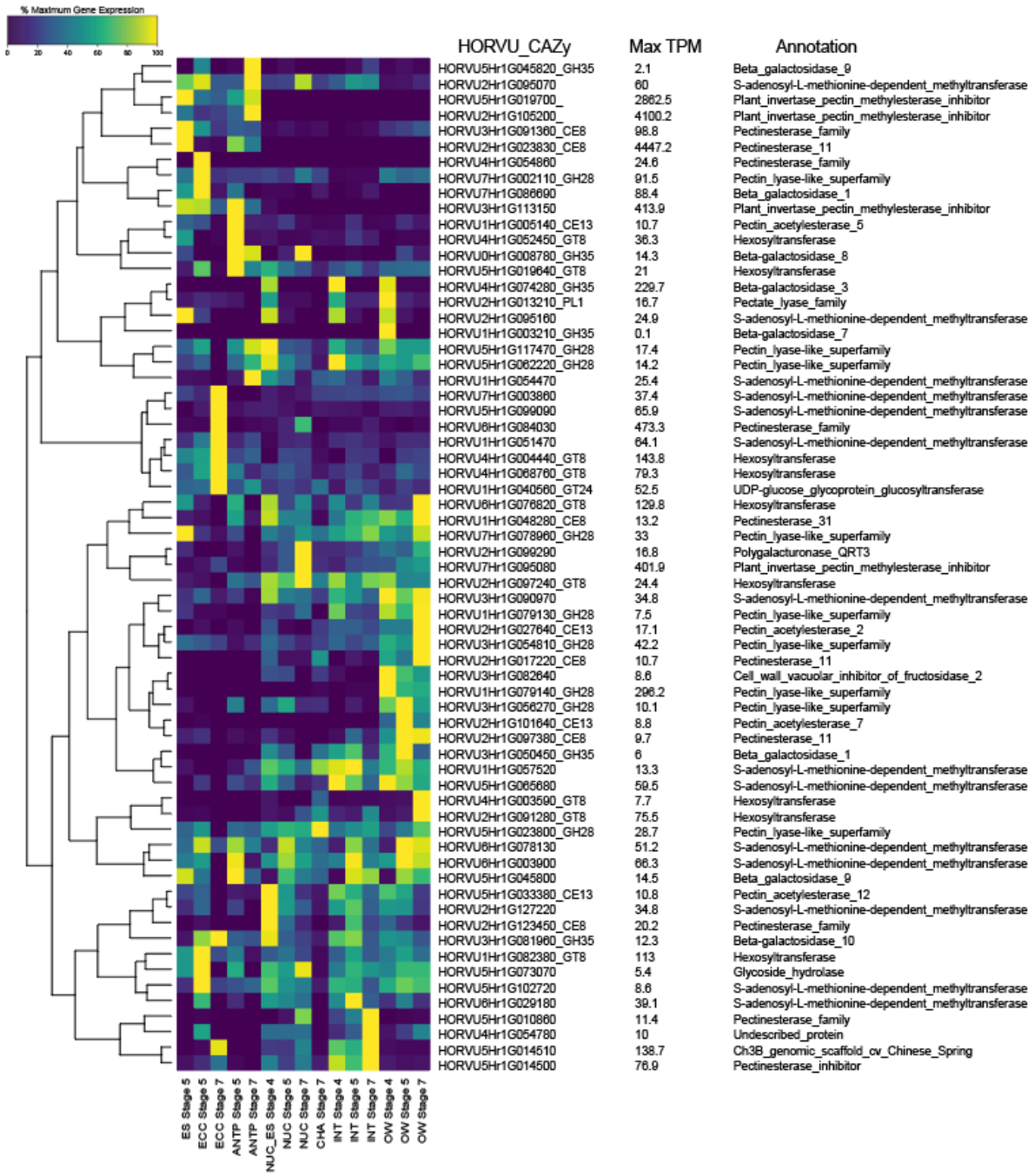

Figure 5-9: Heatmap showing expression of genes involved in pectin biosynthesis and remodelling within specific tissues of the barley ovule at three different stages of reproductive development, as determined by RNA sequencing. Transcript abundance values (TPM) have been normalised to 1. ANTP, antipodal cell cluster; CHLZ, chalaza; ECC, egg apparatus and central cell; ES, embryo sac; INT, integument; NUC, nucellus; NUC_ES, nucellus and embryo sac; OW, ovary wall.

Among the group of non-germline genes, two genes were uniquely abundant in Stage 4 tissue-specific samples, a beta-galactosidase and a pectate lyase (HORVU4Hr1G074280 and HORVU2Hr1G013210, respectively). Apart from these genes, the remainder of non-germline genes were expressed in multiple tissues at more than one developmental stage, with varying abundance. For example, six non-germline genes were observed to have maximum abundance in the nucellus. Three of these genes, a general pectinesterase, a pectin methyltransferase and a pectin acetylesterase (HORVU2Hr1G123450, HORVU2Hr1G127220 and HORVU5Hr1G033380, respectively) attained maximum abundance in the Stage 4 nucellus sample, and were observed to decrease in abundance in each of the two subsequent nucellus samples. This pattern of decreasing abundance over time was also observed in the integuments and ovary wall. In contrast, the remaining three genes, a hexosyltransferase, a polygalacturonase known as *QUARTET3* (*QRT3*), and a PMEI (HORVU2Hr1G097240, HORVU2Hr1G099290, and HORVU7Hr1G095080, respectively) were observed to increase in abundance in each subsequent nucellus sample. Of the six genes, the PMEI (HORVU7Hr1G095080) that peaked in abundance in the nucellus was particularly abundant (401.9TPM), while all others peaked with relatively low abundance (~30TPM). Taken together, the expression patterns of these six genes suggests that de-esterification (both methyl-ester and acetyl-ester) of pectin is prominent in the nucellus, and is possibly regulated via simultaneous reduction of PMEs and increase in PMEIs.

The “germline genes” could be further divided into specific egg apparatus plus central cell, and antipodal genes, as well as few that are abundant in both. Genes that reached maximum abundance in germline samples included two within the top 10% most highly abundant genes identified within the entire tissue-specific data set. Moreover, genes that reached maximum abundance in the egg apparatus plus central cell samples tended to be expressed at relatively low abundance in other germline tissues. Among these genes two general pectinesterase genes (HORVU4Hr1G054860, HORVU6Hr1G084030) and four methyltransferase family

genes were present (HORVU1Hr1G082380, HORVU1Hr1G051470, HORVU7Hr1G003860 and HORVU5Hr1G099090), of which the pectinesterase HORVU6Hr1G084030 was the most abundant (473.3TPM). Similarly, enzymes required for de-esterification were represented among the genes that attained maximum abundance in antipodal cell samples, specifically, two methyltransferase family members (HORVU2Hr1G095070, HORVU1Hr1G054470) and an acetylesterase (HORVU1Hr1G005140). However, none of these three genes exhibited high transcript abundance. The most abundant pectin-related "germline" gene was a pectinesterase "11" gene (HORVU2Hr1G023830, 4447.2TPM), which reached maximum abundance in the whole-ES sample. Transcripts of this pectinesterase were barely identified within egg apparatus plus central cell samples, but were highly abundant within the antipodal tissue samples, particularly at Stage 5. Three additional PMEIs were also highly abundant within the whole-ES sample (HORVU5Hr1G019700, 2862.5TPM), and the antipodal cell samples at both Stage 5 (HORVU3Hr1G113150, 413TPM) and Stage 7 (HORVU2Hr1G105200, 4100.2TPM). Finally, there is also evidence for activity of pectin biosynthetic and remodelling machinery beyond the modifications performed by esterification, as expression of pectin lyase genes was found within egg/central-cell samples, and hexosyltransferase genes were found to be abundant in all germline tissue types.

Together these results indicate that pectin is highly modified within the germline cells throughout development, in a tightly regulated manner whereby pectin at the distal/micropylar end of the embryo sac is subject to the activity of numerous low-abundance PMEs, while pectin at the proximal/antipodal end of the embryo sac, close to the antipodal cell cluster, is more likely to be methylesterified due to exceptionally high abundance of PMEIs.

Discussion

The ovule is particularly important for seed development, since it gives rise to the female gametophyte and nourishes it before and after fertilisation. Studies in barley have focussed

on the role of the ovule around the time or fertilisation and beyond (Radchuk et al. 2006; Thiel et al. 2008; Tran et al. 2014), while limited genetic information is available regarding earlier stages when the ovule is established. Genes that contribute to ovule growth might be utilised to control floret fertility for breeding purposes, to protect against stress or to influence downstream aspects of seed development. In this study, four genotypes representing “small” (Forum and Gant) and “large” (Salka and Wren) mature ovule phenotypes (Chapter 4) were selected for further study, driven by the questions: 1) How early in ovule development does the variation in mature phenotype arise?; 2) How does the cellular organisation of each ovule tissue contribute to mature phenotype?; and 3) What is occurring with respect to gene expression throughout barley ovule development? In order to address these questions, two microscopic techniques were employed to assess ovule development in the four genotypes of interest, and RNA sequencing was used to investigate gene expression in whole pistil tissue and in specific ovule tissues using laser microdissection.

Microscopy of whole mounted pistil tissue reveals distinct reproductive stages

Previous analysis of mature ovule traits identified that the size of the embryo sac and nucellus are independently controlled, i.e. it is possible for an ovule to have both a small embryo sac and a small nucellus, resulting in a small ovule, while it is similarly possible for an average sized ovule to have a large embryo sac and small nucellus, or vice versa (Chapter 4). As the nucellus of model dicots only consists of a single layer (Schneitz et al. 1995), little research has been undertaken regarding at what developmental stage the nucellus proliferates and expands into a substantial component of the ovule, and how this growth might affect developmental progression of the female gametophyte. In order to address this, morphology of ovule tissue was studied between Waddington Scale 7 and 10 (Waddington et al. 1983), in four two-row spring barley genotypes representing varied small (Forum, Gant) and large (Salka, Wren) mature ovule phenotypes. Following morphological analysis, nine distinct

stages of reproductive development were identified, here called Stages 0 to 8. Of these, Stages 0 to 3 describe the initiation of the reproductive lineage of the ovule, in which the megaspore mother cell (MMC) has been selected at Stage 1, the MMC undergoes meiosis during Stage 2, and the functional megaspore (FM) undergoes mitosis at Stage 3. Stages 4 to 7 describe the maturation of the female gametophyte (FG), wherein the micropyle is formed by the inner integuments and the FG is established at Stage 4, the nucellus begins expanding and the antipodal cells undergo rapid proliferation at Stage 5, the nucellus and embryo sac cells expand at Stage 6, and the ovule reaches anthesis, or reproductive maturity, at Stage 7. Stage 8 was used to describe ovules that had been fertilised. These stages may be regarded as an addition to previously established scales used to categorise floral development in cereal crops, such as the Waddington Scale, and thus improves the accuracy of these scales in staging female reproductive development in barley.

Progression of reproductive development is subject to genotypic variation

Quantification of ovule traits from Stages 2 to 7 revealed genotypic differences in the rate of growth of the embryo sac, nucellus, and thus the overall size of the ovule. The genotypes selected to represent the “small” ovule phenotype at maturity, Forum and Gant, behaved differently with respect to each other. Ovules of Forum overall rapidly developed in size between Stages 4 and 6, leading to a plateau in its growth between Stages 6 and 7. In comparison, ovules of Gant did not increase in size as rapidly throughout Stages 4 to 6, and continued to increase in size toward Stage 7. When specific tissues were assessed, the plateau of growth in Forum was found to be due to a minimal increase in nucellus area. This supports the hypothesis that the embryo sac and nucellus are able to develop independently. This hypothesis was further supported by the difference between the final ovule sizes of Forum and Gant, which demonstrated the key contribution of the nucellus in determining mature ovule size, and emphasised the question of what genetic signals regulate ovule growth. Of the

genotypes selected to represent the “large” mature ovule phenotype, Salka and Wren, the small nucellus area of Wren during Stages 2 to 5 meant that in the initial stages of development it appeared to have a small-ovule phenotype, until rapid growth of the nucellus from Stages 5 to 7 led to its mature ovule size being the largest of the four genotypes. The increase in nucellus size was matched by increased size of the embryo sac, whereby a relatively small embryo sac in Wren at Stage 5 developed into the largest observed at Stage 7. The sudden increase of nucellus and embryo sac area in Wren, and the lack of increase in nucellus area in Forum, produced mature morphology of ovules in these two genotypes that agreed with previously quantified phenotypes, and suggests that both the embryo sac and nucellus may be responding to independent stimulatory and inhibitory growth signals at different stages of ovule development. Further, the difference in the timing of growth of each tissue in Forum and Wren suggests that the diming of these developmental cues may genotypically vary. While the development of Forum, Gant and Salka supported the hypothesis that the size of the ovule at early developmental stages would determine the size of the ovule at maturity, the data from Wren indicates that this is not always true. This data emphasises the question of how tissue growth is achieved with respect to regulation of cell proliferation and expansion.

Discrete zones of the nucellus may differentially contribute to cell proliferation and expansion

The two major factors contributing to the size of any biological tissue are the number of cells and the size of these cells. Therefore, in this study we considered that differences between the four genotypes of interest might relate to differences in cell proliferation (cell number) and/or cell expansion (cell size). Semi-thin sections of flowers at Stages 3, 5 and 7 were labelled with antibodies that bind (1,3;1,4)-ß-glucan (BG) and different forms of pectin including de-esterified homogalacturonan (LM19) and methylesterified homogalacturonan (LM20). This immunolabelling, combined with observation of autofluorescence of cellular

contents, allowed visualisation of the cell walls within the developing ovule, thus facilitating study of the cellular arrangement of ovule tissues and measurement of two-dimensional ovule area and nucellus cell number.

Sections taken from mature ovules revealed that the nucellus consists of three domains, identifiable by cell size, shape and density of cellular contents. These domains included the nucellus epidermis, the peripheral nucellus and the inner nucellus. While the epidermal layer and peripheral nucellus consisted of small cells with dense cytoplasm, cells of the inner nucellus were large, highly vacuolated and often irregularly shaped. These cells were present in a region occupying the centre of the ovule and surrounding the embryo sac. The inner nucellus domain was visible in sections taken through both the egg apparatus and the antipodal cell cluster at Stages 5 and 7, being most prominent around the antipodal cell cluster at Stage 7.

Analysis of ovule area, the number of cells within the nucellus, and the average area of cells within the nucellus was undertaken using transverse sections taken at the distal tip of the ovule, i.e. through the egg apparatus, and at the centre of the ovule, i.e. through the antipodal cell cluster. It was found that little proliferation or expansion occurred in the nucellus cells surrounding the egg apparatus throughout the later stages of development, which maintained a peripheral nucellus phenotype. In contrast, both cell expansion and proliferation was found to occur in the nucellus surrounding the antipodal cells from Stage 5 to Stage 7, indicating that this region of the nucellus is responsible for driving the growth of nucellus, observed throughout these developmental stages from whole-mount microscopy. Further to this, while the nucellus cell area measurements presented refer to the average of all nucellus cells, given the notable difference in cell sizes between peripheral and inner nucellus, it is suggested that cell expansion in the nucellus specifically occurs within the inner nucellus and cell proliferation occurs in the peripheral nucellus. In Forum the number of nucellus cells around the antipodal

cell cluster increased by 160%, from 397 ± 29 at Stage 5 to 635 ± 34 at Stage 7. In contrast, in Wren the number of nucellus cells in this same region increased by 356%, from 217 ± 4 at Stage 5 to 773 ± 14 at Stage 7. When considered with the data obtained from whole-mounted tissue, this nucellus cell number data indicates that, regarding the contribution of the nucellus to overall ovule area, the relatively little and large increase in ovule area of the genotypes Forum and Wren may be attributed to differential regulation of cell proliferation in the nucellus. Further study is required to thoroughly characterise the different domains of the nucellus, to address speculation of their discrete contribution to ovule growth through proliferation and expansion, and to determine the role of discrete ovule tissues in supporting development of the embryo sac.

LM19 specifically labels nucellus cells flanking the reproductive lineage throughout ovule development

Previous studies have shown that pectin epitopes are present in the cell walls of the nucellus of diverse species including Arabidopsis, *Hieracium pilosella,* avocado (*Persea americana*) and larch (*Larix decidua* Mill; Juranić et al. 2018; Lora et al. 2017; Rafińska et al. 2014). In the present study, LM19 was found to predominate in the cell walls of the nucellus surrounding the embryo sac, at Stages 3, 5 and 7. Notably, at Stages 5 and 7 the cells labelled with LM19 were consistently those of the inner nucellus, and cell layers of intermediate phenotype, i.e. regularly shaped but slightly enlarged and more vacuolated as compared to peripheral nucellus. As such, LM19 may be used as a marker for the reproductive lineage and the nucellus at the distal tip of the ovule during early stages of development, and as a marker of the embryo sac and inner nucellus at later stages of development. In the absence of functional data, we can only speculate what the role of de-methylesterified pectin within the cell walls of the inner nucellus might be. Demethylesterification of pectin in the presence of Ca^{2+} allows increased crosslinking of pectin, increasing the mechanical strength of the plant cell wall,

however in the absence of Ca^{2+} demethylesterification contributes to cell wall flexibility (Bidhendi and Geitmann 2015). Although Ca^{2+} levels were not measured here, previous studies in lettuce suggest that there is a concentration of Ca^{2+} within or near the developing female gametophyte (Qiu et al. 2008). If this feature is conserved in barley, the abundance of LM19 labelling may indicate that the walls of the embryo sac and surrounding cells are being reinforced to enhance rigidity. Conversely, it is not entirely clear how this can be reconciled with the massive expansion of the embryo sac and the role of the nucellus as a transfer tissue. After fertilisation, the nucellus of cereal crops forms the nucellar projection, facilitating transfer of nutrients to the developing endosperm, and undergoing programmed cell death (Tran et al. 2014; Wang et al. 1994). Ostensibly, due to its positioning around the embryo sac, the inner nucellus may contribute a more nutritive role to sustain development of the embryo sac. The LM19-labelled walls of the inner nucellus and embryo sac may therefore equally reflect the flexibility required for rapid growth of the ovule, or the need for a rigid cell wall structure such that the cells can withstand the turgor pressure associated with accumulation of solutes prior to death and nutrient transfer (Beauzamy et al. 2014).

Intricacies of the relationship between the ovule and the ovary remain to be explored

While previous work (see Chapter 4) does not support a direct relationship between the size of the ovule and grain traits, other studies in barley have established links between increased cell number along a transverse line spanning the carpel and the dry weight of the spike after grain maturation (Guo et al. 2016). Ovary size was not assessed across the whole panel in this study, but based upon histological data from four genotypes at three stages, the relationship between the width of the carpel and the width of the ovule appears to be subject to stage and genotype-specific variation. Future studies might assess this relationship in a greater number of genotypes. As it stands, we propose that while any size of ovule provides

the capacity for grain to be produced, variation in carpel traits (Guo et al. 2016) and other reproductive features (Fahy et al. 2018) have a greater influence over the downstream events of grain development. It is important to note, however, that variations in ovule size may contribute to other features of reproductive development not investigated here, such as floret fertility or abiotic stress tolerance (Barnabás et al. 2008). In this context, the molecular basis for ovule development and variation in ovule morphology are still of considerable interest. In order to begin to address this, data was generated to describe the dynamics of gene expression during barley ovule development.

Generation of tissue-specific and whole-pistil transcriptional data profiling ovule development in different genotypes and at developmental stages

This study presents transcriptional data for discrete ovule cell types and for the whole pistil at five stages of reproductive development in barley, complementing data sets relating to the developing ovule currently available for Arabidopsis, rice and maize (Chettoor et al. 2014; Ohnishi et al. 2011; Wuest et al. 2010). Analysis of the data demonstrated the validity and necessity of utilising fine dissection techniques to analyse RNA from small tissues undergoing rapid change, such as those within the germline/ovule. This supports previous studies in diverse species and developmental models that have used tissue-specific transcriptional data to analyse gene expression (Okada et al. 2013; Thiel et al. 2008; Tucker et al. 2012). Importantly, the relatively low transcript abundance of ovule cell type-specific genes in the whole-pistil data suggests that the level of transcript abundance required for important reproductive processes may be too low to be reproducibly detected when these small tissues are examined as part of a larger floral organ. This study also demonstrated that isolation of tissues as small as the egg apparatus and central cell from a single ovule at a midpoint-stage of reproductive development yields sufficient RNA to permit sequencing, but only when RNA is prepared with amplification steps. It is difficult to judge whether amplification bias or variation

in reproductive developmental stage have a greater influence upon the stage-specific accuracy of the sequencing data obtained. To overcome this, we chose to use different developmental stages as tissue “replicates”, favouring identification of tissue-specific genes over stage-specific genes. In the future, these tissue specific genes could be used as bait to identify other “co-expressed” genes within this data set, to provide more ovule tissue specific markers for barley and cereal crops.

MADS box gene expression in the barley ovule coincides with a stage of rapid growth and development

MADS-box genes are well characterised to be crucial for ovule identity, however their role during subsequent stages of ovule development has not been considered in great detail (reviewed by Callens et al. 2018; Theißen et al. 2016). Some evidence from maize, rice and wheat suggest that several MADS-box genes influence female reproductive development (Favaro et al. 2002; Li et al. 2010; Zhao et al. 2006). Moreover, several studies have considered the potential importance of MADS box genes in controlling organ size (reviewed in Dornelas et al., 2011). The RNAseq data generated here provided an excellent opportunity to investigate MADS box gene expression in the context of barley ovule development, and determine stages and tissues where function might be important.

Based on the data presented here, expression of HvMADS genes is most abundant during Stage 5 of pistil development, when ovule tissues were shown to undergo a rapid increase in size and the differentiation of inner nucellus cells begins to become prominent. Furthermore, HvMADS gene expression is predominantly restricted to the maternal tissue, i.e. somatic cells outside of the embryo sac. The single exception to this is the gene *HvAGL1*, the putative barley orthologue of wheat AGL1 (Zhao et al. 2006), which is known as *SHATTERPROOF1* (*SHP1*) in Arabidopsis (Flanagan et al. 1996; Liljegren et al. 2000). In Arabidopsis, SHP1

interacts with SHP2 and other developmental regulators such as AINTEGUMENTA and CRABS CLAW (ANT, CRC) and MADS13, MADS29 and MADS31 (Class D and two B_{sister} transcription factors, respectively) to redundantly specify ovule identity, and regulate correct integument formation and carpel development (Colombo et al. 2010; Ehlers et al. 2016; Liljegren et al. 2000). In rice, expression of *OsMADS13* is required for ovule development (Dreni et al. 2007), and requires interaction with the AGL6 transcription factor MADS6 (Li et al. 2011). In the present data, *HvAGL1*, *MADS13*, *MADS29* and *MADS31* were observed to be expressed in distinct ovule tissues; *HvAGL1* in the embryo sac, *MADS13* in the integument, and *MADS29* and *MADS31* in the nucellus. Additionally, *MADS6* was found to be predominantly expressed in the ovary wall. These results indicate that *HvAGL1* may have a unique role in development of the egg apparatus or central cell in barley. Additionally, tissue-specific expression of these MADS-box genes indicates that, should their function be conserved between rice and barley, the products of these genes must be mobile in order to interact. The relative expression levels of *MADS29* and *MADS31* suggest that the roles of these genes may be reversed with respect to rice, where only *MADS29* is considered to be functional (Yin and Xue 2012). However, based on their nucellus-specific pattern of expression, the functional role of B_{sister} genes as putative regulators of programmed cell death in the nucellus and nucellar projection may be conserved in barley (Nayar et al. 2013; Yang et al. 2012; Yin and Xue 2012). This data set provides a basis for future work aimed at thoroughly translating the ABC model of floral development to barley.

Auxin-related genes are abundant during multiple stages of ovule and pistil development

In rice, mutants in the auxin pathway have pleiotropic effects on reproductive development, ranging from decreased fertility and seed abortion to increased seed size and increased grain weight (Fujita et al. 2013; Jun et al. 2011; Liu et al. 2015). A number of studies have addressed

the critical role of auxin signalling during Arabidopsis ovule development (reviewed in Lora et al., 2019; Shirley et al., 2018). Here, the transcript profiles of barley genes potentially involved in auxin signalling revealed dynamic patterns across development. Overall, differential presence of specific TIR/AFB, ARF, Aux/IAA and PIN family members in specific tissues and at each developmental stage points toward specific, developmentally regulated auxin responses and multiple discrete roles of auxin in the ovule and ovary wall as development progresses. Particularly within the female gametophyte, the egg apparatus and central cell were observed to express key auxin machinery in the form of *HvPIN1a* and *HvIAA1*, complemented by high abundance of *HvPIN1c* and *HvARF4c* in the pooled early nucellus and embryo sac. Further investigation of these genes using techniques such as *in situ* hybridisation may reveal a similar expression pattern of *HvPIN1* and *HvIAA* in the embryo sac and nucellus cells at the micropylar tip of the developing ovule as has been described in maize and Arabidopsis (Chettoor and Evans 2015; Panoli et al. 2015). Collectively, the data regarding “ovary wall” and “non-germline” genes suggests most of the signalling machinery, ranging from TIR/AFB family genes to IAA/ARF complexes that regulate auxin-responsive gene expression, is abundant within the nucellus and ovary wall at Stage 4. High and exclusive expression of *HvTIR1, HvIAA1* and *HvIAA3* in the chalaza sample indicates that this tissue, positioned at the junction of nucellus, integument and ovary wall, may play an important role in coordinating auxin flux and responses between the ovule and the surrounding ovary wall. Interestingly, this site coincides with the future location of the nucellar projection, and the location of DR5v2:3xnlsYFP expression (Shirley et al. 2018) which acts as a putative reporter for auxin accumulation (Ulmasov et al. 1997). None of the putative barley PIN auxin efflux transporters were observed to be abundant in the chalaza. This raises general questions regarding the role of auxin signalling during the late stages of ovule development in the *Triticeae*. However, much work is required to experimentally determine whether the function of orthologues of auxin-related genes are conserved between species.

Pectin accumulation reveals a specific domain within the barley nucellus that surrounds the germline

Immunohistological assays were used to assess whether differences in cell number or expansion might contribute to the differences in ovule size between the four selected barley genotypes. These assays revealed remarkable details of the barley ovule, and indicated that a combination of cell division and expansion contributes to overall ovule size at maturity. Perhaps of greater significance was the identification of specific cell wall epitopes that define sub-domains within the barley ovule. Specific LM19 labelling was detected in cells surrounding the germline from the earliest stages of development. Since pectin is usually synthesised in a methyesterified form (detected by LM20), the presence of de-methylesterified pectin (labelled by LM19) suggests that specific genes are induced in the ovule to support and/or potentiate cells undergoing germline development. Diverse pectin-related genes were identified in the RNAseq datasets, and perhaps the most interesting of these are the pectinmethylesterases (PME), the PME inhibitors (PMEI) and the polygalacturonases (PG) that were abundant in embryo sac-derived samples. One possibility is that these enzymes are secreted from the embryo sac to modify the cell walls of surrounding cells. Oligogalacturonic acids (OGAs) released by PG have been shown to antagonise IAA, thus disrupting auxin signalling and inhibiting organ elongation in pea stem and developing tobacco roots (Bellincampi et al. 1993; Branca et al. 1988). Further, the methylation status of pectin influences cell-cell signalling mediated by wall associated kinases (WAK), both by providing an anchor point to WAKs under Ca^{2+} rich conditions (Anderson et al. 2001; Decreux and Messiaen 2005), and direct activation of WAK1 signalling by OGAs (Brutus et al. 2010). Additionally, regulation of PME activity has been shown to be the molecular basis of auxin-mediated valve elongation in Arabidopsis carpels (Anderson et al. 2001). While the present data is insufficient to draw firm conclusions, it may be speculated that regulation of pectin methylesterification may play a role in mediating signalling among nucellus cells, and potentially between the nucellus and the cells of the

reproductive lineage, through interaction with auxin and receptor signalling pathways. Future studies of gene expression in the developing nucellus would benefit from isolating the inner and peripheral nucellus, in addition to modifying the activity of pectin-modifying genes in mutants or transgenic plants. It also remains unclear whether differential regulation of discrete groups of pectin machinery throughout ovule development confers changes in the mechanical properties of the cell walls. As discussed previously, further investigation of the abundance of Ca^{2+} in the ovule would be specifically required to determine the likely structural properties of pectin, as well as broader investigation of the overall cell wall rigidity and presence of other cell wall polysaccharides within the ovule using techniques such as FTIT-microscopy, atomic force microscopy (AFM) and high performance liquid chromatography (HPLC).

Conclusion

In sum, this study presents morphological and transcriptional data that may be used as a foundation for future studies of the developing barley ovule. Microscopic analysis revealed genotypic variation in the rate at which discrete domains of the ovule grow and contribute to overall ovule size, and demonstrated that the size of the ovule at stages early in female gametophyte development does not necessarily dictate the size of the mature ovule. Further, discrete regions of the nucellus were identified, and labelling of de-methylestereified pectin revealed a sub-domain within the nucellus surrounding the reproductive lineage. Following investigation of the expression profiles of genes involved in auxin signalling and regulation of the pectin content of cell walls, it is clear that groups of genes within these functional categories are differentially regulated throughout development, and in different cell types of the ovule. However, further study is required to determine whether differential regulation is responsible for developmental cues that influence ovule development in a genotype-dependent manner. Investigation of the barley MADS-box transcription factors revealed uniquely high expression of *HvAGL1* within the egg apparatus, and suggested a reversal of

the roles of the B_{sister} genes *MADS29* and *MADS31* within the nucellus with respect to rice based on the increased expression of *MADS31*.

References

Anderson CM, Wagner TA, Perret M, He Z-H, He D, Kohorn BD (2001) WAKs: cell wall-associated kinases linking the cytoplasm to the extracellular matrix. Plant Molecular Biology 47 (1):197-206. doi:10.1023/A:1010691701578

Andres-Robin A, Reymond MC, Dupire A, Battu V, Dubrulle N, Mouille G, Lefebvre V, Pelloux J, Boudaoud A, Traas J, Scutt CP, Monéger F (2018) Evidence for the regulation of gynoecium morphogenesis by *ETTIN* via cell wall dynamics. Plant Physiology 178 (3):1222. doi:10.1104/pp.18.00745

Arora R, Agarwal P, Ray S, Singh AK, Singh VP, Tyagi AK, Kapoor S (2007) MADS-box gene family in rice: genome-wide identification, organization and expression profiling during reproductive development and stress. BMC Genomics 8 (1):242

Atmodjo MA, Sakuragi Y, Zhu X, Burrell AJ, Mohanty SS, Atwood JA, 3rd, Orlando R, Scheller HV, Mohnen D (2011) Galacturonosyltransferase (GAUT)1 and GAUT7 are the core of a plant cell wall pectin biosynthetic homogalacturonan:galacturonosyltransferase complex. Proceedings of the National Academy of Sciences 108 (50):20225-20230. doi:10.1073/pnas.1112816108

Barnabás B, Jäger K, Fehér A (2008) The effect of drought and heat stress on reproductive processes in cereals. Plant, Cell & Environment 31 (1):11-38. doi:doi:10.1111/j.1365-3040.2007.01727.x

Beauzamy L, Nakayama N, Boudaoud A (2014) Flowers under pressure: ins and outs of turgor regulation in development. Annals of Botany 114 (7):1517-1533. doi:10.1093/aob/mcu187

Bellincampi D, Salvi G, De Lorenzo G, Cervone F, Marfà V, Eberhard S, Darvill A, Albersheim P (1993) Oligogalacturonides inhibit the formation of roots on tobacco explants. The Plant Journal 4 (1):207-213. doi:doi:10.1046/j.1365-313X.1993.04010207.x

Bidhendi AJ, Geitmann A (2015) Relating the mechanics of the primary plant cell wall to morphogenesis. Journal of Experimental Botany 67 (2):449-461. doi:10.1093/jxb/erv535

Bowman J, Mansfield S, Modrusan Z, Reiser L, Fischer R, Haughn G, Feldman K, Webb M (1994) Ovules. In: Arabidopsis. Springer, pp 297-331

Bowman JL, Smyth DR, Meyerowitz EM (2012) The ABC model of flower development: then and now. Development 139 (22):4095-4098. doi:10.1242/dev.083972

Branca C, Lorenzo GD, Cervone F (1988) Competitive inhibition of the auxin-induced elongation by α-D-oligogalacturonides in pea stem segments. Physiologia Plantarum 72 (3):499-504. doi:doi:10.1111/j.1399-3054.1988.tb09157.x

Briggs D (1978) Barley Chapman & Hall, London 6l2 pp

Brink RA, Cooper DC (1944) The antipodals in relation to abnormal endosperm behavior in Hordeum jubatum x Secale cereale hybrid seeds. Genetics 29 (4):391-406

Brutus A, Sicilia F, Macone A, Cervone F, De Lorenzo G (2010) A domain swap approach reveals a role of the plant wall-associated kinase 1 (WAK1) as a receptor of oligogalacturonides. Proceedings of the National Academy of Sciences 107 (20):9452-9457. doi:10.1073/pnas.1000675107

Burton RA, Jobling SA, Harvey AJ, Shirley NJ, Mather DE, Bacic A, Fincher GB (2008) The genetics and transcriptional profiles of the cellulose synthase-like *HvCslF* gene family in barley. Plant Physiology 146 (4):1821-1833

Callens C, Tucker MR, Zhang D, Wilson ZA (2018) Dissecting the role of MADS-box genes in monocot floral development and diversity. Oxford University Press UK,

Carraro N, Forestan C, Canova S, Traas J, Varotto S (2006) *ZmPIN1a* and *ZmPIN1b* encode two novel putative candidates for polar auxin transport and plant architecture determination of maize. Plant Physiology 142 (1):254-264

Cheng Y, Dai X, Zhao Y (2006) Auxin biosynthesis by the YUCCA flavin monooxygenases controls the formation of floral organs and vascular tissues in Arabidopsis. Genes & Development 20 (13):1790-1799. doi:10.1101/gad.1415106

Chettoor AM, Evans MMS (2015) Correlation between a loss of auxin signaling and a loss of proliferation in maize antipodal cells. Frontiers in Plant Science 6 (187). doi:10.3389/fpls.2015.00187

Chettoor AM, Evans MMS (2017) Live-cell imaging of auxin and cytokinin signaling in maize female gametophytes. In: Schmidt A (ed) Plant Germline Development: Methods and Protocols. Springer New York, New York, NY, pp 95-101. doi:10.1007/978-1-4939-7286-9_9

Chettoor AM, Givan SA, Cole RA, Coker CT, Unger-Wallace E, Vejlupkova Z, Vollbrecht E, Fowler JE, Evans MM (2014) Discovery of novel transcripts and gametophytic functions via RNA-seq analysis of maize gametophytic transcriptomes. Genome Biology 15 (7):414-414. doi:10.1186/s13059-014-0414-2

Cho M, Lee SH, Cho H-T (2007) P-Glycoprotein4 displays auxin efflux transporter–like action in *Arabidopsis* root hair cells and tobacco cells. The Plant Cell 19 (12):3930-3943

Coen ES, Meyerowitz EM (1991) The war of the whorls: genetic interactions controlling flower development. Nature 353 (6339):31

Colombo M, Brambilla V, Marcheselli R, Caporali E, Kater MM, Colombo L (2010) A new role for the SHATTERPROOF genes during *Arabidopsis* gynoecium development. Developmental Biology 337 (2):294-302. doi:https://doi.org/10.1016/j.ydbio.2009.10.043

Cosgrove DJ (1999) Enzymes and other agents that enhance cell wall extensibility. Annual Review of Plant Physiology and Plant Molecular Biology 50 (1):391-417. doi:10.1146/annurev.arplant.50.1.391

Crhak Khaitova L, Mroue S, Robert HS, Benková E (2015) The importance of localized auxin production for morphogenesis of reproductive organs and embryos in *Arabidopsis*. Journal of Experimental Botany 66 (16):5029-5042. doi:10.1093/jxb/erv256

Decreux A, Messiaen J (2005) Wall-associated kinase WAK1 interacts with cell wall pectins in a calcium-induced conformation. Plant and Cell Physiology 46 (2):268-278. doi:10.1093/pcp/pci026

Dharmasiri N, Dharmasiri S, Weijers D, Lechner E, Yamada M, Hobbie L, Ehrismann JS, Jürgens G, Estelle M (2005) Plant development is regulated by a family of auxin receptor f box proteins. Developmental Cell 9 (1):109-119. doi:https://doi.org/10.1016/j.devcel.2005.05.014

Dornelas MC, Patreze CM, Angenent GC, Immink RG (2011) MADS: the missing link between identity and growth? Trends in Plant Science 16 (2):89-97

Dreni L, Jacchia S, Fornara F, Fornari M, Ouwerkerk PBF, An G, Colombo L, Kater MM (2007) The D-lineage MADS-box gene OsMADS13 controls ovule identity in rice. The Plant Journal 52 (4):690-699. doi:doi:10.1111/j.1365-313X.2007.03272.x

Dreni L, Pilatone A, Yun D, Erreni S, Pajoro A, Caporali E, Zhang D, Kater MM (2011) Functional analysis of all AGAMOUS subfamily members in rice reveals their roles in

reproductive organ identity determination and meristem determinacy. The Plant Cell 23 (8):2850-2863. doi:10.1105/tpc.111.087007

Dreni L, Zhang D (2016) Flower development: the evolutionary history and functions of the AGL6 subfamily MADS-box genes. Journal of Experimental Botany 67 (6):1625-1638. doi:10.1093/jxb/erw046

Drula E, Golaconda Ramulu H, Coutinho PM, Lombard V, Henrissat B (2013) The carbohydrate-active enzymes database (CAZy) in 2013. Nucleic Acids Research 42 (D1):D490-D495. doi:10.1093/nar/gkt1178

Ehlers K, Bhide AS, Tekleyohans DG, Wittkop B, Snowdon RJ, Becker A (2016) The MADS box genes *ABS*, *SHP1*, and *SHP2* are essential for the coordination of cell divisions in ovule and seed coat development and for endosperm formation in *Arabidopsis thaliana*. PLOS ONE 11 (10):e0165075-e0165075. doi:10.1371/journal.pone.0165075

Endress PK (2011) Angiosperm ovules: diversity, development, evolution. Annals of Botany 107 (9):1465-1489. doi:10.1093/aob/mcr120

Engell K (1994) Embryology of barley. IV. Ultrastructure of the antipodal cells of *Hordeum vulgare* L. cv. Bomi before and after fertilization of the egg cell. Sexual Plant Reproduction 7 (6):333-346

Fahy B, Siddiqui H, David LC, Powers SJ, Borrill P, Uauy C, Smith AM (2018) Final grain weight is not limited by the activity of key starch-synthesising enzymes during grain filling in wheat. Journal of Experimental Botany 69 (22):5461-5475. doi:10.1093/jxb/ery314

Favaro R, Immink R, Ferioli V, Bernasconi B, Byzova M, Angenent G, Kater M, Colombo L (2002) Ovule-specific MADS-box proteins have conserved protein-protein interactions in monocot and dicot plants. Molecular Genetics and Genomics 268 (2):152-159

Favaro R, Pinyopich A, Battaglia R, Kooiker M, Borghi L, Ditta G, Yanofsky MF, Kater MM, Colombo L (2003) MADS-box protein complexes control carpel and ovule development in *Arabidopsis*. The Plant Cell 15 (11):2603-2611. doi:10.1105/tpc.015123

Flanagan CA, Hu Y, Ma H (1996) Specific expression of the *AGL1* MADS-box gene suggests regulatory functions in *Arabidopsis* gynoecium and ovule development. The Plant Journal 10 (2):343-353. doi:doi:10.1046/j.1365-313X.1996.10020343.x

Friml J (2010) Subcellular trafficking of PIN auxin efflux carriers in auxin transport. European Journal of Cell Biology 89 (2):231-235. doi:https://doi.org/10.1016/j.ejcb.2009.11.003

Fujita D, Trijatmiko KR, Tagle AG, Sapasap MV, Koide Y, Sasaki K, Tsakirpaloglou N, Gannaban RB, Nishimura T, Yanagihara S, Fukuta Y, Koshiba T, Slamet-Loedin IH, Ishimaru T, Kobayashi N (2013) *NAL1* allele from a rice landrace greatly increases yield in modern *indica* cultivars. Proceedings of the National Academy of Sciences 110 (51):20431-20436. doi:10.1073/pnas.1310790110

Goldberg R, Morvan C, Jauneau A, Jarvis MC (1996) Methyl-esterification, de-esterification and gelation of pectins in the primary cell wall. In: Visser J, Voragen AGJ (eds) Progress in Biotechnology, vol 14. Elsevier, pp 151-172. doi:https://doi.org/10.1016/S0921-0423(96)80253-X

Guo Z, Slafer GA, Schnurbusch T (2016) Genotypic variation in spike fertility traits and ovary size as determinants of floret and grain survival rate in wheat. Journal of Experimental Botany 67 (14):4221-4230. doi:10.1093/jxb/erw200

Haagen-Smit A, Dandliker W, Wittwer S, Murneek A (1946) Isolation of 3-indoleacetic acid from immature corn kernels. American Journal of Botany:118-120

Hongo S, Sato K, Yokoyama R, Nishitani K (2012) Demethylesterification of the primary wall by PECTIN METHYLESTERASE35 provides mechanical support to the Arabidopsis stem. The Plant Cell 24 (6):2624-2634. doi:10.1105/tpc.112.099325

IBSC IBGSC (2012) A physical, genetic and functional sequence assembly of the barley genome. Nature 491 (7426):711

Ito T, Meyerowitz EM (2000) Overexpression of a gene encoding a cytochrome P450, *CYP78A9*, induces large and seedless fruit in *Arabidopsis*. The Plant Cell 12 (9):1541-1550

Iwai H, Masaoka N, Ishii T, Satoh S (2002) A pectin glucuronyltransferase gene is essential for intercellular attachment in the plant meristem. Proceedings of the National Academy of Sciences 99 (25):16319-16324

Jack T (2001) Plant development going MADS. Plant Molecular Biology 46 (5):515-520. doi:10.1023/A:1010689126632

Jain M, Khurana JP (2009) Transcript profiling reveals diverse roles of auxin-responsive genes during reproductive development and abiotic stress in rice. The FEBS Journal 276 (11):3148-3162

Johnston AJ, Meier P, Gheyselinck J, Wuest SE, Federer M, Schlagenhauf E, Becker JD, Grossniklaus U (2007) Genetic subtraction profiling identifies genes essential for Arabidopsisreproduction and reveals interaction between the female gametophyte and the maternal sporophyte. Genome Biology 8 (10):R204. doi:10.1186/gb-2007-8-10-r204

Jun N, Gaohang W, Zhenxing Z, Huanhuan Z, Yunrong W, Ping W (2011) OsIAA23-mediated auxin signaling defines postembryonic maintenance of QC in rice. The Plant Journal 68 (3):433-442

Juranić M, Tucker MR, Schultz CJ, Shirley NJ, Taylor JM, Spriggs A, Johnson SD, Bulone V, Koltunow AM (2018) Asexual female gametogenesis involves contact with a sexually-fated megaspore in apomictic *Hieracium*. Plant Physiology 177 (3):1027-1049. doi:10.1104/pp.18.00342

Kaethner TM (1977) Conformational change theory for auxin structure–activity relationships. Nature 267 (5606):19-23. doi:10.1038/267019a0

Kellogg EA (2015) Flowering plants. monocots: Poaceae, vol 13. Springer,

Kubo T, Fujita M, Takahashi H, Nakazono M, Tsutsumi N, Kurata N (2013) Transcriptome analysis of developing ovules in rice isolated by laser microdissection. Plant and cell physiology 54 (5):750-765

Larsson E, Sundberg E, Franks RG (2013) Auxin and the *Arabidopsis thaliana* gynoecium. Journal of Experimental Botany 64 (9):2619-2627. doi:10.1093/jxb/ert099

Lee DS, Chen LJ, Li CY, Liu Y, Tan XL, Lu B-R, Li J, Gan SX, Kang SG, Suh HS, Zhu Y (2013) The Bsister MADS gene *FST* determines ovule patterning and development of the zygotic embryo and endosperm. PLOS ONE 8 (3):e58748-e58748. doi:10.1371/journal.pone.0058748

Li H, Liang W, Hu Y, Zhu L, Yin C, Xu J, Dreni L, Kater MM, Zhang D (2011) Rice *MADS6* interacts with the floral homeotic genes *SUPERWOMAN1*, *MADS3, MADS58, MADS13,* and *DROOPING LEAF* in specifying floral organ identities and meristem fate. The Plant Cell 23 (7):2536-2552. doi:10.1105/tpc.111.087262

Li H, Liang W, Jia R, Yin C, Zong J, Kong H, Zhang D (2010) The *AGL6*-like gene *OsMADS6* regulates floral organ and meristem identities in rice. Cell Research 20 (3):299

Liljegren SJ, Ditta GS, Eshed Y, Savidge B, Bowman JL, Yanofsky MF (2000) *SHATTERPROOF* MADS-box genes control seed dispersal in *Arabidopsis*. Nature 404:766. doi:10.1038/35008089

Liu L, Tong H, Xiao Y, Che R, Xu F, Hu B, Liang C, Chu J, Li J, Chu C (2015) Activation of Big Grain1 significantly improves grain size by regulating auxin transport in rice. Proceedings of the National Academy of Sciences 112 (35):11102-11107

Lloyd FE (1899) The comparative embryology of the rubiaceae. Memoirs of the Torrey Botanical Club 8 (1):1-112

Lora J, Herrero M, Tucker MR, Hormaza JI (2017) The transition from somatic to germline identity shows conserved and specialized features during angiosperm evolution. New Phytologist 216 (2):495-509. doi:doi:10.1111/nph.14330

Lora J, Laux T, Hormaza JI (2019) The role of the integuments in pollen tube guidance in flowering plants. New Phytologist 221 (2):1074-1089

Maheswari P (1950) An introduction to the embryology of angiosperms. Tata Mcgraw-Hill Publishing Company Ltd; Bombay; New Delhi,

Mizzotti C, Ezquer I, Paolo D, Rueda-Romero P, Guerra RF, Battaglia R, Rogachev I, Aharoni A, Kater MM, Caporali E, Colombo L (2014) *SEEDSTICK* is a master regulator of development and metabolism in the *Arabidopsis* seed coat. PLoS Genetics 10 (12):e1004856-e1004856. doi:10.1371/journal.pgen.1004856

Morris ER, Powell DA, Gidley MJ, Rees DA (1982) Conformations and interactions of pectins: I. Polymorphism between gel and solid states of calcium polygalacturonate. Journal of Molecular Biology 155 (4):507-516. doi:https://doi.org/10.1016/0022-2836(82)90484-3

Mouille G, Ralet M-C, Cavelier C, Eland C, Effroy D, Hématy K, McCartney L, Truong HN, Gaudon V, Thibault J-F, Marchant A, Höfte H (2007) Homogalacturonan synthesis in Arabidopsis thaliana requires a Golgi-localized protein with a putative methyltransferase domain. The Plant Journal 50 (4):605-614. doi:doi:10.1111/j.1365-313X.2007.03086.x

Murai K (2013) Homeotic genes and the ABCDE model for floral organ formation in wheat. Plants (Basel, Switzerland) 2 (3):379-395. doi:10.3390/plants2030379

Nayar S, Kapoor S, Sharma R, Tyagi AK (2013) Functional delineation of rice MADS29 reveals its role in embryo and endosperm development by affecting hormone homeostasis. Journal of Experimental Botany 64 (14):4239-4253. doi:10.1093/jxb/ert231

Noh B, Murphy AS, Spalding EP (2001) Multidrug resistance–like genes of *Arabidopsis* required for auxin transport and auxin-mediated development. The Plant Cell 13 (11):2441-2454

Nonomura K-I, Miyoshi K, Eiguchi M, Suzuki T, Miyao A, Hirochika H, Kurata N (2003) The *MSP1* gene is necessary to restrict the number of cells entering into male and female sporogenesis and to initiate anther wall formation in rice. The Plant Cell 15 (8):1728-1739

Nonomura K-I, Morohoshi A, Nakano M, Eiguchi M, Miyao A, Hirochika H, Kurata N (2007) A germ cell specific gene of the ARGONAUTE family is essential for the progression of premeiotic mitosis and meiosis during sporogenesis in rice. The Plant cell 19 (8):2583-2594. doi:10.1105/tpc.107.053199

O'NEILL M, ALBERSHEIM P, DARVILL A (1990) The pectic polysaccharides of primary cell walls. In: Methods in Plant Biochemistry, vol 2. Elsevier, pp 415-441

Ohnishi T, Takanashi H, Mogi M, Takahashi H, Kikuchi S, Yano K, Okamoto T, Fujita M, Kurata N, Tsutsumi N (2011) Distinct gene expression profiles in egg and synergid cells of rice as revealed by cell type-specific microarrays. Plant Physiology 155 (2):881-891. doi:10.1104/pp.110.167502

Okada T, Hu Y, Tucker MR, Taylor JM, Johnson SD, Spriggs A, Tsuchiya T, Oelkers K, Rodrigues JCM, Koltunow AMG (2013) Enlarging cells initiating apomixis in *Hieracium praealtum* transition to an embryo sac program prior to entering mitosis. Plant Physiology 163 (1):216-231. doi:10.1104/pp.113.219485

Pagnussat GC, Alandete-Saez M, Bowman JL, Sundaresan V (2009) Auxin-dependent patterning and gamete specification in the *Arabidopsis* female gametophyte. Science 324 (5935):1684-1689. doi:10.1126/science.1167324

Panoli A, Martin MV, Alandete-Saez M, Simon M, Neff C, Swarup R, Bellido A, Yuan L, Pagnussat GC, Sundaresan V (2015) Auxin import and local auxin biosynthesis are required for mitotic divisions, cell expansion and cell specification during female gametophyte development in *Arabidopsis thaliana*

PLOS ONE 10 (5):e0126164-e0126164. doi:10.1371/journal.pone.0126164

Parry G, Calderon-Villalobos LI, Prigge M, Peret B, Dharmasiri S, Itoh H, Lechner E, Gray WM, Bennett M, Estelle M (2009) Complex regulation of the TIR1/AFB family of auxin receptors. Proceedings of the National Academy of Sciences 106 (52):22540-22545. doi:10.1073/pnas.0911967106

Peaucelle A, Louvet R, Johansen JN, Höfte H, Laufs P, Pelloux J, Mouille G (2008) *Arabidopsis* phyllotaxis is controlled by the methyl-esterification status of cell-wall pectins. Current Biology 18 (24):1943-1948. doi:https://doi.org/10.1016/j.cub.2008.10.065

Pinto SC, Mendes MA, Coimbra S, Tucker MR (2019) Revisiting the female germline and its expanding toolbox. Trends in Plant Science *in press*

Pinyopich A, Ditta GS, Savidge B, Liljegren SJ, Baumann E, Wisman E, Yanofsky MF (2003) Assessing the redundancy of MADS-box genes during carpel and ovule development. Nature 424:85. doi:10.1038/nature01741

https://www.nature.com/articles/nature01741#supplementary-information

Qiu YL, Liu RS, Xie CT, Russell SD, Tian HQ (2008) Calcium changes during megasporogenesis and megaspore degeneration in lettuce (*Lactuca sativa* L.). Sexual Plant Reproduction 21 (3):197-204

Radchuk V, Borisjuk L, Radchuk R, Steinbiss H-H, Rolletschek H, Broeders S, Wobus U (2006) *Jekyll* encodes a novel protein involved in the sexual reproduction of barley. The Plant Cell 18 (7):1652-1666. doi:10.1105/tpc.106.041335

Rafińska K, Świdziński M, Bednarska-Kozakiewicz E (2014) Homogalacturonan deesterification during pollen-ovule interaction in *Larix decidua* Mill.: an immunocytochemical study. Planta 240 (1):195-208. doi:10.1007/s00425-014-2074-6

Ray A, Lang JD, Golden T, Ray S (1996) *SHORT INTEGUMENT (SIN1)*, a gene required for ovule development in Arabidopsis, also controls flowering time. Development 122 (9):2631-2638

Ridley BL, O'Neill MA, Mohnen D (2001) Pectins: structure, biosynthesis, and oligogalacturonide-related signaling. Phytochemistry 57 (6):929-967. doi:https://doi.org/10.1016/S0031-9422(01)00113-3

Schneitz K, Hülskamp M, Pruitt RE (1995) Wild-type ovule development in *Arabidopsis thaliana:* a light microscope study of cleared whole-mount tissue. The Plant Journal 7 (5):731-749. doi:doi:10.1046/j.1365-313X.1995.07050731.x

Sechet J, Marion-Poll A, North H (2018) Emerging functions for cell wall polysaccharides accumulated during Eudicot seed development. Plants 7 (4):81

Sénéchal F, Habrylo O, Hocq L, Domon J-M, Marcelo P, Lefebvre V, Pelloux J, Mercadante D (2017) Structural and dynamical characterization of the pH-dependence of the pectin methylesterase-pectin methylesterase inhibitor complex. The Journal of Biological Chemistry 292 (52):21538-21547. doi:10.1074/jbc.RA117.000197

Sénéchal F, L'Enfant M, Domon J-M, Rosiau E, Crépeau M-J, Surcouf O, Esquivel-Rodriguez J, Marcelo P, Mareck A, Guérineau F, Kim H-R, Mravec J, Bonnin E, Jamet E, Kihara D, Lerouge P, Ralet M-C, Pelloux J, Rayon C (2015) Tuning of pectin methylesterification: PECTIN METHYLESTERASE INHIBITOR 7 modulates the processive activity of co-expressed PECTIN METHYLESTERASE 3 in a pH-dependent manner. The Journal of Biological Chemistry 290 (38):23320-23335. doi:10.1074/jbc.M115.639534

Shirley NJ, Aubert MK, Wilkinson LG, Bird DC, Lora J, Yang X, Tucker MR (2018) Translating auxin responses into ovules, seeds and yield: Insight from Arabidopsis and the cereals. Journal of Integrative Plant Biology

Sobry S, Havelange A, Van Cutsem P (2005) Immunocytochemistry of pectins in shoot apical meristems: consequences for intercellular adhesion. Protoplasma 225 (1-2):15-22

Spiro MD, Bowers JF, Cosgrove DJ (2002) A comparison of oligogalacturonide- and auxin-induced extracellular alkalinization and growth responses in roots of intact cucumber seedlings. Plant Physiology 130 (2):895-903. doi:10.1104/pp.006064

Sprunck S, Rademacher S, Vogler F, Gheyselinck J, Grossniklaus U, Dresselhaus T (2012) Egg cell–secreted EC1 triggers sperm cell activation during double fertilization. Science 338 (6110):1093-1097. doi:10.1126/science.1223944

Steffen JG, Kang I-H, Macfarlane J, Drews GN (2007) Identification of genes expressed in the Arabidopsis female gametophyte. The Plant Journal 51 (2):281-292. doi:doi:10.1111/j.1365-313X.2007.03137.x

Stepanova AN, Robertson-Hoyt J, Yun J, Benavente LM, Xie D-Y, Doležal K, Schlereth A, Jürgens G, Alonso JM (2008) TAA1-mediated auxin biosynthesis is essential for hormone crosstalk and plant development. Cell 133 (1):177-191. doi:https://doi.org/10.1016/j.cell.2008.01.047

Swarup K, Benková E, Swarup R, Casimiro I, Péret B, Yang Y, Parry G, Nielsen E, De Smet I, Vanneste S (2008) The auxin influx carrier LAX3 promotes lateral root emergence. Nature Cell Biology 10 (8):946

Theißen G, Kim JT, Saedler H (1996) Classification and phylogeny of the MADS-box multigene family suggest defined roles of MADS-box gene subfamilies in the morphological evolution of eukaryotes. Journal of Molecular Evolution 43 (5):484-516. doi:10.1007/BF02337521

Theißen G, Melzer R, Rümpler F (2016) MADS-domain transcription factors and the floral quartet model of flower development: linking plant development and evolution. Development 143 (18):3259-3271. doi:10.1242/dev.134080

Thiel J, Weier D, Sreenivasulu N, Strickert M, Weichert N, Melzer M, Czauderna T, Wobus U, Weber H, Weschke W (2008) Different hormonal regulation of cellular differentiation and function in nucellar projection and endosperm transfer cells: a microdissection-based transcriptome study of young barley grains. Plant Physiology 148 (3):1436-1452. doi:10.1104/pp.108.127001

Thimann KV (1958) Auxin activity of some indole derivatives. Plant Physiology 33 (5):311-321

Tiwari SB, Hagen G, Guilfoyle TJ (2004) Aux/IAA proteins contain a potent transcriptional repression domain. The Plant Cell 16 (2):533-543. doi:10.1105/tpc.017384

Tran V, Weier D, Radchuk R, Thiel J, Radchuk V (2014) Caspase-like activities accompany programmed cell death events in developing barley grains. PLOS ONE 9 (10):e109426-e109426. doi:10.1371/journal.pone.0109426

Tucker MR, Lou H, Aubert MK, Wilkinson LG, Little A, Houston K, Pinto SC, Shirley NJ (2018) Exploring the role of cell wall-related genes and polysaccharides during plant development. Plants (Basel, Switzerland) 7 (2):42. doi:10.3390/plants7020042

Tucker MR, Okada T, Hu Y, Scholefield A, Taylor JM, Koltunow AMG (2012) Somatic small RNA pathways promote the mitotic events of megagametogenesis during female reproductive development in *Arabidopsis*. Development 139 (8):1399-1404. doi:10.1242/dev.075390

Ulmasov T, Hagen G, Guilfoyle TJ (1999) Activation and repression of transcription by auxin-response factors. Proceedings of the National Academy of Sciences 96 (10):5844-5849. doi:10.1073/pnas.96.10.5844

Ulmasov T, Murfett J, Hagen G, Guilfoyle TJ (1997) Aux/IAA proteins repress expression of reporter genes containing natural and highly active synthetic auxin response elements. The Plant Cell 9 (11):1963-1971. doi:10.1105/tpc.9.11.1963

Untergasser A, Cutcutache I, Koressaar T, Ye J, Faircloth BC, Remm M, Rozen SG (2012) Primer3—new capabilities and interfaces. Nucleic Acids Research 40 (15):e115-e115

Vandesompele J, De Preter K, Pattyn F, Poppe B, Van Roy N, De Paepe A, Speleman F (2002) Accurate normalization of real-time quantitative RT-PCR data by geometric averaging of multiple internal control genes. Genome biology 3 (7):research0034. 0031

Verhertbruggen Y, Marcus SE, Haeger A, Ordaz-Ortiz JJ, Knox JP (2009) An extended set of monoclonal antibodies to pectic homogalacturonan. Carbohydrate Research 344 (14):1858-1862

Vincken J-P, Schols HA, Oomen RJFJ, McCann MC, Ulvskov P, Voragen AGJ, Visser RGF (2003) If homogalacturonan were a side chain of rhamnogalacturonan I. Implications for cell wall architecture. Plant Physiology 132 (4):1781-1789. doi:10.1104/pp.103.022350

Waddington S, Cartwright P, Wall P (1983) A quantitative scale of spike initial and pistil development in barley and wheat. Annals of Botany 51 (1):119-130

Wang C-JR, Nan G-L, Kelliher T, Timofejeva L, Vernoud V, Golubovskaya IN, Harper L, Egger R, Walbot V, Cande WZ (2012) Maize MULTIPLE ARCHESPORIAL CELLS 1 (MAC1), an ortholog of rice TDL1A, modulates cell proliferation and identity in early anther development. Development 139 (14):2594-2603

Wang HL, Offler CE, Patrick JW (1994) Nucellar projection transfer cells in the developing wheat grain. Protoplasma 182 (1):39-52. doi:10.1007/BF01403687

Weatherwax P (1926) Persistence of the antipodal tissue in the development of the seed of maize. Bulletin of the Torrey Botanical Club 53 (6):381-384. doi:10.2307/2481150

Wilkinson LG, Bird DC, Tucker MR (2018) Exploring the role of the ovule in cereal grain development and reproductive stress tolerance. Annual Plant Reviews:1-35

Wilkinson LG, Tucker MR (2017) An optimised clearing protocol for the quantitative assessment of sub-epidermal ovule tissues within whole cereal pistils. Plant Methods 13 (1):67

Willemse M, De Boer-de M (1981) Megasporogenesis and early megagametogenesis. Acta Societatis Botanicorum Poloniae 50 (1-2):111-120

Wolf S, Greiner S (2012) Growth control by cell wall pectins. Protoplasma 249 (2):169-175. doi:10.1007/s00709-011-0371-5

Wolf S, Mouille G, Pelloux J (2009) Homogalacturonan methyl-esterification and plant development. Molecular Plant 2 (5):851-860. doi:https://doi.org/10.1093/mp/ssp066

Won C, Shen X, Mashiguchi K, Zheng Z, Dai X, Cheng Y, Kasahara H, Kamiya Y, Chory J, Zhao Y (2011) Conversion of tryptophan to indole-3-acetic acid by TRYPTOPHAN AMINOTRANSFERASES OF ARABIDOPSIS and YUCCAs in Arabidopsis. Proceedings of the National Academy of Sciences 108 (45):18518-18523. doi:10.1073/pnas.1108436108

Wuest SE, Vijverberg K, Schmidt A, Weiss M, Gheyselinck J, Lohr M, Wellmer F, Rahnenführer J, von Mering C, Grossniklaus U (2010) Arabidopsis female gametophyte gene expression map reveals similarities between plant and animal gametes. Current Biology 20 (6):506-512. doi:https://doi.org/10.1016/j.cub.2010.01.051

Yang J, Yuan Z, Meng Q, Huang G, Périn C, Bureau C, Meunier A-C, Ingouff M, Bennett MJ, Liang W, Zhang D (2017) Dynamic regulation of auxin response during rice development revealed by newly established hormone biosensor markers. Frontiers in Plant Science 8:256-256. doi:10.3389/fpls.2017.00256

Yang X, Wu F, Lin X, Du X, Chong K, Gramzow L, Schilling S, Becker A, Theißen G, Meng Z (2012) Live and let die-the Bsister MADS-box gene *OsMADS29* controls the degeneration of cells in maternal tissues during seed development of rice *(Oryza sativa)*. PLOS ONE 7 (12):e51435

Yin L-L, Xue H-W (2012) The MADS29 transcription factor regulates the degradation of the nucellus and the nucellar projection during rice seed development. The Plant Cell 24 (3):1049-1065. doi:10.1105/tpc.111.094854

Yoshida H, Nagato Y (2011) Flower development in rice. Journal of Experimental Botany 62 (14):4719-4730. doi:10.1093/jxb/err272

You R, Jensen WA (1985) Ultrastructural observations of the mature megagametophyte and the fertilization in wheat (*Triticum aestivum*). Canadian Journal of Botany 63 (2):163-178

Yu H-J, Hogan P, Sundaresan V (2005) Analysis of the female gametophyte transcriptome of arabidopsis by comparative expression profiling. Plant Physiology 139 (4):1853-1869. doi:10.1104/pp.105.067314

Zhang R, Tucker MR, Burton RA, Shirley NJ, Little A, Morris J, Milne L, Houston K, Hedley PE, Waugh R, Fincher GB (2016) The dynamics of transcript abundance during cellularization of developing barley endosperm. Plant Physiology 170 (3):1549-1565. doi:10.1104/pp.15.01690

Zhao T, Ni Z, Dai Y, Yao Y, Nie X, Sun Q (2006) Characterization and expression of 42 MADS-box genes in wheat (*Triticum aestivum* L.). Molecular Genetics and Genomics 276 (4):334. doi:10.1007/s00438-006-0147-3

Supplementary Data

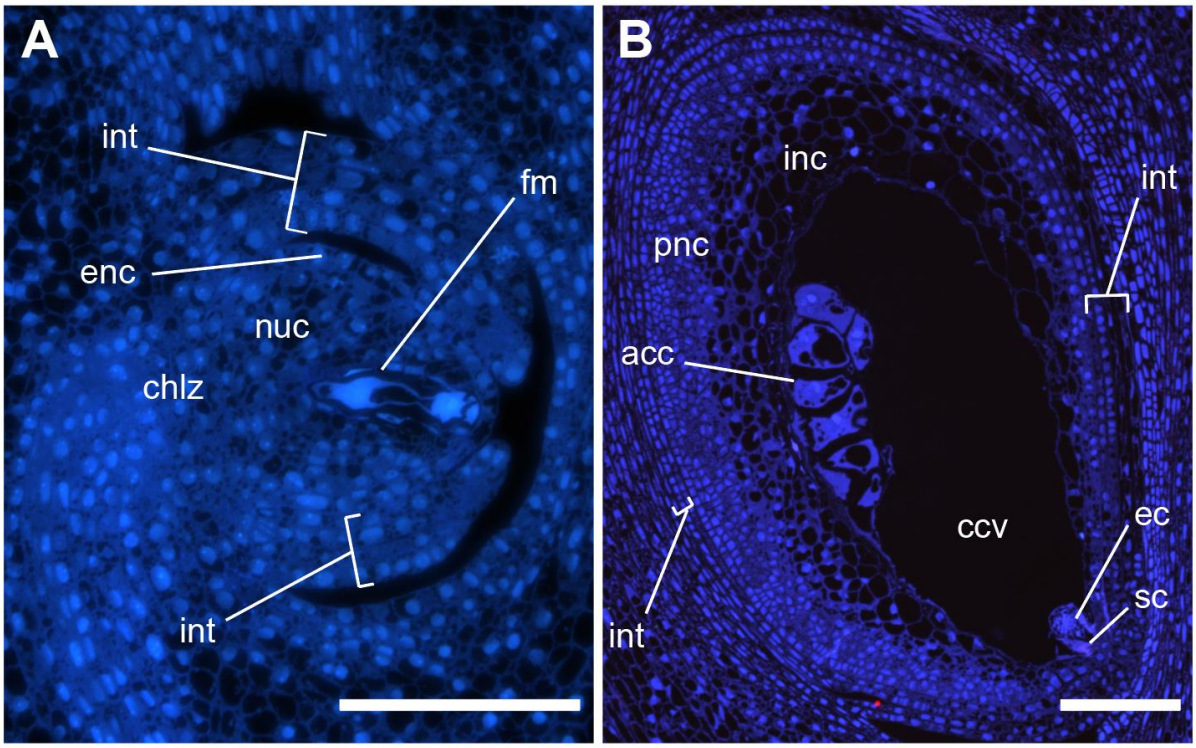

Figure 5-S1: Negative controls for immunohistochemical staining of barley ovules at (A) Stage 3, as the functional megaspore begins development of the embryo sac, and (B) Stage 7, at reproductive maturity, for presence of demethylesterified (LM19) and methylesterified (LM20) pectin. Negative control was performed by exclusion of primary antibody while secondary antibody (AlexaFluor 555 anti-rat monoclonal IgG) was applied. Autofluorescence at 461nm is shown in blue. Sections were taken in the saggital aspect, 0.8μm thickness. Scale bars = 100μm. acc, antipodal cell cluster; ccv, central cell vacuole; chlz, chalaza; ec, egg cell; enc, epithelial nucellus cells; fm, functional megaspore; inc; inner nucellus cells; int, integument; nuc, nucellus; pnc, peripheral nucellus cells; sc, synergid cell.

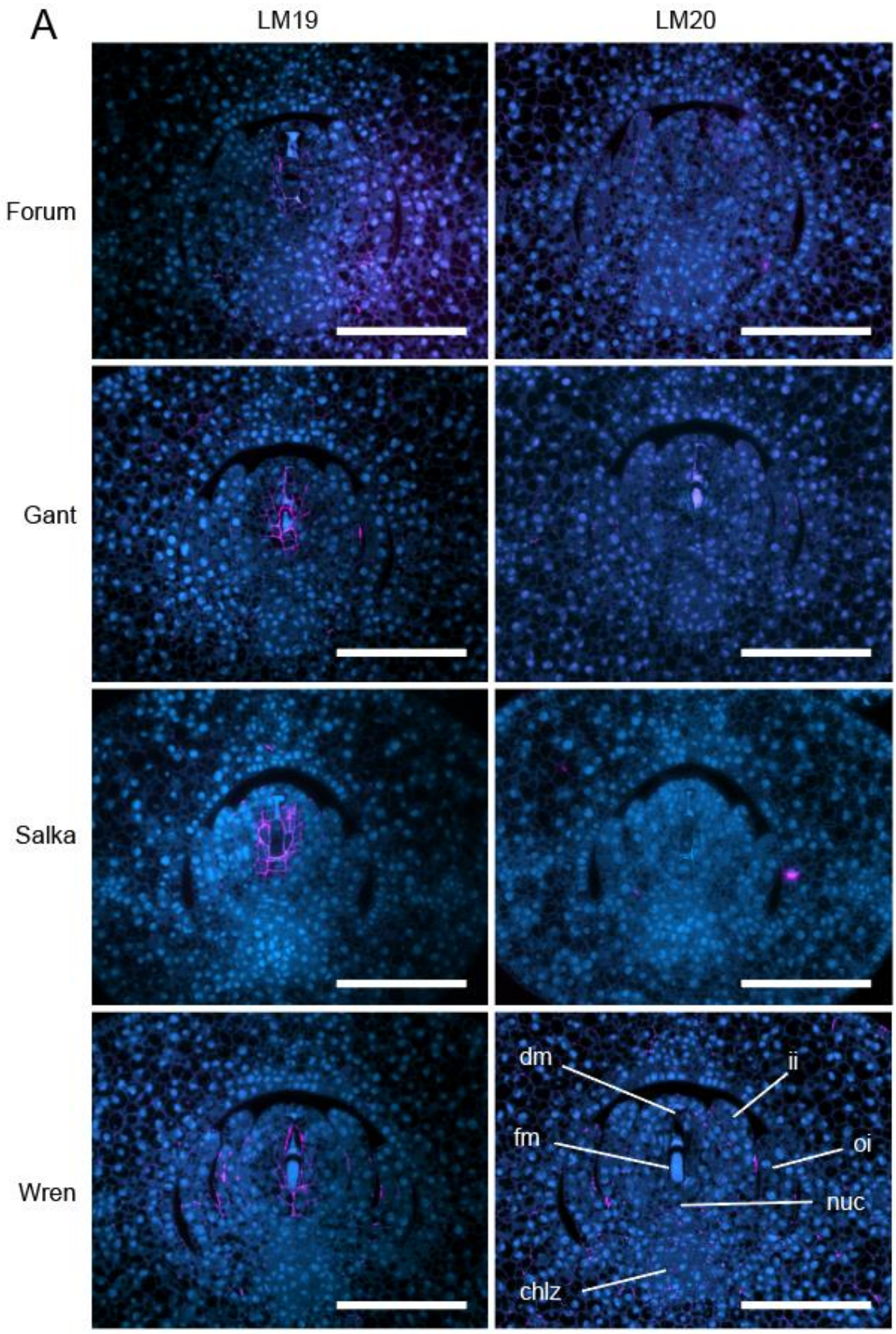
A
LM19
LM20
Forum
Gant
Salka
Wren
dm
ii
fm
oi
nuc
chlz

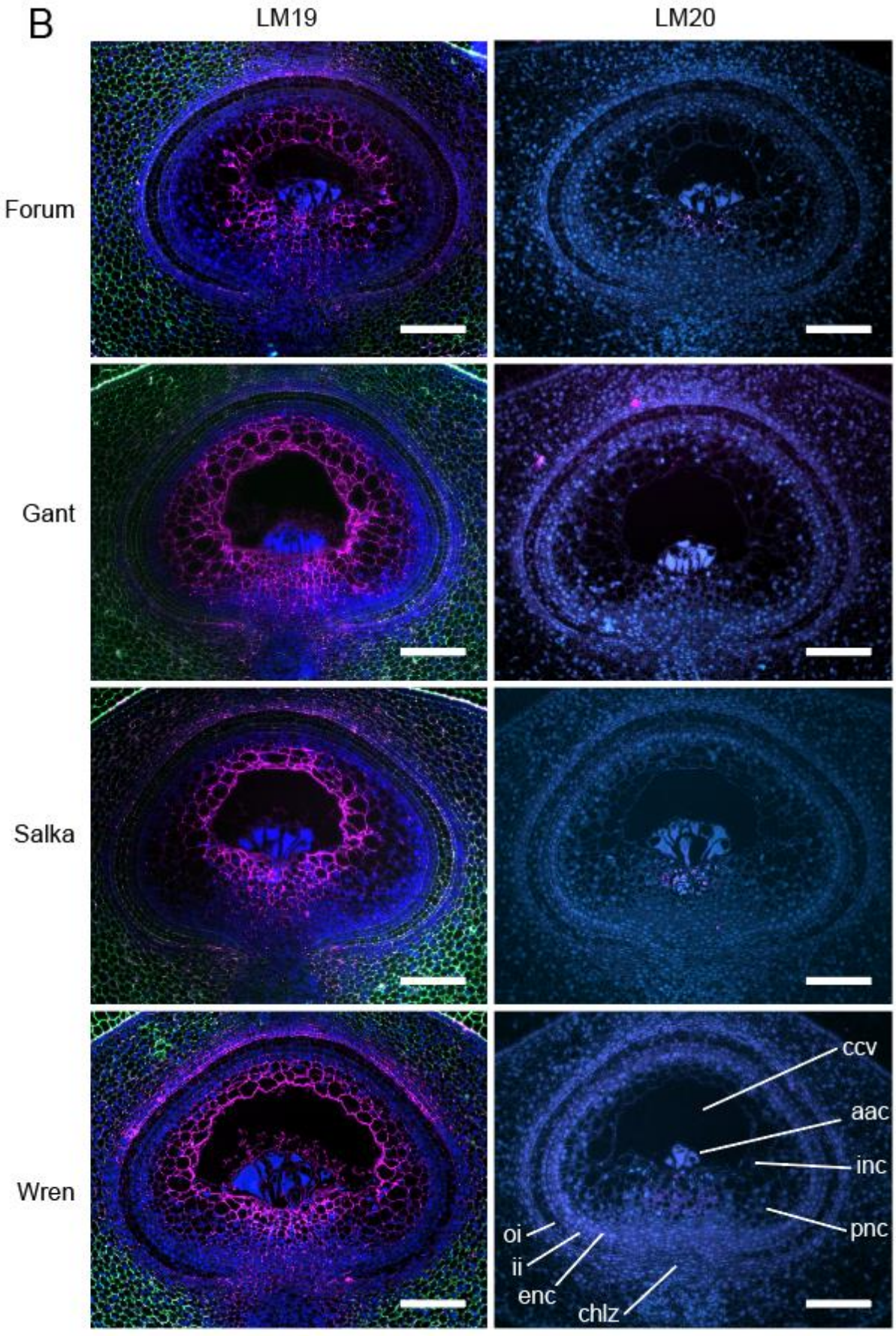
B
LM19
LM20
Forum
Gant
Salka
Wren
ccv
aac
inc
pnc
oi
ii
enc
chlz

Figure 5-S2: Immunohistochemical microscopic comparison of demethylesterified (LM19) and methylesterified (LM20) pectin localisation in barley ovules of four genotypes, at (A) Stage 3, as the functional megaspore begins development of the embryo sac and (B) Stage 7, as the ovule becomes reproductively mature. De-methylesterified pectin was labelled with LM19, methylesterified pectin was labelled with LM20, and both are shown in magenta. At Stage 7 (B) sections labelled with LM19 were additionally labelled with BG1, visualising ß-(1,3;1,4)-glucan, shown in green. Autofluorescence at 461nm is shown in blue. Sections were taken in the transverse aspect, with 0.8μm thickness. aac, archesporial cell; ccv, central cell vacuole; chlz, chalaza; dm, degenerating megaspore; enc = epithelial nucellus cells; ii, inner integument; inc; inner nucellus cells; nuc, nucellus; oi, outer integument; pnc, peripheral nucellus cells. Scale bars = 100μm.

Table 5-S1: Total number of unique HORVUs identified, and HORVUs with transcript abundance (TPM), following sequencing of RNA extracted from whole pistils of four genotypes of barley (Forum, Gant, Salka and Wren) at five stages spanning initiation of the embryo sac to reproductive maturity (Stages 3-7), each with two replicates. RNA quality of replicate samples of Forum Stage 3, Salka at Stage 3, and Wren at Stages 5 and 7 was too poor to allow sequencing.

Cultivar	Stage	Rep	# HORVUs	# HORVUs TPM>5
Forum	3	1	31616	11379
Forum	3	n/a	n/a	n/a
Forum	4	1	31980	11456
Forum	4	2	31427	11496
Forum	5	1	32163	11639
Forum	5	2	30912	11139
Forum	6	1	31676	11308
Forum	6	2	32956	11645
Forum	7	1	33033	11772
Forum	7	2	32558	11708
Gant	3	1	30820	11368
Gant	3	2	32037	11883
Gant	4	1	30356	10705
Gant	4	2	30838	11231
Gant	5	1	30950	11338
Gant	5	2	31483	11610
Gant	6	1	31006	11354
Gant	6	2	31941	11812
Gant	7	1	31718	11459
Gant	7	2	31760	11418
Salka	3	1	32039	11647
Salka	3	n/a	n/a	n/a
Salka	4	1	32340	11911
Salka	4	2	30707	11193
Salka	5	1	31015	11320
Salka	5	2	32980	12048
Salka	6	1	32708	11782
Salka	6	2	32974	11715
Salka	7	1	30994	11432
Salka	7	2	32998	11708
Wren	3	1	30739	10994
Wren	3	2	31010	10967

Wren	4	1	32896	11754
Wren	4	2	32554	11700
Wren	5	n/a	n/a	n/a
Wren	5	2	32723	11780
Wren	6	1	30144	11180
Wren	6	2	29607	11024
Wren	7	1	26809	10396
Wren	7	n/a	n/a	n/a

Table 5-S2: Total number of unique HORVUs identified following sequencing of RNA extracted from specific ovule tissues isolated using laser capture microdissection from ovules of barley genotype Sloop, at three stages of ovule development (Stages 4, 5 and 7).

Tissue	Developmental Stage	# HORVUs	# HORVUs TPM>5
Embryo Sac + Nucellus	Stage 4	26967	12552
Embryo Sac	Stage 5	16480	7836
Egg Apparatus + Central Cell	Stage 5	18130	8925
Egg Apparatus + Central Cell	Stage 7	11921	5703
Antipodal Cells	Stage 5	19638	9503
Antipodal Cells	Stage 7	14226	6885
Nucellus	Stage 5	24789	10725
Nucellus	Stage 7	21234	9872
Chalaza	Stage 7	17112	8677
Integument	Stage 4	25451	10947
Integument	Stage 5	26406	11874
Integument	Stage 7	21301	10101
Ovary Wall	Stage 4	29905	11178
Ovary Wall	Stage 5	27897	12130
Ovary Wall	Stage 7	26294	11661
All Tissues	All Stages	40476	19143

Table 5-S3 Total number of unique HORVUs identified following sequencing of RNA extracted from whole pistils of four genotypes of barley (Forum, Gant, Salka and Wren) at five stages spanning initiation of the embryo sac to reproductive maturity (Stages 3- 7).

Identity	# HORVUs	# HORVUS with TPM >5	% Total with TPM >5
All genotypes	51800	15594	30.1
Forum	42981	13219	30.8
Gant	42131	13132	31.2
Salka	43386	13705	31.6
Wren	42284	13968	33.0
Stage 3	40967	13330	32.5
Stage 4	43036	13499	31.4
Stage 5	42608	13505	31.7
Stage 6	43358	13604	31.4
Stage 7	42494	13481	31.7

Table 5-S4 Average number of unique HORVUs identified in each sample following sequencing of RNA extracted from whole pistils of four genotypes of barley (Forum, Gant, Salka and Wren) at five stages spanning initiation of the embryo sac to reproductive maturity (Stages 3- 7).

Sample	# HORVUs	# HORVUs with TPM > 5
Forum	32035.7 ± 672.7	11504.7 ± 194.7
Gant	31290.9 ± 540.1	11417.8 ± 310.9
Salka	32083.9 ± 889.1	11639.6 ± 261.6
Wren	30810.3 ± 1903.8	11224.4 ± 455.9
Stage 3	31376.8 ± 545.1	11373 ± 327.5
Stage 4	31637.3 ± 882.2	11430.8 ± 359.8
Stage 5	31746.6 ± 809.2	11553.4 ± 287.6
Stage 6	31626.5 ± 1199.8	11477.5 ± 280
Stage 7	31410 ± 2001.2	11413.3 ± 437.5
Forum Stage 3	31616 ± 0	11379 ± 0
Forum Stage 4	31703.5 ± 276.5	11476 ± 20
Forum Stage 5	31537.5 ± 625.5	11389 ± 250
Forum Stage 6	32316 ± 640	11476.5 ± 168.5
Forum Stage 7	32795.5 ± 237.5	11740 ± 32
Gant Stage 3	31428.5 ± 608.5	11625.5 ± 257.5
Gant Stage 4	30597 ± 241	10968 ± 263
Gant Stage 5	31216.5 ± 266.5	11474 ± 136
Gant Stage 6	31473.5 ± 467.5	11583 ± 229
Gant Stage 7	31739 ± 21	11438.5 ± 20.5
Salka Stage 3	32039 ± 0	11647 ± 0
Salka Stage 4	31523.5 ± 816.5	11552 ± 359
Salka Stage 5	31997.5 ± 982.5	11684 ± 364
Salka Stage 6	32841 ± 133	11748.5 ± 33.5
Salka Stage 7	31996 ± 1002	11570 ± 138
Wren Stage 3	30874.5 ± 135.5	10980.5 ± 13.5
Wren Stage 4	32725 ± 171	11727 ± 27
Wren Stage 5	32723 ± 0	11780 ± 0
Wren Stage 6	29875.5 ± 268.5	11102 ± 78

Wren Stage 7	26809 ± 0	10396 ± 0

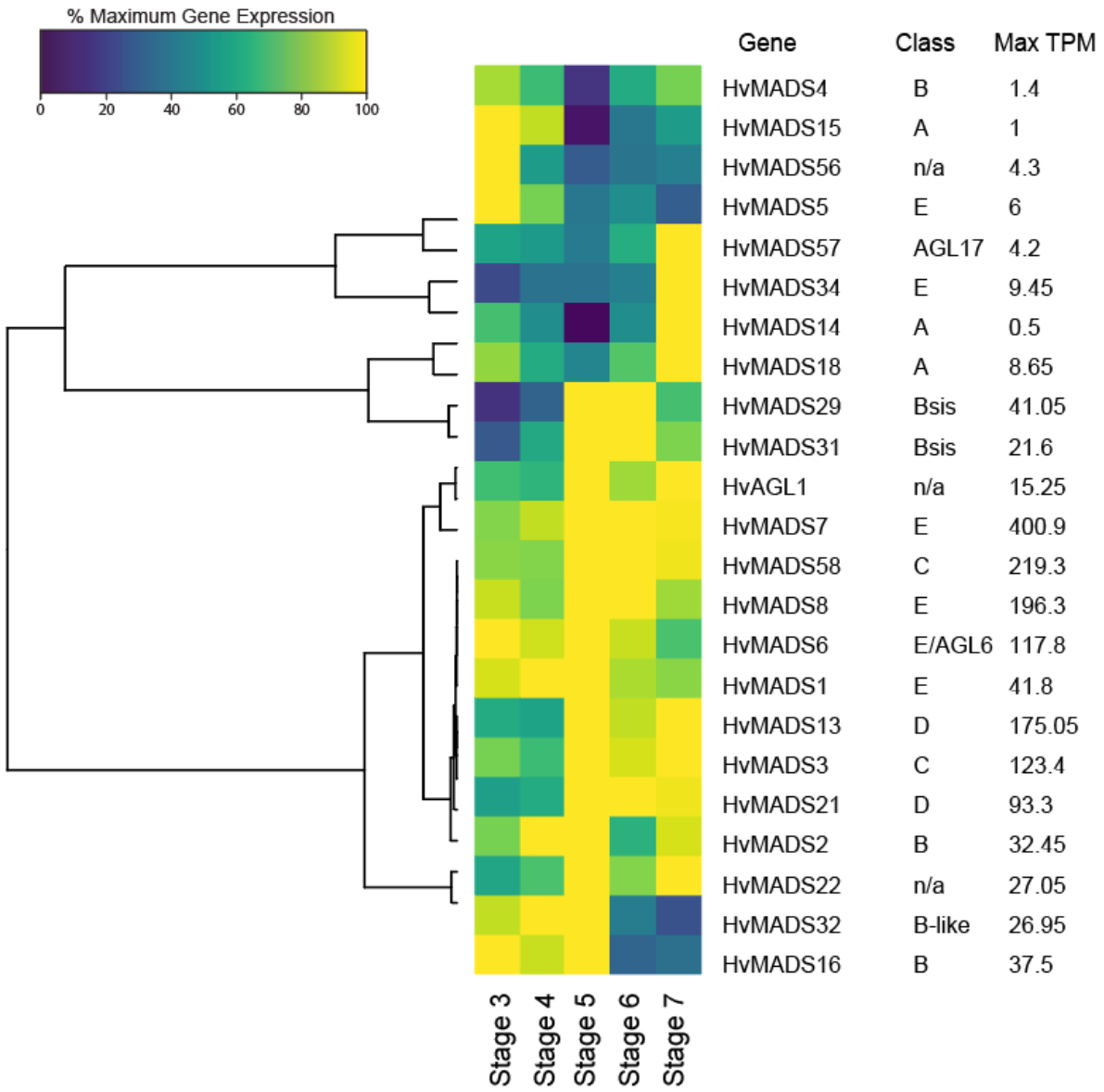

Figure 5-S3: Heatmap showing average expression of putative barley genes encoding MADS-box transcription factors at five stages of ovule development in four barley genotypes, as determined by RNA sequencing of whole pistils. Transcript abundance values (TPM) have been normalised to 1.

Table 5-S5: Locus identifiers for barley genes putatively encoding MADS-box transcription factors found to be expressed within whole-pistil and tissue-specific RNA-sequencing data sets, with transcript abundance (TPM) greater than 5.

Class	Name	Barley	Barley MLOC	Rice	Arabidopsis	Tissue-specific maximum TPM	Whole-pistil maximum TPM
A	HvBM14	HORVU1Hr1G047560		LOC_Os03g54160	At1g69120	0.7	0.5
A	HvBM15	HORVU2Hr1G063800	MLOC_61901	LOC_Os07g01820	At1g69120	0.2	1.0
A	HvBM18	HORVU2Hr1G069820	MLOC_36644	LOC_Os04g31804	At5g60910	6.5	8.7
AGL17	HvBM57	HORVU6Hr1G073040		LOC_Os02g49840	At3g57230	24.2	4.2
B	HvBM16	HORVU7Hr1G091210		LOC_Os06g49840	At3g54340	2.7	37.5
B	HvBM2	HORVU3Hr1G091000	MLOC_59262	LOC_Os01g66030	At5g20240	12.9	32.5
B	HvBM4	HORVU4Hr1G077850	MLOC_65665	LOC_Os03g08754	At2g22540	1.1	1.4
B-like	HvBM32	HORVU3Hr1G068900	MLOC_80902	LOC_Os01g52680	At5g60910	134.4	27.0
Bsis	HvBM29	HORVU6Hr1G032220	MLOC_65966	LOC_Os02g07430	At1g26310	61.4	41.1
Bsis	HvBM31	HORVU2Hr1G098930	MLOC_12133	LOC_Os04g52410	At5g23260	327.4	21.6
C	HvBM3	HORVU3Hr1G026650	MLOC_5375	LOC_Os01g10504	At4g18960	135.7	123.4
C	HvBM58	HORVU1Hr1G029220	MLOC_57700	LOC_Os05g11414	At4g18960	170.8	219.3
D	HvBM13	HORVU1Hr1G023620	MLOC_57890	LOC_Os12g10540	At3g58780	432.2	175.1
D	HvBM21	HORVU1Hr1G064150	MLOC_65843	LOC_Os01g66290	At4g09960	339.6	93.3
E	HvBM1	HORVU4Hr1G067680		LOC_Os03g11614	At3g02310	39.3	41.8
E	HvBM34	HORVU5Hr1G095710	MLOC_64157	LOC_Os03g54170	At5g15800	2.0	9.5
E	HvBM5	HORVU7Hr1G025700		LOC_Os06g06750	At3g02310	4.5	6.0
E	HvBM7	HORVU7Hr1G054220	MLOC_56472	LOC_Os08g41950	At1g24260	417.9	400.9
E	HvBM8	HORVU5Hr1G076400	MLOC_37733	LOC_Os09g32948	At1g24260	63.0	196.3
E/AGL6	HvBM6	HORVU6Hr1G066140	MLOC_52944	LOC_Os02g45770	At2g45650	78.7	117.8
n/a	HvAGL1	HORVU6Hr1G002330	MLOC_54256	LOC_Os02g01355		245.5	15.3
n/a	HvBM22	HORVU6Hr1G077300	MLOC_47708	LOC_Os02g52340	At2g22540	46.9	27.1
n/a	HvBM56	HORVU1Hr1G051660		LOC_Os10g39130	At2g45660	0.3	4.3

Table 5-S6. Expression of barley genes putatively encoding MADS-box transcription factors at five stages of ovule development, in four barley genotypes (Forum, Gant, Salka and Wren), as determined by RNA-sequencing of whole pistils. Expression values are transcripts per million (TPM).

Class	Gene	Stage 3	Stage 4	Stage 5	Stage 6	Stage 7
A	HvMADS14	0.4 ± 0.1	0.3 ± 0.1	0.2 ± 0.1	0.3 ± 0	0.5 ± 0.2
A	HvMADS15	1 ± 0.2	0.9 ± 0.1	0.5 ± 0.2	0.4 ± 0.1	0.6 ± 0.2
A	HvMADS18	7.2 ± 1.6	5.3 ± 0.7	4.1 ± 0.6	6.4 ± 1	8.7 ± 3
AGL17	HvMADS57	2.5 ± 0.3	2.3 ± 0.4	3.6 ± 0.8	2.6 ± 0.5	4.2 ± 1.3
B	HvMADS16	37.5 ± 10.1	34.2 ± 8.4	30.2 ± 8	12.3 ± 1.6	14.1 ± 3.4
B	HvMADS2	25.6 ± 5.7	32.5 ± 7.4	28.2 ± 3.5	21 ± 2.1	30.4 ± 10.7
B	HvMADS4	1.2 ± 0.4	1 ± 0.3	1.4 ± 0.3	0.9 ± 0.2	1.1 ± 0.3
B-like	HvMADS32	24.3 ± 7.9	27 ± 6.8	18.8 ± 4.8	11.5 ± 2.8	6.8 ± 2.1
Bsis	HvMADS29	6 ± 0.4	12.9 ± 2.9	28.4 ± 6.7	41.1 ± 11.8	28.9 ± 10.1
Bsis	HvMADS31	6 ± 0.9	13.1 ± 3.1	20 ± 3.1	21.6 ± 6.3	17.3 ± 6.9
C	HvMADS3	97.5 ± 14.2	84 ± 7.3	84 ± 3.5	115.5 ± 6.9	123.4 ± 8.1
C	HvMADS58	179.9 ± 11.1	176.8 ± 11.1	200.8 ± 7	219.3 ± 28	214.5 ± 27.4
D	HvMADS13	107.2 ± 10.6	101.9 ± 8.3	118.1 ± 6.4	157.7 ± 12.2	175.1 ± 18.5
D	HvMADS21	52.3 ± 7.2	56.6 ± 8.8	62.2 ± 8.5	93.3 ± 8.8	91.3 ± 6.8
E	HvMADS1	38.8 ± 7.5	41.8 ± 8.6	39.8 ± 7.1	36.3 ± 5.4	34 ± 5.5
E	HvMADS34	2.2 ± 0.3	3.6 ± 0.9	3.3 ± 1	4.1 ± 1.3	9.5 ± 3.7
E	HvMADS5	6 ± 1.2	4.8 ± 0.6	3.5 ± 0.4	3 ± 0.6	1.8 ± 0.4
E	HvMADS7	325.4 ± 24.3	363 ± 32.4	384 ± 18	400.9 ± 24	394.1 ± 17.1
E	HvMADS8	179.7 ± 16.6	156.3 ± 8.9	167.7 ± 11.6	196.3 ± 16.1	165.7 ± 8.8
E/AGL6	HvMADS6	117.8 ± 5.4	109.2 ± 7.4	95.6 ± 12.7	107.6 ± 16.1	84.4 ± 11.1
n/a	HvAGL1	10.5 ± 2	9.9 ± 2.2	11.7 ± 2.9	12.9 ± 2.3	15.3 ± 2.4
n/a	HvMADS22	15.8 ± 0.7	19.4 ± 2.7	21 ± 2.4	21.7 ± 3	27.1 ± 2.8
n/a	HvMADS56	4.3 ± 1.2	2.4 ± 0.4	2.5 ± 0.6	1.7 ± 0.5	1.9 ± 0.5

Table 5-S7: Expression of barley genes putatively encoding MADS-box transcription factors within fifteen tissue-specific RNA-sequencing samples, collected from the genotype Sloop. Expression values are given as transcripts per million (TPM). ANTP, antipodal cell cluster; CHLZ, chalaza; ECC, egg apparatus and central cell; ES, embryo sac; INT, integument; NUC, nucellus; NUCES, nucellus and embryo sac; OW, ovary wall.

Class	Gene	ES	ECC		ANTP		NUC			CHLZ	INT			OW		
		Stage 5	Stage 5	Stage 7	Stage 5	Stage 7	NUCES Stage 4	Stage 5	Stage 7	Stage 7	Stage 4	Stage 5	Stage 7	Stage 4	Stage 5	Stage 7
A	HvMADS14	0.0	0.0	0.7	0.0	0.0	0.0	0.0	0.0	0.0	0.0	0.0	0.0	0.0	0.0	0.0
A	HvMADS15	0.0	0.1	0.0	0.0	0.0	0.1	0.0	0.0	0.2	0.0	0.0	0.0	0.1	0.0	0.0
A	HvMADS18	0.7	0.1	0.0	0.2	0.0	2.2	3.1	1.8	0.2	2.6	4.3	1.8	2.5	6.5	4.2
AGL17	HvMADS57	2.4	8.9	4.6	3.0	0.0	2.2	7.1	0.2	4.4	0.4	24.2	0.8	0.9	10.2	0.8
B	HvMADS16	0.0	0.0	0.0	0.0	0.0	1.3	0.0	0.0	0.0	0.2	0.2	0.0	0.3	1.2	2.7
B	HvMADS2	0.4	3.4	0.0	1.2	0.0	3.5	3.7	11.2	12.9	5.2	6.7	9.7	1.2	2.6	7.9
B	HvMADS4	0.0	0.0	0.0	0.0	0.0	0.0	0.4	0.0	1.1	0.0	0.6	0.0	0.1	0.5	0.3
B-like	HvMADS32	0.0	4.9	0.1	1.1	0.0	0.7	28.7	18.4	1.7	95.6	134.4	47.8	6.7	5.4	2.1
Bsis	HvMADS29	3.1	10.3	0.1	23.3	0.0	61.4	53.9	6.3	1.5	7.7	7.9	0.6	0.0	0.0	0.0
Bsis	HvMADS31	74.1	122.4	83.1	143.0	4.2	327.4	215.3	153.9	3.6	16.1	20.2	7.6	0.7	1.4	1.2
C	HvMADS3	5.5	35.5	32.6	17.7	2.7	99.7	60.1	28.3	83.1	85.5	135.7	58.3	35.8	65.2	55.3
C	HvMADS58	1.0	9.3	16.5	10.4	0.7	62.0	27.8	11.1	56.8	62.4	146.0	61.4	170.8	160.1	152.8
D	HvMADS13	13.4	107.7	151.6	52.4	0.9	171.7	253.3	184.0	204.5	153.2	432.2	355.9	24.4	45.3	31.7
D	HvMADS21	0.5	28.5	8.9	5.6	0.0	9.5	8.0	0.9	56.4	144.9	339.6	334.5	1.8	10.9	4.9
E	HvMADS1	0.0	0.1	0.0	5.2	0.0	0.3	4.2	1.2	32.6	0.0	0.8	1.1	0.9	37.2	39.3
E	HvMADS34	0.0	0.0	0.0	0.0	0.0	0.0	0.0	0.0	0.0	0.0	0.0	0.0	2.0	0.9	1.7
E	HvMADS5	0.0	0.3	0.0	1.7	0.0	4.5	3.2	0.6	0.0	1.1	3.7	2.7	1.4	3.9	2.2
E	HvMADS7	25.6	69.8	69.2	65.3	0.0	178.7	181.8	245.5	297.9	149.0	417.9	399.8	91.0	232.2	294.9
E	HvMADS8	6.7	20.2	0.1	5.5	0.0	38.6	26.9	11.8	7.6	49.2	63.0	14.3	35.7	34.8	14.3
E/AGL6	HvMADS6	0.2	0.2	0.0	0.4	0.0	32.6	25.0	14.5	69.9	65.2	43.0	37.4	78.7	78.2	65.1
n/a	HvAGL1	79.8	105.2	245.5	34.7	44.6	12.6	18.9	11.9	9.3	16.9	36.2	22.7	4.9	5.5	3.0
n/a	HvMADS22	8.3	25.4	6.3	21.3	25.3	3.5	1.0	0.4	23.2	12.2	27.9	20.4	11.6	21.1	46.9
n/a	HvMADS56	0.0	0.0	0.0	0.0	0.0	0.0	0.0	0.0	0.0	0.0	0.0	0.2	0.2	0.1	0.3

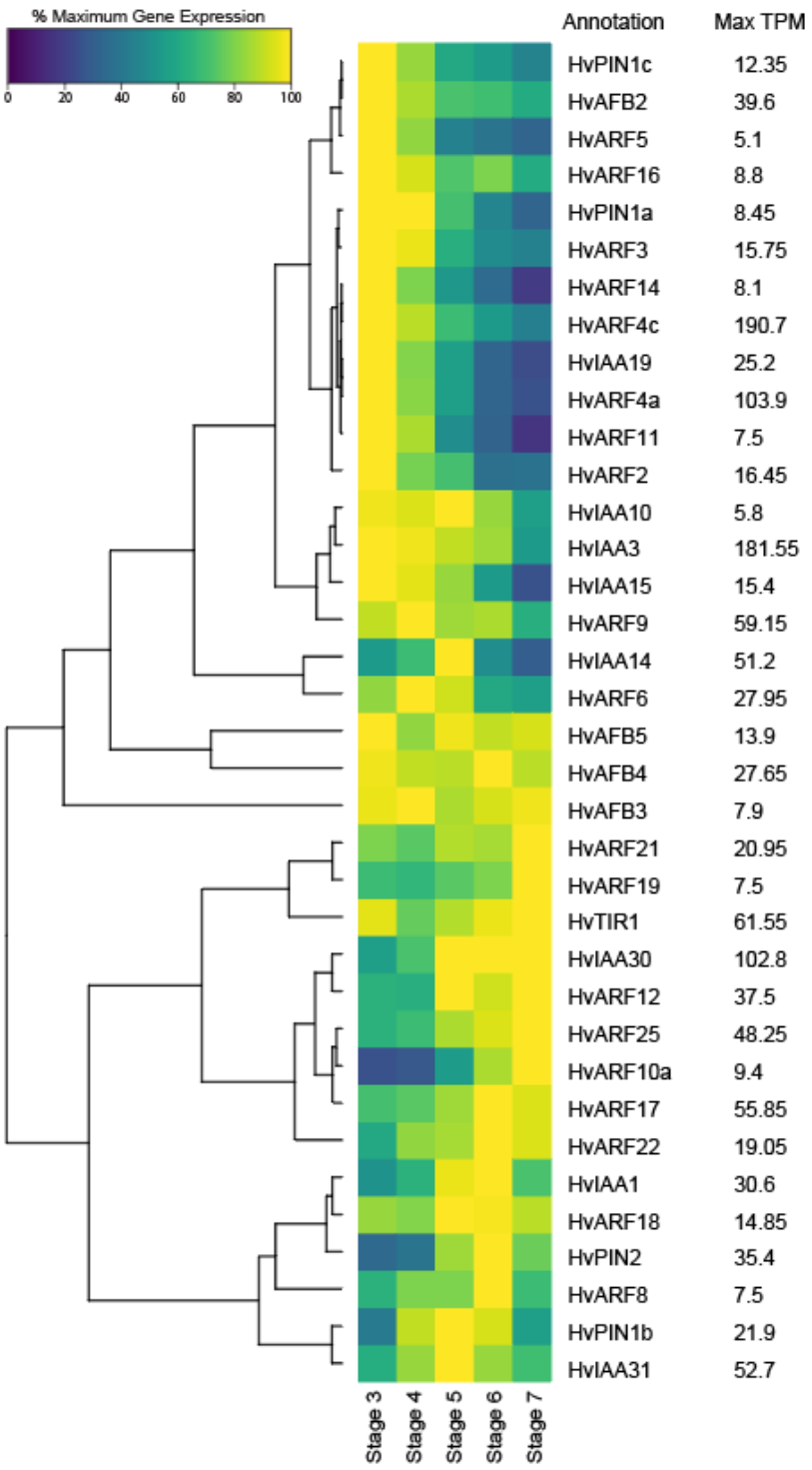

Figure 5-S4. Heatmap showing average expression of putative barley genes involved in auxin biosynthesis and transport at five stages of ovule development in four barley genotypes, as determined by RNA sequencing of whole pistils. Transcript abundance values (TPM) have been normalised to 1.

Table 5-S8: Locus identifiers for barley genes putatively involved in auxin biosynthesis and trnasport found to be expressed within whole-pistil and tissue-specific RNA-sequencing data sets, with transcript abundance (TPM) greater than 5.

Gene	HORVU	Barley MLOC	Rice	Arabidopsis	Tissue-specific maximum TPM	Whole-pistil maximum TPM
HvAFB2	HORVU2Hr1G070800	MLOC_56088	LOC_Os04g32460	At3g26810	28.9	39.6
HvAFB3	HORVU5Hr1G075620	MLOC_52024	LOC_Os11g31620	At1g12820	25.9	7.9
HvAFB4	HORVU6Hr1G077570	MLOC_66474	LOC_Os02g52230	At5g49980	65.3	27.7
HvAFB5	HORVU4Hr1G078120	MLOC_73542	LOC_Os03g08850	At5g49980	25.5	13.9
HvARF10a	HORVU2Hr1G089670		LOC_Os04g43910	At2g28350	11.0	9.4
HvARF11	HORVU2Hr1G109650	MLOC_55345	LOC_Os04g56850	At1g19850	9.9	7.5
HvARF12	HORVU2Hr1G121110	MLOC_51932	LOC_Os04g57610	At1g30330	19.7	37.5
HvARF14	HORVU1Hr1G076690	MLOC_38232	LOC_Os05g43920	At2g33860	14.2	8.1
HvARF16	HORVU7Hr1G033820	MLOC_5871	LOC_Os06g09660	At1g19220	14.9	8.8
HvARF17	HORVU7Hr1G106280	MLOC_58330	LOC_Os06g46410	At1g30330	58.1	55.9
HvARF18	HORVU7Hr1G101270	MLOC_69988	LOC_Os06g47150	At4g30080	30.8	14.9
HvARF19	HORVU7Hr1G096460	MLOC_63194	LOC_Os02g04810	At1g19220	33.5	7.5
HvARF2	HORVU1Hr1G087460	MLOC_17721	LOC_Os05g48870	At2g33860	19.4	16.5
HvARF21	HORVU7Hr1G051930	MLOC_14584	LOC_Os08g40900	At1g19220	28.8	21.0
HvARF22	HORVU1Hr1G041770	MLOC_64795	LOC_Os10g33940	At4g30080	91.0	19.1
HvARF25	HORVU5Hr1G009650	MLOC_63938	LOC_Os12g41950	At1g30330	21.6	48.3
HvARF3	HORVU3Hr1G072340	MLOC_66439	LOC_Os01g54990	At2g33860	9.7	15.8
HvARF4a	HORVU3Hr1G097200	MLOC_18401	LOC_Os01g70270	At5g62000	88.4	103.9
HvARF4c	HORVU3Hr1G096510		LOC_Os01g70270	At5g62000	103.2	190.7
HvARF5	HORVU6Hr1G020330	MLOC_73144	LOC_Os02g04810	At1g19220	5.3	5.1
HvARF6	HORVU6Hr1G026730		LOC_Os02g06910	At1g30330	17.3	28.0

HvARF8	HORVU6Hr1G058890	MLOC_77438	LOC_Os02g41800	At4g30080	7.2	7.5
HvARF9	HORVU2Hr1G076920	MLOC_64596	LOC_Os04g36054	At1g59750	80.9	59.2
HvIAA1	HORVU3Hr1G022540		LOC_Os01g08320	At1g04250	228.1	30.6
HvIAA10	HORVU6Hr1G091260	MLOC_65332	LOC_Os02g57250	At2g33310	12.3	5.8
HvIAA14	HORVU5Hr1G106350	MLOC_57434	LOC_Os03g58350	At4g29080	34.6	51.2
HvIAA15	HORVU1Hr1G025670		LOC_Os05g08570	At2g22670	32.1	15.4
HvIAA19	HORVU1Hr1G086070	MLOC_10203	LOC_Os05g48590	At2g22670	46.7	25.2
HvIAA3	HORVU3Hr1G031460	MLOC_54255	LOC_Os05g14180	At4g29080	222.0	181.6
HvIAA30	HORVU5Hr1G014300	MLOC_73033	LOC_Os12g40890	At3g04730	342.0	102.8
HvIAA31	HORVU5Hr1G014290	MLOC_60624	LOC_Os12g40900	At1g04240	86.6	52.7
HvTIR1	HORVU1Hr1G021550	MLOC_9864	LOC_Os05g05800	At3g62980	242.4	61.6
HvPIN1a	HORVU7Hr1G038700	MLOC_12686	LOC_Os06g12610	At2g01420	99.9	8.5
HvPIN1b	HORVU6Hr1G076110	MLOC_64867	LOC_Os02g50960	At1g23080	32.8	21.9
HvPIN1c	HORVU4Hr1G026680	MLOC_293	LOC_Os11g04190	At2g01420	144.7	12.4
HvPIN2	HORVU7Hr1G110470		LOC_Os06g44970	At5g57090	76.7	35.4

Table 5-S9: Expression of barley genes putatively involved in auxin biosynthesis and transport at five stages of ovule development, in four barley genotypes (Forum, Gant, Salka and Wren), as determined by RNA-sequencing of whole pistils. With the exception of Forum at Stage 3, Salka at Stage 3, and Wren at Stages 5 and 7, all data presented is the average of two replicate samples. Expression values are given as transcripts per million (TPM).

Gene	Stage 3	Stage 4	Stage 5	Stage 6	Stage 7
HvAFB2	31.5 ± 4.7	29.9 ± 5.7	26.6 ± 1.2	23.6 ± 3	20.6 ± 2.6
HvAFB3	6.9 ± 0.7	7 ± 0.5	6.5 ± 0.5	7 ± 0.2	7 ± 0.4
HvAFB4	24.3 ± 2.7	22.9 ± 1.8	21.6 ± 1.9	22.9 ± 2.8	20.8 ± 2.6
HvAFB5	12.3 ± 1.8	10.6 ± 1.3	11.6 ± 1.4	12 ± 0.8	10.6 ± 2
HvARF10a	2 ± 0.4	2.2 ± 0.2	4.2 ± 0.6	6.4 ± 1.1	6.4 ± 1.9
HvARF11	5.9 ± 2	5 ± 1.5	3 ± 0.6	1.6 ± 0.5	1 ± 0.2
HvARF12	19.3 ± 3.3	20 ± 3.3	28.1 ± 5.3	29.3 ± 3.7	28.1 ± 8.2
HvARF14	6.5 ± 1.8	5.2 ± 1	3.6 ± 0.8	1.9 ± 0.6	1.1 ± 0.4
HvARF16	5.9 ± 1.8	5.2 ± 1.8	5.4 ± 0.8	5 ± 1.3	4.5 ± 1.1
HvARF17	34.6 ± 3.4	37.7 ± 3.5	42.6 ± 3.3	49.6 ± 4	50.6 ± 2.2
HvARF18	10.1 ± 2	10.3 ± 1.4	13 ± 1.8	13.5 ± 1.2	10.5 ± 2.3
HvARF19	4.4 ± 0.7	4.6 ± 0.4	4.9 ± 0.5	5.2 ± 1.1	6.4 ± 0.6
HvARF2	15.1 ± 0.9	11.8 ± 1	9.5 ± 1.3	5.9 ± 0.4	4.7 ± 1.4
HvARF21	13.8 ± 2.9	13.5 ± 2.4	16 ± 1.5	15.7 ± 2.8	16.2 ± 4.6
HvARF22	9.9 ± 1.1	11.4 ± 2.8	15.9 ± 0.5	15.7 ± 2.4	12.5 ± 3.8
HvARF25	25 ± 3.8	29.6 ± 4.5	36.1 ± 3.7	40.1 ± 4.3	42 ± 7.7
HvARF3	12.2 ± 3.7	10.8 ± 2.9	8.3 ± 1.2	5.5 ± 1.3	5 ± 1.4
HvARF4a	79 ± 14.8	74.8 ± 11.8	53.3 ± 3.7	29.3 ± 4.7	21.3 ± 3.5
HvARF4c	175.3 ± 12.5	153.4 ± 14	122 ± 4.4	88.7 ± 8.7	66 ± 12.1
HvARF5	4.3 ± 0.6	3 ± 0.7	1.9 ± 0.4	1.3 ± 0.5	1.2 ± 0.4
HvARF6	15.5 ± 4.9	21.4 ± 6.2	20.6 ± 3.7	12.9 ± 3.3	12.9 ± 2.7
HvARF8	3.7 ± 0.7	3.9 ± 1.5	4.8 ± 1	5.9 ± 1	4 ± 0.9
HvARF9	48.7 ± 3.7	48.7 ± 7.8	47.2 ± 2.9	38.7 ± 8.1	27.8 ± 7.3
HvIAA1	14.6 ± 1	18.3 ± 0.7	24.3 ± 3	23.8 ± 4	19.6 ± 1.5
HvIAA10	5.3 ± 0.4	4.7 ± 0.7	5.1 ± 0.5	3.5 ± 0.8	2.8 ± 0.4
HvIAA14	20.4 ± 10	24.1 ± 10.2	33.6 ± 13.2	13.5 ± 6.9	6.8 ± 4.9
HvIAA15	10.6 ± 2.8	11.4 ± 2.3	11.8 ± 1	5.8 ± 1.7	2.8 ± 1
HvIAA19	20.1 ± 3.2	17.3 ± 2.6	11.8 ± 2.4	6.9 ± 1.4	5.3 ± 0.9
HvIAA3	150.1 ± 29.1	153 ± 20.7	153.6 ± 11.7	113.4 ± 27.2	94.8 ± 2.6
HvIAA30	47.3 ± 7.4	62.7 ± 9.5	86.5 ± 15.3	81.4 ± 14.4	63.3 ± 32.3
HvIAA31	24.8 ± 4.9	34.2 ± 6.3	40.7 ± 9.2	34.2 ± 7.5	25 ± 8.9
HvTIR1	46.6 ± 7.6	41.5 ± 3.2	43.7 ± 7.3	49 ± 6.3	49.1 ± 8.2
HvPIN1a	5.8 ± 2.3	6.1 ± 1.8	4.6 ± 1.3	2.4 ± 0.9	1.5 ± 0.8
HvPIN1b	8 ± 0.7	11.6 ± 4.7	14.5 ± 4.4	14 ± 3.9	9.3 ± 1.9
HvPIN1c	8.3 ± 2.7	7.5 ± 1.7	6.3 ± 0.8	5 ± 1	3.8 ± 1.2
HvPIN2	8 ± 3.1	10.9 ± 2.6	21.9 ± 5.3	27.9 ± 6.5	20.1 ± 4.3

Table 5-S10: Expression of barley genes putatively involved in auxin biosynthesis and transport within fifteen tissue-specific RNA-sequencing samples, collected from the genotype Sloop. Expression values are given as transcripts per million (TPM). ANTP, antipodal cell cluster; CHLZ, chalaza; ECC, egg apparatus and central cell; ES, embryo sac; INT, integument; NUC, nucellus; NUCES, nucellus and embryo sac; OW, ovary wall.

Gene	ES	ECC		ANTP		NUC			CHLZ	INT			OW		
	Stage 5	Stage 5	Stage 7	Stage 5	Stage 7	NUCES Stage 4	Stage 5	Stage 7	Stage 7	Stage 4	Stage 5	Stage 7	Stage 4	Stage 5	Stage 7
HvAFB2	5.4	2.2	0.0	3.4	20.9	16.5	3.8	4.6	5.7	36.8	32.2	12.1	83.9	77.0	100.0
HvAFB3	6.4	0.2	0.1	0.6	0.3	100.0	29.5	13.0	2.5	78.8	33.2	15.1	72.6	31.1	14.2
HvAFB4	5.0	0.4	0.0	5.1	0.0	100.0	15.6	8.5	2.8	60.2	31.6	10.8	42.2	29.6	23.8
HvAFB5	0.0	0.4	8.7	50.2	0.1	29.5	14.8	37.4	8.1	39.9	15.1	21.6	100.0	48.7	71.8
HvARF10a	12.9	89.4	44.2	29.2	0.6	9.4	77.4	100.0	0.8	5.7	79.0	87.8	1.2	16.4	34.6
HvARF11	0.0	0.0	0.0	0.1	0.0	0.0	0.7	0.0	10.2	0.0	2.1	0.0	88.4	100.0	38.4
HvARF12	0.0	0.7	20.2	10.7	3.4	11.9	46.1	32.5	6.9	10.3	28.0	15.4	20.4	74.4	100.0
HvARF14	0.1	0.0	0.0	0.0	0.1	23.7	3.4	0.1	20.4	50.4	17.9	5.8	100.0	30.4	38.7
HvARF16	15.3	16.8	100.0	14.4	0.1	89.0	25.5	33.3	34.8	26.8	29.5	20.5	18.9	19.7	50.5
HvARF17	0.0	0.0	5.8	2.3	1.3	2.2	11.0	25.2	0.3	3.2	8.5	6.6	26.5	46.3	100.0
HvARF18	0.0	0.9	2.3	22.9	0.0	100.0	52.4	46.5	5.8	25.5	18.9	12.3	79.3	36.3	28.8
HvARF19	20.3	100.0	53.1	51.2	0.0	25.3	9.3	25.5	3.6	11.9	2.8	7.3	20.8	7.9	6.3
HvARF2	0.0	0.0	0.0	24.5	0.0	25.8	8.1	0.7	22.3	83.3	21.9	11.4	100.0	32.1	18.5
HvARF21	2.1	10.8	2.9	7.6	0.0	100.0	39.3	22.1	29.5	45.2	34.6	14.1	39.9	39.5	24.0
HvARF22	19.0	17.5	13.3	11.7	0.0	54.2	38.7	23.6	1.4	54.4	100.0	38.6	36.0	44.5	28.6
HvARF25	1.6	2.8	0.1	16.1	15.4	17.3	13.6	17.3	15.2	7.0	14.3	6.3	73.3	94.6	100.0
HvARF3	1.4	0.2	0.0	18.4	39.9	43.2	15.3	3.7	10.8	69.1	42.0	6.4	100.0	72.1	59.8
HvARF4a	15.1	20.3	2.5	20.5	22.0	70.6	46.7	17.1	5.3	72.6	68.3	41.6	100.0	71.5	33.1
HvARF4c	0.5	8.4	0.0	4.8	0.0	100.0	5.5	0.5	0.0	60.5	7.8	0.2	91.3	9.8	0.9

HvARF5	0.0	0.0	0.0	0.4	12.8	34.1	3.1	12.7	0.0	35.1	3.6	0.0	100.0	33.0	4.0
HvARF6	0.0	0.0	13.5	2.8	0.0	5.7	2.7	6.5	0.0	3.6	9.4	3.8	68.1	58.6	100.0
HvARF8	0.0	0.0	0.0	0.0	0.0	100.0	25.2	30.2	0.0	38.5	69.8	25.9	50.7	55.3	40.8
HvARF9	7.5	25.2	0.2	13.0	3.1	77.3	56.2	18.6	8.2	76.8	58.0	25.3	100.0	67.1	40.6
HvIAA1	38.0	100.0	21.0	59.3	1.0	43.6	60.3	49.2	37.5	15.7	30.0	20.4	17.2	22.4	22.0
HvIAA10	100.0	39.0	0.0	18.9	0.0	0.2	6.2	0.0	7.1	0.2	2.6	0.0	1.6	3.7	0.0
HvIAA14	3.6	1.4	28.6	29.8	0.0	1.7	3.9	40.7	16.5	2.2	2.7	1.5	94.8	100.0	67.6
HvIAA15	31.4	100.0	21.9	40.0	0.0	32.2	12.9	6.7	0.8	35.2	37.7	20.9	33.5	36.8	39.2
HvIAA19	0.1	1.8	46.7	18.0	0.0	72.3	33.7	37.8	18.4	100.0	65.3	26.3	95.8	50.5	30.4
HvIAA3	10.3	14.5	0.7	7.3	8.1	2.0	54.2	49.0	94.9	1.9	65.4	46.4	2.8	100.0	83.2
HvIAA30	0.0	0.1	0.0	0.0	0.0	1.1	1.6	3.7	27.2	7.1	16.7	26.5	24.2	43.8	100.0
HvIAA31	0.0	0.1	0.1	0.0	0.0	3.3	0.9	15.0	8.8	2.3	14.8	24.8	65.3	88.3	100.0
HvTIR1	10.0	10.6	0.0	22.7	6.2	80.2	28.1	15.4	100.0	82.7	35.2	36.1	79.4	40.6	52.1
HvPIN1a	14.3	100.0	74.8	4.4	0.0	12.3	0.2	0.0	16.9	0.0	0.2	0.0	68.4	9.4	3.4
HvPIN1b	0.1	0.2	0.4	0.0	0.0	22.5	4.3	0.0	0.0	19.3	0.2	0.0	100.0	8.4	7.9
HvPIN1c	0.0	0.0	0.0	2.4	0.0	100.0	16.9	4.7	10.7	18.2	4.9	1.5	28.1	9.6	1.8
HvPIN2	0.0	0.0	0.0	0.0	0.0	0.0	0.0	0.0	0.0	0.0	0.3	0.0	20.1	50.9	100.0

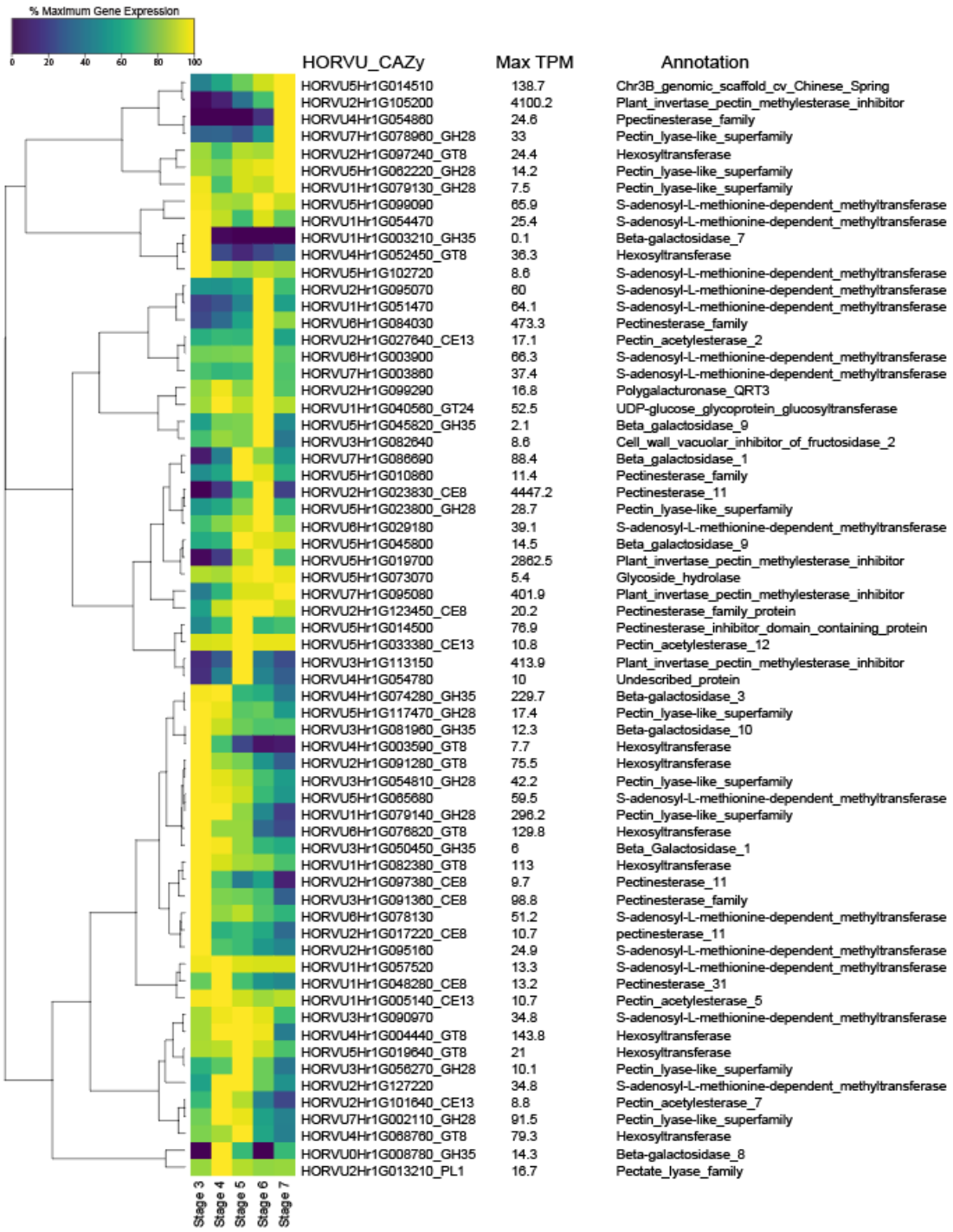

Figure 5-S5. Heatmap showing average expression genes involved in pectin biosynthesis and remodelling at five stages of ovule development in four barley genotypes, as determined by RNA sequencing of whole pistils. Transcript abundance values (TPM) have been normalised to 1.

Table 5-S11: Locus identifiers for barley genes involved in pectin biosynthesis and remodelling found to be expressed within whole-pistil and tissue-specific RNA-sequencing data sets, with transcript abundance (TPM) greater than 5.

HORVU	Rice	Arabidopsis	Annotation	Tissue-specific maximum TPM	Whole-pistil maximum TPM
HORVU0Hr1G008780	LOC_Os03g15020	At2g28470	Beta-galactosidase 8	14.3	0.2
HORVU1Hr1G003210	LOC_Os01g34920	At5g20710	Beta-galactosidase 7	0.1	5.1
HORVU1Hr1G005140	LOC_Os05g02120	At3g09410	Pectin acetylesterase 5	10.7	5.7
HORVU1Hr1G040560	LOC_Os02g44510	At1g71220	UDP-glucose:glycoprotein glucosyltransferase	52.5	30.1
HORVU1Hr1G048280	LOC_Os10g26680	At3g29090	Pectinesterase 31	13.2	20.3
HORVU1Hr1G051470	LOC_Os02g45310	At4g19120	S-adenosyl-L-methionine-dependent methyltransferase	64.1	21.7
HORVU1Hr1G054470	LOC_Os10g41970	At1g26850	S-adenosyl-L-methionine-dependent methyltransferase	25.4	6.9
HORVU1Hr1G057520	LOC_Os05g31480	At5g04060	S-adenosyl-L-methionine-dependent methyltransferase	13.3	17.9
HORVU1Hr1G079130	LOC_Os05g46520	At1g80170	Pectin lyase-like	7.5	7.8
HORVU1Hr1G079140	LOC_Os05g46520	At1g80170	Pectin lyase-like	296.2	107.7
HORVU1Hr1G082380	LOC_Os08g23780	At5g47780	Hexosyltransferase	113.0	49.7
HORVU2Hr1G013210	LOC_Os01g36620	At3g55140	Pectate lyase family	16.7	12.7
HORVU2Hr1G017220	LOC_Os01g53990	At5g19730	Pectinesterase 11	10.7	9.4
HORVU2Hr1G023830	LOC_Os07g46190	At2g47280	Pectinesterase 11	4447.2	11.7
HORVU2Hr1G027640	LOC_Os07g44070	At1g57590	Pectin acetylesterase 2	17.1	38.2
HORVU2Hr1G091280	LOC_Os04g44850	At3g28340	Hexosyltransferase	75.5	33.9
HORVU2Hr1G095070	LOC_Os04g48230	At4g00750	S-adenosyl-L-methionine-dependent methyltransferase	60.0	48.2
HORVU2Hr1G095160	LOC_Os04g48140	At4g00740	S-adenosyl-L-methionine-dependent methyltransferase	24.9	18.9
HORVU2Hr1G097240	LOC_Os04g46750	At2g35710	Hexosyltransferase	24.4	12.6
HORVU2Hr1G097380	LOC_Os04g46740	At5g47500	Pectinesterase 11	9.7	32.6
HORVU2Hr1G099290	LOC_Os04g52320	At4g20050	Polygalacturonase QRT3	16.8	7.3
HORVU2Hr1G101640	LOC_Os04g51340	At4g19410	Pectin acetylesterase 7	8.8	15.1
HORVU2Hr1G105200	LOC_Os04g49730	At5g46960	Plant invertase/pectin methylesterase inhibitor	4100.2	30.4

HORVU2Hr1G123450	LOC_Os11g08750	At3g10720	Pectinesterase family	20.2	14.3
HORVU2Hr1G127220	LOC_Os04g59590	At5g64030	S-adenosyl-L-methionine-dependent methyltransferase	34.8	26.1
HORVU3Hr1G050450	LOC_Os01g39830	At3g13750	Beta galactosidase 1	6.0	8.5
HORVU3Hr1G054810	LOC_Os01g43160	At4g23820	Pectin lyase-like	42.2	23.8
HORVU3Hr1G056270	LOC_Os01g44970	At1g60590	Pectin lyase-like	10.1	13.5
HORVU3Hr1G081960	LOC_Os01g65460	At5g63810	Beta-galactosidase 10	12.3	26.0
HORVU3Hr1G081980	LOC_Os05g35360	At1g77410	Beta-galactosidase 16	98.3	0.0
HORVU3Hr1G082640	LOC_Os08g01670	At5g64620	Cell wall / vacuolar inhibitor of fructosidase 2	8.6	8.1
HORVU3Hr1G090970	LOC_Os01g66110	At5g64030	S-adenosyl-L-methionine-dependent methyltransferase	34.8	47.2
HORVU3Hr1G091360	LOC_Os01g65790	At5g09760	Pectinesterase family	98.8	20.0
HORVU3Hr1G113150	LOC_Os08g25070	n/a	Plant invertase/pectin methylesterase inhibitor	413.9	5.2
HORVU4Hr1G003590	LOC_Os03g47530	At3g50760	Hexosyltransferase	7.7	10.7
HORVU4Hr1G004440	LOC_Os06g49810	At3g61130	Hexosyltransferase	143.8	9.2
HORVU4Hr1G052450	LOC_Os03g20120	At2g47180	Hexosyltransferase	36.3	5.8
HORVU4Hr1G054780	LOC_Os03g18890	At4g02130	Undescribed protein	10.0	5.8
HORVU4Hr1G054860	LOC_Os03g18860	At5g27870	Pectinesterase family	24.6	9.2
HORVU4Hr1G068760	LOC_Os03g11330	At5g15470	Hexosyltransferase	79.3	25.9
HORVU4Hr1G074280	LOC_Os03g06940	At4g36360	Beta-galactosidase 3	229.7	101.1
HORVU5Hr1G010860	LOC_Os01g21034	At3g14310	Pectinesterase family	11.4	5.9
HORVU5Hr1G014500	LOC_Os12g40750	n/a	Pectinesterase inhibitor domain containing protein	76.9	14.5
HORVU5Hr1G014510	LOC_Os12g40760	n/a	Ch3B genomic scaffold cv. Chinese Spring	138.7	8.2
HORVU5Hr1G019640	LOC_Os12g38930	At3g01040	Hexosyltransferase	21.0	16.2
HORVU5Hr1G019700	LOC_Os04g49730	At5g46940	Plant invertase/pectin methylesterase inhibitor	2862.5	11.0
HORVU5Hr1G023800	LOC_Os12g36810	At3g16850	Pectin lyase-like	28.7	26.7
HORVU5Hr1G033380	LOC_Os01g74330	At3g05910	Pectin acetylesterase 12	10.8	9.1
HORVU5Hr1G045800	LOC_Os12g24170	At2g32810	Beta galactosidase 9	14.5	17.6
HORVU5Hr1G045820	LOC_Os12g24170	At2g32810	Beta galactosidase 9	2.1	16.6
HORVU5Hr1G062220	LOC_Os09g26800	At3g42950	Pectin lyase-like	14.2	8.2

HORVU5Hr1G065680	LOC_Os09g24900	At1g26850	S-adenosyl-L-methionine-dependent methyltransferase	59.5	60.2
HORVU5Hr1G073070	LOC_Os09g31270	At3g57790	Gycoside hydrolase	5.4	6.3
HORVU5Hr1G099090	LOC_Os03g56380	At1g19430	S-adenosyl-L-methionine-dependent methyltransferase	65.9	14.7
HORVU5Hr1G102720	LOC_Os03g26200	At1g26850	S-adenosyl-L-methionine-dependent methyltransferase	8.6	10.7
HORVU5Hr1G117470	LOC_Os03g61800	At3g62110	Pectin lyase-like	17.4	21.1
HORVU6Hr1G003900	LOC_Os10g36690	At4g10440	S-adenosyl-L-methionine-dependent methyltransferase	66.3	56.6
HORVU6Hr1G029180	LOC_Os01g62800	At2g39750	S-adenosyl-L-methionine-dependent methyltransferase	39.1	7.6
HORVU6Hr1G076820	LOC_Os02g50600	At1g70090	Hexosyltransferase	129.8	26.4
HORVU6Hr1G078130	LOC_Os02g51860	At1g78240	S-adenosyl-L-methionine-dependent methyltransferase	51.2	35.5
HORVU6Hr1G084030	LOC_Os08g34900	At3g43270	Pectinesterase family	473.3	19.3
HORVU7Hr1G002110	LOC_Os06g01760	At3g61490	Pectin lyase-like	91.5	23.7
HORVU7Hr1G003860	LOC_Os06g01450	At4g10440	S-adenosyl-L-methionine-dependent methyltransferase	37.4	12.5
HORVU7Hr1G078960	LOC_Os05g20020	At1g48100	Pectin lyase-like	33.0	31.6
HORVU7Hr1G086690	LOC_Os06g37560	At3g13750	Beta galactosidase 1	88.4	8.4
HORVU7Hr1G095080	LOC_Os06g49760	At1g62770	Plant invertase/pectin methylesterase inhibitor	401.9	98.4

Table 5-S12. Expression of barley genes involved in pectin biosynthesis and remodelling at five stages of ovule development, in four barley genotypes (Forum, Gant, Salka and Wren), as determined by RNA-sequencing of whole pistils. With the exception of Forum at Stage 3, Salka at Stage 3, and Wren at Stages 5 and 7, all data presented is the average of two replicate samples. Expression values are given as transcripts per million (TPM).

HORVU	Stage 3	Stage 4	Stage 5	Stage 6	Stage 7
HORVU0Hr1G008780	0 ± 0	0.1 ± 0.1	0 ± 0	0 ± 0	0.1 ± 0.1
HORVU1Hr1G003210	1.4 ± 2.2	0.1 ± 0.1	0 ± 0	0 ± 0	0 ± 0
HORVU1Hr1G005140	4.4 ± 0.8	4.7 ± 0.8	4.9 ± 0.5	4.2 ± 0.5	4.6 ± 0.4
HORVU1Hr1G040560	23.8 ± 1.7	24.8 ± 3.4	24.7 ± 1.4	25.6 ± 2.7	24.5 ± 1.7
HORVU1Hr1G048280	13.8 ± 1.4	15 ± 3.6	11.6 ± 2	9.8 ± 0.7	8.7 ± 0.7
HORVU1Hr1G051470	3.2 ± 1.2	4.2 ± 1.3	8.2 ± 1.5	13.3 ± 5.2	10 ± 1.9
HORVU1Hr1G054470	5.1 ± 1.1	4.8 ± 0.9	4.6 ± 0.3	5 ± 1	4.6 ± 0.8
HORVU1Hr1G057520	14.7 ± 2	15.7 ± 1.8	15.6 ± 1.3	15.2 ± 1.6	15 ± 1.2
HORVU1Hr1G079130	5.1 ± 1.5	4.3 ± 0.9	5.1 ± 1.3	6.4 ± 0.6	6.5 ± 1
HORVU1Hr1G079140	67.4 ± 31	72 ± 21.5	54.4 ± 20.7	25.7 ± 14.6	15.3 ± 5.7
HORVU1Hr1G082380	37.3 ± 14.3	36.6 ± 12	35 ± 11.2	33.6 ± 10.4	30.4 ± 7.5
HORVU2Hr1G013210	9.1 ± 1	10.2 ± 1.7	10.6 ± 0.4	10 ± 0.4	9.5 ± 1.2
HORVU2Hr1G017220	6 ± 2.3	5.1 ± 0.8	5.4 ± 0.9	3.6 ± 1.2	2.5 ± 0.5
HORVU2Hr1G023830	0 ± 0	0.7 ± 0.7	4.3 ± 2.4	3.8 ± 4.6	1.3 ± 0.9
HORVU2Hr1G027640	16.5 ± 4.7	17.9 ± 4.7	20.2 ± 4.6	23.6 ± 9.3	17.9 ± 4.4
HORVU2Hr1G091280	25.5 ± 5	22.6 ± 3.9	21.5 ± 4.2	12.4 ± 3.5	9.1 ± 0.5
HORVU2Hr1G095070	17.1 ± 4.6	16.7 ± 5	22.3 ± 3.4	29.6 ± 11	26.3 ± 4.3
HORVU2Hr1G095160	13.6 ± 3.4	12.1 ± 1	11.7 ± 0.9	9.3 ± 0.5	8.3 ± 0.5
HORVU2Hr1G097240	9.2 ± 1.2	8 ± 0.6	8.8 ± 1.6	10.1 ± 0.4	11.5 ± 0.6
HORVU2Hr1G097380	20 ± 8.5	16.1 ± 4.8	11.6 ± 2.6	8.2 ± 6	2.6 ± 0.4
HORVU2Hr1G099290	4.9 ± 0.7	4.4 ± 1.9	4.3 ± 1.7	4 ± 2	3.4 ± 1.4
HORVU2Hr1G101640	5.9 ± 2.5	7.7 ± 4.4	9.1 ± 2.5	5.9 ± 1.1	2.6 ± 0.6
HORVU2Hr1G105200	0.7 ± 0.3	1.6 ± 1	7.5 ± 3.8	11.6 ± 9.8	15.6 ± 11.7
HORVU2Hr1G123450	4.6 ± 2.3	7 ± 3.6	9.4 ± 3.1	9.2 ± 3.8	10.4 ± 2.1
HORVU2Hr1G127220	14.6 ± 0.3	16.6 ± 5.6	17.6 ± 5	15.3 ± 3.1	11.5 ± 1.3
HORVU3Hr1G050450	7.6 ± 0.6	7.9 ± 0.3	6.2 ± 0.7	5.3 ± 0.4	4.8 ± 0.4
HORVU3Hr1G054810	20.6 ± 2.3	19.7 ± 2.2	17.7 ± 1.9	14.9 ± 1.2	12.7 ± 0.3
HORVU3Hr1G056270	8 ± 0.6	9.9 ± 0.2	10.6 ± 2	8.4 ± 2.1	4.2 ± 1.4
HORVU3Hr1G081960	18.3 ± 4.7	18.2 ± 4	15.3 ± 2.9	11.7 ± 4.4	11.7 ± 4.7
HORVU3Hr1G081980	0 ± 0	0 ± 0	0 ± 0	0 ± 0	0 ± 0
HORVU3Hr1G082640	4.3 ± 1.5	5.7 ± 0.7	5.6 ± 0.8	4.1 ± 2.4	2.4 ± 0.6
HORVU3Hr1G090970	35.6 ± 3.4	38.8 ± 4.4	40.5 ± 4.7	35.1 ± 6	25.9 ± 4.3
HORVU3Hr1G091360	12.1 ± 4.8	12.3 ± 2.9	10.4 ± 3.7	7.9 ± 3.7	6 ± 0.3
HORVU3Hr1G113150	0.3 ± 0.2	0.9 ± 0.5	2.2 ± 1.9	1 ± 0.8	0.7 ± 0.5

HORVU4Hr1G003590	6 ± 2.9	4.2 ± 2.2	1.5 ± 0.7	0.4 ± 0.2	0.6 ± 0.3
HORVU4Hr1G004440	5.6 ± 1.4	6.5 ± 2.3	6.5 ± 1.7	4.6 ± 2.6	2.4 ± 1.3
HORVU4Hr1G052450	2.1 ± 2.1	1 ± 0.4	0.6 ± 0.2	0.7 ± 0.4	1.2 ± 0.6
HORVU4Hr1G054780	0.6 ± 0.1	1.1 ± 0.8	2.2 ± 2.1	1.4 ± 0.8	1 ± 0.5
HORVU4Hr1G054860	0 ± 0	0 ± 0	0 ± 0	0.4 ± 0.6	4.5 ± 3.6
HORVU4Hr1G068760	17.7 ± 2.2	19.3 ± 2.1	20.7 ± 4.5	13.4 ± 1.8	9.8 ± 0.8
HORVU4Hr1G074280	76.4 ± 22.4	76.7 ± 22.7	59.6 ± 5	50.5 ± 7.7	36.5 ± 2.8
HORVU5Hr1G010860	1.8 ± 0.8	2.4 ± 0.7	4.3 ± 1.6	4.2 ± 1.4	2.3 ± 0.9
HORVU5Hr1G014500	5 ± 1.7	7.2 ± 2.1	9.8 ± 3.1	7.6 ± 1.3	7 ± 2.3
HORVU5Hr1G014510	2.7 ± 0.8	4.1 ± 0.8	5.1 ± 1.5	5.8 ± 1.2	6.1 ± 1.5
HORVU5Hr1G019640	13 ± 1.6	13.6 ± 0.9	14.4 ± 1.3	11.4 ± 2.5	8.8 ± 2.9
HORVU5Hr1G019700	0.1 ± 0.1	0.9 ± 0.8	5.4 ± 2.9	4.7 ± 4.4	4.9 ± 3.1
HORVU5Hr1G023800	11.9 ± 2.1	14 ± 1.3	18.7 ± 2	19.1 ± 6.7	11.5 ± 5
HORVU5Hr1G033380	7.6 ± 0.7	7.5 ± 0.9	8.4 ± 0.9	7.6 ± 0.9	7.6 ± 1.2
HORVU5Hr1G045800	8.5 ± 1.4	9.4 ± 2.4	11.5 ± 3.9	12.8 ± 3.1	13.6 ± 1.7
HORVU5Hr1G045820	6.1 ± 2	7.7 ± 4.3	7.1 ± 3.6	7.6 ± 5.6	4.8 ± 2.3
HORVU5Hr1G062220	6 ± 1.2	6 ± 0.4	6.6 ± 0.7	6.4 ± 1.1	6.4 ± 1.6
HORVU5Hr1G065680	53.3 ± 4.5	54.4 ± 4.9	45.4 ± 6	33.8 ± 4	27.3 ± 3.3
HORVU5Hr1G073070	4.5 ± 0.6	4.8 ± 0.6	5.6 ± 0.5	5.7 ± 0.5	5 ± 0.9
HORVU5Hr1G099090	11.9 ± 1.6	11.4 ± 1.1	11.1 ± 1.3	11.8 ± 2.2	11.9 ± 1.4
HORVU5Hr1G102720	9.8 ± 1	8.9 ± 0.6	8.5 ± 0.4	8.6 ± 0.8	8.4 ± 0.7
HORVU5Hr1G117470	15.5 ± 3.4	16.9 ± 2.5	15.4 ± 0.3	12.8 ± 2.8	8.7 ± 2.7
HORVU6Hr1G003900	39.7 ± 4	43.1 ± 1.3	43.4 ± 1	43.5 ± 8	38.7 ± 3.3
HORVU6Hr1G029180	1.8 ± 2	2.1 ± 2.4	2.2 ± 2.8	2.4 ± 3	2.1 ± 2.4
HORVU6Hr1G076820	17.4 ± 5.4	15.6 ± 4.5	13.8 ± 5.1	7 ± 1.7	5.4 ± 1.2
HORVU6Hr1G078130	28.9 ± 4.4	28.1 ± 1.4	28.7 ± 1.8	23.1 ± 2.7	19.1 ± 2.7
HORVU6Hr1G084030	3.4 ± 0.8	4.2 ± 1.6	8.1 ± 2.2	10.5 ± 5.2	10.1 ± 4
HORVU7Hr1G002110	15.5 ± 2.5	20.3 ± 2.7	18.2 ± 3.1	11.9 ± 2.1	6.9 ± 2.2
HORVU7Hr1G003860	5.8 ± 2.8	5.8 ± 2.3	6.3 ± 2.1	7.1 ± 3.7	5.6 ± 2.7
HORVU7Hr1G078960	7 ± 3	6.7 ± 2.5	6.6 ± 1.3	10.2 ± 5.3	15.5 ± 9.9
HORVU7Hr1G086690	0.5 ± 0.1	1.7 ± 1.2	4.7 ± 2.4	5.4 ± 0.9	3.6 ± 0.8
HORVU7Hr1G095080	39.3 ± 1.9	52.7 ± 7.8	66.7 ± 17.3	68.3 ± 16.1	63.2 ± 25.8

Table 5-S13. Expression of barley genes involved in pectin biosynthesis and remodelling within fifteen tissue-specific RNA-sequencing samples, collected from the genotype Sloop. Expression values are given as transcripts per million (TPM). ANTP, antipodal cell cluster; CHLZ, chalaza; ECC, egg apparatus and central cell; ES, embryo sac; INT, integument; NUC, nucellus; NUC_ES, nucellus and embryo sac; OW, ovary wall.

HORVU	ES	ECC		ANTP		NUC			CHLZ	INT			OW		
	Stage 5	Stage 5	Stage 7	Stage 5	Stage 7	NUCES Stage 4	Stage 5	Stage 7	Stage 7	Stage 4	Stage 5	Stage 7	Stage 4	Stage 5	Stage 7
HORVU0Hr1G008780	3.3	0.0	0.0	14.1	13.3	0.0	1.4	14.3	0.0	0.0	0.2	0.1	0.0	3.1	0.9
HORVU1Hr1G003210	0.0	0.0	0.0	0.0	0.0	0.0	0.0	0.0	0.0	0.0	0.0	0.0	0.1	0.0	0.0
HORVU1Hr1G005140	3.4	2.7	0.2	10.7	1.1	1.0	2.0	0.4	0.2	0.3	1.5	0.1	0.3	1.5	0.7
HORVU1Hr1G040560	17.3	18.4	52.5	13.3	26.8	8.6	12.0	8.7	20.1	3.7	14.3	10.0	4.2	10.8	6.7
HORVU1Hr1G048280	1.1	0.7	0.0	7.4	0.9	11.9	6.0	5.8	0.3	5.3	8.4	9.3	10.6	8.2	13.2
HORVU1Hr1G051470	8.8	26.2	64.1	7.1	15.2	0.9	6.9	8.3	1.9	8.3	10.1	6.9	3.5	8.2	8.4
HORVU1Hr1G054470	1.1	0.9	0.0	2.1	25.4	13.5	8.9	1.7	7.5	8.6	5.5	1.8	10.9	7.4	3.4
HORVU1Hr1G057520	0.7	0.0	0.0	0.8	3.5	9.9	8.2	4.7	11.0	12.6	13.3	5.7	8.8	11.8	8.3
HORVU1Hr1G079130	1.2	0.2	0.2	0.0	0.0	1.4	1.1	2.6	0.0	5.8	1.7	1.3	6.6	4.9	7.5
HORVU1Hr1G079140	0.0	0.0	0.0	0.2	0.0	0.1	1.8	0.0	7.3	0.4	4.7	4.8	296.2	193.7	180.5
HORVU1Hr1G082380	59.5	113.0	27.1	48.0	4.9	32.8	43.4	24.9	2.6	33.5	64.9	30.9	46.6	64.4	40.2
HORVU2Hr1G013210	1.2	2.1	1.7	1.1	0.0	9.4	0.5	0.6	0.0	10.3	1.8	1.9	16.7	2.1	1.2
HORVU2Hr1G017220	0.0	0.0	0.0	0.0	0.0	3.3	0.5	0.5	5.5	0.0	0.9	0.3	6.3	4.3	10.7
HORVU2Hr1G023830	4447.2	193.2	110.8	3600.7	1838.0	0.0	0.2	0.2	0.0	0.0	0.1	0.4	0.0	0.1	0.0
HORVU2Hr1G027640	0.1	0.9	0.0	0.6	0.0	4.5	0.4	0.2	3.1	5.2	5.2	3.9	7.1	7.1	17.1
HORVU2Hr1G091280	1.2	1.6	0.0	0.6	0.0	4.8	2.8	19.2	39.0	8.1	6.3	36.8	3.5	5.8	75.5
HORVU2Hr1G095070	46.1	56.3	16.9	16.4	60.0	11.6	13.1	53.1	11.5	17.4	31.6	29.3	2.8	3.2	7.3
HORVU2Hr1G095160	24.9	5.0	0.0	0.1	0.0	22.6	1.5	0.0	0.2	21.6	1.3	0.1	22.4	1.5	0.0
HORVU2Hr1G097240	1.9	1.1	0.0	9.3	6.4	20.8	18.0	24.4	10.4	20.3	12.3	19.0	20.2	11.2	11.7

HORVU2Hr1G097380	1.0	1.4	0.0	0.4	0.1	1.6	0.4	0.0	0.1	0.4	3.3	0.8	5.0	9.7	9.4
HORVU2Hr1G099290	2.2	0.0	0.1	1.0	0.0	2.3	4.7	16.8	2.2	2.2	2.9	4.7	6.6	5.1	10.7
HORVU2Hr1G101640	0.0	0.1	0.0	0.0	0.0	0.0	0.0	0.0	0.0	0.0	0.0	0.0	2.9	8.8	4.1
HORVU2Hr1G105200	1652.5	647.2	839.1	1305.6	4100.2	31.6	0.8	0.6	0.0	0.0	0.0	0.1	0.0	0.0	0.0
HORVU2Hr1G123450	0.0	1.0	0.0	0.0	0.0	20.2	7.3	2.4	0.0	1.5	14.2	4.4	6.6	3.4	1.2
HORVU2Hr1G127220	4.6	11.3	0.0	6.9	0.0	34.8	18.8	10.2	2.1	19.1	25.9	10.8	18.5	17.9	5.9
HORVU3Hr1G050450	0.0	0.0	0.0	0.0	0.0	3.0	1.7	0.0	2.3	3.4	4.4	0.8	3.9	6.0	1.9
HORVU3Hr1G054810	14.2	11.6	8.4	2.1	5.5	14.9	9.2	4.8	8.6	13.9	9.5	12.9	26.4	22.0	42.2
HORVU3Hr1G056270	0.6	0.0	0.0	4.4	0.0	3.5	6.0	1.3	1.4	0.0	0.8	0.2	7.7	10.1	5.6
HORVU3Hr1G081960	0.7	10.2	12.3	3.7	3.1	11.9	3.6	2.6	1.0	9.0	9.9	3.4	6.4	5.9	3.3
HORVU3Hr1G081980	0.0	0.0	98.3	0.0	0.0	0.3	0.0	0.0	0.0	0.0	0.0	0.0	0.1	0.0	0.0
HORVU3Hr1G082640	0.0	0.0	0.0	0.0	0.0	2.2	2.0	0.1	1.6	0.4	0.1	0.0	8.6	6.0	4.6
HORVU3Hr1G090970	5.1	11.5	2.6	6.8	0.5	29.7	14.9	12.9	6.6	22.7	17.8	11.0	34.8	26.4	34.2
HORVU3Hr1G091360	98.8	50.8	16.7	28.8	25.9	2.4	5.9	3.1	4.5	0.1	1.5	3.9	15.0	19.7	27.8
HORVU3Hr1G113150	377.5	366.2	119.1	413.9	149.1	14.7	0.0	0.0	0.0	0.0	0.0	0.0	0.0	0.0	0.0
HORVU4Hr1G003590	0.0	0.0	0.0	0.0	0.0	0.5	0.1	0.0	2.4	0.1	0.2	0.2	0.3	0.4	7.7
HORVU4Hr1G004440	67.0	82.1	143.8	32.9	44.7	0.2	33.6	30.4	4.9	0.2	25.4	23.8	0.4	28.2	30.0
HORVU4Hr1G052450	19.9	0.0	0.5	36.3	1.9	2.5	0.6	1.0	2.0	1.5	6.6	3.1	0.3	0.6	0.6
HORVU4Hr1G054780	0.0	5.8	0.0	0.0	0.0	3.5	3.5	3.7	0.0	1.3	2.8	10.0	0.5	1.9	4.5
HORVU4Hr1G054860	0.0	24.6	0.0	0.0	0.0	0.0	0.1	0.0	0.0	0.0	0.0	0.0	0.0	0.0	0.0
HORVU4Hr1G068760	21.8	46.2	79.3	33.7	9.2	18.6	22.6	16.4	5.1	12.0	18.2	6.3	11.0	28.1	18.4
HORVU4Hr1G074280	0.0	0.0	0.0	0.4	0.0	196.9	1.0	0.7	0.0	229.7	1.7	2.2	219.7	3.3	3.3
HORVU5Hr1G010860	0.0	0.1	0.0	0.0	0.0	0.1	0.7	9.1	0.0	2.4	5.0	11.4	0.1	0.2	0.2
HORVU5Hr1G014500	3.7	9.7	29.6	1.8	0.1	33.1	14.9	31.2	6.6	69.5	53.4	76.9	6.0	3.3	4.6
HORVU5Hr1G014510	0.1	3.0	132.2	0.0	0.1	25.4	23.3	63.4	2.0	102.7	87.0	138.7	5.7	3.4	3.6
HORVU5Hr1G019640	1.7	15.6	0.7	21.0	9.6	13.5	8.0	5.5	2.0	5.4	7.2	3.4	6.9	7.1	7.2
HORVU5Hr1G019700	2862.5	1088.0	859.6	1591.9	2641.1	5.2	0.4	0.1	0.0	0.0	0.2	0.1	0.0	0.1	0.0
HORVU5Hr1G023800	9.1	14.9	0.1	9.8	8.4	16.0	18.6	17.5	28.7	11.3	14.2	16.3	6.5	11.8	21.3

HORVU5Hr1G033380	2.4	3.4	0.0	0.8	0.6	10.8	5.7	1.7	0.7	8.4	6.9	3.5	7.8	6.4	2.0
HORVU5Hr1G045800	13.3	5.6	0.0	14.5	4.5	0.7	10.0	5.9	4.7	0.4	13.6	12.0	0.5	12.1	9.7
HORVU5Hr1G045820	0.0	1.0	0.0	0.1	2.1	0.0	0.1	0.0	0.0	0.0	0.1	0.4	0.0	0.1	0.0
HORVU5Hr1G062220	2.9	4.4	0.0	5.0	9.3	13.5	6.8	3.8	0.8	14.2	8.3	6.1	8.7	7.8	10.0
HORVU5Hr1G065680	0.1	9.9	0.0	14.3	7.7	36.2	18.3	4.9	9.8	59.5	45.3	18.8	58.8	49.4	35.4
HORVU5Hr1G073070	2.8	5.4	0.0	3.3	0.0	3.7	3.0	5.2	0.1	2.2	3.5	2.8	2.5	3.6	3.6
HORVU5Hr1G099090	0.1	5.4	65.9	3.2	5.6	6.4	4.0	1.4	5.0	4.3	4.0	1.4	5.7	6.5	3.9
HORVU5Hr1G102720	1.3	8.6	1.7	2.2	2.8	6.4	4.3	3.6	0.7	5.6	5.5	2.3	5.2	6.6	6.0
HORVU5Hr1G117470	5.2	10.1	0.0	8.9	16.1	17.4	4.8	4.3	1.6	10.8	5.7	3.6	13.6	9.6	9.5
HORVU6Hr1G003900	28.3	36.4	0.2	64.9	3.8	33.3	56.5	37.6	23.9	28.4	65.1	29.2	35.7	66.3	59.4
HORVU6Hr1G029180	0.0	26.5	0.0	4.9	0.0	20.9	18.7	14.5	0.0	19.0	39.1	11.7	6.1	17.5	5.9
HORVU6Hr1G076820	67.9	13.3	0.0	82.0	0.2	112.8	29.5	63.9	12.1	62.6	21.8	56.8	21.1	22.9	129.8
HORVU6Hr1G078130	18.0	46.6	12.6	43.4	22.3	6.9	46.0	24.0	17.0	4.7	41.7	19.2	4.7	51.2	48.0
HORVU6Hr1G084030	12.2	5.6	473.3	2.2	10.0	17.5	49.6	322.3	3.9	13.0	11.0	42.8	7.1	2.4	11.9
HORVU7Hr1G002110	35.6	91.5	14.1	17.8	17.6	20.0	14.8	38.0	20.8	1.9	2.3	2.7	38.8	30.2	32.6
HORVU7Hr1G003860	7.8	4.7	37.4	0.4	0.3	3.2	1.9	2.9	7.5	8.0	8.8	7.6	9.5	9.8	7.7
HORVU7Hr1G078960	33.0	5.2	1.6	8.2	0.0	13.8	10.3	17.0	12.4	18.8	21.8	26.7	17.5	15.5	29.7
HORVU7Hr1G086690	47.8	88.4	4.8	34.7	0.0	2.5	2.8	0.5	6.7	0.5	1.6	6.6	0.1	0.1	0.4
HORVU7Hr1G095080	8.5	21.2	89.7	9.1	0.0	49.3	112.2	401.9	57.2	41.1	93.2	104.4	107.0	196.0	216.7

Chapter 6

Differential expression analysis of candidate genes underlying quantitative trait loci influencing mature ovule morphology in barley

Statement of Authorship

Title of Paper	Differential expression analysis of genes expressed within quantitative trait loci influencing mature ovule morphology in barley
Publication Status	☐ Published ☐ Accepted for Publication ☐ Submitted for Publication ☑ Unpublished and Unsubmitted work written in manuscript style
Publication Details	Laura G. Wilkinson[1,2], Neil J. Shirley[1,2], Rachel A. Burton[1,2] and Matthew. R Tucker[1]

Principal Author

Name of Principal Author (Candidate)	Laura G. Wilkinson		
Contribution to the Paper	Performed experiments, analysed all samples, interpreted data and wrote manuscript.		
Overall percentage (%)	80%		
Certification:	This paper reports on original research I conducted during the period of my Higher Degree by Research candidature and is not subject to any obligations or contractual agreements with a third party that would constrain its inclusion in this thesis. I am the primary author of this paper.		
Signature		Date	14/2/19

Co-Author Contributions

By signing the Statement of Authorship, each author certifies that:

i. the candidate's stated contribution to the publication is accurate (as detailed above);
ii. permission is granted for the candidate in include the publication in the thesis; and
iii. the sum of all co-author contributions is equal to 100% less the candidate's stated contribution.

Name of Co-Author	Neil J. Shirley		
Contribution to the Paper	Assisted with differential gene analysis. I hereby certify that the statement of authorship is accurate.		
Signature		Date	14/2/19

Name of Co-Author	Rachel A. Burton		
Contribution to the Paper	Assisted with project conception and experimental design. I hereby certify that the statement of authorship is accurate.		
Signature		Date	24/02/2019

Name of Co-Author	Matthew R. Tucker		
Contribution to the Paper	Conceived project and designed experiments. Contributed to the preparation of the manuscript. I hereby certify that the statement of authorship is accurate.		
Signature		Date	14/2/19

Abbreviations

AGP	Arabinogalactan protein
ANTP	Antipodal cell cluster
BLAST	Basic local alignment search tool
CAZy	Carbohydrate-Active enZYmes
DEG	Differentially expressed gene
ECC	Egg and central cell
ES	Embryo sac
ES_A	Two-dimensional embryo sac area
ES_L	Embryo sac longitude
ES_T	Embryo sac transverse
FG	Female gametophyte
FM	Functional megaspore
GWAS	Genome wide association study
HORVU	*Hordeum vulgare* gene identifier
I_W	Integument width
INT	Integument
LCM	Laser capture microdissection
MLOC	Morex loci
MMC	Megaspore mother cell
N_P	Two dimensional nucellus area
N_P	Nucellus proportion (%)
NUC	Nucellus
NUC_ES	Nucellus and embryo sac
O_A	Two-dimensional ovule area
O_L	Ovule longitude
O_T	Ovule transverse
OW	Ovary wall
PFAM	Protein family
QTL	Quantitative trait locus

QTL1H_ES	QTL located on Ch 1H associated with embryo sac area
QTL2H_NUC	QTL located on Ch 2H associated with nucellus area
QTL2H_OV	QTL located on Ch 2H associated with ovule area
QTL4H_INT	QTL located on Ch 4H associated with integument width
snoRNP	Small nucleolar ribonucleoprotein
SNP	Single nucleotide polymorphism
TPM	Transcripts per million

Abstract

Ovule formation is a critical process for grain production. Genetic and molecular characterisation of the processes required for initiation and successful development of the ovule in agriculturally important cereal crops is far from complete. This study aimed to identify candidate genes contributing to natural variation in *Horduem vulgare* (barley) ovule development in a population of 127 2-row spring genotypes. Global transcriptional profiles of developing pistils from four divergent barley genotypes (Chapter 5) were interrogated to identify 6,656 differentially expressed genes (DEGs) at comparable stages in four genotypes, or between sequential stages within individual genotypes. This list of DEGs was filtered further for expression within a second transcriptional data set, consisting of 15 samples isolated from specific ovule cell types by laser microdissection (LCM) in a reference cultivar. This identified 2377 differentially expressed genes for which tissue-specific expression data was available. Of these genes, 82 were located within four putative QTL regions previously identified to be associated with mature ovule morphology (Chapter 4). Annotations were identified for approximately half of these genes. Interesting candidates include a pentatricopeptide protein involved in cytoplasmic male sterility, a trio of genes encoding putative H/ACA small nucleolar ribonucleoprotein (snoRNP) complex subunit 4 proteins, and His-rich arabinogalactan protein (AGP), HISTIDINE-RICH ARABINOGALACTAN PROTEIN (HvHRA1). Although these genes were not analysed in further detail in this study, their putative functions are discussed in the context of barley ovule development and their possible roles in organ size.

Introduction

Barley ovules consist of discrete tissues that each play a distinct role in grain development; the integuments give rise to the seed coat, the chalaza connects the seed to the pistil, the nucellus acts as a nutrient transfer tissue and the embryo sac gives rise to the embryo and

endosperm (Engell 1988; Linnestad et al. 1998). The embryo sac, also called the female gametophyte (FG), contains several specific cell types that arise by mitosis of a single haploid cell, the functional megaspore (Willemse and De Boer-de 1981). The cells within the embryo sac are similar in eudicot and monocotyledonous species, and include two synergid cells, an egg cell, two polar nuclei within a central cell, and a cluster of antipodal cells (Schneitz et al 1995). The process of double fertilisation occurs within the FG and involves the fusion of two male sperm nuclei, one with the egg cell, which thus forms the zygotic embryo, and one with the polar nuclei of the central cell, which goes on to form the endosperm (Engell 1994). Following fertilisation, the nucellus acts as a nutrient transfer tissue, to support embryonic development and nutrient storage in the endosperm (Thiel et al. 2008).

Evidence suggests that developmental events occurring within the ovule tissues prior to fertilisation have an impact on downstream seed development. Many maternal factors that are expressed in the Arabidopsis ovule, such as AINTEGUMENTA (ANT; Mizukami and Fischer 2000)), APETALA2 (AP2; Ohto et al. 2005)) and KLUH (Zhao et al. 2018) have an effect on seed size (reviewed in Li and Li, 2015; JXB). In wheat (*Triticum aestivum*) it has also been suggested that signals that accumulate in the ovule may play an important a role in grain fill, if not more important that the activity of nutrient storage genes expressed after fertilisation has occurred (Fahy et al. 2018). This hypothesis is supported by evidence in maize (*Zea mays*), where expression of *EMBRYO-SAC BASAL-ENDOSPERM LAYER EMBRYO-SURROUNDING-REGION* (*ZmEBE*) within the central cell prior to fertilisation is critical to enable correct formation of the basal endosperm transfer cells upon fertilisation, thus playing a major role in grain fill (Magnard et al. 2003). Similarly, it has been found that DNA hypomethylation characteristic of maternal imprinting in the endosperm is initiated by demethylation in the central cell of both the model eudicot *Arabidopsis thaliana* and the monocot cereal rice (*Oryza sativa*), the level of which can impact seed weight and size (Park et al. 2016). Another component of the developing embryo sac, the antipodal cell cluster, has

been hypothesised for several decades to function as a conduit for developmental cues and nutrition required for maintenance of embryo sac development prior to fertilisation, and to support endosperm and embryonic development after fertilisation, however conclusive evidence is lacking (Chaban et al. 2011; Lloyd 1899).

Surrounding the embryo sac, the nucellus of wheat and barley has also been considered for its role in seed development (Wilkinson et al., 2018). The nucellus is reported to undergo programmed cell death after fertilisation in a manner mediated by vacuolar processing enzymes (Dominguez et al. 2001; Linnestad et al. 1998; Tran et al. 2014). Prior to fertilisation, the nucellus of model dicots including Arabidopsis and *Hieracium pilosella* is involved in auxin signalling, gives rise to a germline precursor (Pinto et al., 2019) and is suggested to mediate cross-talk between the somatic maternal tissue and the developing embryo sac (Juranić et al. 2018; Pagnussat et al. 2009; Panoli et al. 2015). However, in *Triticeae* monocot species such as barley, the role of the nucellus from FG initiation to ovule maturity remains unclear, as does the reason for its enlarged size relative to many modern angiosperms (Lora et al. 2017; Wilkinson and Tucker 2017). One way to investigate this is via compositional and transcriptional profiling, which can reveal structural and molecular details of tissue identity (Chapter 5). However, determining whether these genes or structural components play a functional role in ovule development via reverse genetic approaches, such as CRISPR or transgenic knock down, is particularly time consuming in the cereal monocots. Moreover, ovule development is a highly multigenic process, requiring coordinated input from many different regulatory pathways (Endress 2011; Jack 2001; Larsson et al. 2013; Yoshida and Nagato 2011). Modification of many ovule pathways often results in female sterility, which reveals little regarding specific functions in the ovule or during downstream seed development (Chettoor et al. 2016; Cui et al. 2010; Dreni et al. 2011). These limitations are one possible reason why, to date, few genes have been identified that function specifically within the

developing ovule of cereal crops such as wheat and barley, compromising our ability to investigate the influence that different ovule tissues have over grain developmental processes.

One way to overcome these limitations is to make use of natural diversity present within a large panel of related genotypes. Due to its long history of human cultivation, there is great diversity among barley and the combined number of known barley genotypes, including agriculturally utilised cultivars, breeding lines and wild relatives, exceeds 460,000 (Sato et al. 2014). A number of these genotypes have been genetically characterised (Comadran et al. 2012), providing suitable material for genome wide association studies (GWAS), a common method of identifying quantitative trait loci (QTL) that contribute to phenotypic diversity. Although the identification of causative genes underlying QTL is not trivial, studies show that it is possible to find them when combined with parallel approaches such as transcriptional profiling or variant mapping (Hassan et al. 2017; Houston et al. 2014; Garcia et al. 2019). Moreover, alleles contributing to features of ovule development are not expected to be overly deleterious, since the source material reflects elite European germplasm that has been selected for predictable yield and quality.

In a previous study, features of ovule development were shown to vary among a population of 127 two-row spring barleys (Chapter 4). This variation was used to perform GWAS, which confirmed ovule development in barley is a multigenic trait, likely influenced by a large number of small effect QTL. Despite this, four QTL that appear to influence morphology of the overall ovule, the embryo sac, the nucellus, and the integument in mature barley ovules, were identified. These QTL are known as QTL1H_ES, QTL2H_NUC, QTL2H_OV, and QTL4H_INT. Rather than initiating traditional bi-parental mapping to narrow down candidate genes, an alternative RNA sequencing (RNAseq) based approach was used to identify candidate causative genes. Gene expression data was generated from whole pistils at five discrete stages of reproductive development, and from four barley genotypes from the panel with “big”

(Salka, Wren) or “small” (Forum, Gant) mature ovule morphological traits (Chapter 5). Additionally, tissue-specific gene expression data was obtained for specific cell types within the ovule, including the egg apparatus and central cell, the antipodal cell cluster, the nucellus, the integuments, the chalaza and the ovary wall (Chapter 5). These RNAseq datasets form a powerful resource to identify possible candidate genes underlying natural variation in barley ovule development.

With the aim of identifying candidate genes, this study investigated differential expression of genes located within the four QTL identified in Chapter 4. Analysis revealed significant temporally and genotypically differential expression of 82 unique genes among the four QTL, of which 11 were within QTL1H_ES, 8 were within QTL2H_NUC, 8 were within QTL2H_OV, and 55 were within QTL4H_INT.

Methods

Genome wide association study and HORVU list identification

A population of 127 genotypes of European two-row spring barleys was grown and screened for ovule morphological traits at reproductive maturity, including ovule area, ovule width/transverse, ovule height/longitude, embryo sac area, embryo sac width/transverse, embryo sac height/longitude, nucellus area, nucellus proportion, and integument width. As described in Chapter 4, these data were used to perform a genome wide association study (GWAS). Quantitative trait loci (QTL) were identified on the basis of markers showing higher association with ovule traits as indicated by logarithm of the odds (LOD) scores. Genes within these QTL were identified using Barleymap (Cantalapiedra et al. 2015), and are referred to using HORVU identities. Three of the QTL identified have been investigated in this study, QTL1H_ES, QTL2H_NUC, and QTL2H_OV.

Generation of gene expression data

Whole pistil

Whole pistils were collected from four genotypes, Forum, Gant, Salka and Wren, as described in Chapter 5. For all four genotypes, samples were collected at five developmental stages, known as Stages 3 to 7. With respect to pistil development, these stages correspond to between Waddington Stages 7.5 and 9.5 (Waddington et al. 1983), and cover, with respect to ovule development, a timepoint shortly after selection of the functional megaspore until anthesis. For each stage, in each genotype, RNA was extracted from two replicate samples, yielding a total of forty RNA samples, of which poor RNA quality excluded four from being sequenced. The samples excluded were: Forum at Stage 3, Salka at Stage 3, and Wren at Stages 5 and 7.

Laser capture microdissection (LCM)

Discrete cell types were isolated using laser capture microdissection from ovules from cv. Sloop at three stages of development, and prepared for RNA sequencing as described in Chapter 5. The developmental stages included: (1) early female gametophyte development, equal to Stage 4 of the whole-pistil data, (2) a stage at which the nucellus and embryo sac are about to begin rapid expansion, equal to Stage 5 of the whole-pistil data, and (3) a stage at reproductive maturity, known as anthesis and equivalent to Stage 7 of the whole-pistil data. The specific tissues isolated varied between each developmental stage, with emphasis being placed on collecting replicates of each tissue at different developmental timepoints. The tissues collected included, from Stage 4: pooled nucellus and embryo sac (Stage 4_NUC_ES), integument (Stage 4_INT) and ovary wall (Stage 4_OW); from Stage 5: whole embryo sac (Stage 5_ES), the egg apparatus and central cell (Stage 5_ECC), the antipodal cell cluster (Stage 5_ANTP), nucellus (Stage 5_NUC), integument (Stage 5_INT), and ovary wall (Stage 5_OW); from anthesis: the egg apparatus and central cell (Stage 7_ECC), the antipodal cell

cluster (Stage 7_ANTP), nucellus (Stage 7_NUC), chalaza (Stage 7_CHL), integuments (Stage 7_INT) and ovary wall (Stage 7_OW).

Differential gene expression (DEG) analysis

Whole-pistil gene expression data were used to assess differential gene expression. Transcripts per million (TPM) values for the two replicates at each developmental stage, in each genotype, were averaged in order to yield a single expression value for all five developmental stages, in the four genotypes. Differential analysis was performed with respect to genotype and developmental stage, also referred to as temporal expression. Differentially expressed genes (between genotypes) were required to have a log2 fold change of magnitude equal or greater than 2 and a p-value below 0.05 for at least one comparison at equivalent developmental stages. Temporal DEGs were required to fulfil the same log2 fold change and p-value criteria for comparisons of samples at sequential developmental stages (e.g. 3 vs. 4 or 4 vs. 5, but not 3 vs. 5) within at least one genotype. Samples at the same developmental stage, within each genotype, were considered as replicates to perform two-tailed t-tests. Due to the single replicate of sequencing data for four samples, differential expression could not be assessed between several genotypes due to inability to calculate a p-value. Differential expression analysis was performed in CLC Genomics Workbench (Qiagen, Germany) and Microsoft Excel (Microsoft Corporation, USA). Venn diagrams used to visualise data were generated in Venn Painter (Lin et al. 2016).

Annotation and identification of candidate genes

Candidate genes were shortlisted by identifying those that were predicted to be located within each QTL regions (Chapter 4), exhibited a transcript abundance of TPM>5 in at least one of the fifteen samples of tissue-specific expression data and exhibited for differential expression, as described above. Annotations were assigned to each shortlisted gene as given in the Barlex Genome Explorer (Colmsee et al. 2015) when available, or by using the nucleotide and protein

sequences provided in the Barlex Genome Explorer to perform basic local alignment searches (BLASTs) with the NCBI BLAST portal (https://blast.ncbi.nlm.nih.gov/Blast.cgi), followed by a reciprocal BLAST of the best matching sequence identified back in the Barlex Genome Explorer.

Results

Comparison of temporal and genotypic differentially expressed genes (DEGs)

Comparison of whole pistil samples at sequential timepoints revealed differential expression of 2004 unique HORVUs, of which 1770 were differentially expressed only within one genotype, and 234 were differentially expressed throughout development in multiple genotypes (Table 6-1). Of these, 341 genes were identified to be differentially expressed over time in Forum, 503 in Gant, 779 in Salka and 612 in Wren. Comparison of developmentally equivalent samples revealed genotypic differential expression of 5958 unique HORVUs, of which 1306 were also differentially expressed over time. Therefore, the initial list of differentially expressed genes identified from genotypic and temporal comparisons of whole-pistil RNA-seq data included 6656 unique HORVUs. This initial list of 6656 HORVUs was filtered such that all HORVUs must have expression of TPM>5 in at least one sample of the ovule tissue-specific RNAseq data set, in order to eliminate genes predominantly expressed outside of the ovule (Figure 6-1). Filtering in this manner reduced the total number of differentially expressed HORVUs to 2377, of which 238 were only differentially expressed with respect to developmental stage, 1763 were only differentially expressed with respect to genotype, and 376 were differentially expressed both over time and between genotypes.

Table 6-1: Comparison of temporally and genotypically differentially expressed genes (DEGs). Genes were considered to be differentially expressed on the basis of greater than ±2 $\log_2$ fold change and $p < 0.05$. Genotypic DEGs were determined by comparison of samples at equivalent developmental stages from four different genotypes: Forum, Gant, Salka and Wren. Temporal DEGs were determined by comparison of samples at sequential developmental stages within individual genotypes.

DEG category	Number of DEGs
Genotypic	5958
Temporal: Forum	341
Temporal: Gant	503
Temporal: Salka	779
Temporal: Wren	612
Temporal: All genotypes	2004

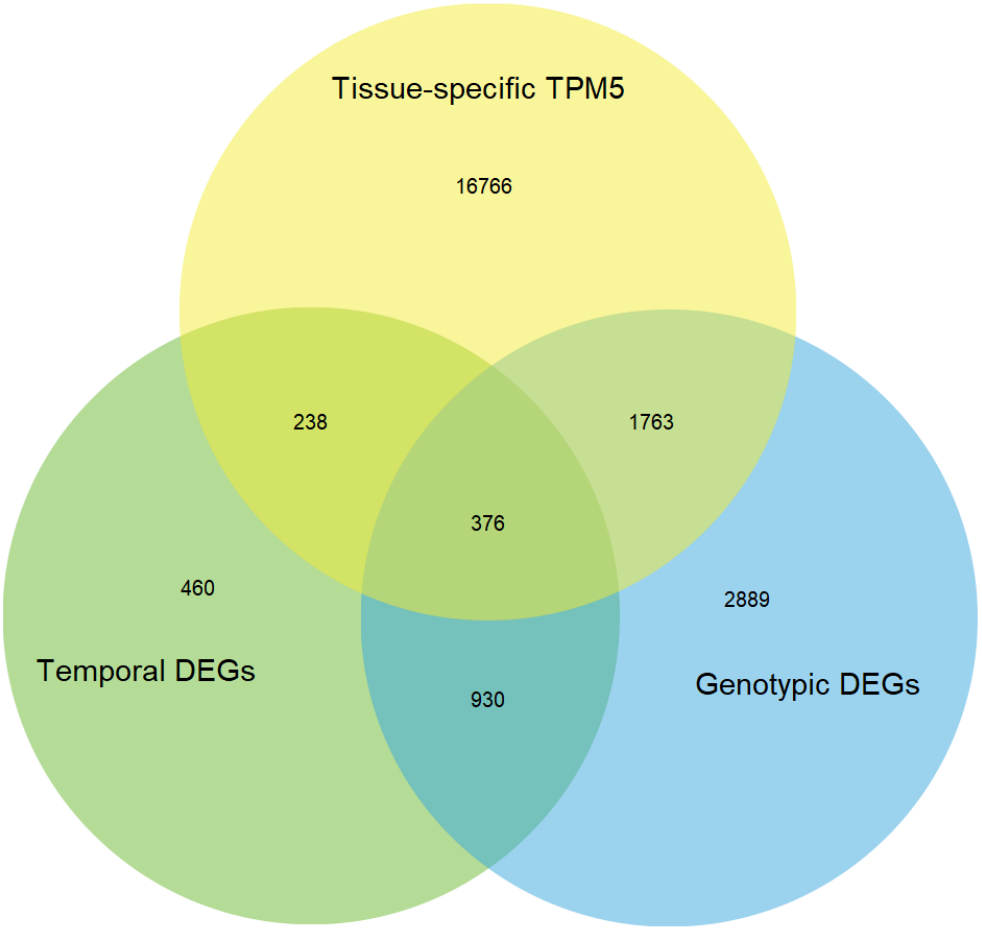

Figure 6-1: Venn diagram visualising the alignment of the genes identified in whole-pistil RNA-seq data to be differentially expressed among genotypes, among different developmental timepoints, and the genes identified to have TPM>5 among tissue-specific RNA-seq data. Genes were considered to be differentially expressed on the basis of greater than ±2 $\log_2$ fold change and $p < 0.05$. Genotypic DEGs were determined by comparison of samples at equivalent developmental stages from four different genotypes: Forum, Gant, Salka and Wren. Temporal DEGs were determined by comparison of samples at sequential developmental stages within individual genotypes.

Alignment of transcriptional data with quantitative trait loci

In order to identify genes potentially involved in natural phenotypic differences in ovule development, DEGs were cross-checked against the genes predicted to be present within four QTL associated with mature ovule morphological traits, as described in Chapter 4. Previously, a total of 4211 HORVUs were found to be located within the four QTL. Of these, 399 were located in the region associated with embryo sac traits, QTL1H_ES; 187 were located the region associated with nucellus area, QTL2H_NUC; 152 were located the region associated with ovule traits, QTL2H_OV; and 3473 were located the region associated with integument width, QTL4H_INT (Chapter 4).

Of the 4211 HORVUs within QTL regions, 82 were found to be differentially expressed (Table 6-2; Figure 6-2A). An additional 777 HORVUs within these QTL were abundant at a level of TPM>5 among the tissue specific data, but were not differentially expressed. Eleven differentially expressed genes (DEGs) were identified within QTL1H_ES, of which nine were genotypic DEGs and two were both genotypic and temporal DEGs (Figure 6-2B). Within QTL2H_NUC eight DEGs were identified, all of which were genotypic DEGs. Eight DEGs were identified within QTL2H_OV, of which five were genotypic DEGs and three were both genotypic and temporal DEGs. Fifty five DEGs were identified within QTL4H_INT, of which forty were genotypic DEGs, ten were temporal DEGs, and five were both temporal and genotypical DEGs. Thus, the majority of the 82 differentially expressed genes (DEGs) within the QTL regions were differentially expressed with respect to genotype only. HORVUs that were only differentially expressed with respect to developmental timepoint were exclusively located within QTL4H_INT. Data for identification of temporal and genotypic DEGs within the QTLs is presented in Tables 6-S1 and 6-S2, respectively.

Table 6-2. Summary of differentially expressed genes (DEGs) within four quantitative trait loci (QTLs) associated with morphological traits of mature barley ovules. Genes were considered to be differentially expressed on the basis of greater than ±2 log_2 fold change and $p < 0.05$. Genotypic DEGs were determined by comparison of samples at equivalent developmental stages from four different genotypes: Forum, Gant, Salka and Wren. Temporal DEGs were determined by comparison of samples at sequential developmental stages within individual genotypes. All DEGs considered were expressed in the tissue-specific data generated from the genotype Sloop with a transcript per million (TPM) abundance of greater than 5.

	Number of genes within QTLs					
	Total	All QTLs	QTL1H_ES	QTL2H_NUC	QTL2H_OV	QTL4H_INT
Genes within QTLs	4211	4211	399	187	152	3473
Genotypic DEGs	1763	62	9	8	5	40
Temporal DEGs	238	10	0	0	0	10
Genotypic and temporal DEGs	376	10	2	0	3	5
All DEGs	2377	82	11	8	8	55
Genes with TPM>5 in tissue specific data	19,143	777	40	37	36	664

A.

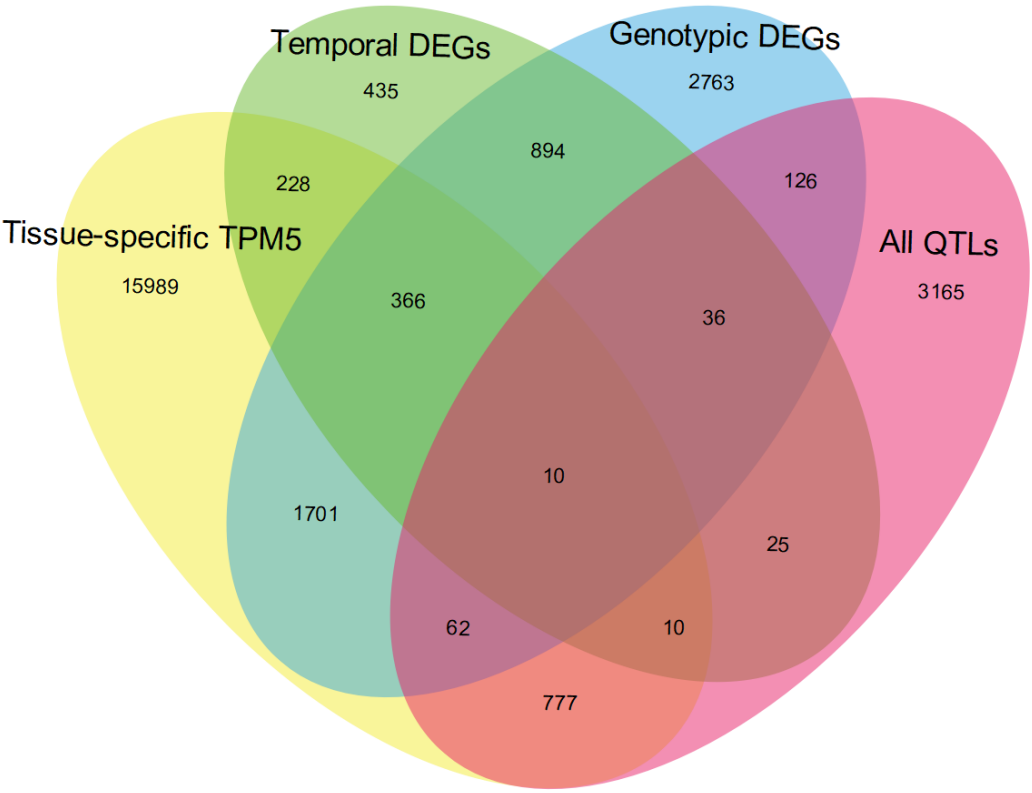
Temporal DEGs
435
Genotypic DEGs
2763
894
228
126
Tissue-specific TPM5
15989
All QTLs
3165
366
36
10
1701
25
62
10
777

B.

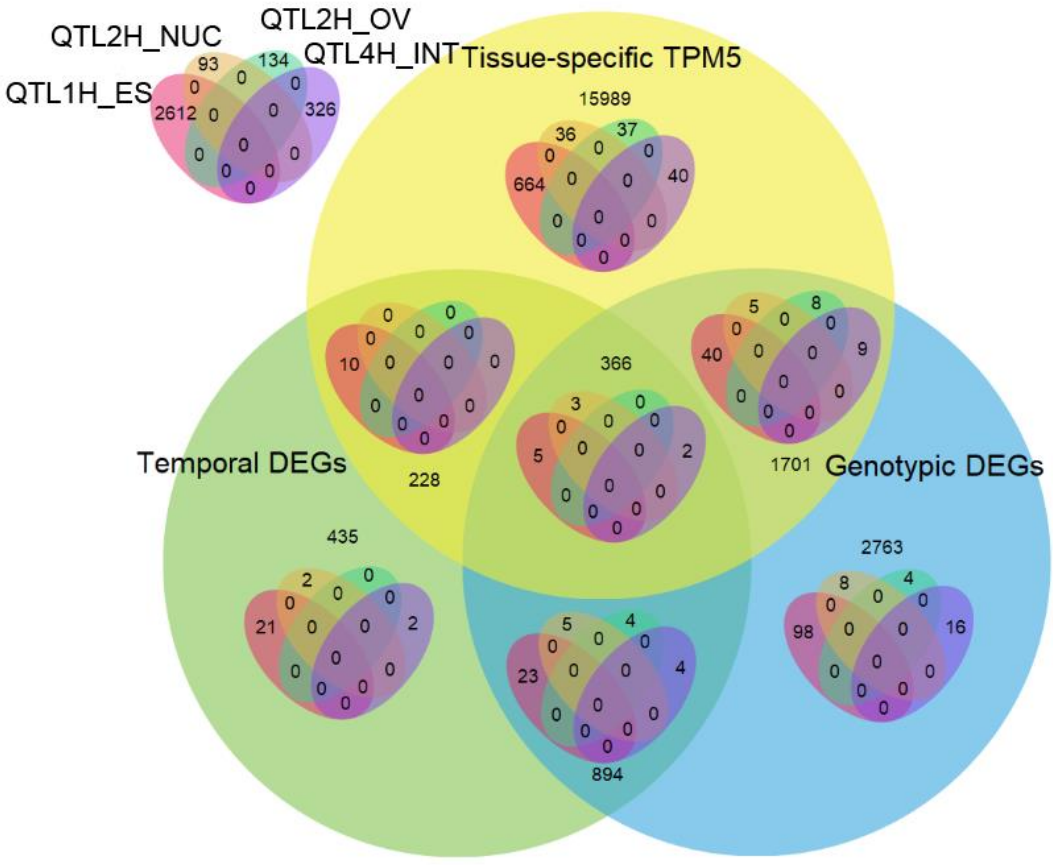
QTL2H_NUC
QTL2H_OV
QTL4H_INT
QTL1H_ES
Tissue-specific TPM5
15989
Temporal DEGs
228
366
1701
Genotypic DEGs
435
2763
894

Figure 6-2. Venn diagram visualising the identification of candidate differentially expressed genes (DEGs) within four quantitative trait loci (QTL) associated with variation in mature ovule morphology. Genes meeting the DEG criteria under (A) all four QTLs, and (B) each specific QTL are presented. Genotypic DEGs were determined by comparison of samples at equivalent developmental stages from four different genotypes: Forum, Gant, Salka and Wren. Temporal DEGs were determined by comparison of samples at sequential developmental stages within individual genotypes. Genes were considered to be differentially expressed on the basis of greater than ±2 $\log_2$ fold change and $p < 0.05$. Expression within tissue-specific RNAseq data of greater than 5 transcripts per million (TPM) was used to filter the candidate genes further.

Functional annotation of differentially expressed genes underlying QTLs

To annotate HORVUs of interest, the FASTA sequence for each HORVU was extracted from the Barlex Genome Browser (Colmsee et al. 2015). The sequence was used to perform a BLASTn within the cv. Morex genes database hosted by the James Hutton Institute (JHI, Scotland; (Bayer et al. 2017)), yielding Morex loci (MLOC) identifiers and predicted coding and protein sequences for some HORVUs. Coding sequences obtained from the Barlex Genome Explorer and the JHI database were used to perform BLASTn and BLASTp searches within both the MSU rice database and the NBCI database (Kawahara et al. 2013); https://blast.ncbi.nlm.nih.gov/Blast) in order to assess similarity with genes from other species. The MLOCs, LOCs, and annotations were cross-checked by performing a reciprocal BLAST of the MLOC and/or LOC coding sequences against the Barlex Genome Browser in order to reach a consensus gene identity and function where possible. This data is presented in Table 6-S3. Localisation of gene expression within the ovule was assessed using tissue-specific transcript data (Chapter 5).

Eleven differentially expressed HORVUs were identified within QTL1H_ES (Table 6-2). Specifically, nine were differentially expressed between genotypes and two were differentially expressed between both genotypes and developmental timepoints. The average expression abundance of these HORVUs among all tissue specific samples was 46.0 TPM, and among whole-pistil samples was 8.9TPM. The maximum expression among tissue specific samples was 209.9TPM, and among the whole pistil samples the maximum expression observed was 29.5TPM (Table 6-S3).

Functional annotations were determined for four of the eleven genes (Table 6-S3). In brief, these included a beta-glucosidase (HORVU1Hr1G010010), an alcohol dehydrogenase (HORVU1Hr1G010130), a putative transmembrane protein (HORVU1Hr1G010940), and

pentatricopeptide repeat protein 336 (PRR; HORVU1Hr1G011240). While HORVU1Hr1G011270 was found to be a low-confidence gene in the Barley genome explorer, using BLAST it was found to align to the same rice gene as PPR 336, LOC_Os04g28300.1, annotated as the precursor to RESTORATION OF FERTILITY 1 (RF1; Akagi et al. 2004).

Of the eleven genes identified within QTL1H_ES, three were specifically expressed within a single ovule tissue (Figure 6-3A). HORVU1HrG008900 was present within ES-derived samples, HORVU1Hr1G012660 was present in the nucellus, HORVU1Hr1G009760 was present in the chalaza. Of these, HORVU1HrG008900 was found to specifically be expressed in samples dissected at the Stage 5, corresponding the developmental point at which the embryo sac and nucellus rapidly begins to expand in two-dimensional area (Chapter 5). Whole-pistil expression data revealed that, on average among the four genotypes, expression of these eleven genes was not biased toward a particular developmental stage (Figure 6-3B). Three genes, HORVU1Hr1G110240, HORVU1Hr1G010240 and HORVU1Hr1G010010, were found to be consistently genotypically differentially expressed throughout all developmental stages such that expression was greater in Forum and Gant, the genotypes representing small mature ovule phenotypes.

Eight differentially expressed HORVUs were identified within QTL2H_NUC, on the basis of genotypically differential expression (Table 6-2). None of the eight genes were differentially expressed with respect to developmental stage. The maximum expression abundance of these eight genes was attained by HORVU2Hr1G027360, found to be 1578.4TPM in the tissue-specific data and 96.9TPM within the whole-pistil developmental series data (Table 6-S3). The average expression abundance of these HORVUs among all tissue specific samples was 272.5TPM, or 85.9TPM when HORVU2Hr1G027360 was excluded.

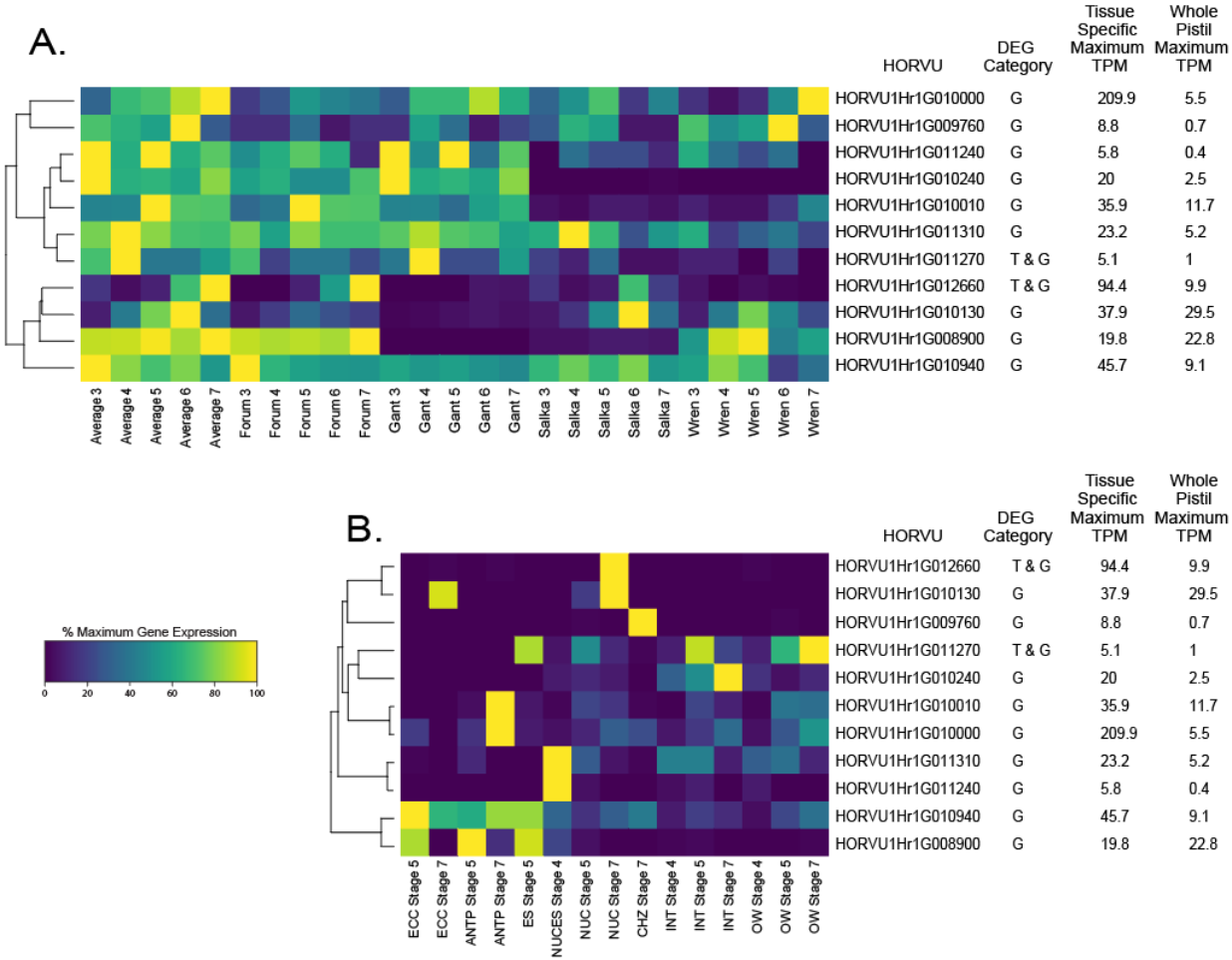

Figure 6-3: Heatmap visualisation of the expression of differentially expressed located within QTL1H_ES within (A) specific ovule tissues, and (B) at five stages of ovule development within the whole pistil in four barley genotypes.

Functional annotations were determined for six genes (Table 6-S3). In brief, these included three ribosomal L7Ae/L30e/S12e/Gadd45 family proteins (HORVU2Hr1G027230, HORVU2Hr1G027360, HORVU2Hr1G027410), a haloacid dehalogenase-like hydrolase (HAD) superfamily protein (HORVU2Hr1G027680), and CWC15-like protein A (HORVU2Hr1G026610).

Four of these eight HORVUs attained maximum expression in the Stage 4_NUC_ES sample (Figure 6-4A). Two HORVUs reach their maximum expression in ECC samples, one at the Stage 5 and one at anthesis, and the final two HORVUs attained maximum expression in the whole-ES sample and the integument sample, both at Stage 5. Only two of the eight HORVUs were found to reach more than 50% of their maximum abundance within the tissue-specific ovary wall samples. Within the whole-pistil data, these eight genes tended to reach maximum expression at later stages of development (Figure 6-4B).

Eight differentially expressed HORVUs were identified within QTL2H_OV, of which five were genotypic DEGs and three were both genotypic and temporal DEGs (Table 6-2). The maximum expression abundance of these eight genes was 8547.7TPM among the tissue specific samples and 74.9TPM among the whole-pistil samples, attained by HORVU2Hr1G085020 and HORVU2Hr1G085270, respectively (Table 6-S3). Among the laser dissected samples the average transcript abundance value was 1822.7TPM when all eight samples were considered, or 39.7TPM when the two samples with TPM values over 5000 were excluded. Among the whole-pistil samples the average transcript abundance of all eight HORVUs was 23.3TPM.

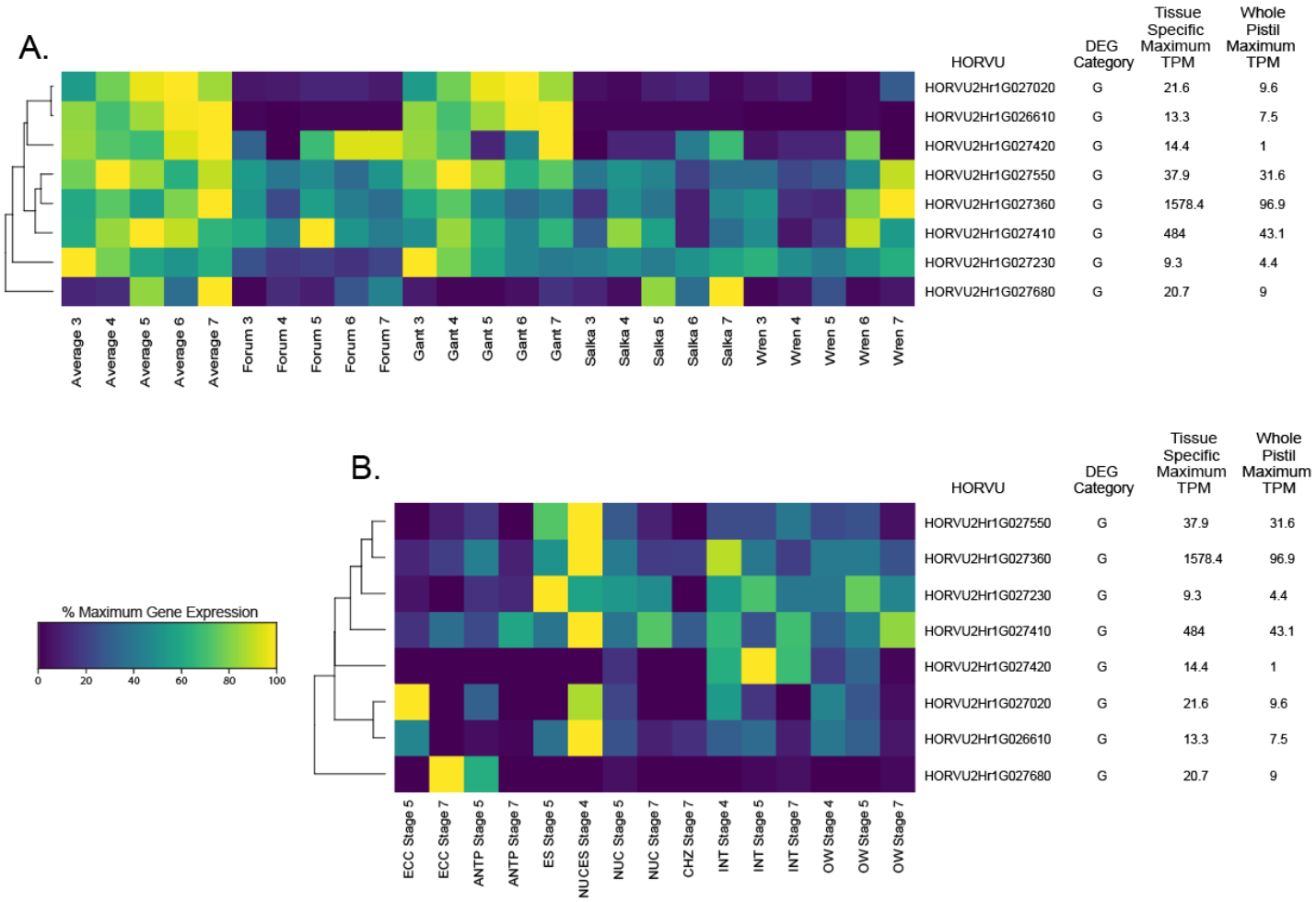

Figure 6-4: Heatmap visualisation of the expression of differentially expressed located within QTL2H_NUC within (A) specific ovule tissues, and (B) at five stages of ovule development within the whole pistil in four barley genotypes.

Functional annotations were determined for six genes (Table 6-S3). In brief, these included cyclin-dependent kinase G2 (HORVU2Hr1G084400), a B-box zinc finger family protein (HORVU2Hr1G085000), a chitinase (HORVU2Hr1G085270), and the most abundantly expressed gene within the QTL was identified as HvHRA1, a cereal-specific histidine-rich arabinogalactan protein 1 (HORVU2Hr1G085020). Notably, expression of this HvHRA1 gene as well as the second most abundant gene, HORVU2Hr1G085050, was found to be specific to embryo sac-derived samples, with a heavy bias toward the antipodal cells at anthesis (Figure 6-5A). Among the eight genes identified within QTL2H_OV, whole-pistil gene expression data revealed that maximum transcript abundance tended to occur at later developmental stages, and that few genes maintained greater than 50% maximum transcript abundance over multiple developmental stages (Figure 6-5B).

Fifty five differentially expressed HORVUs were identified within QTL4H_INT, of which forty were genotypic DEGs, ten were temporal DEGs, and five were differentially expressed with respect to both genotype and developmental timepoint (Table 6-2). Among the tissue-specific data, the maximum and average transcript abundance attained by these genes was 824TPM and 60.1TPM, respectively (Table 6-S3). Among whole-pistil data, the maximum and average transcript abundance attained by these genes was 303.9TPM and 20.9TPM, respectively. Due to the relatively large number of genes identified within this QTL, tissue-specific transcription data revealed groups of genes for which expression was biased towards embryo sac-derived cell types, the nucellus, the ovary wall, or specifically toward each of the three developmental stages from which RNA was extracted. None of the 55 genes were found to be specifically expressed in the integuments (Figure 6-6A). Analysis of whole-pistil expression data revealed that expression of the genes shortlisted within QTL4H_INT was not biased towards any developmental stage (Figure 6-6B). Only a single gene, HORVU4Hr1G037050, was found to be consistently genotypically differentially expressed throughout all five developmental stages in a manner reflecting the different phenotypes of Forum and Gant, and Salka and Wren.

Functional annotations were determined for twenty five of the fifty five HORVUs within QTL4H_INT, as presented in Table 6-S3.

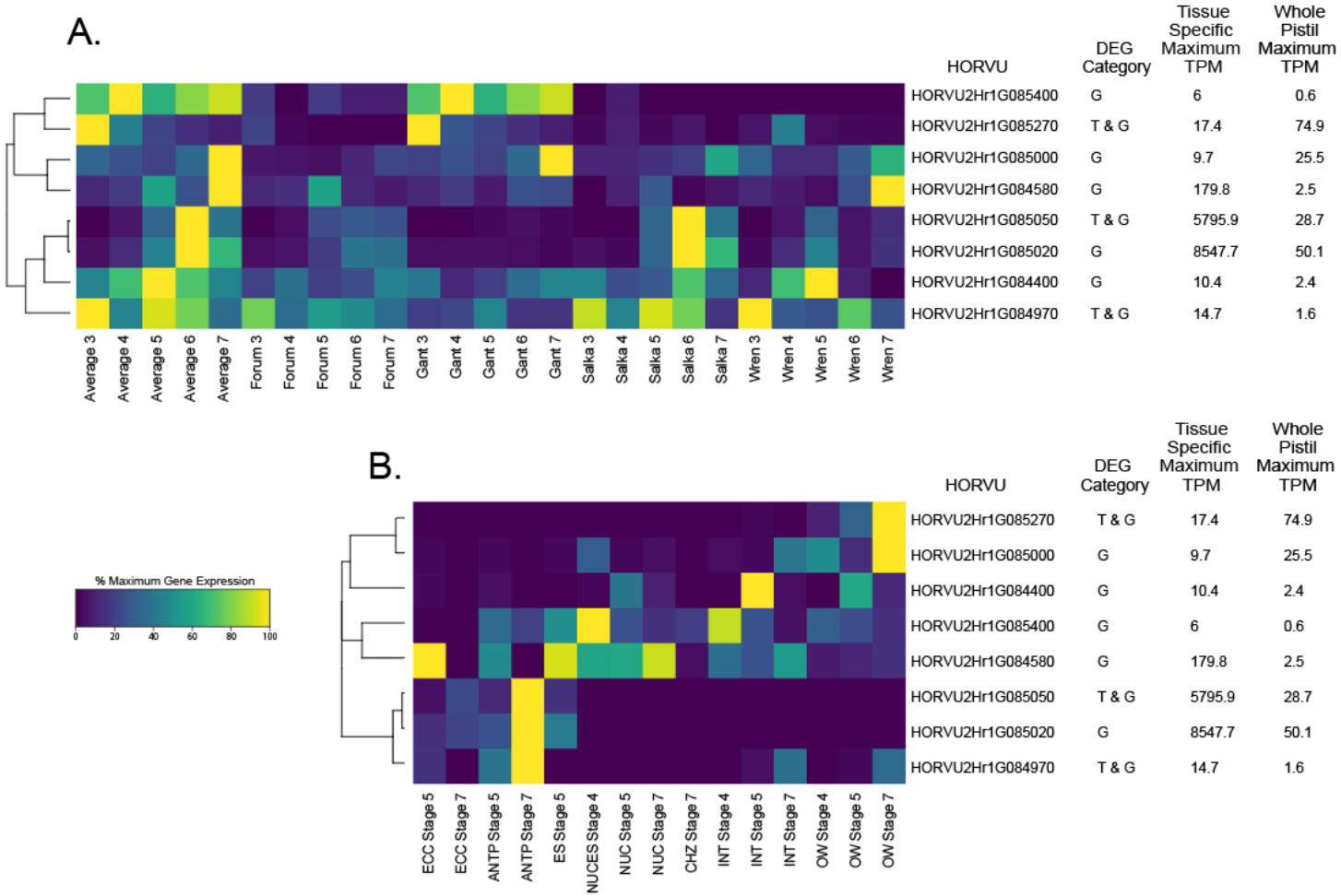

Figure 6-5: Heatmap visualisation of the expression of differentially expressed located within QTL2H_OV within (A) specific ovule tissues, and (B) at five stages of ovule development within the whole pistil in four barley genotypes.

A.

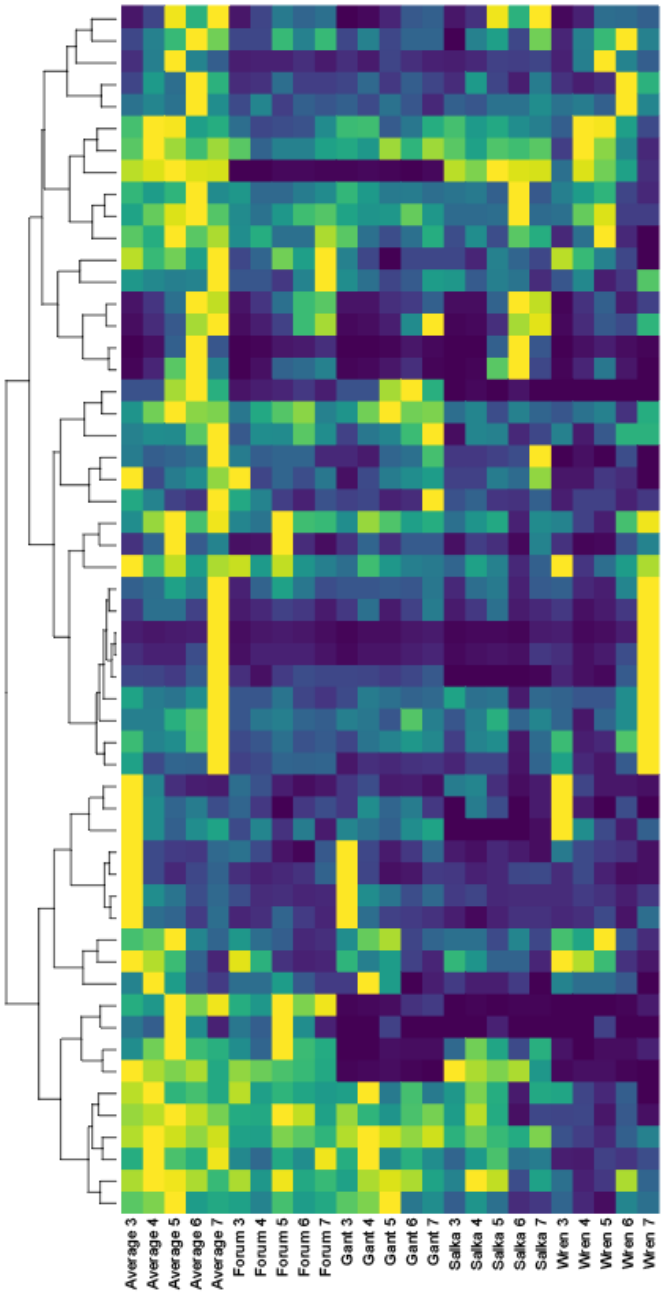

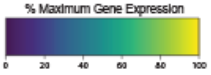

HORVU	DEG Category	Tissue Specific Maximum TPM	Whole Pistil Maximum TPM
HORVU4Hr1G044040	G	46.1	45.9
HORVU4Hr1G021390	G	12.4	0.5
HORVU4Hr1G054780	T & G	10	5.8
HORVU4Hr1G048540	G	187	2.4
HORVU4Hr1G034670	G	11.5	1.3
HORVU4Hr1G054850	G	14.1	33.4
HORVU4Hr1G030730	T	8.5	1.6
HORVU4Hr1G037050	G	5.7	3.5
HORVU4Hr1G028720	G	14	167.8
HORVU4Hr1G054970	G	14.8	22.4
HORVU4Hr1G024480	G	35.2	0.4
HORVU4Hr1G051590	G	47.2	0.5
HORVU4Hr1G039160	G	10.4	2.3
HORVU4Hr1G027180	G	151.1	15
HORVU4Hr1G026150	T	143.1	18.6
HORVU4Hr1G040510	G	6.5	48.7
HORVU4Hr1G040520	T & G	10.2	20.3
HORVU4Hr1G035330	G	10.7	1.8
HORVU4Hr1G034730	G	9.3	2.3
HORVU4Hr1G043630	G	95.1	2.5
HORVU4Hr1G023980	G	55.8	1.2
HORVU4Hr1G052660	T	14.7	3
HORVU4Hr1G021320	T	5.2	15.4
HORVU4Hr1G041600	G	22.9	8.9
HORVU4Hr1G035540	T	205.2	4.7
HORVU4Hr1G035100	T	21.5	11.8
HORVU4Hr1G046970	G	80.6	8
HORVU4Hr1G055110	T & G	30.6	1.2
HORVU4Hr1G025580	G	9.7	42.3
HORVU4Hr1G025470	G	6.6	129.1
HORVU4Hr1G046000	G	5.2	3.5
HORVU4Hr1G040350	T	41	1.9
HORVU4Hr1G030420	G	28.4	1.5
HORVU4Hr1G027940	G	824	8.7
HORVU4Hr1G035670	G	7.7	16.1
HORVU4Hr1G049550	G	16.7	8.7
HORVU4Hr1G042040	T	421.2	0.6
HORVU4Hr1G050560	G	7.6	1.3
HORVU4Hr1G046350	G	29.4	13.5
HORVU4Hr1G052450	T & G	36.3	5.8
HORVU4Hr1G022780	G	92.5	303.9
HORVU4Hr1G054200	G	12.4	9.7
HORVU4Hr1G054470	T	55	40.6
HORVU4Hr1G054770	T	62.7	54.8
HORVU4Hr1G021590	T & G	7.6	0.6
HORVU4Hr1G052260	G	169.1	14.6
HORVU4Hr1G029240	G	6	0.5
HORVU4Hr1G034030	G	12	6.2
HORVU4Hr1G055560	G	68.8	9
HORVU4Hr1G030780	G	19.6	3.3
HORVU4Hr1G030980	G	20.3	6.1
HORVU4Hr1G031060	G	11.1	5.7
HORVU4Hr1G052290	G	14.7	4.9
HORVU4Hr1G037240	G	9.3	2.4
HORVU4Hr1G040730	G	29.9	3

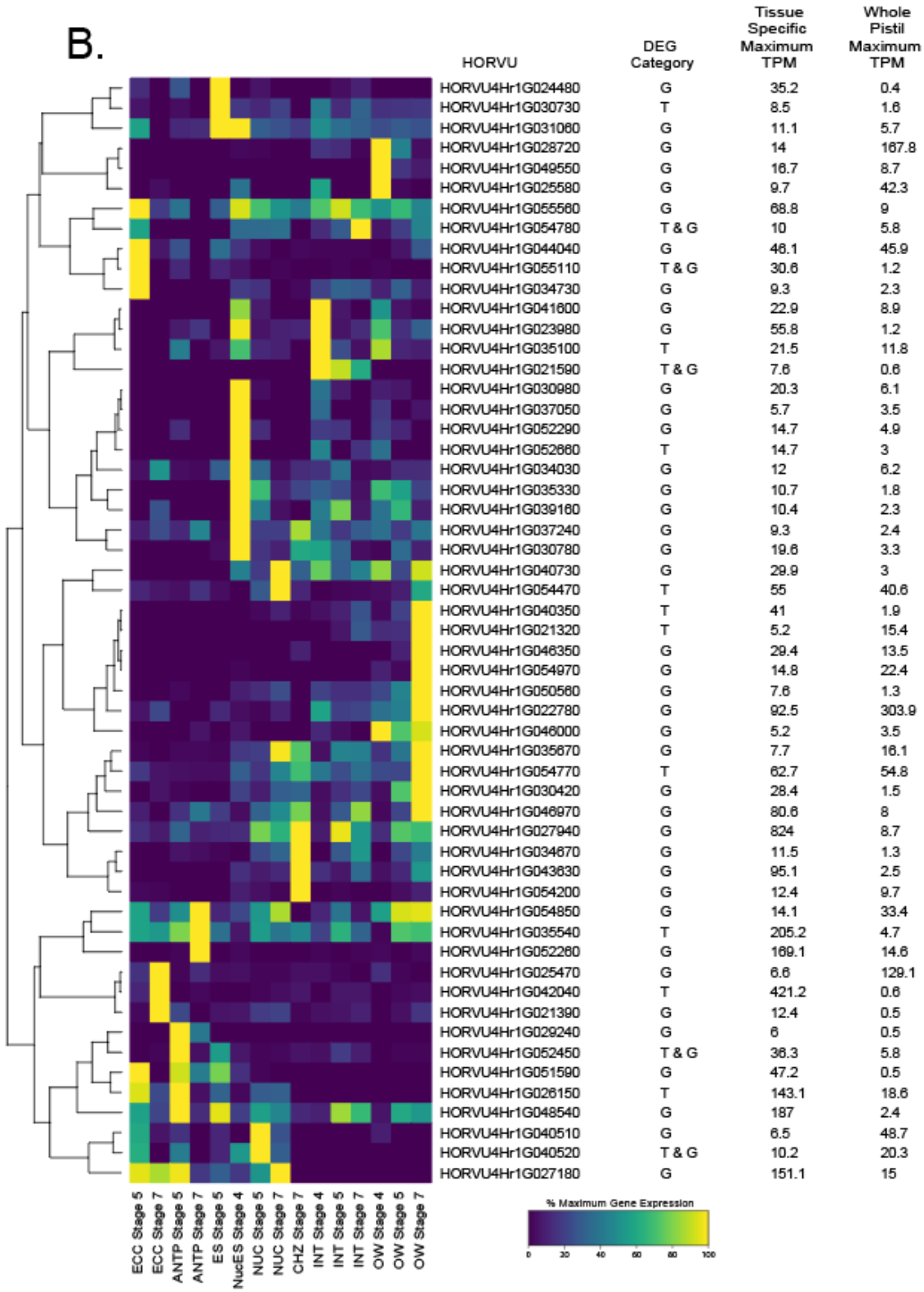

Figure 6-6. Heatmap visualisation of the expression of differentially expressed located within QTL4H_INT within (A) specific ovule tissues, and (B) at five stages of ovule development within the whole pistil in four barley genotypes.

Discussion

Differential gene expression analysis as a tool for GWAS QTL candidate discovery

This study used transcriptional data to investigate genes located near four quantitative trait loci (QTL), which are associated with variation in morphological traits of mature barley ovules. The four QTLs were previously identified by performing a genome wide association study (GWAS) on a population of 127 two-row spring barley genotypes, presented in Chapter 4. Variation in embryo sac morphology was associated with QTL1H_ES, variation in nucellus area was associated with QTL2H_NUC, variation in ovule morphology was associated with QTL2H_OV, and variation in integument width was associated with QTL4H_INT. Two sets of transcriptional data were utilised for downstream analysis, presented in Chapter 5. The first transcriptional data set included twenty samples, representing ovule development at five specific stages between mitosis of the functional megaspore to anthesis (Stages 3 to 7) in four genotypes that were identified to have large (Salka and Wren) or small (Forum and Gant) mature ovule phenotypes. Each of the twenty samples presented the average expression (as transcripts per million, TPM) of two combined individual replicates, with the exception of four samples, thus allowing calculation of the significance of differential expression between any two developmental stages or genotypes. The second transcriptional data set included fifteen samples isolated from specific ovule cell types, using laser capture microdissection. This data was collected from a fifth genotype, cv. Sloop, a representative Australian established as a system for gene expression analysis (Burton et al. 2011).

Differential expression analysis is a standard technique that has been used in many studies of wild-type and mutant ovule development to identify candidate genes involved in gametogenesis (Schmidt et al. 2014; Wu et al. 2015; Yu et al. 2005). For example, a recent differential screen in Arabidopsis led to the identification of the cytochrome P450 gene *KLUH*

(Zhao et al. 2014), which was shown to be involved in integument growth and female germline development. In barley, differential expression analysis of *vrs3* mutants, which regulate floret fertility, showed that VRS3 likely acts upstream of *VRS1* and *VRS5* (van Esse et al. 2017). Despite this, global gene expression profiling to find candidate genes underlying GWAS QTL is a relatively new approach and one that carries many caveats. It relies on the assumption that the causative polymorphism(s) underlying QTL have an effect on transcript abundance, rather than a change in function that do not impact mRNA levels. Also, when multiple cultivars are compared to find DEGs, care must be taken to ensure that similar phenotypes equate to similar haplotypes, particularly at the QTL of interest. Finally, population screens for genes that influence ovule development, and hence fertility, might be expected to show bias towards "weak" alleles, since "strong" alleles that severely compromise fertility are unlikely to be present in in elite genotypes. Data in the preceding Chapters confirmed that ovule development in barley is under the control of multiple genes, is influenced by multiple component tissues and varies between genotypes in terms of when differences appear. Hence, the multi-faceted gene expression approach reported here was essentially used as a test-case to: 1) document general gene expression profiles during barely ovule development, 2) speed up QTL characterisation without additional genetic studies and 3) provide target genes for further "knock-out" analysis.

In order to be considered to be differentially expressed, each gene had to pass the threshold of showing at least 2 $\log_2$-fold change in expression between two samples assessed, with a p-value of <0.05. Comparisons were made between samples of different genotypes at equivalent developmental stages, and samples at subsequent developmental stages of a single genotype, thus yielding "genotypic" and "temporal" differentially expressed genes. In this manner, among all expressed genes identified within the whole-pistil transcript data, 5958 genes were found to be genotypically differentially expressed, and 2004 genes were found to be temporally differentially expressed (Table 6-1; Figure 6-1). From these differentially

expressed genes, shortlists of candidate genes that might be causative of the phenotypes associated with each QTL were selected using the following criteria: 1) located within the QTL region as per the most recent annotation of the Morex genome (Mascher et al. 2017); 2) transcript abundance of greater than 5TPM in at least one sample of the tissue-specific transcript data set. A total of 82 differentially expressed genes were found to pass these criteria (Table 6-2; Figure 6-2), of which 11 were located within QTL1H_ES, 8 were located within QTL2H_NUC, 8 were located within QTL2H_OV, and 55 were located within QTL4H_INT. Functional annotations were identified for each of these genes where possible using the Barlex genome explorer (Colmsee et al. 2015), and by performing basic local alignment searches (BLASTs) of the nucleotide and protein sequences using the NCBI BLAST portal (https://blast.ncbi.nlm.nih.gov/Blast.cgi). Functional annotations were identified for approximately half of the shortlisted candidate genes (Figure 6-S3), and the annotations were utilized to prioritize candidate genes located within three QTLs. The large number of shortlisted candidate genes within QTL4H_INT constrained further selection of specific candidate genes. Identification of candidate genes in this manner demonstrates the application of novel transcriptional data sets describing ovule development in cereal crops, and may guide the direction of future studies that improve our genetic and molecular understanding of the cues influencing ovule development in barley.

Differential expression analysis reveals genes involved in mRNA processing within a QTL associated with embryo sac morphology

Eleven genes were found to be differentially expressed within the QTL1H_ES region associated with variation in mature embryo sac morphology. Of these eleven genes, HORVU1Hr1G010940 was abundant in all ES-derived RNA-seq samples, and showed differential expression between genotypes at Stage 6. The rice homologue, LOC_Os05g02990, encodes a transmembrane protein that is highly expressed in the

inflorescence, pistil and anther, although no function has been reported. Perhaps of greater interest were the HORVU1Hr1G011240 and HORVU1Hr1G011270 genes, both of which were found to align to the same rice sequence, LOC_Os04g28300, which is annotated as a PPR 336 protein, specifically, RESTORATION OF FERTILITY 1 (RF1, Akagi et al. 2004). Based on tissue-specific RNA-seq in barley, the HORVU1Hr1G011240 and HORVU1Hr1G011270 transcripts reached maximum abundance in the nucellus during an early reproductive developmental stage and in the ovary wall at reproductive maturity, respectively, thus supporting independent identities. In rice, *RF1* processes mRNA of the cytotoxic factor ORF79 that causes cytoplasmic male sterility (CMS) in Bacillus thuringiensis (BT) rice, preventing its accumulation and thus permitting production of fertile pollen (Itabashi et al. 2009; Wang et al. 2006). As CMS is a useful tool for hybrid production, RF1 plays an important role in rice breeding programs (reviewed by Fan et al. 2017). Similar roles for other members of the PPR family in restoring CMS have been identified in sorghum (*Sorghum bicolor*) and canola (*Brassica napus;* Klein et al. 2005; Liu et al. 2017). At the cellular level in rice, *rf1* mutants show defects during male gametophyte development (Kazama and Toriyama 2003), but there is no effect reported on female fertility. In general, the 35-amino acid repeat sequence that forms the PPR motif confers capacity for binding and modification of mRNAs (Small and Peeters 2000). Other members of the PPR family have been found to be involved in regulating mitochondrial function required for embryonic and endosperm development in maize and rice (Cui et al. 2010; Qi et al. 2017; Sun et al. 2018). From these studies, it is not abundantly clear what the function of PPR protein might be during female gametophyte development in barley. A decrease in transcript abundance during pistil development indicates that the gene product may have a regulatory role during early stages of embryo sac growth. Interestingly, expression of both genes was found to be lower in Salka and Wren, the genotypes with large mature ovule phenotypes, compared to the two genotypes with smaller ovules, Forum and Gant, suggesting a possible general association between higher expression of these genes and a small embryo sac phenotype. Although the overall transcript abundance of both

HORVU1Hr1G011240 and HORVU1Hr1G011270 was relatively low, with either gene reaching a maximum of only 5.8 TPM within the tissue-specific RNAseq data and 1.0 TPM within the whole-pistil data, this may indicate a restricted expression location within the ovule or ovary wall. While lower expression within the whole-pistil data was expected, relative to that of the tissue-specific data, this raises the question of how abundant transcripts, and the gene product, of a gene must be in order to have an appreciable effect on phenotype. In the case of small tissues that are rapidly undergoing change, such as within the developing ovule, it may be that very little gene product is required. Future work will be required to verify the expression of these sequences and determine a novel function for PPR 336 and its precursor within or around the developing female gametophyte of barley.

Genes involved in mRNA splicing and non-coding RNA function are potentially involved in the nucellus development

Eight genes were found to be differentially expressed within the QTL associated with variation in nucellus area, QTL2H_NUC, all of which were found to vary genotypically but not with respect to developmental timepoint. Among the six genes for which functional annotations were determined, four were notable. First, genes encoding CWF15/CWC15 cell cycle control family (CWC15)-like protein A, HORVU2Hr1G026610, and then three sequences that were found to encode H/ACA ribonucleoprotein complex subunit 4-like proteins (H/ACA snoRNPs), HORVU2Hr1G027360, HORVU2Hr1G027410 and HORVU2Hr1G027420. Of the latter three, HORVU2Hr1G027410 and HORVU2Hr1G027420 occupy consecutive positions on the genome scaffold and thus may be part of the same sequence.

In Arabidopsis, CWC15-like protein A is annotated as EMBRYO DEFECTIVE 2769 (EMB2769, AT3G13200; Patton et al. 1998), a factor involved in biotin metabolism required for embryogenesis. Additionally, there is evidence that suggests that locus AT3G13200 may

act downstream of SPOROCYTELESS/NOZZLE (SPL/NZZ), a key transcription factor in both male and female reproductive development (Xing and Zachgo 2008; Yang et al. 1999). Protein-protein BLAST search through NCBI (https://blast.ncbi.nlm.nih.gov/Blast.cgi) indicate that the CWC15-like protein A shares homology with sequences in wheat (*Triticum urartu*), rice, sorghum, millet (*Panicum miliaceum*) and *Aegilops tauschii*. In rice, the gene LOC_Os06g01700.1 encodes an orthologous protein that is expressed in multiple tissues, including the pistil. Based on annotation, the rice CWC15-like protein A may be involved in pre-mRNA splicing (Ouyang et al. 2006). In principal, a gene involved in splicing and cell cycle regulation that is expressed in a range of ovule tissues might be an exciting candidate for further research. One puzzle is that HORVU2Hr1G026610 expression is specifically in the whole-pistil sequence data for the genotype Gant. Thus, although the gene exhibits differential expression between genotypes, it is not a promising candidate that fits the broader big/small genotype profile for a causative gene within this QTL.

The trio of genes that were functionally annotated as H/ACA snoRNPs, HORVU2Hr1G027360, HORVU2Hr1G027410 and HORVU2Hr1G027420, were designated low confidence, unannotated genes within the Barlex Genome Browser. However, nucleotide BLAST search through the NCBI portal identified matches to genes predicted to encode H/ACA ribonucleoprotein complex subunit 4 in several other grasses, including rice, wheat (*Triticum aestivum*), maize, sorghum, setaria (*Setaria italica*), *Panicum hallii*, and *Brachypodium distachyon*. Generally, in both plants and animals snoRNPs are known to be involved in mRNA processing (as reviewed by Brant and Budak 2018; Filipowicz and Pogačić 2002; Scott and Ono 2011). As *in-vitro* confirmation of these *in silico* annotations is yet to be achieved, it is not possible to verify the function of these sequences in barley or determine their role in ovule development. However, due to the relatively high transcript abundance of HORVU2Hr1G027360, which reaches a maximum of 1578.4 TPM in the tissue-specific data and 96.4TPM in the whole-pistil data, and the demonstrated roles of other small non-coding

RNA in plant development (Ohtani et al. 2008; Tucker et al. 2012), these sequences may be considered as candidates for future investigation.

A role for the antipodal cells in micronutrient accumulation and ovule size?

Eight genes were found to be differentially expressed within the QTL2H_OV region associated with variation in ovule area. Of these, functional annotations were found for four genes, including a cyclin-dependent kinase G2 (CDK G2; HORVU2Hr1G084400), a B-box zinc finger family protein (HORVU2Hr1G085000), a histidine rich arabinogalactan protein (His-rich AGP; HORVU2Hr1G085020), and a chitinase (HORVU2Hr1G085270). While the functional annotation of the genes encoding a CDK G2 protein, a B-box zinc finger protein, and a chitinase are promising with respect to a potential role in regulating ovule development, no specific functions could be predicted based on a lack of characterised homologues in other species. As such, these genes present candidates for future investigation.

The transcript abundance of two of the QTL2H_OV genes, HORVU2Hr1G085020 and HORVU2Hr1G085050, was particularly notable due to relatively high and specific expression within the embryo sac, particularly in the antipodal cell cluster at anthesis. HORVU2Hr1G085020 was found to have a transcript abundance of 8547.7TPM in the antipodals, while HORVU2Hr1G085050 was also abundant at 5795.9TPM. Despite being specifically expressed in a very small tissue, transcript of these two HORVUs was also observed in the whole-pistil data, whereby transcript abundance of HORVU2Hr1G085020 and HORVU2Hr1G085050 reached 50.1TPM and 28.7TPM, respectively. This may indicate that high transcript abundance of these genes uniquely within the embryo sac was sufficient for detection within the whole-pistil data. While these genes were described as low-confidence unannotated sequences in the Barlex genome browser, nucleotide BLAST search through the NCBI portal identified that HORVU2Hr1G085020 matched the sequence of a specific barley

His-rich AGP (HvHRA1, accession no. TC147437; match: 99% query cover, E value: 0.0, identity: 96.4%). Alignment searches with the coding sequence of HORVU2Hr1G085050 were not successful in identifying any annotated genes, thus it cannot be determined whether this gene is of similar function to *HvHRA1* or is simply co-expressed. HvHRA1 has been found to be involved in micronutrient storage, and its expression has previously been identified in the developing pistil and within the grain from 3 to 10 days after fertilisation (Aizat et al. 2011). The function of the antipodal cells in ovule development has been debated for many years, whereby some studies dismiss them as having no role, and others propose that the antipodal cells fulfil a key role in maintaining the supply of nutrition and cues required for embryo sac formation, embryogenesis and endosperm development (Chaban et al. 2011; Lloyd 1899; Maeda and Miyake 1996, 1997). The existence of a large cluster of antipodal cells that persists until after fertilisation has long been documented in cereal crops (Brink and Cooper 1944; Diboll 1968; Engell 1994), while the notion that the three antipodal cells of Arabidopsis degenerate prior to fertilisation has only recently been disproved (Song et al. 2014). AGPs have been widely characterised to be involved in both male and female sexual reproduction processes in plants (reviewed by Leszczuk et al. 2019), however within the ovule their role has thus far been predominantly characterised as a required marker of the functional megaspore (Acosta-García and Vielle-Calzada 2004; Juranić et al. 2018). Transcript abundance of HvHRA1 and HORVU2Hr1G085050 was found to increase on average throughout the whole-pistil developmental series data until Stage 6, which was described in Chapter 5 as the developmental point at which the nucellus and embryo sac, presumably driven by the central cell and antipodal cell cluster, rapidly expand in two-dimensional area. Given the putative role of HvHRA1 in micronutrient accumulation, we speculate that this data agrees with previous reports suggesting the antipodal cells are required for accumulation of nutrients within the embryo sac prior to fertilisation in order to support the initial stages of endosperm development (Chaban et al. 2011; Lloyd 1899). Investigation of the metabolic activity and nutrient accumulation within discrete tissues of the developing ovule and grain is

required to address this hypothesis. Additionally, future work in barley may benefit from verification and detailed characterisation of *HvHRA1* expression within the developing ovule such that it might be used as a marker of germline or antipodal cell identity.

Model of cause and effect: do we have enough information to predict the expression pattern of candidate effector genes?

Tissue-specific data profiling of gene expression within discrete ovule cell types is a powerful tool to test the relevance of candidate genes identified from more generalized data. This is particularly important before progressing to generation of transgenic plants with altered expression of candidate genes. In species such as Arabidopsis and rice, tissue-specific data is available for the developing ovule in the form of microarrays and RNA sequencing (Ohnishi et al. 2011; Steffen et al. 2007; Tucker et al. 2012; Wuest et al. 2010), while in barley, only early stages of seed development have been analyzed in detail (Thiel et al. 2008). Hence, the resource generated here appears to be unique for the *Triticeae* cereals. Not only does data of this kind allow exclusion of shortlisted candidate genes that are not expressed within the tissues of interest, but, as with other techniques such as *in situ* hybridization, observation of the precise pattern of expression may yield further clues about the role of the gene of interest. For example, based upon the association of QTL1H_ES with embryo sac morphology, it could be hypothesized that a candidate gene influencing this trait might encode a stimulatory factor expressed within the embryo sac tissues, or encode an inhibitory factor expressed within the nucellus. In this context, expression of HORVU1Hr1G008900 specifically within tissues derived from the embryo sac at “FG” stages of development indicates that it may be a good candidate for future analysis. One limitation in barley remains the lack of suitable annotation. For example, HORVU1Hr1G008900 is annotated as “Chromosome 3B scaffold cv. Chinese Spring”, i.e. it is a sequence used to mark a region of chromosome 3B within the wheat genotype Chinese Spring. As such, full utility of the transcript data presented here will require

support from new genomic scaffold releases, annotations and gene models. Equally, based on the data available it is not possible to assess the relationship between transcript abundance and protein level, making it difficult to establish a transcript cutoff that indicates whether or not an expressed gene product will induce a measurable effect. Although linear amplification was used to generate the RNA libraries for sequencing, and patterns of known marker genes look promising, novel low-abundance candidate genes will need to be tested using other means, such as q-PCR and *in situ* hybridization, in order to verify that the expression observed is not an artefact of amplification.

Conclusion

This study identified 82 HORVUs that fulfil strict criteria as differentially expressed genes, and underlie four QTL associated with variation in mature ovule traits. Of these genes, several promising candidates were highlighted based on their functional annotation in barley and other species. Future work may consider using additional criteria to investigate genes underlying QTL regions. This might include analysis of RNA sequence variation between the four genotypes, identification of ovule "tissue-enriched" genes that are not necessarily differentially expressed, and generation of co-expression networks to identify genes that may function together during pistil development.

References

Acosta-García G, Vielle-Calzada J-P (2004) A classical arabinogalactan protein is essential for the initiation of female gametogenesis in *Arabidopsis*. The Plant Cell 16 (10):2614-2628. doi:10.1105/tpc.104.024588

Aizat WM, Preuss JM, Johnson AAT, Tester MA, Schultz CJ (2011) Investigation of a His-rich arabinogalactan-protein for micronutrient biofortification of cereal grain. Physiologia Plantarum 143 (3):271-286. doi:doi:10.1111/j.1399-3054.2011.01499.x

Akagi H, Nakamura A, Yokozeki-Misono Y, Inagaki A, Takahashi H, Mori K, Fujimura T (2004) Positional cloning of the rice Rf-1 gene, a restorer of BT-type cytoplasmic male sterility that encodes a mitochondria-targeting PPR protein. Theoretical and Applied Genetics 108 (8):1449-1457

Bayer MM, Rapazote-Flores P, Ganal M, Hedley PE, Macaulay M, Plieske J, Ramsay L, Russell J, Shaw PD, Thomas W, Waugh R (2017) Development and evaluation of a barley 50k iSelect SNP array. Frontiers in Plant Science 8 (1792). doi:10.3389/fpls.2017.01792

Brant EJ, Budak H (2018) Plant small non-coding RNAs and their roles in biotic stresses. Frontiers in Plant Science 9:1038-1038. doi:10.3389/fpls.2018.01038

Brink RA, Cooper DC (1944) The antipodals in relation to abnormal endosperm behavior in Hordeum jubatum x Secale cereale hybrid seeds. Genetics 29 (4):391-406

Burton RA, Collins HM, Kibble NA, Smith JA, Shirley NJ, Jobling SA, Henderson M, Singh RR, Pettolino F, Wilson SM (2011) Over‐expression of specific *HvCslF* cellulose synthase‐like genes in transgenic barley increases the levels of cell wall (1, 3; 1, 4)‐β‐d‐glucans and alters their fine structure. Plant Biotechnology Journal 9 (2):117-135

Cantalapiedra CP, Boudiar R, Casas AM, Igartua E, Contreras-Moreira B (2015) BARLEYMAP: physical and genetic mapping of nucleotide sequences and annotation of surrounding loci in barley. Molecular Breeding 35 (1):13. doi:10.1007/s11032-015-0253-1

Chaban I, Lazareva E, Kononenko N, Polyakov VY (2011) Antipodal complex development in the embryo sac of wheat. Russian Journal of Developmental Biology 42 (2):79-91

Chettoor AM, Phillips AR, Coker CT, Dilkes B, Evans MMS (2016) Maternal gametophyte effects on seed development in maize. Genetics 204 (1):233-248. doi:10.1534/genetics.116.191833

Colmsee C, Beier S, Himmelbach A, Schmutzer T, Stein N, Scholz U, Mascher M (2015) BARLEX–the barley draft genome explorer. Molecular Plant 8 (6):964-966

Comadran J, Kilian B, Russell J, Ramsay L, Stein N, Ganal M, Shaw P, Bayer M, Thomas W, Marshall D, Hedley P, Tondelli A, Pecchioni N, Francia E, Korzun V, Walther A, Waugh R (2012) Natural variation in a homolog of Antirrhinum *CENTRORADIALIS* contributed to spring growth habit and environmental adaptation in cultivated barley. Nature Genetics 44:1388. doi:10.1038/ng.2447

https://www.nature.com/articles/ng.2447#supplementary-information

Cui R, Han J, Zhao S, Su K, Wu F, Du X, Xu Q, Chong K, Theißen G, Meng Z (2010) Functional conservation and diversification of class E floral homeotic genes in rice (*Oryza sativa*). The Plant Journal 61 (5):767-781. doi:10.1111/j.1365-313X.2009.04101.x

Diboll AG (1968) Fine structural development of the megagametophyte of *Zea mays* following fertilization. American Journal of Botany 55 (7):787-806

Dominguez F, Moreno J, Cejudo FJ (2001) The nucellus degenerates by a process of programmed cell death during the early stages of wheat grain development. Planta 213 (3):352-360

Dreni L, Pilatone A, Yun D, Erreni S, Pajoro A, Caporali E, Zhang D, Kater MM (2011) Functional analysis of all AGAMOUS subfamily members in rice reveals their roles in reproductive organ identity determination and meristem determinacy. The Plant Cell 23 (8):2850-2863. doi:10.1105/tpc.111.087007

Endress PK (2011) Angiosperm ovules: diversity, development, evolution. Annals of Botany 107 (9):1465-1489. doi:10.1093/aob/mcr120

Engell K (1988) Embryology of barley II: synergids and egg cell, zygote and embryo development. In: Sexual Reproduction in Higher Plants. Springer, pp 383-388

Engell K (1994) Embryology of barley. IV. Ultrastructure of the antipodal cells of *Hordeum vulgare* L. cv. Bomi before and after fertilization of the egg cell. Sexual Plant Reproduction 7 (6):333-346

Fahy B, Siddiqui H, David LC, Powers SJ, Borrill P, Uauy C, Smith AM (2018) Final grain weight is not limited by the activity of key starch-synthesising enzymes during grain filling in wheat. Journal of Experimental Botany 69 (22):5461-5475. doi:10.1093/jxb/ery314

Fan F, Li N, Chen Y, Liu X, Sun H, Wang J, He G, Zhu Y, Li S (2017) Development of elite BPH-resistant wide-spectrum restorer lines for three and two line hybrid rice. Frontiers in Plant Science 8:986

Filipowicz W, Pogačić V (2002) Biogenesis of small nucleolar ribonucleoproteins. Current Opinion in Cell Biology 14 (3):319-327. doi:https://doi.org/10.1016/S0955-0674(02)00334-4

Garcia M, Eckermann P, Haefele S, Satija S, Sznajder B, Timmins A, Baumann U, Wolters P, Mather DE, Fleury D (2019) Genome-wide association mapping of grain yield in a diverse collection of spring wheat (*Triticum aestivum* L.) evaluated in southern Australia. PLOS ONE 14 (2):e0211730. doi:10.1371/journal.pone.0211730

Hassan AS, Houston K, Lahnstein J, Shirley N, Schwerdt JG, Gidley MJ, Waugh R, Little A, Burton RA (2017) A Genome Wide Association Study of arabinoxylan content in 2-row spring barley grain. PLOS ONE 12 (8):e0182537

Houston K, Russell J, Schreiber M, Halpin C, Oakey H, Washington JM, Booth A, Shirley N, Burton RA, Fincher GB, Waugh R (2014) A genome wide association scan for (1,3;1,4)-β-glucan content in the grain of contemporary 2-row Spring and Winter barleys. BMC Genomics 15 (1):907. doi:10.1186/1471-2164-15-907

Itabashi E, Kazama T, Toriyama K (2009) Characterization of cytoplasmic male sterility of rice with Lead Rice cytoplasm in comparison with that with Chinsurah Boro II cytoplasm. Plant Cell Reports 28 (2):233-239. doi:10.1007/s00299-008-0625-7

Jack T (2001) Plant development going MADS. Plant Molecular Biology 46 (5):515-520. doi:10.1023/A:1010689126632

Juranić M, Tucker MR, Schultz CJ, Shirley NJ, Taylor JM, Spriggs A, Johnson SD, Bulone V, Koltunow AM (2018) Asexual female gametogenesis involves contact with a sexually-fated megaspore in apomictic *Hieracium*. Plant Physiology 177 (3):1027-1049. doi:10.1104/pp.18.00342

Kawahara Y, de la Bastide M, Hamilton JP, Kanamori H, McCombie WR, Ouyang S, Schwartz DC, Tanaka T, Wu J, Zhou S (2013) Improvement of the *Oryza sativa* Nipponbare reference genome using next generation sequence and optical map data. Rice 6 (1):4

Klein R, Klein P, Mullet J, Minx P, Rooney W, Schertz K (2005) Fertility restorer locus Rf1 of sorghum (*Sorghum bicolo*r L.) encodes a pentatricopeptide repeat protein not present in the colinear region of rice chromosome 12. Theoretical and Applied Genetics 111 (6):994-1012

Larsson E, Sundberg E, Franks RG (2013) Auxin and the *Arabidopsis thaliana* gynoecium. Journal of Experimental Botany 64 (9):2619-2627. doi:10.1093/jxb/ert099

Leszczuk A, Szczuka E, Zdunek A (2019) Arabinogalactan proteins: Distribution during the development of male and female gametophytes. Plant Physiology and Biochemistry 135:9-18. doi:https://doi.org/10.1016/j.plaphy.2018.11.023

Lin G, Chai J, Yuan S, Mai C, Cai L, Murphy RW, Zhou W, Luo J (2016) VennPainter: A tool for the comparison and identification of candidate genes based on Venn diagrams. PLOS ONE 11 (4):e0154315-e0154315. doi:10.1371/journal.pone.0154315

Linnestad C, Doan DNP, Brown RC, Lemmon BE, Meyer DJ, Jung R, Olsen O-A (1998) Nucellain, a barley homolog of the dicot vacuolar-processing protease, is localized in nucellar cell walls. Plant Physiology 118 (4):1169-1180. doi:10.1104/pp.118.4.1169

Liu Z, Dong F, Wang X, Wang T, Su R, Hong D, Yang G (2017) A pentatricopeptide repeat protein restores nap cytoplasmic male sterility in Brassica napus. Journal of Experimental Botany 68 (15):4115-4123. doi:10.1093/jxb/erx239

Lloyd FE (1899) The comparative embryology of the rubiaceae. Memoirs of the Torrey Botanical Club 8 (1):1-112

Lora J, Herrero M, Tucker MR, Hormaza JI (2017) The transition from somatic to germline identity shows conserved and specialized features during angiosperm evolution. New Phytologist 216 (2):495-509. doi:doi:10.1111/nph.14330

Maeda E, Miyake H (1996) Ultrastructure of antipodal cells of rice (*Oryza sativa*) after anthesis, as related to nutrient transport in embryo sac. Japanese Journal of Crop Science 65 (2):340-351

Maeda E, Miyake H (1997) Ultrastructure of antipodal cells of rice (oryza sativa) before anthesis with special reference to concentric configuration of endoplasmic reticula. Japanese Journal of Crop Science 66 (3):488-496. doi:10.1626/jcs.66.488

Magnard J-L, Lehouque G, Massonneau A, Frangne N, Heckel T, Gutierrez-Marcos JF, Perez P, Dumas C, Rogowsky PM (2003) *ZmEBE* genes show a novel, continuous expression pattern in the central cell before fertilization and in specific domains of the resulting endosperm after fertilization. Plant Molecular Biology 53 (6):821-836

Mascher M, Gundlach H, Himmelbach A, Beier S, Twardziok SO, Wicker T, Radchuk V, Dockter C, Hedley PE, Russell J, Bayer M, Ramsay L, Liu H, Haberer G, Zhang X-Q, Zhang Q, Barrero RA, Li L, Taudien S, Groth M, Felder M, Hastie A, Šimková H, Staňková H, Vrána J, Chan S, Muñoz-Amatriaín M, Ounit R, Wanamaker S, Bolser D, Colmsee C, Schmutzer T, Aliyeva-Schnorr L, Grasso S, Tanskanen J, Chailyan A, Sampath D, Heavens D, Clissold L, Cao S, Chapman B, Dai F, Han Y, Li H, Li X, Lin C, McCooke JK, Tan C, Wang P, Wang S, Yin S, Zhou G, Poland JA, Bellgard MI, Borisjuk L, Houben A, Doležel J, Ayling S, Lonardi S, Kersey P, Langridge P, Muehlbauer GJ, Clark MD, Caccamo M, Schulman AH, Mayer KFX, Platzer M, Close TJ, Scholz U, Hansson M, Zhang G, Braumann I, Spannagl M, Li C, Waugh R, Stein N (2017) A chromosome conformation capture ordered sequence of the barley genome. Nature 544:427. doi:10.1038/nature22043

https://www.nature.com/articles/nature22043#supplementary-information

Mizukami Y, Fischer RL (2000) Plant organ size control: AINTEGUMENTA regulates growth and cell numbers during organogenesis. Proceedings of the National Academy of Sciences 97 (2):942-947

Ohnishi T, Takanashi H, Mogi M, Takahashi H, Kikuchi S, Yano K, Okamoto T, Fujita M, Kurata N, Tsutsumi N (2011) Distinct gene expression profiles in egg and synergid cells of rice as revealed by cell type-specific microarrays. Plant Physiology 155 (2):881-891. doi:10.1104/pp.110.167502

Ohtani M, Demura T, Sugiyama M (2008) Differential requirement for the function of SRD2, an snRNA transcription activator, in various stages of plant development. Plant Molecular Biology 66 (3):303-314. doi:10.1007/s11103-007-9271-7

Ohto M-a, Fischer RL, Goldberg RB, Nakamura K, Harada JJ (2005) Control of seed mass by APETALA2. Proceedings of the National Academy of Sciences 102 (8):3123-3128

Ouyang S, Zhu W, Hamilton J, Lin H, Campbell M, Childs K, Thibaud-Nissen F, Malek RL, Lee Y, Zheng L (2006) The TIGR rice genome annotation resource: improvements and new features. Nucleic acids research 35 (suppl_1):D883-D887

Pagnussat GC, Alandete-Saez M, Bowman JL, Sundaresan V (2009) Auxin-dependent patterning and gamete specification in the *Arabidopsis* female gametophyte. Science 324 (5935):1684-1689. doi:10.1126/science.1167324

Panoli A, Martin MV, Alandete-Saez M, Simon M, Neff C, Swarup R, Bellido A, Yuan L, Pagnussat GC, Sundaresan V (2015) Auxin import and local auxin biosynthesis are required for mitotic divisions, cell expansion and cell specification during female gametophyte development in *Arabidopsis thaliana*

PLOS ONE 10 (5):e0126164-e0126164. doi:10.1371/journal.pone.0126164

Park K, Kim MY, Vickers M, Park J-S, Hyun Y, Okamoto T, Zilberman D, Fischer RL, Feng X, Choi Y, Scholten S (2016) DNA demethylation is initiated in the central cells of *Arabidopsis* and rice. Proceedings of the National Academy of Sciences:201619047. doi:10.1073/pnas.1619047114

Patton DA, Schetter AL, Franzmann LH, Nelson K, Ward ER, Meinke DW (1998) An embryo-defective mutant of arabidopsis disrupted in the final step of biotin synthesis. Plant Physiology 116 (3):935-946

Qi W, Yang Y, Feng X, Zhang M, Song R (2017) Mitochondrial function and maize kernel development requires Dek2, a pentatricopeptide repeat protein involved in *nad1* mRNA splicing. Genetics 205 (1):239-249. doi:10.1534/genetics.116.196105

Sato K, Flavell A, Russell J, Börner A, Valkoun J (2014) Genetic diversity and germplasm management: wild barley, landraces, breeding materials. In: Biotechnological Approaches to Barley Improvement. Springer, pp 21-36

Schmidt A, Schmid MW, Klostermeier UC, Qi W, Guthörl D, Sailer C, Waller M, Rosenstiel P, Grossniklaus U (2014) Apomictic and sexual germline development differ with respect to cell cycle, transcriptional, hormonal and epigenetic regulation. PLoS genetics 10 (7):e1004476-e1004476. doi:10.1371/journal.pgen.1004476

Scott MS, Ono M (2011) From snoRNA to miRNA: Dual function regulatory non-coding RNAs. Biochimie 93 (11):1987-1992. doi:10.1016/j.biochi.2011.05.026

Small ID, Peeters N (2000) The PPR motif–a TPR-related motif prevalent in plant organellar proteins. Trends in Biochemical Sciences 25 (2):45-47

Song X, Yuan L, Sundaresan V (2014) Antipodal cells persist through fertilization in the female gametophyte of Arabidopsis. Plant Reproduction 27 (4):197-203

Steffen JG, Kang I-H, Macfarlane J, Drews GN (2007) Identification of genes expressed in the Arabidopsis female gametophyte. The Plant Journal 51 (2):281-292. doi:doi:10.1111/j.1365-313X.2007.03137.x

Sun F, Jiang R, Zhang X, Zhang X, Yang Y-Z, Liu Y, Wang Y, Xiu Z, Tan B-C, Li X (2018) The mitochondrial pentatricopeptide repeat protein EMP12 is involved in the splicing of three *nad2* introns and seed development in maize. Journal of Experimental Botany 70 (3):963-972. doi:10.1093/jxb/ery432

Thiel J, Weier D, Sreenivasulu N, Strickert M, Weichert N, Melzer M, Czauderna T, Wobus U, Weber H, Weschke W (2008) Different hormonal regulation of cellular differentiation and function in nucellar projection and endosperm transfer cells: a microdissection-based transcriptome study of young barley grains. Plant Physiology 148 (3):1436-1452. doi:10.1104/pp.108.127001

Tran V, Weier D, Radchuk R, Thiel J, Radchuk V (2014) Caspase-like activities accompany programmed cell death events in developing barley grains. PLOS ONE 9 (10):e109426-e109426. doi:10.1371/journal.pone.0109426

Tucker MR, Okada T, Hu Y, Scholefield A, Taylor JM, Koltunow AMG (2012) Somatic small RNA pathways promote the mitotic events of megagametogenesis during female reproductive development in *Arabidopsis*. Development 139 (8):1399-1404. doi:10.1242/dev.075390

van Esse GW, Walla A, Finke A, Koornneef M, Pecinka A, von Korff M (2017) Six-Rowed Spike3 (VRS3) Is a Histone Demethylase That Controls Lateral Spikelet Development in Barley. Plant Physiology 174 (4):2397-2408. doi:10.1104/pp.17.00108

Waddington S, Cartwright P, Wall P (1983) A quantitative scale of spike initial and pistil development in barley and wheat. Annals of Botany 51 (1):119-130

Wang Z, Zou Y, Li X, Zhang Q, Chen L, Wu H, Su D, Chen Y, Guo J, Luo D (2006) Cytoplasmic male sterility of rice with boro II cytoplasm is caused by a cytotoxic peptide and is restored by two related PPR motif genes via distinct modes of mRNA silencing. The Plant Cell 18 (3):676-687

Wilkinson LG, Tucker MR (2017) An optimised clearing protocol for the quantitative assessment of sub-epidermal ovule tissues within whole cereal pistils. Plant Methods 13 (1):67

Willemse M, De Boer-de M (1981) Megasporogenesis and early megagametogenesis. Acta Societatis Botanicorum Poloniae 50 (1-2):111-120

Wu Y, Yang L, Cao A, Wang J (2015) Gene Expression Profiles in Rice Developing Ovules Provided Evidence for the Role of Sporophytic Tissue in Female Gametophyte Development. PLOS ONE 10 (10):e0141613. doi:10.1371/journal.pone.0141613

Wuest SE, Vijverberg K, Schmidt A, Weiss M, Gheyselinck J, Lohr M, Wellmer F, Rahnenführer J, von Mering C, Grossniklaus U (2010) Arabidopsis female gametophyte gene expression map reveals similarities between plant and animal gametes. Current Biology 20 (6):506-512. doi:https://doi.org/10.1016/j.cub.2010.01.051

Xing S, Zachgo S (2008) ROXY1 and ROXY2, two Arabidopsis glutaredoxin genes, are required for anther development. The Plant Journal 53 (5):790-801. doi:doi:10.1111/j.1365-313X.2007.03375.x

Yang W-C, Ye D, Xu J, Sundaresan V (1999) The *SPOROCYTELESS* gene of Arabidopsis is required for initiation of sporogenesis and encodes a novel nuclear protein. Genes & Development 13 (16):2108-2117

Yoshida H, Nagato Y (2011) Flower development in rice. Journal of Experimental Botany 62 (14):4719-4730. doi:10.1093/jxb/err272

Yu H-J, Hogan P, Sundaresan V (2005) Analysis of the female gametophyte transcriptome of arabidopsis by comparative expression profiling. Plant Physiology 139 (4):1853-1869. doi:10.1104/pp.105.067314

Zhao L, Cai H, Su Z, Wang L, Huang X, Zhang M, Chen P, Dai X, Zhao H, Palanivelu R (2018) KLU suppresses megasporocyte cell fate through SWR1-mediated activation of *WRKY28* expression in Arabidopsis. Proceedings of the National Academy of Sciences 115 (3):E526-E535

Zhao L, He J, Cai H, Lin H, Li Y, Liu R, Yang Z, Qin Y (2014) Comparative expression profiling reveals gene functions in female meiosis and gametophyte development in Arabidopsis. The Plant Journal 80 (4):615-628. doi:doi:10.1111/tpj.12657

Supplementary Data

Table 6-S1: Data for identification of temporally differentially expressed genes (DEGs) within four quantitative trait loci (QTL) using an RNA-sequencing data set from whole pistils collected at five stages of ovule development (Stages 3-7) in four barley genotypes: Forum, Gant, Salka and Wren. Temporal DEGs (T) were determined by comparison of samples at sequential developmental stages within individual genotypes. Genotypic DEGs (G) were determined by comparison of samples at equivalent developmental stages from the four genotypes. Genes were considered to be differentially expressed on the basis of greater than ± 2 $\log_2$ fold change and $p < 0.05$. Expression data is presented in transcripts per million (TPM), barley gene identifiers are given as HORVUs.

			Forum								Gant								Salka								Wren							
QTL	**DEG**	**Horvul**	3v4	p	4v5	p	5v6	p	6v7	p	3v4	p	4v5	p	5v6	p	6v7	p	3v4	p	4v5	p	5v6	p	6v7	p	3v4	p	4v5	p	5v6	p	6v7	p
QTL01	T&G	HORVU1Hr1G011270	1.8	nd	-1.0	0.293	0.0	1.000	0.7	0.543	-1.3	0.027	2.0	0.022	0.0	1.000	-1.1	0.486	1.0	nd	-1.8	0.238	2.8	0.198	0.0	1.000	0.0	1.000	_	nd	_	nd	_	nd
QTL01	T&G	HORVU1Hr1G012660	_	nd	-4.3	0.199	-2.4	0.109	-0.9	0.100	_	_	_	_	_	0.364	0.3	0.831	2.0	nd	-0.9	0.720	-3.2	0.015	1.9	0.005	3.5	0.461	-3.0	nd	1.4	nd	_	nd
QTL03	T&G	HORVU2Hr1G085270	3.6	nd	3.8	0.319	0.0	1.000	_	0.423	1.9	0.353	0.3	0.729	0.5	0.516	0.7	0.082	-2.1	nd	1.9	0.432	-1.4	0.049	2.9	0.011	-2.9	0.448	3.6	nd	0.1	nd	1.4	nd
QTL03	T&G	HORVU2Hr1G084970	1.1	nd	-0.6	0.051	0.2	0.733	0.4	0.629	-0.2	0.860	-1.0	0.296	1.5	0.161	0.0	1.000	1.0	nd	-1.1	0.245	0.3	0.642	2.3	0.014	1.8	0.090	0.2	nd	-1.5	nd	1.5	nd
QTL03	T&G	HORVU2Hr1G085050	-3.5	nd	-2.7	0.033	-0.1	0.785	0.1	0.925	_	_	_	0.027	-1.3	0.533	1.3	0.560	0.0	nd	-6.6	0.423	-1.6	0.178	1.3	0.257	_	0.423	-2.2	nd	2.4	nd	-1.2	nd
QTL04	T&G	HORVU4Hr1G052450	0.4	nd	-0.2	0.423	-0.3	0.633	-1.1	0.192	2.2	0.160	2.3	0.042	-0.7	0.609	-1.4	0.179	0.7	nd	-0.2	0.423	-0.9	0.115	-0.1	0.890	-0.8	0.232	1.2	nd	1.6	nd	-0.6	nd
QTL04	T&G	HORVU4Hr1G040520	_	nd	-2.9	0.054	-0.1	0.872	-0.3	0.786	-0.8	0.333	-1.5	0.054	-1.1	0.537	2.8	0.351	-1.8	nd	-5.4	0.427	-0.4	0.757	2.2	0.015	-2.8	0.482	-1.9	nd	2.6	nd	_	nd
QTL04	T&G	HORVU4Hr1G054780	-0.3	nd	0.0	1.000	-0.4	0.698	0.8	0.477	0.8	0.296	-1.5	0.260	0.6	0.457	0.4	0.553	-0.5	nd	-0.7	0.403	0.1	0.918	-0.2	0.846	-2.2	0.045	-1.2	nd	1.1	nd	0.6	nd
QTL04	T&G	HORVU4Hr1G055110	-0.6	nd	-0.7	0.293	0.3	0.698	1.0	0.423	-1.2	0.038	2.2	0.020	-1.3	0.423	-1.0	0.238	-1.0	nd	-1.2	0.038	2.2	0.089	-0.6	0.698	2.0	0.543	-1.0	nd	-1.0	nd	-2.6	nd
QTL04	T&G	HORVU4Hr1G021590	0.0	nd	-0.6	0.423	1.0	0.423	0.6	0.771	-2.5	0.012	0.9	0.349	_	0.272	_	0.423	1.0	nd	0.0	1.000	-1.0	0.423	_	_	0.3	0.860	0.0	nd	0.4	nd	_	nd
QTL04	T	HORVU4Hr1G035100	0.8	nd	-0.8	0.441	0.8	0.402	0.3	0.775	-0.9	0.174	0.4	0.341	0.3	0.598	0.1	0.818	-0.8	nd	0.4	0.751	1.9	0.189	-1.4	0.233	2.6	0.019	-1.1	nd	-0.6	nd	-0.7	nd
QTL04	T	HORVU4Hr1G021320	0.4	nd	1.2	0.080	1.0	0.102	-1.3	0.160	-0.2	0.610	1.1	0.136	-0.3	0.620	-3.0	0.006	-0.3	nd	1.0	0.227	0.1	0.911	-1.0	0.522	-1.2	0.096	0.0	nd	1.1	nd	-0.8	nd
QTL04	T	HORVU4Hr1G035540	-0.3	nd	-4.2	0.391	3.0	0.426	2.0	0.480	-1.1	0.467	1.3	0.498	-1.1	0.530	0.0	1.000	-2.2	nd	0.5	0.788	2.7	0.423	-4.4	0.403	3.8	0.028	-1.0	nd	-3.6	nd	-0.8	nd
QTL04	T	HORVU4Hr1G026150	-1.4	nd	-1.2	0.233	-1.7	0.187	-0.3	0.646	-0.5	0.423	-1.2	0.057	-2.5	0.009	-1.0	0.315	-0.4	nd	-2.7	0.368	-2.6	0.026	-0.1	0.854	-2.2	0.392	-1.1	nd	0.3	nd	-1.5	nd
QTL04	T	HORVU4Hr1G042040	1.0	nd	_	_	_	0.423	-0.6	0.698	-1.6	0.423	0.6	0.698	-0.3	0.698	1.3	0.095	_	nd	0.7	0.592	_	0.095	_	0.423	3.6	0.008	_	nd	_	nd	_	nd
QTL04	T	HORVU4Hr1G054770	0.6	nd	2.1	0.048	0.5	0.459	-0.1	0.655	0.6	0.597	-0.3	0.651	1.4	0.016	0.9	0.164	0.3	nd	0.7	0.345	0.0	0.988	1.6	0.002	0.2	0.716	0.4	nd	2.2	nd	1.1	nd
QTL04	T	HORVU4Hr1G054470	0.5	nd	0.3	0.648	1.3	0.255	-0.2	0.719	-0.6	0.521	-0.2	0.741	2.0	0.014	-0.7	0.258	0.0	nd	0.7	0.287	-1.0	0.110	1.1	0.124	0.3	0.396	-0.8	nd	1.9	nd	1.1	nd
QTL04	T	HORVU4Hr1G052660	2.2	nd	-0.6	0.192	0.4	0.642	-0.7	0.609	-2.2	0.039	-0.8	0.491	-0.3	0.843	-0.1	0.905	0.0	nd	-1.1	0.006	0.3	0.515	-1.3	0.045	0.0	_	-1.3	nd	0.3	nd	_	nd
QTL04	T	HORVU4Hr1G030730	1.3	nd	-0.5	0.184	0.0	1.000	-0.4	0.676	0.2	0.764	-0.7	0.228	0.4	0.767	-0.4	0.761	0.4	nd	-0.4	0.642	0.1	0.924	-0.1	0.860	-2.4	0.028	0.3	nd	0.8	nd	1.9	nd
QTL04	T	HORVU4Hr1G040350	0.0	nd	-0.6	0.238	0.9	0.145	0.4	_	-0.8	0.145	0.2	0.423	0.2	0.863	-0.1	0.932	0.7	nd	-0.1	0.934	2.3	0.232	-2.1	0.019	0.3	0.844	0.0	nd	-0.9	nd	-1.0	nd
QTL01	G	HORVU1Hr1G011240	-0.3	nd	-0.3	0.423	0.3	0.771	2.3	0.333	1.0	0.184	-1.0	0.592	1.4	0.497	-1.0	0.095	_	nd	0.6	0.423	0.0	_	1.0	0.423	0.7	0.592	0.6	nd	-0.6	nd	_	nd
QTL01	G	HORVU1Hr1G010240	-0.1	nd	0.4	0.477	0.0	1.000	-0.5	0.039	0.7	0.246	-0.1	0.757	0.1	0.686	-0.5	0.294	_	nd	_	_	_	_	_	0.423	_	_	_	nd	_	nd	_	nd
QTL01	G	HORVU1Hr1G011310	0.5	nd	-0.5	0.358	0.2	0.382	0.0	1.000	-0.2	0.303	0.3	0.030	0.1	0.493	0.3	0.457	-0.7	nd	0.6	0.511	1.4	0.172	-1.0	0.290	1.8	0.109	-0.8	nd	-0.4	nd	0.9	nd
QTL01	G	HORVU1Hr1G010940	0.6	nd	0.2	0.527	0.1	0.522	0.0	0.968	0.2	0.463	-0.1	0.513	0.1	0.687	0.1	0.911	-0.2	nd	0.2	0.310	-0.3	0.214	0.6	0.202	-0.5	0.371	0.2	nd	1.9	nd	-1.0	nd
QTL01	G	HORVU1Hr1G008900	0.0	nd	0.0	0.625	0.1	0.790	-0.2	0.292	_	0.423	_	0.423	_	_	_	_	-0.2	nd	-0.6	0.232	0.0	0.885	0.2	0.760	-0.8	0.004	-0.1	nd	1.2	nd	-0.4	nd
QTL01	G	HORVU1Hr1G010010	-0.2	nd	-1.3	0.363	0.5	0.610	0.0	0.889	-0.1	0.906	0.4	0.424	-0.7	0.002	-0.2	0.636	0.5	nd	-1.4	0.306	-0.1	0.918	0.8	0.200	1.3	0.296	-0.3	nd	-1.8	nd	-1.4	nd
QTL01	G	HORVU1Hr1G010000	-0.5	nd	-1.0	0.375	0.2	0.787	0.2	0.798	-1.2	0.075	0.0	1.000	-0.4	0.729	0.5	0.693	-0.6	nd	-0.5	0.788	2.0	0.466	-1.4	0.412	1.8	0.143	-1.5	nd	-2.0	nd	-1.0	nd
QTL01	G	HORVU1Hr1G009760	0.0	nd	-1.3	0.095	2.3	0.106	-1.0	0.423	-2.0	0.312	0.7	0.609	2.3	0.333	-1.6	0.293	-1.2	nd	0.2	0.698	3.0	0.089	0.0	1.000	0.5	0.312	-0.2	nd	-0.8	nd	1.8	nd
QTL01	G	HORVU1Hr1G010130	-1.3	nd	-1.0	0.203	0.5	0.072	0.4	0.572	-0.4	0.493	-1.1	0.053	-0.6	0.216	0.5	0.270	-1.2	nd	-1.7	0.194	-1.0	0.120	1.5	0.062	-2.2	0.328	-0.9	nd	0.7	nd	1.0	nd
QTL02	G	HORVU2Hr1G027550	0.4	nd	-0.3	0.435	0.5	0.293	-0.5	0.283	-0.4	0.097	0.2	0.146	0.4	0.050	-0.2	0.417	-0.4	nd	0.2	0.599	1.1	0.070	-0.8	0.444	0.7	0.041	-0.2	nd	-0.9	nd	-0.9	nd
QTL02	G	HORVU2Hr1G027230	0.6	nd	-0.2	0.764	0.4	0.333	-0.5	0.051	0.4	0.014	0.4	0.207	0.4	0.380	0.2	0.553	-0.2	nd	0.2	0.558	-0.2	0.296	-0.2	0.145	0.4	0.069	0.3	nd	-0.3	nd	-0.3	nd
QTL02	G	HORVU2Hr1G027680	-3.6	nd	0.6	0.659	-1.6	0.394	-0.8	0.370	2.2	0.306	0.0	1.000	-1.6	0.051	-1.6	0.030	1.7	nd	-4.6	0.428	1.2	0.618	-1.5	0.526	-2.3	0.434	-2.2	nd	3.2	nd	-1.3	nd
QTL02	G	HORVU2Hr1G027360	1.1	nd	-1.2	0.331	0.4	0.650	0.2	0.716	-0.3	0.327	0.6	0.161	0.5	0.229	-0.3	0.618	-1.6	nd	0.3	0.800	1.9	0.417	-2.2	0.313	1.9	0.094	0.2	nd	-2.7	nd	-0.3	nd
QTL02	G	HORVU2Hr1G027020	-0.2	nd	-0.5	0.553	-0.1	0.961	0.6	0.727	-0.5	0.321	-0.3	0.563	-0.1	0.905	0.2	0.274	1.0	nd	-2.0	0.051	-0.3	0.592	2.3	0.157	-0.6	0.513	3.1	nd	-1.6	nd	-3.2	nd
QTL02	G	HORVU2Hr1G026610	1.0	nd	-1.0	0.698	0.0	1.000	-0.6	0.423	0.3	0.452	-0.3	0.427	-0.2	0.619	0.0	0.932	-0.6	nd	0.0	1.000	0.6	0.423	-0.6	0.423	0.0	1.000	_	nd	_	nd	_	nd
QTL02	G	HORVU2Hr1G027420	_	nd	_	0.359	-0.5	0.694	0.0	_	0.2	0.771	2.8	_	-2.2	0.296	-1.1	0.434	_	nd	0.0	1.000	-2.0	0.312	-0.7	0.349	-1.0	0.698	0.0	nd	-2.9	nd	_	nd
QTL02	G	HORVU2Hr1G027410	0.4	nd	-1.1	0.361	1.0	0.443	0.3	0.746	-0.7	0.035	0.4	0.207	0.4	0.507	-0.5	0.701	-1.5	nd	0.5	0.721	2.5	0.316	-1.9	0.372	2.8	0.130	-1.3	nd	-2.4	nd	0.7	nd
QTL03	G	HORVU2Hr1G085400	_	nd	_	_	1.0	0.423	0.0	1.000	-0.5	0.095	0.7	0.106	-0.4	0.293	-0.2	0.698	_	nd	_	0.423	_	_	_	_	_	_	_	nd	_	nd	_	nd
QTL03	G	HORVU2Hr1G084400	-0.8	nd	1.0	0.295	-0.4	0.633	-0.8	0.057	1.7	0.137	-0.6	0.633	-0.9	0.257	-0.4	0.598	0.9	nd	-0.1	0.918	-1.4	0.035	1.0	0.198	-2.5	0.095	-0.5	nd	3.3	nd	_	nd
QTL03	G	HORVU2Hr1G084580	-0.2	nd	-2.1	0.443	2.3	0.424	0.6	0.553	-0.6	0.493	1.2	0.238	-1.7	0.214	0.1	0.860	_	nd	-1.5	0.277	3.8	0.166	-1.6	0.293	0.6	0.423	1.0	nd	-2.7	nd	-1.9	nd
QTL03	G	HORVU2Hr1G085020	-0.9	nd	-1.6	0.127	-1.1	0.308	0.1	0.935	-0.5	0.534	-0.1	0.846	0.5	0.426	1.4	0.314	1.2	nd	-3.8	0.421	-1.6	0.162	0.6	0.631	-2.1	0.340	-1.8	nd	2.8	nd	-1.2	nd
QTL03	G	HORVU2Hr1G085000	0.1	nd	0.3	0.553	-1.2	0.119	-1.0	0.045	-0.3	0.404	0.3	0.085	-0.7	0.500	-1.6	0.055	0.1	nd	-0.5	0.525	-0.3	0.620	-1.6	0.054	1.4	0.172	-0.1	nd	-1.1	nd	-1.1	nd
QTL04	G	HORVU4Hr1G034730	-0.6	nd	-0.3	0.576	-0.2	0.702	0.9	0.003	-0.6	0.564	-0.4	0.684	0.4	0.574	0.0	0.885	-0.4	nd	0.9	0.568	-0.9	0.432	0.4	0.642	-0.5	0.497	-0.2	nd	1.5	nd	-2.0	nd
QTL04	G	HORVU4Hr1G021390	0.0	nd	-1.6	0.184	0.6	0.423	-0.6	0.423	-1.0	0.423	1.0	0.553	-0.6	0.698	0.0	1.000	_	nd	-0.3	0.698	1.3	0.095	-1.8	0.423	-2.0	0.312	-0.6	nd	-0.6	nd	1.2	nd
QTL04	G	HORVU4Hr1G054200	-0.3	nd	-1.2	0.237	0.8	0.375	0.7	0.404	1.5	0.085	0.8	0.360	0.1	0.950	0.3	0.866	1.6	nd	-1.7	0.303	-0.6	0.430	0.0	1.000	-0.3	0.811	-0.7	nd	2.1	nd	-2.7	nd
QTL04	G	HORVU4Hr1G022780	0.9	nd	-0.1	0.781	0.4	0.434	-0.2	0.086	1.0	0.047	0.4	0.500	0.7	0.482	-0.5	0.614	-0.2	nd	0.9	0.170	-0.2	0.260	0.1	0.794	-0.4	0.014	0.2	nd	0.7	nd	-0.9	nd
QTL04	G	HORVU4Hr1G040730	0.3	nd	-0.6	0.204	0.3	0.576	-0.1	0.882	-0.1	0.827	-0.3	0.283	1.3	0.015	-0.3	0.400	-0.8	nd	0.5	0.711	1.5	0.518	-0.3	0.423	1.5	0.122	1.8	nd	-3.8	nd	0.3	nd
QTL04	G	HORVU4Hr1G044040	-1.6	nd	-0.9	0.433	0.3	0.747	-0.2	0.702	-1.4	0.204	-2.1	0.072	-1.3	0.129	-0.2	0.679	-1.1	nd	-2.7	0.058	0.6	0.248	-0.6	0.124	-2.2	0.378	-1.8	nd	0.1	nd	0.2	nd
QTL04	G	HORVU4Hr1G054970	0.3	nd	-0.5	0.299	-0.4	0.058	-0.1	0.880	0.2	0.589	0.0	0.930	-0.5	0.503	0.5	0.531	0.0	nd	0.0	0.946	-1.5	0.068	1.5	0.097	-1.0	0.210	-0.3	nd	2.3	nd	-0.1	nd
QTL04	G	HORVU4Hr1G039160	0.0	nd	0.6	0.184	-1.4	0.294	-1.1	0.126	0.4	0.293	0.8	0.296	-0.4	0.789	-0.9	0.527	0.9	nd	-0.6	0.465	0.2	0.836	1.6	0.198	-0.9	0.451	2.5	nd	-1.0	nd	-2.1	nd
QTL04	G	HORVU4Hr1G043630	-0.8	nd	0.1	0.890	-0.6	0.248	0.6	0.256	-1.0	0.155	-0.2	0.776	-0.6	0.639	-0.6	0.647	-3.5	nd	0.1	0.959	1.9	0.030	-0.9	0.563	2.5	0.277	-1.8	nd	-1.2	nd	0.0	nd
QTL04	G	HORVU4Hr1G029240	0.4	nd	-1.7	0.020	1.0	0.038	2.3	0.106	_	_	_	_	_	_	_	_	_	nd	_	0.423	_	0.423	_	_	_	_	_	nd	_	nd	_	nd
QTL04	G	HORVU4Hr1G027180	-1.4	nd	-1.2	0.368	-0.9	0.367	-0.1	0.819	-0.1	0.918	-1.3	0.026	-0.4	0.176	-0.7	0.104	-0.1	nd	-3.1	0.313	-1.7	0.125	0.2	0.746	-3.2	0.372	-1.0	nd	2.0	nd	-1.4	nd
QTL04	G	HORVU4Hr1G037050	_	nd	_	_	0.0	_	1.0	0.423	-1.0	0.423	1.0	0.423	_	0.423	_	_	0.1	nd	-0.3	0.584	0.1	0.846	0.0	0.698	-1.3	0.247	0.3	nd	0.4	nd	2.0	nd
QTL04	G	HORVU4Hr1G052290	0.5	nd	-0.8	0.181	0.3	0.689	-1.0	0.128	-0.7	0.318	1.0	0.164	-0.4	0.678	0.3	0.704	-0.7	nd	-0.4	0.630	0.9	0.332	-0.1	0.914	0.2	0.808	-1.3	nd	0.3	nd	-0.6	nd
QTL04	G	HORVU4Hr1G030980	0.0	nd	-0.7	0.444	0.2	0.654	0.7	0.096	0.4	0.439	0.3	0.400	-0.5	0.283	-0.1	0.295	-0.7	nd	0.5	0.629	3.6	0.091	-2.2	0.300	-0.1	0.966	1.8	nd	-2.0	nd	2.5	nd
QTL04	G	HORVU4Hr1G052260	0.2	nd	-0.9	0.166	0.3	0.440	-0.3	0.493	-0.5	0.592	-0.8	0.423	-1.8	0.088	-0.3	0.826	-1.0	nd	_	0.423	_	0.423	-0.3	0.860	0.0	1.000	_	nd	_	nd	-2.6	nd
QTL04	G	HORVU4Hr1G031060	0.0	nd	-0.5	0.234	0.1	0.746	0.2	0.349	-0.2	0.448	0.1	0.538	0.2	0.463	-0.2	0.511	-0.3	nd	0.2	0.409	0.1	0.499	-0.4	0.326	0.4	0.406	0.7	nd	-1.3	nd	-0.5	nd
QTL04	G	HORVU4Hr1G035670	-0.3	nd	-0.5	0.498	0.1	0.913	0.0	0.929	-1.0	0.262	0.2	0.686	-0.3	0.349	-0.1	0.941	-0.9	nd	0.0	1.000	1.8	0.222	-2.5	0.256	2.2	0.304	0.8	nd	-2.1	nd	-1.8	nd
QTL04	G	HORVU4Hr1G046970	-1.6	nd	-0.8	0.383	0.5	0.632	0.7	0.515	0.0	1.000	-0.1	0.827	0.1	0.846	-0.6	0.740	-1.5	nd	-0.2	0.831	2.1	0.276	-1.6	0.362	1.3	0.463	0.5	nd	-2.4	nd	-1.1	nd
QTL04	G	HORVU4Hr1G051590	-0.6	nd	-1.2	0.333	0.5	0.592	-0.8	0.515	1.0	0.423	_	0.423	_	_	0.0	_	1.0	nd	-2.0	0.312	0.4	0.698	0.6	0.698	0.4	0.667	0.6	nd	1.0	nd	_	nd
QTL04	G	HORVU4Hr1G040510	-2.7	nd	-2.3	0.059	-0.3	0.122	-0.9	0.378	_	0.272	-1.6	0.443	-1.9	0.474	1.5	0.513	_	nd	_	0.417	-1.7	0.165	1.9	0.072	_	0.423	-1.0	nd	1.2	nd	1.1	nd
QTL04	G	HORVU4Hr1G023980	0.5	nd	-0.2	0.860	0.0	1.000	1.4	0.497	0.6	0.423	-2.0	0.095	-0.2	0.698	-0.9	0.127	0.0	nd	-0.3	0.771	-0.3	0.808	-2.0	0.465	_	0.423	_	nd	_	nd	_	nd
QTL04	G	HORVU4Hr1G025470	-1.1	nd	0.1	0.952	0.0	0.971	0.8	0.398	-0.9	0.047	0.0	0.950	-0.7	0.482	-0.3	0.590	-0.6	nd	-0.4	0.728	0.4	0.710	-2.0	0.247	1.4	0.006	-0.6	nd	-1.7	nd	-2.0	nd
QTL04	G	HORVU4Hr1G035330	-0.6	nd	-0.4	0.423	-0.6	_	1.0	0.095	0.0	1.000	-1.7	0.036	-0.2	0.349	0.7	0.028	_	nd	_	0.423	_	_	_	_	_	_	_	nd	_	nd	_	nd
QTL04	G	HORVU4Hr1G041600	0.2	nd	-1.3	0.276	0.5	0.545	0.0	0.936	-0.8	0.045	0.2	0.333	0.4	0.148	-0.2	0.626	-0.5	nd	-0.2	0.805	2.6	0.205	-2.3	0.316	1.1	0.293	1.2	nd	-3.0	nd	-0.5	nd
QTL04	G	HORVU4Hr1G046350	0.7	nd	2.1	0.184	1.6	0.293	-3.9	0.417	2.2	0.435	1.4	0.255	-1.1	0.657	-1.0	0.432	0.5	nd	-1.2	0.609	0.7	0.746	0.9	0.584	0.8	0.416	0.3	nd	0.3	nd	1.6	nd
QTL04	G	HORVU4Hr1G034670	-1.0	nd	1.3	0.232	-0.7	0.543	0.2	0.831	0.4	0.698	-0.7	0.592	0.5	0.671	1.2	0.106	0.2	nd	-0.5	0.493	0.0	1.000	-0.4	0.095	-0.1	0.423	0.5	nd	-1.7	nd	1.1	nd
QTL04	G	HORVU4Hr1G049550	0.5	nd	1.6	0.036	1.3	0.214	-0.9	0.349	-0.5	0.294	1.7	0.015	-0.3	0.493	1.0	0.057	-0.1	nd	1.7	0.145	1.8	0.448	-1.0	0.192	2.2	0.066	1.7	nd	0.1	nd	0.5	nd
QTL04	G	HORVU4Hr1G050560	-1.0	nd	1.6	0.106	-1.5	0.192	2.5	0.130	0.3	0.808	0.3	0.782	-0.7	0.155	-0.2	0.733	_	nd	_	_	_	_	_	0.423	1.0	0.192	1.1	nd	1.6	nd	-2.0	nd
QTL04	G	HORVU4Hr1G055560	0.1	nd	0.1	0.360	0.1	0.333	0.2	0.601	-0.4	0.698	-0.8	0.312	1.2	0.106	_	0.095	0.2	nd	0.1	0.720	-0.1	0.697	0.7	0.128	-1.0	0.184	0.0	nd	2.0	nd	_	nd
QTL04	G	HORVU4Hr1G030780	0.7	nd	-0.2	0.658	0.1	0.746	0.1	0.865	-0.9	0.190	1.3	0.048	-0.8	0.121	0.8	0.014	-0.6	nd	0.4	0.684	3.0	0.192	-3.0	0.307	1.4	0.360	0.8	nd	-1.2	nd	_	nd
QTL04	G	HORVU4Hr1G027940	-0.2	nd	-0.5	0.684	0.5	0.573	-0.2	0.863	-0.9	0.124	-0.2	0.598	-0.2	0.593	0.1	0.779	-1.2	nd	-0.1	0.912	2.8	0.306	-2.3	0.319	2.9	0.102	-0.3	nd	-2.7	nd	-0.5	nd
QTL04	G	HORVU4Hr1G024480	-0.3	nd	0.7	0.293	0.0	1.000	-1.2	0.106	1.0	0.312	0.6	0.423	-0.6	0.423	-0.7	0.293	-1.0	nd	1.0	0.553	-1.6	0.184	0.3	0.771	-1.6	0.293	-1.4	nd	3.0	nd	_	nd
QTL04	G	HORVU4Hr1G046000	1.7	nd	-2.1	0.461	-0.4	0.752	0.1	0.698	0.1	0.808	0.2	0.684	-0.3	0.493	-0.2	0.633	_	nd	_	_	_	_	_	0.423	1.4	0.349	0.6	nd	-3.3	nd	-1.8	nd
QTL04	G	HORVU4Hr1G034030	0.6	nd	-1.6	0.320	0.5	0.594	0.2	0.385	_	0.423	_	0.095	0.3	0.808	0.3	0.771	-1.2	nd	0.4	0.681	1.3	0.245	-1.4	0.244	2.8	0.198	-2.0	nd	-0.3	nd	-1.3	nd
QTL04	G	HORVU4Hr1G054850	0.7	nd	-0.2	0.658	0.0	0.945	-0.9	0.324	0.0	0.982	1.2	0.363	-0.5	0.637	-0.6	0.400	0.4	nd	-0.2	0.783	0.3	0.371	0.2	0.416	-1.8	0.015	0.0	nd	0.8	nd	1.3	nd
QTL04	G	HORVU4Hr1G037240	0.7	nd	-0.9	0.391	0.7	0.456	-0.1	0.633	-0.6	0.221	-0.1	0.804	0.1	0.746	0.6	0.258	-1.1	nd	0.2	0.831	1.8	0.251	-1.2	0.095	1.8	0.192	-0.7	nd	-2.4	nd	1.4	nd
QTL04	G	HORVU4Hr1G025580	-0.8	nd	-0.2	0.872	0.1	0.934	1.0	0.458	-0.8	0.063	-0.2	0.423	-0.9	0.203	-0.1	0.914	-0.4	nd	-0.3	0.679	0.7	0.423	-2.1	0.194	1.9	0.012	-0.4	nd	-1.5	nd	-3.5	nd
QTL04	G	HORVU4Hr1G048540	-0.2	nd	-1.3	0.320	0.9	0.375	0.0	1.000	-0.7	0.168	1.0	0.333	-0.8	0.443	0.5	0.184	-2.1	nd	1.3	0.451	1.3	0.423	-2.3	0.423	0.8	0.095	-0.6	nd	-3.0	nd	0.6	nd
QTL04	G	HORVU4Hr1G030420	-0.6	nd	-0.1	0.870	0.4	0.609	0.2	0.423	0.1	0.698	0.6	0.293	-1.5	0.869	0.8	0.533	-0.7	nd	-0.5	0.293	0.9	0.130	-0.5	0.293	2.3	0.057	-2.3	nd	-0.6	nd	-1.0	nd
QTL04	G	HORVU4Hr1G028720	0.6	nd	0.0	0.928	-0.3	0.490	-0.2	0.586	0.3	0.109	0.4	0.155	0.0	0.952	0.2	0.688	-0.1	nd	0.4	0.430	-1.7	0.021	1.8	0.028	-0.3	0.557	-0.2	nd	1.6	nd	0.8	nd

Table 6-S2: Data for identification of genotypically differentially expressed genes within four quantitative trait loci (QTL) using an RNA-sequencing data set from whole pistils collected at five stages of ovule development (Stages 3-7) in four barley genotypes: Forum, Gant, Salka and Wren. Genotypic DEGs (G) were determined by comparison of samples at equivalent developmental stages from the four genotypes. Temporal DEGs (T) were determined by comparison of samples at sequential developmental stages within individual genotypes. Genes were considered to be differentially expressed on the basis of greater than ±2 $\log_2$ fold change and $p < 0.05$. Expression data is presented in transcripts per million (TPM), barley gene identifiers are given as HORVUs.

			Forum vs Gant										Forum vs Salka										Forum vs Wren										Gant vs Salka										Gant vs Wren										Salka vs Wren									
QTL	**DEG**	**Horvul**	3v3	p	4v4	p	5v5	p	6v6	p	7v7	p	3v3	p	4v4	p	5v5	p	6v6	p	7v7	p	3v3	p	4v4	p	5v5	p	6v6	p	7v7	p	3v3	p	4v4	p	5v5	p	6v6	p	7v7	p	3v3	p	4v4	p	5v5	p	6v6	p	7v7	p	3v3	p	4v4	p	5v5	p	6v6	p	7v7	p
QTL01	T&G	HORVU1Hr1G011270	0.8	nd	-2.3	0.030	0.7	0.312	0.7	0.543	-1.1	0.486	1.8	nd	1.0	0.423	0.2	0.808	3.0	0.232	2.3	0.106	2.8	nd	1.0	0.553	_	_	1.0	0.465	_	_	1.0	nd	3.3	0.012	-0.5	0.592	2.3	0.106	3.5	0.293	2.0	_	3.3	0.024	_	nd	0.3	0.698	_	nd	1.0	nd	0.0	1.000	_	_	-2.0	0.312	_	nd
QTL01	T&G	HORVU1Hr1G012660	_	nd	_	0.423	_	0.184	2.9	0.101	4.2	0.001	_	nd	-3.0	0.477	0.4	0.808	-0.3	0.438	2.4	0.002	_	nd	0.0	1.000	1.3	_	5.2	0.073	_	_	_	nd	_	0.423	_	0.423	-3.3	0.010	-1.8	0.057	_	0.423	_	0.423	_	nd	2.2	0.468	_	nd	1.5	nd	3.0	0.477	0.9	_	5.5	0.001	_	nd
QTL03	T&G	HORVU2Hr1G085270	-2.2	nd	-3.9	0.164	-7.3	0.124	-6.8	0.009	_	0.007	3.3	nd	-2.4	0.397	-4.2	0.095	-5.7	0.008	_	0.020	1.9	nd	-4.6	0.411	-4.7	_	-4.6	0.040	_	_	5.5	nd	1.5	0.332	3.0	0.152	1.1	0.038	3.3	0.009	4.2	0.257	-0.7	0.727	2.6	nd	2.2	0.018	2.9	nd	-1.3	nd	-2.2	0.495	-0.5	_	1.1	0.048	-0.4	nd
QTL03	T&G	HORVU2Hr1G084970	2.0	nd	0.7	0.333	0.3	0.543	1.6	0.189	1.1	0.486	-0.2	nd	-0.3	0.312	-0.8	0.316	-0.7	0.237	1.1	0.360	-0.4	nd	0.3	0.293	1.1	_	-0.6	0.304	0.5	_	-2.2	nd	-1.0	0.192	-1.1	0.267	-2.3	0.014	0.0	1.000	-2.4	0.090	-0.4	0.592	0.8	nd	-2.2	0.030	-0.7	nd	-0.1	nd	0.6	0.155	1.9	_	0.1	0.808	-0.7	nd
QTL03	T&G	HORVU2Hr1G085050	_	nd	_	0.423	3.6	0.001	2.4	0.143	3.6	0.147	0.0	nd	3.5	0.459	-0.4	0.821	-1.9	0.015	-0.6	0.764	_	nd	-0.9	0.731	-0.4	_	2.2	0.137	1.0	_	_	nd	_	_	-4.0	0.444	-4.3	0.003	-4.2	0.434	_	_	_	0.423	-3.9	nd	-0.1	0.928	-2.6	nd	_	nd	-4.3	0.442	0.1	_	4.1	0.002	1.6	nd
QTL04	T&G	HORVU4Hr1G052450	-2.8	nd	-1.1	0.049	1.5	0.130	1.1	0.295	0.8	0.260	-0.3	nd	0.0	_	0.0	1.000	-0.6	0.295	0.5	0.434	0.1	nd	-1.2	0.004	0.2	_	2.1	0.122	2.6	_	2.5	nd	1.1	0.049	-1.5	0.130	-1.7	0.086	-0.4	0.486	2.9	0.138	-0.1	0.592	-1.3	nd	1.0	0.423	1.8	nd	0.4	nd	-1.2	0.004	0.2	_	2.7	0.032	2.2	nd
QTL04	T&G	HORVU4Hr1G040520	_	nd	0.9	0.602	2.3	0.051	1.4	0.374	4.5	0.235	_	nd	1.3	0.523	-1.2	0.625	-1.5	0.061	1.0	0.489	_	nd	-1.3	0.621	-0.3	_	2.4	0.227	_	_	1.3	nd	0.4	0.293	-3.5	0.452	-2.9	0.013	-3.5	0.160	-0.3	0.860	-2.3	0.512	-2.7	nd	1.0	0.553	_	nd	-1.6	nd	-2.6	0.491	0.9	_	3.9	0.001	_	nd
QTL04	T&G	HORVU4Hr1G054780	-0.7	nd	0.4	0.686	-1.1	0.318	0.0	1.000	-0.4	0.543	0.0	nd	-0.2	0.844	-0.9	0.159	-0.5	0.649	-1.5	0.284	-0.1	nd	-2.1	0.051	-3.3	_	-1.7	0.451	-1.9	_	0.7	nd	-0.6	0.649	0.1	0.853	-0.5	0.571	-1.1	0.382	0.5	0.238	-2.5	0.049	-2.2	nd	-1.7	0.445	-1.5	nd	-0.1	nd	-1.8	0.086	-2.3	_	-1.3	0.518	-0.4	nd
QTL04	T&G	HORVU4Hr1G055110	-1.0	nd	-1.6	0.051	1.3	0.095	-0.3	0.808	-2.3	_	0.0	nd	-0.4	0.423	-0.8	0.106	1.0	0.553	-0.6	0.423	-1.0	nd	1.6	0.293	1.3	_	0.0	1.000	-3.6	_	1.0	nd	1.2	0.038	-2.2	0.020	1.3	0.493	1.7	0.020	0.0	1.000	3.2	0.030	0.0	nd	0.3	0.771	-1.3	nd	-1.0	nd	2.0	0.095	2.2	_	-1.0	0.423	-3.0	nd
QTL04	T&G	HORVU4Hr1G021590	1.0	nd	-1.5	0.089	0.0	1.000	_	0.423	1.0	0.423	1.0	nd	2.0	0.312	2.6	0.038	0.6	0.771	_	_	-0.3	nd	0.0	1.000	0.6	_	0.0	1.000	_	_	0.0	nd	3.5	0.019	2.6	0.349	_	_	_	0.423	-1.3	0.423	1.5	0.232	0.6	nd	_	0.423	_	nd	-1.3	nd	-2.0	0.543	-2.0	_	-0.6	0.771	_	nd
QTL04	T	HORVU4Hr1G035100	1.3	nd	-0.4	0.454	0.8	0.417	0.2	0.640	0.0	0.961	1.5	nd	-0.1	0.928	1.0	0.345	2.1	0.116	0.5	0.672	-0.1	nd	1.7	0.203	1.3	_	-0.1	0.936	-1.0	_	0.1	nd	0.3	0.753	0.3	0.684	1.9	0.123	0.4	0.240	-1.5	0.048	2.1	0.058	0.5	nd	-0.3	0.769	-1.1	nd	-1.6	nd	1.8	0.369	0.3	_	-2.2	0.315	-1.5	nd
QTL04	T	HORVU4Hr1G021320	1.6	nd	1.0	0.109	0.9	0.160	-0.3	0.470	-2.0	0.015	1.2	nd	0.5	0.204	0.3	0.754	-0.5	0.395	-0.3	0.827	2.7	nd	1.2	0.089	0.0	_	0.1	0.592	0.6	_	-0.4	nd	-0.5	0.148	-0.6	0.629	-0.2	0.741	1.7	0.079	1.1	0.022	0.1	0.758	-1.0	nd	0.4	0.402	2.6	nd	1.5	nd	0.7	0.083	-0.3	_	0.6	0.353	0.8	nd
QTL04	T	HORVU4Hr1G035540	-1.8	nd	-2.6	0.309	2.8	0.431	-1.2	0.493	-3.2	0.375	0.0	nd	-1.8	0.404	2.8	0.431	2.6	0.423	-3.8	0.414	-1.8	nd	2.3	0.333	5.5	_	-1.0	0.523	-3.8	_	1.8	nd	0.8	0.621	0.0	1.000	3.8	0.238	-0.6	0.763	0.0	1.000	5.0	0.256	2.7	nd	0.2	0.890	-0.6	nd	-1.8	nd	4.2	0.294	2.7	_	-3.6	0.208	0.0	nd
QTL04	T	HORVU4Hr1G026150	0.3	nd	1.2	0.237	1.2	0.209	0.5	0.496	-0.2	0.788	1.0	nd	2.0	0.138	0.5	0.665	-0.3	0.533	-0.1	0.875	0.1	nd	-0.6	0.686	-0.5	_	1.6	0.195	0.4	_	0.7	nd	0.8	0.272	-0.7	0.645	-0.8	0.030	0.1	0.938	-0.1	0.771	-1.8	0.425	-1.7	nd	1.1	0.032	0.6	nd	-0.9	nd	-2.6	0.362	-1.0	_	1.9	0.009	0.6	nd
QTL04	T	HORVU4Hr1G042040	1.0	nd	-1.6	0.423	_	0.184	-1.3	0.312	0.6	0.423	_	nd	-1.3	0.423	_	0.095	_	0.423	1.6	0.293	-1.6	nd	1.0	0.423	_	_	-0.6	0.808	_	_	_	nd	0.3	0.860	0.4	0.698	_	0.038	1.0	0.423	-2.6	_	2.6	0.349	_	nd	0.7	0.592	_	nd	_	nd	2.3	0.333	_	_	_	0.423	_	nd
QTL04	T	HORVU4Hr1G054770	0.6	nd	0.5	0.480	-1.9	0.016	-1.0	0.136	-0.1	0.684	0.5	nd	0.3	0.369	-1.1	0.402	-1.7	0.002	0.0	0.941	-0.1	nd	-0.5	0.517	-2.2	_	-0.6	0.550	0.6	_	0.0	nd	-0.3	0.735	0.8	0.292	-0.6	0.113	0.1	0.620	-0.6	0.316	-1.0	0.344	-0.3	nd	0.4	0.587	0.7	nd	-0.6	nd	-0.8	0.342	-1.1	_	1.1	0.143	0.6	nd
QTL04	T	HORVU4Hr1G054470	0.1	nd	-1.1	0.317	-1.5	0.040	-0.8	0.328	-1.2	0.091	0.5	nd	-0.1	0.836	0.3	0.691	-1.9	0.014	-0.6	0.521	-0.4	nd	-0.7	0.144	-1.7	_	-1.1	0.308	0.2	_	0.4	nd	1.0	0.339	1.9	0.016	-1.1	0.089	0.6	0.346	-0.5	0.308	0.3	0.659	-0.2	nd	-0.3	0.718	1.4	nd	-0.9	nd	-0.7	0.202	-2.1	_	0.8	0.216	0.8	nd
QTL04	T	HORVU4Hr1G052660	4.3	nd	-0.1	0.808	-0.3	0.740	-1.0	0.534	-0.5	0.662	2.3	nd	0.1	0.771	-0.3	0.155	-0.5	0.619	-1.1	0.176	3.9	nd	1.7	0.095	1.0	_	0.9	0.551	_	_	-2.0	nd	0.2	0.423	0.0	1.000	0.5	0.678	-0.6	0.338	-0.4	0.423	1.8	0.038	1.3	nd	1.9	0.355	_	nd	1.6	nd	1.6	_	1.3	_	1.4	0.179	_	nd
QTL04	T	HORVU4Hr1G030730	0.3	nd	-0.8	0.145	-0.9	0.137	-0.6	0.722	-0.6	0.403	0.0	nd	-0.8	0.314	-0.7	0.342	-0.7	0.333	-0.4	0.649	2.0	nd	-1.7	0.032	-0.9	_	-0.1	0.808	2.2	_	-0.3	nd	-0.1	0.895	0.2	0.688	-0.1	0.961	0.2	0.759	1.7	0.137	-0.9	0.095	0.1	nd	0.5	0.761	2.8	nd	2.0	nd	-0.8	0.192	-0.2	_	0.6	0.406	2.6	nd
QTL04	T	HORVU4Hr1G040350	0.2	nd	-0.7	_	0.1	0.808	-0.6	0.728	-1.1	0.145	-1.1	nd	-0.5	0.667	0.0	1.000	1.4	0.038	-1.1	0.020	-0.3	nd	0.0	1.000	0.6	_	-1.2	0.423	-2.7	_	-1.3	nd	0.2	0.826	-0.1	0.903	2.0	0.465	0.0	1.000	-0.4	0.759	0.7	0.272	0.5	nd	-0.7	0.684	-1.5	nd	0.9	nd	0.5	0.698	0.6	_	-2.7	0.284	-1.5	nd
QTL01	G	HORVU1Hr1G011240	-1.0	nd	0.3	0.698	-0.4	0.771	0.7	0.592	-2.6	0.038	_	nd	0.7	0.293	1.6	_	1.3	0.423	0.0	1.000	-0.3	nd	0.7	0.293	1.6	_	0.7	0.684	_	_	_	nd	0.4	0.698	2.0	0.423	0.6	0.423	2.6	0.038	0.7	0.423	0.4	0.698	2.0	nd	0.0	1.000	_	nd	_	nd	0.0	1.000	0.0	_	-0.6	0.771	_	nd
QTL01	G	HORVU1Hr1G010240	-0.8	nd	0.0	0.913	-0.4	0.293	-0.3	0.451	-0.2	0.497	_	nd	_	0.047	_	0.027	_	0.007	5.1	0.002	_	nd	_	0.047	_	_	_	0.007	_	_	_	nd	_	0.017	_	0.015	_	0.028	5.3	0.023	_	0.047	_	0.017	_	nd	_	0.028	_	nd	_	nd	_	_	_	_	_	_	_	nd
QTL01	G	HORVU1Hr1G011310	0.1	nd	-0.6	0.226	0.2	0.505	0.0	0.860	0.3	0.481	0.4	nd	-0.8	0.401	0.3	0.579	1.4	0.020	0.4	0.467	0.3	nd	1.6	0.187	1.4	_	0.8	0.017	1.7	_	0.3	nd	-0.2	0.782	0.1	0.793	1.4	0.016	0.1	0.884	0.3	0.546	2.3	0.010	1.2	nd	0.8	0.009	1.4	nd	0.0	nd	2.5	0.159	1.1	_	-0.6	0.095	1.3	nd
QTL01	G	HORVU1Hr1G010940	0.8	nd	0.3	0.335	0.0	0.746	0.0	0.900	0.1	0.924	0.6	nd	-0.2	0.369	-0.2	0.338	-0.6	0.048	0.0	0.958	0.8	nd	-0.3	0.482	-0.3	_	1.4	0.072	0.5	_	-0.2	nd	-0.5	0.009	-0.3	0.308	-0.7	0.101	-0.1	0.856	0.0	0.923	-0.6	0.221	-0.3	nd	1.4	0.124	0.4	nd	0.2	nd	-0.1	0.793	-0.1	_	2.1	0.014	0.5	nd
QTL01	G	HORVU1Hr1G008900	_	nd	8.6	0.000	_	0.001	_	0.012	_	0.001	4.4	nd	4.1	0.000	3.5	0.001	3.5	0.015	4.0	0.002	0.8	nd	-0.1	0.136	-0.2	_	1.0	0.051	0.8	_	_	nd	-4.5	0.090	_	0.001	_	0.030	_	0.155	_	0.001	-8.7	0.000	_	nd	_	0.003	_	nd	-3.6	nd	-4.2	0.001	-3.7	_	-2.5	0.005	-3.1	nd
QTL01	G	HORVU1Hr1G010010	-0.4	nd	-0.2	0.832	1.5	0.287	0.4	0.011	0.1	0.727	3.0	nd	3.7	0.261	3.7	0.178	3.2	0.001	3.9	0.006	1.7	nd	3.2	0.276	4.3	_	2.1	0.001	0.6	_	3.4	nd	4.0	0.064	2.2	0.016	2.8	0.001	3.8	0.066	2.1	0.030	3.4	0.072	2.8	nd	1.7	0.001	0.5	nd	-1.3	nd	-0.5	0.746	0.6	_	-1.1	0.035	-3.3	nd
QTL01	G	HORVU1Hr1G010000	-0.7	nd	-1.4	0.040	-0.4	0.647	-1.0	0.489	-0.6	0.580	-0.8	nd	-0.9	0.456	-0.4	0.803	1.4	0.097	-0.2	0.880	0.2	nd	2.5	0.118	2.1	_	-0.1	0.838	-1.3	_	-0.2	nd	0.4	0.587	-0.1	0.959	2.4	0.292	0.4	0.721	0.9	0.368	3.9	0.001	2.4	nd	0.8	0.545	-0.7	nd	1.1	nd	3.5	0.210	2.5	_	-1.5	0.202	-1.1	nd
QTL01	G	HORVU1Hr1G009760	0.0	nd	-2.0	0.272	0.0	1.000	0.0	1.000	-0.6	0.423	-1.0	nd	-2.2	0.020	-0.7	0.312	0.0	1.000	1.0	0.423	-2.3	nd	-1.8	0.038	-0.7	_	-3.8	0.028	-1.0	_	-1.0	nd	-0.2	0.831	-0.7	0.493	0.0	1.000	1.6	0.293	-2.3	0.106	0.2	0.831	-0.7	nd	-3.8	0.028	-0.4	nd	-1.3	nd	0.4	0.293	0.0	_	-3.8	0.028	-2.0	nd
QTL01	G	HORVU1Hr1G010130	2.1	nd	3.0	0.219	2.9	0.005	1.9	0.014	2.0	0.215	0.1	nd	0.3	0.805	-0.5	0.480	-2.0	0.015	-0.9	0.426	-0.3	nd	-1.2	0.470	-1.2	_	-0.9	0.016	-0.3	_	-1.9	nd	-2.8	0.217	-3.4	0.114	-3.8	0.010	-2.8	0.161	-2.4	0.253	-4.2	0.255	-4.1	nd	-2.8	0.003	-2.2	nd	-0.5	nd	-1.5	0.412	-0.7	_	1.1	0.030	0.6	nd
QTL02	G	HORVU2Hr1G027550	-0.5	nd	-1.3	0.021	-0.8	0.034	-0.8	0.081	-0.5	0.233	0.4	nd	-0.4	0.349	0.1	0.752	0.8	0.160	0.5	0.519	0.5	nd	0.8	0.131	0.9	_	-0.5	0.435	-0.8	_	1.0	nd	1.0	0.038	0.9	0.026	1.6	0.017	1.0	0.195	1.1	0.010	2.1	0.008	1.7	nd	0.4	0.421	-0.3	nd	0.1	nd	1.2	0.070	0.8	_	-1.3	0.155	-1.3	nd
QTL02	G	HORVU2Hr1G027230	-2.0	nd	-2.2	0.010	-1.6	0.070	-1.6	0.023	-0.9	0.054	-0.8	nd	-1.5	0.083	-1.1	0.075	-1.8	0.001	-1.4	0.010	-1.3	nd	-1.5	0.041	-1.1	_	-1.8	0.010	-1.5	_	1.2	nd	0.7	0.075	0.5	0.307	-0.1	0.423	-0.5	0.095	0.6	0.005	0.7	0.020	0.5	nd	-0.2	0.423	-0.6	nd	-0.6	nd	0.0	1.000	0.0	_	0.0	0.771	-0.1	nd
QTL02	G	HORVU2Hr1G027680	-2.8	nd	3.0	0.223	2.4	0.325	2.4	0.295	1.6	0.037	-3.3	nd	2.0	0.291	-3.2	0.457	-0.4	0.607	-1.2	0.579	0.0	nd	1.3	0.434	-1.5	_	3.2	0.260	2.7	_	-0.5	nd	-1.0	0.543	-5.6	0.420	-2.8	0.021	-2.7	0.420	2.8	0.283	-1.7	0.477	-3.9	nd	0.8	0.106	1.2	nd	3.3	nd	-0.7	0.698	1.7	_	3.7	0.018	3.9	nd
QTL02	G	HORVU2Hr1G027360	-0.2	nd	-1.6	0.061	0.2	0.800	0.3	0.622	-0.3	0.697	1.7	nd	-1.1	0.419	0.5	0.683	2.0	0.109	-0.4	0.745	0.0	nd	0.7	0.393	2.2	_	-0.9	0.224	-1.5	_	1.9	nd	0.6	0.434	0.3	0.755	1.7	0.054	-0.1	0.925	0.2	0.609	2.4	0.029	2.0	nd	-1.2	0.146	-1.2	nd	-1.7	nd	1.8	0.281	1.7	_	-2.9	0.065	-1.1	nd
QTL02	G	HORVU2Hr1G027020	-3.1	nd	-3.4	0.017	-3.2	0.077	-3.2	0.022	-3.5	0.001	0.6	nd	1.8	0.255	0.3	0.592	0.1	0.961	1.8	0.219	0.1	nd	-0.3	0.776	3.3	_	1.8	0.473	-1.9	_	3.7	nd	5.2	0.014	3.5	0.073	3.3	0.013	5.3	0.001	3.3	0.084	3.1	0.019	6.5	nd	5.0	0.010	1.6	nd	-0.5	nd	-2.1	0.216	3.0	_	1.7	0.157	-3.8	nd
QTL02	G	HORVU2Hr1G026610	-6.0	nd	-6.7	0.039	-6.0	0.006	-6.2	0.043	-5.6	0.000	0.0	nd	-1.6	0.293	-0.6	0.698	0.0	_	0.0	1.000	1.0	nd	0.0	1.000	_	_	-1.0	0.423	_	_	6.0	nd	5.1	0.040	5.4	0.006	6.2	0.043	5.6	0.000	7.0	0.002	6.7	0.039	_	nd	5.2	0.044	_	nd	1.0	nd	1.6	0.293	_	_	-1.0	0.423	_	nd
QTL02	G	HORVU2Hr1G027420	-1.4	nd	_	_	2.7	0.423	1.0	0.214	-0.1	0.922	_	nd	_	_	2.7	0.429	1.2	0.130	0.5	0.038	2.6	nd	_	0.423	2.7	_	0.3	0.771	_	_	_	nd	2.8	_	0.0	1.000	0.2	0.890	0.5	0.576	4.0	0.133	2.8	0.027	0.0	nd	-0.7	0.619	_	nd	_	nd	0.0	1.000	0.0	_	-0.9	0.551	_	nd
QTL02	G	HORVU2Hr1G027410	0.3	nd	-0.9	0.023	0.7	0.518	0.2	0.874	-0.6	0.625	1.0	nd	-0.9	0.545	0.8	0.539	2.4	0.191	0.2	0.853	0.4	nd	2.7	0.002	2.6	_	-0.8	0.254	-0.4	_	0.7	nd	0.0	0.992	0.1	0.882	2.2	0.192	0.8	0.583	0.0	0.931	3.6	0.006	1.9	nd	-1.0	0.189	0.3	nd	-0.7	nd	3.6	0.281	1.8	_	-3.2	0.023	-0.6	nd
QTL03	G	HORVU2Hr1G085400	-2.0	nd	_	0.008	-1.8	0.038	-3.2	0.030	-3.3	0.057	_	nd	_	0.423	_	_	_	0.423	_	0.423	_	nd	_	_	_	_	_	0.423	_	_	_	nd	3.5	0.019	_	0.020	_	0.012	_	0.038	_	_	_	0.008	_	nd	_	0.012	_	nd	_	nd	_	0.423	_	_	_	_	_	nd
QTL03	G	HORVU2Hr1G084400	-0.9	nd	1.6	0.115	0.0	1.000	-0.5	0.155	-0.1	0.913	-1.1	nd	0.6	0.571	-0.5	0.564	-1.5	0.024	0.3	0.702	0.7	nd	-0.9	0.267	-2.4	_	1.3	0.089	_	_	-0.2	nd	-1.0	0.543	-0.5	0.564	-1.0	0.030	0.4	0.718	1.7	0.122	-2.5	0.099	-2.4	nd	1.8	0.014	_	nd	1.9	nd	-1.5	0.223	-1.9	_	2.8	0.011	_	nd
QTL03	G	HORVU2Hr1G084580	0.0	nd	-0.4	0.684	2.9	0.391	-1.1	0.323	-1.6	0.057	_	nd	0.5	0.592	1.1	0.593	2.6	0.155	0.4	0.698	0.0	nd	0.8	0.493	3.9	_	-1.1	0.089	-3.6	_	_	nd	0.8	0.333	-1.8	0.238	3.7	0.143	2.0	0.012	0.0	1.000	1.2	0.300	1.0	nd	0.0	1.000	-2.1	nd	_	nd	0.3	0.698	2.8	_	-3.7	0.014	-4.1	nd
QTL03	G	HORVU2Hr1G085020	0.0	nd	0.3	0.794	1.8	0.061	3.4	0.136	4.7	0.164	-0.7	nd	1.4	0.419	-0.8	0.691	-1.4	0.062	-0.8	0.687	0.1	nd	-1.1	0.523	-1.2	_	2.6	0.160	1.3	_	-0.7	nd	1.1	0.325	-2.7	0.460	-4.8	0.005	-5.6	0.397	0.2	0.714	-1.4	0.433	-3.1	nd	-0.9	0.493	-3.4	nd	0.8	nd	-2.5	0.319	-0.4	_	3.9	0.006	2.1	nd
QTL03	G	HORVU2Hr1G085000	-1.7	nd	-2.1	0.007	-2.1	0.010	-1.6	0.305	-2.2	0.002	-0.9	nd	-0.9	0.085	-1.7	0.224	-0.8	0.069	-1.4	0.064	-2.4	nd	-1.1	0.108	-1.5	_	-1.4	0.040	-1.5	_	0.8	nd	1.2	0.011	0.4	0.525	0.8	0.467	0.8	0.055	-0.7	0.344	1.0	0.037	0.6	nd	0.2	0.809	0.7	nd	-1.5	nd	-0.2	0.495	0.2	_	-0.6	0.080	-0.1	nd
QTL04	G	HORVU4Hr1G034730	-0.4	nd	-0.4	0.648	-0.4	0.564	0.1	0.293	-0.8	0.117	0.2	nd	0.4	0.691	1.6	0.193	0.9	0.108	0.4	0.549	0.6	nd	0.7	0.019	0.7	_	2.4	0.002	-0.5	_	0.5	nd	0.7	0.554	2.0	0.176	0.8	0.133	1.3	0.150	0.9	0.416	1.0	0.354	1.2	nd	2.3	0.003	0.4	nd	0.4	nd	0.3	0.788	-0.9	_	1.5	0.166	-0.9	nd
QTL04	G	HORVU4Hr1G021390	0.0	nd	-1.0	0.423	1.6	0.293	0.4	0.423	1.0	0.312	_	nd	-1.0	0.423	0.3	0.698	1.0	_	-0.2	0.870	1.0	nd	-1.0	0.423	0.0	_	-1.2	0.038	0.6	_	_	nd	0.0	1.000	-1.3	0.312	0.6	0.423	-1.2	0.515	1.0	0.423	0.0	1.000	-1.6	nd	-1.6	0.051	-0.4	nd	_	nd	0.0	1.000	-0.3	_	-2.2	0.020	0.8	nd
QTL04	G	HORVU4Hr1G054200	-3.1	nd	-1.4	0.074	0.7	0.522	0.0	0.982	-0.5	0.404	0.3	nd	2.2	0.060	1.7	0.206	0.2	0.740	-0.5	0.480	-0.1	nd	-0.1	0.958	0.5	_	1.7	0.207	-1.7	_	3.4	nd	3.5	0.030	1.0	0.528	0.3	0.883	0.0	0.942	3.1	0.047	1.3	0.169	-0.2	nd	1.7	0.559	-1.3	nd	-0.4	nd	-2.2	0.306	-1.2	_	1.4	0.014	-1.2	nd
QTL04	G	HORVU4Hr1G022780	-2.0	nd	-2.0	0.007	-1.5	0.199	-1.2	0.352	-1.5	0.177	0.4	nd	-0.7	0.201	0.2	0.599	-0.3	0.080	-0.1	0.794	0.9	nd	-0.5	0.022	-0.2	_	0.2	0.003	-0.5	_	2.5	nd	1.2	0.034	1.7	0.169	0.9	0.438	1.4	0.190	2.9	0.015	1.5	0.009	1.3	nd	1.4	0.318	1.0	nd	0.4	nd	0.2	0.541	-0.4	_	0.5	0.039	-0.4	nd
QTL04	G	HORVU4Hr1G040730	-0.4	nd	-0.8	0.121	-0.5	0.161	0.5	0.522	0.3	0.720	0.9	nd	-0.2	0.752	0.9	0.417	2.0	0.151	1.8	0.207	0.8	nd	1.9	0.059	4.4	_	0.2	0.805	0.7	_	1.3	nd	0.6	0.338	1.4	0.171	1.6	0.057	1.6	0.047	1.2	0.109	2.8	0.049	4.9	nd	-0.2	0.809	0.4	nd	-0.2	nd	2.1	0.185	3.5	_	-1.8	0.289	-1.1	nd
QTL04	G	HORVU4Hr1G044040	2.8	nd	3.0	0.002	1.9	0.280	0.2	0.583	0.3	0.530	0.0	nd	0.5	0.490	-1.3	0.178	-1.0	0.070	-1.4	0.053	1.6	nd	1.0	0.264	0.2	_	-0.1	0.795	0.3	_	-2.9	nd	-2.5	0.238	-3.1	0.048	-1.2	0.060	-1.7	0.030	-1.2	0.391	-2.0	0.392	-1.7	nd	-0.3	0.392	0.0	nd	1.7	nd	0.5	0.692	1.4	_	0.9	0.052	1.7	nd
QTL04	G	HORVU4Hr1G054970	-0.3	nd	-0.4	0.429	0.0	1.000	-0.1	0.832	0.5	0.544	0.5	nd	0.1	0.763	0.6	0.187	-0.5	0.191	1.1	0.333	0.4	nd	-1.0	0.243	-0.8	_	1.9	0.044	1.9	_	0.7	nd	0.6	0.201	0.6	0.188	-0.4	0.533	0.6	0.470	0.6	0.094	-0.5	0.394	-0.8	nd	2.0	0.200	1.4	nd	-0.1	nd	-1.1	0.183	-1.4	_	2.4	0.048	0.8	nd
QTL04	G	HORVU4Hr1G039160	-0.9	nd	-0.5	0.238	-0.3	0.698	0.7	0.594	0.9	0.263	-1.0	nd	-0.1	0.860	-1.3	0.198	0.2	0.808	2.9	0.012	0.0	nd	-0.9	0.423	1.0	_	1.4	0.294	0.4	_	-0.1	nd	0.4	0.564	-1.0	0.300	-0.5	0.689	2.1	0.285	0.9	0.159	-0.4	0.679	1.3	nd	0.7	0.642	-0.4	nd	1.0	nd	-0.8	0.505	2.3	_	1.2	0.255	-2.5	nd
QTL04	G	HORVU4Hr1G043630	0.5	nd	0.3	0.451	0.1	0.928	0.1	0.891	-1.0	0.410	2.8	nd	0.1	0.920	0.1	0.698	2.6	0.051	1.2	0.207	-0.7	nd	2.6	0.060	0.8	_	0.2	0.849	-0.4	_	2.3	nd	-0.2	0.877	0.1	0.924	2.5	0.262	2.2	0.259	-1.1	0.443	2.3	0.030	0.7	nd	0.1	0.950	0.6	nd	-3.5	nd	2.5	0.383	0.7	_	-2.4	0.360	-1.5	nd
QTL04	G	HORVU4Hr1G029240	_	nd	_	0.095	2.3	_	_	0.038	_	0.423	_	nd	_	0.095	3.3	0.012	_	0.038	_	0.423	_	nd	_	0.095	2.3	_	_	0.038	_	_	_	nd	_	_	1.0	0.423	_	_	_	_	_	_	_	_	0.0	nd	_	_	_	nd	_	nd	_	_	-1.0	_	_	_	_	nd
QTL04	G	HORVU4Hr1G027180	0.2	nd	1.5	0.328	1.4	0.302	1.9	0.141	1.3	0.053	0.8	nd	2.1	0.266	0.3	0.842	-0.5	0.366	-0.3	0.596	1.8	nd	0.1	0.950	0.3	_	3.2	0.107	1.9	_	0.7	nd	0.6	0.293	-1.1	0.498	-2.4	0.041	-1.5	0.120	1.7	0.306	-1.4	0.509	-1.1	nd	1.3	0.180	0.6	nd	1.0	nd	-2.0	0.435	0.0	_	3.7	0.035	2.2	nd
QTL04	G	HORVU4Hr1G037050	_	nd	_	_	1.0	0.423	_	_	-1.0	0.423	_	nd	_	0.043	-5.1	0.063	-5.0	0.001	-6.0	0.000	_	nd	_	0.111	-4.8	_	-4.3	0.063	-3.3	_	-6.0	nd	-4.8	0.046	-6.1	0.062	_	0.001	-5.0	0.000	-4.7	0.054	-5.0	0.117	-5.8	nd	_	0.057	-2.3	nd	1.3	nd	-0.2	0.745	0.4	_	0.7	0.126	2.7	nd
QTL04	G	HORVU4Hr1G052290	-0.4	nd	-1.6	0.110	0.3	0.468	-0.3	0.740	1.0	0.027	0.5	nd	-0.7	0.593	-0.3	0.468	0.4	0.755	1.2	0.129	2.4	nd	2.0	0.020	1.5	_	1.6	0.260	2.0	_	0.9	nd	0.9	0.356	-0.6	0.035	0.7	0.595	0.2	0.779	2.7	0.089	3.6	0.061	1.2	nd	1.9	0.280	1.0	nd	1.8	nd	2.7	0.281	1.8	_	1.2	0.517	0.8	nd
QTL04	G	HORVU4Hr1G030980	-0.5	nd	-0.1	0.910	1.0	0.141	0.3	0.233	-0.5	0.047	0.2	nd	-0.6	0.679	0.7	0.247	4.2	0.016	1.4	0.111	1.5	nd	1.4	0.450	3.9	_	1.7	0.139	3.5	_	0.6	nd	-0.5	0.656	-0.3	0.702	3.8	0.003	1.8	0.050	2.0	0.112	1.5	0.074	3.0	nd	1.4	0.212	4.0	nd	1.3	nd	2.0	0.297	3.2	_	-2.5	0.451	2.2	nd
QTL04	G	HORVU4Hr1G052260	5.2	nd	4.5	0.015	4.6	0.046	2.4	0.005	2.4	0.089	6.5	nd	5.3	0.015	_	0.042	5.9	0.002	5.8	0.047	5.9	nd	5.7	0.014	_	_	5.9	0.002	3.6	_	1.3	nd	0.8	0.609	_	0.095	3.4	0.058	3.4	0.345	0.7	0.592	1.2	0.333	_	nd	3.4	0.052	1.1	nd	-0.6	nd	0.4	0.831	_	_	0.0	1.000	-2.3	nd
QTL04	G	HORVU4Hr1G031060	-0.6	nd	-0.8	0.019	-0.2	0.535	-0.1	0.342	-0.5	0.173	-0.2	nd	-0.5	0.077	0.2	0.516	0.3	0.053	-0.3	0.465	1.1	nd	1.5	0.021	2.7	_	1.3	0.012	0.6	_	0.5	nd	0.4	0.120	0.5	0.160	0.4	0.088	0.2	0.556	1.8	0.029	2.4	0.010	2.9	nd	1.4	0.021	1.1	nd	1.3	nd	2.0	0.020	2.4	_	1.0	0.028	0.8	nd
QTL04	G	HORVU4Hr1G035670	1.5	nd	0.7	0.228	1.4	0.183	1.0	0.179	1.0	0.213	0.8	nd	0.2	0.686	0.6	0.466	2.4	0.082	0.0	1.000	-1.5	nd	1.0	0.138	2.3	_	0.1	0.756	-1.6	_	-0.6	nd	-0.6	0.294	-0.8	0.438	1.4	0.005	-1.0	0.472	-3.0	0.269	0.2	0.595	0.9	nd	-0.9	0.011	-2.6	nd	-2.3	nd	0.8	0.155	1.6	_	-2.3	0.003	-1.6	nd
QTL04	G	HORVU4Hr1G046970	-1.4	nd	0.2	0.780	1.0	0.292	0.6	0.592	-0.7	0.689	-0.3	nd	-0.2	0.806	0.4	0.649	2.1	0.273	-0.2	0.814	-1.6	nd	1.3	0.344	2.7	_	-0.2	0.816	-2.0	_	1.1	nd	-0.4	0.507	-0.5	0.625	1.5	0.146	0.5	0.792	-0.2	0.882	1.1	0.301	1.7	nd	-0.8	0.150	-1.3	nd	-1.3	nd	1.5	0.213	2.2	_	-2.3	0.025	-1.8	nd
QTL04	G	HORVU4Hr1G051590	-1.0	nd	0.6	0.698	_	0.145	1.3	0.095	2.2	0.296	0.0	nd	1.6	0.293	0.8	0.493	0.7	0.293	2.2	0.323	-2.0	nd	-1.0	0.095	0.8	_	1.3	0.095	_	_	1.0	nd	1.0	0.698	_	0.184	-0.6	0.423	0.0	1.000	-1.0	0.423	-1.6	0.184	_	nd	0.0	_	_	nd	-2.0	nd	-2.6	0.038	0.0	_	0.6	0.423	_	nd
QTL04	G	HORVU4Hr1G040510	_	nd	1.1	0.658	1.8	0.062	0.2	0.902	2.5	0.172	0.0	nd	_	0.423	-2.2	0.509	-3.7	0.014	-0.9	0.588	_	nd	-1.7	0.573	-0.5	_	1.0	0.019	2.9	_	_	nd	_	0.272	-4.1	0.442	-3.8	0.018	-3.4	0.313	_	_	-2.8	0.482	-2.3	nd	0.9	0.641	0.4	nd	_	nd	_	0.423	1.8	_	4.7	0.013	3.8	nd
QTL04	G	HORVU4Hr1G023980	1.7	nd	1.8	0.238	0.0	1.000	-0.2	0.885	-2.5	0.047	1.3	nd	0.8	0.423	0.7	0.609	0.4	0.782	-3.0	0.404	_	nd	2.8	0.198	_	_	0.4	0.836	_	_	-0.4	nd	-1.0	_	0.7	0.493	0.6	0.312	-0.5	0.762	_	0.095	1.0	0.423	_	nd	0.6	0.671	_	nd	_	nd	2.0	0.095	_	_	0.0	1.000	_	nd
QTL04	G	HORVU4Hr1G025470	0.7	nd	0.9	0.517	0.8	0.462	0.2	0.845	-0.9	0.083	0.7	nd	1.2	0.437	0.7	0.556	1.2	0.266	-1.6	0.293	-1.5	nd	1.0	0.463	0.4	_	-1.3	0.194	-4.1	_	0.0	nd	0.4	0.518	-0.1	0.944	1.0	0.371	-0.6	0.516	-2.2	0.004	0.2	0.373	-0.4	nd	-1.5	0.178	-3.1	nd	-2.2	nd	-0.2	0.760	-0.3	_	-2.5	0.099	-2.5	nd
QTL04	G	HORVU4Hr1G035330	-2.2	nd	-1.6	0.051	-2.9	0.023	-2.5	0.001	-2.9	0.014	_	nd	1.6	0.293	_	_	1.6	_	_	0.095	_	nd	_	0.095	_	_	_	_	_	_	_	nd	3.2	0.030	_	0.017	4.1	0.001	_	0.008	_	0.214	_	0.012	_	nd	_	0.001	_	nd	_	nd	_	0.423	_	_	_	_	_	nd
QTL04	G	HORVU4Hr1G041600	-0.1	nd	-1.1	0.028	0.5	0.572	0.3	0.439	0.1	0.795	0.3	nd	-0.4	0.491	0.7	0.493	2.9	0.051	0.5	0.608	0.0	nd	0.9	0.098	3.5	_	0.0	0.944	-0.5	_	0.4	nd	0.7	0.143	0.3	0.689	2.5	0.000	0.4	0.699	0.1	0.824	2.0	0.008	3.0	nd	-0.3	0.003	-0.6	nd	-0.3	nd	1.3	0.149	2.7	_	-2.9	0.000	-1.0	nd
QTL04	G	HORVU4Hr1G046350	-1.4	nd	0.1	0.925	-0.6	0.752	-3.2	0.449	-0.3	0.830	2.4	nd	2.2	0.167	-1.1	0.636	-2.0	0.339	2.8	0.454	-0.1	nd	0.0	1.000	-1.7	_	-3.0	0.412	2.4	_	3.7	nd	2.1	0.103	-0.5	0.802	1.2	0.621	3.1	0.022	1.3	0.543	-0.1	0.925	-1.2	nd	0.2	0.926	2.7	nd	-2.5	nd	-2.2	0.167	-0.6	_	-1.0	0.628	-0.3	nd
QTL04	G	HORVU4Hr1G034670	-0.4	nd	1.0	0.312	-1.0	0.497	0.2	0.831	1.2	0.106	-0.4	nd	0.8	0.423	-1.0	0.155	-0.3	0.667	-0.9	0.051	-0.7	nd	0.1	0.831	-0.7	_	-1.7	0.182	-0.8	_	0.0	nd	-0.2	0.808	0.0	1.000	-0.5	0.095	-2.1	0.019	-0.3	0.667	-0.9	0.155	0.3	nd	-1.9	0.143	-2.0	nd	-0.3	nd	-0.7	0.333	0.3	_	-1.4	0.184	0.1	nd
QTL04	G	HORVU4Hr1G049550	1.1	nd	0.1	0.633	0.2	0.684	-1.4	0.155	0.5	0.095	-0.3	nd	-0.8	0.143	-0.7	0.655	-0.2	0.860	-0.3	0.312	-1.5	nd	0.2	0.849	0.3	_	-0.9	0.711	0.5	_	-1.4	nd	-0.9	0.115	-0.9	0.596	1.2	0.130	-0.8	0.095	-2.6	0.019	0.1	0.912	0.1	nd	0.5	0.698	0.0	nd	-1.2	nd	1.1	0.352	1.1	_	-0.7	0.759	0.8	nd
QTL04	G	HORVU4Hr1G050560	-1.0	nd	0.3	0.782	-1.0	0.293	-0.2	0.592	-2.9	0.137	_	nd	_	0.027	_	0.184	_	0.067	1.0	0.698	-2.1	nd	-0.1	0.808	-0.6	_	2.5	0.095	-2.0	_	_	nd	_	0.238	_	0.057	_	0.006	3.9	0.111	-1.1	0.192	-0.4	0.698	0.4	nd	2.7	0.008	0.9	nd	_	nd	_	0.049	_	_	_	_	-3.0	nd
QTL04	G	HORVU4Hr1G055560	5.6	nd	5.1	0.002	4.2	0.003	5.3	0.000	_	0.036	-0.3	nd	-0.2	0.214	-0.2	0.633	-0.4	0.037	0.2	0.723	5.2	nd	4.1	0.002	4.0	_	5.9	0.001	_	_	-5.9	nd	-5.3	0.003	-4.4	0.039	-5.7	0.002	_	0.059	-0.4	0.423	-1.0	0.293	-0.2	nd	0.6	0.698	_	nd	5.5	nd	4.3	0.003	4.2	_	6.3	0.002	_	nd
QTL04	G	HORVU4Hr1G030780	0.7	nd	-0.9	0.065	0.6	0.344	-0.3	0.216	0.4	0.648	0.8	nd	-0.5	0.488	0.1	0.931	2.9	0.015	-0.2	0.903	0.6	nd	1.4	0.093	2.4	_	1.0	0.390	_	_	0.1	nd	0.3	0.558	-0.6	0.570	3.2	0.003	-0.5	0.679	-0.1	0.942	2.2	0.015	1.8	nd	1.3	0.255	_	nd	-0.2	nd	1.9	0.175	2.3	_	-1.9	0.497	_	nd
QTL04	G	HORVU4Hr1G027940	0.1	nd	-0.6	0.566	-0.3	0.686	-1.0	0.150	-0.7	0.409	0.2	nd	-0.8	0.429	-0.4	0.761	1.9	0.148	-0.3	0.835	-1.6	nd	1.5	0.443	1.7	_	-1.5	0.194	-1.8	_	0.1	nd	-0.2	0.625	-0.1	0.911	2.9	0.043	0.5	0.644	-1.7	0.140	2.1	0.080	2.0	nd	-0.5	0.513	-1.1	nd	-1.8	nd	2.3	0.073	2.1	_	-3.4	0.106	-1.5	nd
QTL04	G	HORVU4Hr1G024480	-0.6	nd	0.7	0.293	0.6	0.423	0.0	1.000	0.5	0.293	1.0	nd	0.3	0.698	0.6	0.698	-1.0	0.095	0.5	0.592	2.0	nd	0.7	0.293	-1.4	_	1.6	0.293	_	_	1.6	nd	-0.4	0.698	0.0	1.000	-1.0	0.095	0.0	1.000	2.6	0.155	0.0	1.000	-2.0	nd	1.6	0.293	_	nd	1.0	nd	0.4	0.698	-2.0	_	2.6	0.038	_	nd
QTL04	G	HORVU4Hr1G046000	-0.7	nd	-2.3	0.063	0.0	1.000	0.1	0.698	-0.2	0.633	_	nd	_	0.095	_	0.359	_	0.003	4.0	0.022	0.3	nd	0.0	1.000	2.7	_	-0.2	0.543	-2.1	_	_	nd	_	0.038	_	0.049	_	0.015	4.2	0.072	1.0	0.216	2.3	0.063	2.7	nd	-0.3	0.465	-1.9	nd	_	nd	_	0.095	_	_	_	0.038	-6.1	nd
QTL04	G	HORVU4Hr1G034030	6.0	nd	_	0.130	4.4	0.197	4.1	0.002	4.2	0.016	0.6	nd	-1.3	0.323	0.8	0.529	1.6	0.001	-0.1	0.932	3.1	nd	5.3	0.135	5.0	_	4.1	0.000	2.6	_	-5.4	nd	_	0.138	-3.6	0.132	-2.5	0.017	-4.3	0.132	-2.8	0.198	_	0.423	0.6	nd	0.0	1.000	-1.6	nd	2.6	nd	6.6	0.141	4.2	_	2.5	0.003	2.7	nd
QTL04	G	HORVU4Hr1G054850	-0.9	nd	-1.6	0.300	-0.2	0.662	-0.7	0.530	-0.4	0.523	-1.0	nd	-1.3	0.244	-1.3	0.060	-1.0	0.044	0.2	0.804	0.3	nd	-2.2	0.012	-2.0	_	-1.1	0.197	1.0	_	-0.1	nd	0.4	0.729	-1.0	0.082	-0.3	0.684	0.5	0.116	1.2	0.254	-0.5	0.467	-1.8	nd	-0.5	0.602	1.4	nd	1.3	nd	-0.9	0.158	-0.7	_	-0.2	0.753	0.9	nd
QTL04	G	HORVU4Hr1G037240	0.6	nd	-0.7	0.251	0.1	0.930	-0.5	0.179	0.2	0.676	0.9	nd	-0.9	0.163	0.1	0.895	1.3	0.117	0.2	0.300	1.2	nd	2.3	0.120	2.6	_	-0.5	0.593	1.0	_	0.3	nd	-0.2	0.649	0.1	0.930	1.8	0.034	0.1	0.918	0.6	0.312	3.1	0.049	2.5	nd	0.0	1.000	0.8	nd	0.3	nd	3.3	0.037	2.4	_	-1.8	0.279	0.8	nd
QTL04	G	HORVU4Hr1G025580	1.1	nd	1.0	0.487	1.0	0.401	0.0	0.959	-1.2	0.366	1.0	nd	1.4	0.413	1.3	0.351	1.9	0.300	-1.3	0.306	-1.2	nd	1.4	0.411	1.2	_	-0.4	0.661	-4.9	_	-0.1	nd	0.4	0.293	0.3	0.633	1.9	0.095	-0.1	0.913	-2.3	0.010	0.4	0.198	0.2	nd	-0.3	0.553	-3.7	nd	-2.2	nd	0.0	1.000	-0.1	_	-2.3	0.070	-3.6	nd
QTL04	G	HORVU4Hr1G048540	-0.7	nd	-1.2	0.130	1.1	0.432	-0.6	0.155	-0.2	0.860	0.0	nd	-1.8	0.360	0.8	0.527	1.2	0.038	-1.2	0.579	-0.2	nd	0.8	0.423	1.5	_	-2.4	0.268	-1.7	_	0.7	nd	-0.6	0.612	-0.3	0.836	1.8	0.038	-1.0	0.596	0.5	0.312	2.0	0.027	0.4	nd	-1.7	0.319	-1.6	nd	-0.2	nd	2.6	0.296	0.7	_	-3.6	0.228	-0.6	nd
QTL04	G	HORVU4Hr1G030420	-0.7	nd	0.0	1.000	0.7	0.451	-1.1	0.423	-0.5	0.106	0.0	nd	-0.1	0.808	-0.5	0.412	0.0	1.000	-0.6	0.155	-0.3	nd	2.6	0.038	0.4	_	-0.6	0.038	-1.7	_	0.7	nd	-0.1	0.808	-1.2	0.093	1.1	0.428	-0.1	0.698	0.4	0.312	2.6	0.038	-0.3	nd	0.6	0.620	-1.2	nd	-0.3	nd	2.7	0.067	0.9	_	-0.6	0.155	-1.1	nd
QTL04	G	HORVU4Hr1G028720	-0.3	nd	-0.6	0.000	-0.3	0.500	0.0	0.995	0.4	0.307	0.4	nd	-0.3	0.060	0.1	0.874	-1.3	0.013	0.8	0.299	0.3	nd	-0.7	0.303	-1.0	_	-1.0	0.155	2.0	_	0.8	nd	0.4	0.021	0.4	0.476	-1.3	0.041	0.4	0.585	0.6	0.107	-0.1	0.911	-0.7	nd	1.0	0.269	1.6	nd	-0.2	nd	-0.4	0.457	-1.1	_	2.2	0.007	1.2	nd

Table 6-S3: List of the differentially expressed barley genes (HORVUs) within four quantitative trait loci (QTL) associated with variation in mature barley phenotypes. Genotypic DEGs (G) were determined by comparison of samples at equivalent developmental stages from four different genotypes: Forum, Gant, Salka and Wren. Temporal DEGs (T) were determined by comparison of samples at sequential developmental stages within individual genotypes. Genes were considered to be differentially expressed on the basis of greater than ±2 $\log_2$ fold change and $p < 0.05$. Expression data is presented in transcripts per million (TPM).

QTL	DEG category	HORVU	Annotation	Tissue-specific maximum TPM	Whole-pistil maximum TPM
QTL1H_ES	G	HORVU1Hr1G008900	Chromosome 3B scaffold cv Chinese Spring	19.8	22.8
QTL1H_ES	G	HORVU1Hr1G009760	unknown function	8.8	0.7
QTL1H_ES	G	HORVU1Hr1G010000	undescribed protein	209.9	5.5
QTL1H_ES	G	HORVU1Hr1G010010	beta-glucosidase 47	35.9	11.7
QTL1H_ES	G	HORVU1Hr1G010130	alcohol dehydrogenase 1	37.9	29.5
QTL1H_ES	G	HORVU1Hr1G010240	undescribed protein	20	2.5
QTL1H_ES	G	HORVU1Hr1G010940	Transmembrane protein putative	45.7	9.1
QTL1H_ES	G	HORVU1Hr1G011240	Pentatricopeptide repeat 336 – mitochondrial Rf1 precursor protein	5.8	0.4
QTL1H_ES	T & G	HORVU1Hr1G011270	Pentatricopeptide repeat 336 – mitochondrial Rf1 precursor protein	5.1	1
QTL1H_ES	G	HORVU1Hr1G011310	undescribed protein	23.2	5.2
QTL1H_ES	T & G	HORVU1Hr1G012660	unknown function	94.4	9.9
QTL2H_NUC	G	HORVU2Hr1G026610	Protein CWC15-like protein A	13.3	7.5
QTL2H_NUC	G	HORVU2Hr1G027020	unknown protein	21.6	9.6
QTL2H_NUC	G	HORVU2Hr1G027230	Ribosomal protein L7Ae/L30e/S12e/Gadd45 family	9.3	4.4
QTL2H_NUC	G	HORVU2Hr1G027360	H/ACA ribonucleoprotein complex subunit 4-like protein	1578.4	96.9
QTL2H_NUC	G	HORVU2Hr1G027410	H/ACA ribonucleoprotein complex subunit 4-like protein	484	43.1
QTL2H_NUC	G	HORVU2Hr1G027420	H/ACA ribonucleoprotein complex subunit 4-like protein	14.4	1
QTL2H_NUC	G	HORVU2Hr1G027550	undescribed protein	37.9	31.6

QTL2H_NUC	G	HORVU2Hr1G027680	Haloacid dehalogenase-like hydrolase (HAD) superfamily	20.7	9
QTL2H_OV	G	HORVU2Hr1G084400	Cyclin-dependent kinase G-2	10.4	2.4
QTL2H_OV	G	HORVU2Hr1G084580	undescribed protein	179.8	2.5
QTL2H_OV	T & G	HORVU2Hr1G084970	undescribed protein	14.7	1.6
QTL2H_OV	G	HORVU2Hr1G085000	B-box zinc finger family protein	9.7	25.5
QTL2H_OV	G	HORVU2Hr1G085020	His-rich AGP, HvHRA1	8547.7	50.1
QTL2H_OV	T & G	HORVU2Hr1G085050	undescribed protein, co-expressed with HvHRA1	5795.9	28.7
QTL2H_OV	T & G	HORVU2Hr1G085270	Chitinase	17.4	74.9
QTL2H_OV	G	HORVU2Hr1G085400	undescribed protein	6	0.6
QTL4H_INT	T & G	HORVU4Hr1G052450	Hexosyltransferase	36.3	5.8
QTL4H_INT	T & G	HORVU4Hr1G040520	undescribed protein	10.2	20.3
QTL4H_INT	T & G	HORVU4Hr1G054780	undescribed protein	10	5.8
QTL4H_INT	T & G	HORVU4Hr1G055110	Core-2/I-branching beta-16-N-acetylglucosaminyltransferase family	30.6	1.2
QTL4H_INT	T & G	HORVU4Hr1G021590	unknown function	7.6	0.6
QTL4H_INT	T	HORVU4Hr1G035100	undescribed protein	21.5	11.8
QTL4H_INT	T	HORVU4Hr1G021320	early nodulin-like protein 20	5.2	15.4
QTL4H_INT	T	HORVU4Hr1G035540	undescribed protein	205.2	4.7
QTL4H_INT	T	HORVU4Hr1G026150	alpha-L-arabinofuranosidase 2	143.1	18.6
QTL4H_INT	T	HORVU4Hr1G042040	undescribed protein	421.2	0.6
QTL4H_INT	T	HORVU4Hr1G054770	COBRA-like protein 7	62.7	54.8
QTL4H_INT	T	HORVU4Hr1G054470	Long cell-linked locus protein	55	40.6
QTL4H_INT	T	HORVU4Hr1G052660	NADH-quinone oxidoreductase subunit H	14.7	3
QTL4H_INT	T	HORVU4Hr1G030730	undescribed protein	8.5	1.6
QTL4H_INT	T	HORVU4Hr1G040350	undescribed protein	41	1.9
QTL4H_INT	G	HORVU4Hr1G034730	undescribed protein	9.3	2.3
QTL4H_INT	G	HORVU4Hr1G021390	HVA22-like protein J	12.4	0.5
QTL4H_INT	G	HORVU4Hr1G054200	Adenine nucleotide alpha hydrolases-like superfamily	12.4	9.7
QTL4H_INT	G	HORVU4Hr1G022780	Non-specific lipid-transfer protein 4	92.5	303.9

QTL4H_INT	G	HORVU4Hr1G040730	undescribed protein	29.9	3
QTL4H_INT	G	HORVU4Hr1G044040	Nucleoside diphosphate kinase family	46.1	45.9
QTL4H_INT	G	HORVU4Hr1G054970	Wound-induced protein 1	14.8	22.4
QTL4H_INT	G	HORVU4Hr1G039160	undescribed protein	10.4	2.3
QTL4H_INT	G	HORVU4Hr1G043630	undescribed protein	95.1	2.5
QTL4H_INT	G	HORVU4Hr1G029240	undescribed protein	6	0.5
QTL4H_INT	G	HORVU4Hr1G027180	proline transporter 1	151.1	15
QTL4H_INT	G	HORVU4Hr1G037050	unknown function	5.7	3.5
QTL4H_INT	G	HORVU4Hr1G052290	undescribed protein	14.7	4.9
QTL4H_INT	G	HORVU4Hr1G030980	undescribed protein	20.3	6.1
QTL4H_INT	G	HORVU4Hr1G052260	undescribed protein	169.1	14.6
QTL4H_INT	G	HORVU4Hr1G031060	Paired amphipathic helix protein Sin3-like 3	11.1	5.7
QTL4H_INT	G	HORVU4Hr1G035670	undescribed protein	7.7	16.1
QTL4H_INT	G	HORVU4Hr1G046970	undescribed protein	80.6	8
QTL4H_INT	G	HORVU4Hr1G051590	Pyruvate kinase family protein	47.2	0.5
QTL4H_INT	G	HORVU4Hr1G040510	undescribed protein	6.5	48.7
QTL4H_INT	G	HORVU4Hr1G023980	undescribed protein	55.8	1.2
QTL4H_INT	G	HORVU4Hr1G025470	Senescence-associated protein	6.6	129.1
QTL4H_INT	G	HORVU4Hr1G035330	Tryptophan synthase beta chain 2	10.7	1.8
QTL4H_INT	G	HORVU4Hr1G041600	undescribed protein	22.9	8.9
QTL4H_INT	G	HORVU4Hr1G046350	undescribed protein	29.4	13.5
QTL4H_INT	G	HORVU4Hr1G034670	Retrotransposon protein, putative, unclassified	11.5	1.3
QTL4H_INT	G	HORVU4Hr1G049550	transcription regulators	16.7	8.7
QTL4H_INT	G	HORVU4Hr1G050560	undescribed protein	7.6	1.3
QTL4H_INT	G	HORVU4Hr1G055560	unknown function	68.8	9
QTL4H_INT	G	HORVU4Hr1G030780	undescribed protein	19.6	3.3
QTL4H_INT	G	HORVU4Hr1G027940	CLIP-associated protein	824	8.7
QTL4H_INT	G	HORVU4Hr1G024480	Double-stranded RNA-binding protein 7	35.2	0.4

QTL4H_INT	G	HORVU4Hr1G046000	undescribed protein	5.2	3.5
QTL4H_INT	G	HORVU4Hr1G034030	undescribed protein	12	6.2
QTL4H_INT	G	HORVU4Hr1G054850	Chaperone protein DnaJ	14.1	33.4
QTL4H_INT	G	HORVU4Hr1G037240	Protein BRASSINOSTEROID INSENSITIVE 1	9.3	2.4
QTL4H_INT	G	HORVU4Hr1G025580	mRNA RefSeq: XM_372959.1	9.7	42.3
QTL4H_INT	G	HORVU4Hr1G048540	0	187	2.4
QTL4H_INT	G	HORVU4Hr1G030420	undescribed protein	28.4	1.5
QTL4H_INT	G	HORVU4Hr1G028720	xyloglucan endotransglucosylase/hydrolase 5	14	167.8

Chapter 7

Thesis Summary and Future Directions

Thesis Summary

Improving our fundamental knowledge of ovule development in cereal crops is important for understanding the processes underlying grain production, and will provide valuable information regarding the optimisation of female fertility to breeding programs globally. The ovule is key to grain production, yet research in *Triticeae* cereal crops has not thoroughly characterised (1) the genetic and molecular cues that regulate ovule development, (2) the significance of developmental processes occurring before fertilisation upon grain development, or (3) the significance of differences in ovule structure among various genotypes of individual cereal species. The research in this thesis has addressed ovule development in barley, identifying natural variation in ovule morphology, key reproductive phases, and candidate genes within genomic regions associated with variant ovule phenotypes. Further, this thesis has generated phenotypic and genetic resources that provide a fundamental platform for analysis of ovule development in barley, complementing similar resources currently emerging for other cereal crops.

A major limitation of research into understanding ovule development in cereal crops is the technical difficulty in accessing the ovule tissue. This difficulty compromises observation of phenotypes, ability for accurate staging to be performed, and makes collection of sufficient ovule tissue for genetic or molecular analyses challenging. Historically, investigation of the internal structure of ovule morphology in cereal crops has been undertaken using microscopic techniques that rely on sectioning of material, such as histological staining with toluidine blue, transmission electron microscopy, and more recently, *in situ* hybridisation. While this information is valuable, sectioning is a time consuming technique, especially when considering that only a single ovule exists in each sample of cereal crops, and thus the study of ovule morphology in a large number of genotypes, mutants, or following various treatments has not been feasible. The adaption of a clearing method using Hoyer's solution such that whole barley

pistils can be made sufficiently clear to allow observation of ovule structures using DIC light microscopy, as presented in Chapter 3, thus marks a significant technical advance. As demonstrated in Chapter 3 and subsequent chapters, this method may be used to process samples in a much more high-throughput manner than methods relying on sectioning, and the resolution of ovule structures is sufficient to capture phenotypic data that can identify genotypic variation in a population screen, as was undertaken in Chapter 4.

In Chapter 4, mature ovule morphology was assessed in a population of 150 genotypes of European two-row spring barley. Analysis of images of cleared tissue revealed that several genotypes were not sampled correctly, as many examples of immature and fertilised ovules were identified, thus eliminating 23 genotypes from further assessment and suggesting that assessment of anther dehiscence may not be sufficient for precise staging of ovule maturity in all genotypes. The remaining 127 genotypes were used to establish the “average” phenotype of nine mature ovule features (traits), and thus identified several large and small outlier genotypes for each. Correlation analysis revealed that the embryo sac was the most variable ovule component, and it was less tightly coupled to overall ovule dimensions as compared to the correlation between the ovule and nucellus dimensions, suggesting that the germline cells may respond to more varied, or in a more variable manner to, developmental cues than the surrounding somatic nucellus. Further, there were few correlations between ovule and grain traits across the whole population, suggesting that under ideal growth conditions, pre-fertilisation variation in ovule development may not have a significant impact on grain morphology. However,s it must be acknowledged that this should be repeated with subsequent generations of the population, and under sub-optimal conditions. Analysis of ovule area in this population raised several questions. First, at what stage of growth do differences in ovule phenotypes appear? In the case of the nucellus, the size of ovule primordium may determine the number of cells in the young ovule and hence the size of the nucellus at reproductive maturity, or differences may appear with time. In contrast, the embryo sac in

every genotype arises as a single cell at a relatively late stage of ovule development, suggesting there must be a developmental stage at which variable embryo sac morphology becomes apparent. Second, how does variation in ovule tissues arise with respect to cell proliferation and cell expansion? In the case of the crassinucellate nucellus of barley, this could potentially arise through cell expansion, division or a combination of both. Third, what is the genetic basis for genotype-dependent differential regulation of cellular proliferation or expansion at a particular developmental stage, and is this sufficient to produce an “outlier” phenotype. While each of these questions could be addressed with developmental study of an individual genotype or a pair of genotypes, we made use of the whole population to screen for genomic regions that influence ovule development, by GWAS. The analysis suggests that most features of ovule development are controlled by multiple small-effect QTL. Only a few regions, associated with ~66 markers, made a significant contribution to the nine ovule traits, and many markers were associated with multiple traits. Markers tended to be grouped in six genomic regions, of which three were notable in containing markers with the strongest associations, and a fourth was notably enriched for markers associated with variation in integument width. Over 2000 genes were located within these four QTL. Further analysis of these loci might involve re-mapping with additional genetic markers to refine the QTL, or generation of bi-parental populations to assess the contribution of different alleles to ovule development. In the case of this study, an alternative method was used, based on transcriptional profiling.

In Chapter 5, morphological phenotypes and transcriptional data were generated at five stages of ovule development in four genotypes with variant mature ovule morphology, thus establishing the resources required to begin addressing the questions raised in Chapter 4. Among the four genotypes, nine stages of ovule development were identified based on morphological features of several ovule tissues. These nine stages were aligned to a previously existing cereal floral staging scale, the Waddington scale, and thus may be used in

the future to improve the accuracy of staging female reproductive development in barley. Comparison of ovule tissue traits throughout development in the four genotypes revealed that while in some cases the initial tissue was reflected in the size of the tissue at maturity, this was not always true. Further, it was found that different genotypes appear to progress through reproductive development at different rates, attaining mature ovule size relatively early or late during the nine developmental stages. These results strongly suggest that there are multiple genotypically distinct regulatory processes governing ovule development, and that these may include signals that vary over time. This may explain why the GWAS study of Chapter 4 only identified small effect QTL for ovule traits, rather than a single prominent locus as has been detected for other traits in this panel. Although this diversity does not appear to impact ovule function or downstream seed development, the impact upon reproductive fitness in sub-optimal conditions remains unclear.

Variation was also observed within sub-domains of the ovule tissues of interest. Immunolabelling of cell wall polysaccharides on transverse semi-thin sections of ovules in the four genotypes was performed to address how cell proliferation and cell expansion contribute to growth of the nucellus and thus the ovule overall. In species such as Arabidopsis, this feature might normally be addressed through the use of fluorescent reporters, but such resources are either not available or not entirely feasible in barley. Despite this, the immunolabelling facilitated three remarkable findings, the first being the differentiation of the (non-epidermal) nucellus into two discrete domains, the inner and peripheral nucellus; the second being that the peripheral nucellus is responsible for driving nucellus growth through cell proliferation, and that the inner nucellus contributes toward nucellus growth through cellular expansion; the third being that the cell walls of the nucellus flanking the reproductive cells specifically contains de-methylesterified pectin, and that at later stages of development these cells differentiate into the inner nucellus. From the data presented, neither the role of the differentiated inner nucellus nor the reason for such a specific pattern of pectin

demethylesterification from such an early stage is clear. The observation of these features directly flanking the reproductive lineage suggests they may provide specific regulatory or mechanical support to guide development of the embryo sac. Alternatively, they may reflect a biochemical state that prevents initiation of additional reproductive cells. The origin of pectin methylesterase enzymes that presumably control the specific LM19 labelling is also unclear. Because no gene expression resources related to ovule development in barley were available to address this question, or their possible relevance to QTL identified in Chapter 4, RNA sequencing was undertaken to generate two transcriptional data sets.

The first transcriptional data set described gene expression in whole pistils at five different stages of ovule development, in the four genotypes previously analysed in Chapter 5. The second transcriptional data set described gene expression in discrete ovule tissues, isolated using laser capture microdissection from a fifth genotype. Therefore, between the two sets of data, expression dynamics could be assessed throughout ovule development, compared between variant genotypes, and the specific localisation of gene expression could be assessed. Given the lack of knowledge regarding the fundamental processes regulating ovule development in barley, the utility of this data set was demonstrated by identification of the barley orthologues of genes known to influence ovule development in other species, such as the MADS-box transcription factors, and genes involved in auxin biosynthesis and transport. In the case of MADS-box genes, expression patterns of individual genes were generally similar between barley and rice, with the exception of a potential swap between *MADS29* and *MADS31* in terms of transcript abundance. This work thus confirms expression patterns of putative barley MADS-box genes, and provides information about the expression of these genes in wildtype genotypes that may be useful for designing and assessing future mutational studies to confirm the functionality of these genes. Analysis of the expression of genes involved in auxin signalling indicated that auxin signalling is generally more abundant at earlier stages of ovule development than late, and that the embryo sac is highly involved in auxin

signalling. Tissue- and timepoint-specific regulation of members of gene families within the ovule was observed, such as expression of *HvPIN1c* within the pooled nucellus and embryo sac sample at Stage 4 as compared to expression of *HvPIN1a* within the egg apparatus and central cell. A discrete group of genes was observed to be specific to the ovary, suggesting that while auxin signalling is simultaneously occurring in the ovary and the ovule, and potentially between the two organs, the mechanisms of signalling and likely the responses elicited are different. Notably, the two genes found to be expressed within the chalaza, *HvTIR1* and *HvIAA3*, were highly abundant, which may indicate either that this tissue has a very specific role in auxin signalling, or that the barley orthologues for other components of the auxin signalling machinery in this tissue are yet to be identified. As such, further study is required to identify and functionally characterise additional genes involved in auxin signalling in barley, and this dataset may be used as a reference point for future work. Expression analysis of genes underlying pectin biosynthesis and modification was also examined, revealing (in a similar manner to the auxin pathway), discrete groups of genes specifically expressed within the embryo sac, or within the surrounding somatic tissues. While expression of genes involved in auxin signalling was found to be greater at the earliest stage observed, Stage 4, in both the embryo sac and the somatic tissues, expression of pectin-related genes was found to be abundant and dynamic at all three stages observed. Notably, the discrete tissues within the embryo sac, the egg and central cell, and the antipodal cell cluster, were found to have distinct expression profiles of pectin methylesterase inhibitors (PMEIs) and pectinesterases (PEs), suggesting a strong signal for synthesis and methylesterification of pectin, while the nucellus was slightly biased toward expression of pectin methylesterases (PMEs), consistent with LM19 labelling. While further data is required to draw firm conclusions, in conjunction with the pattern of pectin de/methylesterification within the nucellus cell walls revealed by immunolabelling, this data suggests that there may be an antagonistic relationship between the embryo sac and the inner nucellus, whereby a balance between methylesterifciation and demethylesterification contributes to growth and cell identity. Given

previous associations between auxin signalling and the products of pectin degradation, which are released from demethylestereified pectin, future work may reveal a key role for a relationship between these two systems in regulating ovule development in barley, or give insight into the specific role of the inner nucellus in supporting successful maturation of the embryo sac. Taken together, Chapter 5 demonstrates morphological and transcriptional data that will be a valuable tool for future work charcterising ovule development in barley, and assessing functional conservation of orthologues genes identified in other species.

In order to identify novel genes involved in ovule development, a differential expression analysis was performed in Chapter 6. Comparison of the expression levels of genes within QTLs identified in Chapter 4 at different stages of ovule development, and between variant genotypes revealed differential expression of 82 genes. Of these, functional annotations gathered from genomic annotation resources suggested a small selection of interesting candidate genes from three QTL regions. These include a putative orthologue of the precursor to OsRF1, a component of male cytoplasmic sterility in rice, as a candidate influencer of embryo sac area; three putative H/ACA ribonucleoprotein complex subunit 4 genes involved in post-transcriptional gene regulation, as candidate influencers of nucellus area; and an arabinogalactan protein known as HvHRA1 as a candidate influencer of overall ovule area. Additionally, several unannotated genes were identified and may be considered novel candidates influencing ovule development. Tissue-specific expression data indicated that these differentially expressed candidate genes are likely to affect the associated ovule phenotype indirectly, either by inducing developmental cues that are cell-to-cell mobile, or by initiating a regulatory change early in development that subsequently causes variation of tissue developmental progress.

Overall, this thesis presents a morphological and transcriptional description of the developing barley ovule, compiled from a combination of microscopic, molecular and bioinformatic

analyses with the aim of genetically and phenotypically quantifying variation in barley ovule development. In summary, the findings indicate that: (1) details of ovule structure within whole-mounted cereal floral tissue may be observed using light microscopy; (2) the cell walls of nucellus cells flanking the female reproductive lineage specifically contain demethylestereified homogalacturonan, and as development progresses the nucellus differentiates into discrete domains; (3) both overall ovule morphology, and the individual contribution of discrete ovule tissues varies among genotypes of barley. Further, the size of the nucellus and embryo sac may only have a small impact grain development under ideal conditions; (4) multiple regions of the genome are associated with variation in mature ovule morphology, and within these regions several candidate genes are differentially expressed between “large” and “small” ovule genotypes. This thesis also establishes fundamental resources for future investigation of ovule development in barley, including: (1) a microscopic technique; (2) morphological developmental staging references for wildtype genotypes with naturally variant ovule developmental programs; (3) two transcriptional data sets characterising both tissue-specific gene expression within the ovule, and the transcriptional profiles of whole pistils from four genotypes at five developmental stages. In conclusion, the work presented in this thesis will facilitate future translation of knowledge of the molecular and genetic cues influencing ovule development between species, and thus contributes to future efforts of improving cereal crop production.

Future Perspectives

Optimisation of cereal crop yield is a core aim of global plant breeding efforts, and it is likely to become imperative for ensuring food security in future years as the global population grows and environmental conditions become more challenging. This thesis demonstrates that it is possible to investigate the intimate details of female reproduction in barley and provides initial fundamental resources to do so. This thesis also leaves several questions regarding ovule

development to be answered. As such, future avenues of investigation may include the following:

1) *What are the genes required for ovule initiation and development in barley?*

Genetic and molecular factors required for ovule initiation and development have been widely studied in Arabidopsis, rice and maize. As demonstrated in this study, knowledge from other systems may be utilised to broadly identify similar genes in barley. Following this study, there is enormous scope for utilisation of the transcriptional data presented in confirmation of the expression patterns of putative orthologues of genes identified in other species, that may be used as a proof of concept alongside, or as an alternative to, other techniques such as *in situ* hybridisation, before time and money is invested in generation of transgenic plants. The data presented also provides several candidate genes for non-lethal regulation of ovule developmental processes, which may be investigated with transgenic overexpression or CRISPR/Cas9 lines, or used as bait further co-expression analysis of the transcriptional data in order to identify other components of the regulatory pathways that lie outside of the identified QTL. Identification of genes both required for successful ovule development, and influential in regulation of these processes, may be useful in the future for understanding and optimising ovule development in barley for survival under sub-optimal environmental conditions.

2) *What is the role of the nucellus specifically with regard to development of the initial functional megaspore into the mature embryo sac?*

The roles of the nucellus during initiation of the female reproductive lineage at the beginning of ovule development, and as a transfer tissue to support filling of the endosperm with nutrients, have been characterised in diverse species. Meanwhile, the function of the nucellus throughout maturation of the embryo sac is less clearly defined. Logically, communication of developmental signals and transfer of nutrients would occur between the two tissues, as the nucellus completely surrounds the embryo sac. Data presented in this thesis regarding expression of auxin signalling pathways and pectin remodelling may be seen to support this

hypothesis, however, this exchange has yet to be characterised. Thus, in the future, the transcriptional data presented in this study may be used to identify expression of components of cell-to-cell signal transduction pathways. Additionally, future work may consider isolation of the inner and peripheral nucellus, in order to elucidate the reason for differentiation of the inner nucellus and its significance to development of the embryo sac.

3) *To what extent do pre-fertilisation developmental processes in the embryo sac and maternal tissue influence grain development under normal conditions?*

While three-dimensional and whole pistil traits were not addressed in this study, they may be considered in future studies addressing the relationship between the ovule and grain morphology. Future work may also consider using the current data to compare differential tissue morphology and gene expression among smaller subsets of the genotypes, particularly those showing extreme variation in grain qualities. This may also include increasing the number of grain traits assessed, and including compositional analyses to assess whether nutritional aspects of grain, such as the relative proportions of protein and carbohydrates, are influenced by developmental factors. Further, future study may consider analysis of ovule and grain traits over several generations, in order to assess the heritability of traits over generations, and to contribute resources for study of the epigenetic components of grain development.

4) *How does each component of the ovule respond to environmental stress?*

The ovule is known to be more resilient to environmental stresses than pollen, however the underlying reasons why have not been determined. Further, studies have generally measured the overall effect upon the ovule, or even pistil, as whether or not female fertility is maintained, without assessing the specific factors contributing toward survival or abortion. As such, both the morphological and transcriptional data presented in this study provide a reference point for normal ovule developmental processes among naturally variant genotypes, with which

future studies involving drought, heat, or salt stress may be compared. Study of this nature, involving drought stress, is currently being pursued at the University of Adelaide, guided by the data presented in this thesis.

5) Development of future tools

This study provides genetic resources that may be used to begin selection of appropriate genes for use driving fluorescent reporters, and transgenic constructs in a tissue specific manner. These resources would be valuable for future studies as it would facilitate both the generation of CRISPR/Cas9 or overexpression mutants for functional characterisation of candidate genes, and greatly improve our ability to assess the subsequent consequences to ovule morphology.

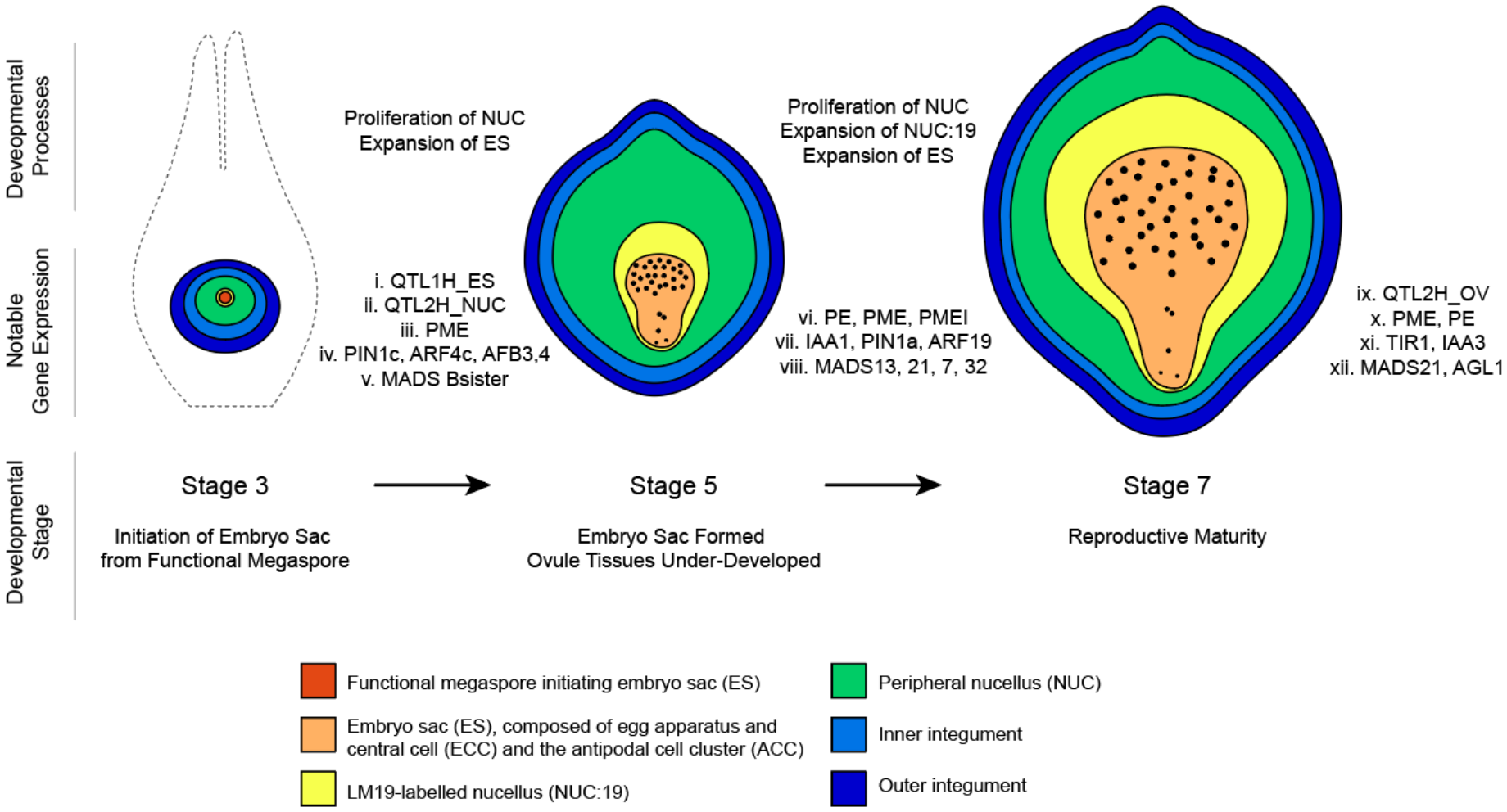
Deveopmental Processes
Notable Gene Expression
Developmental Stage
Proliferation of NUC
Expansion of ES
Proliferation of NUC
Expansion of NUC:19
Expansion of ES
i. QTL1H_ES
ii. QTL2H_NUC
iii. PME
iv. PIN1c, ARF4c, AFB3,4
v. MADS Bsister
vi. PE, PME, PMEI
vii. IAA1, PIN1a, ARF19
viii. MADS13, 21, 7, 32
ix. QTL2H_OV
x. PME, PE
xi. TIR1, IAA3
xii. MADS21, AGL1
Stage 3
Stage 5
Stage 7
Initiation of Embryo Sac
from Functional Megaspore
Embryo Sac Formed
Ovule Tissues Under-Developed
Reproductive Maturity
Functional megaspore initiating embryo sac (ES)
Embryo sac (ES), composed of egg apparatus and central cell (ECC) and the antipodal cell cluster (ACC)
LM19-labelled nucellus (NUC:19)
Peripheral nucellus (NUC)
Inner integument
Outer integument

Figure 7-1: Schematic model integrating data from Chapters 4, 5 and 6. Annotations: i. Expression of the QTL1H_ES candidate PRR-336 in the nucellus/ES at Stage 4; ii. Expression of the QTL2H_NUC candidate H/ACA snoRNPs in the nucellus/ES at Stage 4; iii. Expression of pectinmethylesterase within the nucellus/ES at Stage 4; iv. Expression of PIN1c, ARF4c, ARF18, ARF21, AFB3, and AFB4 in the nucellus/ES at Stage 4; v. Expression of the MADS-box Bsister genes MADS29 and 31 within the nucellus/ES at Stage 4 vi. Expression of PE in the ES and ACC, PMEI in the ES, and PME in the ECC at Stage 5; vii. Expression of IAA1, PIN1a, and ARF19 in the ES and ECC at Stage 5; vii. Expression of MADS13, MADS21, MADS7 and MADS32 in the integuments at Stage 5; ix. Expression of the QTL2H_OV candidate HvHRA1 in the antipodal cells at Stage 7; x. Expression of PME in the ECC and PE in the ACC at Stage 7; xi. Expression of TIR1 and IAA3 in the Chalaza (not shown on schematic) at Stage 7; xii. Expression of AGL1 in the ECC and MADS21 in the integument at Stage 7.

Appendix I

Exploring the role of the ovule in cereal grain development and reproductive stress tolerance

ꕥ • ꕥ

Statement of Authorship

Title of Paper	Exploring the Role of the Ovule in Cereal Grain Development and Reproductive Stress Tolerance
Publication Status	☑ Published ☐ Accepted for Publication ☐ Submitted for Publication ☐ Unpublished and Unsubmitted work written in manuscript style
Publication Details	Laura G. Wilkinson[1,2], Dayton C. Bird[1,2], Matthew R. Tucker[1,*]

Principal Author

Name of Principal Author (Candidate)	Laura G. Wilkinson		
Contribution to the Paper	Compiled information and wrote the manuscript. I hereby certify that the statement of authorship is accurate.		
Overall percentage (%)	70%		
Certification:	This paper reports on original research I conducted during the period of my Higher Degree by Research candidature and is not subject to any obligations or contractual agreements with a third party that would constrain its inclusion in this thesis. I am the primary author of this paper.		
Signature		Date	14/2/19

Co-Author Contributions

By signing the Statement of Authorship, each author certifies that:

iv. the candidate's stated contribution to the publication is accurate (as detailed above);

v. permission is granted for the candidate in include the publication in the thesis; and

vi. the sum of all co-author contributions is equal to 100% less the candidate's stated contribution.

Name of Co-Author	Dayton C. Bird		
Contribution to the Paper	Compiled information and contributed to the preparation of the manuscript. I hereby certify that the statement of authorship is accurate.		
Signature		Date	14/2/19

Name of Co-Author	Matthew R. Tucker		
Contribution to the Paper	Compiled information and contributed to the preparation of the manuscript. I hereby certify that the statement of authorship is accurate.		
Signature		Date	14/2/19

Annual Plant Reviews (2018) **1**, 1–35
doi: 10.1002/9781119312994.apr0609

http://onlinelibrary.wiley.com

EXPLORING THE ROLE OF THE OVULE IN CEREAL GRAIN DEVELOPMENT AND REPRODUCTIVE STRESS TOLERANCE

Laura G. Wilkinson[1,2], Dayton C. Bird[1,2] and Matthew R. Tucker[1]

[1]*School of Agriculture, Food and Wine, University of Adelaide, Waite Campus, Urrbrae, South Australia, Australia*
[2]*ARC Centre of Excellence in Plant Cell Walls, University of Adelaide, Waite Campus, Urrbrae, South Australia, Australia*

Abstract: Maintaining and enhancing grain production in cereal crops is a key priority for global research efforts. The formation of floral organs impacts the number and quality of grain produced, and is an important component of cereal yield. The grain is derived predominantly from the ovule, a multifunctional tissue located in the ovary of the flower that specifies and nurtures the female germline, pro- duces a female gametophyte, and supports embryo and endosperm development after fertilisation. Grain cannot form without successful production and fertilisa- tion of the female gametophyte, and the stages of floral development encompass- ing gametophyte formation are particularly sensitive to environmental fluctua- tions. A deeper fundamental understanding of female reproductive development from a tissue- and cell-type-specific perspective may provide opportunities to sus- tain and increase grain yields. In this article, we consider flower and ovule development, with a particular focus on pre-fertilisation stages in cereals and their role in stress tolerance and downstream grain formation.

Keywords: ovule, ovary, development, nucellus, cereal, grain, programmed cell death, fertilisation, stress

1 The Plant Ovule: Where, What, and Why?

Plant reproduction in angiosperms begins with the formation of a flower and ends with the formation of seed. In general, the floral organs of both monocot and dicot species are arranged similarly, forming rings (whorls) that surround the central reproductive structures (Figure 1). Distinct differences can be found, however, in the identity, arrangement, and the number of organs present in each whorl. In dicot species such as *Arabidopsis thaliana* (Arabidopsis), the outer whorls form sepals and petals (Figure 1a), whereas in monocot species such as *Hordeum vulgare* (barley) they are occupied by the palea and lemma (Figure 1b). The inner whorls consist of the stamens, which support the anthers, and carpels, which house the ovule(s). The number of floral organs varies between species. Arabidopsis flowers produce two carpels that fuse to form the pistil, six stamens, four petals, and four sepals. Florets of barley and *Triticum aestivum* (wheat) consist of a single pistil, which terminates in two styles, three stamens, and two lodicules, enclosed by two

Figure 1 Flower and ovule development in Arabidopsis and barley. (a) In Arabidopsis, a representative of the dicots, the flower is arranged into concentric whorls of organs, each of which fulfils a specific role during reproductive development. The female reproductive organs are located in the centre of the flower. (b) In barley, a member of the monocots, a whorl arrangement is also present, but organ types differ from those in Arabidopsis and show distinct identity relative to their position in the flower. The female reproductive organs are present in the centre of the flower. (c) Ovule development in Arabidopsis initiates from the placenta (at the junction of the two carpels) and requires the establishment of three distinct domains, the nucellus (which produces the germline), the chalaza (which produces the integuments), and the funiculus (which connects the ovule to the placenta and maternal plant). The nucellus can be divided into epidermal and sub-epidermal cell types. The accompanying legend uses colour coding to indicate the identity of the different cell types. (d) As the ovule grows, the megaspore mother cell undergoes meiosis to produce four megaspores in a linear or tetrahedral arrangement. The proximal megaspore initiates female gametophyte development. (e) At anthesis, the female gametophyte contains seven cells that represent four distinct cell types. The nucellus is restricted mainly to the chalazal end of the female gametophyte and is heavily reduced compared to species such as barley. (f) During early stages of ovule development in barley, the ovule appears similar to that of Arabidopsis, as indicated by the similar shading colours. However, a true funiculus is lacking, and the chalaza connects directly to the placental tissue. (g) As ovule development continues, the nucellus proliferates and expands, forming the bulk of the ovule. (h) Barley, similar to Arabidopsis, produces a Polygonum-type female gametophyte containing four different cell types. However, unlike Arabidopsis, the central cell nuclei do not fuse prior to fertilisation, and the antipodals continue proliferating independently of other gametophyte cells. se, sepal; pe, petal; st, stamen; ov, ovule; ca, carpel (ovary); sti, stigma; an, anther; pd, pedicel; le, lemma; pa, palea; lo, lodicule; gl, glume; ra, rachis; fg, female gametophyte; mmc, megaspore mother cell; lc, locule; mp, micropyle; ch, chalaza.

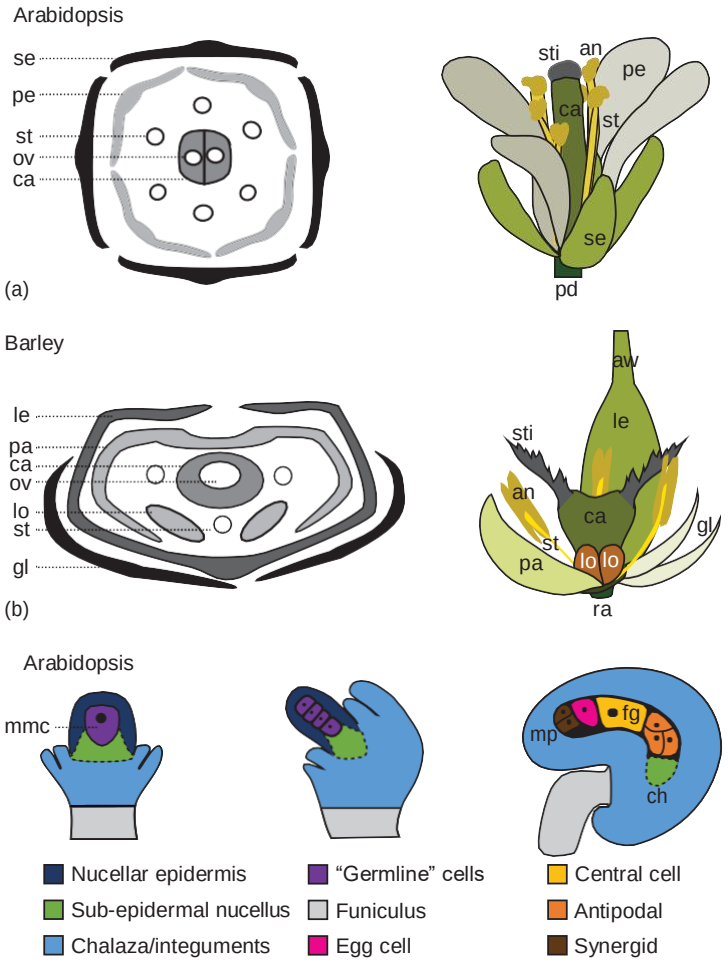
Arabidopsis
se
pe
st
ov
ca
(a)
sti
an
pe
ca
st
se
pd
Barley
le
pa
ca
ov
lo
st
gl
(b)
aw
le
sti
an
ca
gl
st
pa
lo
lo
ra
Arabidopsis
mmc
mp
fg
ch
Nucellar epidermis
Sub-epidermal nucellus
Chalaza/integuments
"Germline" cells
Funiculus
Egg cell
Central cell
Antipodal
Synergid

'empty glume' organs, the palea and lemma (Figure 1b; De Vries, 1971). The *Oryza sativa* (rice) floret is similar except that it includes six stamens (Itoh et al., 2005). *Zea mays* (maize) florets initiate development of three carpels, which fuse to form a single pistil that bears two silks, three stamens, and two lodicules, enclosed by the palea and lemma. However, during maturation, maize inflorescences become monoecious, meaning florets on the tassel abort the pistil, becoming male, and florets on the ear abort the stamens, becoming female (Bonnett, 1940; Nickerson, 1954). Despite this inter-species variation, a common feature within the cereals is the development of a single ovule within each pistil.

The ovule is located in the ovary and at maturity consists of a haploid embryo sac (female gametophyte, FG) surrounded by diploid maternal nucel- lus tissue and one or two integuments (Figure 1c–h). Both Arabidopsis and barley ovules are bitegmic, meaning that two integuments form around the ovule, eventually giving rise to the seed coat. The mature FG is composed of an egg cell, two synergid cells, two polar nuclei within the central cell, and a cluster of between 3 (Arabidopsis) and ~100 (maize) antipodal cells (Diboll, 1968; Engell, 1994; Evans and Grossniklaus, 2009). The FG is located towards the distal, micropylar end of the ovule and oriented such that the synergids, egg cell, and central cell are most proximal to the micropyle. The synergid cells lack a complete cell wall whereby the plasma membrane con- tacts that of the egg cell (Jensen, 1973). The role of the synergids is to guide the pollen tube towards the ovule, and upon pollen burst the egg cell and the polar nuclei are both fertilised, giving rise to the zygote and the endosperm (Higashiyama et al., 2001). The enlarged, persistent nucellus and a high num- ber of antipodal cells are a distinguishing feature of cereal ovules compared to the three antipodal cells and reduced nucellus of Arabidopsis (compare Figure 1e and h).

1.1 Genes involved in ovule development

Using forward and reverse genetics, diverse genes have been identified that influence ovule development. Table 1 lists a number of these from different species, dividing them into categories based on their role in floral meristem development, ovule formation and patterning, germline formation, and early gametophyte development. Many of these genes are potentially useful for the modification of flower, ovule, and seed development, affecting seed mor- phology or yield, and this has been discussed in various reviews (Cucinotta et al., 2014; Itoh et al., 2005; Noman et al., 2017). For the purposes of this arti- cle, we will mainly consider genes involved in the development of the most prominent somatic tissue within the ovule, the nucellus. The nucellus plays a multifunctional role in providing signals to support germline development prior to fertilisation, as well as establishing an environment that sustains and

Table 1 Selected genes involved in flower, ovary, and ovule development in species including Arabidopsis, rice, wheat, and maize.

Class	Gene	Species	Type	Function	Impact of altered function	Reference
Meristem development	KNOTTED1	*Z. mays*	HD TF	Regulator of meristem development	Additional carpels, altered ovule nucellus growth	Kerstetter et al. (1997)
	SUPERWOMAN (OsMADS16)	*O. sativa*	MADS TF (AP3)	Regulator of whorl-specific proliferation	Stamens and lodicules transformed into carpels and palea-like organs, altered ovule nucellus growth	Nagasawa et al. (2003)
	SILKY1	*Z. mays*	MADS TF (AP3)	Regulator of whorl-specific proliferation	Stamens and lodicules transformed into carpels and palea/lemma-like organs	Ambrose et al. (2000), Whipple et al. (2004)
	TaMADS51	*T. aestivum*	MADS TF (AP3)	Regulator of whorl-specific proliferation	Stamens transformed into pistil-like structures	Yamada et al. (2009), Zhao et al. (2006)
	PHOTOPERIOD DETERMINANT 1	*T. aestivum*	PRR	Regulator of circadian clock	Modified architecture, additional paired spikelets (acts via FT)	Boden et al. (2015)
	INDETERMINATE FLORAL APEX1	*Z. mays*	YABBY TF	Regulator of meristem determinacy	Increased spikelets, ovule primordia	Laudencia-Chingcuanco and Hake (2002), Strable et al. (2017)

Table 2 *(continued)*

Class	Gene	Species	Type	Function	Impact of altered function	Reference
	TASSEL SEED 1 and 2	*Z. mays*	Putative alcohol dehydrogenase	Regulator of tassel pistil abortion	Carpels in tassel survive	Irish (1997)
	TASSEL SEED 4 and 6	*Z. mays*	miR172	Regulator of meristem development	Additional florets, tassel pistils, floral meristem indeterminacy	Chuck et al. (2007)
	REQUIRED TO MAINTAIN REPRESSION6	*Z. mays*	RNA polymerase d1	Regulator of tassel pistil abortion	Carpels in tassel survive, SILKY1 deregulated	Parkinson et al. (2007)
	INCOMPLETEY FUSED CARPELS	*Z. mays*	Unknown	Regulates carpel fusion, nucellus proliferation	Unfused carpels, protruding nucellus growth	Li et al. (2016), Li et al. (2017)
Ovule formation	SEEDSTICK	*A. thaliana*	MADS TF	Regulator of ovule identity	Ovules transformed to leaf- and carpel-like structures, elongated funiculus	Pinyopich et al. (2003)
	OsMADS13	*O. sativa*	MADS TF (STK)	Regulator of ovule identity	Ovule transformed to carpelloid structure	Dreni et al. (2007), Li et al. (2011)
	TaAGL2	*T. aestivum*	MADS TF (STK)	Regulator of ovule identity	Ectopic ovule growth in pistil-like stamens	Yamada et al. (2009), Zhao et al. (2006)

Annual Plant Reviews Online, Volume 1. Edited by Jeremy Roberts.

Ovule patterning	SPOROCYTELESS	*A. thaliana*	TF	Regulator of transcription and megasporocyte development	Nucellus fails to elongate, FG development is blocked	Be (2C Sch (19 (19
	WUSCHEL	*A. thaliana*	HD TF	Regulator of MMC development, nucellus formation, and integument formation	Integuments do not form, MMC development terminates	Gr (2C (2C
	WINDHOSE1, WINDHOSE2	*A. thaliana*	Small peptides	Regulator of MMC formation	Disrupted MMC development, ovule cell morphology	Lie
	DICER-LIKE 1	*A. thaliana*	RNAse III	Involved in miRNA production	Pleiotropic defects, short integuments, FG abortion	Ku Wa Sch (2C
	CORONA, PHABULOSA, PHAVOLUTA	*A. thaliana*	HD-ZIP III TF	Regulator of integument development and chalaza formation, repress WUSCHEL expression	Abnormal integument development, extra carpels	Ya (2C

(co

Table 4 *(continued)*

Class	Gene	Species	Type	Function	Impact of altered function	Reference
	ARGONAUTE1	*A. thaliana*	AGO	Effector of gene silencing	Altered ovule polarity	Lynn et al. (1999), Morel et al. (2002)
	ARGONAUTE10	*A. thaliana*	AGO	Modulator of gene silencing	Altered ovule polarity	Mallory et al. (2009), Moussian et al. (1998)
	PIN-FORMED1	*A. thaliana*	PIN	Auxin efflux facilitator	Loss of integuments, FG abortion	Ceccato et al. (2013)
	INNER NO OUTER	*A. thaliana*	YABBY TF	Regulator of integument development	Lacking outer integument, impaired FG development	Baker et al. (1997)
	AINTEGUMENTA	*A. thaliana*	AP2-like TF	Regulator of integument development	No integument growth, failed meiosis and FG development	Klucher et al. (1996)
	BEL1	*A. thaliana*	HD TF	Regulator of integument specification and patterning, and chalaza development	Single integument formation which is converted into a carpel-like structure, disrupted FG formation	Brambilla et al. (2007), Ray et al. (1994), Robinson-Beers et al. (1992)

Annual Plant Reviews Online, Volume 1. Edited by Jeremy Roberts.

Female germline formation	ARGONAUTE9	*A. thaliana*	AGO	Effector of gene silencing	Extra germline-like cells	Olmedo-Monfil et al. (2010)
	RNA-DEPENDENT RNA POLYMERASE 6	*A. thaliana*	RDRP	Component of gene silencing pathways	Extra germline-like cells	Olmedo-Monfil et al. (2010), Peragine et al. (2004)
	SUPPRESSOR OF GENE SILENCING 3	*A. thaliana*	Uncharacterised protein	Component of gene silencing pathways	Extra germline-like cells	Olmedo-Monfil et al. (2010), Peragine et al. (2004)
	AUXIN RESPONSE FACTOR 3 (ETTIN)	*A. thaliana*	ARF TF	Regulator of gynoecium and integument development	Fused integuments, ovule abortion, extra germline-like cells	Sessions et al. (1997), Su et al. (2017)
	RETINOBLASTOMA1	*A. thaliana*	RB-like	Transcriptional repressor, regulator of MMC differentiation	Pleiotropic defects, extra germline-like cells	Ebel et al. (2004), Zhao et al. (2017)
	MULTIPLE SPOROCYTES 1	*O. sativa*	RLK	Suppressor of sporocyte differentiation	Extra germline-like cells	Nonomura et al. (2003)
	TAPETUM DETERMINANT-LIKE 1A (MAC1)	*Z. mays*	SP	Intercellular signalling component	Multiple nucellar cells adopt MMC identity	Sheridan et al. (1996), Wang et al. (2012a,b)
	AMEIOTIC1	*Z. mays*	AtSWI1-like	Regulator of meiosis: zygotene-leptotene transition	MMC undergoes mitosis instead of meiosis	Pawlowski et al. (2009)

Table 6 *(continued)*

Class	Gene	Species	Type	Function	Impact of altered function	Reference
Early gametophyte development	ARABIDOPSIS HISTIDINE KINASE1,2,3,4,5	*A. thaliana*	HK	Cytokinin receptor(s)	Knockouts lead to FG abortion	Cheng et al. (2013)
	ARABINOGALACTAN PROTEIN 18	*A. thaliana*	AGP	Cell wall glycoprotein, putative signalling molecule	Overexpression leads to multiple megaspores surviving	Demesa-Arevalo and Vielle-Calzada (2013)
	INDETERMINATE GAMETOPHYTE1	*Z. mays*	LBD TF	Regulator of cell identity	Additional egg cells, polar nuclei, and synergids	Evans (2007)
	DiSUMO-LIKE	*Z. mays*	SUMO	Regulates ubiquitylation/protein function	FG nuclei fail to polarise at stage FG5	Dresselhaus et al. (2010)
	ARGONAUTE5	*A. thaliana*	AGO	Effector of gene silencing	Dominant-negative version compromises FG development	Tucker et al. (2012)

Annual Plant Reviews Online, Volume 1. Edited by Jeremy Roberts.

nourishes the downstream events of seed development after fertilisation has taken place.

1.2 The Nucellus Fulfils Critical Roles as a Generative and Nutritive Tissue

The nucellus is also referred to as the megasporangium, and its main roles are to produce a germline progenitor cell, the megasporocyte (megaspore mother cell, MMC), and support the downstream events of germline development (megasporogenesis; Yadegari and Drews, 2004). In Arabidopsis, the nucel- lus is separated from maternal placental tissues through the growth of the chalaza and funiculus (Figure 1c). However, in species such as barley and wheat, a true funiculus is absent (Figure 1f–h). Similarly, in maize the funicu- lus is absent and the nucellus directly contacts the maternal plant through the pedicel, which is the site of sucrose supply from the phloem and selective uptake into the ovule (McLaughlin and Boyer, 2004; Tang and Boyer, 2013). Nucellar morphology varies greatly between species with regard to size and cell number (Lora et al., 2016). Evolutionary-derived angiosperms such as Arabidopsis produce tenuinucellar ovules with a prominent unicellular layer surrounding the MMC (Figure 1c) and a small number of hypodermal nucel- lar cells (Lora et al., 2016). Cereals such as maize are crassinucellar, producing a large MMC deep within a multilayered nucellus (Rudall, 1997; Voronova et al., 2003). There are varying reports that describe the barley ovule as being crassinucellar, intermediate between those with massive and delicate nucelli (Norstog, 1974), as nearly tenuinucellate at anthesis (Engell, 1989), tenuin- ucellate (Bennett et al., 1973), or as medionucellate, syndermal, and multi- layered (Shamrov, 1998). Despite this variation in terminology, it is clear that prior to fertilisation of the female gametophyte in barley, the nucellus is much more prominent than in tenuinucellate species such as Arabidopsis (compare Figure 1e and h). The role of an enlarged nucellus has been debated from an evolutionary perspective (Endress, 2011), but the question of how it forms in the cereals and acts to balance MMC formation, megasporogenesis, and downstream reproductive development, relative to what is known from Ara- bidopsis, is yet to be clearly addressed.

1.3 A One-way Street Ending in Female Gametophyte Production?

At the mechanistic level, most of our molecular knowledge regarding nucellus development has been derived from Arabidopsis. In brief, the young ovule is produced through redundant activities of the MADS-box transcription factors SEEDSTICK (STK; Table 1) and SHATTERPROOF (SHP1/2) in the placenta, the tissue formed through fusion of the two carpels. Ovule primordia consist of three domains including the distal

nucellus where the germline initiates, the central chalaza, and proximal funiculus (Figure 1c; Grossniklaus and Schneitz, 1998). These domains are initially defined by distinct gene expression patterns, rather than obvious differences in cellular morphology. In wild-type Arabidopsis, a single germline precursor cell (Megaspore mother cell; MMC) forms in the centre of the nucellus and expands much faster than the surrounding cells (Figure 1c; Lora et al., 2016). During expansion, the MMC exhibits a unique gene expression profile compared to the surrounding cells (Schmidt et al., 2011). Remarkably, many genes that influence female germline development in Arabidopsis are expressed in nucellar cells surrounding the MMC. In this sense, the nucellus appears to mimic the function of escort stem cells found in the drosophila ovary stem cell niche, which provide specific signals to maintain female gametogenesis (Decotto and Spradling, 2005). The Ara- bidopsis 'nucellus genes' include both positive and negative regulators of germline development (Table 1); for example, the nuclear protein encoded by *SPOROCYTLESS* (SPL) maintains nucellar cell identity (Wei et al., 2015; Yang et al., 1999), the WUSCHEL (WUS) transcription factor establishes the boundary between the distal and central ovule domains (Groß-Hardt et al., 2002) with support from HD-ZIP Class III genes and BEL1 (Yamada et al., 2016), and the small WINDHOSE (WIH) proteins appear to influence aspects of nucellar cell shape (Lieber et al., 2011). Plants lacking SPL, WUS, or WIH1/2 fail to form a functional female germline. Conversely, small RNA pathways acting downstream of ARGONAUTE9 (AGO9) restrict germline development, and mutants display additional germline-like cells in the ovule (Olmedo-Monfil et al., 2010). AGO9 appears to act with RNA-DEPENDENT RNA POLYMERASE 6 (RDR6) and a small RNA intermediate to regulate gene expression via RNA-dependent DNA methylation (RdDM). The protein-coding targets of this pathway have proven elusive, but a recent report indicates that trans-acting small interfering RNA (tasiRNA)-mediated regulation of ETTIN/AUXIN RESPONSE FACTOR 3 (ARF3) is likely to be involved (Su et al., 2017). Regulation of phytohormone transport and response has also been linked to SPL, which modulates expression of the auxin efflux carrier PIN FORMED1 (PIN1), and WUS, which controls cytokinin response through the *ARABIDOPSIS RESPONSE REGULATOR* genes (Bencivenga et al., 2012; Leibfried et al., 2005). It is tempting to speculate that AGO9, SPL, and WUS form an interrelated regulatory net- work controlling signal flow and response in the developing ovule. Such a system would ensure a number of basic criteria: responsive cell types (the nucellus), positional information to direct the response (auxin flow through the epidermis and/or cytokinin accumulation), pathways that restrict the response to a single cell (sRNA molecules), and secondary signals that drive differentiation (such as cell wall genes; reviewed in Tucker and Koltunow, 2014).

To date it remains unclear whether a similar molecular framework supports nucellus development in the cereals. Various MADS-box genes including *OsMADS13*, the rice D-class homologue of Arabidopsis *STK* (Dreni et al., 2007; Groß-Hardt et al., 2002), and the B_{sister} gene *OsMADS29* (Yang et al., 2012) impact ovule development. In terms of germline development, mutations in the maize *AGO104* gene (a homologue of Arabidopsis AGO9) lead to defects in female meiosis and megagametogenesis, despite being expressed outside the germline in nucellar cells (Singh et al., 2011). AGO104 is required for correct DNA methylation, suggesting that RdDM pathways may be conserved during ovule development between the dicots and the monocots. The *MULTIPLE SPOROCYTES* (*MSP1*) gene from rice encodes a leucine-rich repeat receptor-like protein kinase (Nonomura et al., 2003), while *MULTIPLE ARCHESPORIAL CELLS1* (*MAC1*) encodes the maize homologue of TAPETUM DETERMINANT-LIKE 1A (TDL1a; Sheridan et al., 1996; Wang et al., 2012a,b), a small peptide that appears to act as a ligand for MSP1-like receptors (Zhao et al., 2008). Mutations in these genes lead to the formation of extra germline-like cells. Although homologues of these receptors and ligands are expressed in the Arabidopsis ovule, and ectopic expression causes infertility (Huang et al., 2015), a precise loss-of-function phenotype has yet to be demonstrated.

2. Life After Death: the Nutritive Role of the Nucellus

In species such as Arabidopsis, the epidermal layer of the nucellus collapses during germline development, and sub-epidermal nucellar cells are difficult to trace after the completion of gametogenesis. Xu et al. (2016) suggest that a cluster of cells positioned at the chalazal end of the ovule represent persistent nucellar cells, and these degenerate after fertilisation in a process dependent on AGAMOUS-like 62 (AGL62) and central cell fertilisation. Degradation of these cells is possibly required to make space for development of the chalazal endosperm.

In cereal ovules, the bulk of the nucellus persists until after fertilisa- tion, switching from a tissue that supports gametogenesis to one that transfers maternal nutrients to the nascent grain (Figure 2). During this transition, nucellus morphology changes dramatically; by 6 days after pollination (DAP), the majority of nucellar tissue is no longer present as it has undergone programmed cell death (PCD). However, the region of nucellus between the main vascular bundle and the ventral crease of the developing grain is retained and differentiates into the nucellar projection (NP; Figure 2a,b; Duffus and Cochrane, 1992). Instigated by an increase in the ratio of gibberellic acid to abscisic acid (Weier et al., 2014), differentiation of the NP is crucial for survival of the ovule and grain after fertilisation.

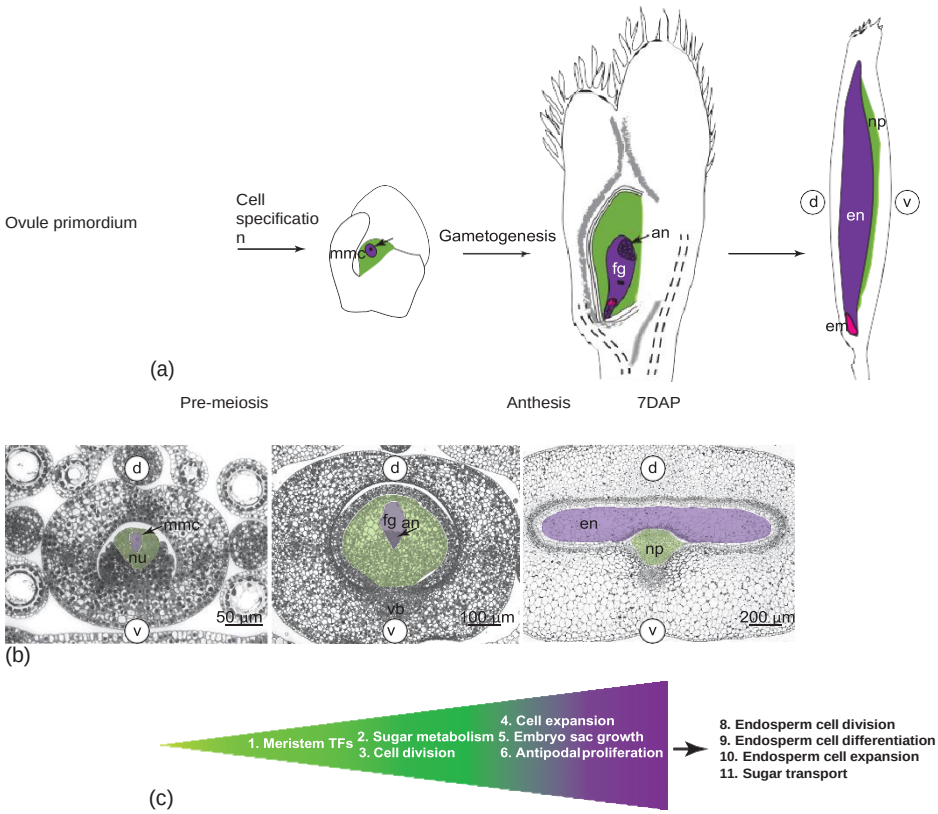

Figure 2 Nucellus development in barley. (a) A schematic representation of barley carpel, ovule, and grain development, presented in the sagittal plane. Different ovule tissues including the nucellus (green) and female gametophyte/embryo sac (purple) are indicated. (b) Transverse sections of barley ovules at pre-meiosis and anthesis stages, and a developing grain at 7 days after pollination. The ovule in barley forms from placental tissue, and the nucellus can be easily distinguished after integument initiation, consisting of both L1 and L2 cell types. Nucellar cells undergo divisions and expansion, concurrent with integument growth and female gametophyte development, and at anthesis contribute most of the ovule tissue. After fertilisation, the majority of the nucellar tissue degenerates via programmed cell death, and the remainder differentiates to form the nucellar projection that funnels maternal nutrients into the endosperm through the endosperm transfer cells. (c) Many pathways contribute to ovule and nucellus development and function. Variation in the size of the nucellus might be explained by primary differences in floral meristem size or secondary changes in sugar metabolism, nucellar cell division and/or expansion, or variation in the size of other ovule tissues including the embryo sac, antipodals, and integuments. After fertilisation, the nucellus continues to influence grain development through control of sugar transport and endosperm division, differentiation, and expansion. an, antipodals; em, embryo; fg, female gametophyte; d, dorsal; en, endosperm; v, ventral; np, nucellar projection; DAP, days after pollination; nu, nucellus; mmc, megaspore mother cell; vb, main provascular bundle. Bars indicate the relative size of each transverse section.

2.1 Molecular Components of Nucellar Degeneration

Components of post-fertilisation nucellus development have been examined in several species. *OsMADS29* is expressed in the nucellus, NP, tapetum, and vascular bundle of the anther and stimulates production of a cysteine protease (LOC_Os02g07430) integral to nucellar PCD, as well as regulating other PCD-associated genes and auxin signalling pathways (Yin and Xue, 2012). Initially characterised in rice (Yin and Xue, 2012), homologues of *MADS29* have been isolated in maize (Chen et al., 2015) and barley (Thiel et al., 2008). Also in barley, eight vacuolar processing enzyme (VPE) iso- forms have been characterised (HvVPE1, HvVPE2a, HvVPE2b, HvVPE2c, HvVPE2d, HvVPE3, HvVPE4, and LEG8; Radchuk et al., 2011; Julián et al., 2013) that participate in post-fertilisation ovary development. Initially called 'nucellain', *HvVPE2a*, a cysteine protease of the C13 protease family, was one of the initial genes identified in the barley ovule (Doan et al., 1996; Linnestad et al., 1998). Alongside research describing similar roles for the four *VPE* genes in Arabidopsis (Nakaune et al., 2005; Shimada et al., 2003), there is strong support for nucellain *HvVPE2b* and *HvVPE2d* acting in barley nucellar PCD.

Most of the nucellar degeneration events initiate rapidly upon fertilisa- tion. DNA fragmentation assays suggest that in barley, PCD initiates in the inner nucellus layers and spreads to outer layers within 2 days of pollina- tion (Radchuk et al., 2011). At 2–4 DAP, an aspartic protease called 'nucellin' is expressed in nucellar tissues surrounding the vascular bundle (Chen and Foolad, 1997; Gubatz et al., 2007), as well as in the embryo, pollen, and apical meristems (Bi et al., 2005). A rice orthologue, *OsAsp1,* shows similar spatial and temporal expression (Bi et al., 2005) suggesting a conserved role in nucel- lar degeneration, although the targets of proteolysis remain unclear. Uniquely in barley, a protein encoded by *Jekyll* is expressed in the maternal tissue sur- rounding the male and female gametophytes (Radchuk et al., 2006). Peak expression of *Jekyll* occurs in the nucellar tissue around the vascular bundle at 4–6 DAP, concurrent with NP differentiation and nucellar PCD. Severe dis- ruption of grain fill in *Jekyll* knockdown plants, in which differentiation and PCD of the nucellar tissue is impaired, demonstrates that PCD of nucellar tissues is crucial for later stages of grain development (Radchuk et al., 2006).

2.2 The Nucellar Projection Feeds the Seed

Research in barley, wheat, and maize indicates that the NP (Figure 2b) is the site of release of photoassimilates and other nutrients from the mater- nal tissue for uptake by adjacent endosperm transfer cells (Sreenivasulu et al., 2002; Tang and Boyer, 2013; Thiel et al., 2009; Weschke et al., 2003). Sucrose, the major photoassimilate, is an essential source of carbon required for development of different cell types and energy reserves (e.g. starch)

within the developing grain (reviewed by Ludewig and Flügge, 2013). Once unloaded from the phloem, invertase (INV), and sucrose synthase (SuSy) enzymes hydrolyse sucrose into its constituent hexoses, fructose, and glucose. This metabolism reduces the local sucrose concentration, thus maintaining a high concentration gradient between source and sink tissues, osmotically driving sucrose unloading (McLaughlin and Boyer, 2004; Ruan et al., 2012). Different invertase isoforms locate to the cell wall (CWIN), cytoplasm (CIN), or vacuole (VINs) and have their activity regulated by specific inhibitors (INVINH/PMEI). Expression of the sucrose transporters SUT1 and SUT2, and HvCWIN1/2, have been observed from 1 to 6 DAP in the NP, endosperm transfer cells, and nucellar tissues of barley and maize (Cheng et al., 1996; Weschke et al., 2000, 2003). A recent report suggests that HvSUT2 and HvSUT1 control sucrose homeostasis during grain fill, and downregulation leads to reduced endosperm starch content and dry weight (Radchuk et al., 2017). Other members of these sugar metabolism-related families accumulate in developing ovules of cotton (Wang et al., 2014) and the grass species *Brachiaria* (Dusi and Willemse, 1999). Furthermore, recent studies suggest that photoassimilates interact with hormonal pathways to regulate aspects of development, an area that has not been explored in detail in the cereals (see Liu et al., 2013 for review).

2.3 What does Nucellus PCD Achieve?

Although studies have demonstrated that changes in nucellus PCD can have negative impacts on grain development (Radchuk et al., 2006), the specific role of early post-fertilisation PCD remains elusive. This is partly due to the difficulty in disentangling the events of PCD from NP differentiation and early endosperm development. Concurrent with nucellar degeneration, the NP differentiates, which is critical for maternal nutrient transfer into the endosperm (Radchuk et al., 2006). In barley, however, the NP does not fully differentiate until around five DAP, suggesting that nutrients supporting the initial endosperm divisions may come from a local source rather than from the phloem. In the grasses, these nutrients may already be available within the embryo sac, where a large number of transient antipodal cells reside (Chettoor and Evans, 2015). Alternatively, it is also possible that remobilisa- tion of reserves from nucellar cells by PCD provides a local nutrient source for early endosperm divisions and cellularisation, which would require local transport into the embryo sac. As discussed earlier, collapse of the nucellar cells coincides with expression of a diverse array of proteolytic enzymes, α-amylase and phosphoenolpyruvate carboxylase (Domínguez and Cejudo, 2014; Sreenivasulu et al., 2006; Tran et al., 2014; Van Hautegem et al., 2015), suggesting that specific amino acids and glucose may support differentiation of the NP and/or rapid endosperm proliferation. Alternatively (but not mutually exclusively), nucellus PCD may release physical constraints on

the embryo sac, permitting expansion during endosperm divisions. Studies in barley suggest that nucellus size at anthesis varies between cultivars (Wilkinson and Tucker, 2017), but the mechanistic basis and contribution to grain development remains unclear (Figure 2c).

3. The Role of Pre-anthesis Female Tissues in Downstream Grain Development

The size of cereal carpels (ovaries) and grain varies along the inflorescence. In wheat (Benincasa et al., 2017; Calderini and Reynolds, 2000; Xie et al., 2015), barley (Guo et al., 2015, 2016; Scott et al., 1983), and sorghum (Yang et al., 2009), grain weight has a strong genetic component determined before anthe- sis, which is in part due to carpel size. Florets in the middle of the spike tend to be bigger, make bigger grain, and are less influenced by environmental stress than those at the tips (Guo et al., 2015), while the size of barley carpels at distal positions along the spike is positively correlated with the number of grains per spike (Guo et al., 2015, 2016; Scott et al., 1983; Yang et al., 2009; Benincasa et al., 2017; Calderini and Reynolds, 2000; Xie et al., 2015). In a recent study, Reale et al. (2017) found that variation in wheat ovary size was due to increased cell numbers rather than cell size. In barley, the size of carpels during meiosis is positively correlated with carpel weight at anthesis (Scott et al., 1983), while in sorghum, floret meristem size is positively linked to ovary volume (Yang et al., 2009). In the same sorghum study, a positive cor- relation was identified between the number of ovary cells and grain weight (Yang et al., 2009). These studies indicate that changes in growth during early (pre-anthesis) stages of floral development impact downstream grain pro- duction. The basis for variation might range from the control of primordial size through to modified sugar metabolism, tissue-specific cell division, cell expansion, antipodal proliferation, and/or integument growth (Figure 2c). The genes underlying this variation may therefore be of interest for down- stream application in breeding programs.

4. A Role for the Ovary in Stress Tolerance

The events of floral initiation, germline development, fertilisation, and grain fill may be compromised by environmental stress (Barnabas et al., 2008; Driedonks et al., 2016; Saini and Westgate, 1999).

The specific effects of stress during early reproductive development have been most closely examined in anthers, and these include meiotic arrest, microspore abortion, and heat-induced differential expression of many genes (Giorno et al., 2013; Jain et al., 2010; Oshino et al., 2007). With regard

to the ovary, less information is available, although studies indicate that both pre- and post-fertilisation stages of ovary development are sensitive (Bac-Molenaar et al., 2015; Sun et al., 2004; Zinn et al., 2010).

In Arabidopsis, single treatments of heat stress compromise meiosis in both male and female reproductive organs, leading to severe reductions in yield (Bac-Molenaar et al., 2015). Similarly in wheat, both male and female tissues are particularly sensitive to heat stress in the week preceding anthesis, which encapsulates meiosis and gametophyte development (Saini et al., 1983). In general, there is a negative correlation between ambient temperatures over 15 °C in the 30 days preceding anthesis and yield in cereal species (Ferris et al., 1998; Fischer, 1985; Sage et al., 2015). At the cellular level, Arabidopsis ovules show defects in megagametogenesis (Sun et al., 2004), ovule abortion, and reduced ovule number (Bac-Molenaar et al., 2015) after heat or salt stress. In one of the few studies to report cytological details of female development in cereals under stress, wheat exposed to severe heat stress at the start of meiosis experienced disrupted nucellus and integument development, or complete ovule abortion at a frequency of 30% (Saini et al., 1983). In both wheat and rice, heat stress also affects stigma receptivity and length, reflecting alteration of stigma structural development under conditions of stress (Jagadish et al., 2010; Saini et al., 1983).

Similar to heat stress, pre-fertilisation water stress can have severe effects on downstream grain development (Bac-Molenaar et al., 2015; Saini et al., 1983; Ferris et al., 1998; Fischer, 1985; Sage et al., 2015; Giorno et al., 2013; Jain et al., 2010; Oshino et al., 2007; Sun et al., 2004; Zinn et al., 2010; Jagadish et al., 2010). Waterlogging during anthesis, for example reduces barley and wheat grain number by up to 79% and 92%, respectively (de San Celedonio et al., 2014). At the other extreme, wheat subjected to water deficit during meiosis exhibited a high level of pollen sterility and a 50% reduction in grain yield (Dorion et al., 1996). In general, the wheat anther is less tolerant of drought conditions than the ovary, and ovary tissue is better able to recover from short-term (4 days) water deficit upon water re-availability (Ji et al., 2010). Saini and Aspinall (1981) reported that wheat ovaries are unaffected by water deficit during meiosis, while pollen development aborts during microsporogenesis. In a recent study, however, Onyemaobi et al. (2016) examined the effect of water stress in 13 wheat genotypes and found that 4 showed reduced seed set as a result of reduced female fertility. Although the genetic basis for this variability remains unclear, molecular evidence suggests that wheat ovaries from different cultivars show differential responses to stress. For example, in a study comparing sensitive and tolerant cultivars, Ji et al. (2010) showed that upon drought stress at the 'young microspore' stage, expression of cell wall invertase *IVR1* and sucrose 1-fructosyl-transferase (1-SST) are downregulated in the ovary of drought sensitive wheat cultivars, while in drought-tolerant cultivars, 1-SST is upregulated (Zinn et al., 2010).

4.1 Sugar as a Mediator of Pre-anthesis Female Stress Tolerance

Photoassimilates are an important determinant of reproductive resilience in both male and female tissues. Sugar limitation under heat and/or water stress is a major component of fruit and seed abortion (Barnabas et al., 2008; Boyer and McLaughlin, 2007), and studies show that modified sugar accumulation through the manipulation of INV or INVINH levels can alleviate some of these defects (see Liu et al., 2013 for review). In maize, for example water deficit imposed throughout anthesis leads to simultaneous accumulation of sucrose and depletion of sucrose metabolites in the ovary (Zinselmeier et al., 1995). This is accompanied by a reduction in invertase activity and increased ovule abortion, resulting in kernel number being reduced by 60% (Zinselmeier et al., 1999). Maize soluble acid invertase *IVR2* is expressed at the site of phloem unloading in the pedicel and within the basal region of the nucellus and is repressed by drought imposed 6 days before fertilisation (Andersen et al., 2002). Other studies show that invertase is active within the nucellus of diverse species including *Brachiaria* (Dusi and Willemse, 1999), *Gasteria* (Wittich and Willemse, 1999) and maize (McLaughlin and Boyer, 2004), creating a glucose gradient that enhances the sink strength of the ovule. McLaughlin and Boyer (2004) found that low water potential within the maize plant reduced photosynthesis and glucose and starch levels within the floret stem (pedicel) and led to high levels of ovule abortion. However, by feeding sucrose into water-deprived maize plants during anthesis, ovule abortion could be alleviated.

Similar sugar-related pathways appear to modulate the response to salt stress. In maize, salt stress inhibits invertase activity and has a stronger effect on kernel number than drought stress (Hütsch et al., 2015), limiting yield by reducing kernel number by 50% (Hütsch et al., 2014). Under salt stress condi- tions, plasma membrane H + ATPase activity is greatly inhibited within the ovary, lowering the pH gradient across the plasma membrane sufficiently to prevent proper function of hexose transporters and hexose metabolism within the maize ovary at anthesis and in the initial days of grain filling (Jung et al., 2017).

Collectively these studies suggest that photoassimilate accumulation and metabolism prior to fertilisation moderate the female response to stress. In the context of maize at least, water deficit and altered sugar metabolism during pre-anthesis stages have a more severe impact upon yield (grain number) than deficit after anthesis, as pre-anthesis stress causes female abortion rather than a reduction in kernel size. Based on the prominent size and position of the nucellus in the ovule surrounding the germline cells, and its role in nutrient accumulation and metabolism, it may represent a central component of female stress tolerance in different cereal species and cultivars.

5 Technical Advances to Expand Understanding of Germline Formation, Sugar Metabolism, and Stress Tolerance in Cereal Ovules

The diverse ovule signals and effectors balancing germline formation and nutrient flow have been difficult to identify, mainly because the tiny tissues involved are buried deep within the flower and are challenging to access for high-throughput imaging and molecular and cell biological analysis. How- ever, recent technological advances have seen methods evolve to the level where interactions between ovule cell types can be examined in greater detail, both in model dicots and commercially relevant cereal species.

Cells within the ovule can be observed at high resolution through advances in whole-mount clearing (Kurihara et al., 2015; Wilkinson and Tucker, 2017) and deep-tissue live imaging (Kimata et al., 2016). The chemical composi- tion of ovule cells can potentially be assessed through mass spectroscopy (MS) imaging (Peukert et al., 2016) or infrared (IR) microscopy (Warren et al., 2015), while molecular signatures can be generated through laser capture microdissection (LCM; also known as laser-assisted microdissection, LAM) and high-throughput transcriptomics (Okada et al., 2013; Tucker et al., 2012; Wuest and Grossniklaus, 2014). In cereals such as rice, LCM has been used to generate stage-specific profiles of ovule development, which reveal the dynamic transcriptional behaviour of many regulatory (Figure 3a–d) and metabolic (Figure 3e–f) genes discussed in this article (Kubo et al., 2013). For example, specific members of the MADS-box (Figure 3a), WUSCHEL-RELATED HOMEOBOX (Figure 3b), and ARG-

ONAUTE (Figure 3d) families show stage-specific expression patterns that may reflect important general or cell-type-specific roles in ovule and nucellus development.

As an alternative to LCM, cell sorting via flow cytometry (fluorescence acti- vated cell sorting; FACS) has recently been used to generate cell-type-specific profiles from the Arabidopsis placenta (Villarino et al., 2016) and MMC (Zhao et al., 2014). Although suited mainly to the diverse fluorescent marker gene resources available for Arabidopsis, the increased availability and flexibil- ity of fluorescent tags provides an avenue by which FACS techniques might be applied more generally in cereal species (Yang et al., 2017). Even greater cell-type-specific resolution is available through the application of microflu- idic systems such as the Fluidigm C1 (Clark et al., 2016), which has the poten- tial to provide unique transcriptomic, genomic, and epigenetic profiles for individual reproductive cells.

Once identified, key molecular signatures of the female reproductive cells can be dissected using genetic resources such as CRISPR/Cas9 (Zong et al., 2017), natural diversity panels (Muñoz-Amatriaín et al., 2014), and sequenced mutant resources (Cavanagh et al., 2008; Wang et al., 2012a,b).

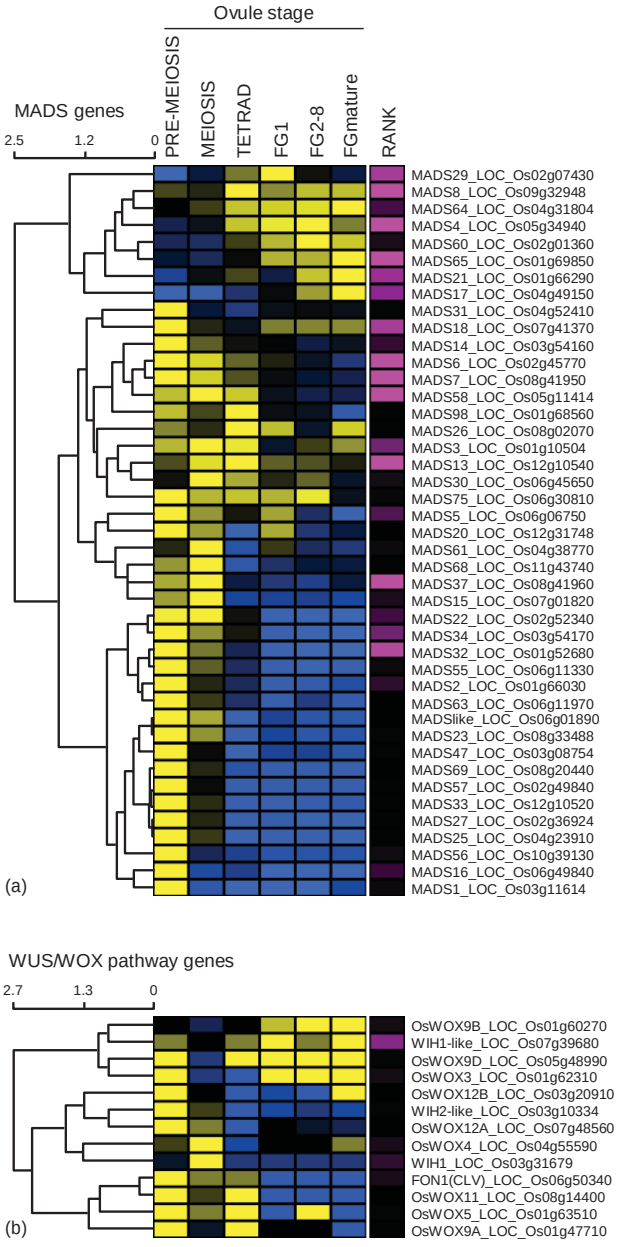
Ovule stage
PRE-MEIOSIS
MEIOSIS
TETRAD
FG1
FG2-8
FGmature
RANK
MADS genes
2.5
1.2
0
MADS29_LOC_Os02g07430
MADS8_LOC_Os09g32948
MADS64_LOC_Os04g31804
MADS4_LOC_Os05g34940
MADS60_LOC_Os02g01360
MADS65_LOC_Os01g69850
MADS21_LOC_Os01g66290
MADS17_LOC_Os04g49150
MADS31_LOC_Os04g52410
MADS18_LOC_Os07g41370
MADS14_LOC_Os03g54160
MADS6_LOC_Os02g45770
MADS7_LOC_Os08g41950
MADS58_LOC_Os05g11414
MADS98_LOC_Os01g68560
MADS26_LOC_Os08g02070
MADS3_LOC_Os01g10504
MADS13_LOC_Os12g10540
MADS30_LOC_Os06g45650
MADS75_LOC_Os06g30810
MADS5_LOC_Os06g06750
MADS20_LOC_Os12g31748
MADS61_LOC_Os04g38770
MADS68_LOC_Os11g43740
MADS37_LOC_Os08g41960
MADS15_LOC_Os07g01820
MADS22_LOC_Os02g52340
MADS34_LOC_Os03g54170
MADS32_LOC_Os01g52680
MADS55_LOC_Os06g11330
MADS2_LOC_Os01g66030
MADS63_LOC_Os06g11970
MADSlike_LOC_Os06g01890
MADS23_LOC_Os08g33488
MADS47_LOC_Os03g08754
MADS69_LOC_Os08g20440
MADS57_LOC_Os02g49840
MADS33_LOC_Os12g10520
MADS27_LOC_Os02g36924
MADS25_LOC_Os04g23910
MADS56_LOC_Os10g39130
MADS16_LOC_Os06g49840
MADS1_LOC_Os03g11614
(a)
WUS/WOX pathway genes
2.7
1.3
0
OsWOX9B_LOC_Os01g60270
WIH1-like_LOC_Os07g39680
OsWOX9D_LOC_Os05g48990
OsWOX3_LOC_Os01g62310
OsWOX12B_LOC_Os03g20910
WIH2-like_LOC_Os03g10334
OsWOX12A_LOC_Os07g48560
OsWOX4_LOC_Os04g55590
WIH1_LOC_Os03g31679
FON1(CLV)_LOC_Os06g50340
OsWOX11_LOC_Os08g14400
OsWOX5_LOC_Os01g63510
OsWOX9A_LOC_Os01g47710
(b)

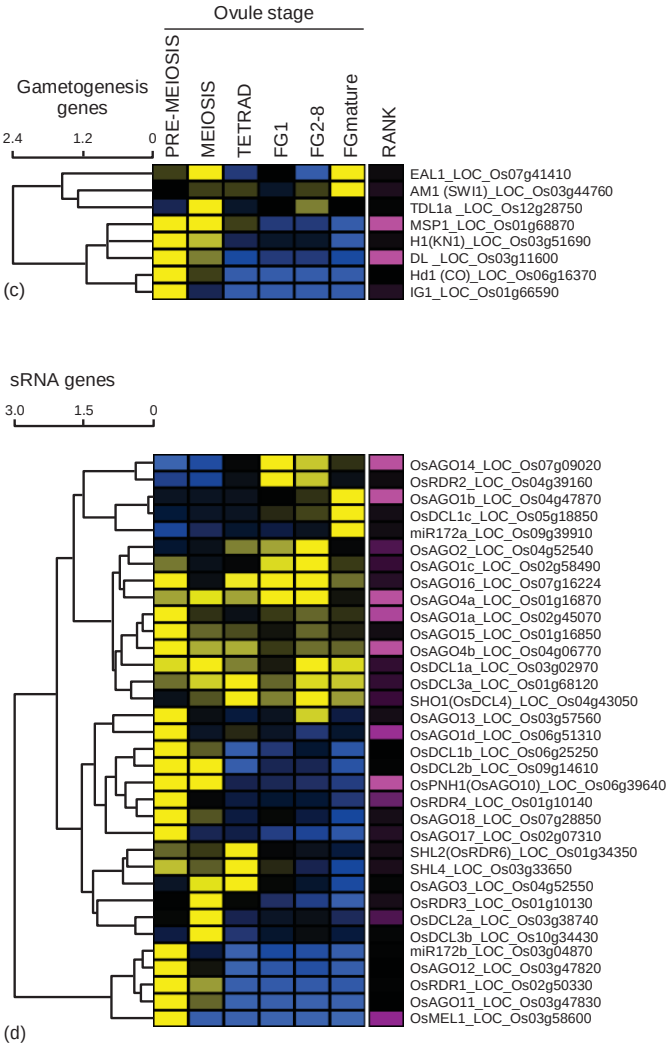
Ovule stage
PRE-MEIOSIS
MEIOSIS
TETRAD
FG1
FG2-8
FGmature
RANK
Gametogenesis genes
2.4
1.2
0
EAL1_LOC_Os07g41410
AM1 (SWI1)_LOC_Os03g44760
TDL1a _LOC_Os12g28750
MSP1_LOC_Os01g68870
H1(KN1)_LOC_Os03g51690
DL _LOC_Os03g11600
Hd1 (CO)_LOC_Os06g16370
IG1_LOC_Os01g66590
(c)
sRNA genes
3.0
1.5
0
OsAGO14_LOC_Os07g09020
OsRDR2_LOC_Os04g39160
OsAGO1b_LOC_Os04g47870
OsDCL1c_LOC_Os05g18850
miR172a_LOC_Os09g39910
OsAGO2_LOC_Os04g52540
OsAGO1c_LOC_Os02g58490
OsAGO16_LOC_Os07g16224
OsAGO4a_LOC_Os01g16870
OsAGO1a_LOC_Os02g45070
OsAGO15_LOC_Os01g16850
OsAGO4b_LOC_Os04g06770
OsDCL1a_LOC_Os03g02970
OsDCL3a_LOC_Os01g68120
SHO1(OsDCL4)_LOC_Os04g43050
OsAGO13_LOC_Os03g57560
OsAGO1d_LOC_Os06g51310
OsDCL1b_LOC_Os06g25250
OsDCL2b_LOC_Os09g14610
OsPNH1(OsAGO10)_LOC_Os06g39640
OsRDR4_LOC_Os01g10140
OsAGO18_LOC_Os07g28850
OsAGO17_LOC_Os02g07310
SHL2(OsRDR6)_LOC_Os01g34350
SHL4_LOC_Os03g33650
OsAGO3_LOC_Os04g52550
OsRDR3_LOC_Os01g10130
OsDCL2a_LOC_Os03g38740
OsDCL3b_LOC_Os10g34430
miR172b_LOC_Os03g04870
OsAGO12_LOC_Os03g47820
OsRDR1_LOC_Os02g50330
OsAGO11_LOC_Os03g47830
OsMEL1_LOC_Os03g58600
(d)

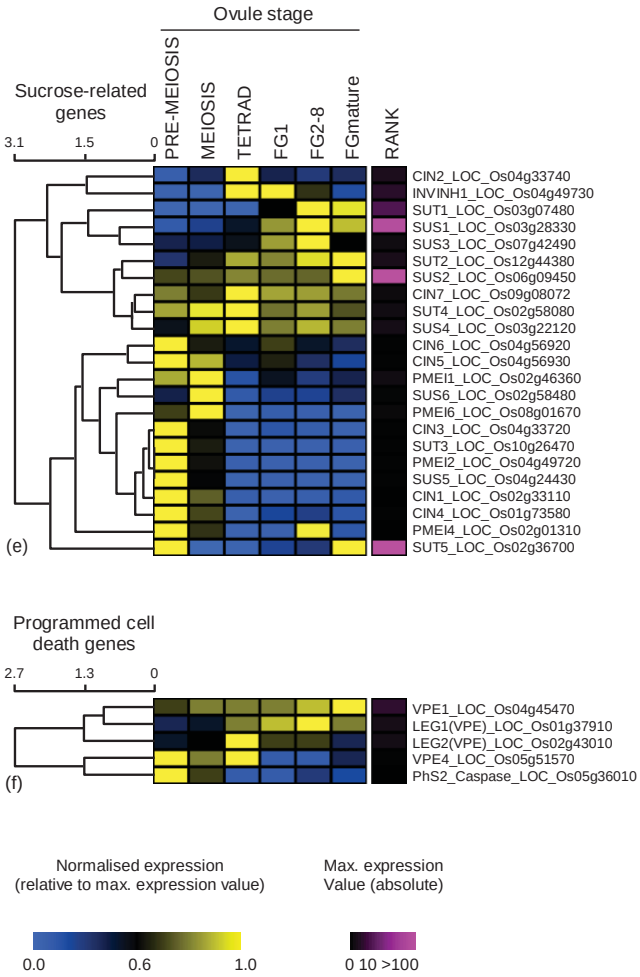
Ovule stage
PRE-MEIOSIS
MEIOSIS
TETRAD
FG1
FG2-8
FGmature
RANK
Sucrose-related genes
3.1
1.5
0
CIN2_LOC_Os04g33740
INVINH1_LOC_Os04g49730
SUT1_LOC_Os03g07480
SUS1_LOC_Os03g28330
SUS3_LOC_Os07g42490
SUT2_LOC_Os12g44380
SUS2_LOC_Os06g09450
CIN7_LOC_Os09g08072
SUT4_LOC_Os02g58080
SUS4_LOC_Os03g22120
CIN6_LOC_Os04g56920
CIN5_LOC_Os04g56930
PMEI1_LOC_Os02g46360
SUS6_LOC_Os02g58480
PMEI6_LOC_Os08g01670
CIN3_LOC_Os04g33720
SUT3_LOC_Os10g26470
PMEI2_LOC_Os04g49720
SUS5_LOC_Os04g24430
CIN1_LOC_Os02g33110
CIN4_LOC_Os01g73580
PMEI4_LOC_Os02g01310
SUT5_LOC_Os02g36700
(e)
Programmed cell death genes
2.7
1.3
0
VPE1_LOC_Os04g45470
LEG1(VPE)_LOC_Os01g37910
LEG2(VPE)_LOC_Os02g43010
VPE4_LOC_Os05g51570
PhS2_Caspase_LOC_Os05g36010
(f)
Normalised expression
(relative to max. expression value)
0.0
0.6
1.0
Max. expression
Value (absolute)
0 10 >100

Figure 3 Transcript accumulation patterns of regulatory and metabolic genes during ovule development in rice. Kubo et al. (2013) used laser microdissection to capture tissues from consecutive stages of *O. sativa* ovule development. Transcript accumulation patterns are shown for various gene families discussed in this article, which have been implicated in ovule development, gametogenesis, and/or nucellus growth. The stage names are assigned based on the staging reported in Kubo et al. (2013). Heatmaps show the expression at each stage relative to the maximum expression value for each gene (yellow indicates a stage where transcript is abundant) and the relative rank of each gene based on the absolute abundance of the maximum expression value (pink shows highly abundant genes). Genes were clustered using hierarchical clustering and Manhattan distance in Multiexperiment Viewer. Families examined include (a) MADS-box transcription factors, which have been shown to influence ovule and ovary development in many species (see Table 1); (b) WUSCHEL-related homeobox (WOX) genes that influence cell differentiation; (c) genes that are known to influence gametogenesis; (d) small-RNA pathway-related genes that influence many developmental events; (e) sucrose metabolism and transport-related genes, and (f) programmed cell death-related genes. Many of the genes examined are abundant during the earliest stage of ovule development examined. However, distinct clusters show stage-specific expression or gradual changes in transcript level over time, accompanying the progression of gametogenesis and nucellus development. Source: Kubo et al. (2013). Reproduced with permission of Oxford University Press.

Moreover, nowadays routine biochemical techniques such as chromatin immuno-precipitation sequencing (ChIPSeq) can be used to identify cell-type-specific targets of regulatory transcription factors (Zhang et al., 2017). Techniques that were once suited solely to simple 'model' species are now broadly applicable, presenting new opportunities for fundamental discovery and application in relevant crops.

6 Conclusion

The ovule is a complex organ that facilitates seed development and thus allows plant reproduction. Many years of research suggest that the ovule nucellus is a multifunctional tissue that balances generative and nutritive functions. Despite this, the capacity of the young growing nucellus to influence downstream events of seed development has not been explored in great detail. Avenues are now available to investigate this tissue further, with the overall aim of improving reproductive stress tolerance and grain traits.

Acknowledgements

We apologise to colleagues whose work we did not cite in this article. We wish to thank Matthew Aubert, Neil Shirley, Rachel Burton, Caitlin Byrt, Geoff Fincher, and Vincent Bulone for advice and support. Research in the Tucker lab is supported by an ARC Future Fellowship and DP180104092. L.G.W. is supported by a Research Training Program Scholarship and a top-up schol- arship from the ARC Centre of Excellence in Plant Cell Walls.

Related Articles

The Genetic and Molecular Control of Ovule Development The Central Role of the Ovule in Apomixis and Parthenocarpy The Ins and Outs of Ovule Development
Combinatorial Control of Floral Organ Identity by MADS-Domain Transcrip- tion Factors
Gynoecium Patterning in Arabidopsis: A Basic Plan Behind a Complex Struc- ture
Intercellular Communication during Floral Initiation and Development Floral Architecture: Regulation and Diversity of Floral Shape and Pattern Inflorescence Architecture
Floral Induction
Floral Patterning and Control of Floral Organ Formation Parthenocarpy in Crop Plants

References

Ambrose, B.A., Lerner, D.R., Ciceri, P. et al. (2000). Molecular and genetic analyses of the silky1 gene reveal conservation in floral organ specification between eudicots and monocots. *Molecular Cell* **5** (**3**): 569–579.

Andersen, M.N., Asch, F., Wu, Y. et al. (2002). Soluble invertase expression is an early target of drought stress during the critical, abortion-sensitive phase of young ovary development in Maize. *Plant Physiology* **130** (**2**): 591–604.

Bac-Molenaar, J.A., Fradin, E.F., Becker, F.F.M. et al. (2015). Genome-wide asso- ciation mapping of fertility reduction upon heat stress reveals developmental stage-specific QTLs in *Arabidopsis thaliana*. *The Plant Cell* **27**: 1857–1874.

Baker, S.C., Robinson-Beers, K., Villanueva, J.M. et al. (1997). Interactions among genes regulating ovule development in *Arabidopsis thaliana*. *Genetics* **145**: 1109–1124.

Barnabas, B., Jager, K., and Feher, A. (2008). The effect of drought and heat stress on reproductive processes in cereals. *Plant Cell and Environment* **31** (**1**): 11–38.

Bencivenga, S., Simonini, S., Benkova, E., and Colombo, L. (2012). The transcription factors BEL1

and SPL are required for cytokinin and auxin signaling during ovule development in Arabidopsis. *The Plant Cell* **24** (**7**): 2886–2897.
Benincasa, P., Reale, L., Tedeschini, E. et al. (2017). The relationship between grain and ovary size in wheat: an analysis of contrasting grain weight cultivars under different growing conditions. *Field Crops Research* **210**: 175–182.
Bennett, M., Rao, M., Smith, J., and Bayliss, M. (1973). Cell development in the anther, the ovule, and the young seed of *Triticum aestivum* L. var. Chinese Spring. *Philosoph- ical Transactions of the Royal Society of London Series B, Biological Sciences* 39–81.
Bi, X.Z., Khush, G.S., and Bennett, J. (2005). The rice nucellin gene ortholog *OsAsp1* encodes an active aspartic protease without a plant-specific insert and is strongly expressed in early embryo. *Plant and Cell Physiology* **46** (**1**): 87–98.
Boden, S.A., Cavanagh, C., Cullis, B.R. et al. (2015). Ppd-1 is a key regulator of inflo- rescence architecture and paired spikelet development in wheat. *Nature Plants* **1**: 14016.
Bonnett, O. (1940). Development of the staminate and pistillate inflorescences of sweet corn. *Journal of Agricultural Research* **60**: 25–37.
Boyer, J.S. and McLaughlin, J.E. (2007). Functional reversion to identify controlling genes in multigenic responses: analysis of floral abortion. *Journal of Experimental Botany* **58** (**2**): 267–277.
Brambilla, V., Battaglia, R., Colombo, M. et al. (2007). Genetic and molecular interac- tions between BELL1 and MADS box factors support ovule development in Ara- bidopsis. *The Plant Cell* **19** (**8**): 2544–2556.
Calderini, D.F. and Reynolds, M.P. (2000). Changes in grain weight as a consequence of de-graining treatments at pre- and post-anthesis in synthetic hexaploid lines of wheat *Triticum durum* x *T. tauschii*. *Functional Plant Biology* **27** (**3**): 183–191.
Cavanagh, C., Morell, M., Mackay, I., and Powell, W. (2008). From mutations to MAGIC: resources for gene discovery, validation and delivery in crop plants. *Current Opinion in Plant Biology* **11** (**2**): 215–221.
Ceccato, L., Masiero, S., Sinha Roy, D. et al. (2013). Maternal control of PIN1 is required for female gametophyte development in Arabidopsis. *PLoS One* **8** (**6**): e66148.
Chen, F. and Foolad, M.R. (1997). Molecular organization of a gene in barley which encodes a protein similar to aspartic protease and its specific expression in nucellar cells during degeneration. *Plant Molecular Biology* **35** (**6**): 821–831.
Chen, J., Yi, Q., Song, Q. et al. (2015). A highly efficient maize nucellus protoplast system for transient gene expression and studying programmed cell death-related processes. *Plant Cell Reports* **34** (**7**): 1239–1251.
Cheng, C.Y., Mathews, D.E., Schaller, G.E., and Kieber, J.J. (2013). Cytokinin- dependent specification of the functional megaspore in the Arabidopsis female gametophyte. *The Plant Journal* **73** (**6**): 929–940.
Cheng, W.H., Taliercio, E.W., and Chourey, P.S. (1996). The *Miniature1 Seed* locus of maize encodes a cell wall invertase required for normal development of endosperm and maternal cells in the pedicel. *The Plant Cell* **8** (**6**): 971–983.
Chettoor, A.M. and Evans, M.M. (2015). Correlation between a loss of auxin signaling and a loss of proliferation in maize antipodal cells. *Frontiers in Plant Science* **6**: 186. Chuck, G., Meeley, R., Irish, E. et al. (2007). The maize tasselseed4 microRNA controls sex determination and meristem cell fate by targeting Tasselseed6/indeterminate
spikelet1. *Nature Genetics* **39** (**12**): 1517–1521.
Clark, S.J., Lee, H.J., Smallwood, S.A. et al. (2016). Single-cell epigenomics: powerful new methods for understanding gene regulation and cell identity. *Genome Biology* **17** (**1**): 72.

Cucinotta, M., Colombo, L., and Roig-Villanova, I. (2014). Ovule development, a new model for lateral organ formation. *Frontiers in Plant Science* **5**: 117.
de San Celedonio, R.P., Abeledo, L.G., and Miralles, D.J. (2014). Identifying the critical period for waterlogging on yield and its components in wheat and barley. *Plant and Soil* **378** (**1**): 265–277.
De Vries, A.P. (1971). Flowering biology of wheat, particularly in view of hybrid seed production—a review. *Euphytica* **20** (**2**): 152–170.
Decotto, E. and Spradling, A.C. (2005). The Drosophila ovarian and testis stem cell niches: similar somatic stem cells and signals. *Developmental Cell* **9** (**4**): 501–510.
Demesa-Arevalo, E. and Vielle-Calzada, J.P. (2013). The classical arabinogalactan pro- tein AGP18 mediates megaspore selection in Arabidopsis. *The Plant Cell* **25** (**4**): 1274–1287.
Diboll, A.G. (1968). Fine structural development of the megagametophyte of *Zea mays* following fertilization. *American Journal of Botany* **55** (**7**): 797–806.
Doan, D.N.P., Linnestad, C., and Olsen, O.A. (1996). Isolation of molecular markers from the barley endosperm coenocyte and the surrounding nucellus cell layers. *Plant Molecular Biology* **31** (**4**): 877–886.
Domínguez, F. and Cejudo, F.J. (2014). Programmed cell death (PCD): an essential process of cereal seed development and germination. *Frontiers in Plant Science* **5**: 366.
Dorion, S., Lalonde, S., and Saini, H.S. (1996). Induction of male sterility in wheat by meiotic-stage water deficit is preceded by a decline in invertase activity and changes in carbohydrate metabolism in anthers. *Plant Physiology* **111** (**1**): 137–145.
Dreni, L., Jacchia, S., Fornara, F. et al. (2007). The D-lineage MADS-box gene OsMADS13 controls ovule identity in rice. *The Plant Journal* **52** (**4**): 690–699.
Dresselhaus, T., Srilunchang, K.O., and Krohn, N.G. (2010). DiSUMO-like DSUL is required for nuclei positioning, cell specification and viability during female game- tophyte maturation in maize. *Development* **137** (**2**): 333–345.
Driedonks, N., Rieu, I., and Vriezen, W.H. (2016). Breeding for plant heat tolerance at vegetative and reproductive stages. *Plant Reproduction* **29** (**1–2**): 67–79.
Duffus, C. and Cochrane, M. (1992). Grain structure and composition. In: *Barley: Genetics, Biochemistry, Molecular Biology and Biotechnology* (ed. P.R. Shewry), 291–317. Wallingford: CAB International.
Dusi, D.M.A. and Willemse, M.T.M. (1999). Activity and localisation of sucrose syn- thase and invertase in ovules of sexual and apomictic *Brachiaria decumbens*. *Proto- plasma* **208** (**1–4**): 173–185.
Ebel, C., Mariconti, L., and Gruissem, W. (2004). Plant retinoblastoma homologues control nuclear proliferation in the female gametophyte. *Nature* **429** (**6993**): 776–780. Endress, P.K. (2011). Angiosperm ovules: diversity, development, evolution. *Annals of Botany* **107** (**9**): 1465–1489.
Engell, K. (1989). Embryology of barley: time course and analysis of controlled fertil- ization and early embryo formation based on serial sections. *Nordic Journal of Botany* **9** (**3**): 265–280.
Engell, K. (1994). Embryology of barley. IV. Ultrastructure of the antipodal cells of *Hordeum vulgare* L. cv. Bomi before and after fertilization of the egg cell. *Sexual Plant Reproduction* **7** (**6**): 333–346.
Evans, M.M.S. (2007). The indeterminate gametophyte1 gene of maize encodes a LOB domain protein required for embryo sac and leaf development. *The Plant Cell* **19** (**1**): 46.

Evans, M.M.S. and Grossniklaus, U. (2009). *Handbook of Maize: Its Biology*. New York: Springer.
Ferris, R., Ellis, R., Wheeler, T., and Hadley, P. (1998). Effect of high temperature stress at anthesis on grain yield and biomass of field-grown crops of wheat. *Annals of Botany* **82** (**5**):

631–639.
Fischer, R. (1985). Number of kernels in wheat crops and the influence of solar radia- tion and temperature. *The Journal of Agricultural Science* **105** (**2**):447–461.
Giorno, F., Wolters-Arts, M., Mariani, C., and Rieu, I. (2013). Ensuring reproduction at high temperatures: the heat stress response during anther and pollen development. *Plants* **2** (**3**): 489–506.
Gray-Mitsumune, M. and Matton, D.P. (2006). The egg apparatus 1 gene from maize is a member of a large gene family found in both monocots and dicots. *Planta* **223** (**3**): 618–625.
Groß-Hardt, R., Lenhard, M., and Laux, T. (2002). WUSCHEL signaling functions in interregional communication during Arabidopsis ovule development. *Genes & Development* **16** (**9**): 1129–1138.
Grossniklaus, U. and Schneitz, K. (1998). The molecular and genetic basis of ovule and megagametophyte development. *Seminars in Cell & Developmental Biology* **9** (**2**): 227–238.
Gubatz, S., Dercksen, V.J., Brüß, C. et al. (2007). Analysis of barley (Hordeum vulgare) grain development using three-dimensional digital models. *The Plant Journal* **52** (**4**): 779–790.
Guo, Z., Chen, D., and Schnurbusch, T. (2015). Variance components, heritability and correlation analysis of anther and ovary size during the floral development of bread wheat. *Journal of Experimental Botany* **66** (**11**): 3099–3111.
Guo, Z., Slafer, G.A., and Schnurbusch, T. (2016). Genotypic variation in spike fertility traits and ovary size as determinants of floret and grain survival rate in wheat. *Journal of Experimental Botany* **67** (**14**): 4221–4230.
Higashiyama, T., Yabe, S., Sasaki, N. et al. (2001). Pollen tube attraction by the synergid cell. *Science* **293** (**5534**): 1480–1483.
Huang, J., Wijeratne, A.J., Tang, C. et al. (2015). Ectopic expression of TAPE- TUM DETERMINANT1 affects ovule development in Arabidopsis. *Journal of Experimental Botany* **67** (**5**): 1311–1326.
Hütsch, B., Jung, S., and Schubert, S. (2015). Comparison of salt and drought stress effects on Maize growth and yield formation with regard to acid invertase activity in the kernels. *Journal of Agronomy and Crop Science* **201** (**5**):353–367.
Hütsch, B.W., Saqib, M., Osthushenrich, T., and Schubert, S. (2014). Invertase activity limits grain yield of maize under salt stress. *Journal of Plant Nutrition and Soil Science* **177** (**2**): 278–286.
Irish, E. (1997). Class II tassel seed mutations provide evidence for multiple types of inflorescence meristems in maize (Poaceae). *American Journal of Botany* **84** (**11**): 1502. Irish, E.E., Szymkowiak, E.J., and Garrels, K. (2003). The wandering carpel mutation of *Zea mays* (Gramineae) causes misorientation and loss of zygomorphy in flowers
and two-seeded kernels. *American Journal of Botany* **90** (**4**): 551–560.
Itoh, J.-I., Nonomura, K.-I., Ikeda, K. et al. (2005). Rice plant development: from zygote to spikelet. *Plant and Cell Physiology* **46** (**1**): 23–47.
Jagadish, S., Muthurajan, R., Oane, R. et al. (2010). Physiological and proteomic approaches to address heat tolerance during anthesis in rice (*Oryza sativa* L.). *Journal of Experimental Botany* **61** (**1**): 143–156.
Jain, M., Chourey, P.S., Boote, K.J., and Allen, L.H. (2010). Short-term high temperature growth conditions during vegetative-to-reproductive phase transition irreversibly compromise cell wall invertase-mediated sucrose catalysis and microspore meiosis in grain sorghum (*Sorghum bicolor*). *Journal of Plant Physiology* **167** (**7**): 578–582.
Jensen, W.A. (1973). Fertilization in flowering plants. *BioScience* **23** (**1**): 21–27.

Ji, X., Shiran, B., Wan, J. et al. (2010). Importance of pre-anthesis anther sink strength for maintenance of grain number during reproductive stage water stress in wheat. *Plant, Cell & Environment* **33** (**6**): 926–942.
Julián, I., Gandullo, J., Santos-Silva, L.K. et al. (2013). Phylogenetically distant barley legumains have a role in both seed and vegetative tissues. *Journal of Experimental Botany* **64** (**10**): 2929–2941.
Jung, S., Hütsch, B.W., and Schubert, S. (2017). Salt stress reduces kernel number of corn by inhibiting plasma membrane H+-ATPase activity. *Plant Physiology and Bio- chemistry* **113**: 198–207.
Kerstetter, R.A., Laudencia-Chingcuanco, D., Smith, L.G., and Hake, S. (1997). Loss-of-function mutations in the maize homeobox gene, knotted1, are defective in shoot meristem maintenance. *Development* **124** (**16**): 3045–3054.
Kimata, Y., Higaki, T., Kawashima, T. et al. (2016). Cytoskeleton dynamics control the first asymmetric cell division in Arabidopsis zygote. *Proceedings of the National Academy of Sciences* **101** (**49**): 14157–14162.
Klucher, K.M., Chow, H., Reiser, L., and Fischer, R.L. (1996). The AINTEGUMENTA gene of Arabidopsis required for ovule and female gametophyte development is related to the floral homeotic gene APETALA2. *The Plant Cell* **8** (**2**): 137–153.
Kubo, T., Fujita, M., Takahashi, H. et al. (2013). Transcriptome analysis of developing ovules in rice isolated by laser microdissection. *Plant Cell Physiology* **54** (**5**): 750–765. Kurihara, D., Mizuta, Y., Sato, Y., and Higashiyama, T. (2015). ClearSee: a rapid opti- cal clearing reagent for whole-plant fluorescence imaging. *Development* **142** (**23**):
4168–4179.
Kurihara, Y. and Watanabe, Y. (2004). Arabidopsis micro-RNA biogenesis through Dicer-like 1 protein functions. *Proceedings of the National Academy of Sciences* **101** (**34**): 12753–12758.
Laudencia-Chingcuanco, D. and Hake, S. (2002). The indeterminate floral apex1 gene regulates meristem determinacy and identity in the maize inflorescence. *Develop- ment* **129** (**11**): 2629–2638.
Leibfried, A., To, J.P, Busch, W. et al. (2005). WUSCHEL controls meristem function by direct regulation of cytokinin-inducible response regulators. *Nature* **438** (**7071**): 1172–1175.
Li, H., Liang, W., Yin, C. et al. (2011). Genetic interaction of OsMADS3, DROOPING LEAF, and OsMADS13 in specifying rice floral organ identities and meristem deter- minacy. *Plant Physiology* **156** (**1**): 263–274.
Li, H., Wu, Y., Zhao, Y. et al. (2016). Differential morphology and transcriptome profile between the incompletely fused carpels ovary and its wild-type in maize. *Science Reports* **6**: 32652.
Li, H., Peng, T., Wang, Q. et al. (2017). Development of incompletely fused carpels in maize ovary revealed by miRNA, target gene and phytohormone analysis. *Frontiers in Plant Science* **8**: 463.
Lieber, D., Lora, J., Schrempp, S. et al. (2011). Arabidopsis WIH1 and WIH2 genes act in the transition from somatic to reproductive cell fate. *Current Biology* **21** (**12**): 1009–1017.
Linnestad, C., Doan, D.N., Brown, R.C. et al. (1998). Nucellain, a barley homolog of the dicot vacuolar-processing protease, is localized in nucellar cell walls. *Plant Physiol- ogy* **118** (**4**): 1169–1180.
Liu, Y.-H., Offler, C.E., and Ruan, Y.-L. (2013). Regulation of fruit and seed response to heat and drought by sugars as nutrients and signals. *Frontiers in Plant Science* **4**: 282.
Lora, J., Herrero, M., Tucker, M.R., and Hormaza, J.I. (2016). The transition from somatic to germline identity shows conserved and specialized features during angiosperm evolution. *New Phytologist* **216** (**2**): 495–509.
Ludewig, F. and Flügge, U.-I. (2013). Role of metabolite transporters in source-sink carbon allocation. *Frontiers in Plant Science* **4**: 231.

Lynn, K., Fernandez, A., Aida, M. et al. (1999). The PINHEAD/ZWILLE gene acts pleiotropically in Arabidopsis development and has overlapping functions with the ARGONAUTE1 gene. *Development* **126** (**3**): 469–481.
Mallory, A.C., Hinze, A., Tucker, M.R. et al. (2009). Redundant and specific roles of the ARGONAUTE proteins AGO1 and ZLL in development and small RNA-directed gene silencing. *PLoS Genetics* **5** (**9**): e1000646.
McLaughlin, J.E. and Boyer, J.S. (2004). Sugar-responsive gene expression, invertase activity, and senescence in aborting maize ovaries at low water potentials. *Annals of Botany* **94** (**5**): 675–689.
Morel, J.B., Godon, C., Mourrain, P. et al. (2002). Fertile hypomorphic ARGONAUTE (ago1) mutants impaired in post-transcriptional gene silencing and virus resistance. *The Plant Cell* **14** (**3**): 629–639.
Moussian, B., Schoof, H., Haecker, A. et al. (1998). Role of the ZWILLE gene in the regulation of central shoot meristem cell fate during Arabidopsis embryogenesis. *EMBO Journal* **17** (**6**): 1799–1809.
Muñoz-Amatriaín, M., Cuesta-Marcos, A., Endelman, J.B. et al. (2014). The USDA barley core collection: genetic diversity, population structure, and potential for genome-wide association studies. *PLoS One* **9** (**4**): e94688.
Nagasawa, N., Miyoshi, M., Sano, Y. et al. (2003). SUPERWOMAN1 and DROOPING LEAF genes control floral organ identity in rice. *Development* **130** (**4**):705–718.
Nakaune, S., Yamada, K., Kondo, M. et al. (2005). A vacuolar processing enzyme, δVPE, is involved in seed coat formation at the early stage of seed development. *The Plant Cell* **17** (**3**): 876–887.
Nickerson, N.H. (1954). Morphological analysis of the maize ear. *American Journal of Botany* **41** (**2**): 87–92.
Noman, A., Fahad, S., Aqeel, M. et al. (2017). miRNAs: Major modulators for crop growth and development under abiotic stresses. *Biotechnology Letters* **39** (**5**): 685–700.
Nonomura, K.-I., Miyoshi, K., Eiguchi, M. et al. (2003). The MSP1 gene is necessary to restrict the number of cells entering into male and female sporogenesis and to initiate anther wall formation in rice. *The Plant Cell* **15** (**8**): 1728–1739.
Norstog, K. (1974). Nucellus during early embryogeny in barley: fine structure. *Botan- ical Gazette* **135** (**2**): 97–103.
Okada, T., Hu, Y., Tucker, M.R. et al. (2013). Enlarging cells initiating apomixis in *Hieracium praealtum* transition to an embryo sac program prior to Entering Mitosis. *Plant Physiology* **163** (**1**): 216.
Olmedo-Monfil, V., Durán-Figueroa, N., Arteaga-Vandázquez, M. et al. (2010). Con- trol of female gamete formation by a small RNA pathway in Arabidopsis. *Nature* **464** (**7288**): 628.
Onyemaobi, I., Liu, H., Siddique, K.H.M., and Yan, G. (2016). Both male and female malfunction contributes to yield reduction under water stress during meiosis in bread wheat. *Frontiers in Plant Science* **7**: 2071.
Oshino, T., Abiko, M., Saito, R. et al. (2007). Premature progression of anther early developmental programs accompanied by comprehensive alterations in tran- scription during high-temperature injury in barley plants. *Molecular Genetics and Genomics* **278** (**1**): 31–42.
Parkinson, S.E., Gross, S.M., and Hollick, J.B. (2007). Maize sex determination and abaxial leaf fates are canalized by a factor that maintains repressed epigenetic states. *Developmental Biology* **308** (**2**): 462–473.
Pawlowski, W.P., Wang, C.J., Golubovskaya, I.N. et al. (2009). Maize AMEIOTIC1 is essential for multiple early meiotic processes and likely required for the initiation of meiosis. *Proceedings of the National Academy of Sciences* **106** (**9**): 3603–3608.

Peragine, A., Yoshikawa, M., Wu, G. et al. (2004). SGS3 and SGS2/SDE1/RDR6 are required for juvenile development and the production of trans-acting siRNAs in Arabidopsis. *Genes & Development* **18** (**19**): 2368–2379.
Peukert, M., Lim, W.L., Seiffert, U., and Matros, A. (2016). Mass spectrometry imaging of metabolites in barley grain tissues. *Current Protocols in Plant Biology* **1**: 574–591.
Pinyopich, A., Ditta, G.S., Savidge, B. et al. (2003). Assessing the redundancy of MADS-box genes during carpel and ovule development. *Nature* **424** (**6944**): 85–88.
Radchuk, V., Borisjuk, L., Radchuk, R. et al. (2006). *Jekyll* encodes a novel protein involved in the sexual reproduction of barley. *The Plant Cell* **18** (**7**): 1652–1666.
Radchuk, V., Weier, D., Radchuk, R. et al. (2011). Development of maternal seed tissue in barley is mediated by regulated cell expansion and cell disintegration and coor- dinated with endosperm growth. *Journal of Experimental Botany* **62** (**3**): 1217–1227.
Radchuk, V., Riewe, D., Peukert, M. et al. (2017). Down-regulation of the sucrose trans- porters HvSUT1 and HvSUT2 affects sucrose homeostasis along its delivery path in barley grains. *Journal of Experimental Botany* **68** (**16**): 4595–4612.
Ray, A., Robinson-Beers, K., Ray, S. et al. (1994). *Arabidopsis* floral homeotic gene *BELL* (*BEL1*) controls ovule development through negative regulation of *AGAMOUS* gene (*AG*). *Proceedings of the National Academy of Sciences* **91**:5761–5765.
Reale, L., Rosati, A., Tedeschini, E. et al. (2017). Ovary size in wheat (*Triticum aestivum* L.) is related to cell number. *Crop Science* **57**: 914–925.
Robinson-Beers, K., Pruitt, R.E., and Gasser, C.S. (1992). Ovule development in wild-type Arabidopsis and two female-sterile mutants. *The Plant Cell* **4** (**10**): 1237–1249.
Ruan, Y.L., Patrick, J.W., Bouzayen, M. et al. (2012). Molecular regulation of seed and fruit set. *Trends in Plant Science* **17** (**11**): 656–665.
Rudall, P.J. (1997). The nucellus and chalaza in monocotyledons: structure and sys- tematics. *The Botanical Review* **63** (**2**): 140–181.
Sage, T.L., Bagha, S., Lundsgaard-Nielsen, V. et al. (2015). The effect of high temper- ature stress on male and female reproduction in plants. *Field Crops Research* **182**: 30–42.
Saini, H. and Aspinall, D. (1981). Effect of water deficit on sporogenesis in wheat (*Triticum aestivum* L.). *Annals of Botany* **48** (**5**): 623–633.
Saini, H., Sedgley, M., and Aspinall, D. (1983). Effect of heat stress during floral devel- opment on pollen tube growth and ovary anatomy in wheat (*Triticum aestivum* L.). *Functional Plant Biology* **10** (**2**): 137–144.
Saini, H.S. and Westgate, M.E. (1999). Reproductive development in grain crops dur- ing drought. *Advances in Agronomy* **68**: 59–96.
Schauer, S.E., Jacobsen, S.E., Meinke, D.W., and Ray, A. (2002). DICER-LIKE1: blind men and elephants in Arabidopsis development. *Trends in Plant Science* **7** (**11**): 487–491.
Schiefthaler, U., Balasubramanian, S., Sieber, P. et al. (1999). Molecular analysis of NOZZLE, a gene involved in pattern formation and early sporogenesis during sex organ development in Arabidopsis thaliana. *Proceedings of the National Academy of Sciences* **96** (**20**): 11664–11669.
Schmidt, A., Wuest, S.E., Vijverberg, K. et al. (2011). Transcriptome analysis of the Arabidopsis megaspore mother cell uncovers the importance of RNA helicases for plant germline development. *PLoS Biology* **9** (**9**): e1001155.
Scott, W., Appleyard, M., Fellowes, G., and Kirby, E. (1983). Effect of genotype and position in the ear on carpel and grain growth and mature grain weight of spring barley. *The Journal of Agricultural Science* **100** (**2**): 383–391.
Sessions, A., Nemhauser, J.L., McColl, A. et al. (1997). *ETTIN* patterns the *Arabidopsis*

floral meristem and reproductive organs. *Development* **124**: 4481–4491.
Shamrov, I. (1998). Ovule classification in flowering plants-new approaches and con- cepts. *Botanische Jahrbücher* **120**: 377–407.
Sheridan, W.F., Avalkina, N.A., Shamrov, I.I. et al. (1996). The mac1 gene: controlling the commitment to the meiotic pathway in maize. *Genetics* **142** (**3**):1009–1020.
Shimada, T., Yamada, K., Kataoka, M. et al. (2003). Vacuolar processing enzymes are essential for proper processing of seed storage proteins in Arabidopsis thaliana. *Journal of Biological Chemistry* **278** (**34**): 32292–32299.
Singh, M., Goel, S., Meeley, R.B. et al. (2011). Production of viable gametes without meiosis in maize deficient for an ARGONAUTE protein. *The Plant Cell Online* **23** (**2**): 443–458.
Sreenivasulu, N., Altschmied, L., Panitz, R. et al. (2002). Identification of genes specif- ically expressed in maternal and filial tissues of barley caryopses: a cDNA array analysis. *Molecular Genetics and Genomics* **266** (**5**): 758–767.
Sreenivasulu, N., Radchuk, V., Strickert, M. et al. (2006). Gene expression patterns reveal tissue-specific signaling networks controlling programmed cell death and ABA-regulated maturation in developing barley seeds. *The Plant Journal* **47** (**2**): 310–327.
Strable, J., Wallace, J.G., Unger-Wallace, E. et al. (2017). Maize YABBY genes drooping leaf1 and drooping leaf2 regulate plant architecture. *The Plant Cell* **29** (**7**): 1622–1641. Su, Z., Zhao, L., Zhao, Y. et al. (2017). The THO complex non-cell-autonomously represses female germline specification through the TAS3-ARF3 module. *Current Biology* **27** (**11**): 1597–1609.

Sun, K., Hunt, K., and Hauser, B.A. (2004). Ovule abortion in *Arabidopsis* triggered by stress. *Plant Physiology* **135** (**4**): 2358–2367.
Tang, A.-C. and Boyer, J.S. (2013). Differences in membrane selectivity drive phloem transport to the apoplast from which maize florets develop. *Annals of Botany* **111** (**4**): 551–562.
Thiel, J., Weier, D., Sreenivasulu, N. et al. (2008). Different hormonal regulation of cellular differentiation and function in nucellar projection and endosperm transfer cells: a microdissection-based transcriptome study of young barley grains. *Plant Physiology* **148** (**3**): 1436–1452.
Thiel, J., Müller, M., Weschke, W., and Weber, H. (2009). Amino acid metabolism at the maternal–filial boundary of young barley seeds: a microdissection-based study. *Planta* **230** (**1**): 205–213.
Tran, V., Weier, D., Radchuk, R. et al. (2014). Caspase-like activities accompany pro- grammed cell death events in developing barley. *PLoS One* **9** (**10**): e109426.
Tucker, M.R., Okada, T., Hu, Y. et al. (2012). Somatic small RNA pathways promote the mitotic events of megagametogenesis during female reproductive development in Arabidopsis. *Development* **139** (**8**): 1399–1404.
Tucker, M.R. and Koltunow, A.M. (2014). Traffic monitors at the cell periphery: the role of cell walls during early female reproductive cell differentiation in plants. *Current Opinions in Plant Biology* **17**: 137–145.
Van Hautegem, T., Waters, A.J., Goodrich, J., and Nowack, M.K. (2015). Only in dying, life: programmed cell death during plant development. *Trends in Plant Science* **20** (**2**): 102–113.
Villarino, G.H., Hu, Q., Manrique, S. et al. (2016). Transcriptomic signature of the SHATTERPROOF2 expression domain reveals the meristematic nature of Arabidopsis gynoecial medial domain. *Plant Physiology* **171** (**1**): 42–61.
Vollbrecht, E., Springer, P.S., Goh, L. et al. (2005). Architecture of floral branch systems in maize and related grasses. *Nature* **436** (**7054**): 1119–1126.
Voronova, O.N., Shamrov, I.I., and Batygina, T.B. (2003). Ovule morphogenesis in nor- mal and mutant *Zea mays*. *Acta Biologica Cracoviensia Series Botanica* **45** (**1**): 155–160. Wang, C.-J.R., Nan, G.-L., Kelliher, T. et al. (2012a). Maize multiple archesporial cells 1 (mac1), an ortholog of rice TDL1A, modulates cell proliferation and identity in
early anther development. *Development* **139** (**14**): 2594–2603.
Wang, L., Cook, A., Patrick, J.W. et al. (2014). Silencing the vacuolar invertase gene GhVIN1 blocks cotton fiber initiation from the ovule epidermis, probably by sup- pressing a cohort of regulatory genes via sugar signaling. *The Plant Journal* **78** (**4**): 686–696.
Wang, T.L., Uauy, C., Robson, F., and Till, B. (2012b). TILLING in extremis. *Plant Biotechnology Journal* **10** (**7**): 761–772.
Warren, F.J., Perston, B.B., Galindez-Najera, S.P. et al. (2015). Infrared microspectro- scopic imaging of plant tissues: spectral visualization of *Triticum aestivum* kernel and Arabidopsis leaf microstructure. *The Plant Journal* **84** (**3**): 634–646.
Wei, B., Zhang, J., Pang, C. et al. (2015). The molecular mechanism of SPOROCYTE- LESS/NOZZLE in controlling Arabidopsis ovule development. *Cell Research* **25** (**1**): 121.
Weier, D., Thiel, J., Kohl, S. et al. (2014). Gibberellin-to-abscisic acid balances govern development and differentiation of the nucellar projection of barley grains. *Journal of Experimental Botany* **65** (**18**): 5291–5304.

Weschke, W., Panitz, R., Sauer, N. et al. (2000). Sucrose transport into barley seeds: molecular characterization of two transporters and implications for seed develop- ment and starch accumulation. *The Plant Journal* **21** (**5**): 455–467.
Weschke, W., Panitz, R., Gubatz, S. et al. (2003). The role of invertases and hexose trans- porters in controlling sugar ratios in maternal and filial tissues of barley caryopses during early development. *The Plant Journal* **33** (**2**): 395–411.
Whipple, C.J., Ciceri, P., Padilla, C.M. et al. (2004). Conservation of B-class floral homeotic gene function between maize and Arabidopsis. *Development* **131** (**24**): 6083–6091.
Wilkinson, L.G. and Tucker, M.R. (2017). An optimised clearing protocol for the quan- titative assessment of sub-epidermal ovule tissues within whole cereal pistils. *Plant Methods* **13** (**1**): 67.
Wittich, P. and Willemse, M. (1999). Sucrose utilization during ovule and seed devel- opment of *Gasteria verrucosa* (Mill.) H. Duval as monitored by sucrose synthase and invertase localization. *Protoplasma* **208** (**1**): 136–148.
Wuest, S.E. and Grossniklaus, U. (2014). Laser-assisted microdissection applied to flo- ral tissues. *Flower Development. Methods in Molecular Biology (Methods and Protocols)* **1110**: 329–344.
Xie, Q., Mayes, S., and Sparkes, D.L. (2015). Carpel size, grain filling, and morphology determine individual grain weight in wheat. *Journal of Experimental Botany* **66** (**21**): 6715–6730.
Xu, W., Fiume, E., Coen, O. et al. (2016). Endosperm and nucellus develop antagonis- tically in Arabidopsis seeds. *The Plant Cell* **28** (**6**): 1343–1360.
Yadegari, R. and Drews, G.N. (2004). Female gametophyte development. *The Plant Cell* **16**: S133–S141.
Yamada, K., Saraike, T., Shitsukawa, N. et al. (2009). Class D and Bsister MADS-box genes are associated with ectopic ovule formation in the pistil-like stamens of allo- plasmic wheat (*Triticum aestivum* L.). *Plant Molecular Biology* **71** (**1**): 1–14.
Yamada, T., Sasaki, Y., Hashimoto, K. et al. (2016). CORONA, PHABULOSA and PHAVOLUTA collaborate with BELL1 to confine WUSCHEL expression to the nucellus in Arabidopsis ovules. *Development* **143** (**3**): 422–426.
Yang, J., Yuan, Z., Meng, Q. et al. (2017). Dynamic regulation of auxin response dur- ing rice development revealed by newly established hormone biosensor markers. *Frontiers in Plant Science* **8**: 256.
Yang, W.C., Ye, D., Xu, J., and Sundaresan, V. (1999). The *SPOROCYTELESS* gene of *Arabidopsis* is required for initiation of sporogenesis and encodes a novel nuclear protein. *Genes & Development* **13**: 2108–2117.
Yang, X., Wu, F., Lin, X. et al. (2012). Live and let die – The B(sister) MADS-box gene OsMADS29 controls the degeneration of cells in maternal tissues during seed devel- opment of rice (*Oryza sativa*). *PLoS One* **7** (**12**): e51435.
Yang, Z., van Oosterom, E.J., Jordan, D.R., and Hammer, G.L. (2009). Pre-anthesis ovary development determines genotypic differences in potential kernel weight in sorghum. *Journal of Experimental Botany* **60** (**4**): 1399–1408.
Yin, L.-L. and Xue, H.-W. (2012). The MADS29 transcription factor regulates the degra- dation of the nucellus and the nucellar projection during rice seed development. *The Plant Cell* **24** (**3**): 1049–1065.

Zhang, J., Tang, W., Huang, Y. et al. (2015). Down-regulation of a LBD-like gene, OsIG1, leads to occurrence of unusual double ovules and developmental abnormalities of various floral organs and megagametophyte in rice. *Journal of Experimental Botany* **66** (**1**): 99–112.
Zhang, S.-S., Yang, H., Ding, L. et al. (2017). Tissue-specific transcriptomics reveals an important role of the unfolded protein response in maintaining fertility upon heat stress in Arabidopsis. *The Plant Cell* **29** (**5**): 1007–1023.
Zhao, L., He, J., Cai, H. et al. (2014). Comparative expression profiling reveals gene functions in female meiosis and gametophyte development in Arabidopsis. *The Plant Journal* **80** (**4**): 615–628.
Zhao, T., Ni, Z., Dai, Y. et al. (2006). Characterization and expression of 42 MADS-box genes in wheat (*Triticum aestivum* L.). *Molecular Genetics and Genomics* **276** (**4**): 334.
Zhao, X., De Palma, J., Oane, R. et al. (2008). OsTDL1A binds to the LRR domain of rice receptor kinase MSP1, and is required to limit sporocyte numbers. *The Plant Journal* **54** (**3**): 375–387.
Zhao, X., Bramsiepe, J., Van Durme, M. et al. (2017). RETINOBLASTOMA RELATED1 mediates germline entry in Arabidopsis. *Science* **356** (**6336**).
Zinn, K.E., Tunc-Ozdemir, M., and Harper, J.F. (2010). Temperature stress and plant sexual reproduction: uncovering the weakest links. *Journal of Experimental Botany* **61** (**7**): 1959–1968.
Zinselmeier, C., Lauer, M.J., and Boyer, J.S. (1995). Reversing drought-induced losses in grain-yield - sucrose maintains embryo growth in maize. *Crop Science* **35** (**5**): 1390–1400.
Zinselmeier, C., Jeong, B.R., and Boyer, J.S. (1999). Starch and the control of kernel number in maize at low water potentials. *Plant Physiology* **121** (**1**): 25–35.
Zong, Y., Wang, Y., Li, C. et al. (2017). Precise base editing in rice, wheat and maize with a Cas9-cytidine deaminase fusion. *Nature Biotechnology* **35** (**5**): 438–440.

Appendix II

An optimised clearing protocol for the quantitative assessment of sub-epidermal ovule tissues within whole cereal pistils

Statement of Authorship

Title of Paper	Exploring the Role of the Ovule in Cereal Grain Development and Reproductive Stress Tolerance
Publication Status	☑ Published ☐ Accepted for Publication ☐ Submitted for Publication ☐ Unpublished and Unsubmitted work written in manuscript style
Publication Details	Laura G. Wilkinson[1] and Matthew R. Tucker[2,*]

Principal Author

Name of Principal Author (Candidate)	Laura G. Wilkinson		
Contribution to the Paper	Compiled information and wrote the manuscript. I hereby certify that the statement of authorship is accurate.		
Overall percentage (%)	90%		
Certification:	This paper reports on original research I conducted during the period of my Higher Degree by Research candidature and is not subject to any obligations or contractual agreements with a third party that would constrain its inclusion in this thesis. I am the primary author of this paper.		
Signature		Date	14/2/19

Co-Author Contributions

By signing the Statement of Authorship, each author certifies that:

i. the candidate's stated contribution to the publication is accurate (as detailed above);
ii. permission is granted for the candidate in include the publication in the thesis; and
iii. the sum of all co-author contributions is equal to 100% less the candidate's stated contribution.

Name of Co-Author	Matthew R. Tucker		
Contribution to the Paper	Conceived project and designed experiments. Contributed to the preparation of the manuscript. I hereby certify that the statement of authorship is accurate.		
Signature		Date	14/2/19

Wilkinson and Tucker *Plant Methods (2017) 13:67*
DOI 10.1186/s13007-017-0217-z

Plant Methods

METHODOLOGY ARTICLE

Open Access

An optimised clearing protocol for the quantitative assessment of sub-epidermal ovule tissues within whole cereal pistils

Laura G. Wilkinson[1] and Matthew R. Tucker[2*]

Abstract

Background: Seed development in the angiosperms requires the production of a female gametophyte (embryo sac) within the ovule. Many aspects of female reproductive development in cereal crops are yet to be described, largely due to the technical difficulty in obtaining phenotypic information at the cellular or sub-cellular level. Hoyer's solution is currently well established as a solution for clearing thin tissues samples, such as sections or whole tissues of bryophytes, mycorrhizal fungi, and small model organisms (e.g. *Arabidopsis thaliana*).

Results: Here we report a Hoyer's solution-based clearing method to facilitate clearing of the whole barley pistil, with high reproducibility. The clearing process takes 10 days from fixation to visualisation, whereupon tissue is sufficiently clear to obtain multiple phenotypic measurements from sub-epidermal tissues and cells within the ovule.

Conclusion: Visualisation of cereal ovules that have not been dissected from the pistil allows an unprecedented capability to collect quantitative morphological information from the developing ovule, integument, nucellus and embryo sac. This will enable comparisons with genetic data to reveal the contribution of pre-fertilisation ovule tissues towards downstream seed development.

Keywords: Microscopy, Hoyer's solution, Barley, Ovule, Monocot, Development, Cereal, Clearing

Background

Sustaining food production above the level of food demand is a growing global challenge. Estimates suggest that crop yields will need to increase by 25–75% to ensure sufficient food production for the world's population in 2050 [1]. Cereal crop production is highly reliant upon development of flowers. In particular, the single ovule within each flower is essential, as it is the site of gametogenesis, fertilisation and downstream grain development. Environmental events such as drought, high temperatures and frost are known to disrupt flower and seed development, causing a reduction in both grain number and grain quality, thus compromising yield [2–4].

Our understanding of floral development and seed formation in flowering plants has been dramatically expanded by research in diverse model dicots, such as *Arabidopsis thaliana*, *Hieracium* sp., and *Torenia fournieri* [5–7]. The formation of ovule primordia, the differentiation of a megaspore mother cell from somatic precursors and the production and fertilisation of an embryo sac have been described in intimate molecular, genetic and morphological detail [8]. Research in rice, maize, wheat and barley has contributed significant molecular and genetic knowledge of monocot inflorescence and flower development [9–12]. Despite this, remarkably little is known about ovule development in these important cereal species, particularly in regards to how different tissues contribute to eventual seed size, composition and shape. Studies have shown that ovary size is an important component of floret and grain survival [13], but the contribution of constituent tissues remains unclear. Determining the role of these tissues for downstream seed

*Correspondence: matthew.tucker@adelaide.edu.au
[2] School of Agriculture, Food and Wine, University of Adelaide, Waite Campus, Urrbrae, SA, Australia
Full list of author information is available at the end of the article

development requires robust, high throughput methods for quantitative two and three-dimensional analysis of developing ovule tissues, such that phenotypic information can be extracted and assessed.

Observation of the internal morphology of cleared floral organs is a powerful tool that allows examination of phenotypic alterations in internal structures following genetic or environmental modification, without the need for thin-sectioning. Chemical treatment to clear small tissue samples is a well-established practice, with reagents ranging from the more traditional methyl salicylate, lactic acid and chloral hydrate based solutions [14–16] to recently developed methods such as ClearSee [17, 18] and PEA-CLARITY [19]. Despite this, observation of female reproductive tissues in cereal monocots remains technically challenging, contributing to a lack of specific genetic and mechanistic information about gametogenesis and ovule development. Two key technical challenges include the relatively large size of the pistils, which are sufficiently thick to remain opaque when treated using previously published clearing protocols designed for substantially smaller tissues (e.g. [20]), and the ease by which the physical structure of the ovule may be damaged during the process of dissection.

Here we report a robust method for clearing whole cereal pistils with Hoyer's Solution [14], allowing visualisation of wheat and barley ovule ultrastructure in a manner that preserves the physical integrity of internal structures. Experimental variation of incubation time offers flexibility in sample preparation, yielding exceptionally clear tissue after a minimum of 10 days post tissue collection and up to a maximum of 16 weeks. The utility of the method was demonstrated by using optical sections through cleared pistils to measure the dimensions of component tissues, enabling phenotypic variation in ovule development to be captured within a panel of barley cultivars.

Methods

Reagents

Chloral Hydrate C-IV (#15307, Sigma-Aldrich, Australia)
Ethanol (#EA043-2.5L, Chem-Supply, Australia)
Formaldehyde (#809, Ajax Finechem, Australia)
Glacial Acetic Acid (#2335, Ajax Finechem, Australia)
Glycerol (#242, Ajax Finechem, Australia)

Solutions

FAA fixative [21] 50% Ethanol (v/v), 10% Formaldehyde (37% solution, also called formalin), 5% glacial acetic acid (v/v), and 35% sterile water (v/v).
Ethanol Series 100% analytical grade EtOH diluted in water to a concentration of 70, 80 and 90%, and 100% EtOH filtered through a molecular sieve.
Chloral hydrate solution 250 g chloral hydrate dissolved in 100 mL sterile water
Hoyer's Solution [14] A 3.0:0.8:0.2 mixture of chloral hydrate:water:glycerol.

Equipment

Greenhouse facility
Standard laboratory 4 °C refrigerator
Fume cupboard
Compound microscope with differential contrast (DIC) and Nomarski filter for a ×10, ×20 and/or ×40 objective
Computer and free ZEN 2011 Blue (Zeiss) LE software
Ventilated microscopy slide box
Small exhaust fan
Glass pipettes
Fine point tweezers (Dumont #5, Emgrid, Australia)
Liquid scintillation vials (#Z190535, SigmaAldrich, Australia)
Polysine Slides (#P4981, ThermoFisher Scientific, Australia)
22 × 40 mm Cover slips (#G422, ProSciTech, Australia)
Microflex 93-260 chemical resistant gloves (Ansell, Australia)

Plant growth and staging

Barley plants were grown in greenhouse facilities at The Plant Accelerator (Adelaide, Australia), under 22 °C (day) and 17 °C (night) temperatures without addition of supplemental light (Fig. 1a). Florets were identified to be at anthesis by removing them from spikes (Fig. 1b), gently reaching inside the palea and lemma with tweezers then assessing the colour of the anthers and how readily pol- len was released upon gentle squashing. At anthesis, the anthers are a rich yellow colour and have yet to shed pollen, but readily release pollen with minimal application of pressure when pressed against a thumbnail (Fig. 1c). Any florets that contained green or green/yellow anthers, or anthers that had already shed pollen, were discarded.

Sample collection and fixation (timing: 10 min per tiller + overnight fixation)

Whole pistils were removed from anthesis barley flow- ers by reaching inside the flower with fine tweezers and pinching the base of the pistil as low as possible (Fig. 1c). Care was taken to avoid tearing the base of the pistil where the ovule is located. Lodicules were gently removed from the outside of the pistil before placing it in

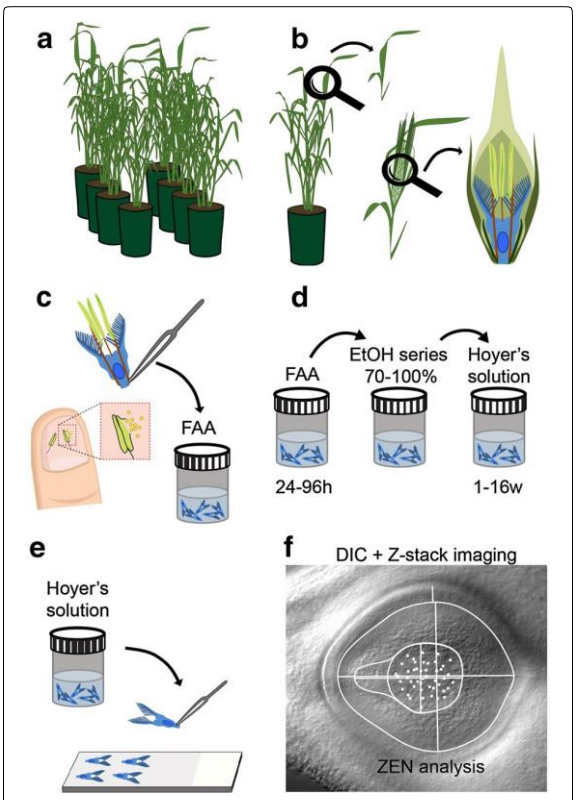

Fig. 1 Schematic representation of the steps involved in visualising the internal structures of ovules within cleared cereal pistils. **a** Plants were examined to identify tillers containing developing spikes. **b**, **c** Individual florets were removed from spikes to identify those at anthesis stage, achieved via observation of pollen on fingernails after anther squashing. **c**, **d** Whole pistils and anthers were gently removed and placed in fixative, followed by dehydration in an ethanol series and clearing in Hoyer's solution. **e** Pistils were transferred to glass slides and covered with glass coverslips. **f** Samples were examined using DIC microscopy and Zeiss ZEN software

a flat bottomed glass scintillation vial containing 2 mL of ice cold FAA fixative.

Sample dehydration (timing: 4 h + overnight dehydration + 4 to 120 days incubation)

Within 1 week of fixation barley pistils were dehydrated through an ethanol series and placed into Hoyer's solution (Fig. 1d), using fine-tipped glass pipettes for each fluid exchange to minimise the possibility of damage to tissue samples. The EtOH series comprised of 3 × 20 min washes at 70, 80, 90 and 100% EtOH at room temperature. Samples were left in the final 100% EtOH wash overnight before transfer into 4 mL Hoyer's Solution. Samples must remain immersed in Hoyer's solution at room temperature for a minimum of 4 days.

Long protocol Samples may remain gently infiltrating in Hoyer's solution for up to 16 weeks. Incubation for 4 weeks preserves tissue quality ideally for imaging of embryo sac features. Vials must be tightly sealed if samples are to be stored for longer than 2 weeks.

Sample mounting (timing: 15 min per slide + 2 to 4 days incubation)

Pistil tissues were manipulated with fine point tweezers and only held by the stigma in order to avoid crushing the ovary wall, ovule or surrounding tissue. Pistils were placed on flat Poly-Lys coated glass microscopy slides with either the dorsal or ventral side down so that both stigma of each pistil lay "flat", rather than one stigma pointing up into the air (Fig. 1e). On each slide, pistils were placed equidistantly in a symmetrical arrangement and gently covered with a 22 × 40 mm coverslip. This arrangement allows the pistils to lie flat, ensures that variation in the relative viewing angle of the ovule is limited, and preserves the structural integrity of the ovule by preventing any damage to the tissue. Following sample arrangement and application of the cover slip, Hoyer's Solution was pipetted underneath the cover slip onto the slide until all air was evacuated. Slides were then placed flat into a slide storage box that allowed limited ventilation and left in a fume cupboard for 4 days. Samples stored in a well ventilated location are cleared in 24–48 h depending upon the degree of ventilation. Conversely, samples stored after mounting with insufficient or no ventilation required up to 14 days to clear sufficiently to allow visualisation. Therefore, the degree of ventilation can be used to tailor the method to suit the user's time constraints.

Long protocol Samples incubated in 4 mL Hoyer's Solution for longer than 2 weeks typically require less than 4 days to clear completely once mounted on the microscopy slide. For example, tissue stored in Hoyer's Solution for 8–16 weeks generally does not require a period of ventilated storage longer than 12 h, and in some cases may be visualised immediately after mount- ing on slides.

Imaging (timing: 2 min per piece of tissue)

Pistils were imaged using differential contrast microscopy (DIC) at ×10 magnification with a Zeiss AxioImager M2 equipped with a Nomarski filter. For comprehensive data collection, optical slices spanning from the dorsal to ventral integument were taken as a z-stack image, using Zeiss ZEN 2011 (Blue) software.

Image analysis (timing: 10 to 15 min per image)

Data were analysed using the Zeiss ZEN 2011 (Blue) software package. Diverse measurements were taken including the 2-dimensional area (μm^2) of each ovule tissue of interest, using the "contour (spline)" graphics tool to encircle the tissue, as well as the longitudinal and transverse dimensions (μm) of the same tissues, using the "line" graphics tool, and the antipodal nuclei were counted using the "event marker" graphics tool (Fig. 4c). Measurements were taken by following tissue boundaries for each given trait throughout optical sections and placing contour markers at the widest point. Two-dimensional ovule area was measured at the boundary between integument and nucellus. Embryo sac area was measured by tracing the outline of the structure from the micropyle to the chalazal region. The residual somatic cell (nucellus) area was measured by subtracting the embryo sac area from the whole ovule area.

Results

Protocol timing optimisation

Clearing was most successful when fixative was removed through an ethanol dehydration series prior to a 4-day infiltration step in Hoyer's solution, followed by a 4-day rest after mounting on microscopy slides (Fig. 2a). Equally clear images were obtained from samples that were dehydrated, left to gently infiltrate in Hoyer's solu- tion for 4 weeks, then imaged directly after mounting on microscopy slides (Additional file 1: Fig S1A). The maximum period of incubation that achieved acceptable clearing was approximately 16 weeks (Additional file 1: Fig S1B). Deterioration of cellular morphology was seen when samples were left in scintillation vials to gently infiltrate with Hoyer's solution for longer than 5 months (Fig. 2b), or when samples were mounted on microscopy slides and stored in a well ventilated area for multiple days, or were imaged after 10 days in a semi-ventilated storage box (Additional file 1: Fig S1C). Evaporation of the Hoyer's solution was also a factor that prevented acquisition of acceptable images if the samples were over-ventilated.

Protocol reagent optimisation

Clearing was not successful when ethanol dehydration was omitted and fixed samples were placed directly in Hoyer's solution (Fig. 2c). Similarly, it was found that use of pure chloral hydrate solution rather than Hoyer's solution yields unacceptably murky images (Fig. 2d), a factor of both the harsher degradation process when chloral hydrate is used in isolation and the lack of glycerol lowering the refractive index of the mounting fluid. Rough sample collection or handling of tissue throughout the dehydration

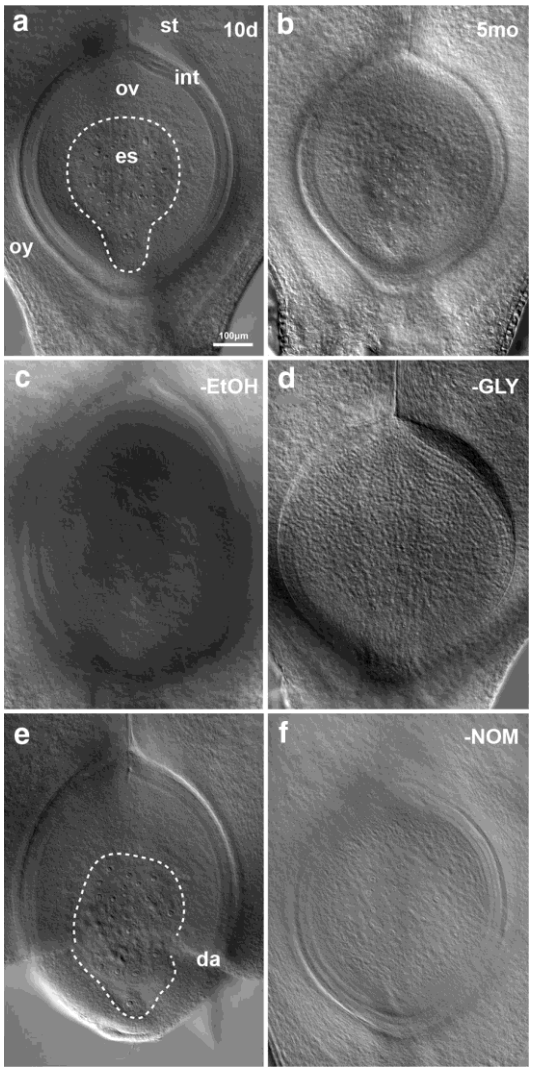

Fig. 2 Barley ovules imaged at ×10 showing the outcomes of variations to the clearing protocol. Images presented as composites, generated by merging optical sections. **a** A 10-day (10d) method incorporating ethanol dehydration prior to a 4-day infiltration with Hoyer's solution, then a 4-day rest after mounting on microscopy slides produced the greatest clarity of results within a reasonably short time frame. es = embryo sac, ov = ovule, oy = ovary wall, st = style, int = integuments. **b** Samples gently infiltrated with Hoyer's solution for over 5 months (5mo) deteriorated, resulting in unacceptably murky images. **c** Omitting ethanol (-EtOH) dehydration prior to incubation in Hoyer's solution results in the tissue becoming grainy and unacceptably murky. **d** Incubation of the sample in chloral hydrate without glycerol (-GLY) after fixation and dehydration results in the tissue becoming unacceptably murky. **e** Rough sample collection and careless handling of the tissues results in damaged ovaries, which may disrupt the internal morphology of the ovule. da = damaged region. **f** Samples cannot be imaged without a Nomarski filter (-NOM)

process often resulted in structural disruption of the sample (Fig. 2e; Additional file 1: Fig. S1D). In addition, a Nomarski filter is essential for image acquisition (Fig. 2f).

Optimised method results

Cleared pistils offer an excellent opportunity to visualise internal components of the ovule in their native spatial arrangement using a DIC microscope with a Nomar- ski filter (Figs. 3, 4). Imaging the entire ovule within the ovary is easily possible at ×10 magnification, and is particularly powerful when captured in a series of optical sections, allowing construction of composite images and videos that represent all internal features of the ovule's cellular arrangement (Fig. 3a; Additional file 2: Fig. S2) and measurement of some three-dimensional features such as embryo sac depth. At ×40 magnification, intimate cellular details of the embryo sac and other ovule components could be obtained (Fig. 3b, c), such as clear, prominent nuclei in the egg cell, central cell and antipodal cells. The quality of tissue resolution was similar in pistils that were infiltrated in Hoyer's solution for 10 days (Fig. 3d) and 10 weeks (Fig. 3b).

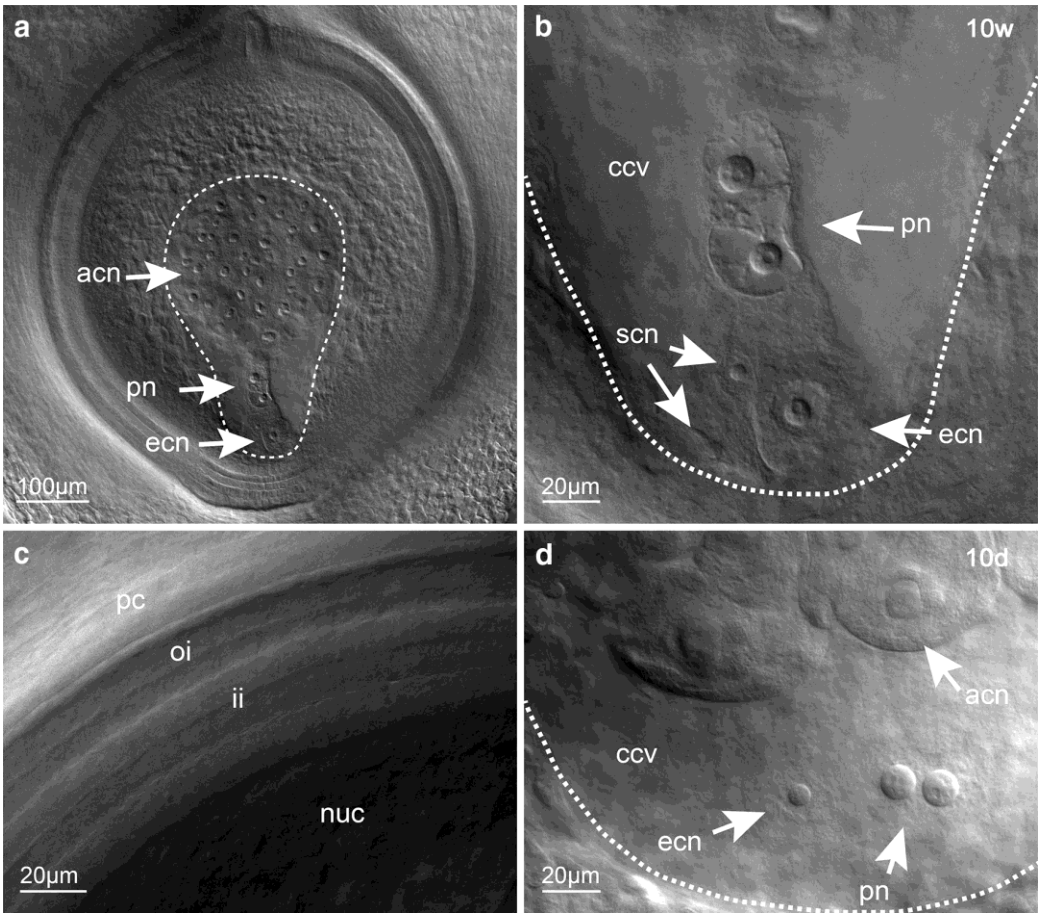

Fig. 3 Structural details of the ovule are visible in cleared barley pistils (*H. vulgare* cv. Host). Images presented as composites, generated by merging optical sections. **a** Mature barley ovule imaged at ×10 magnification without dissection from the pistil. **b**–**d** Cellular resolution may be achieved with a ×40 objective, allowing clear visualisation of the egg cell nucleus, synergid nuclei, polar nuclei and antipodal cell nuclei using the"long method" i.e. incubation for at least 10 weeks (10w) in Hoyer's solution (**b**). The integument layers are also visible (**c**). Similar cellular resolution may also be achieved in samples processed with a 10-day (10d) "short" method (**d**). acn = antipodal cell nuclei, ccv = central cell vacuole, ecn = egg cell nucleus, ii = inner integument, nuc = nucellus, oi = outer integument, pn = polar nuclei, pc = pericarp, scn = synergid cell nuclei. The embryo sac is indicated by a *dashed white line*

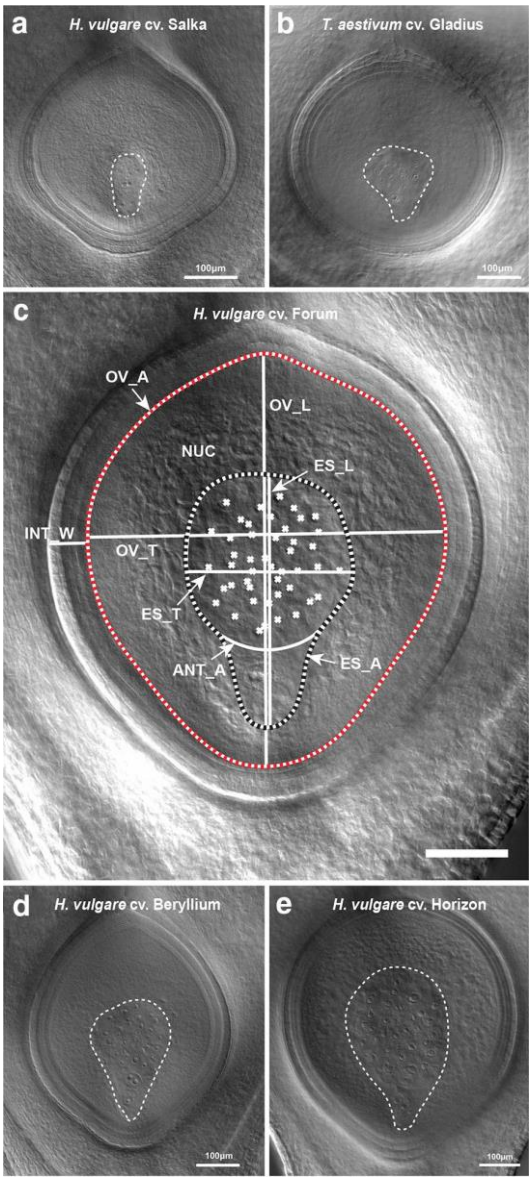

Fig. 4 Ovule morphology after clearing. Ovule images are presented as composites, generated by merging optical sections. The method worked equally well for barley (**a**) and wheat (**b**) pistils at various stages. Pre-anthesis ovules are shown. **c** Measurement of traits at anthesis, including ovule area (OV_A), embryo sac area (ES_A), ovule and embryo sac transverse and longitudinal dimensions (OV_L, OV_T, ES_L, ES_T), integument width (INT_W), antipodal number (*marked with crosses*) and antipodal cluster area (ANT_A), using Zeiss ZEN software. The ovule area is indicated with a *dashed red* and *white line*, while the embryo sac area is indicated by a *dashed black* and *white line*. NUC = nucellus. Small (**d**) and large (**e**) mature barley ovules after clearing imaged at ×10 magnification without dissection from the pistil. *Bar* 100 µm

Sup-epidermal details of ovule development differ between cultivars

A fundamental understanding of reproductive organ development in cereals ultimately aims to support breeding programs in generating high-yielding, high-quality cultivars. To demonstrate the utility of this clearing technique, we examined pistils from barley and wheat (Fig. 4a, b). In both species, sub-epidermal details of ovule tissues, including the embryo sac, egg cell, central cell, antipodals, integument and nucellus could be dis- cerned and measured (Fig. 4c). To determine if intraspe- cific differences in ovule development could be identified, we examined a selection of 2-row spring barley culti- vars. Quantification of morphological features such as tissue area, thickness and cell number in nine cultivars revealed natural variation in most traits (Table 1; Figs. 4d, e, 5). For example, ovule area in *H. vulgare* cv Horizon was almost twofold larger than *H. vulgare* cv Beryllium (Figs. 4d, e, 5a), antipodal number was lowest in *H. vulgare* cv. Toucan (~32 ± 5) compared to *H. vulgare* cv. Horizon (~49 ± 4) and integument width was thickest in *H. vulgare* cv Agenda (~50 ± 4 µm) and thinnest in *H. vulgare* cv Rainbow (~41 ± 3 µm). Correlation analysis indicated that multiple traits showed strong positive correlations, such as ovule area, embryo sac area and ovule height (Fig. 5b, c), suggesting that these features are intimately related. However, other traits showed weak or no correlations with other ovule features, including integument width, antipodal number, nucellus area and ovule transverse width (Fig. 5b, c).

Discussion

In this study a method for clearing tissue using Hoyer's solution has been designed to suit cereal pistils such that internal structures of the ovule may be imaged with a high degree of clarity. Chloral hydrate-based clearing solutions have been successfully used in a wide range of biological fields [14, 22, 23], permitting a great deal of fundamental morphological and phenotypic informa- tion to be gathered. However, in our hands, previously reported protocols incorporating chloral hydrate that work well in Arabidopsis (e.g. [20, 24]) did not result in sufficient clearing of barley pistils to enable quantita- tive measurement of individual ovule tissues. Moreover, alternative methods that incorporate methyl salicylate [16, 25–27], lactic acid [28], sodium hypochlorite [29] or sodium hydroxide [30], lack the convenience and/or efficiency of our established Arabidopsis chloral hydrate-based method [20]. Other recently reported clearing reagents such as ClearSEE [17], PEA-CLARITY [19] and FocusClear [31] are designed to clear tissue while preserving fluorescent labelling, but are either too expensive

Table 1 Phenotypic measurements of ovule tissues from nine *H. vulgare* cultivars

Cultivar	n	Ovule			Embryo sac			Integument	Nucellus		Antipodal	
		Area (μm²)	Trans (μm)	Long (μm)	Area (μm²)	Trans (μm)	Long (μm)	Width (μm)	Area (μm²)	%	#	Area (μm²)
Beryllium	6	138,197.8	396.9	484.3	30,462.7	174.6	270.1	44.9	107,735.1	78.1	37.7	25,829.6
STDEV		15,888.7	28.7	21.7	5597.7	26.0	25.5	5.7	11,329.2	2.2	2.7	5562.9
Novello	12	154,239.1	413.1	505.6	33,330.3	171.7	298.0	43.9	120,908.9	78.5	35.0	27,401.0
STDEV		16,522.7	19.1	42.8	6097.1	16.7	37.4	3.2	12,418.2	2.5	4.7	6447.3
Orbit	6	161,883.0	451.7	487.3	33,816.5	182.2	281.0	46.4	128,066.6	78.9	36.5	28,026.6
STDEV		20,556.0	32.4	20.9	4352.4	17.3	10.6	3.0	18,494.2	2.6	6.6	4934.9
Extract	11	164,652.1	448.3	497.6	34,479.2	188.9	284.0	46.7	130,172.9	79.1	36.0	29,457.8
STDEV		14,406.3	22.8	21.5	7094.9	25.8	27.4	2.7	11,537.1	3.5	2.9	7992.9
Toucan	11	177,561.6	444.7	554.2	45,330.7	210.7	320.3	46.1	132,230.9	74.7	32.6	42,617.2
STDEV		21,683.1	25.0	44.8	9374.7	22.8	46.4	2.1	14,255.4	3.3	4.7	5469.6
Saloon	13	199,385.6	456.7	598.7	70,066.1	266.1	382.3	43.6	129,319.5	64.9	41.8	65,125.7
STDEV		11,367.7	19.1	25.6	9071.9	21.7	25.0	1.7	10,869.6	3.9	4.8	8283.8
Rainbow	6	221,620.1	488.6	598.6	65,471.9	242.4	375.2	41.0	156,148.2	70.6	36.8	57,424.8
STDEV		14,500.2	20.3	19.8	8707.8	16.8	23.0	3.0	8030.2	2.5	3.5	7982.3
Agenda	6	227,499.2	483.4	625.2	75,121.6	272.9	367.9	49.5	152,377.7	66.7	45.2	72,000.8
STDEV		42,467.0	42.0	60.6	13,856.8	28.5	53.2	4.9	32,315.5	4.3	8.5	14,718.3
Horizon	6	241,310.7	519.2	607.2	72,158.9	268.8	371.9	43.0	169,151.8	70.0	48.8	66,487.6
STDEV		48,703.9	48.0	59.0	14,691.2	29.0	48.1	1.5	35,130.8	2.2	3.6	14,851.0

Trans transverse width, *Long* longitudinal height

for high-throughput analysis or provide insufficient cellular resolution without additional staining.

Although the chloral hydrate-based method we describe is not compatible with visualisation of fluorescently-tagged proteins, it can be applied to diverse cereals, allows customisable incubation times, requires minimal tissue handling, and consistently provided excellent clearing and an ability to detect quantitative differences in tissue development in unstained cereal ovary samples. The Zeiss ZEN software used for image analysis is freely available for download and easy to use, while the FIJI software suite was used to extract similar results [32]. In our pilot study of barley ovules at anthesis, 75 pistils were examined from 9 cultivars. The method was not specifically tested on a microscope containing a motorised 8-slide mounting frame or image stitching software, but such an approach would almost certainly be compatible, suggesting that image acquisition might be automated in future to allow for high-throughput data collection. Whether the scale of analysis required for germplasm screens in breeding populations can be achieved is currently unclear. However, the method is compatible with pre-breeding efforts to dissect pre-fertilisation traits that contribute to downstream seed development and morphology. Furthermore, we anticipate that the method will be particularly useful for the rapid characterisation of mutant phenotypes and transgenic plants that effect ovule development in barley and wheat.

Conclusions

A clearing technique typically used in the analysis of tissues from dicot model organisms was successfully adapted to clear the much larger cereal pistil. This paves the way for further interrogation of sup-epidermal fea- tures of ovule development in barley and other cereal crop species. The application of this method to a large panel of genetically distinct or genetically modified cereal varieties may assist the identification of novel genes con- trolling ovule phenotypes as well as components of seed yield and quality.

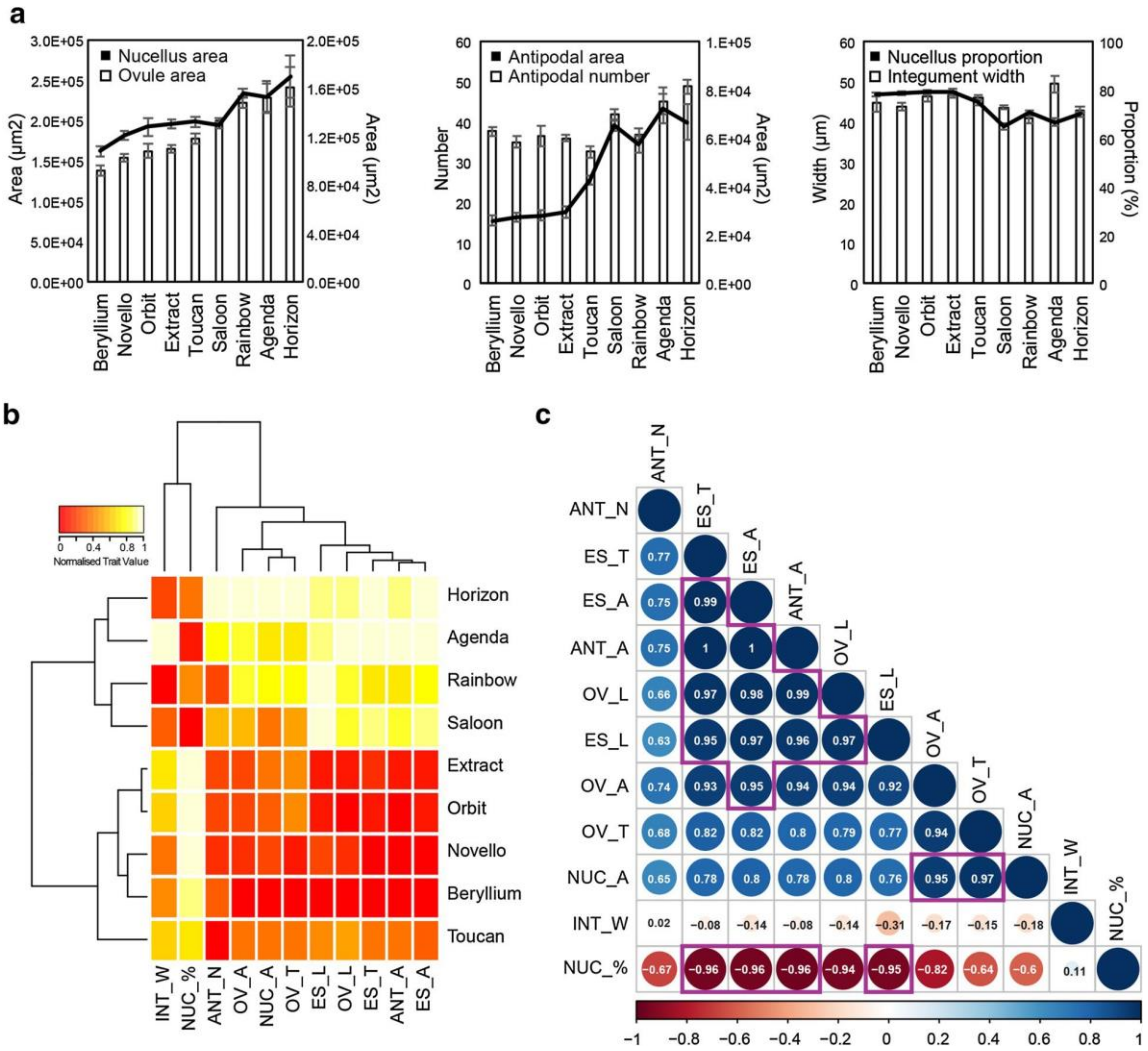

Fig. 5 Analysis of barley ovule traits by pistil clearing. **a** Ovule phenotypes were examined in nine cultivars of 2-row spring barley. Traits such as ovule area, nucellus area, antipodal number, antipodal area, nucellus proportion and integument width (see Fig. 4) were compared between the cultivars. *Error bars* show standard error. **b** Heat map showing the normalised trait values (between 0 and 1) for 11 ovule traits in the 9 examined cultivars. Cultivars and traits were clustered via hierarchical clustering. **c** Correlation analysis of 11 different ovule traits. The *size* and *colour* of the *circles* indicates the degree of trait correlation, which is also indicated via a numerical value. R-squared values greater than 0.95 are indicated via *purple boxes*. INT_W = integument width, NUC_% = nucellus proportion, ANT_N = antipodal number, OV_A = ovule area, NUC_A = nucellus area, OV_T = ovule transverse width, ES_L = embryo sac longitudinal height, OV_L = ovule longitudinal height, ES_T = embryo sac transverse width, ANT_A = entire antipodal area, ES_A = embryo sac area

Additional files

Additional file 1: Fig. S1. Barley ovules imaged at ×10 showing the outcomes of variations to the clearing protocol. Images presented as composites, generated by merging optical sections. **A** Ethanol dehydration prior to a 4-week (4w) gentle infiltration with Hoyer's solution, then imaging samples directly after mounting on microscopy slides produced high clarity results in a longer time frame. **B** Samples gently infiltrated with Hoyer's solution for 16 weeks (16w) then immediately imaged produced high-quality results. **C** Samples left mounted on microscope slides in a well ventilated storage box or for too long were not able to be imaged properly due to evaporation (+Evap) of the Hoyer's solution, causing uneven illumination of the sample and in some cases accelerated degradation of the tissue, resulting in an unacceptably grainy image. **D** Rough sample collection and careless handling of the tissues results in damaged ovaries, which may disrupt the internal morphology of the ovule. The embryo sac is indicated by a dashed white line.

Additional file 2: Fig. S2. Sequential 2.4 µm optical slices (n = 50) of a cleared *H. vulgare* cv. Gant ovule at anthesis were combined to generate a movie file.

Authors' contributions
LGW collected and analysed the data. LGW and MRT designed and tested the method and jointly contributed to writing the manuscript. Both authors read and approved the final manuscript.

Author details
[1] ARC Centre of Excellence in Plant Cell Walls and School of Agriculture, Food and Wine, University of Adelaide, Waite Campus, Urrbrae, SA, Australia. [2] School of Agriculture, Food and Wine, University of Adelaide, Waite Campus, Urrbrae, SA, Australia.

Acknowledgements
We wish to thank Rachel Burton and Caitlin Byrt for advice, Ryan Whitford for wheat samples and Plant Accelerator staff for maintaining plants. We also wish to acknowledge members of the Tucker Laboratory and the ARC Centre of Excellence in Plant Cell Walls for useful discussions and suggestions.

Competing interests
The authors declare that they have no competing interests.

Availability of data and materials
The datasets used and/or analysed during the current study are available from the corresponding author on reasonable request.

Consent for publication
All authors give consent for the data to be published.

Ethics approval and consent to participate
Not applicable.

Funding
This work was supported by an Australian Research Council (ARC) (Grant No. FT140100780) Centre of Excellence in Plant Cell Walls supplementary Ph.D. scholarship (LGW) and an ARC Future Fellowship (MRT).

Publisher's Note

Received: 29 June 2017 Accepted: 8 August 2017
Published online: 15 August 2017

References

1. Hunter MC, Smith RG, Schipanski ME, Atwood LW, Mortensen DA. Agriculture in 2050: recalibrating targets for sustainable intensification. Bioscience. 2017;67(4):386–91.
2. Onyemaobi I, Liu H, Siddique KHM, Yan G. Both male and female malfunction contributes to yield reduction under water stress during meiosis in bread wheat. Front Plant Sci. 2016;7:2071.
3. Saini HS, Westgate ME. Reproductive development in grain crops during drought. Adv Agron. 1999;68:59–96.
4. Thakur P, Kumar S, Malik JA, Berger JD, Nayyar H. Cold stress effects on reproductive development in grain crops: an overview. Environ Exp Bot. 2010;67(3):429–43.
5. Susaki D, Takeuchi H, Tsutsui H, Kurihara D, Higashiyama T. Live imaging and laser disruption reveal the dynamics and cell-cell communication during *Torenia fournieri* female gametophyte development. Plant Cell Physiol. 2015;56(5):1031–41.
6. Tucker MR, Koltunow AMG. Traffic monitors at the cell periphery: the role of cell walls during early female reproductive cell differentiation in plants. Curr Opin Plant Biol. 2014;17:137–45.
7. Yang W-C, Sundaresan V. Genetics of gametophyte biogenesis in Arabidopsis. Curr Opin Plant Biol. 2000;3(1):53–7.
8. Yang W-C, Shi D-Q, Chen Y-H. Female gametophyte development in flowering plants. Annu Rev Plant Biol. 2010;61:89–108.
9. Boden SA, Weiss D, Ross JJ, Davies NW, Trevaskis B, Chandler PM, Swain SM. EARLY FLOWERING3 regulates flowering in spring barley by mediating gibberellin production and FLOWERING LOCUS T expression. Plant Cell. 2014;26(4):1557–69.
10. Yoshida H, Nagato Y. Flower development in rice. J Exp Bot. 2011;62(14):4719–30.
11. Youssef HM, Eggert K, Koppolu R, Alqudah AM, Poursarebani N, Fazeli A, Sakuma S, Tagiri A, Rutten T, Govind G. VRS2 regulates hormone-mediated inflorescence patterning in barley. Nat Genet. 2017;49(1):157–61.
12. Zhang D, Yuan Z. Molecular control of grass inflorescence development. Annu Rev Plant Biol. 2014;65:553–78.
13. Guo Z, Schnurbusch T. Variation of floret fertility in hexaploid wheat revealed by tiller removal. J Exp Bot. 2015;66(19):5945–58.
14. Anderson LE. Hoyer's solution as a rapid permanent mounting medium for bryophytes. Bryologist. 1954;57(3):242–4.
15. Cunningham JL. A miracle mounting fluid for permanent whole-mounts of microfungi. Mycologia. 1972;64(4):906–11.
16. Stelly DM, Peloquin S, Palmer RG, Crane CF. Mayer's hemalum-methyl salicylate: a stain-clearing technique for observations within whole ovules. Stain Technol. 1984;59(3):155–61.
17. Kurihara D, Mizuta Y, Sato Y, Higashiyama T. ClearSee: a rapid optical clearing reagent for whole-plant fluorescence imaging. Development. 2015;142(23):4168–79.
18. Timmers AC. Light microscopy of whole plant organs. J Microsc. 2016;263(2):165–70.
19. Palmer WM, Martin AP, Flynn JR, Reed SL, White RG, Furbank RT, Grof CP. PEA-CLARITY: 3D molecular imaging of whole plant organs. Sci Rep. 2015;5:13492.
20. Tucker MR, Okada T, Hu Y, Scholefield A, Taylor JM, Koltunow AM. Somatic small RNA pathways promote the mitotic events of megagametogenesis during female reproductive development in Arabidopsis. Development. 2012;139(8):1399–404.
21. Young B, Sherwood R, Bashaw E. Cleared-pistil and thick-sectioning techniques for detecting aposporous apomixis in grasses. Can J Bot. 1979;57(15):1668–72.
22. Berleth T, Jurgens G. The role of the monopteros gene in organising the basal body region of the Arabidopsis embryo. Development. 1993;118(2):575–87.
23. Enugutti B, Schneitz K. Microscopic analysis of Arabidopsis ovules. Flower Dev Methods Protocols. 2014;1110:253–61.
24. Franks RG. Histological analysis of the arabidopsis gynoecium and ovules using chloral hydrate clearing and differential interference contrast light microscopy. Oogenesis Methods Protoc. 2016;1457:1–7.
25. Herr J Jr. Recent advances in clearing techniques for study of ovule and female gametophyte development. Angiosperm Pollen Ovules. 1992;149:154.

1. Koltunow AM. Apomixis: embryo sacs and embryos formed without meiosis or fertilization in ovules. Plant Cell. 1993;5(10):1425–37.
2. Ponitka A, Ślusarkiewicz-Jarzina A. Cleared-ovule technique used for rapid access to early embryo development in Secale cereale x Zea mays crosses. Acta Biol Crac Ser Bot. 2004;46:133–7.
3. Desfeux C, Clough SJ, Bent AF. Female reproductive tissues are the primary target of agrobacterium-mediated transformation by the arabidopsis floral-dip method. Plant Physiol. 2000;123(3):895–904.
4. Aditya J, Lewis J, Shirley NJ, Tan HT, Henderson M, Fincher GB, Burton RA, Mather DE, Tucker MR. The dynamics of cereal cyst nematode infection differ between susceptible and resistant barley cultivars and lead to changes in (1, 3; 1, 4)-β-glucan levels and HvCslF gene transcript abundance. New Phytol. 2015;207(1):135–47.
5. Tomer E, Gottreich M, Gazit S. Defective ovules in avocado cultivars. J Am Soc Hortic Sci. 1976;101(5):620–3.
6. Chung K, Wallace J, Kim S-Y, Kalyanasundaram S, Andalman AS, Davidson TJ, Mirzabekov JJ, Zalocusky KA, Mattis J, Denisin AK. Structural and molecular interrogation of intact biological systems. Nature. 2013;497(7449):332–7.
7. Schindelin J, Arganda-Carreras I, Frise E, Kaynig V, Longair M, Pietzsch T, Preibisch S, Rueden C, Saalfeld S, Schmid B. Fiji: an open-source platform for biological-image analysis. Nat Methods. 2012;9(7):676–82.

Appendix III

Exploring the role of cell wall-related genes and polysaccharides during plant development

Statement of Authorship

Title of Paper	Exploring the Role of Cell Wall-Related Genes and Polysaccharides during Plant Development
Publication Status	☑ Published ☐ Accepted for Publication ☐ Submitted for Publication ☐ Unpublished and Unsubmitted work written in manuscript style
Publication Details	Matthew R Tucker[1,*], Haoyu Lou[1,2], Matthew K. Aubert[1,2], Laura G. Wilkinson[1,2], Alan Little[1], Kelly Houston [3], Sara C. Pinto[4], and Neil J. Shirley[1,2].

Principal Author

Name of Principal Author (~~Candidate~~)	Matthew R. Tucker		
Contribution to the Paper	I compiled information and wrote the manuscript. I hereby certify that the statement of authorship is accurate.		
Overall percentage (%)	60%		
Signature		Date	22/2/19

Co-Author Contributions

By signing the Statement of Authorship, each author certifies that:

vii. the candidate's stated contribution to the publication is accurate (as detailed above);

viii. permission is granted for the candidate in include the publication in the thesis; and

ix. the sum of all co-author contributions is equal to 100% less the candidate's stated contribution.

Name of Co-Author	Haoyu Lou		
Contribution to the Paper	Compiled information and contributed to the preparation of the manuscript. I hereby certify that the statement of authorship is accurate.		
Signature		Date	23/11/2018

Name of Co-Author	Matthew K. Aubert		
Contribution to the Paper	Compiled information and contributed to the preparation of the manuscript. I hereby certify that the statement of authorship is accurate.		
Signature		Date	14/02/2019

Name of Co-Author	Laura G. Wilkinson		
Contribution to the Paper	Compiled information and contributed to the preparation of the manuscript. I hereby certify that the statement of authorship is accurate.		
Signature		Date	14/02/19

Name of Co-Author	Alan Little		
Contribution to the Paper	Compiled information and contributed to the preparation of the manuscript. I hereby certify that the statement of authorship is accurate.		
Signature		Date	14/02/19

Name of Co-Author	Kelly Houston		
Contribution to the Paper	Compiled information and contributed to the preparation of the manuscript. I hereby certify that the statement of authorship is accurate.		
Signature		Date	14.02.19

Name of Co-Author	Sara C. Pinto		
Contribution to the Paper	Compiled information and contributed to the preparation of the manuscript. I hereby certify that the statement of authorship is accurate.		
Signature		Date	14/02/2019

Name of Co-Author	Neil J. Shirley		
Contribution to the Paper	Compiled information and contributed to the preparation of the manuscript. I hereby certify that the statement of authorship is accurate.		
Signature		Date	14/2/19

plants

MDPI

Review

Exploring the Role of Cell Wall-Related Genes and Polysaccharides during Plant Development

Matthew R. Tucker [1,*], Haoyu Lou [1,2], Matthew K. Aubert [1,2], Laura G. Wilkinson [1,2], Alan Little [1], Kelly Houston [3], Sara C. Pinto [4] and Neil J. Shirley [1,2]

1 School of Agriculture, Food and Wine, Waite Research Institute, The University of Adelaide, Glen Osmond, SA 5062, Australia; haoyu.lou@adelaide.edu.au (H.L.); matthew.aubert@adelaide.edu.au (M.K.A.); laura.g.wilkinson@adelaide.edu.au (L.G.W.); alan.little@adelaide.edu.au (A.L.); neil.shirley@adelaide.edu.au (N.J.S.)

2 Australian Research Council Centre of Excellence in Plant Cell Walls, The University of Adelaide, Glen Osmond, SA 5062, Australia

3 Cell and Molecular Sciences, The James Hutton Institute, Dundee DD2 5DA, UK; Kelly.Houston@hutton.ac.uk

4 Departamento de Biologia, Faculdade de Ciências da Universidade do Porto, 4169-007 Porto, Portugal; sarapintomendes94@gmail.com

* Correspondence: matthew.tucker@adelaide.edu.au; Tel.: +61-8313-9241

Received: 29 April 2018; Accepted: 29 May 2018; Published: 31 May 2018

Abstract: The majority of organs in plants are not established until after germination, when pluripotent stem cells in the growing apices give rise to daughter cells that proliferate and subsequently differentiate into new tissues and organ primordia. This remarkable capacity is not only restricted to the meristem, since maturing cells in many organs can also rapidly alter their identity depending on the cues they receive. One general feature of plant cell differentiation is a change in cell wall composition at the cell surface. Historically, this has been viewed as a downstream response to primary cues controlling differentiation, but a closer inspection of the wall suggests that it may play a much more active role. Specific polymers within the wall can act as substrates for modifications that impact receptor binding, signal mobility, and cell flexibility. Therefore, far from being a static barrier, the cell wall and its constituent polysaccharides can dictate signal transmission and perception, and directly contribute to a cell's capacity to differentiate. In this review, we re-visit the role of plant cell wall-related genes and polysaccharides during various stages of development, with a particular focus on how changes in cell wall machinery accompany the exit of cells from the stem cell niche.

Keywords: cell wall; polysaccharide; development; glycosyltransferase; glycosyl hydrolase; differentiation; shoot meristem; root meristem

1. Introduction

As plant cells divide away from apical meristems, their molecular and biochemical profiles change. At the molecular level, cells adopt identities through changes in their nuclear morphology, genomic landscape, and transcriptional signatures. Changes also occur at the periphery of the cell, most notably in the abundance and organization of cell wall components such as cellulose, non-cellulosic polysaccharides, phenolic acids, lipids, and proteins [1]. Sometimes this results in terminal differentiation, for example in vascular tissues such as lignified mature fibers [2]. Changes in wall composition influence the downstream function of cells as storage units, structural networks, and solute transporters [3]. In many cases, differentiation also influences the capacity of cells to respond to stresses imparted through pathogens and the environment [4].

Despite its importance for growth and reproduction, plant cell differentiation is infrequently irreversible [5]. Many plant cells, not only those located in the meristems, possess the remarkable ability to adopt new identities. This can be a simple switch in identity between adjoining cells; for example, in the developing maize seed (kernel), where aberrant inward (periclinal) divisions of aleurone cells at the periphery result in one daughter cell retaining aleurone identity and the other adopting inner starchy endosperm identity [6]. The same thing can occur in more complex systems such as apomictic (asexual) plants, where ovule cells that adjoin normal sexual cells can spontaneously adopt germline-like identity and initiate a form of gametophyte development [7,8]. However, the plant meristem remains the epitome of differentiation capacity; meristematic stem cells can give rise to many different cell types, often referred to as pluripotency (the ability to either give rise to all cells and tissues in an organ) or totipotency (the ability to give rise to the entire organism) [9]. At a fundamental level, this indicates that fate is not fixed, and plant cells must maintain flexible cellular properties compatible with differentiation.

Much of our knowledge regarding cell differentiation has come from in vitro studies involving tissue culture, during which plant cells can be induced to de-differentiate (essentially reverse differentiation and lose specialized characteristics [10]), forming protoplasts or callus [11]. Somewhat similar to pluripotent stem cells, these totipotent undifferentiated cells can be stimulated to give rise to entire new tissues and eventually whole plants, depending on the correct exogenous application of growth hormones and vitamin supplements. Importantly, one component of in vitro de-differentiation appears to be modification or removal of the cell wall from the progenitor cell [12,13]. Moreover, in some cell types, the over-accumulation of specific cell wall components even appears to prevent de-differentiation or regeneration [14,15]. Therefore, variation in cell wall composition may contribute to the maintenance of cellular identity in some cases, while promoting the capacity for differentiation in others. How this is determined has yet to be addressed in sufficient detail, since it requires a thorough qualitative and quantitative assessment of cell wall composition at the single cell level.

Prevailing models suggest that there are two types of walls in plants; primary cell walls are relatively thin and flexible and are synthesized during cell growth and division, while secondary cell walls provide strength and rigidity in tissues that are no longer growing [16,17]. In general, the plant cell wall comprises a framework of cellulose microfibrils coated in diverse non-cellulosic polysaccharides. Xyloglucan (XyG) is proposed to cross-link cellulosic microfibrils, while pectins such as homogalacturonan (HG) and rhamnogalacturonan (RG) form a structurally diverse glue that provides flexibility or stiffness depending on chemical modifications [18,19]. Other classes of polymers include 1,3-β-glucan, 1,3;1,4-β-glucan, mannan, arabinan, xylan, and phenolic compounds such as lignin, which vary depending on the cell type, species, and developmental age, and appear to fulfil diverse roles [20–23]. Figure 1 shows thin sections from a number of dicot and monocot tissues labelled with cell wall-related antibodies and/or viewed under UV light, highlighting the diversity of polysaccharides present in growing tissues, as well as specific differences between organs, tissues, and individual cell types. How the different polymers interact within the cell wall matrix is constantly being revisited; direct covalent connections have been reported between pectin and xylan [24], xylan and lignin [25], and xyloglucan and cellulose [26]. However, the nature of the cross-linkages and hydrophobic interactions within the wall are not fully understood, and present significant challenges for the prediction and modelling of cell wall physicochemical properties [27]. Additional complexity is conveyed through glycoproteins such as arabinogalactan proteins (Figure 1), and other cell wall proteins such as proline-rich proteins, extensins, and expansins [28].

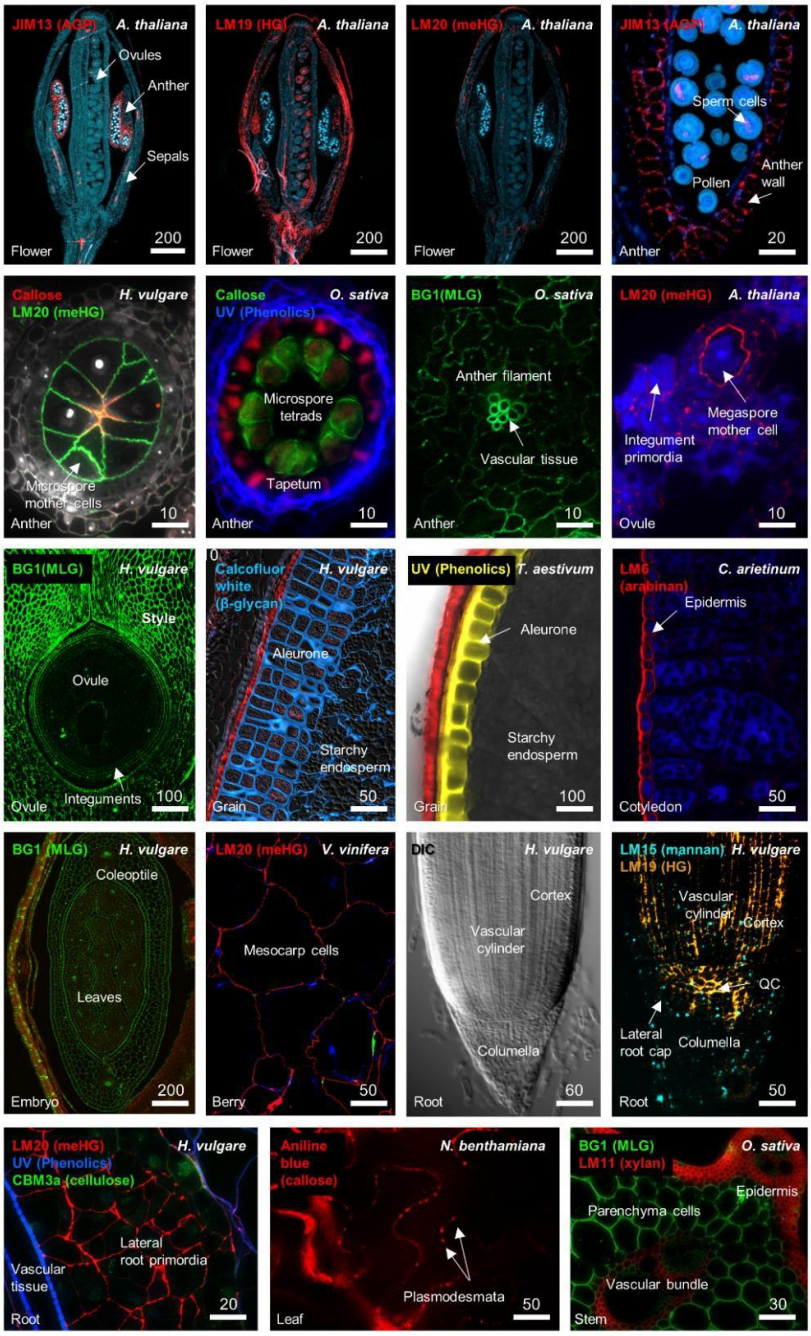

Figure 1. Detection of different cell wall components in distinct tissues of *Arabidopsis thaliana*, *Hordeum vulgare* (barley), *Oryza sativa* (rice), *Cicer arietinum* (chickpea), *Vitis vinifera* (grape), *Nicotiana benthamiana* (tobacco), and *Triticum aestivum* (bread wheat). The tissue origin of each section is indicated at the bottom left of each panel. The antibody or stain is indicated at the top left of each panel. Labelling of polymers was achieved through the use of diverse antibodies including BG1 (1,3;1,4-β-glucan), JIM13 (arabinogalactan proteins, AGP), LM19 (homogalacturonan, HG), LM20 (methylesterified homogalacturonan, meHG), callose (1,3-β-glucan), LM15 (mannan), LM6 (arabinan), LM11 (arabinoxylan), and CBM3a (cellulose), or stains such as aniline blue (1,3-β-glucan) and Calcofluor White (β-glycan), or UV autofluorescence. Differential contrast (DIC) microscopy was used to image the barley root tip and is shown as a reference for the adjoining immunolabelled sample. Images were generated for this review, but further details can be found in previous studies [23,29–32]. Scale bar dimensions are shown in μm.

Classical studies in two-celled embryos of the alga *Fucus* [33] showed that there is a direct role of the cell wall in maintaining cellular fate. Extending this hypothesis to examine the role of the cell wall during differentiation of specialized cells and tissues of higher plants has proved challenging, partially due to compositional complexity and the sub-epidermal location of cells [34]. Moreover, it remains technically challenging to view the cell wall in a high throughput manner, and with enough resolution, to identify specific quantitative and qualitative changes in composition that directly accompany or precede changes in cellular identity. Dogma suggests that as cells divide into new microenvironments they are exposed to new combinations of hormones and signals, which subsequently activate receptors at the plasma membrane to cue signal cascades and downstream transcriptional changes [35,36]. As a result of this feedback, the cell wall is remodeled to introduce new or modified polymers that exhibit different properties and contribute to new cellular identity. This almost certainly involves changes in biomechanical properties, which have been extensively reviewed in recent times [37–39]. However, in order to receive and process a particular differentiation signal, what basic structural or biochemical features are required? Do specific polysaccharides or cell wall proteins enable the preferential accumulation of receptors, transmission of signals or the synthesis of signaling molecules that potentiate differentiation? Is there an ideal wall composition required for cell differentiation? Studies in recent years provide some answers, hinting that the cell wall plays a dynamic role in development, and that cues to initiate remodeling may arise from and depend on the composition of the wall itself. As mentioned above, recent reviews have considered in detail the role of cell wall integrity and sensors in controlling plant growth [40,41]. In this review, we consider molecular and genetic evidence supporting a role for distinct cell wall polysaccharides during plant development, particularly in light of recent studies and technological advances in cell-type specific transcriptional profiling.

2. Cell Wall Modification during Growth, Differentiation, and Development

The molecular determinants of cell wall composition incorporate large families of enzymes including glycosyltransferases (GT), glycosylhydrolases (GH), methyltransferases, and acetylesterases (see the Carbohydrate Active enZyme database; CAZy [42]). The location and presumed site of activity of these enzymes can vary between the Golgi, the plasma membrane or a combination of both [43]. The addition of new polymers to a wall through the action of glycosyltransferases can immediately lead to changes in the pH, providing substrates for de-acetylation [44], de-esterification [19], and transglycosylation [45], and even new binding sites for receptors [46,47]. Specific differences in cell wall composition can be observed at different stages of development, between adjoining cells and tissues, and between monocots and dicots (See Figure 1). Several polymers that are labeled in Figure 1, pectin and callose, have been implicated in key stages of plant development. In the following sections we consider these polysaccharides, in addition to several "structural" polymers, with a view to addressing how their synthesis and/or modification can influence differentiation and development.

2.1. Pectin

Pectin is an important polymer during development since it can undergo considerable modification once it is deposited in the cell wall [48]. Multiple types of pectin are detected in the primary walls of dicots and monocots, including homogalacturonan (HG), rhamnogalacturonan-I (RG-I), rhamnogalacturonan-II (RG-II), and xylogalacturonan (XGA) [48,49]. Immunolabelling shows that pectic polymers are particularly enriched in young flowers, ovules, fruits, and roots (Figure 1). RG-I is detected in a number of tissues and is particularly prominent in the *Arabidopsis* seed coat [50] and the transition zone of developing roots [51]. The tight developmental regulation of RG-I deposition in seedling roots suggests it may play a role in cell expansion [51], but its exact role and the details of its biosynthesis remain unclear [52]. HG is methylesterified (meHG) during synthesis in the Golgi, and this forms a substrate for pectin methylesterase (PME, CE8), which depending on the cellular context can lead to loosening or strengthening of cell walls [19]. Clear roles for PME have been demonstrated in meristem development, seed mucilage biosynthesis, and pollen tube growth [53–55]. In the shoot

meristem, organ primordia initiation requires demethylesterification of HG in sub-epidermal layers through the action of PME [56], which reduces stiffness and promotes outgrowth (Figure 2). Negative regulation of *PME5* in the meristem dome by the BELLRINGER transcription factor ensures that the meHG substrate is only targeted by PME5 at the flanks of the meristem, leading to correct positioning of organ primordial [37]. Similarly, in the root, alterations in PME activity and increased demethylesterification are associated with expansion of cell types in the root tip [57,58].

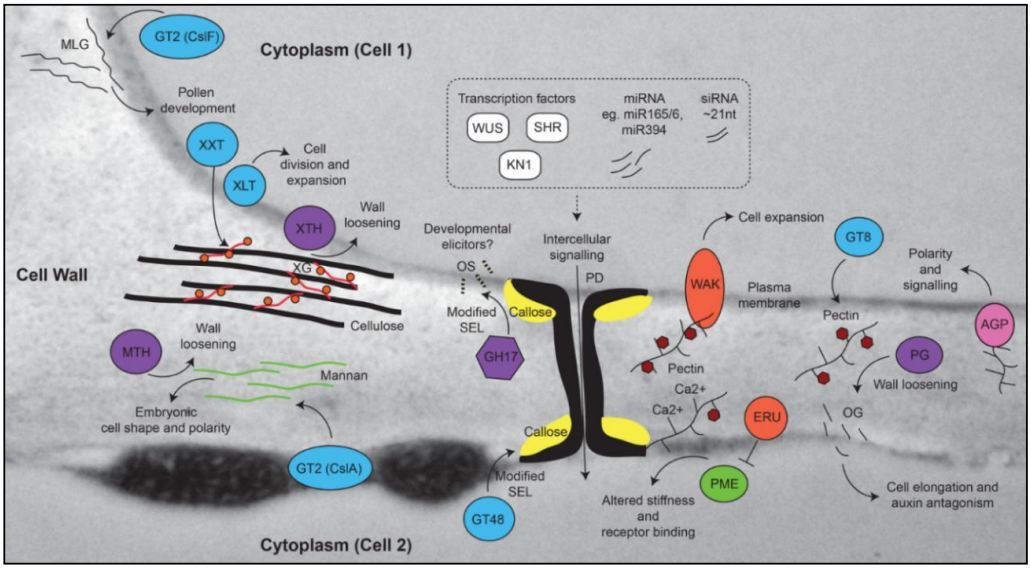

Figure 2. Cell wall components that contribute to growth, development, and differentiation. The model shows polymers superimposed on a TEM image of a leaf cell wall, including 1,3;1,4-β-glucan (MLG), cellulose, xyloglucan (XG), mannan, callose, and pectin. Enzymes that contribute to the biosynthesis or modification of these components are shown. The spatial separation of polymers is only shown for schematic purposes. Biosynthetic enzymes are shown in blue, hydrolytic enzymes are shown in purple, receptors are shown in orange, mobile transcription factors are shown in white, pectin methylesterase (PME) is shown in green, and arabinogalactan protein (AGPs) in pink. Deposition and hydrolysis of callose at the neck of plasmodesmata (PD) can alter the size exclusion limit (SEL) of the PD, hence limiting the mobility of intercellular signaling molecules such as transcription factors (e.g., WUSCHEL [59], SHORT ROOT [60], and KNOTTED [61]), microRNAs (miRNAs [60,62]), and short interfering RNAs (siRNAs [63,64]). Hydrolysis of callose by GH17 enzymes leads to the release of stimulatory oligosaccharides (OS) from the glucan backbone in fungi, but it remains unclear if similar OS contribute to growth and development in plants. By contrast, release of oligogalacturonides (OG) from pectin by polygalacturonase (PG) has been implicated in plant development through antagonistic effects on auxin pathways. The small circles on XG indicate galactosyl residues present due to the activity of XLT2 (xyloglucan galactosyltransferase). GT8 family enzymes contribute to the biosynthesis of pectin, which is usually synthesized in a methylesterified form (e.g., methylesterified homogalacturonan; meHG). Removal of methylesters (red hexagons) through the activity of PME can lead to calcium binding and subsequent cross-linking of pectin polysaccharides, which influences wall stiffness. GT, glycosyltransferase, XXT, xylosyltransferase, MTH, mannan transglycosylase/hydrolase, XTH, xyloglucan transglycosylase/hydrolase, CslF, cellulose synthase-like F, CslA, cellulose synthase-like A, GH, glycosyl hydrolase, WAK, wall-associated kinase, ERU, ERULUS receptor-like kinase.

Other factors that influence cell expansion are the Wall-Associated Kinases (WAKs), which directly bind pectin polymers in the cell wall in a way that is at least partially dependent upon the degree of methylesterification [65,66] (Figure 2). Mutations in several WAK genes suggest they play a role in mediating resistance against various pathogens [67,68], as well as in cell expansion during development [69]. Another putative receptor involved in the pectin pathway is the *Arabidopsis*

Catharanthus roseus receptor-like kinase 1-like (CrRLK1) ERULUS (ERU) protein, which is required for correct root hair formation, and regulates cell wall composition through negative control of PME activity [70] (Figure 2). Interestingly, ERU transcription is downregulated in several mutants showing changes in cell wall composition related to pectin, suggesting a possible feedback mechanism from the wall to regulate pectin composition and root hair development. ERU is part of the FERONIA (FER) family of kinases [41,71] that are implicated in fertilization, cell wall sensing, and root growth. Defects in the FER signaling pathway lead to pronounced defects in pectin composition of pollen tubes and root hairs, and a recent report indicates that FER directly interacts with pectin *in vivo* and in vitro [72]. Curiously, the ability of cell walls to sense change may be restricted to components of the primary wall, since limited signaling and transcriptomic responses were observed in mutants showing altered secondary cell wall biosynthesis in *Arabidopsis* [73].

Finally, modification of pectin by hydrolytic enzymes can lead to the release of small fragments called oligogalacturonides, which are reported to effect plant growth and development [74]. These pectin fragments impact diverse physiological processes, including fruit ripening in tomato [48] and stem elongation in pea [75] via a mechanism that appears to involve antagonism with the plant hormone auxin [76]. In summary, these studies indicate that specific pectic polymers within the wall may predispose cells to respond to stimuli that influence growth and differentiation.

2.2. Callose and Plasmodesmata

Another polymer that influences cellular differentiation is callose. Comprised of a water-insoluble linear form of (1,3)-β-glucan, callose is an atypical cell wall polysaccharide in that it is not often co-extensive throughout cell walls with pectin and cellulose but has specific restricted occurrences and functions in locations such as the cell plate, reproductive tissues, and plasmodesmata (PD). Genes involved in callose biosynthesis and hydrolysis are well characterized and include the 1,3-β-glucan synthases (GT48 family) and 1,3-β-glucan hydrolases (GH17 family), respectively. These enzymes have historically been associated with roles in pathogen response, dormancy, cell division, and plant reproduction [21,77,78], but recent studies emphasize their general importance in controlling intercellular transport of developmental regulators through PD (Figures 1 and 2). PD are intercellular channels embedded in the cell wall that provide a cytoplasmic continuum between cells [79]. Different types of PD can be detected in the cell wall, which vary in terms of their structure and their arrangement within and between cell layers [80,81]. The formation of lateral roots in *Arabidopsis* depends upon restrictive callose deposits in the cell wall adjoining the PD [82], often referred to as the "neck" region. PD also regulate intercellular movement of transcription factors and microRNAs between the stele and endodermis to control xylem development [60]. Although the cues that drive PD formation are unknown, PD are present in many cell types and are accompanied by increased pectin and decreased cellulose deposits in flanking cell wall regions [83]. Enzymes regulating callose biosynthesis and turnover are enriched in the general PD proteome [84] in addition to several PMEs, polygalacturonases and diverse receptor kinases that likely influence PD function [85,86]. The biochemical analysis of PD highlights a potential relationship between pectin and callose that has yet to be explored in significant detail.

The removal of callose from PD and specialized cell walls in the anthers and ovule is mediated by GH17 enzymes, which form a large family found in archaea, bacteria, and eukaryotes [87]. In general, GH17 activity is likely to influence growth and development in several ways by (1) decreasing the size exclusion limit (SEL) of PD and allowing increased symplastic intercellular transport [88]; (2) removing apoplastic barriers that are proposed to insulate cells such as the megaspores or microspores against mobile signals [89,90] and (3) removing a transient matrix for deposition of secondary polymers during cytokinesis and cell division [91]. Consistent with a role in regulating the SEL of PD, studies in the shoot meristem have shown that mobile tracers are free to move between distinct "symplastic fields", which incorporate different zones and layers [92,93]. This indicates that differential regulation of PD conductance is likely to be required for meristem cell identity and function. One key transcription factor involved in meristem maintenance, WUSCHEL, moves from the organizing centre (OC) of the

meristem into above-lying stem cells through PD [59]. Therefore, the presence of PD and associated cell wall polymers is another example by which cells may be predisposed to be responsive to non-cell autonomous stimuli; in essence, the PD and adjoining regions of cell wall provide a substrate for receptor binding as well as for cell wall remodeling activities that can influence intercellular signaling and differentiation (Figure 2).

In addition to these developmental functions, GH17 enzymes also form a defensive barrier during pathogen attack that targets 1,3-β-glucan polymers in the fungal cell wall. A recent study showed that non-branched fungal 1,3-β-glucan oligosaccharides are able to trigger immune responses in *Arabidopsis* via CERK1 (chitin elicitor receptor kinase 1) [94]. It is tempting to speculate that similar to oligogalacturonides, cleavage of endogenous 1,3-β-glucan polymers might release backbone oligosaccharides that elicit responses during growth and development (Figure 2).

2.3. Roles for Other "Structural" Polymers in Growth and Development

1,3;1,4-β-glucan is predominantly found in monocots, particularly the *Poaceae*, where it accumulates in the primary and secondary walls of diverse tissues [95,96] (Figure 1). Evidence suggests that accumulation of 1,3;1,4-β-glucan is required for correct grain fill in barley and wheat [97,98]. However, genetic studies also reveal specific developmental abnormalities, such as male infertility, in rice plants lacking the primary biosynthetic enzyme controlling 1,3;1,4-β-glucan biosynthesis [99] (Cellulose synthase-like F6; CslF6). In barley, tissue-specific over-accumulation of 1,3;1,4-β-glucan appears to inhibit signal and/or solute transmission [29,97] while barley *cslf6* mutants are shorter and show defects in leaf growth [100]. This is perhaps unsurprising given that *CslF6* is expressed in a range of tissues [101], however, the specific role of 1,3;1,4-β-glucan and the *CslF* gene family in plant development requires further investigation.

Unlike 1,3;1,4-β-glucan, xyloglucan (XyG) is a highly branched polysaccharide found in the primary cell wall of many plant tissues and is characterized as a structural cell wall component that binds to cellulose [102] (Figure 2). Remarkably, mutants lacking activity of three xylosyltransferase (*XXT*) genes (*XXT1*, *2* and *5*) contain no detectable xyloglucan in their cell walls, yet develop relatively normally apart from defects in root hairs [103]. By contrast, *murus3* mutants that are deficient for a XyG-specific galactosyltransferase contain normal levels of xyloglucan, but in a form that is depleted of galactosyl substituents, and this results in extreme developmental defects including dwarfism [104]. Hence, while XyG is not required per se for *Arabidopsis* development, incorrect substitution of XyG may compromise interactions between different wall polymers, resulting in a cell wall composition that is incompatible with cell growth.

Similar to xyloglucan, several types of structurally diverse mannans are also linked to the cellulose network providing mechanical support [105], while others are involved in carbohydrate storage. Loss-of-function mutations in the *Cellulose synthase-like A* (*CslA*) 2, 3, and 9 genes, encoding putative glucomannan synthases, result in no detectable glucomannan in stems but plants appear phenotypically normal [106]. However, mutants lacking function of the *CslA7* gene show embryo lethality, suggesting that in some tissues glucomannan is a critical component for growth and differentiation [107]. Although the mechanistic basis for this lethality is unclear, the *csla7* mutant embryos appear remarkably similar to those showing defects in developmental patterning and organ differentiation, such as double mutants of the *WUSCHEL-HOMEOBOX* 8/9 transcription factors [108] and *ARGONAUTE* 1/10 genes involved in post-transcriptional gene silencing [109,110]. This may indicate that targets of these transcriptional and post-transcriptional regulators converge at the cell wall, or that a distinct cell wall composition contributes to downstream function of these regulatory pathways. Interestingly, both mannan and xyloglucan are targets of transglycosylase enzymes activities, which essentially cleave the polysaccharide chain and attach it to a new chain to retain strength in the cell wall (Figure 2). Both mannan endotransglycosylases/hydrolases (MTH) and xyloglucan endotransglycosylases/hydrolases (XET/XTH) have been implicated in fruit development. LeMAN4a, an MTH from tomato, exhibits transglycosylase activity and is expressed in young floral buds where it

is hypothesized to function in tissue softening [111]. Similarly, *XTH* genes are associated with fruit development in persimmon, apple, and tomato [112,113]. Therefore, even in the case of polysaccharides that have historically been associated with structural functions, there is evidence to suggest their presence in the wall may provide a substrate for remodeling enzymes that impact growth and differentiation during diverse stages of plant development.

1. Specific Cell Wall-Related Genes Accompany Differentiation in Meristematic Zones

Antibodies and glyco-arrays are an outstanding resource [114,115] to localize and identify specific cell wall-related epitopes, and this is highlighted by the distinct labelling patterns shown in Figure 1. The limitation of antibodies is that they only provide a limited view of the chemical complexity present in a cell wall at a particular time point. Technologies that enable local qualitative and quantitative assessments of wall complexity, particularly in the case of the shoot and root meristem and reproductive tissues, would provide a significant advantage in understanding cell wall changes during differentiation. Methods such as coherent anti-Stokes Raman scattering (CARS [1]) and FTIR microspectroscopy [116] may enable specific compositional changes to be identified, although they are yet to deliver the required precision for cell-type specific analysis during development. By contrast, at the molecular level, definition of the transcriptional programs underlying cell wall formation has recently become much more accessible. The analysis and identification of cell wall-related genes that define specific cell types and/or show altered expression during development remains a viable approach to assess the role of different cell wall components in facilitating differentiation.

In *Arabidopsis*, studies have utilized the elegant method of fluorescence-assisted cell sorting (FACS) to collect specific populations of cells from developing tissues [117–119]. This approach was used successfully in *Arabidopsis* roots [117,118] to profile RNA from, among others, cell types located in the meristematic zone including the quiescent centre (QC), the adjoining columella, and the lateral root cap (LRC). The QC is marked by the expression of *AGL42* and *WOX5* genes and contains slowly dividing, "undifferentiated" cells that stimulate the formation of adjoining stem cells [120] (Figure 1). Underlying the QC are the columella initials; stem cells that divide periclinally to give rise to one daughter that adopts columella fate and another that retains stem cell identity. Similarly, the LRC initial cells adjoin the QC and give rise to all cells in the lateral root cap. These cell types are in close proximity but assume different identities as soon as they divide away from the QC. Therefore, the cell-type specific transcriptional datasets provide an excellent resource to assess changes in the cell wall machinery during differentiation.

Houston et al. [4] examined transcriptional datasets from *Arabidopsis* and other species to highlight cell wall gene families associated with cell wall remodeling during abiotic stress and pathogen attack. A similar survey of the *Arabidopsis* root cell-type specific RNA profiles [118] reveals a comprehensive set of cell wall genes potentially contributing to growth and differentiation (Figure 3). Relative to the QC (as an undifferentiated reference), cells that adopt LRC or columella fate express different gene families involved in polysaccharide biosynthesis and modification. Examples include the arabinogalactan proteins (AGPs), pectin methylesterases (CE8), glucoronyl/galacturonosyltransferases (GT8), and xylan 1,4-β-xylosyltransferases (GT43). Arabinogalactan proteins are cell wall proteins that have been implicated in many aspects of growth and development [30,31,121,122], while the other families are implicated in pectin and xylan biosynthesis and modification. The majority of these gene families are upregulated as cells adopt columella or LRC identity, consistent with the formation of new wall types compared to the relatively naïve wall in the undifferentiated QC. Notably, within the QC itself, representatives from the pectate lyase (PL1), expansin, 1,3-β-glucanase (GH17), and 1,3-β-glucan synthase (GT48) families are up-regulated, hinting at a key requirement for intercellular signaling and wall flexibility. This analysis exemplifies how transcriptomic studies can enable identification of cell wall-related genes and families that accompany changes in cell identity during differentiation. In many cases, these transcriptional changes directly relate to alterations in root cell wall composition [123] indicating a close link between transcript abundance and putative enzyme activity.

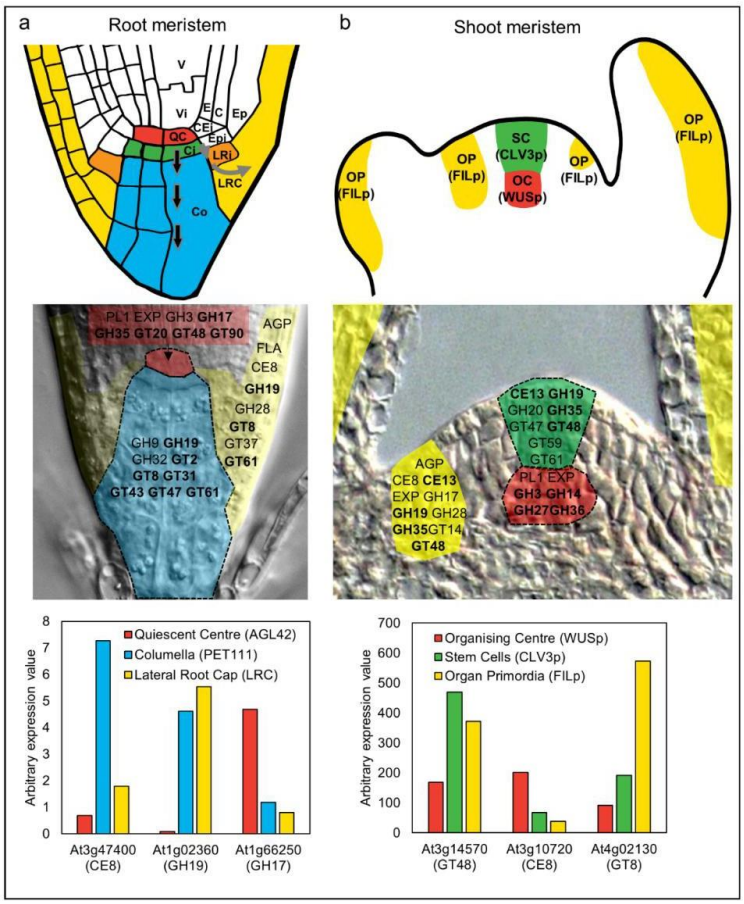

Figure 3. Analysis of cell wall-related gene expression during differentiation of stem cells in the root and shoot meristem of *Arabidopsis thaliana*. The upper panels in (**a**,**b**) show schematic representations of the root and shoot apical meristem [120]. (**a**) In the root meristem, initial cells (stem cells) directly adjoining the QC enter differentiation pathways as they divide away from the niche (shown by arrows for columella and lateral root cap). V, vasculature, Vi, vascular initial, QC, quiescent centre, E, endodermis, C, cortex, CEi, cortex/endodermis initials, Epi, epidermal initials, Ep, epidermis, LRi, lateral root cap initial, LRC, lateral root cap, Ci, columella initial, Co, columella. (**b**) In the shoot meristem, the organizing center (OC) functions via WUSCHEL (WUS) to maintain the stem cells (SC) in an undifferentiated state. The stem cells express the signal peptide CLAVATA3 (CLV3). Divisions of the stem cells provide daughters that enter differentiation pathways at the flanks of the meristem and become organ primordia (OP), which is marked by expression of genes such as *FILAMENTOUS FLOWER* (*FIL*). The second row of panels highlights gene families encoding CAZy carbohydrate-related enzymes [42] that are enriched in each meristem cell type according to FACS-mediated sorting and transcriptional profiling [118,119]. The genes are superimposed on sections of root and shoot meristem tissues. Family names in bold indicate that multiple members from the same family were up-regulated in the QC or OC (depending on the meristem) relative to both of the other cell types. GH, glycosyl hydrolase, GT, glycosyltransferase, PL, pectate lyase, AGP, arabinogalactan protein, EXP, expansin, CE, carbohydrate esterase, FLA, fasciclin-like arabinogalactan protein. See Table 1 for putative functions of enzyme families. The third row of panels shows expression patterns of selected CAZy family members in the different meristem cell types. Several of the individual genes reflect the behavior of the entire family. For example, At1g02360 is up-regulated in the columella and LRC relative to the OC, and this is a pattern shown for many GH19 family members. However, other genes such as At3g47400, At3g10720, and At4g02130 show unique patterns compared to other members of their families. The reason why multiple family members are recruited into some cell-type preferential expression pathways, while in others only individual members are expressed, remains to be elucidated.

In the shoot apical meristem (SAM), Yang et al. (2016) characterized changes in cell wall composition by immunolabelling, in addition to profiling cell wall-related gene expression in different meristematic regions [124]. Their results indicate that as cells divide through the meristem, different enzymes build new walls compared to those that build maturing walls. Complementing this, studies have examined transcriptional changes at the level of individual meristematic cell types (Figure 3). The organizing centre (OC) of the SAM is marked by expression of the *WUSCHEL* gene and is somewhat similar to the root QC, in that it is undifferentiated, slow to divide, and specifies adjoining cells as stem cells [120]. The shoot stem cells express the *CLAVATA3* gene, and as they divide anticlinally, they exit the control of the OC and enter organ differentiation pathways where expression of transcription factors such as *FILAMENTOUS FLOWER* are detected (Figure 3). Yadav et al. (2009) used these cell-type specific markers to isolate and transcriptionally profile shoot stem cell types [119]. Around half of the *Arabidopsis* CAZy cell wall families are up-regulated in organ primordia but downregulated in the stem cells relative to the OC; gene families include the expansins (EXP), fasciclin-like arabinogalactan proteins (FLAs), pectate lyases (PL1), pectin methylesterases (CE8), polygalacturonases (GH28), and endo-arabinanases (GH43). The lack of glycosyltransferases and abundance of cell wall modifying enzymes suggests that, similar to the root meristem, cell wall remodeling is the predominant feature of cell and organ differentiation in the shoot. Interestingly, gene families that are up-regulated in the stem cells relative to the OC and organ primordia include a number of key polysaccharide synthases and hydrolases such as 1,3-β-glucan synthase (GT48), arabinosyl/xylosyltransferase (GT61), and xylanase (GH10). As discussed above, the GT48 genes contribute to callose biosynthesis, and their up-regulation may relate to the formation of symplastic zones through altered PD conductance. Although a direct role for GT61 and GH10 genes during development has not been explicitly reported, GT61 enzymes have been implicated in substitution of polysaccharides to potentially influence wall polymer viscosity in seed-coat epidermal cells [125,126], and some GH10 xylanases are expressed during secondary wall synthesis in poplar [127].

In summary, these studies show that as cells exit the stem cell niche and start differentiating, clear trends are seen in the transcriptional behavior of CAZy families. The CAZy signatures of distinct cell-types within the shoot and root meristem are summarized in Figure 3. It is important to note that despite their grouping via functional domains and proposed carbohydrate-related activities, the vast majority of the CAZy genes remain uncharacterized. The transcriptional profiles of the meristematic cells are remarkably dynamic yet similar between the shoot and root meristems, identifying key activities whose role in differentiation might be addressed in more detail through further mutant and cell-type specific analyses.

3. Perspectives

The basis for this review was to consider the role of the plant cell wall in growth and development, and to assess how cell wall polysaccharides might predispose cells to undergo differentiation. We have focused our attention on polysaccharides including pectin, callose, xyloglucan, and mannan, which fulfil roles during different stages of growth and development. The presence and modification of these polymers correlates with changes in cell identity and function, and their depletion through mutagenesis or transgenic modification results in altered plant development. Callose and pectin in particular provide multiple avenues to influence differentiation, initially through deposition and subsequently through hydrolysis, chemical modification, and receptor binding. Consistent with the chemical complexity of the cell wall, the transcriptional machinery underlying cell wall polysaccharide deposition and modification is intricate. However, common activities are identified in cell types that exit from apical (shoot and root) stem cell niches and initiate differentiation. This overlap suggests that while the cellular context (i.e., roots vs. shoots) and specific gene family members might differ, early stages of differentiation likely depend on a similar wall composition that is compatible with remodeling. In this context, it seems prudent to consider the cell wall in the same light as other

key factors, such as genomic and epigenetic modifications, that facilitate important steps of the cell differentiation process.

Table 1. Protein families potentially involved in polysaccharide biosynthesis and modification in *Arabidopsis*.

CAZy Family	Putative Polysaccharide Target	Gene ID	Enzyme Description
AGP			arabinogalactan protein *
CE13	Pectin		pectin acetylesterase
CE8	Pectin	PME	pectin methylesterase
EXP			expansin
FLA			fasciclin-like arabinogalactan protein
GH3	Glucan/Xylan/Xyloglucan		β-D-glucosidase, α-L-arabinofuranosidase, β-D-xylopyranosidase
GH5	Mannan	MTH	endo-β-mannanase
GH9	Cellulose		cellulase
GH10	Xylan		endo-β-xylanase
GH14	Starch		β-amylase
GH16	Xyloglucan	XTH/XET	xyloglucan:xyloglucosyltransferases
GH17	Callose	GLUC	glucan endo-1,3-β-glucosidase
GH19	Chitin		chitinase; lysozyme
GH20			beta-hexosaminidase
GH27			α-galactosidase
GH28	Pectin	PG	polygalacturonase
GH32			invertase
GH35	Pectin/Xyloglucan		β-galactosidase
GH36			α-galactosidase
GT2	Cellulose/Mannan/1,3;1,4-β-glucan	CslA/CslF	cellulose synthase/cellulose synthase-like
GT8	Pectin/Xylan		homogalacturonan 1,4-α galacturonosyltransferase
GT14	AGP		UDP-GlcA: xylan α-glucuronyltransferase UDP-GlcA: [arabinogalactan] 1,3-β-/1,6-β-galactan 1,6-β-glucuronosyltransferase
GT20			alpha,alpha-trehalose-phosphate synthase [UDP-forming]
GT31	AGP/Pectin		1,3-β-glucuronyltransferase
GT34	Xyloglucan	XXT	xyloglucan 1,6-α-xylosyltransferases
GT37	Xyloglucan		xyloglucan 1,2-α-α-fucosyltransferase
GT43	Xylan		glucuronoxylan glycosyltransferase
GT47	Xylan/Xyloglucan	MUR3	xylosyltransferase/xyloglucan galactosyltransferase
GT48	Callose	GSL	1,3-β-glucan synthase
GT59			1,2-α-glucosyltransferase
GT61	Xylan/Xyloglucan		xylosyltransferase/arabinosyltransferase
GT90	Mannan		UDP-Xyl: (mannosyl) glucuronoxylomannan galactoxylomannan 1,2-β-xylosyltransferase
PL1	Pectin		pectate lyase

Note: * AGPs are not reported to exhibit enzymatic activity. Only families relevant to Figure 2 or the main text are included while genes that are referred to in the text are listed in the Gene ID column.

Author Contributions: All authors contributed to the Investigation, Visualization and Writing-Review & Editing of this review article.

Funding: This work was supported by the Australian Research Council grant numbers FT140100780 and CE110001007, the Grains Research and Development Corporation (GRDC) grant number GRS10938, the H2020-MSCA-RISE-2015 initiative "SEXSEED" and the Scottish Government via Rural Affairs Food and Environment Strategic Research (RESAS).

Acknowledgments: We wish to thank members of the Tucker lab for and four anonymous reviewers for helpful comments.

Conflicts of Interest: The authors declare no conflict of interest.

References

1. Zeng, Y.; Himmel, M.E.; Ding, S.Y. Visualizing chemical functionality in plant cell walls. *Biotechnol. Biofuels* **2017**, *10*, 1–16. [CrossRef] [PubMed]
2. Heo, J.O.; Blob, B.; Helariutta, Y. Differentiation of conductive cells: A matter of life and death. *Curr. Opin. Plant Biol.* **2017**, *35*, 23–29. [CrossRef] [PubMed]
3. Burton, R.A.; Gidley, M.J.; Fincher, G.B. Heterogeneity in the chemistry, structure and function of plant cell walls. *Nat. Chem. Biol.* **2010**, *6*, 724–732. [CrossRef] [PubMed]
4. Houston, K.; Tucker, M.R.; Chowdhury, J.; Shirley, N.; Little, A. The plant cell wall: A complex and dynamic structure as revealed by the responses of genes under stress conditions. *Front. Plant Sci.* **2016**, *7*, 984. [CrossRef] [PubMed]

5. Grafi, G.; Florentin, A.; Ransbotyn, V.; Morgenstern, Y. The stem cell state in plant development and in response to stress. *Front. Plant Sci.* **2011**, *2*, 53. [CrossRef] [PubMed]
6. Becraft, P.W.; Asuncion-Crabb, Y. Positional cues specify and maintain aleurone cell fate in maize endosperm development. *Development* **2000**, *127*, 4039–4048. [PubMed]
7. Tucker, M.R.; Araujo, A.C.; Paech, N.A.; Hecht, V.; Schmidt, E.D.; Rossell, J.B.; De Vries, S.C.; Koltunow, A.M. Sexual and apomictic reproduction in *Hieracium* subgenus *Pilosella* are closely interrelated developmental pathways. *Plant Cell* **2003**, *15*, 1524–1537. [CrossRef] [PubMed]
8. Tucker, M.R.; Okada, T.; Johnson, S.D.; Takaiwa, F.; Koltunow, A.M. Sporophytic ovule tissues modulate the initiation and progression of apomixis in *Hieracium*. *J. Exp. Bot.* **2012**, *63*, 3229–3241. [CrossRef] [PubMed]
9. Gaillochet, C.; Lohmann, J.U. The never-ending story: From pluripotency to plant developmental plasticity. *Development* **2015**, *142*, 2237–2249. [CrossRef] [PubMed]
10. Verdeil, J.L.; Alemanno, L.; Niemenak, N.; Tranbarger, T.J. Pluripotent versus totipotent plant stem cells: Dependence versus autonomy? *Trends Plant Sci.* **2007**, *12*, 245–252. [CrossRef] [PubMed]
11. Fukuda, H.; Ito, M.; Sugiyama, M.; Komamine, A. Mechanisms of the proliferation and differentiation of plant cells in cell culture systems. *Int. J. Dev. Biol.* **1994**, *38*, 287–299. [PubMed]
12. Ikeuchi, M.; Ogawa, Y.; Iwase, A.; Sugimoto, K. Plant regeneration: Cellular origins and molecular mechanisms. *Development* **2016**, *143*, 1442–1451. [CrossRef] [PubMed]
13. Ikeuchi, M.; Sugimoto, K.; Iwase, A. Plant callus: Mechanisms of induction and repression. *Plant Cell* **2013**, *25*, 3159–3173. [CrossRef] [PubMed]
14. Lozovaya, V.; Gorshkova, T.; Yablokova, E.; Zabotina, O.; Ageeva, M.; Rumyantseva, N.; Kolesnichenk, E.; Waranyuwat, A.; Widholm, J. Callus cell wall phenolics and plant regeneration ability. *J. Plant Physiol.* **1996**, *148*, 711–717. [CrossRef]
15. Chen, C.C.; Fu, S.F.; Lee, Y.I.; Lin, C.Y.; Lin, W.C.; Huang, H.J. Transcriptome analysis of age-related gain of callus-forming capacity in *Arabidopsis* hypocotyls. *Plant Cell Physiol.* **2012**, *53*, 1457–1469. [CrossRef] [PubMed]
16. Cosgrove, D.J.; Jarvis, M.C. Comparative structure and biomechanics of plant primary and secondary cell walls. *Front. Plant Sci.* **2012**, *3*, 204. [CrossRef] [PubMed]
17. Hofte, H.; Voxeur, A. Plant cell walls. *Curr. Biol.* **2017**, *27*, R865–R870. [CrossRef] [PubMed]
18. Park, Y.B.; Cosgrove, D.J. Xyloglucan and its interactions with other components of the growing cell wall. *Plant Cell Physiol.* **2015**, *56*, 180–194. [CrossRef] [PubMed]
19. Levesque-Tremblay, G.; Pelloux, J.; Braybrook, S.A.; Muller, K. Tuning of pectin methylesterification: Consequences for cell wall biomechanics and development. *Planta* **2015**, *242*, 791–811. [CrossRef] [PubMed]
20. Rancour, D.M.; Marita, J.M.; Hatfield, R.D. Cell wall composition throughout development for the model grass *Brachypodium distachyon*. *Front. Plant Sci.* **2012**, *3*, 266. [CrossRef] [PubMed]
21. Gibeaut, D.M.; Pauly, M.; Bacic, A.; Fincher, G.B. Changes in cell wall polysaccharides in developing barley (*Hordeum vulgare*) coleoptiles. *Planta* **2005**, *221*, 729–738. [CrossRef] [PubMed]
22. Nunan, K.J.; Sims, I.M.; Bacic, A.; Robinson, S.P.; Fincher, G.B. Changes in cell wall composition during ripening of grape berries. *Plant Physiol.* **1998**, *118*, 783–792. [CrossRef] [PubMed]
23. Wood, J.A.; Tan, H.T.; Collins, H.M.; Yap, K.; Khor, S.; Lim, W.L.; Xing, X.; Bulone, V.; Burton, R.A.; Fincher, G.B.; et al. Genetic and environmental factors contribute to variation in cell wall composition in mature desi chickpea (*Cicer arietinum* L.) cotyledons. *Plant Cell Environ.* **2018**. [CrossRef] [PubMed]
24. Tan, L.; Eberhard, S.; Pattathil, S.; Warder, C.; Glushka, J.; Yuan, C.; Hao, Z.; Zhu, X.; Avci, U.; Miller, J.S.; et al. An *Arabidopsis* cell wall proteoglycan consists of pectin and arabinoxylan covalently linked to an arabinogalactan protein. *Plant Cell* **2013**, *25*, 270–287. [CrossRef] [PubMed]
25. Grabber, J.H.; Ralph, J.; Hatfield, R.D. Cross-linking of maize walls by ferulate dimerization and incorporation into lignin. *J. Agric. Food Chem.* **2000**, *48*, 6106–6113. [CrossRef] [PubMed]
26. Hrmova, M.; Farkas, V.; Lahnstein, J.; Fincher, G.B. A barley xyloglucan xyloglucosyl transferase covalently links xyloglucan, cellulosic substrates, and (1,3;1,4)-β-D-glucans. *J. Biol. Chem.* **2007**, *282*, 12951–12962. [CrossRef] [PubMed]
27. Cosgrove, D.J. Re-constructing our models of cellulose and primary cell wall assembly. *Curr. Opin. Plant Biol.* **2014**, *22*, 122–131. [CrossRef] [PubMed]
28. Jamet, E.; Canut, H.; Boudart, G.; Pont-Lezica, R.F. Cell wall proteins: A new insight through proteomics. *Trends Plant Sci.* **2006**, *11*, 33–39. [CrossRef] [PubMed]

29. Aditya, J.; Lewis, J.; Shirley, N.J.; Tan, H.T.; Henderson, M.; Fincher, G.B.; Burton, R.A.; Mather, D.E.; Tucker, M.R. The dynamics of cereal cyst nematode infection differ between susceptible and resistant barley cultivars and lead to changes in (1,3;1,4)-β-glucan levels and *HvCslF* gene transcript abundance. *New Phytol.* **2015**, *207*, 135–147. [CrossRef] [PubMed]
30. Lora, J.; Herrero, M.; Tucker, M.R.; Hormaza, J.I. The transition from somatic to germline identity shows conserved and specialized features during angiosperm evolution. *New Phytol.* **2017**, *216*, 495–509. [CrossRef] [PubMed]
31. Coimbra, S.; Almeida, J.; Junqueira, V.; Costa, M.L.; Pereira, L.G. Arabinogalactan proteins as molecular markers in *Arabidopsis* thaliana sexual reproduction. *J. Exp. Bot.* **2007**, *58*, 4027–4035. [CrossRef] [PubMed]
32. Yu, J.; Meng, Z.; Liang, W.; Behera, S.; Kudla, J.; Tucker, M.R.; Luo, Z.; Chen, M.; Xu, D.; Zhao, G.; et al. A rice Ca^{2+} binding protein is required for tapetum function and pollen formation. *Plant Physiol.* **2016**, *172*, 1772–1786. [CrossRef] [PubMed]
33. Berger, F.; Taylor, A.; Brownlee, C. Cell fate determination by the cell wall in early *Fucus* development. *Science* **1994**, *263*, 1421–1423. [CrossRef] [PubMed]
34. Fleming, A.J. The co-ordination of cell division, differentiation and morphogenesis in the shoot apical meristem: A perspective. *J. Exp. Bot.* **2006**, *57*, 25–32. [CrossRef] [PubMed]
35. Torii, K.U. Stomatal differentiation: The beginning and the end. *Curr. Opin. Plant Biol.* **2015**, *28*, 16–22. [CrossRef] [PubMed]
36. Benfey, P.N. Defining the path from stem cells to differentiated tissue. *Essays Dev. Biol. Part A* **2016**, *116*, 35–43.
37. Vogler, H.; Felekis, D.; Nelson, B.J.; Grossniklaus, U. Measuring the mechanical properties of plant cell walls. *Plants* **2015**, *4*, 167–182. [CrossRef] [PubMed]
38. Braybrook, S.A.; Jonsson, H. Shifting foundations: The mechanical cell wall and development. *Curr. Opin. Plant Biol.* **2016**, *29*, 115–120. [CrossRef] [PubMed]
39. Cosgrove, D.J. Diffuse growth of plant cell walls. *Plant Physiol.* **2018**, *176*, 16–27. [CrossRef] [PubMed]
40. Wolf, S.; Hematy, K.; Hofte, H. Growth control and cell wall signaling in plants. *Annu. Rev. Plant Biol.* **2012**, *63*, 381–407. [CrossRef] [PubMed]
41. Franck, C.M.; Westermann, J.; Boisson-Dernier, A. Plant malectin-like receptor kinases: From cell wall integrity to immunity and beyond. *Annu. Rev. Plant Biol.* **2018**, *69*, 301–328. [CrossRef] [PubMed]
42. Lombard, V.; Golaconda Ramulu, H.; Drula, E.; Coutinho, P.M.; Henrissat, B. The carbohydrate-active enzymes database (CAZy) in 2013. *Nucleic Acids Res.* **2014**, *42*, D490–D495. [CrossRef] [PubMed]
43. Oikawa, A.; Lund, C.H.; Sakuragi, Y.; Scheller, H.V. Golgi-localized enzyme complexes for plant cell wall biosynthesis. *Trends Plant Sci.* **2013**, *18*, 49–58. [CrossRef] [PubMed]
44. Gou, J.Y.; Miller, L.M.; Hou, G.C.; Yu, X.H.; Chen, X.Y.; Liu, C.J. Acetylesterase-mediated deacetylation of pectin impairs cell elongation, pollen germination, and plant reproduction. *Plant Cell* **2012**, *24*, 50–65. [CrossRef] [PubMed]
45. Bourquin, V.; Nishikubo, N.; Abe, H.; Brumer, H.; Denman, S.; Eklund, M.; Christiernin, M.; Teeri, T.T.; Sundberg, B.; Mellerowicz, E.J. Xyloglucan endotransglycosylases have a function during the formation of secondary cell walls of vascular tissues. *Plant Cell* **2002**, *14*, 3073–3088. [CrossRef] [PubMed]
46. Kohorn, B.D.; Kobayashi, M.; Johansen, S.; Friedman, H.P.; Fischer, A.; Byers, N. Wall-associated kinase 1 (WAK1) is crosslinked in endomembranes, and transport to the cell surface requires correct cell-wall synthesis. *J. Cell Sci.* **2006**, *119*, 2282–2290. [CrossRef] [PubMed]
47. Decreux, A.; Messiaen, J. Wall-associated kinase WAK1 interacts with cell wall pectins in a calcium-induced conformation. *Plant Cell Physiol.* **2005**, *46*, 268–278. [CrossRef] [PubMed]
48. Wolf, S.; Greiner, S. Growth control by cell wall pectins. *Protoplasma* **2012**, *249* (Suppl. 2), S169–S175. [CrossRef] [PubMed]
49. Sorieul, M.; Dickson, A.; Hill, S.J.; Pearson, H. Plant fibre: Molecular structure and biomechanical properties, of a complex living material, influencing its deconstruction towards a biobased composite. *Materials* **2016**, *9*, 618. [CrossRef] [PubMed]
50. Griffiths, J.S.; Tsai, A.Y.; Xue, H.; Voiniciuc, C.; Sola, K.; Seifert, G.J.; Mansfield, S.D.; Haughn, G.W. SALT-OVERLY SENSITIVE5 mediates *Arabidopsis* seed coat mucilage adherence and organization through pectins. *Plant Physiol.* **2014**, *165*, 991–1004. [CrossRef] [PubMed]

51. McCartney, L.; Steele-King, C.G.; Jordan, E.; Knox, J.P. Cell wall pectic (1→4)-β-D-galactan marks the acceleration of cell elongation in the *Arabidopsis* seedling root meristem. *Plant J.* **2003**, *33*, 447–454. [CrossRef] [PubMed]
52. Harholt, J.; Suttangkakul, A.; Vibe Scheller, H. Biosynthesis of pectin. *Plant Physiol.* **2010**, *153*, 384–395. [CrossRef] [PubMed]
53. Turbant, A.; Fournet, F.; Lequart, M.; Zabijak, L.; Pageau, K.; Bouton, S.; Van Wuytswinkel, O. Pme58 plays a role in pectin distribution during seed coat mucilage extrusion through homogalacturonan modification. *J. Exp. Bot.* **2016**, *67*, 2177–2190. [CrossRef] [PubMed]
54. Jiang, L.; Yang, S.L.; Xie, L.F.; Puah, C.S.; Zhang, X.Q.; Yang, W.C.; Sundaresan, V.; Ye, D. Vanguard1 encodes a pectin methylesterase that enhances pollen tube growth in the *Arabidopsis* style and transmitting tract. *Plant Cell* **2005**, *17*, 584–596. [CrossRef] [PubMed]
55. Etchells, J.P.; Moore, L.; Jiang, W.Z.; Prescott, H.; Capper, R.; Saunders, N.J.; Bhatt, A.M.; Dickinson, H.G. A role for *BELLRINGER* in cell wall development is supported by loss-of-function phenotypes. *BMC Plant Biol.* **2012**, *12*, 212. [CrossRef] [PubMed]
56. Peaucelle, A.; Braybrook, S.A.; Le Guillou, L.; Bron, E.; Kuhlemeier, C.; Hofte, H. Pectin-induced changes in cell wall mechanics underlie organ initiation in *Arabidopsis*. *Curr. Biol.* **2011**, *21*, 1720–1726. [CrossRef] [PubMed]
57. Xiong, J.; Yang, Y.; Fu, G.; Tao, L. Novel roles of hydrogen peroxide (H_2O_2) in regulating pectin synthesis and demethylesterification in the cell wall of rice (*Oryza sativa*) root tips. *New Phytol.* **2015**, *206*, 118–126. [CrossRef] [PubMed]
58. Lionetti, V.; Raiola, A.; Camardella, L.; Giovane, A.; Obel, N.; Pauly, M.; Favaron, F.; Cervone, F.; Bellincampi, D. Overexpression of pectin methylesterase inhibitors in *Arabidopsis* restricts fungal infection by *Botrytis cinerea*. *Plant Physiol.* **2007**, *143*, 1871–1880. [CrossRef] [PubMed]
59. Daum, G.; Medzihradszky, A.; Suzaki, T.; Lohmann, J.U. A mechanistic framework for noncell autonomous stem cell induction in *Arabidopsis*. *Proc. Natl. Acad. Sci. USA* **2014**, *111*, 14619–14624. [CrossRef] [PubMed]
60. Vaten, A.; Dettmer, J.; Wu, S.; Stierhof, Y.D.; Miyashima, S.; Yadav, S.R.; Roberts, C.J.; Campilho, A.; Bulone, V.; Lichtenberger, R.; et al. Callose biosynthesis regulates symplastic trafficking during root development. *Dev. Cell* **2011**, *21*, 1144–1155. [CrossRef] [PubMed]
61. Lucas, W.J.; Bouché-Pillon, S.; Jackson, D.P.; Nguyen, L.; Baker, L.; Ding, B.; Hake, S. Selective trafficking of KNOTTED1 homeodomain protein and its mRNA through plasmodesmata. *Science* **1995**, *270*, 1980–1983. [CrossRef] [PubMed]
62. Knauer, S.; Holt, A.L.; Rubio-Somoza, I.; Tucker, E.J.; Hinze, A.; Pisch, M.; Javelle, M.; Timmermans, M.C.; Tucker, M.R.; Laux, T. A protodermal miR394 signal defines a region of stem cell competence in the *Arabidopsis* shoot meristem. *Dev. Cell* **2013**, *24*, 125–132. [CrossRef] [PubMed]
63. Molnar, A.; Melnyk, C.; Baulcombe, D.C. Silencing signals in plants: A long journey for small rnas. *Genome Biol.* **2011**, *12*, 215. [CrossRef] [PubMed]
64. Taochy, C.; Gursanscky, N.R.; Cao, J.; Fletcher, S.J.; Dressel, U.; Mitter, N.; Tucker, M.R.; Koltunow, A.M.G.; Bowman, J.L.; Vaucheret, H.; Carroll, B.J. A genetic screen for impaired systemic RNAi highlights the crucial role of *Dicer-like 2*. *Plant Physiol.* **2017**, *175*, 1424–1437. [CrossRef] [PubMed]
65. Kohorn, B.D.; Johansen, S.; Shishido, A.; Todorova, T.; Martinez, R.; Defeo, E.; Obregon, P. Pectin activation of MAP kinase and gene expression is WAK2 dependent. *Plant J.* **2009**, *60*, 974–982. [CrossRef] [PubMed]
66. Kohorn, B.D.; Kohorn, S.L.; Saba, N.J.; Martinez, V.M. Requirement for pectin methyl esterase and preference for fragmented over native pectins for wall-associated kinase-activated, EDS1/PAD4-dependent stress response in *Arabidopsis*. *J. Biol. Chem.* **2014**, *289*, 18978–18986. [CrossRef] [PubMed]
67. Saintenac, C.; Lee, W.S.; Cambon, F.; Rudd, J.J.; King, R.C.; Marande, W.; Powers, S.J.; Berges, H.; Phillips, A.L.; Uauy, C.; et al. Wheat receptor-kinase-like protein STB6 controls gene-for-gene resistance to fungal pathogen *Zymoseptoria tritici*. *Nat. Genet.* **2018**, *50*, 368–374. [CrossRef] [PubMed]
68. Zhang, N.; Zhang, B.; Zuo, W.; Xing, Y.; Konlasuk, S.; Tan, G.; Zhang, Q.; Ye, J.; Xu, M. Cytological and molecular characterization of *ZmWAK*-mediated head-smut resistance in maize. *Mol. Plant Microbe Interact.* **2017**, *30*, 455–465. [CrossRef] [PubMed]
69. Wagner, T.A.; Kohorn, B.D. Wall-associated kinases are expressed throughout plant development and are required for cell expansion. *Plant Cell* **2001**, *13*, 303–318. [CrossRef] [PubMed]

70. Schoenaers, S.; Balcerowicz, D.; Breen, G.; Hill, K.; Zdanio, M.; Mouille, G.; Holman, T.J.; Oh, J.; Wilson, M.H.; Nikonorova, N.; et al. The auxin-regulated CrRLK1L kinase *ERULUS* controls cell wall composition during root hair tip growth. *Curr. Biol.* **2018**, *28*, 722–732. [CrossRef] [PubMed]
71. Kessler, S.A.; Shimosato-Asano, H.; Keinath, N.F.; Wuest, S.E.; Ingram, G.; Panstruga, R.; Grossniklaus, U. Conserved molecular components for pollen tube reception and fungal invasion. *Science* **2010**, *330*, 968–971. [CrossRef] [PubMed]
72. Lin, W.; Tang, W.; Anderson, C.; Yang, Z. FERONIA's sensing of cell wall pectin activates ROP GTPase signaling in *Arabidopsis*. *bioRxiv* **2018**. [CrossRef]
73. Faria-Blanc, N.; Mortimer, J.C.; Dupree, P. A transcriptomic analysis of xylan mutants does not support the existence of a secondary cell wall integrity system in *Arabidopsis*. *Front. Plant Sci.* **2018**, *9*, 384. [CrossRef] [PubMed]
74. Ferrari, S.; Savatin, D.V.; Sicilia, F.; Gramegna, G.; Cervone, F.; Lorenzo, G.D. Oligogalacturonides: Plant damage-associated molecular patterns and regulators of growth and development. *Front. Plant Sci.* **2013**, *4*, 49. [CrossRef] [PubMed]
75. Branca, C.; Lorenzo, G.D.; Cervone, F. Competitive inhibition of the auxin-induced elongation by α-D-oligogalacturonides in pea stem segments. *Physiol. Plant.* **1988**, *72*, 499–504. [CrossRef]
76. Gramegna, G.; Modesti, V.; Savatin, D.V.; Sicilia, F.; Cervone, F.; De Lorenzo, G. GRP-3 and KAPP, encoding interactors of WAK1, negatively affect defense responses induced by oligogalacturonides and local response to wounding. *J. Exp. Bot.* **2016**, *67*, 1715–1729. [CrossRef] [PubMed]
77. Balasubramanian, V.; Vashisht, D.; Cletus, J.; Sakthivel, N. Plant β-1,3-glucanases: Their biological functions and transgenic expression against phytopathogenic fungi. *Biotechnol. Lett.* **2012**, *34*, 1983–1990. [CrossRef] [PubMed]
78. van der Schoot, C.; Rinne, P.L.H. Dormancy cycling at the shoot apical meristem: Transitioning between self-organization and self-arrest. *Plant Sci.* **2011**, *180*, 120–131. [CrossRef] [PubMed]
79. Sevilem, I.; Miyashima, S.; Helariutta, Y. Cell-to-cell communication via plasmodesmata in vascular plants. *Cell Adhes. Migr.* **2013**, *7*, 27–32. [CrossRef] [PubMed]
80. Kitagawa, M.; Jackson, D. Plasmodesmata-mediated cell-to-cell communication in the shoot apical meristem: How stem cells talk. *Plants* **2017**, *6*, 12. [CrossRef] [PubMed]
81. Amsbury, S.; Kirk, P.; Benitez-Alfonso, Y. Emerging models on the regulation of intercellular transport by plasmodesmata-associated callose. *J. Exp. Bot.* **2017**, *69*, 105–115. [CrossRef] [PubMed]
82. Benitez-Alfonso, Y.; Faulkner, C.; Pendle, A.; Miyashima, S.; Helariutta, Y.; Maule, A. Symplastic intercellular connectivity regulates lateral root patterning. *Dev. Cell* **2013**, *26*, 136–147. [CrossRef] [PubMed]
83. Faulkner, C.; Akman, O.E.; Bell, K.; Jeffree, C.; Oparka, K. Peeking into pit fields: A multiple twinning model of secondary plasmodesmata formation in tobacco. *Plant Cell* **2008**, *20*, 1504–1518. [CrossRef] [PubMed]
84. Fernandez-Calvino, L.; Faulkner, C.; Walshaw, J.; Saalbach, G.; Bayer, E.; Benitez-Alfonso, Y.; Maule, A. *Arabidopsis* plasmodesmal proteome. *PLoS ONE* **2011**, *6*, e18880. [CrossRef] [PubMed]
85. Knox, J.P.; Benitez-Alfonso, Y. Roles and regulation of plant cell walls surrounding plasmodesmata. *Curr. Opin. Plant Biol.* **2014**, *22*, 93–100. [CrossRef] [PubMed]
86. Stavolone, L.; Lionetti, V. Extracellular matrix in plants and animals: Hooks and locks for viruses. *Front. Microbiol* **2017**, *8*, 1760. [CrossRef] [PubMed]
87. Doxey, A.C.; Yaish, M.W.; Moffatt, B.A.; Griffith, M.; McConkey, B.J. Functional divergence in the *Arabidopsis* β-1,3-glucanase gene family inferred by phylogenetic reconstruction of expression states. *Mol. Biol. Evol.* **2007**, *24*, 1045–1055. [CrossRef] [PubMed]
88. Maule, A.; Faulkner, C.; Benitez-Alfonso, Y. Plasmodesmata "in communicado". *Front. Plant Sci.* **2012**, *3*, 30. [CrossRef] [PubMed]
89. Bell, P.R. Megaspore abortion: A consequence of selective apoptosis. *Int. J. Plant Sci.* **1996**, *157*, 1–7. [CrossRef]
90. Bucciaglia, P.A.; Zimmermann, E.; Smith, A.G. Functional analysis of a β-1,3-glucanase gene (*Tag1*) with anther-specific RNA and protein accumulation using antisense RNA inhibition. *J. Plant Physiol.* **2003**, *160*, 1367–1373. [CrossRef] [PubMed]
91. Tucker, M.R.; Koltunow, A.M. Traffic monitors at the cell periphery: The role of cell walls during early female reproductive cell differentiation in plants. *Curr. Opin. Plant Biol.* **2014**, *17*, 137–145. [CrossRef] [PubMed]

92. Gisel, A.; Barella, S.; Hempel, F.D.; Zambryski, P.C. Temporal and spatial regulation of symplastic trafficking during development in *Arabidopsis thaliana* apices. *Development* **1999**, *126*, 1879–1889. [PubMed]
93. Kim, I.; Kobayashi, K.; Cho, E.; Zambryski, P.C. Subdomains for transport via plasmodesmata corresponding to the apical-basal axis are established during *Arabidopsis* embryogenesis. *Proc. Natl. Acad. Sci. USA* **2005**, *102*, 11945–11950. [CrossRef] [PubMed]
94. Melida, H.; Sopena-Torres, S.; Bacete, L.; Garrido-Arandia, M.; Jorda, L.; Lopez, G.; Munoz-Barrios, A.; Pacios, L.F.; Molina, A. Non-branched β-1,3-glucan oligosaccharides trigger immune responses in *Arabidopsis*. *Plant J.* **2018**, *93*, 34–49. [CrossRef] [PubMed]
95. Burton, R.A.; Fincher, G.B. (1, 3;1, 4)-β-D-glucans in cell walls of the *Poaceae*, lower plants, and fungi: A tale of two linkages. *Mol. Plant* **2009**, *2*, 873–882. [CrossRef] [PubMed]
96. Little, A.; Schwerdt, J.G.; Shirley, N.J.; Khor, S.-F.; Neumann, K.; O'Donovan, L.A.; Lahnstein, J.; Collins, H.C.; Henderson, M.; Fincher, G.B.; et al. Revised phylogeny of the cellulose synthase gene superfamily: New insights into cell wall evolution. *Plant Physiol.* **2018**. [CrossRef] [PubMed]
97. Burton, R.A.; Collins, H.M.; Kibble, N.A.; Smith, J.A.; Shirley, N.J.; Jobling, S.A.; Henderson, M.; Singh, R.R.; Pettolino, F.; Wilson, S.M.; et al. Over-expression of specific *HvCslF* cellulose synthase-like genes in transgenic barley increases the levels of cell wall (1, 3;1, 4)-β-D-glucans and alters their fine structure. *Plant Biotechnol. J.* **2011**, *9*, 117–135. [CrossRef] [PubMed]
98. Nemeth, C.; Freeman, J.; Jones, H.D.; Sparks, C.; Pellny, T.K.; Wilkinson, M.D.; Dunwell, J.; Andersson, A.A.M.; Aman, P.; Guillon, F.; et al. Down-regulation of the *CslF6* gene results in decreased (1,3;1,4)-β-D-glucan in endosperm of wheat. *Plant Physiol.* **2010**, *152*, 1209–1218. [CrossRef] [PubMed]
99. Vega-Sanchez, M.E.; Verhertbruggen, Y.; Christensen, U.; Chen, X.W.; Sharma, V.; Varanasi, P.; Jobling, S.A.; Talbot, M.; White, R.G.; Joo, M.; et al. Loss of cellulose synthase-like f6 function affects mixed-linkage glucan deposition, cell wall mechanical properties, and defense responses in vegetative tissues of rice. *Plant Physiol.* **2012**, *159*, 56–69. [CrossRef] [PubMed]
100. Taketa, S.; Yuo, T.; Tonooka, T.; Tsumuraya, Y.; Inagaki, Y.; Haruyama, N.; Larroque, O.; Jobling, S.A. Functional characterization of barley betaglucanless mutants demonstrates a unique role for *CslF6* in (1,3;1,4)-β-D-glucan biosynthesis. *J. Exp. Bot.* **2012**, *63*, 381–392. [CrossRef] [PubMed]
101. Burton, R.A.; Jobling, S.A.; Harvey, A.J.; Shirley, N.J.; Mather, D.E.; Bacic, A.; Fincher, G.B. The genetics and transcriptional profiles of the cellulose synthase-like *HvCslF* gene family in barley. *Plant Physiol.* **2008**, *146*, 1821–1833. [CrossRef] [PubMed]
102. Zabotina, O. Xyloglucan and its biosynthesis. *Front. Plant Sci.* **2012**, *3*, 134. [CrossRef] [PubMed]
103. Zabotina, O.A.; Avci, U.; Cavalier, D.; Pattathil, S.; Chou, Y.H.; Eberhard, S.; Danhof, L.; Keegstra, K.; Hahn, M.G. Mutations in multiple *XXT* genes of *Arabidopsis* reveal the complexity of xyloglucan biosynthesis. *Plant Physiol.* **2012**, *159*, 1367–1384. [CrossRef] [PubMed]
104. Kong, Y.; Pena, M.J.; Renna, L.; Avci, U.; Pattathil, S.; Tuomivaara, S.T.; Li, X.; Reiter, W.D.; Brandizzi, F.; Hahn, M.G.; et al. Galactose-depleted xyloglucan is dysfunctional and leads to dwarfism in *Arabidopsis*. *Plant Physiol.* **2015**, *167*, 1296–1306. [CrossRef] [PubMed]
105. Schröder, R.; Atkinson, R.G.; Redgwell, R.J. Re-interpreting the role of endo-β-mannanases as mannan endotransglycosylase/hydrolases in the plant cell wall. *Ann. Bot.* **2009**, *104*, 197–204. [CrossRef] [PubMed]
106. Goubet, F.; Barton, C.J.; Mortimer, J.C.; Yu, X.; Zhang, Z.; Miles, G.P.; Richens, J.; Liepman, A.H.; Seffen, K.; Dupree, P. Cell wall glucomannan in *Arabidopsis* is synthesised by *CslA* glycosyltransferases, and influences the progression of embryogenesis. *Plant J.* **2009**, *60*, 527–538. [CrossRef] [PubMed]
107. Rodriguez-Gacio Mdel, C.; Iglesias-Fernandez, R.; Carbonero, P.; Matilla, A.J. Softening-up mannan-rich cell walls. *J. Exp. Bot.* **2012**, *63*, 3976–3988. [CrossRef] [PubMed]
108. Ueda, M.; Zhang, Z.; Laux, T. Transcriptional activation of *Arabidopsis* axis patterning genes *WOX8/9* links zygote polarity to embryo development. *Dev. Cell* **2011**, *20*, 264–270. [CrossRef] [PubMed]
109. Mallory, A.C.; Hinze, A.; Tucker, M.R.; Bouche, N.; Gasciolli, V.; Elmayan, T.; Lauressergues, D.; Jauvion, V.; Vaucheret, H.; Laux, T. Redundant and specific roles of the ARGONAUTEe proteins AGO1 and ZLL in development and small RNA-directed gene silencing. *PLoS Genet.* **2009**, *5*, e1000646. [CrossRef] [PubMed]
110. Bohmert, K.; Camus, I.; Bellini, C.; Bouchez, D.; Caboche, M.; Benning, C. *AGO1* defines a novel locus of *Arabidopsis* controlling leaf development. *EMBO J.* **1998**, *17*, 170–180. [CrossRef] [PubMed]
111. Schröder, R.; Wegrzyn, T.F.; Sharma, N.N.; Atkinson, R.G. LeMAN4 endo-β-mannanase from ripe tomato fruit can act as a mannan transglycosylase or hydrolase. *Planta* **2006**, *224*, 1091–1102. [CrossRef] [PubMed]

112. Han, Y.; Ban, Q.; Hou, Y.; Meng, K.; Suo, J.; Rao, J. Isolation and characterization of two persimmon xyloglucan endotransglycosylase/hydrolase (*XTH*) genes that have divergent functions in cell wall modification and fruit postharvest softening. *Front. Plant Sci.* **2016**, *7*, 624. [CrossRef] [PubMed]
113. Muñoz-Bertomeu, J.; Miedes, E.; Lorences, E.P. Expression of xyloglucan endotransglucosylase/hydrolase (*XTH*) genes and XET activity in ethylene treated apple and tomato fruits. *J. Plant Physiol.* **2013**, *170*, 1194–1201. [CrossRef] [PubMed]
114. Knox, J.P. The use of antibodies to study the architecture and developmental regulation of plant cell walls. *Int. Rev. Cytol.* **1997**, *171*, 79–120. [PubMed]
115. Pedersen, H.L.; Fangel, J.U.; McCleary, B.; Ruzanski, C.; Rydahl, M.G.; Ralet, M.C.; Farkas, V.; von Schantz, L.; Marcus, S.E.; Andersen, M.C.; et al. Versatile high resolution oligosaccharide microarrays for plant glycobiology and cell wall research. *J. Biol. Chem.* **2012**, *287*, 39429–39438. [CrossRef] [PubMed]
116. Gierlinger, N. New insights into plant cell walls by vibrational microspectroscopy. *Appl. Spectrosc. Rev.* **2017**. [CrossRef]
117. Birnbaum, K.; Shasha, D.E.; Wang, J.Y.; Jung, J.W.; Lambert, G.M.; Galbraith, D.W.; Benfey, P.N. A gene expression map of the *Arabidopsis* root. *Science* **2003**, *302*, 1956–1960. [CrossRef] [PubMed]
118. Brady, S.M.; Orlando, D.A.; Lee, J.-Y.; Wang, J.Y.; Koch, J.; Dinneny, J.R.; Mace, D.; Ohler, U.; Benfey, P.N. A high-resolution root spatiotemporal map reveals dominant expression patterns. *Science* **2007**, *318*, 801–806. [CrossRef] [PubMed]
119. Yadav, R.K.; Girke, T.; Pasala, S.; Xie, M.; Reddy, G.V. Gene expression map of the *Arabidopsis* shoot apical meristem stem cell niche. *Proc. Natl. Acad. Sci. USA* **2009**, *106*, 4941–4946. [CrossRef] [PubMed]
120. Tucker, M.R.; Laux, T. Connecting the paths in plant stem cell regulation. *Trends Cell Biol.* **2007**, *17*, 403–410. [CrossRef] [PubMed]
121. Nguema-Ona, E.; Coimbra, S.; Vicre-Gibouin, M.; Mollet, J.C.; Driouich, A. Arabinogalactan proteins in root and pollen-tube cells: Distribution and functional aspects. *Ann. Bot.* **2012**, *110*, 383–404. [CrossRef] [PubMed]
122. Lee, K.J.; Sakata, Y.; Mau, S.L.; Pettolino, F.; Bacic, A.; Quatrano, R.S.; Knight, C.D.; Knox, J.P. Arabinogalactan proteins are required for apical cell extension in the moss physcomitrella patens. *Plant Cell* **2005**, *17*, 3051–3065. [CrossRef] [PubMed]
123. Somssich, M.; Khan, G.A.; Persson, S. Cell wall heterogeneity in root development of *Arabidopsis*. *Front. Plant Sci.* **2016**, *7*, 1242. [CrossRef] [PubMed]
124. Yang, W.; Schuster, C.; Beahan, C.T.; Charoensawan, V.; Peaucelle, A.; Bacic, A.; Doblin, M.S.; Wightman, R.; Meyerowitz, E.M. Regulation of meristem morphogenesis by cell wall synthases in *Arabidopsis*. *Curr. Biol.* **2016**, *26*, 1404–1415. [CrossRef] [PubMed]
125. Tucker, M.R.; Ma, C.; Phan, J.; Neumann, K.; Shirley, N.J.; Hahn, M.G.; Cozzolino, D.; Burton, R.A. Dissecting the genetic basis for seed coat mucilage heteroxylan biosynthesis in *Plantago ovata* using gamma irradiation and infrared spectroscopy. *Front. Plant Sci.* **2017**, *8*, 326. [CrossRef] [PubMed]
126. Phan, J.L.; Tucker, M.R.; Khor, S.F.; Shirley, N.; Lahnstein, J.; Beahan, C.; Bacic, A.; Burton, R.A. Differences in glycosyltransferase family 61 accompany variation in seed coat mucilage composition in *Plantago* spp. *J. Exp. Bot.* **2016**, *67*, 6481–6495. [CrossRef] [PubMed]
127. Derba-Maceluch, M.; Awano, T.; Takahashi, J.; Lucenius, J.; Ratke, C.; Kontro, I.; Busse-Wicher, M.; Kosik, O.; Tanaka, R.; Winzéll, A.; et al. Suppression of xylan endotransglycosylase *PtxtXyn10A* affects cellulose microfibril angle in secondary wall in aspen wood. *New Phytol.* **2015**, *205*, 666–681. [CrossRef] [PubMed]

Appendix IV

Translating auxin responses into ovules, seeds and yield: insight from Arabidopsis and the cereals

ꕥ • ꕥ

Statement of Authorship

Title of Paper	Translating auxin responses into ovules, seeds and yield: insights from Arabidopsis and the cereals
Publication Status	☑ Published ☐ Accepted for Publication ☐ Submitted for Publication ☐ Unpublished and Unsubmitted work written in manuscript style
Publication Details	Neil J. Shirley[1], Matthew K. Aubert[1], Laura G. Wilkinson[1], Dayton C. Bird[1], Jorge Lora[2], Xiujuan Yang[1], and Matthew R. Tucker[1,*]

Principal Author

Name of Principal Author (~~Candidate~~)	Neil J. Shirley		
Contribution to the Paper	Compiled information and wrote the manuscript. I hereby certify that the statement of authorship is accurate.		
Overall percentage (%)	60%		
Signature		Date	14/2/19

Co-Author Contributions

By signing the Statement of Authorship, each author certifies that:

i. the candidate's stated contribution to the publication is accurate (as detailed above);
ii. permission is granted for the candidate in include the publication in the thesis; and
iii. the sum of all co-author contributions is equal to 100% less the candidate's stated contribution.

Name of Co-Author	Matthew K. Aubert		
Contribution to the Paper	Compiled information and contributed to the preparation of the manuscript. I hereby certify that the statement of authorship is accurate.		
Signature		Date	14/02/2019

Name of Co-Author	Laura G. Wilkinson		
Contribution to the Paper	Compiled information and contributed to the preparation of the manuscript. I hereby certify that the statement of authorship is accurate.		
Signature		Date	14/02/2019

Name of Co-Author	Dayton C. Bird		
Contribution to the Paper	Compiled information and contributed to the preparation of the manuscript. I hereby certify that the statement of authorship is accurate.		
Signature		Date	14/2/19

Name of Co-Author	Jorge Lora		
Contribution to the Paper	Compiled information and contributed to the preparation of the manuscript. I hereby certify that the statement of authorship is accurate.		
Signature		Date	14/02/2019

Name of Co-Author	Xiujuan Yang		
Contribution to the Paper	Compiled information and contributed to the preparation of the manuscript. I hereby certify that the statement of authorship is accurate.		
Signature		Date	14/2/2019

Name of Co-Author	Matthew R. Tucker		
Contribution to the Paper	Compiled information and contributed to the preparation of the manuscript. I hereby certify that the statement of authorship is accurate.		
Signature		Date	22/2/19

Journal of Integrative Plant Biology

Translating auxin responses into ovules, seeds and yield: insight from Arabidopsis and the cereals

Journal:	*Journal of Integrative Plant Biology*
Manuscript ID	JIPB-2018-0192.R1
Manuscript Type:	Invited Expert Review
Date Submitted by the Author:	22-Oct-2018
Complete List of Authors:	Shirley, Neil; University of Adelaide Aubert, Matthew; University of Adelaide Wilkinson, Laura; University of Adelaide Bird, Dayton; University of Adelaide Lora, Jorge; Instituto de Hortofruticultura Subtropical y Mediterranea 'La Mayora' (IHSM-UMA-CSIC) Yang, Xiujuan; University of Adelaide Tucker, Matthew; University of Adelaide,
Keywords:	Ovule, Seed, Auxin, Barley, Arabidopsis, Development, Plant, Yield, Grain, Phytohormone
TOC Category:	Plant Reproduction Biology, Cell and Developmental Biology

Statement of Authorship

Title of Paper	Translating auxin responses into ovules, seeds and yield: insight from Arabidopsis and the cereals
Publication Status	☐ Published ☑ Accepted for Publication ☐ Submitted for Publication ☐ Unpublished and Unsubmitted work written in manuscript style
Publication Details	Neil. J Shirley, Matthew K. Aubert, Laura G. Wilkinson, Dayton C. Bird, Jorge Lora, Xiujuan Yang and Matthew R. Tucker*

Principal Author

Name of Principal Author (Candidate)	Neil. J Shirley		
Contribution to the Paper	Compiled information and wrote manuscript. I hereby certify that the statement of authorship is accurate.		
Overall percentage (%)	60%		
Certification:	This paper reports on original research I conducted during the period of my Higher Degree by Research candidature and is not subject to any obligations or contractual agreements with a third party that would constrain its inclusion in this thesis. I am the primary author of this paper.		
Signature		Date	21/11/18

Co-Author Contributions

By signing the Statement of Authorship, each author certifies that:

i. the candidate's stated contribution to the publication is accurate (as detailed above);

ii. permission is granted for the candidate in include the publication in the thesis; and

iii. the sum of all co-author contributions is equal to 100% less the candidate's stated contribution.

Name of Co-Author	Matthew K. Aubert		
Contribution to the Paper	Compiled information and contributed to the preparation of the manuscript. I hereby certify that the statement of authorship is accurate.		
Signature		Date	21/11/2018

Name of Co-Author	Laura G. Wilkinson		
Contribution to the Paper	Compiled information and contributed to the preparation of the manuscript. I hereby certify that the statement of authorship is accurate.		
Signature		Date	22/11/2018

Please cut and paste additional co-author panels here as required.

Name of Co-Author	Dayton C. Bird		
Contribution to the Paper	Compiled information and contributed to the preparation of the manuscript. I hereby certify that the statement of authorship is accurate.		
Signature		Date	22/11/2018

Name of Co-Author	Jorge Lora		
Contribution to the Paper	Compiled information and contributed to the preparation of the manuscript. I hereby certify that the statement of authorship is accurate.		
Signature		Date	22/11/2018

Name of Co-Author	Xiujuan Yang		
Contribution to the Paper	Compiled information and contributed to the preparation of the manuscript. I hereby certify that the statement of authorship is accurate.		
Signature		Date	22/11/2018

Name of Co-Author	Matthew R. Tucker		
Contribution to the Paper	Compiled information and contributed to the preparation of the manuscript. I hereby certify that the statement of authorship is accurate.		
Signature		Date	22/11/2018

Translating auxin responses into ovules, seeds and yield: insight from Arabidopsis and the cereals

Neil. J Shirley, Matthew K. Aubert, Laura G. Wilkinson, Dayton C. Bird, Jorge Lora, Xiujuan Yang and Matthew R. Tucker*

School of Agriculture, Food and Wine, Waite Research Institute, The University of Adelaide, Glen Osmond, SA, Australia

*Correspondence: matthew.tucker@adelaide.edu.au; Tel.: +61-8313-9241

Running Title: Auxin signalling during ovule and seed development

Abstract

Grain production in cereal crops depends upon the stable formation of male and female germ cells in the flower. In most angiosperms, the female germ cells are located deep within the ovary, protected by several layers of maternal tissue including the ovary wall, ovule integuments and nucellus. In the field, germline formation and floret fertility are major determinants of yield potential, contributing to traits such as seed number, weight and size. Despite this, viable gametes are not the sole determinants of yield. Stimuli affecting the timing and duration of reproductive phases as well as the viability, size and number of cells within reproductive organs also play a role. One key stimulant is the phytohormone auxin, which influences growth and morphogenesis of female tissues during gynoecium development, gametophyte formation, and endosperm cellularisation. In this review we consider the role of the auxin signalling pathway during ovule and seed development, first in the context of Arabidopsis and then in the cereals. We summarise the gene families involved and highlight distinct expression patterns in barley that suggest a range of roles in reproductive cell specification and fate. This is discussed in terms of seed production and how targeted modification of different tissues might facilitate improvements.

Keywords: grain, seed, barley, ovule, auxin, phytohormone, yield, development, plant, Arabidopsis

Introduction

Plant cells possess an innate developmental plasticity that allows them to adopt different fates dependent on their environment and the signals they perceive (Wolters and Jurgens 2009; Vanstraelen and Benkova 2012; Tucker et al. 2018). Given the vast array of signalling molecules that exist in nature, the architectural limitations of the plant cell wall and the difficulty in accessing sub-epidermal plant cells for molecular analysis, piecing together how a cell actually adopts identity in a complex organ is a remarkably challenging process. This is particularly so in the plant ovule, which develops deep within the flower, but is an essential component of seed formation and therefore plant yield. Since the green revolution, annual yield improvements in cereal crops have plateaued and based on current predictions will not meet global food demands at some point near the middle of this century (Ray et al. 2013). Hence, there is pressing need to develop new strategies that might lead to improvements in grain size, number and/or quality. One area that still holds considerable promise is the detailed study of reproductive organ development at the individual tissue and cellular level, directly in the crops that underlie most of our food, feed and beverage industries. Although many regulators of plant growth and development have already been utilised in the context of germplasm improvement (Sasaki et al. 2002; Mathan et al. 2016; Wurschum et al. 2017), greater understanding of cell and tissue formation in the reproductive organs will provide novel targets for refined genetic improvements and increased yield. For example, the pathways controlling female gamete formation, which depend on interactions between a small subset of epidermal and sub-epidermal cell types in the ovule, are targets for the synthetic control of hybrid production and

heterosis (Sailer et al. 2016). Moreover, the capacity to induce additional germline cells at different stages of ovule development and in different cell types is a target of research into asexual seed formation (apomixis; Hand and Koltunow 2014). Both of these approaches hold potential to significantly increase yields through modification of specific reproductive events.

The central role of the ovule in seed development

The plant ovule hosts processes essential for sexual plant reproduction (Fig. 1A), including the transition from somatic to germline development (megasporogenesis), the formation of a female gametophyte (megagametogenesis), fertilization, embryogenesis, and finally, the generation of the persistent propagule, the seed. In eudicots such as Arabidopsis thaliana (Arabidopsis), the diploid sporophytic tissues of the ovule consists primarily of the proximal funiculus, which connects the ovule to the placenta, the central chalaza and the distal nucellus surrounded by the integuments (Fig. 1B; Reiser and Fischer 1993). The nucellus facilitates the production of a single haploid female gametophyte from a single somatic precursor, which in turn hosts embryo and endosperm development during seed development (reviewed in Wilkinson et al. 2018). After fertilisation in Arabidopsis, division of the central cell within the gametophyte gives rise to a nuclear syncytium that eventually cellularises to form a non-persistent starchy endosperm and persistent peripheral aleurone, while the egg cell is fertilised to give rise to the zygote which divides to form the embryo. At seed maturity, as in most eudicot angiosperms, the embryo consumes most of the endosperm and finally comprises the majority of the seed, leaving only a single layer

of endosperm cells (Brown et al. 1999). At maturity, the embryo makes up over 90% of the seed (Dumas and Rogowsky 2008; Kondou et al. 2008).

In monocots from the grass family such as barley and wheat (i.e. the Poales), the process of ovule initiation and development is similar to Arabidopsis, except that the funiculus is essentially absent, the nucellus is expanded to form the bulk (~65%; Wilkinson and Tucker 2017) of the sporophytic ovule tissue and the female gametophyte accumulates a large number of antipodal cells at the chalazal (proximal) end of the gametophyte (Fig. 1A; Wilkinson et al. 2018). The main difference between eudicots such as Arabidopsis and cereal monocots is observed after fertilisation, during the later stages of endosperm development. Cereal species such as rice (*Oryza sativa*), maize (*Zea mays*) and barley (*Hordeum vulgare*), produce a persistent endosperm that is only consumed during germination by the developing seedling (Yan et al. 2014). The outer layer of the endosperm forms the aleurone, which plays a critical role during germination (Becraft and Yi 2011), while the mature embryo makes up only a fraction (e.g. approximately 10% in barley) of the mature seed.

Variation in reproductive development and possible roles for hormones

Ovule and seed development are under the control of multiple cues that carefully coordinate the reproductive process in space and time (Bencivenga et al. 2011; Tucker and Koltunow 2014). Although all angiosperms produce seed, considerable natural variation is present in the timing of reproductive development and size of constituent organs, which impacts the size and number of seeds both among and within related species (Guo et al. 2015; Guo et al. 2016; Li and Yang 2017). For example, increased ovary size, which is largely due to increased cell number has been positively linked to

the size of mature grains in both wheat and sorghum (Yang et al. 2009; Xie et al. 2015; Reale et al. 2017). In wheat and barley, the greatest potential to establish increased seed number from an individual inflorescence is during the period of the reproductive phase in which spikelet initiation has ended, floret differentiation has begun, and floret death is yet to occur (Alqudah et al. 2014). Therefore, factors that influence the duration of the reproductive phase are likely to have a significant impact on both the size and number of seed (Gonzalez-Navarro et al. 2016). The timing of these phases is undoubtedly due to the interplay of many regulatory factors, of which phytohormones are prime candidates as organisers.

Auxin as a regulator of yield

In Arabidopsis, it is difficult to disentangle the key events of ovule and seed development from auxin, which contributes to growth, morphogenesis and progression through different reproductive stages (Weijers et al. 2006; Pagnussat et al. 2009; Sehra and Franks 2015). Although there are comparatively fewer details known about the relationship between auxin, ovule and seed development in agriculturally important cereal species, evidence points to an important role. In rice, mutants in the auxin pathway have pleiotropic effects on reproductive development, ranging from decreased fertility and seed abortion to increased seed size and increased grain weight (Jun et al. 2011; Ishimaru et al. 2013; Zhang et al. 2015; Hu et al. 2018). In maize, the relative timing of silking and pollen shed, required to coincide for fertilisation to occur, can be altered by overexpression of *PLASTOCHRON1* (*PLA1*), a cytochrome P450 gene in the same group as AtCYP78A5/KLUH (Anastasiou et al. 2007), which disrupts

auxin metabolism and causes substantially increased leaf growth (Sun et al. 2017). Hybrid maize progeny resulting from a cross between ox-KLUH and wild type yield cobs with 7-15% more kernel rows, and kernels that are 6-16% larger than WT (Sun et al. 2017). In contrast, overexpression of the wheat orthologue of *AtCYP78A5*/*KLUH*, *TaCYP78A5*, has been linked to a reduction in cell number in the wheat ovary and developing seed coat, ultimately reducing the size of the mature grain (Ma et al. 2016).

To address the current status of research in this area, in the following sections we summarise the events of auxin biosynthesis, transport and signalling with a primary focus on key stages of ovule and seed development, highlighting the detailed knowledge available for Arabidopsis. We also summarise recent findings from barley, maize and rice, which suggest the tools to investigate and capitalise on the role of auxin in cereal ovule and seed development are rapidly becoming available.

Components of auxin signalling pathways

Auxin can accumulate in a tissue by two methods, through local biosynthesis or transport from a distant source. Studies suggest that the most abundant form of auxin in plants, indole-3-acetic acid auxin (IAA), is synthesised in a number of young tissues via two different pathways, the tryptophan-dependent pathway and the tryptophan-independent pathway (Mano and Nemoto 2012). In Arabidopsis, biosynthesis of auxin requires activity of the *TRYPTOPHAN AMINOTRANSFERASE OF ARABIDOPSIS* (*TAA1*) gene together with *TRYPTOPHAN AMINOTRANSFERASE RELATED* genes (*TAR1* and *TAR2*), to produce indole-3-pyruvic acid (IPA), followed by activity of YUCCA flavin monooxygenase-like enzymes to convert IPA to IAA (Fig. 2; Stepanova

et al. 2008; Mashiguchi et al. 2011; Robert et al. 2015). Models suggest that movement of IAA into cells (influx) can occur passively, or can be bolstered by the AUXIN1/LIKE AUX1 (AUX1/LAX) plasma membrane transporter proteins (Marchant et al. 1999; Enders and Strader 2015), while movement of IAA out of cells (efflux) is mediated by multiple proteins from the PIN-FORMED family (for example, PIN1; Vernoux et al. 2000, Moller et al. 2009, Ganguly et al. 2010) and ATP-BINDING CASSETTE SUBFAMILY B (ABCB) proteins (Noh et al. 2001, Cho et al. 2013). The PIN1 auxin transporter localises to the plasma membrane and shows an asymmetric distribution in cells, which is consistent with its role in polar auxin efflux (reviewed by Remy and Duque 2014).

Within the cell, auxin is initially perceived by the TRANSPORT INHIBITOR RESPONSE 1 / AUXIN SIGNALING F-BOX (TIR1/AFB) proteins, leading to a series of events that activate auxin responsive genes (Fig. 2A,B). There are several models that explain auxin responses (Salehin et al. 2015). In the first model, INDOLE-3-ACETIC ACID INDUCIBLE (Aux/IAA) proteins bind to and repress AUXIN RESPONSE FACTOR (ARF) activator proteins that in turn bind the promoters of auxin-responsive genes; in the absence of auxin, the auxin responsive genes remain untranscribed (Farcot et al. 2015). This repression is partly mediated through recruitment of various co-repressor proteins by the Aux/IAAs, such as TOPLESS/TOPLESS-RELATED (TPL/TPR; Long et al. 2002). The Aux/IAA proteins can also bind TIR1/AFB proteins. When the TIR1/AFBs perceive and bind auxin via their leucine rich repeat repeats, this strengthens their interaction with Aux/IAA proteins and leads to Aux/IAA polyubiquitination and degradation via the proteasome (Worley et al. 2000; Ramos et al. 2001; Mockaitis and Estelle 2008). Hence, when auxin is perceived, the repression

of ARFs by Aux/IAA is lifted, and the ARF proteins are able to regulate transcription of auxin responsive target genes in a positive or negative manner depending on the ARF, the promoter sequence of the target gene and the interaction with additional coactivators or corepressors (Fig. 2; Lee et al. 2009; Farcot et al. 2015).

In the second model, ARF-Aux/IAA dimers are able to sequester ARF activators away from promoters, and upon the perception of auxin this repressive function is lifted, allowing the ARFs to be active on the auxin-responsive promoters (Farcot et al. 2015). In essence, Aux/IAA proteins are the primary responders to auxin and mediate downstream transcriptional responses through interactions with the ARF proteins. In Arabidopsis, 29 Aux/IAA proteins and 23 ARF proteins have been identified, in addition to six TIR1/AFBs (Ulmasov et al. 1997; Guilfoyle et al. 1998b; Parry et al. 2009).

Locating auxin in the reproductive organs and interactions between signalling components

As auxin cannot be directly quantified *in planta* by immunolabelling, various reporter genes have been employed to track its transport and accumulation in plant tissues. A number of these reporters are summarised in Table 1, highlighting cross-species functionality and in some cases, accumulation in specific reproductive tissues. In the Arabidopsis ovule, DR5rev::GFP is reproducibly detected in the young ovule primordia, subsequently in the tip of the nucellus and weakly in the funiculus, and after fertilisation in the integuments adjoining the micropyle and near the chalazal end of the fertilised female gametophyte (Fig. 1B,C; Benkova et al. 2003; Pagnussat et al. 2009). A similar pattern was observed for DR5:nlsGFP in young ovules from the daisy *Hieracium*

piloselloides (Fig. 1D,E; Tucker et al. 2012), in early divergent angiosperms (Lora et al. 2017) and in maize (Forestan and Varotto 2012; Lituiev et al. 2013). In maize, DR5rev::mRFPer shows abundant expression in antipodal cells at the chalazal pole of the female gametophyte (Chettoor and Evans 2015). A recent study in rice indicated that the DR5v2 marker accumulates in meristems and roots, but the pattern in ovule primordia and seeds was not reported (Yang et al. 2017). Moreover, another recent report indicates that in barley, the DR5v2 marker does not respond to auxin (Kirschner et al. 2018), although we have previously observed DR5v2:3xnlsYFP signal in proximal ovule tissues adjoining the female gametophyte in maturing ovules (Fig 1F,G).

In Arabidopsis, regions of the placenta about to give rise to the ovule primordium are marked by PIN3 expression (Larsson et al. 2014), while Pagnussat et al., (2009), showed that PIN1:GFP accumulates in the epidermal cells surrounding the germline until early gametophyte development (FG1 stage). This was later investigated by Bencivenga et al., (2012) in regards to the interactions between auxin signalling and genes involved in ovule patterning, which showed PIN1 is localised towards the apical pole of nucellar epidermal cells. *PIN1* orthologues have been identified in many angiosperm species (Kirschner et al., 2018; Bennett et al., 2014), and the location of expression in ovules has been reported for Arabidopsis, maize (Forestan et al., 2012; Lituiev et al., 2013) and theearly-divergent angiosperms Annona cherimola (custard apple) and *Persea americana* (avocado; Lora et al., 2017a). In all species where ovules have been examined, *PIN1* expression is observed in distal regions of the nucellus, showing polar localisation in epidermal cells, which likely coincides with the accumulation of auxin in the ovule tip prior to megasporogenesis (Forestan et al., 2012; Lituiev et al., 2013; Lora et al., 2017).

The role of auxin in ovule formation

In most angiosperms, the ovule primordium develops through protrusion of the placenta, quickly giving rise to distinct proximal and distal regions. Several studies in Arabidopsis have shown the essential role of auxin in placental protrusion and ovule number. Mutations in the auxin polar transport system, specifically *PIN1* (Vernoux et al. 2000), or inhibition of polar transport by chemical compounds (for example 9-hydroxyfluorene-9-carboxylic acid (HFCA) and 1-N-Naphthylphthalamic acid (NPA)) lead to a reduced number of ovule primordia (Okada et al., 1991). The actual role of auxin accumulation in the distal region of the ovule is not precisely defined, although it clearly accompanies outgrowth from the placenta and thereby mimics the growth of other tissues such as root tips (Friml et al., 2002; Benková et al., 2003).

The action of auxin is dependent upon another phytohormone, cytokinin, which accumulates in the proximal region of the ovule primordium in Arabidopsis (Bartrina et al., 2011). Similar to inhibition of the auxin transport pathway, mutants of the cytokinin receptor genes, *cre1-12 ahk2-2 ahk3-3*, produce fewer ovules (Riefler et al., 2006; Kinoshita-Tsujimura et Kakimoto, 2011), while mutations in the cytokinin oxidase/dehydrogenase (CKK) deactivating enzyme result in a larger number of ovule primordia. Bencivenga et al., (2012) suggest that in Arabidopsis, this relationship is achieved through the cytokinin-dependent regulation of *PIN1* expression; *PIN1* levels are reduced in *cre1-12 ahk2-2 ahk3-3* triple mutants while treatment with exogenous cytokinin increases *PIN1* expression (Bencivenga et al., 2012). Consistent with this, triple mutants of the *cytokinin reponse factor 2* (*crf2*) *crf3 crf6* (Cucinotta et al., 2016)

show a reduced number of ovules and lower *PIN1* expression. In roots, the CRFs modulate *PIN1* expression by binding to a specific *PIN CYTOKININ RESPONSE ELEMENT* (*PCRE*) in the *PIN1* promoter (Šimášková et al., 2015).

Auxin function during germline formation and female gametophyte growth

Apart from its role in ovule formation, auxin also fulfils an important role during subsequent stages of ovule growth. Upon establishment of the primary germline cell (megaspore mother cell; MMC), expression of *TAA1* is detected in the chalazal nucellus and inner integument primordia (Ceccato et al. 2013; Robert et al. 2015), which is complemented by expression of *PIN1* and DR5 markers in the distal nucellar tissue (Pagnussat et al. 2009, Bencivenga et al. 2012). A similar pattern of PIN1 expression has been observed in custard apple, avocado (Lora et al. 2017) and maize (Forestan et al. 2012). This pattern suggests that as ovule development proceeds, auxin is synthesised in the base and transported into the nucellar tissue surrounding the MMC, where it affects a response as the ovule progresses through meiosis and early (FG1 and FG2) stages of gametophyte development.

Genetic and molecular studies indicate that PIN1 expression is organised by the transcription factors *WUSCHEL* (*WUS*), *SPOROCYTLESS* (*SPL*) and *BELL1* (*BEL1*), whereby *WUS* responds to cytokinin, inducing nucellar expression of *SPL* and chalazal expression of *BEL1*. SPL and BEL1 activate and repress PIN1 expression, respectively (Bencivenga et al. 2012). Other studies suggest that genes involved in auxin response may restrict MMC formation to one cell (Su et al. 2017). Mutations in components of the THO/TREX (TRanscription Export) complex, which contributes to the biogenesis

of specific inhibitory small RNA molecules (ta-siRNAs; (Jauvion et al. 2010; Yelina et al. 2010), result in the formation of supernumerary MMC-like cells. Some ta-siRNAs target *ARF* family members for repression, such as *ARF3* and *ARF4*, through tasiR-ARF (Fei et al. 2013). Consistent with incorrect regulation of *ARF3* in THO/TREX mutants, ectopic expression of *ARF3* in wild-type ovules results in supernumerary MMC-like cells (Su et al. 2017).

Auxin also functions during integument formation. *ABERRANT TESTA SHAPE* (*ATS*) is a *KANADI* (*KAN*) transcription factor that maintains tissue boundaries during ovule development (McAbee et al., 2006). Studies have shown that ATS physically interacts with ARF3, otherwise known as *ETTIN* (*ETT*), and both genes are co-expressed within the inner integument. Single or double mutants in *ETT* or *ATS* result in congenital fusion of the integuments, highlighting an auxin-dependent regulatory pathway involved in integument differentiation (Kelley et al., 2012). Further work conducted by Lora et al., (2015) suggests that *ETT* orthologues in *Prunus* species are also required for bitegmic ovule formation. This is consistent with a conserved function of *ATS* and *ETT* during integument growth.

As megagametogenesis proceeds (Figure 1), expression of TAA1 is detected at the micropylar end of the developing female gametophyte in addition to the pre-existing expression in the chalaza and inner integument (Ceccato et al. 2013; Panoli et al. 2015). Concurrently, expression of the *YUCCA* family genes *YUC1*, *YUC2* and *YUC8* begins in the micropylar end of the FG, suggesting that auxin is synthesised in a polar manner (Pagnussat et al. 2009; Panoli et al. 2015; Larsson et al. 2017). Expression of *YUC1*, *YUC2* and *YUC8* is maintained until the FG6 stage of female gametophyte development, whereas *TAA1* expression is maintained until gametogenesis is

complete. In contrast, expression of PIN1 in Arabidopsis has not been observed from the FG3 stage onwards, indicating that auxin required for female gametophyte development may arise in the gametophyte itself, and if transport into the nucellus is required, it may follow a different mechanism. Consistent with these observations, mutations in *YUC8* lead to mitotic arrest during megagametogenesis (Panoli et al. 2015). Moreover, when auxin responses are specifically dampened in the female gametophyte by downregulation of *ARF* genes such as *ARF1* to *8* and *ARF19*, ovules produce defective female gametophytes that cannot be fertilized despite developing to maturity (Pagnussat et al. 2009).

The sustained expression of both *TAA1* and *YUC* throughout Arabidopsis female gametophyte development, and the apparent block of auxin transport from FG3 suggests that the female gametophyte may be enriched for auxin. Contrasting this, recent reports have only described expression of the DR5 auxin marker within the egg cell and synergids, reducing in expression before turning off at FG6 (Panoli et al. 2015), and in the micropylar nucellus from FG6 onward (Lituiev et al. 2013). This is different from that observed in maize, where from FG6 onwards, PIN1 and DR5 are expressed in the nucellar cells flanking the female gametophyte and in the chalazal cluster of antipodals (Chettoor et al. 2015). PIN1 is additionally expressed in the nucellar cells at the chalazal end of the female gametophyte. Hence, it is unclear whether auxin synthesised in the maize gametophyte acts locally, or is transported out of the chalazal end of the female gametophyte and into the surrounding nucellus to elicit auxin-dependent responses.

A role for auxin after fertilisation

Angiosperm seed development initiates when the paternal and maternal gametes fuse to create the diploid embryo and the triploid endosperm (Olsen 2004; Becraft and Yi 2011; Yan et al. 2014). In general, the mature seed consists of three main structures: the seed coat (originating from the integuments), endosperm and embryo (both originating from the gametophyte). Each of these structures comprise multiple tissues derived through synchronised patterns of proliferation and differentiation (Chaudhury et al. 2001). Although the three structures exhibit different morphology and functions, they must coordinate their growth in order to achieve seed viability (Ingram 2010; Figueiredo and Kohler 2018). Two recent studies provide insight regarding the role of auxin during these events. Figueiredo et al. (2018) show that Arabidopsis seeds containing an excess dosage of paternal genomes over-accumulate auxin in the endosperm, and this leads to an inhibition of endosperm cellularisation. Increased activity of DR5v2::VENUS in these seeds was most prominent in the seed coat, consistent with a previous study that showed auxin generated by the fertilization products may be rapidly transported to the seed coat to support sporophytic development (Figueiredo et al. 2016). However, in another study Robert et al. (2018) suggest that auxin biosynthesis in the integuments co-ordinates early development of the embryo, ensuring correct establishment of an apical/basal axis. The authors conclude that the source of auxin in this case is not the endosperm, since only maternal loss of auxin biosynthesis via mutations in *TAA1* (*wei8*) and *TAA-RELATED 1* (*tar1*) induces early defects in embryo development similar to those in which auxin-dependent establishment of apical identity in the proembryo is compromised. Hence,

a complex interplay between auxin synthesis and transport in both maternal and filial tissues coordinates early development of the seed. This is an interesting riddle, particularly in the context of the cereals where the endosperm is a much more prominent component of the seed, grain quality and yield.

Translating knowledge of auxin from Arabidopsis to the cereals

In a recent publication, Locascio et al. (2014) provide a review of auxin function during maize seed development in comparison to Arabidopsis. From this report and others, it is clear that some aspects of the auxin pathway differ across different plant species, especially between monocots and eudicots (McSteen 2010; Poulet and Kriechbaumer 2017). For example, in Arabidopsis, extremely weak or no developmental defects are observed in single auxin biosynthetic gene knockouts due to genetic redundancy (Cheng et al. 2006, 2007; Stepanova et al. 2008; Tao et al. 2008). However in monocot species such as maize, *Brachypodium* and rice, mutations in auxin biosynthetic genes such as *TAA1* lead to dramatic developmental defects (Abu-Zaitoon et al. 2012; Pacheco-Villalobos et al. 2013; Yoshikawa et al. 2014; Pacheco-Villalobos et al. 2016). Conversely in monocots, auxin transporter genes such as PIN1 appear to have more redundant copies than Arabidopsis; for example, two copies of *PIN1* exist in barley, *HvPIN1a* and *HvPIN1b* (O'Connor et al. 2014), versus one for Arabidopsis. Single *pin1* mutants in Arabidopsis fail to develop flowers, while no complete *pin1* knockout phenotypes in the cereals have been reported to date (Galweiler et al. 1998; Xu et al. 2005).

To explore additional aspects of auxin function during cereal grain development, the following sections focus on the role of auxin in somatic tissue (pericarp) at the grain periphery, and in the endosperm tissues located within.

Auxin and the cereal pericarp

The seed coat and hull are derived from the integuments and ovary wall, and protect the endosperm and embryo tissues throughout seed development and after dehiscence. Cell division in the pericarp of barley ceases as early as 2 days after fertilisation and further growth depends on cell expansion (Radchuk et al. 2011), which influences the final shape and size of the caryopsis (Ugarte et al. 2007). Auxin is one of the key drivers of cell expansion (Perrot-Rechenmann 2010; Kutschera and Wang 2016) and induces H+-ATPases, K+ channels, expansins and cell wall remodelling enzymes (Ringli 2010). Expression of various auxin transport and metabolic genes have been detected in barley pericarp tissues, including the biosynthetic *YUCCA* enzymes, the auxin repressor indole-3-acetic acid-amido synthetases, efflux (*PIN*/*ABCB*) and influx (*AUX1*/*LAX*) transporters (Pielot et al. 2015). Array-based transcript profiling during pericarp development showed auxin transporter genes are predominantly expressed during early stages, while auxin biosynthetic enzymes are only expressed during later stages of development (Pielot et al. 2015). This suggests that during early stages of seed growth, auxin is not synthesised in the pericarp but is imported, and PIN- and ABCB-type efflux transporters possibly generate and maintain required auxin levels.

Auxin and the cereal endosperm

The inner parts of the seed adjoining the seed coat and pericarp include the starchy endosperm and aleurone. The aleurone constitutes the epidermal cell layer of the endosperm and separates hull tissues from the inner starchy endosperm. Aleurone cell differentiation occurs in response to surface position but the effect of maternal versus filial signals has been debated (Gruis et al. 2006; Reyes et al. 2010). Several studies suggest that phytohormones fulfil a prominent role in this process (Geisler-Lee and Gallie 2005; Bethke et al. 2006; Forestan et al. 2010). In maize, application of the auxin inhibitor NPA, which inhibits polar auxin transport and disrupts IAA distribution, results in the development of up to four aleurone cell layers instead of the usual one (Forestan et al. 2010). This phenotype may be due to auxin being trapped in the kernel, similar to that seen for NPA-treated ovules in *Hieracium* (Tucker et al. 2012). Each aleurone layer showed ectopic expression of *PIN1* genes and uniform PIN1 distribution, along with auxin accumulation (Forestan et al. 2010). This indicates that auxin accumulation in the aleurone layer in not solely controlled by PIN1 expression and other auxin transporters expressed in the aleurone or pericarp may have a more prominent role in aleurone cell fate.

Adjoining the aleurone, the starchy endosperm is the largest tissue within the cereal seed and accumulates starch and storage proteins to be metabolised by the embryo during germination. Starchy endosperm cells are generated from the first periclinal cell division of the endosperm during cellularisation, while the external cells will differentiate into aleurone (Becraft and Asuncion-Crabb, 2000; Geisler-Lee and Gallie, 2005). Starchy endosperm cells undergo rapid growth, accumulate starch and storage proteins, and initiate endoreduplication (Sabelli 2012), and as such are major

contributors to grain size and grain weight (Li and Yang 2017). In maize and rice, auxin activity is detected during early endosperm development using the *DR5* auxin reporter (Chen et al. 2014; Yang et al. 2017), which correlates with accumulation of IAA in the endosperm (Chourey et al. 2010; Abu-Zaitoon et al. 2012). After fertilisation in maize, PIN1 is up-regulated in the endosperm and localises to the plasma membrane during cellularisation (Forestan et al. 2010). Once the endosperm is fully cellularised, PIN1 becomes confined to the chalazal endosperm region where auxin accumulates, coinciding with the stage when endosperm transfer cells begin to differentiate (Forestan et al. 2010). In the maize mutant *defective endosperm-B18* (*de18*), endosperm IAA levels are severely reduced and the endosperm shows lower total cell number, smaller cell volume and a reduced level of endoreduplication, but defects can be restored by exogenous application of auxin (Torti et al. 1986; Bernardi et al. 2012). Some of the observed defects may be due to abnormal function of the endosperm transfer cells (ETC), which facilitate transport of substances between the maternal tissues and the endosperm (Thiel 2014). The *de18* mutant also shows reduced accumulation of auxin in the transfer cells, and defects in their polarisation and differentiation (Forestan and Varotto 2012). This implicates auxin in maintaining endosperm development in maize by establishing communication pathways between the maternal and filial tissues.

Studies also show an important role for auxin during grain fill in rice. The rice *THOUSAND GRAIN WIGHT 6* (*TGW6*) gene encodes a novel protein with indole-3-acetic acid (IAA)-glucose hydrolase activity. TGW6 controls IAA supply to sink organs, thereby influencing the timing of the syncytial to cellular transition in the endosperm, cell number and grain length (Ishimaru et al. 2013). Also, in rice, mutations in *OsARF4*

lead to an increase in grain size, possibly as a result of de-repression of auxin-responsive genes (Hu et al. 2018). In addition, Liu et al. (2015) isolated a dominant mutant *big grain1-D* (*Bg1-D*) that produces extra-large grains caused by overexpression of the *BG1* gene. *BG1* encodes a novel membrane-localised protein and may physically interact with auxin transporters (Liu et al. 2015; Mishra et al. 2017), and *Bg1-D* mutants exhibit increased basipetal auxin transport and altered auxin distribution suggesting a role in regulating auxin transport.

Taken together, these studies provide compelling evidence for a role of auxin during cereal endosperm development. In light of the recent advances regarding auxin supply during Arabidopsis seed development (discussed above), future studies in the cereals might consider the maternal or filial origin of the auxin in greater detail, while also assessing the tissue-specific nature of auxin responses in different grain tissues.

Expression dynamics of the auxin signalling pathway in barley

The extensive molecular characterisation of the auxin signalling pathway in Arabidopsis provides an opportunity to assess the broader molecular conservation of auxin-related pathways in agriculturally relevant cereal crops. As described in the preceding sections, some insight has already been provided through studies in maize, rice and barley. These confirm that auxin fulfils key functions during reproductive development in a window spanning ovule initiation through to fertilisation, which has a major impact on grain yield (Alqudah et al. 2014; Wurschum et al. 2018). Because auxin plays such a prominent role in cell growth and tissue formation, it is a promising candidate for the regulation of inter cultivar differences in organ size, floret fertility and

the differentiation of tissues in the seed. In the final section of this review, we summarise molecular and phylogenetic details of the auxin signalling pathway (Fig 2). We focus in particular on barley a diploid cereal that has not been extensively studied in terms of auxin responses, but for which considerable transcriptomic, mutant and yield-data resources might be used to highlight key auxin-related genes for further study (Fig. 3).

Auxin perception and the *TIR1*/*AFB* genes

In Arabidopsis, the six TIR1/AFB genes are expressed throughout the plant, particularly in areas of cell division and expansion (Dharmasiri et al. 2005a; Dharmasiri et al. 2005b; Parry et al. 2009). Of these genes, *AtTIR1*, *AtAFB1*, *2*, *3* and *5* have been shown to function as auxin receptors (Dharmasiri et al. 2005a; Dharmasiri et al. 2005b; Kepinski and Leyser 2005; Parry et al. 2009; Calderon Villalobos et al. 2012). Five *TIR1*/*AFB* genes are present in rice, barley and sorghum, while six are present in *Brachypodium* (Fig. 4). Phylogenetic analysis indicates that the cereal genes cluster in five main groups, showing broad homology to the *AtTIR1*/*AtAFB1*, *AtAFB2*/*3* and *AtAFB4*/*5* genes from Arabidopsis. Based on publically available RNAseq data from 8 different barley tissues (IBGS 2012), *HvTIR1*, *HvAFB2* and *HvAFB4* are the most abundant members of this family. Along with *HvAFB3* and *HvAFB5*, they show highest expression in the 5 to 15mm inflorescence samples (Table 2). RNAseq data from developing pistils and seeds (minus embryos; Aubert et al. 2018) indicates that all five *HvTIR*/*AFB* genes are most abundant in the female tissues prior to fertilisation,

although *HvTIR1* and *HvAFB2* maintain expression during the early stages of seed development (Fig 3A,D).

Auxin signalling and the Aux/IAA genes

The Aux/IAA proteins contain four key domains (Paul et al. 2016; Wu et al. 2017; Luo et al. 2018); domain I recruits TPL/TPR co-repressors to enhance repression of ARF target genes, domain II facilitates interaction with the TIR1/AFB proteins (Worley et al. 2000; Ramos et al. 2001; Lee et al. 2009), and domains III and IV facilitate interaction with ARF activator proteins and dimerisation between Aux/IAA proteins (Ulmasov et al. 1997; Guilfoyle et al. 1998a). These domains are sometimes absent, depending on the gene and species (Luo et al. 2018). According to current estimates, 32 Aux/IAA proteins are present in rice (although 31 are reported in some studies; (Jain et al. 2006), 28 in sorghum, 27 in Brachypodium and 27 in barley (excluding a likely pseudogene HORVU2Hr1G027570), compared with the 29 present in Arabidopsis. Despite generally low support values for a number of clades, many of the cereal Aux/IAA sequences show closer homology to each other than to the Arabidopsis genes and mixed Arabidopsis/Poales clades were only found in a few cases; *AtIAA33* - *OsIAA33*, *AtIAA18*/*26*/*28* - *OsIAA7*, *AtIAA10/11/12/13/29/32/34* - *OsIAA10*, and *AtIAA20/30/31* - *OsIAA4/8/9/20* (Fig. 5). Some gene duplication/diversification appears to have occurred in the grasses; for example, *OsIAA22*/*25*, *OsIAA4*/*8* and *OsIAA28*/*29* duplications appear to be restricted to rice, while barley appears to lack *OsIAA17*, *18* and *24* orthologues. In addition, two genes showing high homology to *OsIAA5* are present in

barley but only one is found in Brachypodium, sorghum and rice. Based on tissue RNAseq data (Table 2), multiple *HvIAA* genes are highly expressed in the internodes of barley, but *HvIAA3*, *21*, *28* and *30* are highly abundant during inflorescence and/or caryopsis development. *HvIAA1*, *2*, *10*, *16*, *19* and *31* expression is also detected in the reproductive tissues (Table 2). In the developmental series of pistil and seed samples, expression of *HvIAA3*, *11*, *21*, *28* and *31* is prominent (Fig. 3B). *HvIAA28* and *HvIAA5* show unique patterns that may suggest a role during the early stages of seed development (Fig. 3D).

Auxin response and the *ARF* genes

The ARF transcription factors (Hagen 2015; Li et al. 2016) contain a conserved B3 DNA-binding domain (DBD) at their N-terminus that binds auxin responsive elements (AuxRE; Quint and Gray 2006). A dimerisation domain (DD) is also present within the DBD that facilitates interactions between two ARF proteins (Boer et al. 2014). The middle region of the ARF proteins determines whether they act as an activator or repressor of auxin signalling (Quint and Gray, 2006) and the C-terminus of the ARF proteins contains a protein-protein interaction domain that shares homology with domains III and IV in Aux/IAA proteins. This allows ARF proteins to interact with Aux/IAA proteins in homodimers, heterodimers or large oligomers. ARF proteins are thought to act in several ways as previously summarised (Finet and Jaillais 2012; Finet et al. 2013). ARF activators mediate auxin-dependent transcriptional regulation as shown in Fig. 1, while ARF repressors have limited interactions with other ARF and Aux/IAA proteins (Vernoux et al. 2011). Compared to Arabidopsis where 23 ARF genes

are present, 25 are present in rice (Wang et al. 2007), 25 in sorghum, 24 in Brachypodium and 23 in barley. Phylogenetic analysis highlights a range of clades containing genes from both Arabidopsis and the grasses, while some clades are expanded in the cereals such as *OsARF6*/*17* and *OsARF5*/*19*/*21* in Clade A, *OsARF3*/*14* and *OsARF23*/*24* in Clade B and *OsARF8*/*10* in Clade C (Fig. 6). Although the naming of the proteins is not always consistent between the species based on the clade names (Finet et al., 2012), the clade structure that generally separates activators (Clade A) from repressors (Clades B and C) is maintained in the Arabidopsis/Poales tree. Several notable genomic differences are apparent for the HvARF genes compared to the other grasses; two Clade C *HvARF10* genes appear to be present along with three Clade B *HvARF4* genes, while an *OsARF23* and *OsARF24* homologue appear to be lacking. Most of the *HvARF* genes show maximum expression in the inflorescence and caryopsis tissues (Table 2), and the pistil/seed datasets suggest that most of these are expressed during pre-fertilisation stages (Fig. 3C). The Clade B *ARF* genes *HvARF4c*, *HvARF4*, *HvARF9* and *HvARF17* are the most prominent during pistil development. In contrast to the majority of ARF genes, only a few show patterns of expression that peak after fertilisation (e.g. *HvARF1*, *3*, *10b* and *13*). However, expression of these genes is generally low in the whole organ datasets, suggesting they may fulfil more specific roles in isolated regions of the seed.

Transcriptional signatures of the auxin-signalling pathway during caryopsis development

Based on these published datasets and other studies (Thiel et al. 2011; Pielot et al. 2015), most genes in the auxin signalling pathway are expressed during early stages of barley pistil development, while the number dramatically decreases during the middle stages of grain development. High expression appears to coincide with stages where maternal tissues are actively proliferating to establish an environment suitable for seed development, and/or when early divisions of the endosperm are taking place. The low abundance of most transcripts after fertilisation is intriguing; although comparisons with pre-fertilisation measurements are lacking, auxin (IAA) levels clearly increase during maize endosperm and rice grain development (Lur and Setter, 1993; Abu-Zaitoon et al. 2012), which is consistent with an important role during these stages. One possibility is that there is considerable specialisation of ARF and AuxIAA genes, with multiple family members fulfilling key roles during the diverse processes associated with pre-fertilisation ovule and gametophyte development, and only specific members during the less complex events of endosperm differentiation. Clustering of barley genes based on relative expression (normalised to the maximum expression value for each gene) in the tissue series highlights a number of interesting patterns for specific ARF and Aux/IAA genes (Fig. 3D). For example, the patterns of *HvIAA16*/*19* and *HvARF41*/*b*/*c* genes in young pistils, *HvIAA5b/6/9/12* and *HvARF19*/*21* genes in late pistils, and *HvIAA5a/HvIAA11/HvIAA28* and *HvARF10b*/*13* in young seeds might justify further investigation. One important point to note is that the resolution of the RNA-seq datasets currently available for barley is limited to a few stages of pistil and grain development without separation of tissues. This makes it difficult to propose hypotheses on tissue- and development-specific regulatory processes and is something that might be addressed in future research.

Perspectives

The aim of this review was to consider the role of auxin signalling during ovule and seed development in Arabidopsis and cereal species. The literature provides compelling evidence for key roles in ovule initiation, germline formation and progression, integument growth, endosperm and embryo development. Many aspects of these roles appear to be conserved across the eudicot / monocot (Poales) divide, although the location of auxin synthesis and transport appears to differ due to morphological constraints in ovule and seed development. How these findings might be applied in the context of agriculture is yet to be explored in detail, but there is enough evidence to suggest that new strategies for yield improvement might be achieved through modification of cell-type or tissue-specific pathways during reproduction. Analysis of the auxin signalling pathway provides a number of candidate targets to implement this. Auxin synthesis, transport and response is dynamic during ovule and seed development, with localised pulses occurring in different tissues and stages as development proceeds. If this information can be combined with modern techniques that provide refined cell-type specific gene expression analysis, methylation and chromatin status, it should be possible to tailor specific auxin responses through modification of specific genes and regulatory motifs. In principal, this could allow pleiotropic effects of mutations to be dampened, while the desired effect can be achieved in the cell, tissue or stage of choice.

Acknowledgements

We thank members of the Tucker laboratory, Tobias Würschum and Christopher Davies for fruitful discussions. We apologise to authors whose work we did not cite due to space constraints. We acknowledge funding from the Australian Research Council (FT140100780 & DP180104092), the Grains Research Development Corporation (GRS10938) and the University of Adelaide.

Author contributions

All authors contributed to the writing and editing of the manuscript.

References

Abu-Zaitoon YM, Bennett K, Normanly J, Nonhebel HM (2012) A large increase in IAA during development of rice grains correlates with the expression of tryptophan aminotransferase *OsTAR1* and a grain-specific *YUCCA*. ***Physiologia Plantarum*** 146, 487-499.

Alqudah AM, Sharma R, Pasam RK, Graner A, Kilian B, Schnurbusch T (2014) Genetic dissection of photoperiod response based on GWAS of pre-anthesis phase duration in spring barley. ***PLoS One*** 9, e113120.

Anastasiou E, Kenz S, Gerstung M, MacLean D, Timmer J, Fleck C, Lenhard M (2007) Control of plant organ size by KLUH/CYP78A5-dependent intercellular signaling. ***Dev Cell*** 13, 843-856.

Aubert, MK, Coventry, S, Shirley, NJ, Betts NS, Wurschum, T, Burton RA, Tucker MR (2018). Differences in hydrolytic enzyme activity accompany natural variation in mature aleurone morphology in barley (*Hordeum vulgare* L.). ***Sci Rep*** 8(1): 11025.

Becraft PW, Yi G (2011) Regulation of aleurone development in cereal grains. ***J Exp Bot*** 62, 1669-1675.

Bencivenga S, Colombo L, Masiero S (2011) Cross talk between the sporophyte and the megagametophyte during ovule development. ***Sex Plant Reprod*** 24, 113-121.

Bencivenga S, Simonini S, Benková E, Colombo L (2012) The transcription factors *BEL1* and *SPL* are required for cytokinin and auxin signaling during ovule development in *Arabidopsis*. ***Plant Cell*** 24, 2886-2897.

Bender RL, Fekete ML, Klinkenberg PM, Hampton M, Bauer B, Malecha M, Lindgren K, J AM, Perera MA, Nikolau BJ, Carter CJ (2013) PIN6 is required for nectary auxin response and short stamen development. ***Plant J*** 74, 893-904.

Benkova E, Michniewicz M, Sauer M, Teichmann T, Seifertova D, Jurgens G, Friml J (2003) Local, Efflux-Dependent Auxin Gradients as a Common Module for Plant Organ Formation. ***Cell*** 115, 591-602.

Bernardi J, Lanubile A, Li QB, Kumar D, Kladnik A, Cook SD, Ross JJ, Marocco A, Chourey PS (2012) Impaired auxin biosynthesis in the *defective endosperm18* mutant is due to mutational loss of expression in the *ZmYUC1* gene encoding endosperm-specific YUCCA1 protein in maize. ***Plant Phys*** 160, 1318-1328.

Bethke PC, Hwang YS, Zhu T, Jones RL (2006) Global patterns of gene expression in the aleurone of wild-type and *dwarf1* mutant rice. ***Plant Phys*** 140, 484-498.

Blilou I, Frugier F, Folmer S, Serralbo O, Willemsen V, Wolkenfelt H, Eloy NB, Ferreira PC, Weisbeek P, Scheres B (2002) The *Arabidopsis HOBBIT* gene encodes a *CDC27* homolog that links the plant cell cycle to progression of cell differentiation. ***Genes Dev*** 16, 2566-2575.

Blilou I, Xu J, Wildwater M, Willemsen V, Paponov I, Friml J, Heidstra R, Aida M, Palme K, Scheres B (2005) The PIN auxin efflux facilitator network controls growth and patterning in *Arabidopsis* roots. ***Nature*** 433, 39-44.

Boer DR, Freire-Rios A, van den Berg WA, Saaki T, Manfield IW, Kepinski S, Lopez-Vidrieo I, Franco-Zorrilla JM, de Vries SC, Solano R, Weijers D, Coll M (2014) Structural basis for DNA binding specificity by the auxin-dependent ARF transcription factors. ***Cell*** 156, 577-589.

Brown RC, Lemmon BE, Nguyen H, Olsen OA (1999) Development of endosperm in *Arabidopsis thaliana*. ***Sex Plant Reprod*** 12, 32-42.

Brunoud G, Wells DM, Oliva M, Larrieu A, Mirabet V, Burrow AH, Beeckman T, Kepinski S, Traas J, Bennett MJ, Vernoux T (2012) A novel sensor to map auxin response and distribution at high spatio-temporal resolution. ***Nature*** 482, 103-106.

Calderon Villalobos LI, Lee S, De Oliveira C, Ivetac A, Brandt W, Armitage L, Sheard LB, Tan X, Parry G, Mao H, Zheng N, Napier R, Kepinski S, Estelle M (2012) A combinatorial TIR1/AFB- Aux/IAA co-receptor system for differential sensing of auxin. ***Nat Chem Biol*** 8, 477-485.

Ceccato L, Masiero S, Sinha Roy D, Bencivenga S, Roig-Villanova I, Ditengou FA, Palme K, Simon R, Colombo L (2013) Maternal control of PIN1 is required for female gametophyte development in Arabidopsis. ***PLoS One*** 8, e66148.

Chaudhury AM, Koltunow A, Payne T, Luo M, Tucker MR, Dennis ES, Peacock WJ (2001) Control of early seed development. ***Annu Rev Cell Dev Biol*** 17, 677-699.

Chen JY, Lausser A, Dresselhaus T (2014) Hormonal responses during early embryogenesis in maize. ***Biochemical Society Transactions*** 42, 325-331.

Chen Y, Yordanov YS, Ma C, Strauss S, Busov VB (2013) DR5 as a reporter system to study auxin response in Populus. ***Plant Cell Rep*** 32, 453-463.

Cheng YF, Dai XH, Zhao YD (2006) Auxin biosynthesis by the YUCCA flavin monooxygenases controls the formation of floral organs and vascular tissues in *Arabidopsis*. **Genes Dev** 20, 1790- 678 1799.

Cheng YF, Dai XH, Zhao YD (2007) Auxin synthesized by the YUCCA flavin monooxygenases is essential for embryogenesis and leaf formation in *Arabidopsis*. ***Plant Cell*** 19, 2430-2439.

Chettoor AM, Evans MM (2015) Correlation between a loss of auxin signaling and a loss of proliferation in maize antipodal cells. ***Front Plant Sci*** 6, 187.

Cho, M, Cho H (2013) The function of ABCB transporters in auxin transport. Plant ***Signaling & Behavior*** 8(2): e22990.

Chourey PS, Li QB, Kumar D (2010) Sugar-hormone cross-talk in seed development: Two redundant pathways of IAA biosynthesis are regulated differentially in the *Invertase-deficient miniature1* (*mn1*) seed mutant in maize. ***Mol Plant*** 3, 1026-1036.

Dal Bosco C, Dovzhenko A, Liu X, Woerner N, Rensch T, Eismann M, Eimer S, Hegermann J, Paponov IA, Ruperti B, Heberle-Bors E, Touraev A, Cohen JD, Palme

K (2012) The endoplasmic reticulum localized PIN8 is a pollen-specific auxin carrier involved in intracellular auxin homeostasis. ***Plant J*** 71, 860-870.

Dharmasiri N, Dharmasiri S, Estelle M (2005a) The F-box protein TIR1 is an auxin receptor. ***Nature*** 435, 441-445.

Dharmasiri N, Dharmasiri S, Weijers D, Lechner E, Yamada M, Hobbie L, Ehrismann JS, Jurgens G, Estelle M (2005b) Plant development is regulated by a family of auxin receptor F box proteins. ***Dev Cell*** 9, 109-119.

Dumas C, Rogowsky P (2008) Fertilization and early seed formation. ***Comptes Rendus Biologies*** 331, 715-725.

Enders TA, Strader LC (2015) Auxin activity: Past, present, and future. ***Am J Bot*** 102, 180-196.

Farcot E, Lavedrine C, Vernoux T (2015) A modular analysis of the auxin signalling network. ***PLoS One*** 10, e0122231.

Fei Q, Xia R, Meyers BC (2013) Phased, secondary, small interfering RNAs in post transcriptional regulatory networks. ***Plant Cell*** 25, 2400-2415.

Figueiredo DD, Batista RA, Kohler C (2018) Auxin regulates endosperm cellularization in *Arabidopsis*. ***bioRxiv***.

Figueiredo DD, Batista RA, Roszak PJ, Hennig L, Kohler C (2016) Auxin production in the endosperm drives seed coat development in *Arabidopsis*. ***Elife*** 5.

Figueiredo DD, Kohler C (2018) Auxin: a molecular trigger of seed development. ***Genes & Development*** 32, 479-490.

Finet C, Berne-Dedieu A, Scutt CP, Marletaz F (2013) Evolution of the *ARF* gene family in land plants: old domains, new tricks. ***Mol Biol Evol*** 30, 45-56.

Finet C, Jaillais Y (2012) Auxology: when auxin meets plant evo-devo. ***Dev Biol*** 369, 19-31.

Forestan C, Meda S, Varotto S (2010) ZmPIN1-mediated auxin transport is related to cellular differentiation during maize embryogenesis and endosperm development. ***Plant Physiol*** 152, 1373-1390.

Forestan C, Varotto S (2012) The role of PIN auxin efflux carriers in polar auxin transport and accumulation and their effect on shaping maize development. ***Mol Plant*** 5, 787-798.

Friml J, Benkova E, Blilou I, Wisniewska J, Hamann T, Ljung K, Woody S, Sandberg G, Scheres B, Jurgens G, Palme K (2002) *AtPIN4* mediates sink-driven auxin gradients and root patterning in Arabidopsis. ***Cell*** 108, 661-673.

Gallavotti A, Yang Y, Schmidt RJ, Jackson D (2008) The Relationship between auxin transport and maize branching. ***Plant Physiol*** 147, 1913-1923.

Galweiler L, Guan CH, Muller A, Wisman E, Mendgen K, Yephremov A, Palme K (1998) Regulation of polar auxin transport by *AtPIN1* in *Arabidopsis* vascular tissue. ***Science*** 282, 2226-2230.

Ganguly A, Lee SH, Cho M, Lee OR, Yoo H, Cho H (2010) Differential Auxin-Transporting Activities of PIN-FORMED Proteins in Arabidopsis Root Hair Cells. ***Plant Physiol*** 153, 1046-1061.

Geisler-Lee J, Gallie DR (2005) Aleurone cell identity is suppressed following connation in maize kernels. ***Plant Physiol*** 139, 204-212.

Gonzalez-Navarro OE, Griffiths S, Molero G, Reynolds MP, Slafer GA (2016) Variation in developmental patterns among elite wheat lines and relationships with yield, yield components and spike fertility. ***Field Crops Res*** 196, 294-304.

Gruis D, Guo HN, Selinger D, Tian Q, Olsen OA (2006) Surface position, not signaling from surrounding maternal tissues, specifies aleurone epidermal cell fate in maize. ***Plant Physiol*** 141, 737 898-909.

Guilfoyle T, Hagen G, Ulmasov T, Murfett J (1998a) How does auxin turn on genes? ***Plant Physiol*** 118, 341-347.

Guilfoyle TJ, Ulmasov T, Hagen G (1998b) The ARF family of transcription factors and their role in plant hormone- responsive transcription. ***Cell. Mol. Life. Sci***. 54, 619-627.

Guo Z, Chen D, Schnurbusch T (2015) Variance components, heritability and correlation analysis of anther and ovary size during the floral development of bread wheat. ***J Exp Bot*** 66, 3099-3111.

Guo Z, Slafer GA, Schnurbusch T (2016) Genotypic variation in spike fertility traits and ovary size as determinants of floret and grain survival rate in wheat. ***J Exp Bot*** 67, 4221-4230.

Hagen G (2015) Auxin signal transduction. ***Essays Biochem*** 58, 1-12.

Hand ML, Koltunow AM (2014) The genetic control of apomixis: asexual seed formation. ***GENETICS*** 197, 441-450.

Heisler MG, Ohno C, Das P, Sieber P, Reddy GV, Long JA, Meyerowitz EM (2005) Patterns of auxin transport and gene expression during primordium development revealed by live imaging of the *Arabidopsis* inflorescence meristem. ***Curr Biol*** 15, 1899-1911.

Hu Z, Lu SJ, Wang MJ, He H, Sun L, Wang H, Liu XH, Jiang L, Sun JL, Xin X, Kong W, Chu C, Xue HW, Yang J, Luo X, Liu JX (2018) A Novel QTL *qTGW3* Encodes the GSK3/SHAGGY-Like Kinase *OsGSK5*/*OsSK41* that Interacts with *OsARF4* to Negatively Regulate Grain Size and Weight in Rice. ***Mol Plant*** 11, 736-749.

IBGS (2012) A physical, genetic and functional sequence assembly of the barley genome. ***Nature*** 491, 711-716.

Ingram GC (2010) Family life at close quarters: communication and constraint in angiosperm seed development. ***Protoplasma*** 247, 195-214.

Ishimaru K, Hirotsu N, Madoka Y, Murakami N, Hara N, Onodera H, Kashiwagi T, Ujiie K, Shimizu B, Onishi A, Miyagawa H, Katoh E (2013) Loss of function of the IAA-glucose hydrolase gene *TGW6* enhances rice grain weight and increases yield. ***Nat Genet*** 45, 707-711.

Jain M, Kaur N, Garg R, Thakur JK, Tyagi AK, Khurana JP (2006) Structure and expression analysis of early auxin-responsive *Aux*/*IAA* gene family in rice (Oryza sativa). ***Funct Integr Genomics*** 6, 47-59.

Jauvion V, Elmayan T, Vaucheret H (2010) The conserved RNA trafficking proteins HPR1 and TEX1 are involved in the production of endogenous and exogenous small interfering RNA in Arabidopsis. ***Plant Cell*** 22, 2697-2709.

Jun N, Gaohang W, Zhenxing Z, Huanhuan Z, Yunrong W, Ping W (2011) *OsIAA23*-mediated auxin signaling defines postembryonic maintenance of QC in rice. ***Plant J*** 68, 433-442.

Kepinski S, Leyser O (2005) The Arabidopsis F-box protein TIR1 is an auxin receptor. ***Nature*** 435, 446-451.

Kirschner GK, Stahl Y, Imani J, von Korff M, Simon R (2018) Fluorescent reporter lines for auxin and cytokinin signalling in barley (Hordeum vulgare). ***PLoS One*** 13, e0196086.

Kondou Y, Nakazawa M, Kawashima M, Ichikawa T, Yoshizumi T, Suzuki K, Ishikawa A, Koshi T, Matsui R, Muto S, Matsui M (2008) RETARDED GROWTH OF EMBRYO1, a new basic helix-loop-helix protein, expresses in endosperm to control embryo growth. ***Plant Physiol*** 147, 1924-1935.

Kutschera U, Wang ZY (2016) Growth-limiting proteins in maize coleoptiles and the auxin-brassinosteroid hypothesis of mesocotyl elongation. ***Protoplasma*** 253, 3-14.

Larsson E, Roberts CJ, Claes AR, Franks RG, Sundberg E (2014) Polar auxin transport is essential for medial versus lateral tissue specification and vascular-mediated valve outgrowth in Arabidopsis gynoecia. ***Plant Physiol*** 166, 1998-2012.

Larsson E, Vivian-Smith A, Offringa R, Sundberg E (2017) Auxin Homeostasis in Arabidopsis Ovules Is Anther-Dependent at Maturation and Changes Dynamically upon Fertilization. ***Front Plant Sci*** 8, 1735.

Lee DJ, Park JW, Lee HW, Kim J (2009) Genome-wide analysis of the auxin-responsive transcriptome downstream of *IAA1* and its expression analysis reveal the diversity and complexity of auxin-regulated gene expression. ***J Exp Bot*** 60, 3935-3957.

Li SB, Xie ZZ, Hu CG, Zhang JZ (2016) A Review of Auxin Response Factors (ARFs) in Plants. ***Front Plant Sci*** 7, 47.

Li W, Yang B (2017) Translational genomics of grain size regulation in wheat. ***Theor Appl Genet*** 130, 1765-1771.

Liao CY, Smet W, Brunoud G, Yoshida S, Vernoux T, Weijers D (2015) Reporters for sensitive and quantitative measurement of auxin response. ***Nat Methods*** 12, 207-210

Lituiev DS, Krohn NG, Muller B, Jackson D, Hellriegel B, Dresselhaus T, Grossniklaus U (2013) Theoretical and experimental evidence indicates that there is no detectable auxin gradient in the angiosperm female gametophyte. ***Development*** 140, 4544-4553.

Liu LC, Tong HN, Xiao YH, Che RH, Xu F, Hu B, Liang CZ, Chu JF, Li JY, Chu CC (2015) Activation of *Big Grain1* significantly improves grain size by regulating auxin transport in rice. ***Proc Natl Acad Sci U S A*** 112, 11102-11107.

Locascio A, Roig-Villanova I, Bernardi J, Varotto S (2014) Current perspectives on the hormonal control of seed development in *Arabidopsis* and maize: a focus on auxin. ***Front Plant Sci*** 5, 412.

Long JA, Woody S, Poethig S, Meyerowitz EM, Barton MK (2002) Transformation of shoots into roots in *Arabidopsis* embryos mutant at the *TOPLESS* locus. Development 129, 2797-2806.

Lora J, Herrero M, Tucker MR, Hormaza JI (2017) The transition from somatic to germline identity shows conserved and specialized features during angiosperm evolution. ***New Phytol*** 216, 495-509.

Luo J, Zhou JJ, Zhang JZ (2018) *Aux*/*IAA* Gene Family in Plants: Molecular Structure, Regulation, and Function. ***Int J Mol Sci*** 19.

Ma M, Zhao H, Li Z, Hu S, Song W, Liu X (2016) *TaCYP78A5* regulates seed size in wheat (*Triticum aestivum*). ***J Exp Bot*** 67, 1397-1410.

Ma W, Li J, Qu B, He X, Zhao X, Li B, Fu X, and Tong, Y (2014) Auxin biosynthetic gene *TAR2* is involved in low nitrogen-mediated reprogramming of root architecture in *Arabidopsis*. ***The Plant Journal***, 78(1), pp.70-79.

Mano Y, Nemoto K (2012) The pathway of auxin biosynthesis in plants. ***J Exp Bot*** 63, 2853-2872.

Marchant A, Kargul J, May ST, Muller P, Delbarre A, Perrot-Rechenmann C, Bennett MJ (1999) AUX1 regulates root gravitropism in *Arabidopsis* by facilitating auxin uptake within root apical tissues. ***EMBO J*** 18, 2066-2073.

Marin E, Jouannet V, Herz A, Lokerse AS, Weijers D, Vaucheret H, Nussaume L, Crespi MD, Maizel A (2010) miR390, *Arabidopsis* TAS3 tasiRNAs, and their *AUXIN RESPONSE FACTOR* targets define an autoregulatory network quantitatively regulating lateral root growth. ***Plant Cell*** 22, 1104-1117.

Mashiguchi K, Tanaka K, Sakai T, Sugawara S, Kawaide H, Natsume M, Hanada A, Yaeno T, Shirasu K, Yao H, McSteen P, Zhao Y, Hayashi K, Kamiya Y, Kasahara H (2011) The main auxin biosynthesis pathway in *Arabidopsis*. ***Proc Natl Acad Sci U S A*** 108, 18512-18517.

Mathan J, Bhattacharya J, Ranjan A (2016) Enhancing crop yield by optimizing plant developmental features. ***Development*** 143, 3283-3294.

McSteen P (2010) Auxin and monocot development. ***Cold Spring Harbor Perspectives in Biology*** 2.

Mishra BS, Jamsheer KM, Singh D, Sharma M, Laxmi A (2017) Genome-wide identification and expression, protein-protein interaction and evolutionary analysis of the seed plant-specific *BIG GRAIN* and *BIG GRAIN LIKE* gene family. ***Front Plant Sci*** 8.

Mockaitis K, Estelle M (2008) Auxin receptors and plant development: a new signaling paradigm. ***Annu Rev Cell Dev Biol*** 24, 55-80.

Moller, B, Weijers D (2009) Auxin Control of Embryo Patterning. ***Cold Spring Harbor Perspectives in Biology*** 1(5).

Mravec J, Skupa P, Bailly A, Hoyerova K, Krecek P, Bielach A, Petrasek J, Zhang J, Gaykova V, Stierhof YD, Dobrev PI, Schwarzerova K, Rolcik J, Seifertova D, Luschnig C, Benkova E, Zazimalova E, Geisler M, Friml J (2009) Subcellular homeostasis of phytohormone auxin is mediated by the ER-localized PIN5 transporter. ***Nature*** 459, 1136-1140.

Noh B, Murphy AS, Spalding EP (2001) Multidrug resistance-like genes of *Arabidopsis* required for auxin transport and auxin-mediated development. ***Plant Cell*** 13, 2441-2454.

O'Connor DL, Runions A, Sluis A, Bragg J, Vogel JP, Prusinkiewicz P, Hake S (2014) A division in PIN-mediated auxin patterning during organ initiation in grasses. ***PLoS Comput Biol*** 10, e1003447.

Olsen OA (2004) Nuclear endosperm development in cereals and *Arabidopsis thaliana*. ***Plant Cell*** 16, S214-S227.

Ottenschlager I, Wolff P, Wolverton C, Bhalerao RP, Sandberg G, Ishikawa H, Evans M, Palme K (2003) Gravity-regulated differential auxin transport from columella to lateral root cap cells. ***Proc Natl Acad Sci U S A*** 100, 2987-2991.

Pacheco-Villalobos D, Diaz-Moreno SM, van der Schuren A, Tamaki T, Kang YH, Gujas B, Novak O, Jaspert N, Li ZN, Wolf S, Oecking C, Ljung K, Bulone V, Hardtke CS (2016) The effects of high steady state auxin levels on root cell elongation in *Brachypodium*. Plant Cell 28, 1009-1024.

Pacheco-Villalobos D, Sankar M, Ljung K, Hardtke CS (2013) Disturbed local auxin homeostasis enhances cellular anisotropy and reveals alternative wiring of auxin-ethylene crosstalk in *Brachypodium distachyon* seminal roots. ***Plos Genetics*** 9.

Pagnussat GC, Alandete-Saez M, Bowman JL, Sundaresan V (2009) Auxin-dependent patterning and gamete specification in the *Arabidopsis* female gametophyte. ***Science*** 324, 1684-1689.

Panoli A, Martin MV, Alandete-Saez M, Simon M, Neff C, Swarup R, Bellido A, Yuan L, Pagnussat GC, Sundaresan V (2015) Auxin Import and Local Auxin Biosynthesis Are Required for Mitotic Divisions, Cell Expansion and Cell Specification during Female Gametophyte Development in *Arabidopsis thaliana*. ***PLoS One*** 10, e0126164.

Parry G, Calderon-Villalobos LI, Prigge M, Peret B, Dharmasiri S, Itoh H, Lechner E, Gray WM, Bennett M, Estelle M (2009) Complex regulation of the TIR1/AFB family of auxin receptors. ***Proc Natl Acad Sci U S A*** 106, 22540-22545.

Paul P, Dhandapani V, Rameneni JJ, Li X, Sivanandhan G, Choi SR, Pang W, Im S, Lim YP (2016) Genome-Wide Analysis and Characterization of *Aux*/*IAA* Family Genes in *Brassica rapa*. ***PLoS One*** 11, e0151522.

Perrot-Rechenmann C (2010) Cellular responses to auxin: Division versus expansion. ***Cold Spring Harbor Perspectives in Biology*** 2.

Pielot R, Kohl S, Manz B, Rutten T, Weier D, Tarkowska D, Rolcik J, Strnad M, Volke F, Weber H, Weschke W (2015) Hormone-mediated growth dynamics of the barley pericarp as revealed by magnetic resonance imaging and transcript profiling. ***J Exp Bot*** 66, 6927-6943.

Poulet A, Kriechbaumer V (2017) Bioinformatics analysis of phylogeny and transcription of *TAA*/*YUC* auxin biosynthetic genes. ***Int J Mol Sci*** 18.

Quint M, Gray WM (2006) Auxin signaling. ***Curr Opin Plant Biol*** 9, 448-453.

Radchuk V, Weier D, Radchuk R, Weschke W, Weber H (2011) Development of maternal seed tissue in barley is mediated by regulated cell expansion and cell disintegration and coordinated with endosperm growth. ***J Exp Bot*** 62, 1217-1227.

Ramos JA, Zenser N, Leyser O, Callis J (2001) Rapid degradation of auxin/indoleacetic acid proteins requires conserved amino acids of domain II and is proteasome dependent. ***Plant Cell*** 13, 2349-2360.

Ray DK, Mueller ND, West PC, Foley JA (2013) Yield Trends Are Insufficient to Double Global Crop Production by 2050. ***PLoS One*** 8, e66428.

Reale L, Rosati A, Tedeschini E, Ferri V, Cerri M, Ghitarrini S, Timorato V, Ayano BE, Porfiri O, Frenguelli G, Ferranti F, Benincasa P (2017) Ovary Size in Wheat (*Triticum aestivum* L.) is Related to Cell Number. ***Crop Sci*** 57, 914-925.

Reiser L, Fischer RL (1993) The ovule and the embryo sac. ***Plant Cell*** 5, 1291-1301.

Remy E, Duque P (2014) Beyond cellular detoxification: a plethora of physiological roles for MDR transporter homologs in plants. ***Front Physiol*** 5, 201.

Reyes FC, Sun BM, Guo HN, Gruis D, Otegui MS (2010) *Agrobacterium tumefaciens*-mediated transformation of maize endosperm as a tool to study endosperm cell biology. ***Plant Physiol*** 153, 624-631.

Ringli C (2010) Monitoring the outside: Cell wall-sensing mechanisms. ***Plant Physiol*** 153, 1445-1452.

Robert HS, Grones P, Stepanova AN, Robles LM, Lokerse AS, Alonso JM, Weijers D, Friml J (2013) Local auxin sources orient the apical-basal axis in *Arabidopsis* embryos. ***Curr Biol***, 23(24), pp.2506-2512.

Robert HS, Crhak Khaitova L, Mroue S, Benkova E (2015) The importance of localized auxin production for morphogenesis of reproductive organs and embryos in *Arabidopsis*. ***J Exp Bot*** 66, 5029-5042.

Robert HS, Park C, Gutierrez CL, Wojcikowska B, Pencik A, Novak O, Chen J, Grunewald W, Dresselhaus T, Friml J, Laux T (2018) Maternal auxin supply contributes to early embryo patterning in *Arabidopsis*. ***Nat Plants***.

Sabatini S, Beis D, Wolkenfelt H, Murfett J, Guilfoyle T, Malamy J, Benfey P, Leyser O, Bechtold N, Weisbeek P, Scheres B (1999) An auxin-dependent distal organizer of pattern and polarity in the *Arabidopsis* root. ***Cell*** 99, 463-472.

Sabelli PA (2012) Replicate and die for your own good: Endoreduplication and cell death in the cereal endosperm. ***J Cereal Sci*** 56, 9-20.

Sailer C, Schmid B, Grossniklaus U (2016) Apomixis Allows the Transgenerational Fixation of Phenotypes in Hybrid Plants. ***Curr Biol*** 26, 331-337.

Salehin M, Bagchi R, Estelle M (2015) *SCFTIR1/AFB*-based auxin perception: mechanism and role in plant growth and development. ***Plant Cell*** 27, 9-19.

Sasaki A, Ashikari M, Ueguchi-Tanaka M, Itoh H, Nishimura A, Swapan D, Ishiyama K, Saito T, Kobayashi M, Khush GS, Kitano H, Matsuoka M (2002) Green revolution: a mutant gibberellin-synthesis gene in rice. ***Nature*** 416, 701-702.

Sehra B, Franks RG (2015) Auxin and cytokinin act during gynoecial patterning and the development of ovules from the meristematic medial domain. ***Wiley Interdiscip Rev Dev Biol*** 4, 555-571.

Spiegelman Z, Ham BK, Zhang Z, Toal TW, Brady SM, Zheng Y, Fei Z, Lucas WJ, Wolf S (2015) A tomato phloem-mobile protein regulates the shoot-to-root ratio by mediating the auxin response in distant organs. ***Plant J*** 83, 853-863.

Stepanova AN, Robertson-Hoyt J, Yun J, Benavente LM, Xie DY, Dolezal K, Schlereth A, Jurgens G, Alonso JM (2008) *TAA1*-mediated auxin biosynthesis is essential for hormone crosstalk and plant development. ***Cell*** 133, 177-191.

Su Z, Zhao L, Zhao Y, Li S, Won S, Cai H, Wang L, Li Z, Chen P, Qin Y (2017) The THO Complex Non-Cell-Autonomously Represses Female Germline Specification through the TAS3-ARF3 Module. ***Curr Biol***.

Sun X, Cahill J, Van Hautegem T, Feys K, Whipple C, Novak O, Delbare S, Versteele C, Demuynck K, De Block J, Storme V, Claeys H, Van Lijsebettens M, Coussens G, Ljung K, De Vliegher A, Muszynski M, Inze D, Nelissen H (2017) Altered expression of maize *PLASTOCHRON1* enhances biomass and seed yield by extending cell division duration. ***Nat Commun*** 8, 14752.

Tao Y, Ferrer JL, Ljung K, Pojer F, Hong FX, Long JA, Li L, Moreno JE, Bowman ME, Ivans LJ, Cheng YF, Lim J, Zhao YD, Ballare CL, Sandberg G, Noel JP, Chory J (2008) Rapid synthesis of auxin via a new tryptophan-dependent pathway is required for shade avoidance in plants. ***Cell*** 133, 164-176.

Thiel J (2014) Development of endosperm transfer cells in barley. ***Front Plant Sci*** 5.

Thiel J, Weier D, Weschke W (2011) Laser-capture microdissection of developing barley seeds and cDNA array analysis of selected tissues. ***Methods Mol Biol*** 755, 461-475.

Torti G, Manzocchi L, Salamini F (1986) Free and bound indole-acetic acid is low in the endosperm of the maize mutant *defective-endosperm-b18*. ***Theor Appl Genet*** 72, 602-605.

Tucker MR, Koltunow AM (2014) Traffic monitors at the cell periphery: the role of cell walls during early female reproductive cell differentiation in plants. ***Curr Opin Plant Biol*** 17, 137-145.

Tucker MR, Lou H, Aubert MK, Wilkinson LG, Little A, Houston K, Pinto SC, Shirley NJ (2018) Exploring the Role of Cell Wall-Related Genes and Polysaccharides during Plant Development. ***Plants*** (Basel) 7.

Tucker MR, Okada T, Johnson SD, Takaiwa F, Koltunow AMG (2012) Sporophytic ovule tissues modulate the initiation and progression of apomixis in *Hieracium*. ***J Exp Bot*** 63, 3229-3241.

Ugarte C, Calderini DF, Slafer GA (2007) Grain weight and grain number responsiveness to pre-anthesis temperature in wheat, barley and triticale. ***Field Crops Res*** 100, 240-248.

Ulmasov T, Murfett J, Hagen G, Guilfoyle TJ (1997) Aux / IAA proteins repress expression of reporter genes containing natural and highly active synthetic auxin response elements. ***Plant Cell*** 9, 1963-1971.

Vanstraelen M, Benkova E (2012) Hormonal interactions in the regulation of plant development. ***Annu Rev Cell Dev Biol*** 28, 463-487.

Vernoux T, Brunoud G, Farcot E, Morin V, Van den Daele H, Legrand J, Oliva M, Das P, Larrieu A, Wells D, Guedon Y, Armitage L, Picard F, Guyomarc'h S, Cellier C, Parry G, Koumproglou R, Doonan JH, Estelle M, Godin C, Kepinski S, Bennett M, De Veylder L, Traas J (2011) The auxin signalling network translates dynamic input into robust patterning at the shoot apex. ***Mol Syst Biol*** 7, 508.

Vernoux T, Kronenberger J, Grandjean O, Laufs P, Traas J (2000) *PIN-FORMED 1* regulates cell fate at the periphery of the shoot apical meristem. ***Development*** 127, 5157-5165.

Wang D, Pei K, Fu Y, Sun Z, Li S, Liu H, Tang K, Han B, Tao Y (2007) Genome-wide analysis of the *auxin response factors* (*ARF*) gene family in rice (*Oryza sativa*). ***Gene*** 394, 13-24.

Weijers D, Schlereth A, Ehrismann JS, Schwank G, Kientz M, Jurgens G (2006) Auxin triggers transient local signaling for cell specification in *Arabidopsis* embryogenesis. ***Dev Cell*** 10, 265-270.

Wilkinson LG, Bird DC, Tucker MR (2018) Exploring the Role of the Ovule in Cereal Grain Development and Reproductive Stress Tolerance. ***Annual Plant Reviews***.

Wilkinson LG, Tucker MR (2017) An optimised clearing protocol for the quantitative assessment of sub-epidermal ovule tissues within whole cereal pistils. ***Plant Methods*** 13, 67.

Wolters H, Jurgens G (2009) Survival of the flexible: hormonal growth control and adaptation in plant development. ***Nat Rev Genet*** 10, 305-317.

Worley CK, Zenser N, Ramos J, Rouse D, Leyser O, Theologis A, Callis J (2000) Degradation of Aux / IAA proteins is essential for normal auxin signalling. ***Plant J***. 21, 553-562.

Wu W, Liu Y, Wang Y, Li H, Liu J, Tan J, He J, Bai J, Ma H (2017) Evolution Analysis of the *Aux*/*IAA* Gene Family in Plants Shows Dual Origins and Variable Nuclear Localization Signals. ***Int J Mol Sci*** 18.

Wurschum T, Langer SM, Longin CFH, Tucker MR, Leiser WL (2017) A modern Green Revolution gene for reduced height in wheat. ***Plant J*** 92, 892-903.

Wurschum T, Leiser WL, Langer SM, Tucker MR, Longin CFH (2018) Phenotypic and genetic analysis of spike and kernel characteristics in wheat reveals long-term genetic trends of grain yield components. ***Theor Appl Genet***.

Xie Q, Mayes S, Sparkes DL (2015) Carpel size, grain filling, and morphology determine individual grain weight in wheat. ***J Exp Bot*** 66, 6715-6730.

Xu M, Zhu L, Shou HX, Wu P (2005) A *PIN1* family gene, *OsPIN1*, involved in auxin-dependent adventitious root emergence and tillering in rice. ***Plant Cell Physiol*** 46, 1674-1681.

Yan DW, Duermeyer L, Leoveanu C, Nambara E (2014) The Functions of the Endosperm During Seed Germination. ***Plant Cell Physiol*** 55, 1521-1533.

Yang J, Yuan Z, Meng Q, Huang G, Périn C, Bureau C, Meunier A-C, Ingouff M, Bennett MJ, Liang W (2017a) Dynamic regulation of auxin response during rice development revealed by newly established hormone biosensor markers. ***Front Plant Sci*** 8.

Yang Z, van Oosterom EJ, Jordan DR, Hammer GL (2009) Pre-anthesis ovary development determines genotypic differences in potential kernel weight in sorghum. ***J Exp Bot*** 60, 1399-1408.

Yelina NE, Smith LM, Jones AM, Patel K, Kelly KA, Baulcombe DC (2010) Putative *Arabidopsis* THO/TREX mRNA export complex is involved in transgene and endogenous siRNA biosynthesis. ***Proc Natl Acad Sci U S A*** 107, 13948-13953.

Yoshikawa T, Ito M, Sumikura T, Nakayama A, Nishimura T, Kitano H, Yamaguchi I, Koshiba T, Hibara KI, Nagato Y, Itoh JI (2014) The rice *FISH BONE* gene encodes a tryptophan aminotransferase, which affects pleiotropic auxin-related processes. ***Plant J*** 78, 927-936.

Zhang S, Wang S, Xu Y, Yu C, Shen C, Qian Q, Geisler M, Jiang de A, Qi Y (2015) The auxin response factor, *OsARF19*, controls rice leaf angles through positively regulating *OsGH3-5* and *OsBRI1*. ***Plant Cell Environ*** 38, 638-654.

Zhao FY, Hu F, Zhang SY, Wang K, Zhang CR, Liu T (2013) MAPKs regulate root growth by influencing auxin signaling and cell cycle-related gene expression in cadmium-stressed rice. ***Environ Sci Pollut Res Int*** 20, 5449-5460.

Table 1: Reporter genes for auxin synthesis, distribution and transport available in plants.

					Expression		
Marker type/name	Usage	Mechanism	Reporter	Species	Vegetative Tissues	Reproductive Tissues	Reference
Auxin synthesis							
pTAA1::TAA1-GFP	Indicates the IPA pathway of auxin synthesis	TAA1 is an tryptophan aminotransferase	GFP	Arabidopsis	QC area in root, vasculature of hypocotyls and apical hooks	Young flowers, embryo attachment region, chalaza and funiculus	Stepanova et al., 2008; Robert et al., 2018
pTAR2::GUS	Indicates the IPA pathway of auxin synthesis	TAR2 is a close homolog of TAA1	GUS	Arabidopsis	Nascent leaves, root pericycle and vasculature	The micropylar end of the embryo sac	Ma et al., 2014; Panoli et al., 2015
YUC1::GUS	Indicates the YUC pathway of auxin synthesis	YUCs are flavin monooxygenase-like enzymes	GUS	Arabidopsis	Leaves	Floral meristem, base of floral organs, discrete groups of cells in both stamens and carpels, female gametophyte and neighbouring cells, embryo	Cheng et al., 2006; Cheng et al., 2007; Pagnussat et al., 2009
YUC1::GFP			nuclear targeted 3 X GFP	Arabidopsis		Suspensor cells at 16-cell stage of embryogenesis	Robert et al., 2013
YUC2::GUS			GUS	Arabidopsis		Young flower buds, petals, stamens, and gynoecium of young flowers, nucellus, micropylar end of the embryo sac	Cheng et al., 2006; Pagnussat et al., 2009
YUC4::GFP			nuclear targeted 3 X GFP	Arabidopsis		Protodermal cells from globular and transition stages of embryogenesis, suspensor cells at 16-cell stage of embryogenesis	Robert et al., 2013
YUC4::GUS			GUS	Arabidopsis		Apical meristems and young floral primordia, apical regions of the carpels, stamens, and sepals, inner integument cells close to the micropyle	Cheng et al., 2006; Ceccato et al., 2013
YUC6::GUS			GUS	Arabidopsis		Stamens and pollen	Cheng et al., 2006

YUC8::GFP			GFP	Arabidopsis		Micropylar pole of the female gametophyte, integuments	Panoli et al., 2015
YUC8::GUS			GUS	Arabidopsis		Provascular cells at a late globular stage of embryogenesis	Robert et al., 2013
YUC9::GFP			Cytosolic GFP	Arabidopsis		Suspensor cells at 16-cell stage of embryogenesis	Robert et al., 2013
YUC10::GFP			nuclear targeted 3 X GFP	Arabidopsis		Endosperm	Robert et al., 2013
YUC11::GFP			Cytosolic GFP	Arabidopsis		Endosperm	Robert et al., 2013
Auxin distribution and response							
DR5::GUS	Monitors auxin distribution	7X TGTCTC AuxRE	GUS	Arabidopsis	Seedlings, roots		Ulmasov et al., 1997; Sabatini et al., 1999
				Populus	Leaves, roots, stems		Chen et al., 2013
				Rice		Base of the anther and the mature spikelet	Zhao et al., 2013
DR5::GFP		9X CCTTTTGTCTC AuxRE	GFP	Arabidopsis	Root	Nucellus and embryo sac of the ovule	Ottenschläger et al., 2002; Pagnussat et al., 2009
DR5rev::PEH *A*		9X TGTCTC AuxRE	Phosphonate monoester hydrolase	Arabidopsis		Embryo	Friml et al., 2002
DR5rev::GFP		9X TGTCTC AuxRE	GFP	Arabidopsis	Whole plant	Floral primordia, floral organs, ovule primordia, mature ovules, integuments	Benková et al., 2003
DR5rev::mRFPer		9X TGTCTC AuxRE	ER targeted monomeric RFP	Arabidopsis	Root		Marin et al., 2010

				Maize		Spikelet-pair meristem, glume primordia, floral meristem. L2 micropylar nucellus of ovule	Gallavotti et al., 2008; Lituiev et al., 2013
DR5v2::ntdTomato/3nGFP	Monitors auxin distribution, enhanced sensitivity via the higher affinity of AuxRE	9X TGTCGG AuxRE	Nuclear tandem Tomato or nuclear 3×eGFP	Arabidopsis	Root		Liao et al., 2015
DR5::3XVENUSnls		NA	Nuclear 3XVENUS	Tomato	Root		Spiegelman et al., 2015
DR5rev::3XVENUS-N7		9X TGTCTC AuxRE	Nuclear 3XVENUS (a rapidly folding YFP)	Arabidopsis		Inflorescence meristem, primordial areas	Heisler et al., 2005
				Rice	Root	Inflorescence meristem, spikelet meristems, glume/lemma/lodicule/stamen primordia	Yang et al., 2017
pHvPLT1::HvPLT1-mVENUS	Mirrors auxin distribution	Auxin signailling downstream gene HvPLT	C-terminal mVENUS	Barley	Root		Kirschner et al., 2018
CaV35S::DII-VENUS-NLS	Monitors auxin signalling input by switching off the	Aux/IAA auxin-interaction domain (termed domain II; DII)	VENUS	Arabidopsis		Complementary with DR5-VENUS signals	Brunoud et al., 2012; Vernoux et al., 2011

	signal in the presence of auxin						
R2D2 (ratiometric *version of two DIIs) RPS5A:: DII-n3VENUS fused with RPS5A::mDII-ntdTomato*	Quantitatively measures 'auxin input'	DII and mDII (lack auxin-dependent degradation)	Nuclear tandem Tomato or nuclear 3×eGFP	Arabidopsis	Root		Liao et al., 2015
Auxin transport							
AUX1::GUS	Traces auxin influx	AUX1 is a representative influx carrier of auxin	GUS	Arabidopsis	Major tissue of root		Marchant et al., 1999
PIN1::GUS	Traces auxin efflux		GUS	Arabidopsis	Lateral root		Benková et al., 2003
PIN1::PIN1-GFP		PIN proteins are polar localised in cells, indicaitors of auxin concentration gradient.	GFP	Arabidopsis	Root	Embryo, floral meristem, organ primordia, nucellus of young ovule	Benková et al., 2003; Pagnussat et al., 2009; Gallavotti et al., 2008
ZmPIN1a::PIN1a-YFP			YFP	Maize		Nucellus cell, antipodal cells	Chetoor and Evans, 2015
SoPIN1: SoPIN1-Citrine			Citrine (a variant of YFP)	Brachypodium		Spikelet meristem and lemma primordia	O'Connor et al., 2014
HvpPIN1a:HvPIN1amVENUS			C-terminal cVENUS	Barley	Root		Kirschner et al., 2018

PIN2::GFP	GFP	Arabidopsis	Root	Nucellus	Blilou et al., 2005; Pagnussat et al., 2009
PIN4::GFP	GFP	Arabidopsis	Root	Nucellus	Blilou et al., 2005; Pagnussat et al., 2009
PIN5::GUS	GUS	Arabidopsis	Root		Mravec et al., 2009
PIN6::GFP	GFP	Arabidopsis		Nectary and stamen	Bender et al., 2013
PIN7::GFP	GFP	Arabidopsis	Root		Blilou et al., 2005
PIN8::GFP	GFP	Arabidopsis		Pollen specific	Bosco et al., 2012

PIN5::GUS	GUS	Arabidopsis	Root		Mravec et al., 2009
PIN6::GFP	GFP	Arabidopsis		Nectary and stamen	Bender et al., 2013
PIN7::GFP	GFP	Arabidopsis	Root		Blilou et al., 2005
PIN8::GFP	GFP	Arabidopsis		Pollen specific	Bosco et al., 2012

Table 2: Transcript abundance of TIR/AFB, ARF and Aux/IAA genes in different barley tissues.

ID	Gene	Leaf	Root	Int	Inf 5mm	Inf 15mm	Car 5DAP	Car 15 DAP	Emb 4DAG
HvTIR1	HORVU1Hr1G021550	10.7	17.2	24.2	52.3	80.5	43.4	6.2	28.4
HvAFB2	HORVU2Hr1G070800	24.3	28.7	42.2	110.6	148.6	33.9	21.2	48.1
HvAFB3	HORVU5Hr1G075620	3.8	4.6	8	8.8	12.7	8.5	3.6	5.9
HvAFB4	HORVU6Hr1G077570	12.8	18.9	34.7	65.6	54.2	28.5	5	32.3
HvAFB5	HORVU4Hr1G078120	3.2	6.9	3.9	24.1	21.3	6.7	1.9	13.3
HvARF1	HORVU3Hr1G032230	0.4	8.8	0.1	0.4	1.8	13.6	3.5	4.9
HvARF2	HORVU1Hr1G087460	11.6	8.8	36.1	49.6	61.3	25.5	2	18.6
HvARF3	HORVU3Hr1G072340	6.3	10.6	32.8	29.2	65.3	45.4	4.8	16.8
HvARF4a	HORVU3Hr1G097200	52.6	31	48.7	197	293	56.1	31.9	35.4
HvARF4b	HORVU3Hr1G096410	2.5	2.8	0.7	7.6	9.4	1.8	0.6	2.3
HvARF4c	HORVU3Hr1G096510	84.3	68.4	70.4	334.1	524.5	123.9	29.8	70.9
HvARF5	HORVU6Hr1G020330	11	5.1	24.2	12.3	12.8	1	0.6	5.9
HvARF6	HORVU6Hr1G026730	13	13.8	30.1	37.4	56.3	7.3	4.7	19.6
HvARF8	HORVU6Hr1G058890	4.1	0.7	4.5	3.4	1.1	5.4	0.5	2
HvARF9	HORVU2Hr1G076920	92.8	100.7	77.9	120.7	115.9	53.6	23.6	67.1
HvARF10a	HORVU2Hr1G089670	4.1	6.9	25.1	3.1	2.9	18.5	2.2	7.7
HvARF10b	HORVU2Hr1G089660	0	0	0.3	0	0.1	0.4	0.1	0.1
HvARF11	HORVU2Hr1G109650	0.4	1.2	0.3	42.3	38.8	0.4	3	1.7
HvARF12	HORVU2Hr1G121110	15.1	17.3	82.4	128.4	79.7	50	3.6	42.3
HvARF13	HORVU2Hr1G125740	0	0	0	0	0.5	2.3	1.1	0
HvARF14	HORVU1Hr1G076690	1.4	1.8	1.8	32.3	47.7	6.6	3	3.6
HvARF16	HORVU7Hr1G033820	10.2	4.8	12.9	21.8	17.1	19.1	5.6	11.8
HvARF17	HORVU7Hr1G106280	34	22.1	101.7	127.6	145.1	68.9	11.8	50.9
HvARF18	HORVU7Hr1G101270	24.8	14.4	29.3	7.8	10.8	46.3	6.2	15.5
HvARF19	HORVU7Hr1G096460	10.2	12	17.5	17.8	19.4	7.2	1.4	9.8
HvARF21	HORVU7Hr1G051930	30	26.3	125.4	45.4	47.9	16.3	3	42.8
HvARF22	HORVU1Hr1G041770	7.3	7.5	28	7.5	13.2	83.3	5.7	12.9
HvARF25	HORVU5Hr1G009650	8.3	14.8	31.9	125.2	111	75	6.1	30.9
HvIAA1	HORVU3Hr1G022540	26.2	27.7	446.8	13	17.9	63.6	8.2	26.7
HvIAA2	HORVU3Hr1G019750	11	12.8	48.6	21.6	12.2	37.3	0.8	21.5
HvIAA3	HORVU3Hr1G031460	108.7	78.9	263	127	169.5	102.2	11	103.1
HvIAA4	HORVU1Hr1G017770	2.8	0.3	2.1	0	0	0.9	0.1	0.2
HvIAA5a	HORVU3Hr1G062160	1.5	0.8	0.7	2.5	3.9	1.3	1	0.8
HvIAA5b	HORVU3Hr1G088810	1.5	2.9	2.3	2.4	3.9	1.5	1.4	3.1
HvIAA6	HORVU3Hr1G070620	25.6	14.9	7	14	6.2	0.4	0.8	13.8

HvIAA9	HORVU6Hr1G088140	0.6	1.8	1.3	0.1	0.2	0.1	0	2
HvIAA10	HORVU6Hr1G091260	44.2	14.3	96.1	29.6	43.9	6.7	1.3	11.2
HvIAA11	HORVU5Hr1G093580	2.2	38.5	20.4	1	1.6	23	1.1	32.1
HvIAA12	HORVU5Hr1G093640	21.3	73.6	301	2.4	1.1	2.9	0.6	110.4
HvIAA13	HORVU5Hr1G094220	0.2	0.1	0	0	0.3	0.1	0.2	0.2
HvIAA14	HORVU5Hr1G106350	17.1	3.7	22.5	1.9	2.2	40.5	3.7	8.8
HvIAA15	HORVU1Hr1G025670	25.3	20.3	92.2	12	20.7	13.4	2.6	22.6
HvIAA16	HORVU1Hr1G028170	1.3	3.6	0.1	21.3	20.5	0.4	0.3	4.5
HvIAA19	HORVU1Hr1G086070	13.7	10.5	19.6	29	21.1	1.7	0.4	18.8
HvIAA20	HORVU7Hr1G026970	0	7	0	0	0	0	0	1.6
HvIAA21	HORVU0Hr1G021630	225.4	53	906.7	112.7	190.5	166.6	28	52.5
HvIAA22	HORVU7Hr1G077110	2.1	0.9	8.3	3.8	4.7	2.1	0.3	0.7
HvIAA23	HORVU7Hr1G084940	10.1	19	28.9	16.8	2.4	0.2	0.7	27.5
HvIAA26	HORVU5Hr1G081180	0	0.4	0	2.4	1.1	0	0.2	4.3
HvIAA27	HORVU4Hr1G016160	1.2	4.5	5.8	5.2	5.5	0	0.2	7.1
HvIAA28	HORVU4Hr1G016110	0	0	0	0	0	114.9	0	0
HvIAA30	HORVU5Hr1G014300	87.2	82.2	320.2	30.3	42	104.3	3.3	167.5
HvIAA31	HORVU5Hr1G014290	116.6	69.9	731.1	13.1	17.3	38.9	0.9	156
HvIAA33	HORVU2Hr1G112440	3	0.4	0	0.2	0.9	0	0.1	2

Transcript abundance for the predicted TIR/AFB, ARF and Aux/IAA genes in eight tissues from barley, as determined by RNAseq. Values show TPM and are extracted from public datasets (IBGS 2012). Grey boxes indicate highest TPM value for a given gene. Tissues: Internodes (Int), inflorescences (Inf), caryopsis (Car), embryo (Emb). Days after pollination (DAP); Days after germination (DAG).

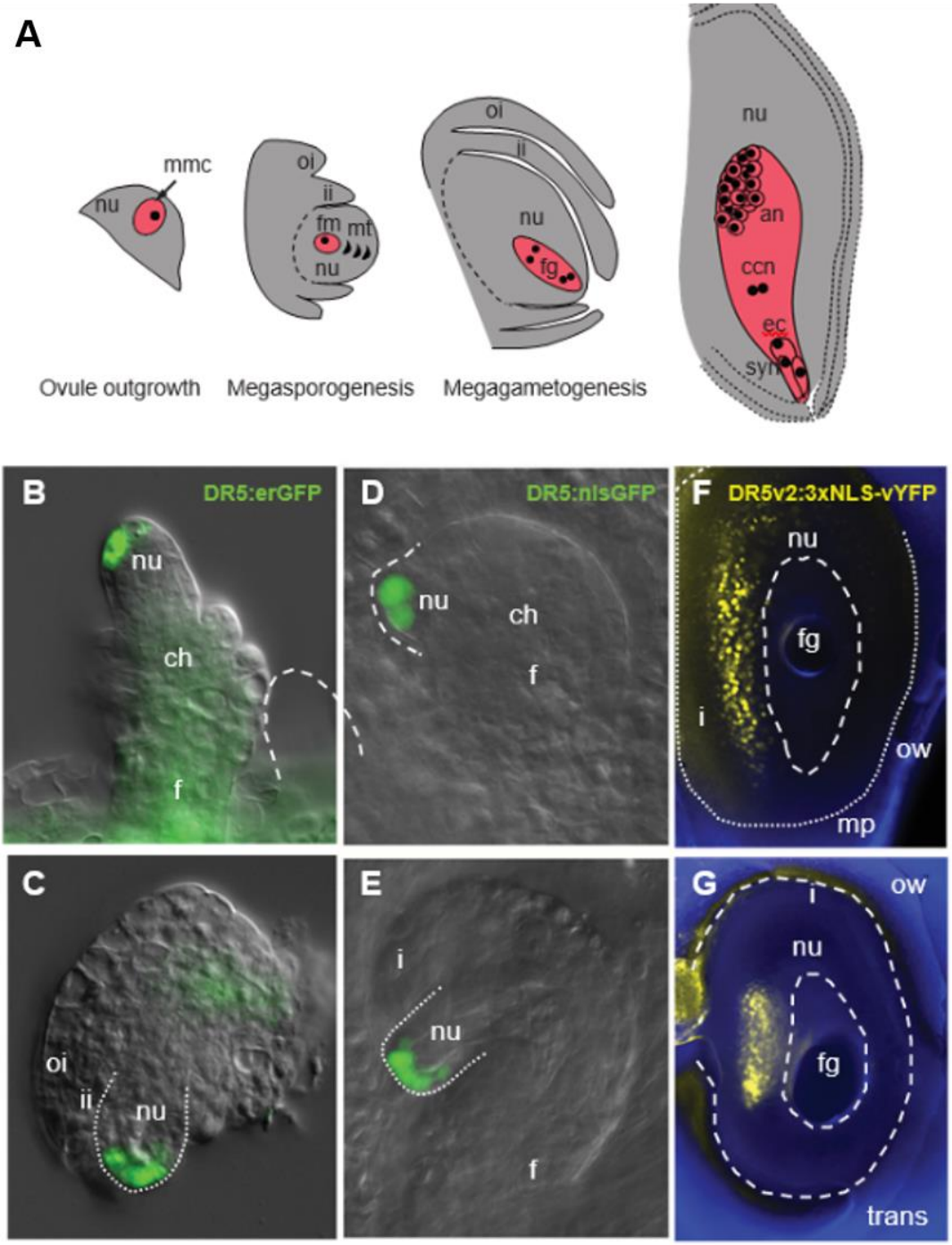

Figure 1: Patterns of auxin accumulation during ovule development. (**A**) Schematic representation of ovule development in barley. Four stages are shown including ovule initiation, megasporogenesis, megagametogenesis and ovule maturity at anthesis. nu, nucellus; mmc, megaspore mother cell; oi, outer integument; ii, inner integument; fm, functional megaspore; fg, female gametophyte; mt, meiotic tetrad; an, antipodals; ccn, central cell nuclei; ec, egg cell; syn, synergids. (**B, C**) DR5:erGFP accumulation in

Arabidopsis during megaspore mother cell expansion and after meiosis. ch, chalaza; f, funiculus. (**D, E**) DR5:nlsGFP accumulation in *Hieracium* during megaspore mother cell initiation and expansion (adapted from Tucker et al. 2012). (**F, G**) DR5v2:3xnlsvYFP expression in mature barley ovules. Panels show a longitudinal and transverse view. ow, ovary wall.

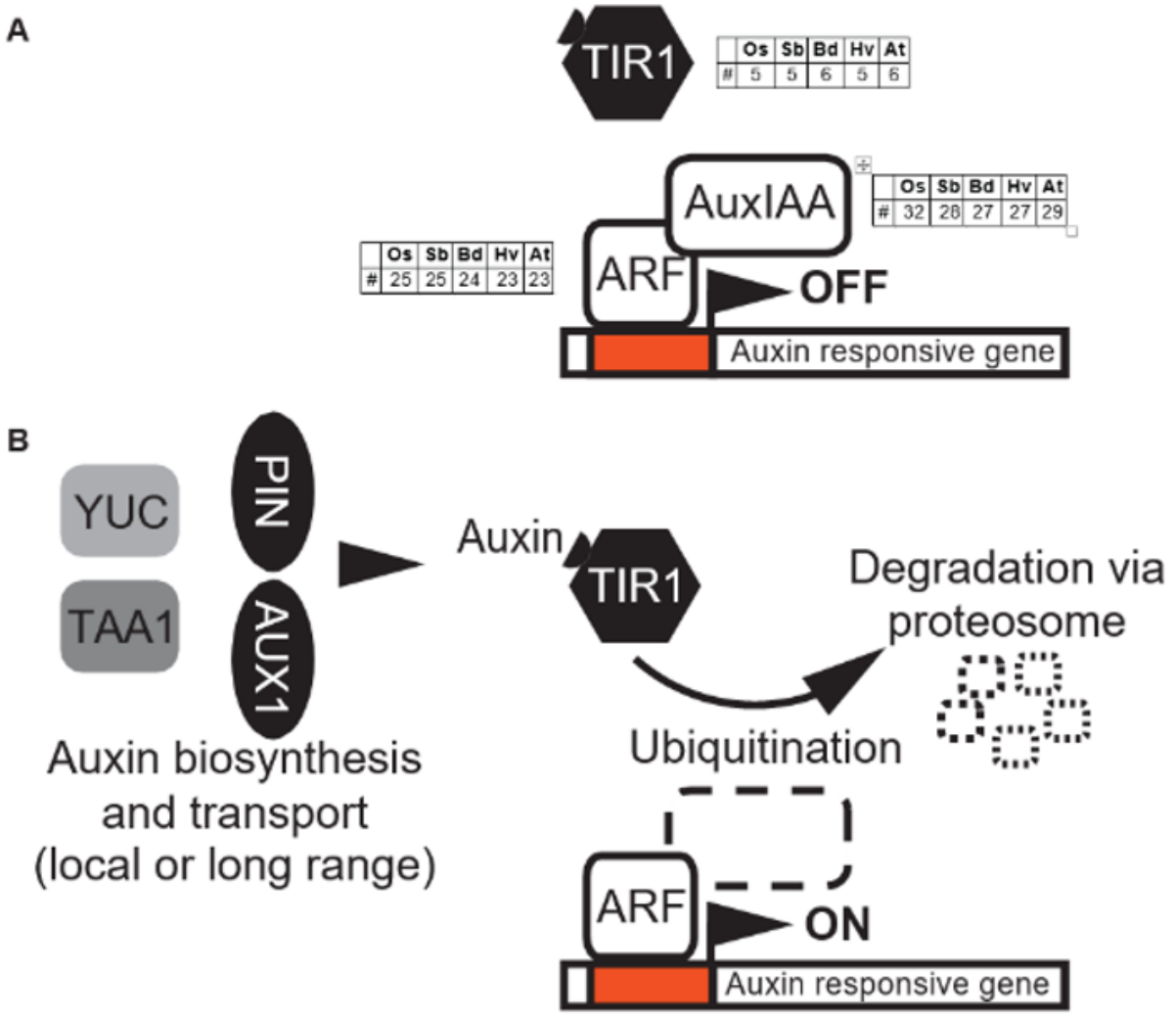

Figure 2: A schematic representation of auxin signalling pathway. (**A**) In the absence of auxin or at low auxin levels, Aux/IAA proteins limit the activity of ARF proteins through recruitment of co-repressors. (**B**) Synthesis of auxin is facilitated by TAA1 and YUC proteins and is transported via diffusion, AUX1 and PIN proteins. The TIR1 protein binds auxin to form a complex which leads to degradation of Aux/IAA and de-repression of ARF target genes. The number of *TIR1*/*AFB*, *ARF* and *Aux*/*IAA* genes in *Oryza sativa* (rice), *Sorghum bicolor*, *Brachypodium distachyon*, *Hordeum vulgare* (barley) and *Arabidopsis thaliana* are indicated.

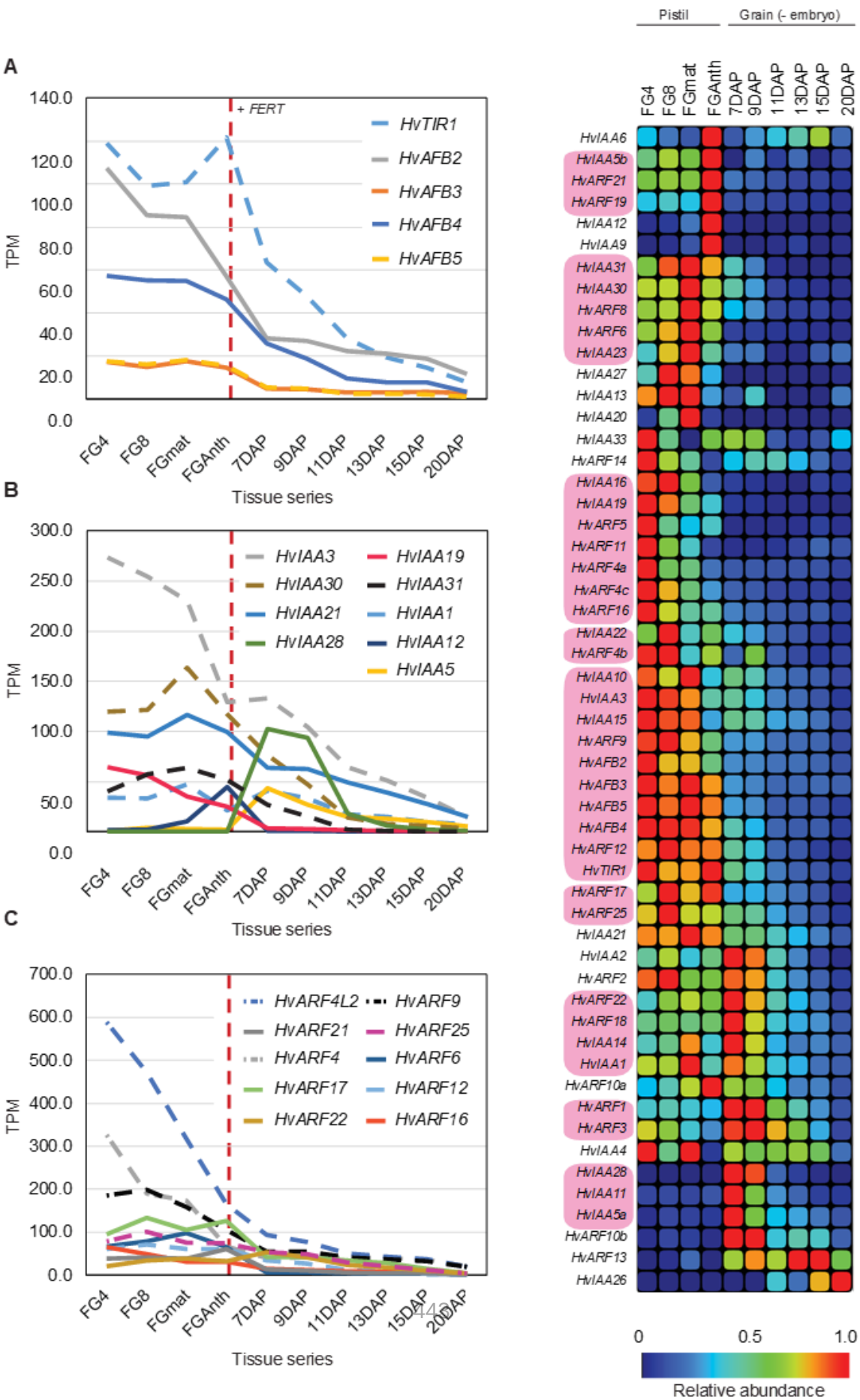
A
140.0
120.0
100.0
80.0
60.0
40.0
20.0
0.0
TPM
+ FERT
HvTIR1
HvAFB2
HvAFB3
HvAFB4
HvAFB5
FG4
FG8
FGmat
FGAnth
7DAP
9DAP
11DAP
13DAP
15DAP
20DAP
Tissue series
B
300.0
250.0
200.0
150.0
100.0
50.0
0.0
TPM
HvIAA3
HvIAA30
HvIAA21
HvIAA28
HvIAA19
HvIAA31
HvIAA1
HvIAA12
HvIAA5
Tissue series
C
700.0
600.0
500.0
400.0
300.0
200.0
100.0
0.0
TPM
HvARF4L2
HvARF21
HvARF4
HvARF17
HvARF22
HvARF9
HvARF25
HvARF6
HvARF12
HvARF16
Tissue series
Pistil
Grain (- embryo)
FG4
FG8
FGmat
FGAnth
7DAP
9DAP
11DAP
13DAP
15DAP
20DAP
HvIAA6
HvIAA5b
HvARF21
HvARF19
HvIAA12
HvIAA9
HvIAA31
HvIAA30
HvARF8
HvARF6
HvIAA23
HvIAA27
HvIAA13
HvIAA20
HvIAA33
HvARF14
HvIAA16
HvIAA19
HvARF5
HvARF11
HvARF4a
HvARF4c
HvARF16
HvIAA22
HvARF4b
HvIAA10
HvIAA3
HvIAA15
HvARF9
HvARF2
HvARF3
HvARF5
HvARF4
HvARF12
HvTIR1
HvARF17
HvARF25
HvIAA21
HvIAA2
HvARF2
HvARF22
HvARF18
HvIAA14
HvIAA1
HvARF10a
HvARF1
HvARF3
HvIAA4
HvIAA28
HvIAA11
HvIAA5a
HvARF10b
HvARF13
HvIAA26
0
0.5
1.0
Relative abundance

Figure 3: Transcript dynamics of the *TIR*, *ARF* and *Aux*/*IAA* (*IAA*) gene families in barley extracted from publically available pistil and seed RNAseq datasets (Aubert et al., 2018). (**A**) TIR1 family. (**B**) ARF family. (**C**) IAA family. In **B** and **C**, only genes showing a transcript value of at least 50TPM in at least one stage are included. The dashed line indicates the approximate timing of fertilisation (FERT). (**D**) Hierarchical cluster analysis of all barley *TIR*, *ARF* and *IAA* genes during pistil and seed development. Values were normalised relative to the highest expression (in TPM) in the dataset. Pink boxes highlight gene clusters showing similar accumulation patterns according to hierarchical clustering.

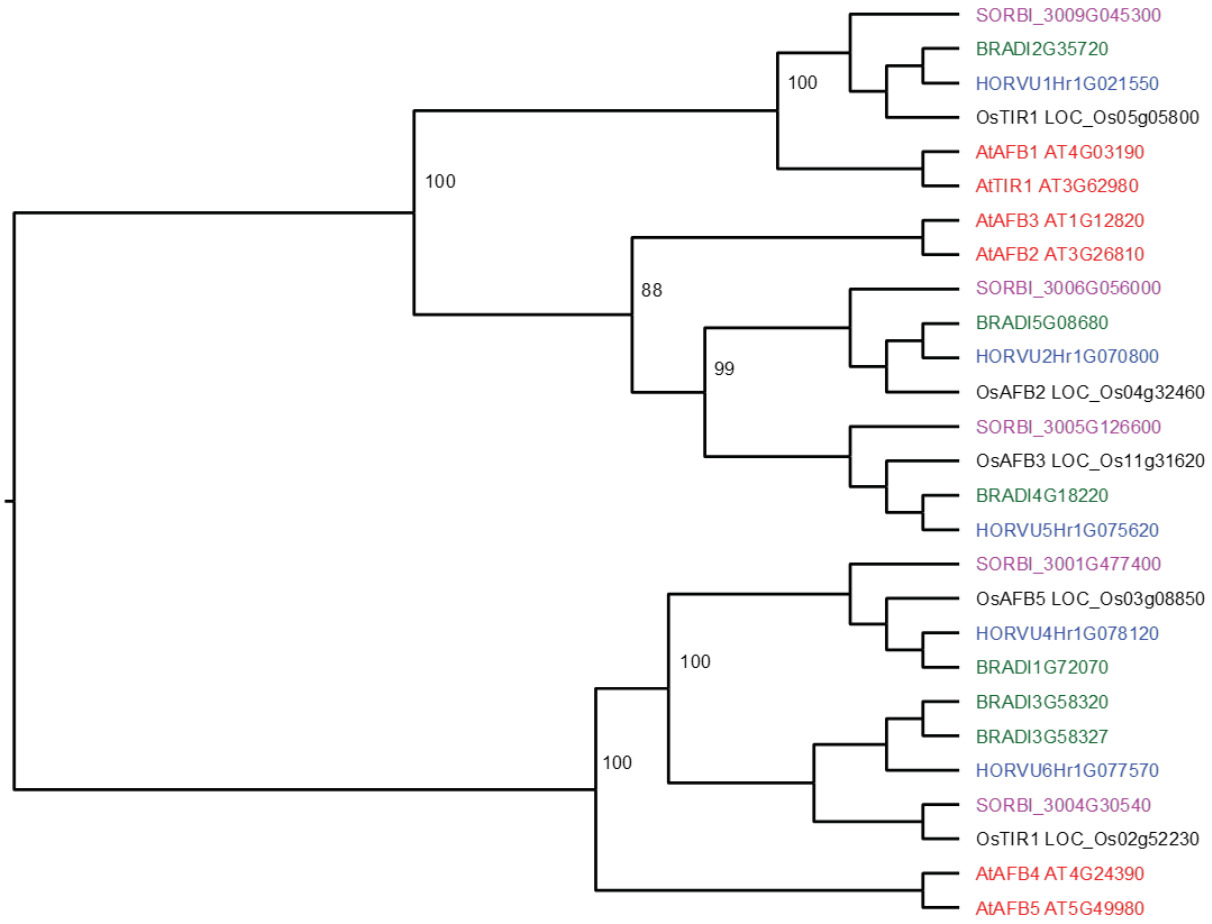

Figure 4: Phylogenetic analysis of the TIR1/AFB family from rice, sorghum, Brachypodium, barley and Arabidopsis. Arabidopsis sequences were obtained from the TAIR website (https://www.arabidopsis.org/). Barley, sorghum, rice and Brachypodium were downloaded from the Ensembl Plants Biomart website (http://plants.ensembl.org/biomart/martview/) using appropriate PFAM (Finn et al., 2014) parameters (Aux/IAA=PFAM02309, Fig 5; ARF=PFAM2309, Fig 6), from the Rice Genome Annotation Project (http://rice.plantbiology.msu.edu/index.shtml) and by BLAST at NCBI (https://blast.ncbi.nlm.nih.gov/Blast.cgi). For each gene family, the coding sequences were curated using the FGENESH+ application (Solovyev, 2007) then aligned by translation after which a tree was constructed in Geneious Pro 8.1.3 ((Biomatters Ltd. Level 2 76 Anzac Avenue Auckland 1010 New Zealand) using RaXML (Stamatakis, 2006) with the GTRGAMMA substitution model and 1000 bootstrap iterations.

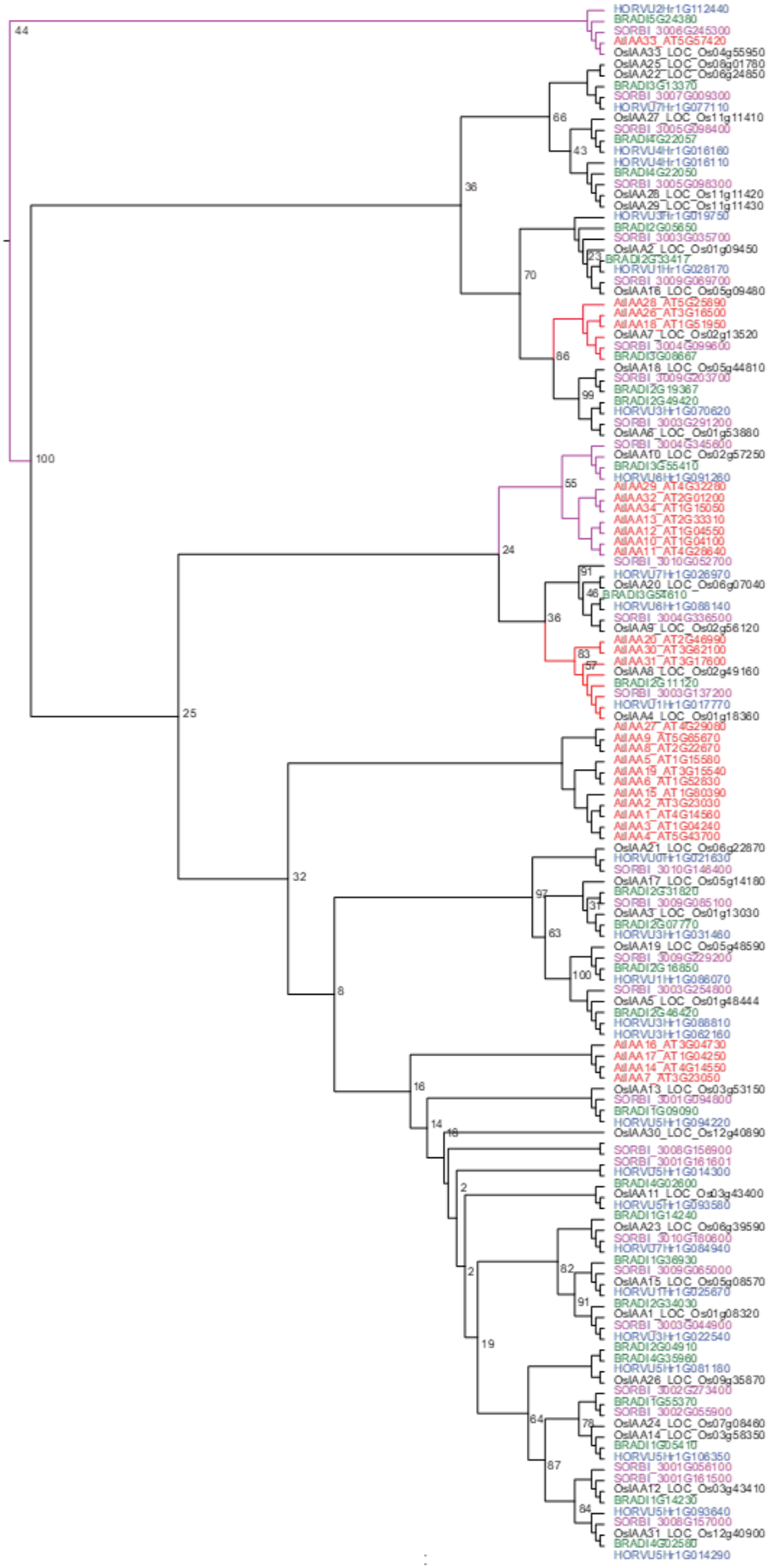
HORVU2Hr1G112440
BRADI5G24380
SORBI_3006G245300
AtIAA33_AT5G57420
OsIAA33_LOC_Os04g55950
OsIAA25_LOC_Os08g01780
OsIAA22_LOC_Os06g24850
BRADI3G13370
SORBI_3007G009300
HORVU7Hr1G077110
OsIAA27_LOC_Os11g11410
SORBI_3005G098400
BRADI4G22057
HORVU4Hr1G016160
HORVU4Hr1G016110
BRADI4G22050
SORBI_3005G098300
OsIAA28_LOC_Os11g11420
OsIAA29_LOC_Os11g11430
HORVU3Hr1G019750
BRADI2G05650
SORBI_3003G035700
OsIAA2_LOC_Os01g09450
BRADI2G33417
HORVU1Hr1G028170
SORBI_3009G069700
OsIAA16_LOC_Os05g09480
AtIAA28_AT5G25890
AtIAA26_AT3G16500
AtIAA18_AT1G51950
OsIAA7_LOC_Os02g13520
SORBI_3004G099600
BRADI3G08867
OsIAA18_LOC_Os05g44810
SORBI_3009G203700
BRADI2G19387
BRADI2G49420
HORVU3Hr1G070620
SORBI_3003G291200
OsIAA6_LOC_Os01g53880
SORBI_3004G345600
OsIAA10_LOC_Os02g57250
BRADI3G55410
HORVU6Hr1G091280
AtIAA29_AT4G32280
AtIAA32_AT2G01200
AtIAA34_AT1G15050
AtIAA13_AT2G33310
AtIAA12_AT1G04550
AtIAA10_AT1G04100
AtIAA11_AT4G28640
SORBI_3010G052700
HORVU7Hr1G026970
OsIAA20_LOC_Os06g07040
BRADI3G57610
HORVU6Hr1G088140
SORBI_3004G336500
OsIAA9_LOC_Os02g56120
AtIAA20_AT2G46990
AtIAA30_AT3G62100
AtIAA31_AT3G17600
OsIAA8_LOC_Os02g49160
BRADI2G11120
SORBI_3003G137200
HORVU1Hr1G017770
OsIAA4_LOC_Os01g18360
AtIAA27_AT4G29080
AtIAA9_AT5G65670
AtIAA8_AT2G22670
AtIAA5_AT1G15580
AtIAA19_AT3G15540
AtIAA6_AT1G52830
AtIAA15_AT1G80390
AtIAA2_AT3G23030
AtIAA1_AT4G14560
AtIAA3_AT1G04240
AtIAA4_AT5G43700
OsIAA21_LOC_Os06g22870
HORVU0Hr1G021630
SORBI_3010G148400
OsIAA17_LOC_Os05g14180
BRADI2G31820
SORBI_3009G085100
OsIAA3_LOC_Os01g13030
BRADI2G07770
HORVU3Hr1G031460
OsIAA19_LOC_Os05g48590
SORBI_3009G229200
BRADI2G16850
HORVU1Hr1G088070
SORBI_3003G254800
OsIAA5_LOC_Os01g48444
BRADI2G46420
HORVU3Hr1G088810
HORVU3Hr1G062160
AtIAA16_AT3G04730
AtIAA17_AT1G04250
AtIAA14_AT4G14550
AtIAA7_AT3G23050
OsIAA13_LOC_Os03g53150
SORBI_3001G094800
BRADI1G09090
HORVU5Hr1G094220
OsIAA30_LOC_Os12g40890
SORBI_3008G156900
SORBI_3001G161601
HORVU5Hr1G014300
BRADI4G02600
OsIAA11_LOC_Os03g43400
HORVU5Hr1G093580
BRADI1G14240
OsIAA23_LOC_Os06g39590
SORBI_3010G180600
HORVU7Hr1G084940
BRADI1G36930
SORBI_3009G065000
OsIAA15_LOC_Os05g08570
HORVU1Hr1G025670
BRADI2G34030
OsIAA1_LOC_Os01g08320
SORBI_3003G044900
HORVU3Hr1G022540
BRADI2G04910
BRADI4G35960
HORVU5Hr1G081180
OsIAA26_LOC_Os09g35870
SORBI_3002G273400
BRADI1G55370
SORBI_3002G055900
OsIAA24_LOC_Os07g08460
OsIAA14_LOC_Os03g58350
BRADI1G05410
HORVU5Hr1G106350
SORBI_3001G056100
SORBI_3001G161500
OsIAA12_LOC_Os03g43410
BRADI1G14230
HORVU5Hr1G093640
SORBI_3008G157000
OsIAA31_LOC_Os12g40900
BRADI4G02580
HORVU5Hr1G014290

Figure 5: Phylogenetic analysis of the Aux/IAA family from rice, sorghum, Brachypodium, barley and Arabidopsis. See Figure 4 legend for construction details. The full-length Aux/IAA gene RAXML tree produced a number of poorly supported nodes with and without partitioning codon position. Because of this, the gene sequence coding for just the PFAM (PF02309) associated with the gene family was extracted and used in a translation alignment. A RAXML tree without codon partitioning was created. A marginal improvement in bootstrap support values was achieved. Red clades are “well supported” and purple clades are poorly supported.

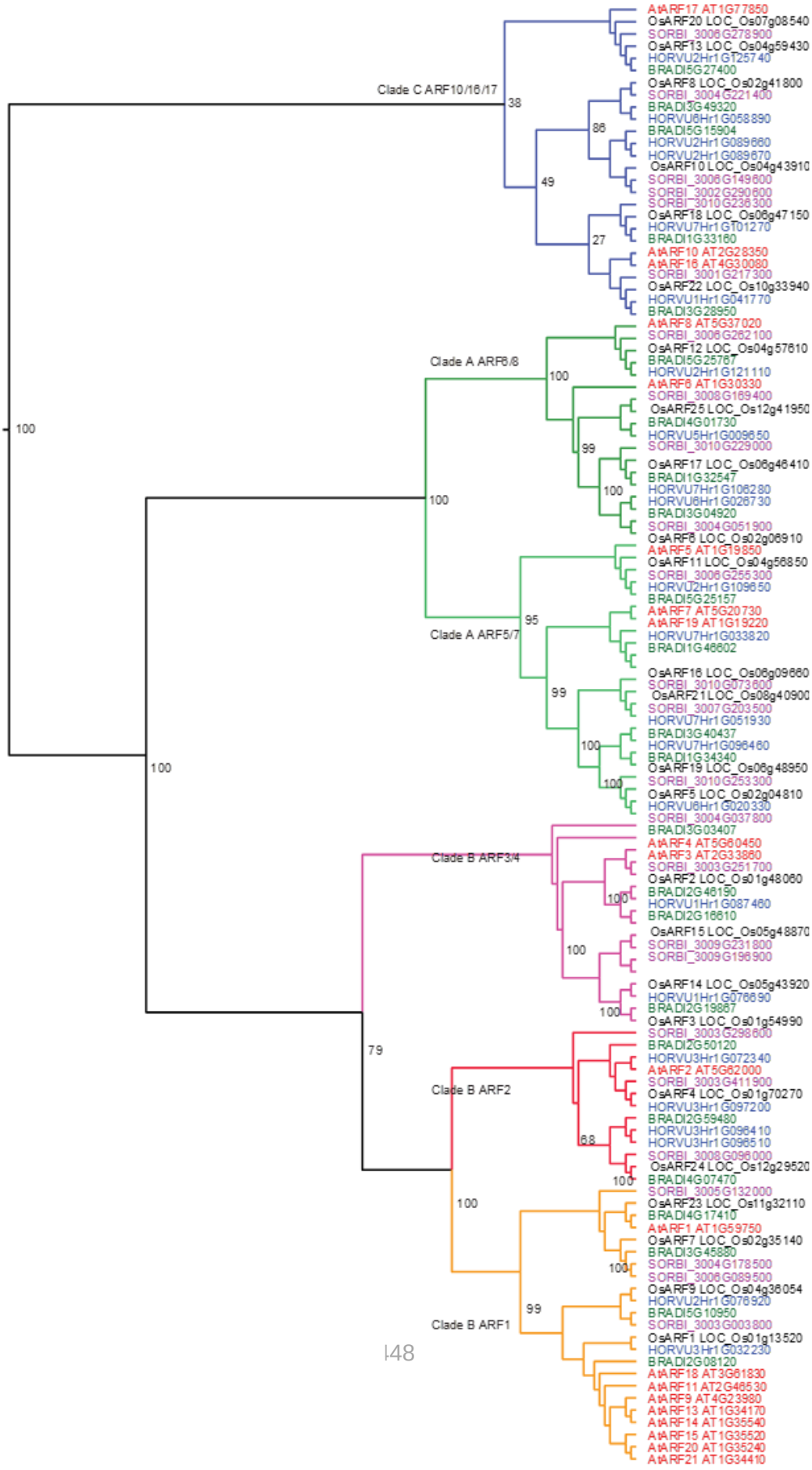
Clade C ARF10/16/17
Clade A ARF6/8
Clade A ARF5/7
Clade B ARF3/4
Clade B ARF2
Clade B ARF1
AtARF17 AT1G77850
OsARF20 LOC_Os07g08540
SORBI_3006G278900
OsARF13 LOC_Os04g59430
HORVU2Hr1GT25740
BRADI5G27400
OsARF8 LOC_Os02g41800
SORBI_3004G221400
BRADI3G49320
HORVU6Hr1G058890
BRADI5G15904
HORVU2Hr1G089660
HORVU2Hr1G089670
OsARF10 LOC_Os04g43910
SORBI_3006G149600
SORBI_3002G290600
SORBI_3010G236300
OsARF18 LOC_Os06g47150
HORVU7Hr1GT01270
BRADI1G33160
AtARF10 AT2G28350
AtARF16 AT4G30080
SORBI_3001G217300
OsARF22 LOC_Os10g33940
HORVU1Hr1G041770
BRADI3G28950
AtARF8 AT5G37020
SORBI_3006G262100
OsARF12 LOC_Os04g57610
BRADI5G25767
HORVU2Hr1G121110
AtARF6 AT1G30330
SORBI_3008G169400
OsARF25 LOC_Os12g41950
BRADI4G01730
HORVU5Hr1G009650
SORBI_3010G229000
OsARF17 LOC_Os06g46410
BRADI1G32547
HORVU7Hr1G106280
HORVU6Hr1G026730
BRADI3G04920
SORBI_3004G051900
OsARF6 LOC_Os02g06910
AtARF5 AT1G19850
OsARF11 LOC_Os04g56850
SORBI_3006G255300
HORVU2Hr1G109650
BRADI5G25157
AtARF7 AT5G20730
AtARF19 AT1G19220
HORVU7Hr1G033820
BRADI1G46602
OsARF16 LOC_Os06g09660
SORBI_3010G073600
OsARF21 LOC_Os08g40900
SORBI_3007G203500
HORVU7Hr1G051930
BRADI3G40437
HORVU7Hr1G096460
BRADI1G34340
OsARF19 LOC_Os06g48950
SORBI_3010G253300
OsARF5 LOC_Os02g04810
HORVU6Hr1G020330
SORBI_3004G037800
BRADI3G03407
AtARF4 AT5G60450
AtARF3 AT2G33860
SORBI_3003G251700
OsARF2 LOC_Os01g48060
BRADI2G46190
HORVU1Hr1G087460
BRADI2G16610
OsARF15 LOC_Os05g48870
SORBI_3009G231800
SORBI_3009G196900
OsARF14 LOC_Os05g43920
HORVU1Hr1G076690
BRADI2G19867
OsARF3 LOC_Os01g54990
SORBI_3003G298600
BRADI2G50120
HORVU3Hr1G072340
AtARF2 AT5G62000
SORBI_3003G411900
OsARF4 LOC_Os01g70270
HORVU3Hr1G097200
BRADI2G59480
HORVU3Hr1G096410
HORVU3Hr1G096510
SORBI_3008G096000
OsARF24 LOC_Os12g29520
BRADI4G07470
SORBI_3005G132000
OsARF23 LOC_Os11g32110
BRADI4G17410
AtARF1 AT1G59750
OsARF7 LOC_Os02g35140
BRADI3G45880
SORBI_3004G178500
SORBI_3006G089500
OsARF9 LOC_Os04g36054
HORVU2Hr1G076920
BRADI5G10950
SORBI_3003G003800
OsARF1 LOC_Os01g13520
HORVU3Hr1G032230
BRADI2G08120
AtARF18 AT3G61830
AtARF11 AT2G46530
AtARF9 AT4G23980
AtARF13 AT1G34170
AtARF14 AT1G35540
AtARF15 AT1G35520
AtARF20 AT1G35240
AtARF21 AT1G34410

Figure 6: Phylogenetic analysis of the ARF family from rice, sorghum, Brachypodium, barley and Arabidopsis. See Fig 4 legend for construction details. Different clades are indicated (Finet et al., 2012) that generally separate activators (Clade A) from repressors (Clades B and C).

Appendix V

Candidature Milestones

ꕥ • ꕥ

December 2014	Offered and accepted an Australian Postgraduate Award
January 2015	Admitted into PhD program at The University of Adelaide
February 2015	Volunteered for the BHP Billiton & CSIRO Aboriginal Summer School for Excellence in Technology and Science (ASSETS)
March 2015	Began PhD
June 2015	Began volunteering for Why Waite
September 2015	Completed the “Core Component of the Structured Program”
April 2016	Completed the “Major Review of Progress for Doctoral Programs” CSIRO-Australian Society of Plant Scientists International Workshop on Developing Crops for the Future, in Kiama NSW
May 2016	Presented a talk at the ARC Centre of Excellence in Plant Cell Walls Annual Meeting, Brisbane, Australia
June 2016	Awarded a Farrer Memorial Travelling Scholarship from the NSW Department of Primary Industries
August 2016	Competed in the local 3 Minute Thesis round, awarded People’s Choice
September 2016	Presented a talk at the 2016 University of Adelaide AFW Postgraduate Symposium, awarded Best Talk in Plant Physiology
November 2016	Presented a talk at the 2016 School of AFW Research Day Presented a talk to the Higashiyama Laboratory Visited the Live Imaging Centre at the Institute of Transformative BioMolecules, Nagoya University, Japan Poster presentation at the Cold Spring Harbour Asia congress on the Latest Advances in Plant Development and Environmental Response, Awaji, Japan

December 2016	Received a Vice Chancellor's certificate of recognition for outstanding volunteer service from the University of Adelaide
March 2017	Presented a talk at the 2017 Waite Barley Research and Development Meeting
April 2017	Awarded the 2017 SARDI Women's Suffrage Centenary Bursary
August 2017	Clearing method paper published (DOI: 10.1186/s13007-017-0217-z) Visited the James Hutton Institute, Scotland, UK
September 2017	Presented a talk at the International Meeting on the Molecular Mechanisms Controlling Flower Development, Padua, Italy
October 2017	Presented poster at ComBio, Adelaide, Australia Honours paper published (DOI: 10.3389/fpls.2017.01872)
February 2018	Selected to participate in the Environmental Institute Leadership Development Program for Early Career Researchers
March 2018	Awarded a Travel Grant from the International Association of Sexual Plant Reproduction Research
April 2018	First-author review paper published (DOI:10.1002/9781119312994.apr0609)
May 2018	Mid-author review paper published (DOI: 10.3390/plants7020042)
June 2018	Presented a poster at the 25th International Congress on Sexual Plant Reproduction, Gifu, Japan
November 2018	Presented a talk at the 2018 School of Agriculture, Food and Wine Research Day Mid-author review paper published (DOI: 10.1111/jipb.12747)
January 2019	Submitted Intention to Submit
February 2019	Submitted thesis for examination
March 2019	Began postdoc at the John Innes Centre
July 2019	Submitted final thesis